

UNIVERSIDAD
NACIONAL
DE COLOMBIA

**DENDRÍMEROS PÉPTIDO-RESORCINARENO:
(i) OBTENCIÓN MEDIANTE REACCIÓN DE CICLOADICIÓN
AZIDA/ALQUINO Y (ii) EVALUACIÓN DE SU POTENCIAL
ANTIBACTERIANO**

**PEPTIDE-RESORCINARENE DENDRIMERS:
(i) OBTAINING THROUGH AZIDE/ALKYNE CYCLOADDITION
REACTION AND (ii) EVALUATION OF ANTIBACTERIAL
POTENTIAL**

Héctor Manuel Pineda Castañeda

Universidad Nacional de Colombia
Facultad de Ciencias, Departamento de Química
Bogotá D.C, Colombia

2023

**DENDRÍMEROS PÉPTIDO-RESORCINARENO:
(i) OBTENCIÓN MEDIANTE REACCIÓN DE CICLOADICIÓN
AZIDA/ALQUINO Y (ii) EVALUACIÓN DE SU POTENCIAL
ANTIBACTERIANO**

Héctor Manuel Pineda Castañeda

Tesis presentada como requisito parcial para optar al título de:

Doctor en Ciencias Químicas

Directora:

Dr. rer. nat. Zuly Jenny Rivera Monroy

Codirector (a):

Ph.D Mauricio Maldonado Villamil

Grupo de Investigación:

Síntesis y Aplicación de Moléculas Peptídicas

Aplicaciones Analíticas de Compuestos orgánicos

Universidad Nacional de Colombia

Facultad de Ciencias, Departamento de Química

Bogotá D, C, Colombia

2023

"Dad... Whatever happens, I want you to know your kid was one of them, dad. One of the best of the best."

~Zack Snyder-Justice League~

Declaración de obra original

Yo declaro lo siguiente:

He leído el Acuerdo 035 de 2003 del Consejo Académico de la Universidad Nacional. «Reglamento sobre propiedad intelectual» y la Normatividad Nacional relacionada al respeto de los derechos de autor. Esta disertación representa mi trabajo original, excepto donde he reconocido las ideas, las palabras, o materiales de otros autores.

Cuando se han presentado ideas o palabras de otros autores en esta disertación, he realizado su respectivo reconocimiento aplicando correctamente los esquemas de citas y referencias bibliográficas en el estilo requerido.

He obtenido el permiso del autor o editor para incluir cualquier material con derechos de autor (por ejemplo, tablas, figuras, instrumentos de encuesta o grandes porciones de texto).

Por último, he sometido esta disertación a la herramienta de integridad académica, definida por la universidad.



Héctor Manuel Pineda Castañeda

Fecha 16/05/2023

Agradecimientos

Agradezco a mis padres y hermanos, mis principales pilares en la vida y con los que puedo contar ante toda dificultad. A mis sobrinos Nicolás, Valentina y Martín, que este producto académico les sea de inspiración en la vida y que sepan que lo que deseen pueden lograrlo.

A mis amigos, Paula, Roger y Alejandro, que se han convertido en mis hermanos y compañeros de viaje, y con quienes compartimos nuestros triunfos, alegrías y tristezas. (Bfsxeveer).

A mi segunda familia, a los integrantes del grupo de investigación Síntesis y Aplicación de Moléculas Peptídicas (SAMP), quienes siempre recurrieron con su apoyo y consejos en pro al desarrollo de mi investigación, un especial agradecimiento a mi colega Natalia Ardila por las innumerables tazas de café sin esas tardes de cotorreo muchas de las ideas aquí plasmadas no se hubieran consolidado.

A mi profesora, tutora y amiga Zuly Rivera quien me ha inspirado, apoyado y contribuido no solo en el desarrollo de esta tesis doctoral si no en muchos aspectos de mi vida personal, muchos de mis triunfos se los debo a ella en gran medida. Solo me queda agradecerle desde mi corazón por todo su tiempo invertido.

A mi codirector Mauricio Maldonado y los integrantes de su grupo de investigación Aplicaciones Analíticas de Compuestos Orgánicos (AACO), por brindarme sus conocimientos en química orgánica y poder ser parte de este gran proyecto.

Al profesor Javier García, quien me ha apoyado con sus incontables consejos siempre buscando fomentar mi formación personal y profesional.

A todos los profesores que como docentes y jurados aportaron sus contribuciones en pro a la mejora de mi proyecto doctoral. En especial a la Doctora Claudia Parra, por abrir las puertas de su laboratorio para desarrollar muchos de los ensayos que fueron involucrados en este proyecto.

A la Universidad Nacional de Colombia, en especial a la Dirección Académica quienes mediante la beca Asistente Docente me brindaron la posibilidad de la continuación de mis estudios de posgrado. Al Ministerio de Ciencias por la financiación del proyecto Diseño y obtención de nuevos agentes antibacterianos basados en dendrímeros péptido-resorcinareno: Una alternativa para combatir la resistencia bacteriana. Y finalmente, al Departamento de Química, en especial al programa de Doctorado en Ciencias-Química. Por abrirme sus espacios, facilitando el debido desarrollo de mis estudios e investigación.

Resumen

La resistencia a los antimicrobianos (RAM) es una de las diez principales amenazas para la salud pública reportadas por la Organización Mundial de la Salud (OMS). Una de las causas del creciente problema de la RAM es la falta de nuevas terapias y/o agentes de tratamiento; en consecuencia, muchas enfermedades infecciosas podrían volverse incontrolables. La necesidad de descubrir nuevos agentes antimicrobianos, que sean alternativos a los existentes, y que permitan mitigar este problema, se ha incrementado debido a la rápida y global expansión de la RAM. En este contexto, se han propuesto como alternativas para combatir la RAM tanto los péptidos antimicrobianos (PAMs) como los dendrímeros que presentan múltiples copias de compuestos antibacterianos en su estructura. Los dendrímeros han exhibido propiedades antifúngicas y antibacterianas y también se han utilizado en terapias antiinflamatorias, antineoplásicas y cardiovasculares y son útiles en sistemas de administración de fármacos y genes. En este trabajo se propuso obtener dendrímeros que presenten cuatro copias de secuencias de PAMs. Específicamente, (i) se exploró la síntesis, purificación y caracterización de dendrímeros de péptido-resorcinareno derivados de las secuencias LfcinB (20-25): RRWQWR y BF (32-35): RLLR, y (ii) la actividad antimicrobiana y citotóxica de estos dendrímeros. Se establecieron las rutas de síntesis que permitieron obtener: a) alquino-resorcinarenos y b) péptidos funcionalizados con el grupo azida; los cuales se usaron para generar c) dendrímeros de péptido-resorcinareno mediante química click de cicloadición de azida-alquino CuAAC. Finalmente, se evaluó la actividad antimicrobiana y citotóxica de los dendrímeros obtenidos frente a cepas de referencia y aislados clínicos. Estos resultados permitieron la identificación de moléculas antimicrobianas prometedoras que pueden conducir a avances en el desarrollo de nuevos agentes terapéuticos.

Palabras clave: Péptidos Antimicrobianos · Lactoferricina Bovina · Buforina · Resorcinareno · Dendrímeros · Química click

Abstract

Antimicrobial resistance (AMR) is one of the top ten threats to public health reported by the World Health Organization (WHO). One of the causes of the growing AMR problem is the lack of new therapies and/or treatment agents; consequently, many infectious diseases could become uncontrollable. The need to discover new antimicrobial agents, which are alternatives to the existing ones, and which allow mitigating this problem, has increased due to the rapid and global expansion of AMR. In this context, both antimicrobial peptides (AMPs) and dendrimers that present multiple copies of antibacterial compounds in their structure have been proposed as alternatives to combat AMR. Dendrimers have exhibited antifungal and antibacterial properties and have also been used in anti-inflammatory, antineoplastic and cardiovascular therapies and are useful in drug and gene delivery systems. In this work, it was proposed to obtain dendrimers that present four copies of AMPs sequences. Specifically, (i) the synthesis, purification, and characterization of peptide-resorcinarene dendrimers derived from the sequences LfcinB (20-25): RRWQWR and BF (32-35): RLLR, and (ii) the antimicrobial and cytotoxic activity were explored. of these dendrimers. The synthesis routes that allowed obtaining: a) alkyne-resorcinarenes and b) peptides functionalized with the azide group were established, which were used to generate c) peptide-resorcinarene dendrimers by azide-alkyne cycloaddition (CuAAC) click chemistry. Finally, the antimicrobial and cytotoxic activity of the dendrimers obtained was evaluated against reference strains and clinical isolates. These results allowed the identification of promising antimicrobial molecules that may lead to breakthroughs in the development of new therapeutic agents.

Keywords: Dendrimers; Resorcinarene; Click chemistry; CuAAC; Antibacterial activity; Anti-fungal activity; Clinical isolate.

Contenido

1. Marco Teórico	18
1.1 Calix[4]resorcinarenos	18
1.1.1 Funcionalización de los resorcinarenos	23
1.1.1.4 Funcionalización mediante química click.....	29
1.2 Péptidos Antimicrobianos (PAMs).....	35
1.2.1 Lactoferrina Bovina	36
1.2.2 Buforina	38
1.2.3 Alcance Clínico de los PAMs.....	39
1.3 Resistencia Bacteriana	40
1.4 Generalidades biológicas de las cepas bacterianas seleccionadas para el proyecto.....	43
1.4.1 <i>Staphylococcus aureus</i>	43
1.4.2 <i>Escherichia coli</i>	44
2. Objetivos	47
2.1 Objetivo General	47
2.2 Objetivos Específicos	47
3. Metodología.....	48
3.1 Diseño experimental	48
3.2 Materiales y Métodos	50
3.2.1 Equipos y Reactivos	50
3.2.2 Síntesis de resorcinarenos base y funcionalización.....	51
3.2.3 Síntesis de péptidos	54
3.2.4 Síntesis de dendrímeros péptido-resorcinareno (química click)	56
3.2.5 Ensayos de actividad biológica	57
3.2.5.1 Determinación Concentración Mínima inhibitoria (CMI) y concentración Mínima Bactericida (CMB)	57
3.2.5.2 Curvas de letalidad-muerte	58
3.2.5.3 Ensayo de sinergia con antibióticos	58
3.2.5.4 Determinación Concentración Mínima inhibitoria (CMI) y Concentración Mínima Fungicida (CMF)	59
4. Resultados y discusión	61

4.1	Síntesis de precursores	61
4.1.1	Síntesis de derivados de Calix[4]resorcinareno	62
a)	CR-8-ALQ (<i>rccc</i>).....	63
b)	CR-4-ALQ (<i>rccc</i> y <i>rctt</i>)	69
4.1.2	Síntesis y caracterización de péptidos.....	75
4.2	Síntesis de dendrímeros mediante química click CuAAC	80
a)	Optimización condiciones química click	80
b)	Reacción click con CR-4-ALQ (<i>rccc</i> y <i>rctt</i>).....	83
4.3	Actividad Antimicrobiana	89
4.3.1	Concentración Mínima Inhibitoria (CMI) y Concentración Mínima Bactericida (CMB)	90
4.3.2	Curvas de Letalidad-Muerte y Sinergia.....	92
4.4	Actividad antifúngica	94
4.5	Actividad citotóxica	95
5.	Conclusiones	97
6.	Productos Académicos	99
7.	Anexo A: Espectros RMN ¹H y ¹³C de derivados de resorcinareno y precursores. Reporte de síntesis de los péptidos sintéticos.	105
8.	Anexo B: Productos Académicos (Artículos).....	129
9.	Anexo C: Certificados.....	247

Lista de figuras

Figura 1. Estructura del calix[4]resorcinareno.	18
Figura 2. Síntesis de calix[4]resorcinarenos.	19
Figura 3. Mecanismo de reacción de la síntesis de calix[4]resorcinarenos.	20
Figura 4. Ciclocondensación entre 2-alkilresorcinoles y 1,3,5-trioxano [16].	20
Figura 5. Síntesis de derivados de calix[4]resorcinarenos a) usando catalizadores de tosيلات de lantánidos (III), b) síntesis normal y c) síntesis asistida por microondas [17-18].	21
Figura 6. a) Isómeros conformacionales reportados para el calix[4]resorcinareno, b) configuración relativa de los sustituyentes en los puentes de metileno [19], [24].	22
Figura 7. Descripción de la estructura de los resorcinarenos de tipo corona (borde superior y borde inferior).	23
Figura 8. Posiciones funcionalizables del calix[4]resorcinareno.	24
Figura 9. Síntesis de dendrímeros supramoleculares derivados de resorcinarenos adaptado de [26].	24
Figura 10. Síntesis de derivados de calix[4]resorcinarenos con grupos alquino.	25
Figura 11. Funcionalización posición orto del anillo aromático de calix[4]resorcinarenos	26
Figura 12. Síntesis de derivados de calix[4]resorcinarenos mediante incorporación de cadenas alifáticas insaturadas con dobles y triples enlaces.	27
Figura 13. Funcionalización de calix[4]resorcinarenos en el puente de metileno.	27
Figura 14. Funcionalización del borde inferior de derivados de calix[4]resorcinarenos. a) incorporación de p-hidroxibenzaldehído y b) 3-bromopropanal.	29
Figura 15. Mecanismo de cicloadición 1,3 dipolar de azidas y alquinos catalizado por cobre (I). [50], [52]. ..	30
Figura 16. Síntesis del macrociclo derivado de calix[4]resorcinareno funcionalizado con tetra-triazol.	31
Figura 17. Ejemplos de dendrímeros a base de calix[4]resorcinareno. a) carbohidrato-resorcinareno, b) polímeros-resorcinareno (copolímeros de estrella), c) bases nitrogenada-resorcinareno, d) radio marcadores-resorcinareno y biomoléculas activas-resorcinareno como e) cumarina y f) ácido fólico.	32
Figura 18. Derivados de calix[4]resorcinarenos evaluados frente a bacterias Gram negativas y Gram positivas.	34
Figura 19. Síntesis de GCR-1 y GCR-2.	35
Figura 20. Secuencia de la Lactoferrina bovina. Se muestra el bucle formado por el puente disulfuro. Los aminoácidos cargados positivamente están en rojo, los números corresponden a la posición en la proteína original [73].	37
Figura 21. Ejemplo del diseño de un dendrímero péptido-resorcinareno derivado de LfcinB (20-25): RRWQWR.	45
Figura 22. Etapas involucradas en el diseño experimental.	48
Figura 23. Derivados del calix[4]resorcinareno sintetizados en este estudio a) CR-8-ALQ modificado en su borde superior y b) CR-4-ALQ modificado en su borde inferior.	62

Figura 24. a) Reacción de cicloadición entre resorcinol y acetaldehído. Análisis de la mezcla de reacción por b) RP-HPLC/UV-Vis, análisis registrado a 210 nm y c) UHPLC-MS (ESI), TIC se presenta el espectro de masas del pico a los 8,7 min.	64
Figura 25. a) Espectros de RMN- ¹ H y b) Perfil cromatográfico de 1a, 1b y 1c.	66
Figura 26. Esquema de reacción para la formación del macrociclo CR-8-ALQ.	67
Figura 27. Seguimiento de la reacción de formación del macrociclo CR-8-ALQ (t= 24 h). Bromuro de propargilo (t _R = 3,9 min), C-tetrametilcalix[4]resorcinareno (1a) (t _R = 9,3 min)	68
Figura 28. Perfil cromatográfico y espectro de masas ESI-Q/TOF del producto octa-funcionalizado puro confórmero <i>rccc</i> (CR-8-ALQ).	68
Figura 29. Seguimiento de la reacción para la síntesis del precursor 4-(prop-2-in-1-iloxi)benzaldehído (<i>p</i> -HF). Perfil cromatográfico de a) <i>p</i> -hidroxibenzaldehído, b) bromuro de propargilo a c) t= 0 h y d) t= 4 h.	70
Figura 30. Caracterización mediante RP-HPLC y LC-MS de 4-(prop-2-in-1-iloxi)benzaldehído.	71
Figura 31. Esquema de la síntesis del macrociclo CR-4-ALQ.	71
Figura 32. Confórmeros obtenidos en la síntesis del CR-4-ALQ funcionalizado con el grupo alquino.	73
Figura 33. Perfil cromatográfico y espectro de masas (MALDI-TOF) del CR-4-ALQ: a) confórmero <i>rctt-silla</i> y b) confórmero <i>rccc-corona</i> purificados.	73
Figura 34. Esquema general de la síntesis de péptidos utilizando la metodología SPPS-Fmoc/tBu. Ejemplo secuencia RRWQWR.	76
Figura 35. Perfiles cromatográficos para el péptido (K(N ₃)-Ahx-RRWQWR) obtenido al usar diferentes condiciones de clivaje: a) EDT/TIPS/H ₂ O/TFA, b) TIPS/H ₂ O/TFA, c) H ₂ O/TFA.	77
Figura 36. TIC y espectro de masas ESI-Q/TOF de a) K(NH ₂)-Ahx-RRWQWR y b) K(N ₃)-Ahx-RRWQWR.	78
Figura 37. Esquema de reacción de la oxidación del grupo tiol presente en la Cys, para la obtención de péptidos tetraméricos a partir de dímeros.	79
Figura 38. Perfil cromatográfico de la reacción de química click de P11: K(N ₃)-AAAA (t _R : 1,7 min) y CR-4-ALQ (<i>rctt</i>) (t _R : 9,6 min), 24 h en a) ACN y b) DMF:H ₂ O (2:1).	82
Figura 39. Perfil cromatográfico (izquierda) y espectro de masas (derecha) del producto de reacción entre el macrociclo CR-4-ALQ (<i>rctt</i>) y a) P4 : K(N ₃)-Ahx-RRWQWR o b) P10 : K(N ₃)-Ahx-RLLRLLR.	85
Figura 40. Perfil cromatográfico del producto de reacción de CuAAC entre a) CR-4-ALQ (<i>rctt</i>) y P7 y b) CR-4-ALQ (<i>rctt</i>) y P3 y c) CR-4-ALQ (<i>rctt</i>) y P9.	86
Figura 41. Esquema de la síntesis del dendrímero DP7: CR-4-ALQ(<i>rctt</i>)-(AAC-(K)-RLLR) ₄	86
Figura 42. Seguimiento, mediante RP-HPLC, de la reacción de obtención del dendrímero DP7: CR-4-ALQ(<i>rctt</i>)-(AAC-(K)-RLLR) ₄	87
Figura 43. a) Perfil cromatográfico y espectro MALDI-TOF MS del dendrímero DP7 purificado: CR-4-ALQ(<i>rctt</i>)-(AAC-(K)-RLLR) ₄ y b) HR-MS del dendrímero DP7, se muestran las señales correspondientes a la distribución isotópica de la especie [M+4H] ⁴⁺ ; monoisotópico experimental M es 3846,28 u.m.a. c) HR-MS del dendrímero DP3, se muestran las señales correspondientes a la distribución isotópica de la especie [M+7H] ⁷⁺ ; monoisotópico experimental M es 5572,84 u.m.a.	88
Figura 44. Curva de cinética de muerte celular. a) Las cepas de <i>E. coli</i> ATCC 25922 y b) <i>S. aureus</i> ATCC 23922 se incubaron con dendrímero DP7 (<i>rctt</i>) durante 48 h utilizando concentraciones de dendrímero correspondientes a 0,5×CMI (línea verde), CMI (línea marrón) y 2×CMI (línea roja). Como antibiótico se empleó en a) Ciprofloxacino y en b) Vancomicina.	92
Figura 45. Actividad hemolítica de dendrímeros peptídicos de resorcinareno derivados de LfcinB (20-25) y BF (32-35).	95

Figura 46. Actividad citotóxica sobre fibroblastos y líneas MCF-7 y HeLa de los dendrímeros a) DP3 y b) DP7 (<i>rcft</i>).....	96
---	----

Lista de tablas

Tabla 1. Calix[4]resorcinarenos funcionalización completa de posiciones R ₁ , R ₂ y R ₃ según Figura 13.	28
Tabla 2. Actividad antimicrobiana (halo de inhibición en mm) de los compuestos 1-4.	34
Tabla 3. Actividad antimicrobiana de GCR-1 y GCR-2.	35
Tabla 4. Actividad antibacteriana de péptidos derivados de la LfcinB.	38
Tabla 5. Actividad antibacteriana de péptidos derivados de la BF.	39
Tabla 6. Péptidos que se encuentran en fase clínica de desarrollo [89].	40
Tabla 7. Péptidos derivados de la LfcinB y BF utilizados en este proyecto. Todos los péptidos en el extremo C-terminal se obtuvieron con función amida.	55
Tabla 8. Dendrímeros derivados de la LfcinB y BF.	56
Tabla 9. Generalidades de las cepas bacterianas.	58
Tabla 10. Generalidades de las Cepas de <i>Candida spp.</i>	59
Tabla 11. Desplazamientos químicos RMN- ¹ H para el precursor 1a (<i>rccc</i>) y CR-8-ALQ (<i>rccc</i>).	69
Tabla 12. Desplazamientos químicos RMN- ¹ H para los derivados CR-4-ALQ (<i>rctt</i>) y CR-4-ALQ (<i>rccc</i>).	73
Tabla 13. Resumen de la caracterización de los precursores y derivados de calix[4]resorcinareno.	74
Tabla 14. Resumen de la caracterización analítica de los péptidos control, azida-péptidos y tetrámeros derivados de la LfcinB y BF obtenidos.	80
Tabla 15. Optimización condiciones química click con precursores	81
Tabla 16. Resumen de las condiciones y caracterización de la síntesis de los dendrímeros péptido-resorcinareno.	84
Tabla 17. Resumen de la caracterización de dendrímeros péptido-resorcinareno.	89
Tabla 18. Actividad antibacteriana de los péptidos control y los dendrímeros péptido-resorcinareno. Los valores de MIC/MBC se expresan en μM.	90
Tabla 19. Actividad antibacteriana contra aislados clínicos de los dendrímeros DP7 (<i>rctt</i>): CR-4-ALQ(<i>rctt</i>)-(AAC-(K)-RLLR) ₄ y DP7 (<i>rccc</i>): CR-4-ALQ(<i>rccc</i>)-(AAC-(K)-RLLR) ₄ . Los valores de CMI/CMB se expresan en concentración μM.	91
Tabla 20. Actividad hemolítica, bacteriostática y bactericida del dendrímero DP7 (<i>rctt</i>): CR-4-ALQ(<i>rctt</i>)-(AAC-(K)-RLLR) ₄ y prueba de sinergia de mezclas de ciprofloxacina CIP (1) y dendrímero DP7 (<i>rctt</i>) (2).	93
Tabla 21. Actividad antifúngica del dendrímero DP7 (<i>rctt</i>): CR-4-ALQ(<i>rctt</i>)-(AAC-(K)-RLLR) ₄	94

Lista de Símbolos y abreviaturas

Termino	Abreviatura	Siglas
Acetonitrilo	ACN	
Acetonitrilo / TFA 0.05%	Solvente B	
Ácido aminohexanoico	Ahx	
Ácido Trifluoroacético	TFA	
Ácido (S)-2-(Fmoc-amino)-4-pentinoico	Fmoc-Pra-OH	
Ácido (S)-6-azido-2-(Fmoc-amino)hexanoico	Fmoc-Lys(N ₃)-OH	
Azide-Alkyne Cycloaddition		AAC
Agar Mueller Hinton		MHA
Agar Standar Plate Count		SPC
Agar tripticasa de soya		TSA
Agua / TFA 0,05%	Solvente A	
American Type Culture Collection		ATCC
Buforina	BF	
Caldo Mueller Hinton		CMH
Ciprofloxacina	CIP	
Concentración Mínima Bactericida		CMB
Concentración Mínima Inhibitoria		CMI
Cromatografía líquida de alta eficiencia en fase reversa		RP-HPLC
N,N'-Diciclohexilcarbodiimida	DCC	
Diclorometano	DCM	
Dimetilsulfóxido	DMSO	
N,N-dimetilformamida	DMF	
Espectrometría de masas		EM (MS)

Etanoditiol	EDT	
Etanol	EtOH	
Extracción en fase sólida		SPE
Concentración Inhibitoria Fraccionada		FIC
9-Fluorenilmetiloxicarbonilo	Fmoc	
1-Hidroxi-6-clorobenzotriazol	6-Cl-HOBt	
Lactoferricina	Lfcin	
Lactoferricina Bovina	LfcinB	
Lactoferricina Humana	LfcinH	
Lactoferrina	LF	
Matrix-Assisted Laser Desorption/Ionization / Time-Of-Flight		MALDI-TOF
Mililitro	mL	
Organización Mundial de la salud		OMS
Palíndromo	Pal	
Péptidos Antimicrobianos	PAMs	
4-(prop-2-in-1-iloxi)benzaldehído	Precursor 1	
Síntesis de Péptidos en Fase Sólida		SPPS
<i>Staphylococcus aureus</i> resistente a la Metilicina		SARM
Temperatura Ambiente		TA
Tetrafluoroborato de O-(Benzo-triazol-1-yl)-N,N,N',N'-tetrametiluronio	TBTU	
Tiempo de retención		t _R
Triisopropilsilano	TIS	
Terbutanol	t-BuOH	
Unidades formadoras de colonias		UFC

Introducción

Desde la introducción de las sulfonamidas y el descubrimiento de la penicilina en 1928, la cantidad de fármacos para tratar infecciones ha crecido exponencialmente, de hecho, los antibióticos se han convertido en los medicamentos empleados con mayor frecuencia y han contribuido a reducir la mortalidad y la morbilidad debidas a enfermedades infecciosas. Desafortunadamente, la utilidad de estos fármacos se ha visto seriamente comprometida por la posterior aparición de bacterias resistentes, claro ejemplo es el ilustrado por la meticilina descubierta en 1959 y posteriormente introducida para tratar el *Staphylococcus aureus* resistente a la penicilina. Sin embargo, dos años más tarde, se aislaron cepas resistentes a meticilina, primero en el Reino Unido y luego en Japón y Australia. La historia ha sido la misma para casi todos los antibióticos, siendo el ejemplo más reciente los lipopéptidos, como la daptomicina introducidos a principios de este siglo [1].

El uso indiscriminado de antibióticos ha sido la principal causa del aumento de la resistencia por parte de las bacterias, en recientes reportes emitidos por la Organización Mundial de la Salud (OMS) se describe la importancia de la búsqueda de moléculas que logren contrarrestar la resistencia antibacteriana, ya que esta problemática es considerada como una amenaza creciente para la salud pública a nivel mundial [2], [3]. El Centro para el Control y la Prevención de Enfermedades (CDC) de USA informó en 2013 que dos millones de personas en este país habían sufrido una infección causada por un patógeno resistente, y al menos 23,000 de estas personas habían muerto debido a la infección. La Sociedad de Enfermedades Infecciosas de América (IDSA) destacó *Enterococcus faecium*, *Staphylococcus aureus*, *Klebsiella pneumoniae*, *Acinetobacter baumannii*, *Pseudomonas aeruginosa* y varias *Enterobacteriaceae* (incluyendo *Klebsiella*, *Escherichia coli*, *Serratia* y *Proteus*) (ESKAPE) como especies capaces de 'escapar' de la acción antibacteriana de los antibióticos. Estas especies constituyen un nuevo paradigma en virulencia, transmisión y resistencia a los antimicrobianos. En 2014, el Centro Europeo para la Prevención y el Control de Enfermedades (ECDC) publicó

un informe sobre la resistencia a los antimicrobianos en Europa, este reporte también se centró en los patógenos *ESKAPE*, e informó sobre el aumento de los niveles de resistencia, especialmente en los países del sur de Europa [3, 4]. En este sentido, se presenta un nuevo reto para el campo de la salud: *la búsqueda de nuevas moléculas con potencial terapéutico que logren combatir infecciones causadas por cepas multidrogoresistentes y que su actividad se base en mecanismos de acción diferentes a los que exhiben los antibióticos convencionales.*

Con el dilema actual de la resistencia generalizada, incluidos los organismos extremadamente resistentes, y la falta de disponibilidad de nuevos agentes antimicrobianos, se comenzó la investigación y el desarrollo de nuevas moléculas con potencial terapéutico derivados de fuentes proteicas, dentro de estas, se ha evidenciado que los péptidos antimicrobianos (PAMs) tanto naturales como sintéticos son una de las opciones para vencer la resistencia. Para la obtención de agentes terapéuticos basados en PAMs que tengan actividad antibacteriana potenciada se han propuesto modificaciones en su estructura, que se han logrado gracias a la versatilidad que presenta la SPPS (por sus siglas en inglés, *Solid Phase Peptide Synthesis*). Dentro de las modificaciones encontramos: i) la incorporación de aminoácidos no naturales [6], ii) secuencias con restricción conformacional [7], iii) estructuras con presentación múltiple del motivo activo [8], iv) estructuras palindrómicas o simétricas [9], [10] v) quimeras entre PAMs y/o moléculas de origen orgánico e inorgánico, haciendo uso de reacciones catalogadas como química click [11]. Dentro de este contexto en este trabajo se exploró la obtención de dendrímeros, o conjugados, en los que péptidos derivados de PAMs fueron unidos a un núcleo (core) polihidroxilado de tipo resorcinareno. Específicamente, (i) Se establecieron las rutas de síntesis que permitieron obtener: a) alquino-resorcinarenos y b) péptidos funcionalizados con el grupo azida, derivados del motivo mínimo de actividad reportado para la LfcinB (RRWQWR) y la buforina (RLLR); los cuales se usaron para generar c) dendrímeros de péptido-resorcinareno mediante química click de cicloadición de azida-alquino CuAAC. Finalmente, se (ii) evaluó la actividad antimicrobiana y citotóxica de los dendrímeros obtenidos frente a cepas de referencia y aislados clínicos

1. Marco Teórico

1.1 Calix[4]resorcinarenos

Los resorcinarenos también conocidos como calix[4]resorcinarenos son compuestos macrocíclicos polihidroxilados derivados del resorcinol, sintetizados por primera vez por Baeyer *et al.* en el año de 1872 a partir de aldehídos alifáticos y aromáticos [12], [13]. Están constituidos por cuatro anillos de resorcinol unidos entre sí en las posiciones 4 y 6 por un enlace metileno (Figura 1); con frecuencia este suele estar sustituido por cadenas alifáticas y/o aromáticas permitiendo la formación de isómeros conformacionales (estereoisomería) [14]. Los calix[4]resorcinarenos pueden obtenerse mediante la condensación del resorcinol con diversos aldehídos que pueden ser alifáticos o aromáticos, esta reacción ocurre al calentar los reactivos a reflujo en una mezcla de etanol y HCl concentrado a tiempos de reacción prolongados, Figura 2.a. Por lo general, el producto es cristalizado de la mezcla de reacción con altos rendimientos (60-90%). Esta reacción requiere de un solo paso, y dependiendo del aldehído existen diferentes condiciones óptimas. Se ha publicado que cuando se utiliza derivados de resorcinol sustituidos en su posición 2 (Figura 2.b) con grupos desactivantes como nitratos (-NO₂) o halógenos (X= Cl, Br, I, F) bajo las mismas condiciones de síntesis no se obtienen productos tetraméricos, es decir derivados de calix[4]resorcinareno [14], [15].

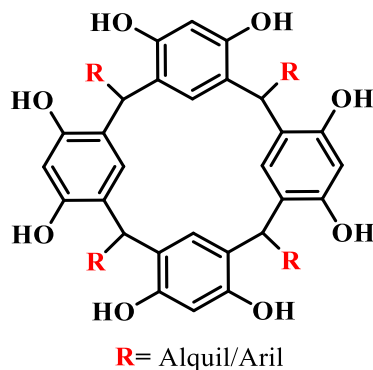


Figura 1. Estructura del calix[4]resorcinareno.

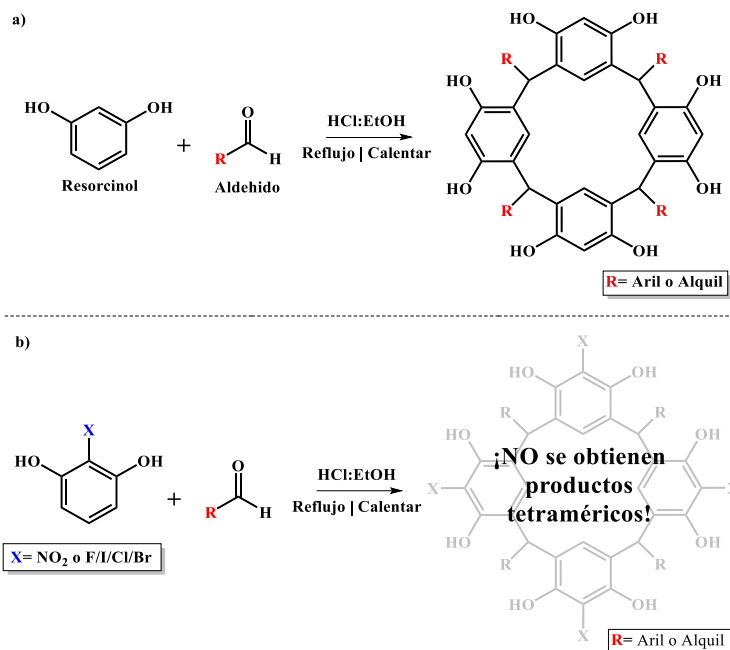


Figura 2. Síntesis de calix[4]resorcinarenos.

De manera general, el mecanismo de síntesis bajo condiciones ácidas se describe a continuación, Figura 3, primero, el aldehído es protonado para servir como el electrófilo inicial, ocurriendo así una primera sustitución electrofílica aromática a una molécula de resorcinol. El hidroxilo alcoholico del aducto subsiguiente es protonado nuevamente para eliminar una molécula de agua. La pérdida de la molécula de agua proporciona un carbocatión intermediario, que por una segunda sustitución electrofílica aromática a la posición orto al hidroxilo de una segunda unidad de resorcinol forma el dímero. Acoplamientos secuenciales del dímero con otras unidades de resorcinol resulta en trímeros, tetrámeros u oligómeros superiores. Dado que la reacción de condensación es reversible bajo condiciones ácidas, la mayoría de los oligómeros superiores se consumen hasta el final de la reacción, aunque estén presentes durante las etapas intermedias de la reacción. El tetrámero lineal se cicla rápidamente para formar calix[4]resorcinarenos, estos se forman demasiado rápido en la mezcla de reacción evitando el aislamiento de tetrámeros lineales. Este proceso de ciclación se ve favorecido debido a la falta de conformación-tensión y por la formación de enlaces de hidrógeno entre los grupos hidroxilo fenólicos proximales de resorcinol en las estructuras plegadas [14].

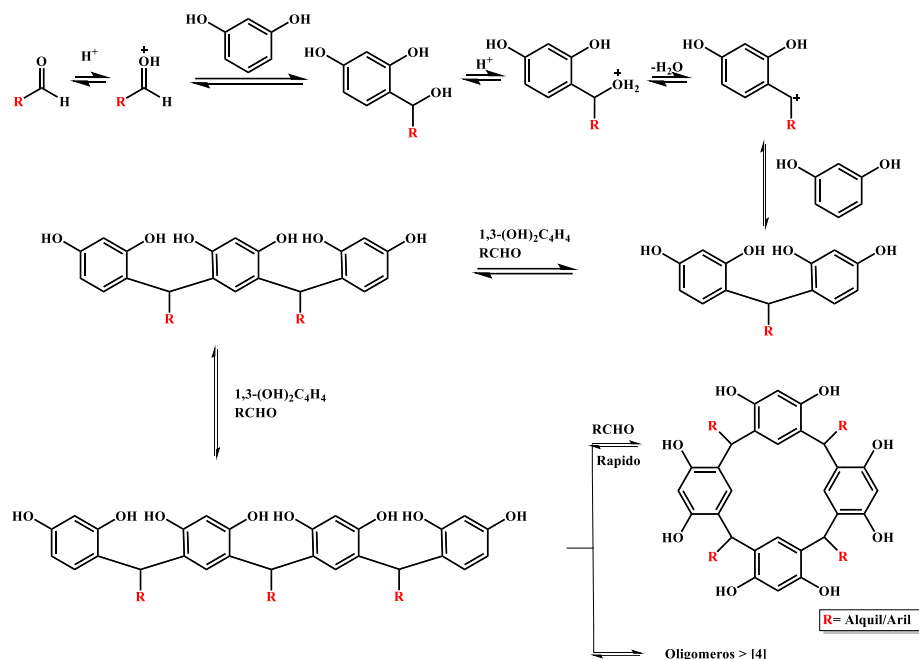


Figura 3. Mecanismo de reacción de la síntesis de calix[4]resorcinarenos.

Aunque las reacciones con aldehídos alifáticos o aromáticos parecen producir solo derivados de calix[4]resorcinareno, se han reportado casos, como el expuesto por Konishi *et. al.*, en el que se producen mezclas que contienen derivados de calix[4]resorcinareno y calix[6]resorcinareno, por la ciclocondensación entre 2-alkilresorcinoles, metil y hexil sustituidos, con 1,3,5-trioxano. El oligómero de 6 unidades puede fácilmente formar el oligómero de 4 unidades por calentamiento prolongado, Figura 4 [16].

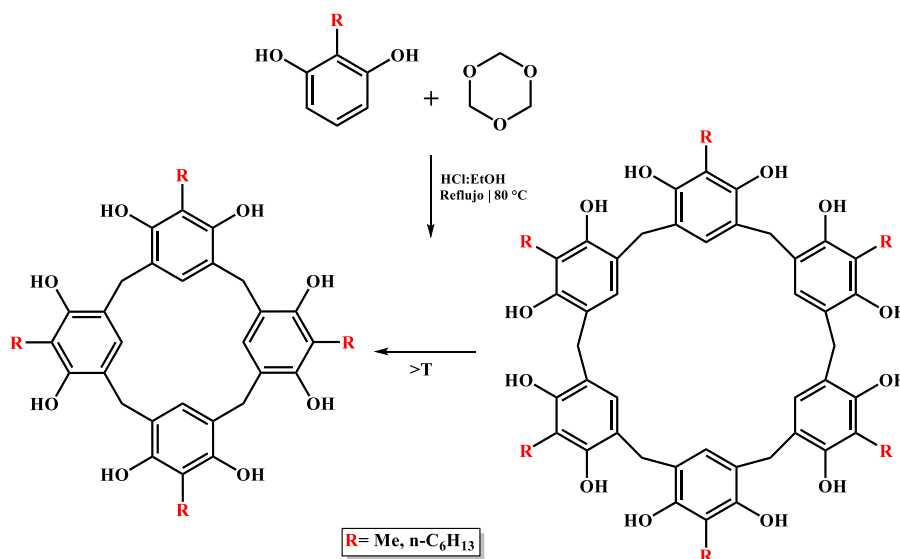


Figura 4. Ciclocondensación entre 2-alkilresorcinoles y 1,3,5-trioxano [16].

Recientemente, se ha estudiado el uso de tosilatos de lantánidos (III), específicamente Iterbio (Yb), Lantano (La), Neodimio (Nd) y Gadolinio (Gd) como catalizadores para la síntesis de derivados de resorcinareno. El uso de estas especies mejora el proceso de síntesis de calix[4]resorcinarenos aumentando el rendimiento de reacción (>80%). Estos nuevos agentes catalizadores presentan ventajas sobre los métodos convencionales debido a que son: i) económicos, ii) reciclables y iii) ecológicos, Figura 5.a, [17]. La síntesis de derivados de calix[4]resorcinarenos a partir de resorcinol y aldehídos catalizada por ácido y asistida por microondas se reportó por primera vez por Hedidi *et. al.* en el 2006, los rendimientos en el proceso sintético presentaron una notable mejora con valores que superaron el 90% a tiempos de reacción cortos, entre 3 a 5 minutos. En la Figura 5.b, se presenta un ejemplo en el cual, por el método tradicional de reflujo la reacción tarda 10 horas y el producto se obtiene con un rendimiento del 60%. Cuando esta reacción es asistida con microondas el tiempo de reacción se reduce a razón de minutos con rendimientos superiores al 80%, Figura 5.c [18].

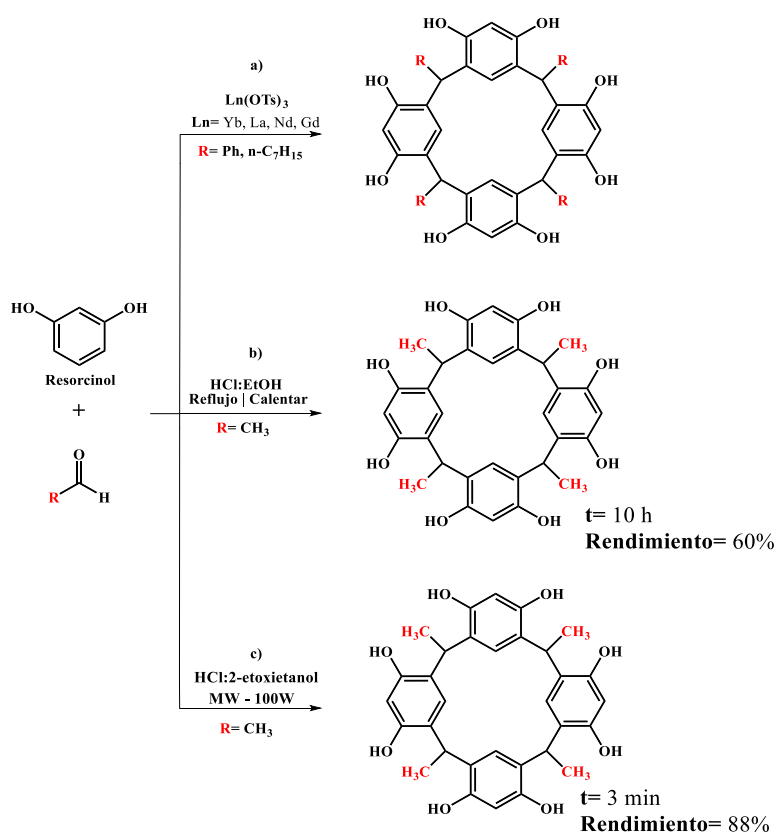


Figura 5. Síntesis de derivados de calix[4]resorcinarenos a) usando catalizadores de tosilatos de lantánidos (III), b) síntesis normal y c) síntesis asistida por microondas [17-18].

Se han reportado cinco posibles conforméromos para el resorcinareno: i) *corona*, ii) *bote*, iii) *silla*, iv) *silla de montar* y v) *diamante* (Figura 6.a) [19]. Cada una de estas conformaciones serán posibles teniendo en cuenta aspectos como la posición de las unidades de resorcinol y los sustituyentes en los puentes de metileno, para la mayoría de los casos reportados en síntesis de derivados de resorcinarenos la conformación más estable ha sido el tipo *corona* establecida a partir de las cavidades profundas formadas y una estabilización mediante puentes de hidrógeno mediada por los grupos hidroxilo presentes [20]–[23].

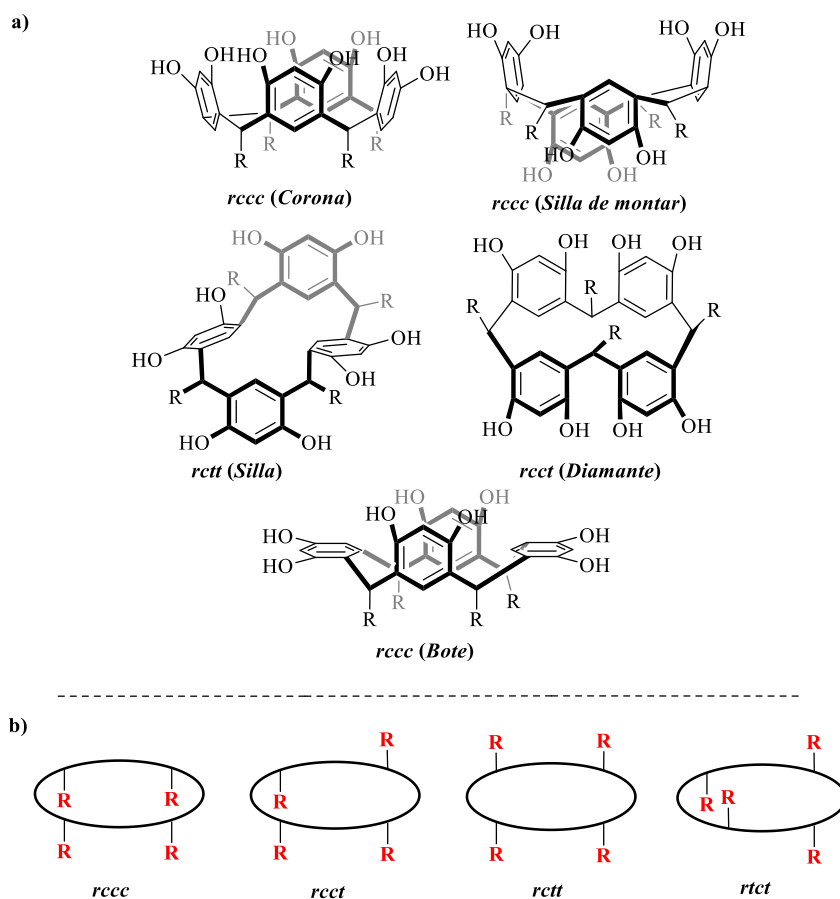


Figura 6. a) Isómeros conformacionales reportados para el calix[4]resorcinareno, b) configuración relativa de los sustituyentes en los puentes de metileno [19], [24].

La estereoquímica generalmente se define por una combinación de tres criterios que no son independientes: el primer criterio es la conformación del macrocíclico, que puede adoptar una de las cinco conformaciones altamente simétricas, *corona*, *silla de montar*, *silla*, *diamante*, y *bote*, Figura 6.a. El segundo criterio es la configuración relativa de los sustituyentes en los puentes de metileno, que pueden ser todos *cis* (*rccc*),

cis+cis+trans (*rcct*), cis+trans+trans (*rcctt*) o trans+cis+trans (*rtct*), Figura 6.b, y el último criterio es la configuración individual de los sustituyentes de puente de metileno, que pueden ser axiales o ecuatoriales en macrociclos con simetría cis. La combinación de estos tres criterios resulta en gran número de posibles estereoisómeros, sin embargo, solo algunos de ellos han sido reportados experimentalmente [14]. En la síntesis de resorcinarenos con conformación del tipo corona sustituidos, con frecuencia se menciona la posición o zona donde se albergan los sitios activos, estos son conocidos como borde superior y borde inferior (Figura 7). La funcionalización del borde inferior se genera mediante el método convencional de catálisis ácida con una posterior ciclocondensación en donde se varía la naturaleza del aldehído involucrado [25]. Por otra parte, la funcionalización del borde superior se realiza una vez el resorcinareno ha sido sintetizado y se genera en los grupos hidroxilos presentes en la unidad del resorcinol mediante reacciones de acetilación y/o sulfometilación o en la posición orto a los grupos hidroxilos [21].

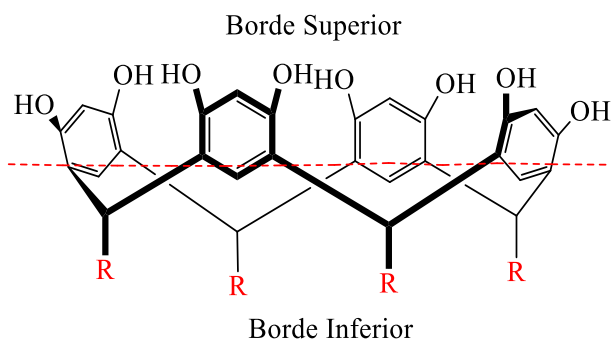


Figura 7. Descripción de la estructura de los resorcinarenos de tipo corona (borde superior y borde inferior).

1.1.1 Funcionalización de los resorcinarenos

Los calix[4]resorcinarenos son una plataforma molecular muy versátil y pueden ser funcionalizados en cuatro ($\times 4$), ocho ($\times 8$) o más sitios dependiendo de las condiciones, el aldehído y el resorcinol utilizado para llevar a cabo la reacción. Para introducir un grupo funcional en la estructura de los calix[4]resorcinarenos se dispone de tres posiciones: i) grupos hidroxilos fenólicos, ii) posición 2 (que es la posición orto a los hidroxilos) o iii) sustituyentes en el puente de metileno, Figura 8. A continuación, se detallan algunos ejemplos de este tipo de funcionalizaciones.

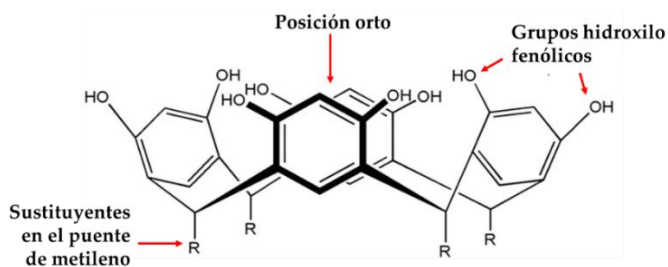


Figura 8. Posiciones funcionalizables del calix[4]resorcinareno.

1.1.1.1 Funcionalización sobre grupos hidroxilo fenólicos

Para este tipo de funcionalización se utiliza la reacción de Williamson para la formación de éteres, en esta reacción se requiere de una base que funciona como catalizador, e.j. carbonato de potasio, se utiliza un halogenuro de alquilo o arilo que será la cadena que se incorpora por la formación del éter. Se ha reportado que este tipo de reacciones dan con buenos rendimientos a tiempos de reacción prolongados. Este tipo de sustitución se ha utilizado para la generación de dendrímeros supramoleculares dada su gran importancia en la conjugación de los electrones π con aplicaciones en la construcción de dendrímeros cromofóricos que permiten la captura eficiente de fotones, Figura 9, [26].

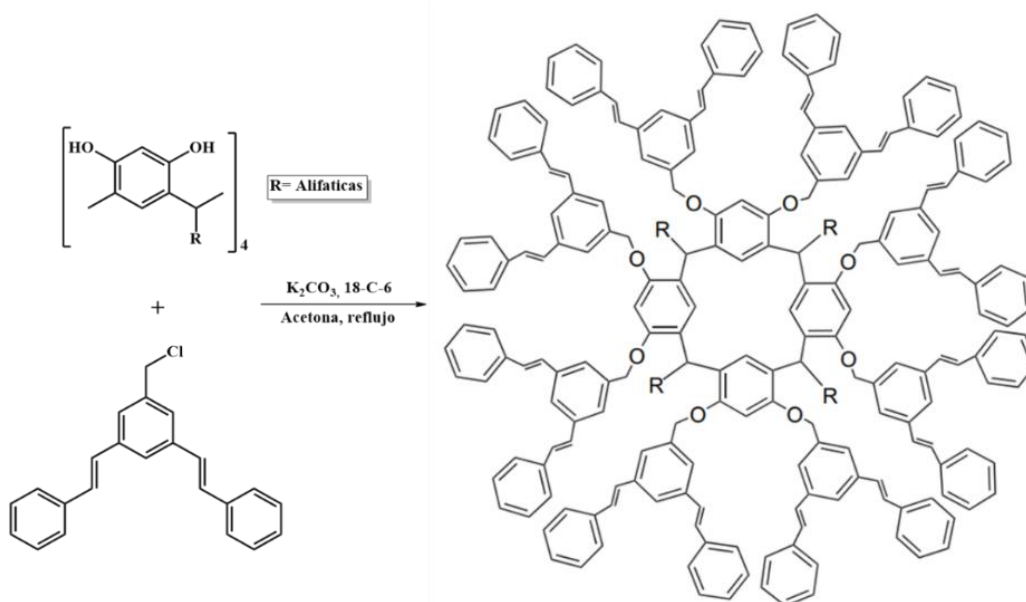


Figura 9. Síntesis de dendrímeros supramoleculares derivados de resorcinarenos adaptado de [26].

Estos grupos hidroxilo han sido utilizados para incorporar nuevos sitios activos sobre el macrociclo, como los alquinos, que se pueden utilizar para reacciones como la cicloadición alquino-azida (química click) la cual

permite seguir explorando la química de este tipo de compuestos. Eisler *et. al.* reportaron nuevos derivados de calix[4]resorcinarenos utilizando dos núcleos de resorcinareno diferentes, uno sustituido en su puente de metileno con un isobutil y otro con etilbenceno, Figura 10. En ambos casos se evidenció la incorporación del grupo alquino [27].

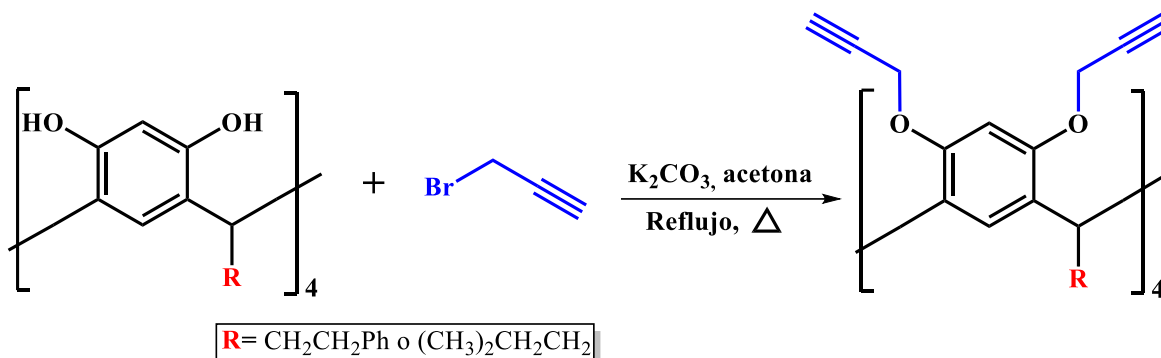


Figura 10. Síntesis de derivados de calix[4]resorcinarenos con grupos alquino.

1.1.1.2 Funcionalización en la posición 2 (orto a los grupos hidroxilo)

Por otro lado, la funcionalización en la posición orto a los grupos hidroxilo se realiza al anillo aromático en su posición 2. Para este tipo de modificación de calix[4]resorcinarenos se han reportado reacciones de i) aminometilación [28], ii) formación de benzoxacinas a partir de aminas primarias [29], iii) unión de péptidos [30], iv) sulfometilación [31], v) tiometilación [32], vi) halogenación [33] y viii) diazotación [34], Figura 11. De manera general en reacciones de aminometilación, los resorcinarenos se comportan como equivalentes enol en reacciones tipo Mannich con formaldehído y aminas (primarias y secundarias). Una amplia gama de aminas secundarias proporciona tetra-(aminometil)resorcinarenos con buenos rendimientos [28], [33]. En condiciones optimizadas, las aminas primarias permiten la síntesis de resorcinarenos de tetrabenzoxazina quirales simétricos. La adición de tioles a la mezcla de reacción da como resultado la formación de tetra-(tiolalquil)resorcinarenos, al reemplazar el precursor tiol por sulfito de sodio da como resultado la formación de análogos de sulfonato de sodio [31]–[33].

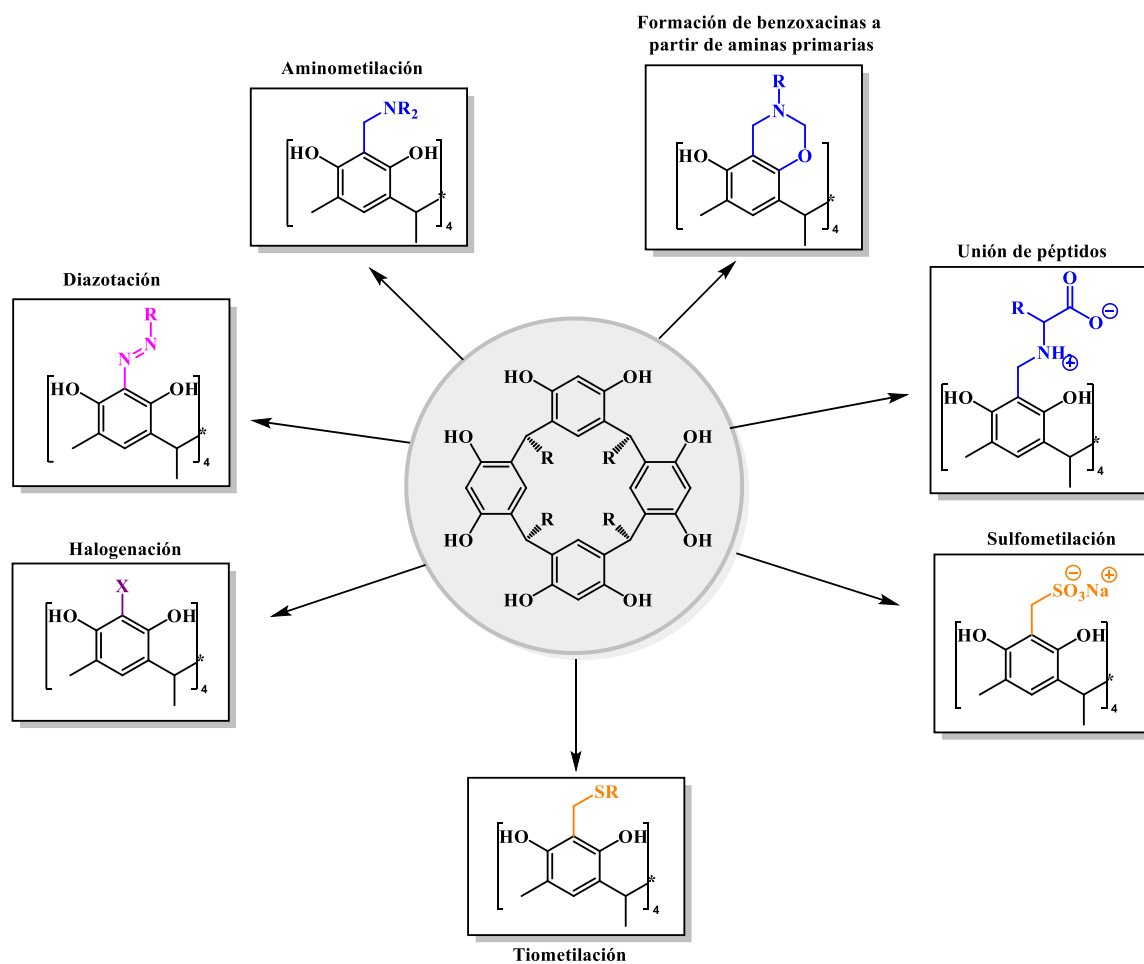


Figura 11. Funcionalización posición orto del anillo aromático de calix[4]resorcinarenos

Urbaniak *et. al.*, realizaron la incorporación de cadenas alifáticas insaturadas con dobles y triples enlaces a partir de alcoholes, Figura 12. Los derivados de calix[4]resorcinarenos modificados con estas cadenas insaturadas han llegado a presentar afinidad en la formación de complejos con cationes de metales pesados, además este tipo de estrategias de funcionalización abre nuevas posibilidades a reacciones específicas sobre estas insaturaciones, como es el caso de la reacción de cicloadición azida-alquino. La síntesis de derivados de resorcinareno con enlaces insaturados presentados en este artículo es efectiva y utilizan sustratos disponibles y de bajo costo [35].

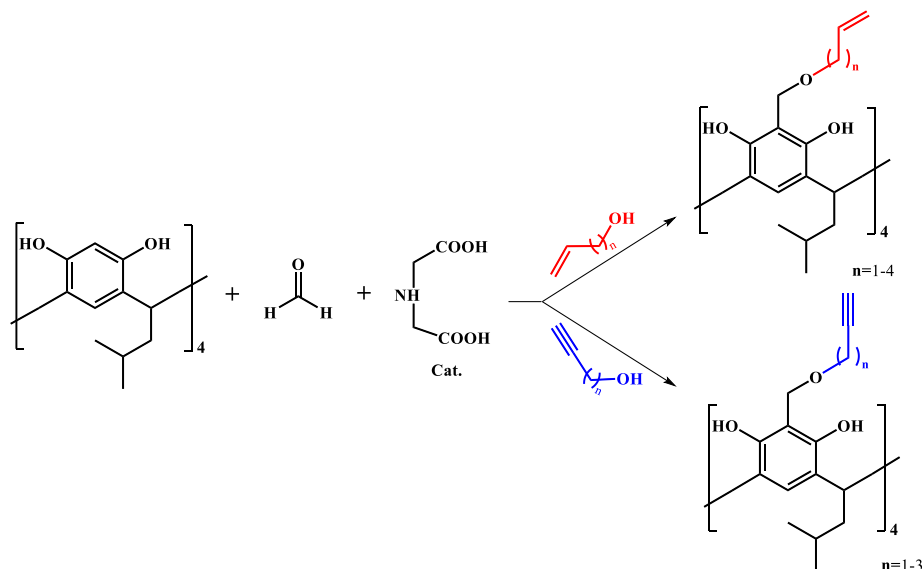


Figura 12. Síntesis de derivados de calix[4]resorcinarenos mediante incorporación de cadenas alifáticas insaturadas con dobles y triples enlaces.

1.1.1.3 Modificaciones sobre el puente de metileno

La funcionalización en el borde inferior del macrociclo surge del aldehído utilizado en la preparación de los derivados de resorcinareno, ya que el grupo unido al aldehído forma el borde inferior. En la preparación de resorcinarenos se utilizan una amplia variedad de aldehídos, incluidos alquil aldehídos saturados, alquil aldehídos insaturados y aldehídos que contienen azufre, Tabla 1. Estos aldehídos funcionalizados conducen a la construcción de resorcinarenos que tienen varias funcionalidades del borde inferior, Figura 13 [36].

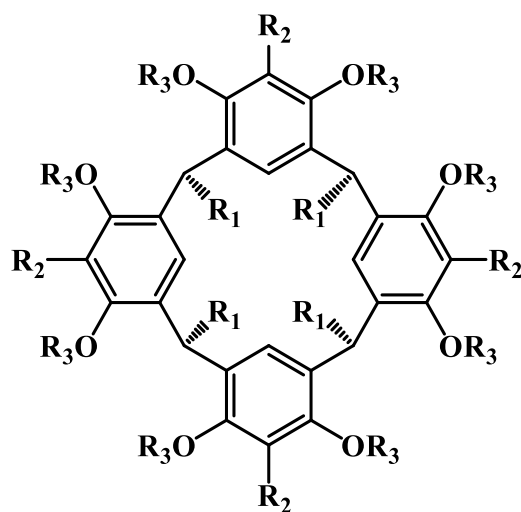
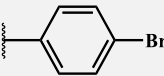
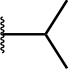
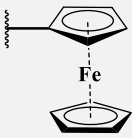
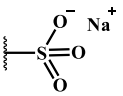
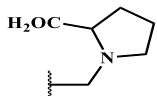
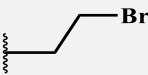
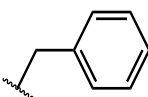
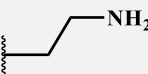
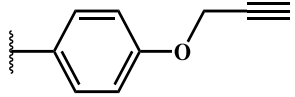
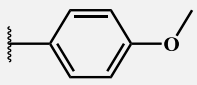
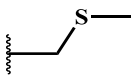


Figura 13. Funcionalización de calix[4]resorcinarenos en el puente de metileno.

Tabla 1. Calix[4]resorcinarenos funcionalización completa de posiciones R₁, R₂ y R₃ según Figura 13.

R ₁	R ₂	R ₃	Ref.
	H	Ac	[37]
	H	Me	[38]
	H	CH ₂ C(O)NEt ₂	[39]
		H	[40]
	H	Me	[41]
	H	PPh ₂	[42]
	H	Me	[41]
	H	Me	[43]
	H	H	[44]
	CH ₂ SO ₃ Na	H	[45]

Así, un aldehído aromático como el p-hidroxibenzaldehído aporta un anillo aromático extra a la estructura del resorcinareno, además de incorporar un nuevo grupo hidroxilo que puede ser funcionalizado, Figura 14.a. Otro ejemplo es la incorporación de halogenuros de alquilo, este tipo de grupos funcionales le proporciona a la estructura del resorcinareno nuevas puntos activos que pueden ser aprovechados para generar nuevos derivados de calix[4]resorcinareno, Figura 14.b [37], [46].

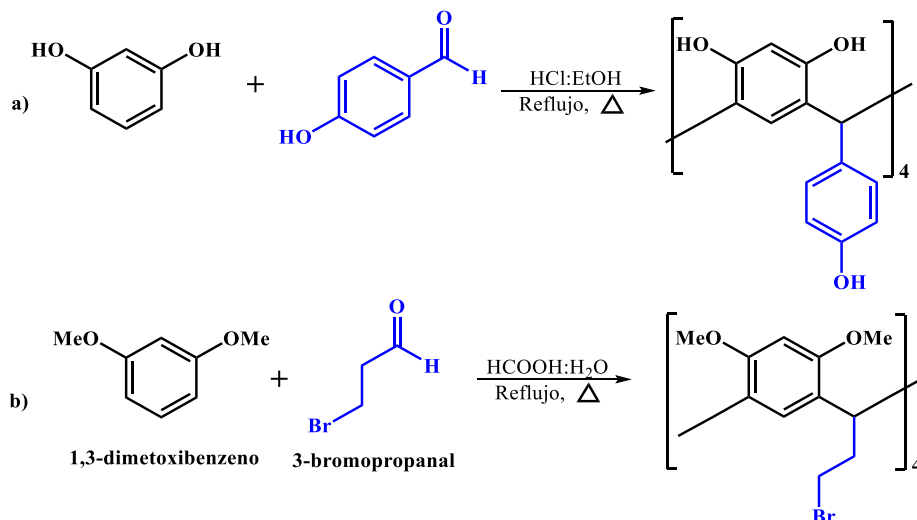


Figura 14. Funcionalización del borde inferior de derivados de calix[4]resorcinarenos. a) incorporación de p-hidroxibenzaldehído y b) 3-bromopropanal.

1.1.1.4 Funcionalización mediante química click

Una de las reacciones que ha ganado relevancia en los últimos años y que se ha empleado en la modificación de este tipo de macrociclos es la química click, la cual es una técnica eficiente implementada en la síntesis de moléculas complejas. El concepto de química click fue incorporado por K. B Sharpless y colaboradores que simplifica el ensamblaje de pequeños bloques para formar estructuras más complejas [47]. Se ha encontrado que la reacción de Huisgen de cicloadición entre un azida y un alquino procede en presencia de un catalizador de cobre bajo condiciones suaves, Figura 15. Este proceso se conoce como CuAAC (por sus siglas en inglés Copper-Catalyzed variant of Huisgen Azide-Alkyne Cycloaddition), y es conocida como una de las principales reacciones de la química click ya que presenta características como: i) estereoespecificidad, ii) facilidad de purificación del producto, iii) uso de reactivos y catalizadores de bajo costo, iv) alta eficiencia y v) condiciones suaves de reacción (es posible llevar este tipo de reacciones en solventes polares y ambientalmente amigables, como el agua) [48], [49].

En la Figura 15, se observa el mecanismo de reacción de CuAAC catalizado por cobre (I), los tres componentes necesarios de una reacción CuAAC son el grupo alquino, el grupo azida y la especie de cobre (I). Sharpless *et. al.* propusieron un mecanismo (ver Figura 15), que comienza con la formación de un acetiluro de cobre (I). La coordinación del grupo azida con el cobre (I) en el nitrógeno alquilado da como resultado un complejo de

los tres componentes (paso a), que se transforma en un metaciclo triazol-cobre de 6 miembros al formar el primer enlace C – N (paso b). En este paso, el centro de cobre se oxida formalmente del estado de oxidación +1 al +3. Sigue la contracción del anillo, junto con la reducción del cobre (III) a cobre (I), para producir triazolido cuproso (paso c). Si no hay otra fuente de protones disponible, el triazolido cuproso tiene que adquirir un protón de una molécula de alquino para completar la formación del triazol (paso d), mientras conduce el siguiente acetiluro de cobre (I) al ciclo catalítico [50], [51].

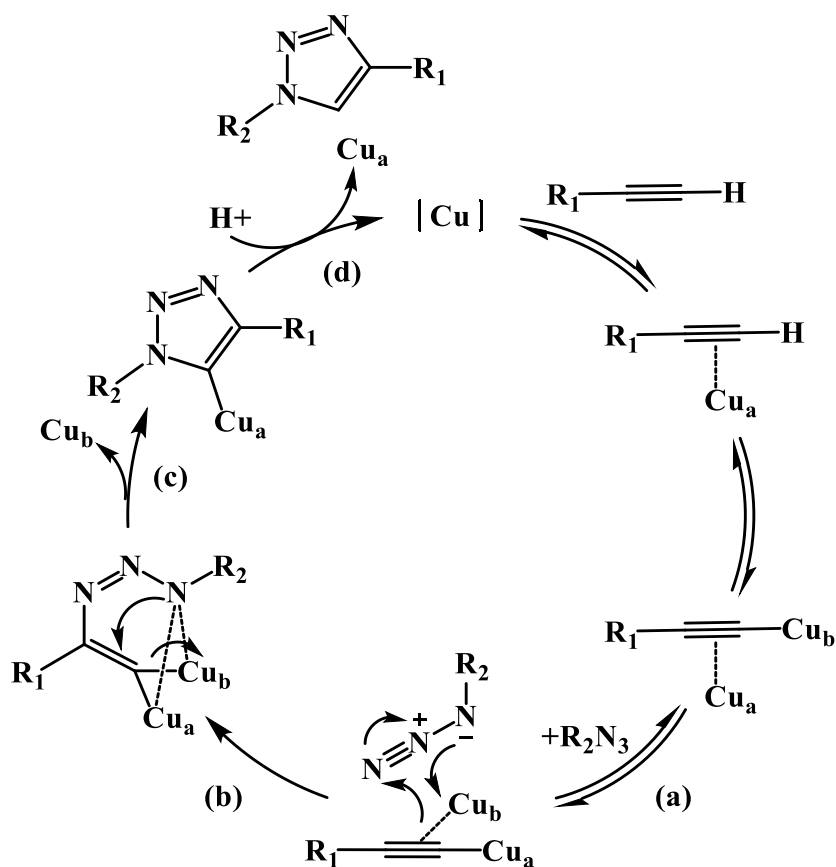


Figura 15. Mecanismo de cicloadición 1,3 dipolar de azidas y alquinos catalizado por cobre (I). [50], [52].

Por ejemplo, Qadri *et. al.* en el 2020 reportaron la síntesis de un nuevo macrociclo derivado de calix[4]resorcinareno funcionalizado con tetra-triazol el cual fue utilizado para la detección de iones en medio acuoso, Figura 16. El potencial fotofísico del compuesto macrocíclico se examinó mediante una variedad de cationes (Ba^{2+} , Ca^{2+} , Co^{2+} , Hg^{2+} , K^+ , Mg^{2+} , Mn^{2+} , Na^+ , NH_4^+ y Pd^{2+}). El macrociclo de calix[4]resorcinareno funcionalizado con triazol interactuó preferentemente con el ion Cu^{2+} , este nuevo compuesto de tetra-triazol

fue sintetizado a partir de un aldehído funcionalizado con una cadena alifática mediante química click para una posterior reacción con resorcinol en medio ácido [53].

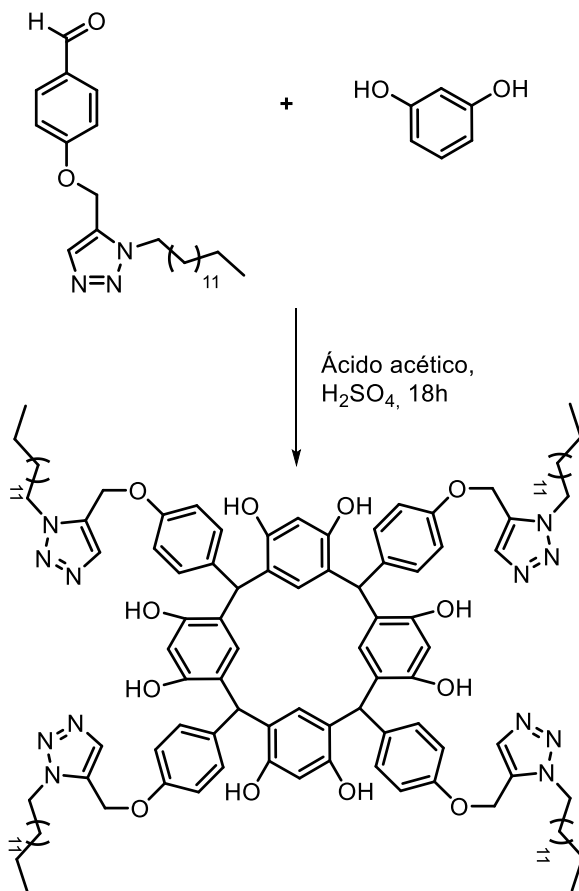


Figura 16. Síntesis del macrociclo derivado de calix[4]resorcinareno funcionalizado con tetra-triazol.

Se han reportado diversos dendrímeros a base de resorcinareno generados mediante química click específicamente CuAAC, por ejemplo, i) unión a carbohidratos [54]–[56], ii) polímeros [57], iii) unión a bases nitrogenadas [58], iv) radio-marcadores [59] y v) unión a biomoléculas activas como cumarina [60], ácido fólico [61], ciclodextrina [62], espiro indolina [63], entre otras, ver Figura 17.

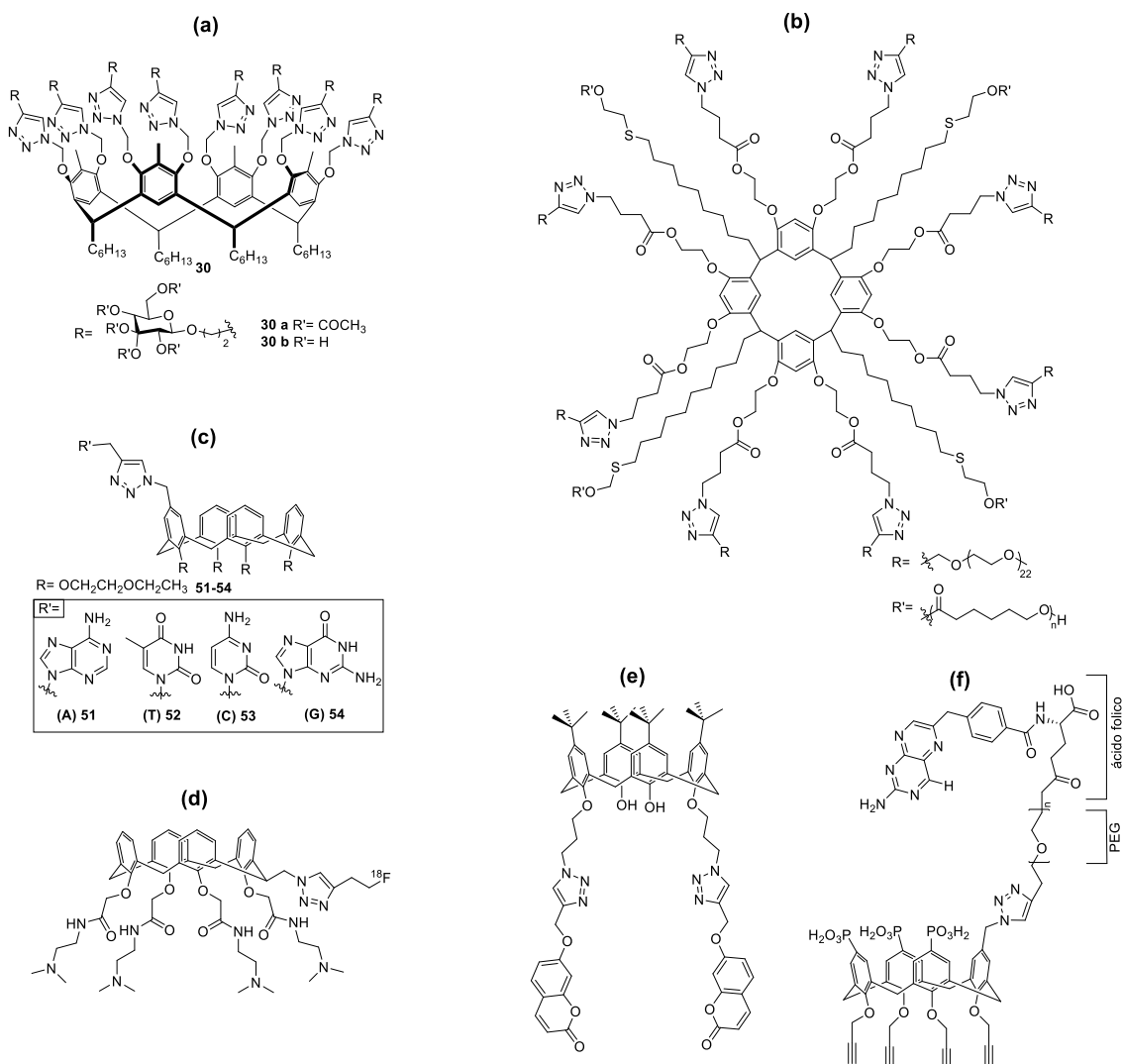


Figura 17. Ejemplos de dendrímeros a base de calix[4]resorcinareno. a) carbohidrato-resorcinareno, b) polímeros-resorcinareno (copolímeros de estrella), c) bases nitrogenada-resorcinareno, d) radio marcadores-resorcinareno y biomoléculas activas-resorcinareno como e) cumarina y f) ácido fólico.

1.1.1.5 Aplicaciones de los Calix[4]resorcinarenos

La aplicación de este tipo de compuestos es limitada debido a sus propiedades hidrofóbicas haciendo que estos macrociclos sean poco solubles en medios acuosos, sin embargo, al presentar sustituciones en sus puentes de metileno se pueden obtener una gran variedad de grupos funcionales con los cuales la molécula original puede modificar parcialmente su hidrofobicidad permitiendo ampliar sus aplicaciones [64]. Estos derivados de resorcinareno funcionalizados son conocidos como dendrímeros, los dendrímeros son macromoléculas con estructuras tridimensionales de construcción ramificada. Los dendrímeros forman parte de los polímeros, pero su principal diferencia radica en que la distribución de las moléculas que constituyen a

los polímeros lineales es probabilística, en tanto que, en el caso de los dendrímeros, se tiene una estructura química precisa, donde los enlaces químicos entre los átomos pueden ser descritos con exactitud [65]. Se han reportado diversos dendrímeros a base de resorcinareno unidos a i) carbohidratos [55], ii) polímeros [57], iii) unión a bases nitrogenadas [66], iv) radio-marcadores [59] y v) unión a biomoléculas activas como péptidos [66], ácido fólico [61], ciclodextrinas [62], entre otras. Dada la gran versatilidad que pueden llegar a presentar las funcionalizaciones en los resorcinarenos, este tipo de derivados presentan aplicaciones como: i) capturador de iones, esta característica se da gracias a su conformación de tipo corona o calix, ii) pueden llegar a tener un efecto sobre la solubilidad, este tipo de compuestos se han implementado para aumentar la solubilidad de moléculas como la testosterona que es altamente insoluble para ensayos de detección [14], iii) como recubrimiento de electrodos, se han implementado resorcinarenos funcionalizados con moléculas conductoras [26], iv) en aplicaciones cromatográficas, como es el caso de la generación de columnas de afinidad [14], v) como sistemas de administración y liberación de medicamentos [67] o vi) como posibles agentes antibacterianos [68].

1.1.1.6 Actividad antibacteriana de derivados de resorcinareno

En el 2014 Makwana *et. al.*, reportaron la actividad antibacteriana de derivados de resorcinareno funcionalizados, compuestos 1-4, Figura 18. Se implementó el ensayo de halo de inhibición utilizando como control de técnica el cloranfenicol. Se encontró que el resorcinareno sin funcionalizar 1 (calix[4]resorcinareno) y funcionalizado compuestos 2 y 4 presentaron una actividad similar a la del control frente a *E. coli* y *S. aureus* a las dos concentraciones evaluadas 50 y 100 ppm, Tabla 2 [68].

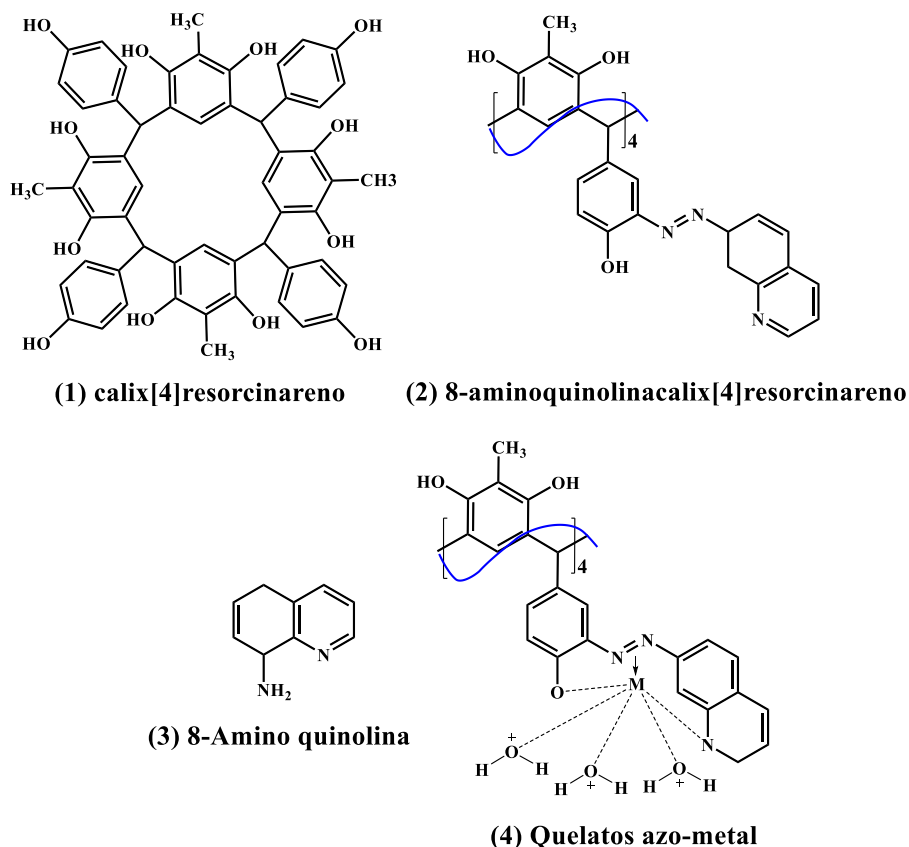


Figura 18. Derivados de calix[4]resorcinarenos evaluados frente a bacterias Gram negativas y Gram positivas.

Tabla 2. Actividad antimicrobiana (halo de inhibición en mm) de los compuestos 1-4.

Nombre del compuesto	Halo de inhibición (mm)							
	<i>E. coli</i>		<i>B. subtilis</i>		<i>S. aureus</i>		<i>B. megaterium</i>	
	50 ppm	100 ppm	50 ppm	100 ppm	50 ppm	100 ppm	50 ppm	100 ppm
A*	9	8	10	10	9	8	9	7
1	6	4	7	4	8	8	6	5
2	6	5	7	7	5	5	6	6
3	7	6	6	6	5	5	6	5
4	9	8	7	8	8	8	9	9

A* = Cloranfenicol (Antibiótico control)

En el 2019 Kashapov *et. al.*, evaluaron la actividad antibacteriana de dos resorcinarenos funcionalizados con 6-(metilamino)hexano-1,2,3,4,5-pentanol, tanto en su borde superior como su borde inferior (GCR-1 y GCR-2, Figura 19). Es de resaltar la actividad que presentaron estos macrociclos frente a *S. aureus* con valores de concentración mínima inhibitoria (CMI) cercanas a 1 mM, Tabla 3. Muchos de los antibióticos usados en la

actualidad presentan una dificultad en el tratamiento de bacterias Gram positivas como lo es *S. aureus*, estos resultados sugieren que este tipo de moléculas macrocíclicas puede ser implementadas como una nueva fuente de exploración de agentes con potencial antibacteriano [69].

Tabla 3. Actividad antimicrobiana de GCR-1 y GCR-2.

Compuesto	Concentración Mínima Inhibitoria (CMI), mM		
	<i>S. aureus</i> 209P	<i>B. cereus</i> 8035	<i>C. albicans</i> 855-653
Actividad bacteriostática y antifúngica			
GCR-1	1,00 ± 0,07	>1	>1
GCR-2	0,13 ± 0,01	0,25	>0,5
Compuesto	Concentración Mínima Bactericida y Fungicida (CMB, CMF), mM		
	Actividad bactericida y antifúngica		
GCR-1	1,00 ± 0,06	>1	>1
GCR-2	1,00 ± 0,08	>1	>0,5

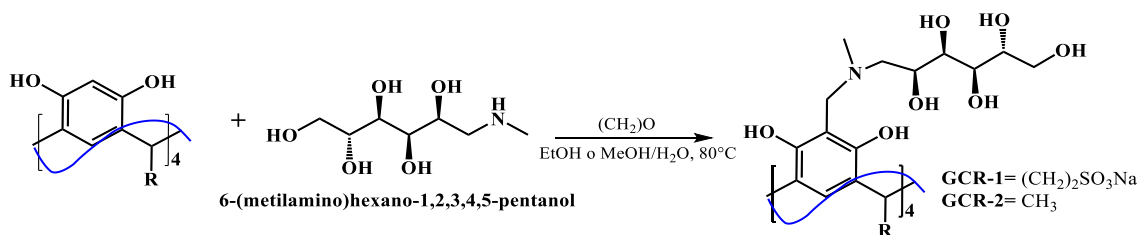


Figura 19. Síntesis de GCR-1 y GCR-2.

1.2 Péptidos Antimicrobianos (PAMs)

Para potenciar la actividad antimicrobiana de moléculas orgánicas se han probado diversas funcionalizaciones con moléculas de origen peptídico, como lo son los PAMs. Los PAMs son producidos por diferentes tipos de células y constituyen un mecanismo primario de defensa contra infecciones causadas por bacterias y otros agentes externos [70]. Los PAMs son una gran fuente de nuevas moléculas biológicas con actividad antimicrobiana, que poseen un amplio espectro de acción y han sido categorizados en cuatro subgrupos, con base a su estructura primaria [71]: Grupo (1), formado principalmente por péptidos aniónicos, a condiciones de pH fisiológico, son PAMs de secuencias cortas con un peso que oscila entre los 700 – 800 Da. Se encuentran con regularidad en fluidos bronquioalveolares y células epiteliales del tracto respiratorio. Se ha

reportado que este tipo de PAMs presentan actividad antibacteriana contra cepas Gram negativas y Gram positivas. Grupo (2), constituido por péptidos catiónicos con un tamaño máximo de 40 aminoácidos, no presentan residuos de Cisteína. No presentan una estructura definida, sin embargo, se han reportado casos como el de la Buforina II donde la extensión de la α -hélice se correlaciona directamente con la actividad antibacteriana. Grupo (3), conformado por péptidos catiónicos ricos en aminoácidos como Prolina, Arginina, Triptófano y Fenilalanina. Estos péptidos carecen de residuos de Cisteína y son particularmente lineales, aunque algunos pueden tomar conformaciones de giros extendidos, similar a la α -hélice. Y Grupo (4), abarca péptidos tanto catiónicos como aniónicos los cuales se diferencian principalmente de los demás subgrupos debido a que presentan residuos de Cisteína, que facilita la formación de puentes disulfuro intramoleculares y estructuras β -plegadas estables; son secuencias que contienen cerca de 30 aminoácidos de los cuales entre 6 a 10 son Cisteínas. La estructura primaria de los PAMs, en la mayoría de los casos, está constituida principalmente por aminoácidos catiónicos que le confieren una mayor capacidad de interacción con las cargas negativas de la membrana externa de las bacterias, esta interacción electrostática conlleva a la desestabilización de su capa estructural externa lo que genera lisis celular [5,16].

1.2.1 Lactoferricina Bovina

La Lactoferrina Bovina (LFB), es una glicoproteína de 703 aminoácidos con un peso molecular de 80 KDa, perteneciente a la familia de las transferrinas (proteínas transportadoras de hierro). Esta proteína presenta en su cadena peptídica una gran variedad de aminoácidos básicos que le confieren propiedades únicas. La LFB se encuentra en su forma libre de hierro, en fluidos corporales, tales como, secreciones de las mucosas, líquido seminal, leche materna, entre otras [72], [73]. Por otra parte, la Lactoferricina bovina (LfcinB: ¹⁷FKCRRWQWRMKKLGAPSITCVRRAF⁴¹) es generada por la hidrólisis de la LFB mediada por la pepsina gástrica [73], este péptido presenta un bucle formado por un enlace disulfuro entre las cisteínas de las posiciones 19 y 36 (Figura 20) que le confiere propiedades estructurales que están asociadas con su efecto como agente antimicrobiano [74]. La LfcinB y fragmentos más cortos han presentado igual o mayor actividad antibacteriana que la LFB; se ha logrado identificar el motivo mínimo de actividad antibacteriana, el cual

corresponde a seis residuos (LfcinB 20-25: ²⁰RRWQWR²⁵), sin embargo, este motivo presenta una menor actividad en comparación a la LfcinB [75].

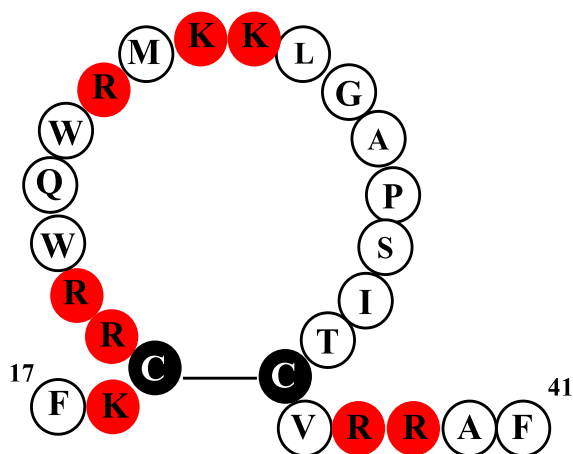


Figura 20. Secuencia de la Lactoferrina bovina. Se muestra el bucle formado por el puente disulfuro. Los aminoácidos cargados positivamente están en rojo, los números corresponden a la posición en la proteína original [73].

La Lactoferrina bovina (LFB) presenta mayor actividad en comparación que sus homologas la Lactoferrinas humana, murina y caprina. La LFB presenta actividad contra parásitos, hongos, bacterias y virus [76]. En estudios *in vitro* se ha demostrado que puede llegar a inhibir el crecimiento de bacterias Gram-positivas y Gram-negativas, entre las que se destacan las cepas resistentes de *S. aureus* y *E. coli* [73]. En la Tabla 4 se muestran algunos ejemplos de la actividad antibacteriana de péptidos homólogos de la LfcinB los cuales han presentado mayor actividad que la LFB, estos son secuencias más cortas, con modificaciones puntuales como incorporación de aminoácidos no presentes en su estructura primaria y un aumento de la polivalencia mediante la generación de dímeros y tetrámeros.

Tabla 4. Actividad antibacteriana de péptidos derivados de la LfcinB.

Secuencia	Actividad Antibacteriana, CMI (μM)					Referencia
	Cepa Bacteriana					
	<i>E. coli</i> ATCC 11775	<i>E. coli</i> ATCC 25922	<i>P. aeruginosa</i> ATCC 27853	<i>S. aureus</i> ATCC 25923	<i>E. faecalis</i> ATCC 29212	
Proteína LFB	>200	25	-	-	25	[6], [77]
$^{17}\text{FKCRRWQWRMKKLGAPSITCVRRAF}^{41}$	102	>102	102	>102	>102	[77], [78]
$^{17}\text{FKARRWQWRMKKLG}^{31}$	>102	102	102	>102	>102	[77], [79]
$(^{17}\text{FKARRWQWRMKKLG}^{31})_2\text{KAhx}$	15	15	15	30	30	[78]
$^{20}\text{RRWQWRMKKLG}^{30}$	130	130	>130	130	>130	[78], [80]
$(^{20}\text{RRWQWRMKKLG}^{30})_2\text{KAhx}$	30	30	15	60	60	
$((^{20}\text{RRWQWRMKKLG}^{30})_2\text{KAhx})_2$	15	15	15	30	30	
$^{20}\text{RRWQWR}^{25}$	203	203	203	203	>203	[77], [78]
$(^{20}\text{RRWQWR}^{25})_2\text{KAhx}$	22	6	23	91	91	
$((^{20}\text{RRWQWR}^{25})_2\text{KAhx})_2$	22	22	11	22	44	
RWQWRWQWR	17	17	67	135	67	[77], [79]
$(\text{RWQWRWQWR})_2\text{KAhx}$	31	16	63	63	31	[78]

1.2.2 Buforina

La Buforina (BF) ha sido descrita como el primer PAM derivado de una histona, se ha reportado que estas solo presentan funciones en el núcleo de la célula como proteínas encargadas del empaquetamiento y regulación de los genes en células eucariotas. En la actualidad se conoce que tienen funciones extracelulares que están relacionadas con el sistema inmune innato. La Buforina I es un PAM constituido por 39 aminoácidos (BF1: $^1\text{AGRKQGGKVRKAKTRSSRAGLQFPVGRVHLLRKGNK}^{39}$) identificado en el tejido estomacal del sapo asiático *Bufo gargarizans*, se ha reportado que este PAM es generado a partir de la proteólisis de la histona H2A dirigida por la catepsina D en donde se libera su región N-terminal en un sitio de reconocimiento específico para inducir una respuesta a lesiones epidérmicas [81].

La Buforina II (BFII) consta de 21 aminoácidos ($^{16}\text{TRSSRAGLQFPVGRVHLLRK}^{37}$), es considerado como un PAM de amplio espectro [82]. Este péptido presentó actividad contra bacterias Gram positivas, Gram negativas, bacterias multirresistentes, hongos y células cancerígenas. La BFII cuenta con un mecanismo de acción independiente del rompimiento de la membrana de la bacteria. Se ha demostrado que la ^{11}Pro está

directamente involucrada en el paso del péptido a través de la membrana de las bacterias, independiente de que exista o no un receptor específico. Luego de atravesar la membrana, la BFII interactúa directamente con el ADN de la bacteria para interrumpir finalmente los procesos vitales de la misma [81], [83], [84]. En la Tabla 5 se muestran a manera de ejemplo la actividad antibacteriana de péptidos análogos a la BF los cuales han presentado mayor actividad que la histona H2A.

Tabla 5. Actividad antibacteriana de péptidos derivados de la BF.

Secuencia	Actividad Antibacteriana, CMI (μM)					Referencia
	Cepa Bacteriana					
	E. coli ATCC 11775	E. coli ATCC 25922	P. aeruginosa ATCC 27853	S. aureus ATCC 25923	E. faecalis ATCC 29212	
TRSSRAGLQFPVGRVHRLLRK (BFII)	-	4	-	4	-	[85]
RAGLQFPVGRLLRLLRLLR (BFIIb)	-	1	-	1	-	[81], [86]
RAGLQFPVGKLLKLLKRLK (Histonin)	-	2	-	2	-	
RAGLQWPIGRLLRLLRLLR (BFIIIa)	-	1	-	1	-	[87]
RAGLQWPIGKLLKLLKLLK (BFIIIc)	-	0,5	-	0,5	-	
RLLR (BF (32-35))	>200	>200	>200	>200	>200	[52], [88]
RLLRLLR (BF (32-35) _{Pal})	100	200	200	>200	>200	

1.2.3 Alcance Clínico de los PAMs

En la actualidad, la Administración de Drogas y Alimentos de los Estados Unidos (FDA) ha aprobado más de 140 fármacos peptídicos los cuales se encuentran en diferentes etapas de ensayos clínicos y más de 500 péptidos terapéuticos en desarrollo preclínico. La mayoría de estos fármacos peptídicos son administrados vía tópica debido a la alta toxicidad que presentan, especialmente, aquellos que provienen de especies animales (e.j anfibios, insectos, reptiles). Como alternativa y buscando la disminución de los efectos adversos se están buscando formas de administración que favorezcan a que el fármaco peptídico actúe sobre la diana objetivo, estas incluyen vías de administración oral, intranasal y transdérmica [89].

Las fases de investigación y desarrollo de un fármaco se presentan a continuación: i) fase de descubrimiento, ii) fase preclínica, iii) fase clínica y iv) fase de aprobación y registro. La fase de descubrimiento consiste en la

identificación de una necesidad médica. En la fase preclínica, se evalúa la seguridad de la forma de administración en un modelo in vivo del compuesto seleccionado. En fase clínica, se determina el método de acción del medicamento en personas, se investiga si se trata de una droga adecuada y eficaz para el tratamiento de la enfermedad. Dentro de esta última etapa se presentan otras tres fases (Fase I, se llevan a cabo los primeros estudios del fármaco en voluntarios, en la fase II ya ha sido evaluada en pacientes y en la última fase se estudia en más de mil pacientes). En la Tabla 6 se presentan algunos péptidos aprobados por la FDA en tratamientos de diversas patologías, se detallan las diferentes etapas en las que se encuentra cada molécula dentro del aspecto de investigación y desarrollo [90].

Tabla 6. Péptidos que se encuentran en fase clínica de desarrollo [89].

Péptido	Descripción	Fase	Indicación	Administración
Pexiganan (MSI-78)	Análogo de Magainina (piel de rana de garra africana)	III	Úlceras de pie diabético infectado	Crema tópica
Omiganan	Derivado de la Indolicidina (bovina)	II / III	Infecciones por catéter y rosácea	Gel tópico
Lytixar (LTX-109)	Peptidomimético sintético antimicrobiano	I / II	Infecciones Gram positivas no complicadas de piel, impétigo y colonización nasal con <i>S. aureus</i>	Hidrogel tópico
HIF1-11	Derivado de la Lactoferricina (humana)	I / II	Bacteriemia e infecciones fúngicas en receptores de trasplantes de células madre hematopoyéticas inmunocomprometidos	Tratamiento intravenoso (Solución salina)
Iseganan (IB-367)	Derivado de Protegrina 1 (leucocitos porcinos)	III	Mucositis oral en pacientes que reciben radioterapia por neoplasia de cabeza y cuello	Solución oral

1.3 Resistencia Bacteriana

Los antibióticos, ya sean citotóxicos o citostáticos para los microorganismos, permiten que las defensas naturales del cuerpo, como el sistema inmunológico, los ataquen con más facilidad y sean eliminados. A menudo estos agentes actúan inhibiendo la síntesis de proteínas, ácido desoxirribonucleico (ADN), ácido ribonucleico (ARN) o generando acción mediante la desestabilización de la membrana bacteriana [91]. Sin duda los antibióticos son considerados como una primera línea de defensa a nivel hospitalario en el tratamiento de diversas enfermedades infecciosas causadas por bacterias [92]. La penicilina descubierta por Sir Alexander Fleming en 1928 fue incorporada por primera vez para tratar infecciones en la década de los 90's, sin embargo,

años más tarde la resistencia a la penicilina fue considerada como un problema de salud pública a nivel mundial. Con esto surgió la necesidad de ampliar el espectro de tratamientos que se encontraban a la fecha, en respuesta a esto se desarrollaron nuevos antibióticos betalactámicos, pero en poco tiempo el primer caso de *Staphylococcus aureus* resistente a la Metilina (SARM) fue identificado en Reino Unido. Desde entonces la resistencia bacteriana se ha presentado frente a casi todos los antibióticos que se han desarrollado; e.j la Vancomicina fue introducida como respuesta a la resistencia bacteriana a la Metilina en *Staphylococcus aureus*. Desde finales de la década de los 60's hasta principios de la década de 80's, la industria farmacéutica introdujo una gran variedad de antibióticos nuevos para resolver el problema de resistencia, sin embargo, esta nueva línea de antibióticos desarrollados comenzó a decaer y se volvieron menos eficaces contra las patologías bacterianas. Como resultado, en la actualidad las infecciones bacterianas siguen siendo una amenaza emergente para la salud pública a nivel mundial [93]. El desarrollo de la resistencia bacteriana a los antibióticos puede ser generado naturalmente a través del tiempo, como parte del proceso de adaptación biológica de las bacterias. Sin embargo, el uso excesivo e inadecuado de estos tratamientos ha acelerado notablemente este proceso. En salud humana, el uso indiscriminado de antibióticos bajo condiciones no requeridas como automedicación, administraciones hospitalarias no requeridas y una inadecuada prescripción en las cantidades empleadas, son consideradas las principales causas del aumento de la resistencia bacteriana [94].

Al igual que con el desarrollo de resistencia a los antibióticos, las bacterias pueden volverse resistentes a los PAMs. La frecuencia difiere ampliamente según la bacteria y el péptido, aunque los mecanismos de resistencia bacteriana a los PAMs aún no están completamente establecidos, la modificación de la interacción fisicoquímica entre el PAM y la membrana para prevenir la permeabilización y el consiguiente desequilibrio osmótico celular es probablemente el primer paso en el desarrollo de la resistencia bacteriana. La producción de enzimas proteolíticas por bacterias Gram negativas o Gram positivas puede resultar en la degradación del PAM activo en fragmentos inactivos y por lo tanto verse reflejado en un aumento de la resistencia. Así, en bacterias Gram negativas, principalmente *Enterobacteriaceae*, la proteína de la membrana externa OmpT de

E. coli es capaz de degradar los PAMs y en Gram positivas como *S. aureus* se ha demostrado lo mismo para la aureolisina. Así surge la necesidad de implementar nuevas estrategias en el diseño de moléculas antibacterianas basadas en PAMs [95], que le confiera estabilidad a la respuesta de las bacterias.

Las pautas regulatorias varían según el país, algunos han actuado con rapidez ofreciendo orientación, mientras que otras naciones aún tienen que avanzar en este campo. La OMS ha ofrecido recomendaciones, como en el caso de los niños de los países en desarrollo, de que los antibióticos sólo deben utilizarse para el tratamiento de la diarrea sanguinolenta grave y el cólera [96], [97]. En la industria del cuidado personal, no hay pautas suficientes para monitorear los productos de higiene del hogar que probablemente causen un mayor riesgo de resistencia porque estos productos contienen una alta concentración de ingredientes antibacterianos [98]. En la actualidad, la obtención de nuevos agentes antibacterianos que no generen resistencia en los patógenos y que puedan ser utilizados como agentes terapéuticos contra infecciones causadas por bacterias resistentes, está siendo el foco de muchas de las investigaciones del campo científico.

La obtención de péptidos cortos de manera rápida es posible mediante la síntesis química de péptidos en fase sólida, SPPS. Esta estrategia permite obtener péptidos con altos rendimientos y de una alta pureza. Una de las principales fuentes para el diseño y desarrollo de nuevos agentes terapéuticos son los péptidos antimicrobianos (PAMs), debido a que estos generalmente forman parte del sistema inmune innato de los organismos [99]. Una de las grandes desventajas de los péptidos sintéticos es su susceptibilidad a proteasas generadas por los patógenos [100], [101]. Con la finalidad de superar este inconveniente en los PAMs se han propuesto diferentes estrategias que favorecen su estabilidad, estas son i) la inclusión de moléculas no naturales para que las enzimas no puedan reconocerlos y que no sean fácilmente degradados y ii) generar péptidos de alto peso molecular con múltiples copias de la secuencia peptídica activa. En este contexto, el presente proyecto propone el diseño, la obtención y evaluación de la actividad antibacteriana de dendrímeros péptido-resorcinareno, derivados de los motivos mínimos de actividad antibacteriana de la LfcinB (RRWQWR) y/o BF (RLLR). Lo anterior permitirá identificar nuevos métodos de presentación polivalente de secuencias peptídicas que puedan llegar a incrementar su actividad antibacteriana.

1.4 Generalidades biológicas de las cepas bacterianas seleccionadas para el proyecto

1.4.1 *Staphylococcus aureus*

Staphylococcus aureus es una bacteria Gram positiva, que tiene forma de cocos (en racimos) que varían de 0,5 a 1,5 μm de diámetro, los cuales pueden o no contener una cápsula de polisacárido. Son anaerobios facultativos, no móviles, que no forman esporas [102], crecen en medios que tienen hasta un 10% de sal y crecen a temperaturas entre 18 y 40 °C [103]. Las pruebas de identificación bioquímicas típicas incluyen catalasa positiva, coagulasa positiva, oxidasa negativa, novobiocina sensible y de fermentación de manitol positiva [104].

Patogenicidad: *S. aureus* se encuentra en el medio ambiente y también como parte de la microbiota de la piel y las membranas mucosas (en el área nasal), normalmente no causa infección en la epidermis sana; sin embargo, si se le permite ingresar al torrente sanguíneo o a los tejidos internos, estas bacterias pueden causar una variedad de infecciones graves; como bacteriemia, endocarditis infecciosa, infecciones de la piel y tejidos blandos (Impétigo, foliculitis, furúnculos, carbunco, celulitis, síndrome de la piel escaldada), osteomielitis, artritis séptica, infecciones por dispositivos protésicos, infecciones pulmonares (neumonía y empiema), gastroenteritis, meningitis, síndrome de shock tóxico e infecciones del tracto urinario. Los mecanismos para la evasión de la respuesta inmune del huésped incluyen la producción de una cápsula antifagocítica, el secuestro de anticuerpos del huésped o el enmascaramiento de antígenos por la proteína A, la formación de biopelículas, la supervivencia intracelular y el bloqueo de la quimiotaxis de los leucocitos [103].

Resistencia-Tratamiento: Aunque el término resistencia a meticilina incluye también a los derivados β -lactámicos, *S. aureus* presenta resistencia a varios grupos de antibióticos como cloranfenicol, tetraciclinas, macrólidos, lincosaminas, aminoglucósidos e, incluso, quinolonas, describiéndose cada vez con mayor frecuencia brotes SARM sensibles sólo a los glucopéptidos [105].

1.4.2 *Escherichia coli*

Escherichia coli es un bacilo Gram negativo, móvil, facultativo, oxidasa negativa, reductor de nitratos [106], fermenta la glucosa y la lactosa con producción de gas. Es una bacteria mesófila, su óptimo desarrollo se encuentra en el entorno de la temperatura corporal de los animales de sangre caliente (35-43 °C). Como todas las bacterias Gram negativas, la cubierta de *E. coli* consta de tres elementos: la membrana citoplasmática, la membrana externa y entre ambas un espacio periplásmico constituido por peptidoglicano, esta última estructura confiere a la bacteria su forma y rigidez, y le permite resistir presiones osmóticas ambientales relativamente elevadas [107].

Patogenicidad: Existen numerosas cepas de *E. coli* que pueden ocasionar patologías en humanos y que presentan una virulencia marcada, estas son conocidas como agentes responsables de gastroenteritis (además de infecciones del tracto urinario), especialmente en países en vías de desarrollo, causando la muerte de cerca de un millón de niños cada año debido a deshidratación y a otras complicaciones. Los principales patógenos intestinales, que se describen en función de los síntomas clínicos que generan y de los factores de patogenicidad que se expresan son los siguientes: *E. coli* enterotoxigénicas (ETEC), *E. coli* enteropatógenas (EPEC), *E. coli* enteroagregativas (EAEC), *E. coli* enterohemorrágicas (EHEC) y *E. coli* enteroinvasivas (EIEC) [107].

E. coli está compuesta por tres antígenos que la caracterizan: i) Antígeno O: Somático. ii) Antígeno K: De superficie. iii) Antígeno H: Flagelar [108]. La patogenicidad es función de los antígenos superficiales y de las toxinas que generan. Así, las fimbrias actúan aportando su capacidad de adherencia, los antígenos O y K presentan propiedades antifagocitarias e inhibidoras de las sustancias bactericidas del suero, presentan una endotoxina ligada al lipopolisacárido, en especial al lípido A, responsable de la acción pirógena. Algunas cepas pueden producir exotoxinas responsables de la producción de diarreas, puede existir, además, una toxina termoestable (TS), de bajo peso molecular y no antigénica, que produce acumulación de líquidos en el intestino. Estas toxinas no producen alteraciones tóxicas ni anatómicas del enterocito, pero sí de tipo funcional (enterotoxinas citotónicas), siendo una característica de las *E. coli* enterotoxigénicas [107].

Resistencia-Tratamiento: *E. coli*, que tiene altos porcentajes de resistencia hacia ampicilina, trimetoprim-sulfametoxazol, tetraciclina, cloranfenicol y ácido nalidíxico, lo que representa grandes complicaciones en el tratamiento antibiótico cuando este es requerido. Este aumento de resistencia antibiótica se debe a la adquisición de diferentes mecanismos moleculares de resistencia mediante mutaciones puntuales a nivel cromosómico o transferencia horizontal de material genético entre especies relacionadas o diferentes, facilitada [109]. Muchas personas con diarrea por *E. coli* requieren la administración por vía intravenosa de líquidos que contengan sales [110], cuando se requiere se utilizan antibióticos sensibles como fosfomicina, betalactámicos, cefixima, cefuroxima y amoxicilina-clavulánico [111].

Dentro de este contexto, el presente proyecto de investigación propuso la síntesis y caracterización de dendrímeros de tipo péptido-resorcinareno derivados de la LfcinB y/o la Buforina. Estrategia con la que se pueden generar moléculas que presenten varias copias de los PAMs seleccionados sobre un núcleo no proteico.

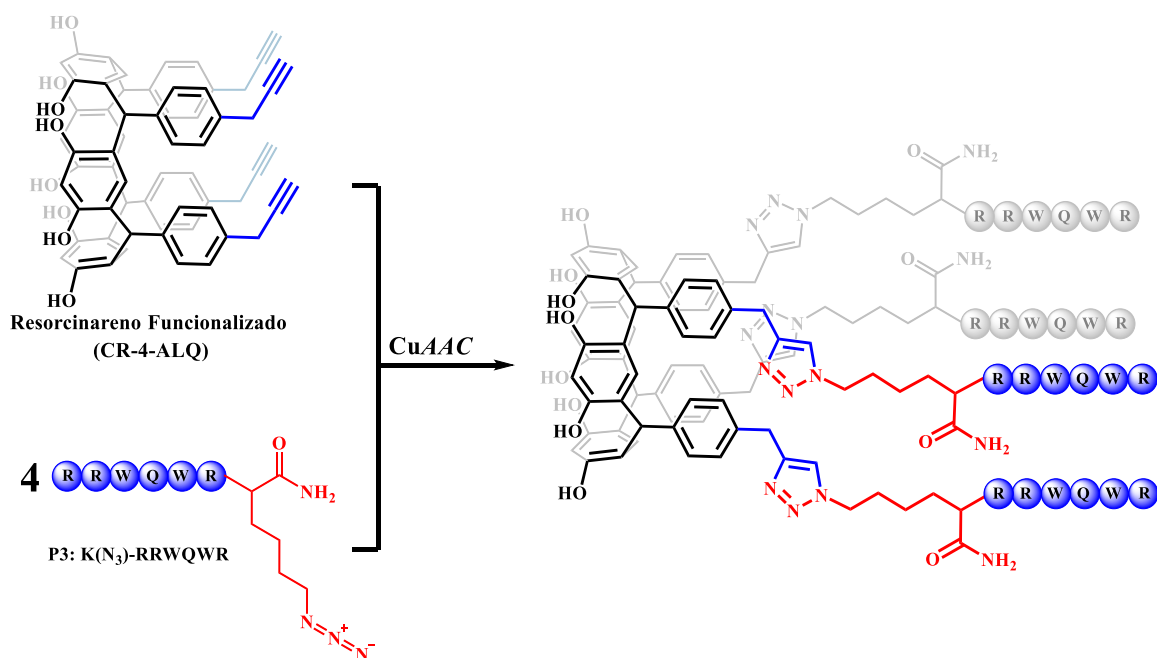


Figura 21. Ejemplo del diseño de un dendrímero péptido-resorcinareno derivado de LfcinB (20-25): RRWQWR.

En la Figura 21, se muestra a manera de ejemplo uno de los diseños de los dendrímeros que se propusieron, en la estructura encontramos: cuatro copias del motivo mínimo de la LfcinB, RRWQWR, unidas mediante un anillo 1,2,3-triazol a una base polihidroxilada de calix[4]resorcinareno. Durante el desarrollo del proyecto se evaluaron cuatro variables: i) las rutas sintéticas que permitan la obtención de resorcinarenos funcionalizados con grupos alquino, ya sea sobre los hidroxilos fenólicos o los sustituyentes en el puente de metileno, ii) viabilidad sintética de péptidos derivados de los motivos mínimos de actividad antibacteriana de la LfcinB y/o Buforina, que contengan un grupo azida en su estructura en el extremo N o C terminal; iii) los parámetros sintéticos (solventes, temperatura, relación molar, catalizador, entre otros) que permitan generar los dendrímeros péptido-resorcinareno mediante cicloadición de azida/alquino, y iv) la actividad antibacteriana de los dendrímeros obtenidos. En este punto, se evaluó la actividad de los dendrímeros péptido-resorcinareno frente a cepas de referencia y aislados clínicos de *Staphylococcus aureus* y *Escherichia coli* y se comparó con la actividad que presentan las secuencias lineales, el resorcinareno base y moléculas polivalentes construidas sobre un núcleo proteico.

2. Objetivos

2.1 Objetivo General

Obtener mediante cicloadición azida/alquino dendrímeros péptido-resorcinareno que contengan secuencias peptídicas derivadas de la LfcinB (20-25): RRWQWR y/o la BF (32-35): RLLR y evaluar su potencial antibacteriano.

2.2 Objetivos Específicos

1. Sintetizar y caracterizar estructuras (núcleos) del tipo resorcinareno funcionalizadas con grupos alquino en su borde inferior y/o grupos hidroxilos aromáticos
2. Obtener y caracterizar péptidos lineales derivados de LfcinB y/o BF que contengan un grupo azida en el extremo N o C terminal.
3. Evaluar las condiciones para la reacción de cicloadición catalizada por cobre (Cu^+), entre el grupo azida introducido en los péptidos antibacterianos y los grupos alquino del resorcinareno funcionalizado.
4. Determinar el potencial antibacteriano de los dendrímeros péptido-resorcinareno obtenidos con mayor rendimiento, frente a cepas de *E. coli* y *S. aureus*.

3. Metodología

3.1 Diseño experimental

Para dar cumplimiento a los objetivos propuestos en la presente tesis doctoral se contempló el diseño experimental que se describe en la Figura 22.



Figura 22. Etapas involucradas en el diseño experimental.

Etapa 1. Obtención de precursores.

- I. Obtención de derivados de calix[4]resorcinareno. Se diseñaron, sintetizaron y caracterizaron dos (2) estructuras, (núcleos) derivadas de calix[4]resorcinareno, funcionalizadas con el grupo alquino en: i) en su puente de metilo, para lo que fue necesario obtener previamente el 4-(prop-2-in-1-iloxi)benzaldehído (p-HF) y ii) en los grupos hidroxilos aromáticos, mediante reacción (sustitución nucleofílica) con 3-bromoprop-1-ino.
- II. Obtención de péptidos, derivados de los motivos mínimos de actividad antibacteriana de la LfcinB y BF, por síntesis de péptidos en fase sólida. Se sintetizaron péptidos lineales funcionalizados con el ácido (S)-2-(Fmoc-amino)-6-azidoheptanoico. Adicionalmente, se obtuvieron péptidos control, específicamente la secuencia lineal del motivo mínimo de los PAMs seleccionados y péptidos polivalentes (tetrámeros), estos últimos generados por el método de dobles dímeros, en donde se empleó un núcleo o core de tipo proteico [80], [112].

Etapa 2. Estandarización de la ruta sintética que permitió la obtención de los dendrímeros péptido-resorcinareno. Se obtuvieron dos (2) dendrímeros del tipo péptido-resorcinareno utilizando química click, específicamente mediante el uso de la reacción de cicloadición catalizada por cobre (I) entre los grupos azida y alquino (CuAAC).

Etapa 3. Determinación de la actividad antimicrobiana de los péptidos control y los dendrímeros péptido-resorcinareno obtenidos (moléculas con una pureza $\geq 80\%$), contra las cepas de referencia y aislados clínicos.

Dentro de esta etapa se desarrollaron cuatro actividades:

- I. Determinación de la concentración mínima inhibitoria (CMI) y concentración mínima bactericida (CMB) contra cepas de referencia de *Escherichia coli* (ATCC 25922) y *Staphylococcus aureus* ATCC 25923.
- II. Determinación del potencial antibacteriano frente a aislados clínicos de *Staphylococcus aureus* (109095, 117719 y 124653) y *Escherichia coli* (1004, 129797 y 301755). Para esta etapa se

seleccionaron los dendrímeros que presentaron los mejores resultados frente a las cepas de referencia.

- III. Construcción de la curva de letalidad, para el dendrímero péptido-resorcinareno que presentó la mayor actividad contra las cepas de referencia y aislados clínicos de *Staphylococcus aureus* y *Escherichia coli*, esto permitió determinar su poder bactericida y/o bacteriostático
- IV. Evaluación del efecto sinérgico. Se evaluó el efecto sinérgico con antibióticos de uso común del dendrímero péptido-resorcinareno que presentó la mayor actividad antibacteriana contra la cepa de *Escherichia coli* ATCC 25922.
- V. Determinación del efecto antifúngico contra cepas de referencia y aislados clínicos de *Candida albicans* y *Candida auris* del dendrímero que presentó la mayor actividad antibacteriana.

Etapa 4. Actividad Citotóxica.

- I. Determinación de la actividad hemolítica de los dendrímeros péptido-resorcinareno sintetizados que presentaron la mejor actividad antimicrobiana.
- II. Evaluación de la actividad citotóxica de los dendrímeros péptido-resorcinareno que presentaron el mayor rendimiento.

A continuación, se describen los métodos empleados en cada una de las etapas.

3.2 Materiales y Métodos

3.2.1 Equipos y Reactivos

Los reactivos, resina Rink amida, Fmoc-Leu-OH, Fmoc-Arg(Pbf)-OH, Fmoc-Trp(Boc)-OH, Fmoc-Gln(Trt)-OH, Diciclohexilcarbodimida (DCC), 1-Hidroxi-6-clorobenzotriazol (6-Cl-HOBt) se adquirió de AAPPTec (Louisville, KY, EE. UU.). Se adquirieron los reactivos acetonitrilo (ACN), ácido trifluoroacético (TFA), diclorometano (DCM), diisopropiletilamina (DIPEA), N,N-dimetilformamida (DMF), Etanoditiol (EDT), isopropanol (IPA),

metanol y triisopropilsilano (TIS) de Merck (Darmstadt, Alemania). Las columnas SPE Supelclean™ LC-18 se adquirieron de Sigma-Aldrich (St. Louis, MO, EE. UU.). Los medios Tripticasa de Soya Agar (TSA), Mueller Hinton Agar (MHA) y Plate Count Agar (PCA) se adquirieron de Scharlau. El medio Mueller Hinton Broth se adquirió de Merck. La cepa bacteriana *Escherichia coli* ATCC 25922 y *Staphylococcus Aureus* ATCC 25923 se adquirió de la ATCC. Las líneas celulares MCF-7 y HeLa se obtuvieron de ATCC® (Manassas, Virginia - Estados Unidos). Todos los reactivos se utilizaron directamente sin purificaciones previas.

Los espectros de RMN-¹H se registraron a 400 MHz en un instrumento Bruker Advance 400. Los análisis de RP-HPLC se realizaron en una columna Chromolith C18 (Merck, Kenilworth, NJ, EE. UU., 50 mm), utilizando un cromatógrafo de líquidos Agilent 1200 (Agilent, Omaha, NE, EE. UU.). Los productos se analizaron en un equipo Bruker Impact II UHPLC Q-TOF MS equipado con ionización por electropulverización (ESI) y/o en un espectrómetro de masas Bruker MicroFlex MALDI-TOF, en ambos casos en modo positivo.

3.2.2 Síntesis de resorcinarenos base y funcionalización

De manera general, la síntesis de los derivados de calix[4]resorcinareno, se realizó mezclando una solución de resorcinol en EtOH:H₂O (1:1), seguido de la adición del aldehído correspondiente en relación equimolar y 10 mL de HCl al 37%, la mezcla de reacción se llevó a reflujo con agitación constante hasta reacción completa, el monitoreo se realizó mediante RP-HPLC, a diferentes tiempos. Finalizada la reacción se enfrió en un baño de hielo y se filtró. El filtrado fue lavado con agua y secado a presión reducida. Los compuestos fueron caracterizados mediante RP-HPLC, espectrometría de masas, RMN-¹H y RMN-¹³C [21].

a) Octa-2-(prop-2-in-1-iloxi)-C-tetrametilcalix[4]resorcinareno (CR-8-ALQ)

Obtención del precursor C-tetrametilcalix[4]resorcinareno, compuesto 1. Se siguió el método reportado por A.G. Sverker *et. al.* [113]. Brevemente, una solución de 1,3-dihidroxibenceno (1 mmol) y acetaldehído (1 mmol) en agua (4,0 mL) se añadió gota a gota a ácido clorhídrico (1,0 mL) y se calentó a reflujo con agitación constante durante 1 h. Se formó rápidamente un precipitado. El precipitado, se enfrió en un baño de hielo y se lavó con agua para eliminar las trazas de ácido. El filtrado se secó a presión reducida y se caracterizó mediante

RMN-¹H. Para la purificación de los productos se utilizaron cartuchos Supelclean ENVI-18 SPE (peso de lecho 5 g, volumen 20 mL). Las columnas SPE se activaron antes de su uso con 30 mL de metanol, 30 mL de ACN (que contenía TFA al 0,1%, disolvente B) y se equilibraron con 30 mL de agua (que contenían TFA al 0,1%, disolvente A). 46 mg de C-tetrametilcalix[4]resorcinareno (mezcla conformacional) disueltos en 1000 µL de ACN:H₂O (50:50), se sembraron en el cartucho de RP-SPE. La elución de la mezcla conformacional se realizó aumentando el porcentaje de disolvente B en el eluyente. Las fracciones recogidas se analizaron mediante RP-HPLC. Las fracciones que contenían el conformero puro se mezclaron y luego se liofilizaron.

C-tetrametilcalix[4]resorcinareno (rccc): sólido blanco con un rendimiento del 37,5%. Punto de Fusión >250°C descomposición. RMN-¹H, δ (DMSO-*d*₆, temperatura ambiente, ppm): CH₃ (1,39, d), CH (4,45, q), CH aromático (6,14, s), CH aromático (6,77, s), OH (8,53, s). Q-TOF MS: calculado *m/z*: 545,21, encontrado: *m/z* 545,2261.

C-tetrametilcalix[4]resorcinareno (rctt): sólido crema con un rendimiento del 6,3 %. Punto de Fusión >250°C descomposición. RMN-¹H, δ (DMSO-*d*₆, temperatura ambiente, ppm): CH₃ (1.15, d), CH (4,37, q), CH aromático (6,08, 6,17, s), CH aromático (6,26, 6,79, s), OH (8,41, .,65, s). Q-TOF MS: calculado *m/z*: 545,21, encontrado: *m/z* 545,2261.

C-tetrametilcalix[4]resorcinareno (rctt): sólido crema con un rendimiento del 3,6%. Punto de Fusión >250°C descomposición. RMN-¹H, δ (DMSO-*d*₆, temperatura ambiente, ppm): CH₃ (1,15, 1,40), CH (4,38-4,46), CH aromático (6,12, 6,16, 6,21, 6,29), CH aromático (6,86, 6,90, 6,98), 7.29), OH (8,50-8,90). Q-TOF MS: calculado *m/z*: 545,21, encontrado: *m/z* 545,2261.

Síntesis del derivado CR-8-ALQ (rccc). El precursor C-tetrametilcalix[4]resorcinareno (rccc) fue funcionalizado mediante una reacción de sustitución nucleofílica. Se disolvió el precursor (0,4 mmol) con carbonato de potasio (11,2 mmol) en 15 mL de ACN, y luego se le adicionó 3-bromoprop-1-ino (11,2 mmol). La mezcla de reacción se llevó a reflujo durante 9 h, transcurrido este tiempo se detuvo el calentamiento y se dejó en agitación durante 15 h. El ACN fue retirado, mediante rotaevaporación, el sólido fue disuelto en

cloroformo y posteriormente la fase orgánica fue lavada con agua (3×), la fase orgánica fue concentrada y finalmente se obtuvo un sólido color amarillo.

CR-8-ALQ (rccc): sólido amarillo, rendimiento del 83,5%. Punto de Fusión >250°C descomposición. RMN-¹H, δ (CDCl₃, temperatura ambiente, ppm): CH aromático (7,26, s), CH aromático (6,72, s), OCH₂ (4,61, d), CH (4,42, d), -C≡CH (2,50-2,48, s), CH₃ (1,44, d), RMN-¹³C (150,9 MHz, CDCl₃, temperatura ambiente, ppm): δ 20,2 (s, C¹), 30,7 (s, C²), 57,6 (s, C³), 75,2 (s, C⁴), 77,5 (s, C⁵), 101,6 (s, C⁶), 125,7 (s, C⁷), 129,7 (s, C⁸), 154,0 (s, C⁹). Q-TOF MS: calculado *m/z*: 848,33, encontrado: *m/z* 849,3285.

b) C-Tetra(4-(prop-2-in-1-iloxi)fenil)calix[4]resorcinareno (CR-4-ALQ):

Síntesis del precursor, 4-(prop-2-in-1-iloxi)benzaldehído (p-HF), el protocolo fue adaptado de de Kivrak *et. al.* [114]. Se disolvió 4-hidroxibenzaldehído (0,032 mmol) en DMF. Luego, se añadieron, a temperatura ambiente, 3-bromoprop-1-ino (0,042 mmol) y carbonato de potasio (0,042 mmol). La mezcla resultante se agitó constantemente a temperatura ambiente durante 4h. Una vez completada la reacción, la mezcla se enfrió a 0 °C, se filtró y se lavó con agua destilada.

4-(prop-2-in-1-iloxi)benzaldehído (p-HF): sólido blanco obtenido con un rendimiento del 88,0%. Punto de fusión 76-78°C. RMN-¹H, δ (DMSO-*d*₆, temperatura ambiente, ppm): 10,08 (s, 1H, CHO), 8,05-8,03 (d, CH aromático 2H), 7,45-7,28 (d, CH aromático 2H), 4,96 (s, 2H, CH₂), 2,76 (s, 1H, HC≡C). Q-TOF MS: calculado *m/z*: 161,05, encontrado: *m/z* 161,0568.

Síntesis de CR-4-ALQ, (10,0 mmol) de resorcinol y (10,0 mmol) del precursor 4-(prop-2-in-1-iloxi)benzaldehído se disolvieron en 25 mL de cloroformo, la mezcla de reacción fue llevada a baño frío. Una vez obtenida la mezcla, lentamente se añadió ácido trifluoroacético, TFA (5,0 mL). Esta mezcla se agitó a 60-65 °C durante 32 h. Transcurrido el tiempo se observó la formación de un precipitado blanco, se lavó con lavados sucesivos de éter dietílico y acetona, se secó con pistola de secado, de la solución de lavado se recristalizó el conformero *rccc* [22], [25].

CR-4-ALQ (rcftf): sólido blanco obtenido con un rendimiento del 58,9%. Punto de fusión > 250°C. RMN-¹H, δ (DMSO-*d*₆, temperatura ambiente, ppm): δ 3,50 (t, 4H, H¹), 4,62 (d, 8H, H²), 5,47 (s, 4H, H¹⁰), 5,51 (s, 2H, H³), 6,12 (s, 2H, H⁴), 6,27 (s, 2H, H⁵), 6,30 (s, 2H, H⁶), 6,50 (br. m, 16H, H⁷), 8,44 (s, 4H, OH⁸), 8,51 (s, 4H, OH⁹). RMN-¹³C (150,9 MHz, DMSO-*d*₆, 30 °C): δ 41,3 (s, C¹), 55,3 (s, C²), 77,8 (s, C³), 79,7 (s, C⁴), 101,7 (s, C⁵), 101,7 (s, C⁶), 113,2 (s, C⁷), 120,9 (s, C⁸), 121,2 (s, C⁹), 129,3 (s, C¹⁰), 129,7 (s, C¹¹), 131,8 (s, C¹²), 137,1 (s, C¹³), 152,4 (s, C¹⁴), 152,6 (s, C¹⁵), 154,5 (s, C¹⁶). Q-TOF MS: calculado *m/z*: 1009,31, encontrado: *m/z* 1009,2943.

CR-4-ALQ (rccc): sólido blanco-amarillo, rendimiento del 20,8%. MP Descomposición > 250°C. RMN-¹H, δ (DMSO-*d*₆, temperatura ambiente, ppm): δ 3,57 (t, 4H, H⁷), 4,73 (d, 8H, H⁶), 5,56 (s, 4H, H⁵), 5,52 (s, 4H, H⁴), 6,50 (s, 4H, H³), 6,63 (br. m, 16H, H²), 8,54 (s, 8H, OH). RMN-¹³C (150,9 MHz, DMSO-*d*₆, 30 °C): δ 40,6 (s, C¹²), 55,3 (s, C¹¹), 77,9 (s, C¹⁰), 79,7 (s, C⁹), 102,0 (s, C⁸), 113,5 (s, C⁷), 120,4 (s, C⁶), 120,6 (s, C⁶), 131,6 (s, C⁵), 138,7 (s, C³), 152,4 (s, C²), 154,6 (s, C¹). Q-TOF MS: calculado *m/z*: 1009,31, encontrado: *m/z* 1008,7142.

3.2.3 Síntesis de péptidos

Los péptidos (Tabla 7) se sintetizaron manualmente utilizando la metodología de síntesis de péptidos en sólida por la estrategia Fmoc/tBu (SPPS-Fmoc/tBu). Se utilizó la resina de Rink Amida (sustitución de 0,46 meq/g), como soporte sólido, y fue acondicionada con DMF por 12 h. i) La eliminación del grupo Fmoc se realizó por tratamiento con 4-metilpiperidina al 2,5% en DMF, 10 min a temperatura ambiente (TA) (×2), luego la resina fue lavada con DMF (×5), IPA (×3) y DCM (×5). Una fracción de la resina se secó y se realizó el test de Kaiser para comprobar la desprotección. ii) Para la reacción de preactivación del Fmoc-aminoácido (0,21 mmol), estese mezcló con DCC/6-CI-HOBt (0,20/0,21 mmol) en DMF por 15 min a TA. Luego la mezcla de reacción fue adicionada a la resina dejándose por 1 h con agitación constante. Entonces, la solución fue desechada y la resina lavada con DMF (×3; 1 min) y DCM (×3; 1 min), una fracción de la resina fue nuevamente secada y se le realizó la prueba de Kaiser. Si la prueba de Kaiser era positiva, se realizaba nuevamente el proceso hasta

que el test fuese negativo [115]. iii) La desprotección de las cadenas laterales y desanclaje del péptido de la resina se realizó tratando la resina-péptido seca con la solución de clivaje que contenía TFA/agua/TIS/EDT (93/2/2,5/2,5 % v/v/v/v), por 4 h con agitación constante a TA. Luego el péptido crudo fue precipitado por tratamiento con éter etílico frío, seguido se realizaron lavados ($\times 5$) con éter etílico frío y el sólido fue secado a TA.

Finalmente, los péptidos crudos fueron caracterizados por RP-HPLC, 10 μ L de una solución de péptido crudo (1 mg/mL) fue inyectada en una columna monolítica Chromolith® C18 (50 \times 4,6 mm), utilizando un cromatógrafo de líquidos Agilent 1200. La elución se realizó con un gradiente lineal de 5/5/50/100/100/5/5 % de solvente B en 0/1/9/9,1/11/11,1/14 min. Solvente B: TFA al 0,05% en ACN y Solvente A: TFA al 0,05% en agua. El flujo usado fue de 2,0 mL/min y longitud de onda de 210 nm. Los productos crudos fueron purificados empleando cartuchos de extracción en fase sólida (RP-SPE). En resumen, las columnas SPE de LC-18 de Supelclean fueron activadas y equilibradas, el péptido/dendrímico péptido-resorcinareno fue cargado y eluido usando un gradiente de disolvente B. Las fracciones recogidas fueron analizadas usando RP-HPLC y MS.

Tabla 7. Péptidos derivados de la LfcinB y BF utilizados en este proyecto. Todos los péptidos en el extremo C-terminal se obtuvieron con función amida.

Familia	Código	Secuencia	Uso
LfcinB (20-25)	P1	RRWQWR	Control lineal
	P2	((RRWQWR) ₂ K-Ahx-C) ₂	Control tetramero con core peptídico
	P3	K(N ₃)-RRWQWR	Azida-péptido
	P4	K(N ₃)-Ahx-RRWQWR	Azida-péptido con espaciador
BF (32-35)	P5	RLLR	Control lineal
	P6	((RLLR) ₂ K-Ahx-C) ₂	Control tetramero con core peptídico
	P7	K(N ₃)-RLLR	Azida-péptido
LfcinB (20-25)_{pal}	P8	RWQWRWQWR	Control lineal
	P9	K(N ₃)-RWQWRWQWR	Azida-péptido
Otros	P10	K(N ₃)-Ahx-RLLRLLR	Azida-péptido BF(32-35) _{pal}
	P11	K(N ₃)-AAAA	Azida-poli-Ala optimización click

3.2.4 Síntesis de dendrímeros péptido-resorcinareno (química click)

Para la optimización de la ruta sintética se adaptaron diferentes protocolos de literatura [88], [116]–[118], se incluyeron parámetros como, solvente, proporciones de precursores, proporciones de catalizador, temperatura y tiempo de reacción. Para ello se realizaron reacciones entre los azida-compuestos (Fmoc-Lys(N₃)-OH, K(N₃)-AAAA, K(N₃)-Ahx-RLLRLLR) y los alquino-compuestos (Fmoc-Pra-OH, CR-4-ALQ (*rcft*), *p*-HF). De manera general la reacción click se llevó mezclando el azida-compuesto con el alquino-compuesto disueltos en el solvente, seguido de una adición del catalizador sulfato de cobre pentahidratado (CuSO₄·5H₂O), y ascorbato de sodio, la mezcla se mantuvo con agitación constante a TA, el seguimiento de la reacción se realizó a través de RP-HPLC. Para la síntesis de los dendrímeros o conjugados péptido-resorcinareno (ver Tabla 8), el péptido crudo funcionalizado con azida (0,064 mmol) y el alquino-resorcinareno (0,016 mmol) fueron disueltos y mezclados en DMF/H₂O (2:1, v/v), luego se adicionó el catalizador sulfato de cobre pentahidratado (CuSO₄·5H₂O) (0,011 mmol) y ascorbato de sodio (0,024 mmol), la mezcla se mantuvo con agitación constante a TA durante 6 h.

Tabla 8. Dendrímeros derivados de la LfcinB y BF.

Dendrímero Código	Resorcinareno base	Secuencia Peptídica	Dendrímero
DP3		K(N ₃)-RRWQWR	CR-4-ALQ-(AAC-(K)-RRWQWR) ₄
DP7 (<i>rcft</i>)	CR-4-ALQ (<i>rcft</i>)	K(N ₃)-RLLR	CR-4-ALQ(<i>rcft</i>)-(AAC-(K)-RLLR) ₄
DP9		K(N ₃)-RWQWRWQWR	CR-4-ALQ-(AAC-(K)-RRWQWR) ₄
DP7 (<i>rccc</i>)	CR-4-ALQ (<i>rccc</i>)	K(N ₃)-RLLR	CR-4-ALQ(<i>rccc</i>)-(AAC-(K)-RLLR) ₄

El progreso de la reacción de formación del dendrímero se controló mediante RP-HPLC, se consideró finalizada la reacción cuando desapareció la especie correspondiente al derivado de resorcinareno. Finalmente, el dendrímero fue lavado con éter etílico (×3) para remover el exceso de solvente, seguido de lavados con agua destilada (×3) para retirar el exceso de catalizador y péptido. Si en el perfil cromatográfico se evidenciaba la presencia del péptido precursor o subproductos, el dendrímero era purificado usando columnas RP-SPE de LC-18 de Supelclean, estas fueron activadas y equilibradas, el producto de reacción fue

cargado y eluido usando un gradiente de disolvente B. Las fracciones recogidas fueron analizadas usando RP-HPLC y MS. El producto puro fue caracterizado por cromatografía líquida (RP-HPLC), los dendrímeros crudos y puros fueron caracterizados usando 10 μL de una solución de dendrímero (1 mg/mL) que fueron inyectados en una columna monolítica Chromolith® C18 (50 \times 4,6 mm), utilizando un cromatógrafo de líquidos Agilent 1200. La elución se realizó con un gradiente lineal de 5 a 100% de solvente B en 18 min. Solvente B: TFA al 0,05% en ACN y Solvente A: TFA al 0,05% en agua. Flujo de 2,0 mL/min y longitud de onda de 210 nm. El producto puro fue caracterizado mediante espectrometría de masas (MALDI-TOF) y/o espectrometría de masas de alta resolución (LC-HRMS).

3.2.5 Ensayos de actividad biológica

3.2.5.1 Determinación Concentración Mínima inhibitoria (CMI) y concentración Mínima Bactericida (CMB)

La Concentración Mínima Inhibitoria (CMI) de los dendrímeros y péptidos control, sobre las diferentes cepas bacterianas (Tabla 9) se determinó mediante un ensayo de microdilución en caldo. Específicamente, Se agregaron 90 μL de caldo Mueller Hinton y 90 μL de péptido (concentración inicial 444 $\mu\text{g/mL}$) en una placa de 96 pozos, y se realizaron diluciones seriadas para obtener concentraciones de 200, 100, 50, 25, 12,5 y 6,2 $\mu\text{g/mL}$. Se adicionaron 10 μL (5×10^5 UFC/mL) de inóculo a cada pocillo, el volumen final en cada pozo fue de 100 μL . Luego se incubaron durante 24 h a 37 °C; y se midió absorbancia a 620 nm usando el lector de ELISA.

Tabla 9. Generalidades de las cepas bacterianas

	Código	Morfología	Origen	Sensible/Resistente/Multiresistente	
<i>E. coli</i>	ATCC 25922	Bacilos	Hemocultivo	Sensible	-
	1004	Bacilos	Hemocultivo	Sensible	-
	129797	Bacilos	Hemocultivo	Resistente	AM, SAM, CEF
	301755	Bacilos	Hemocultivo	Multiresistente	AM, SAM, CPE, CAZ, CAX, CIP, GEN, NIT, NOR, STX
<i>S. aureus</i>	ATCC 25923	Cocos	Hemocultivo	Sensible	-
	109095	Cocos	Hemocultivo	Resistente	P
	117719	Cocos	Hemocultivo	Multiresistente	P, TET
	124653	Cocos	Hemocultivo	Multiresistente	P, ERY, TET

AM: Ampicilina, **SAM:** Ampicilina/sulbactam, **CPE:** Cefepima, **CAZ:** Ceftazidima, **CAX:** Ceftriaxona, **CIP:** Ciprofloxacino, **GEN:** Gentamicina, **NIT:** Nitrofurantoína, **NOR:** Norfloxacino, **STX:** Trimetoprima/sulfametoxazol. **P:** Penicilina, **TET:** Tetraciclina, **ERY:** Eritrosina

Para determinar la Concentración Mínima Bactericida (CMB), se tomó una alícuota de cada pozo y se sembraron sobre una placa de Agar Mueller Hinton. Después de 24 h de incubación a 37 °C, se determinó la CMB. Cada una de estas pruebas se realizó por duplicado (n=2) [6].

3.2.5.2 Curvas de letalidad-muerte

Las curvas de letalidad se realizaron según el protocolo reportado por Vargas *et. al.* [78], [119]. En una caja multipozos, se adicionarán 270 µL de solución de péptido, que fue preparado en Caldo Mueller Hinton (CMH), a diferentes concentraciones (0,5×CMI; CMI y 2×CMI). Posteriormente se agregaron 30 µL del inóculo (concentración final 5×10⁵ UFC/mL). Las muestras se incubaron durante 48 h y la lectura de la absorbancia se realizó cada hora en un equipo Bioscreen C (600 nm). Como control negativo fue utilizado CMH y como control de crecimiento cepa (inóculo) más CMH.

3.2.5.3 Ensayo de sinergia con antibióticos

El efecto sinérgico entre el dendrímero que presentó mayor actividad en *E. coli* ATCC 25922 y el antibiótico (ciprofloxacino) se realizó de acuerdo con el método de tablero de ajedrez [78]. Brevemente, 25 µL del dendrímero junto con 25 µL del antibiótico fueron mezclados, para tener concentraciones finales de: 0; 0,06;

0,12; 0,25; 0,50; 1 y 2 veces la CMI, junto con el inóculo (5×10^5 UFC/mL), luego fue incubado a 37 °C durante 24 h. Para determinar las nuevas CMI, derivadas de este ensayo se utilizó la ecuación 1.

$$\frac{(A)}{CMI_{(A)}} + \frac{(D)}{CMI_{(D)}} = FIC_{(A)} + FIC_{(D)} = \text{Índice FIC} \quad (1)$$

Donde, D corresponde a la CMI del dendrímero y A corresponde a la CMI del antibiótico, determinadas en la mezcla. $CMI_{(A)}$ y $CMI_{(D)}$ son los valores de CMI individuales. FIC es la Concentración Inhibitoria Fraccionada, la cual será interpretada según lo reportado por Saiman *et. al.* donde: índice FIC $\leq 0,5$: sinergia; entre 0,5 y 4: indiferencia; > 4 : antagonismo [120].

3.2.5.4 Determinación Concentración Mínima inhibitoria (CMI) y Concentración Mínima Fungicida (CMF)

Las pruebas de susceptibilidad antifúngica se realizaron utilizando el método de microdilución en caldo (MDC), siguiendo las pautas CLSI M27-A3 con ligeras modificaciones [121]. Brevemente, la suspensión de levadura (Tabla 10) se preparó en solución salina al 0,85% (SS) y se ajustó a $1-5 \times 10^6$ células/mL (0,5 estándar de McFarland). Luego se diluyó en medio líquido RPMI 1640 (Sigma-Aldrich, Saint Louis, MA, EE. UU.) (con MOPS, pH 7,2) y se ajustó a $0,5 \times 10^3-2,5 \times 10^3$ células/mL.

Tabla 10. Generalidades de las Cepas de *Candida spp.*

Cepa	Código	Sensible (S) Resistente (R)	Resistencia a:
<i>C. albicans</i>	SC5314	S	-
	256 HUSI-PUJ	R	FLC
<i>C. auris</i>	435 HUSI-PUJ	S	-
	537 HUSI-PUJ	R	FLC, AmB

FLC: fluconazol, **AmB:** Anfotericina B

Se añadieron 100 μ L de inóculo de levadura a una placa de 96 pocillos que contenía diluciones en serie del dendrímero. Las concentraciones finales utilizadas fueron 200, 100, 50, 25, 12,5 y 6,2 μ g/mL. El fármaco FLC se usó como control (0,125 a 128 μ g/mL). Se visualizaron las Concentraciones Mínimas Inhibitorias (CMI) y se usó densitometría (595 nm, lector de microplacas, iMarkTM, Bio-rad) para determinar la concentración más baja que causó una disminución significativa en comparación con el control de crecimiento no tratado. después

de 48 h de incubación. El criterio de valoración de la CMI se definió como la concentración más baja capaz de inhibir el 80,0% del crecimiento celular en comparación con su respectivo control positivo. Se realizaron tres ensayos independientes (n=3). Para verificar que la molécula analizada podía matar las células de levadura, las placas también se analizaron para determinar la concentración fungicida mínima (CMF). Brevemente, se transfirieron alícuotas de cada pocillo de los ensayos de susceptibilidad a placas que contenían Sabouraud Dextrose Agar (SDA), que luego se incubaron.

3.2.5.5 Actividad Hemolítica

Se centrifugaron 5,0 mL de sangre periférica heparinizada a 1000 rpm durante 7 min. La fracción de eritrocitos se suspendió en 10 mL de solución salina (SS) y se lavó dos veces por centrifugación a 1000 rpm durante 7 min. Los eritrocitos (2% de hematocrito) se incubaron con el dendrímero péptido-resorcinareno (entre 6,2 y 200 µg/mL), durante 2 h a 37 °C. SS se utilizó como control negativo, mientras que el agua destilada se utilizó como control positivo. Las mezclas se centrifugaron, se recogieron los sobrenadantes y se determinó su densitometría mediante absorbancia a una longitud de onda de 540 nm [122], [123]

3.2.5.6 Actividad citotóxica

La actividad citotóxica de los dendrímeros, péptido-resorcinareno, sobre fibroblastos y líneas MCF-7 y HeLa se determinó mediante ensayo de MTT. Brevemente, las células se sembraron con medio completo en placas de 96 pocillos a razón de 10.000 células y 100 µL por pocillo y se permitió que se adhirieran a las placas durante 24 horas. Posteriormente, se eliminó el medio completo y se agregó medio incompleto para sincronizar durante otras 24 h. Las células se incubaron a 37 °C durante 2, 24 o 48 h con 100 µL del dendrímero a las concentraciones a evaluar, 200, 100, 50, 25, 12,5, 6,25 y 3,1 µg/mL. A continuación, se retiró la molécula de la caja y se añadieron 100 µL de medio incompleto con bromuro de 3-4,5-dimetiltiazol-2-il-2,5-difeniltetrazol (MTT) al 10% y se incubó durante 4 h. El medio se reemplazó con 100 µL de isopropanol (IPA), y luego de 30 min de incubación a 37 °C, se midió la absorbancia a 575 nm. Se usó medio de cultivo incompleto con 10% de MTT como control negativo, y células sin tratamiento con MTT se usaron como control positivo [124].

4. Resultados y discusión

4.1 Síntesis de precursores

Los dendrímeros son moléculas que aún se encuentran en fase exploratoria y se han visualizado como candidatos promisorios en el tratamiento de infecciones causadas por bacterias y hongos farmacorresistentes, estas macromoléculas han demostrado amplia actividad antibacteriana y antifúngica, además han presentado potencial como herramientas de diagnóstico, agentes terapéuticos, reconocimiento molecular, vehículos de transporte de genes y fármacos [125]. Los resorcinarenos, han adquirido gran interés debido a que estas moléculas pueden ser modificadas con diversidad de grupos funcionales, y algunos estudios con derivados de resorcinarenos han mostrado actividad antimicrobiana contra bacterias Gram positivas y Gram negativas, así como contra hongos y parásitos, y han sido poco tóxicos contra células humanas [126]. Para esta investigación se planteó la obtención de dendrímeros peptídicos construidos sobre un núcleo no proteico, se seleccionaron los resorcinarenos como núcleo y las secuencias correspondieron a los motivos mínimos de actividad de péptidos antimicrobianos (PAMs), específicamente de la LfcinB (RRWQWR) y la BF (RLLR).

En primera instancia se realizó la síntesis de los precursores: (i) resorcinarenos funcionalizados con el grupo alquino, para lo que se emplearon dos aproximaciones, generar la funcionalización sobre los grupos hidroxilo fenólicos o sobre el puente de metileno (ver Figura 8). (ii) Péptidos modificados con el aminoácido lisina azida (K(N₃)) que fueron obtenidos mediante SPPS. Una vez obtenidos y caracterizados los precursores, se procedió a la optimización de las condiciones de la reacción de química click, cicloadición azida-alquino CuAAC, para la generación de los dendrímeros péptido-resorcinareno, esta optimización incluyó parámetros como, solvente, proporciones, temperatura, entre otros. A continuación, se discuten los resultados obtenidos en las diferentes etapas de síntesis de las moléculas propuestas.

4.1.1 Síntesis de derivados de Calix[4]resorcinareno

Los calix[4]resorcinareno son macromoléculas que presentan una alta versatilidad a nivel sintético ya que se pueden realizar modificaciones o funcionalizaciones en tres partes de la estructura, a nivel del puente de metileno. En la posición orto a los grupos hidroxilo del anillo aromático de estos macrociclos, o en los grupos hidroxilo fenólicos. Sin embargo, se sabe que las conformaciones de resorcinareno (sin sustituir) se modulan con bastante facilidad por las condiciones de reacción cuando se sintetiza el huésped. Se han reportado cinco posibles conformaciones: i) *corona*, ii) *bote*, iii) *silla de montar*, iv) *silla* y v) *diamante* [19].

Para esta investigación, Se propusieron dos núcleos derivados de calix[4]resorcinareno (CR) los cuales fueron funcionalizados con el grupo propargilo: i) en los grupos hidroxilo del resorcinol, introduciendo ocho grupos alquino en la estructura; este derivado, por facilidad se nombrará como CR-8-ALQ; y ii) en el puente de metileno, usando para la reacción de formación del resorcinareno el 4-(prop-2-in-1-iloxi)benzaldehído; mediante esta estrategia se introducen cuatro grupos alquino al macrociclo, CR-4-ALQ, ver Figura 23.

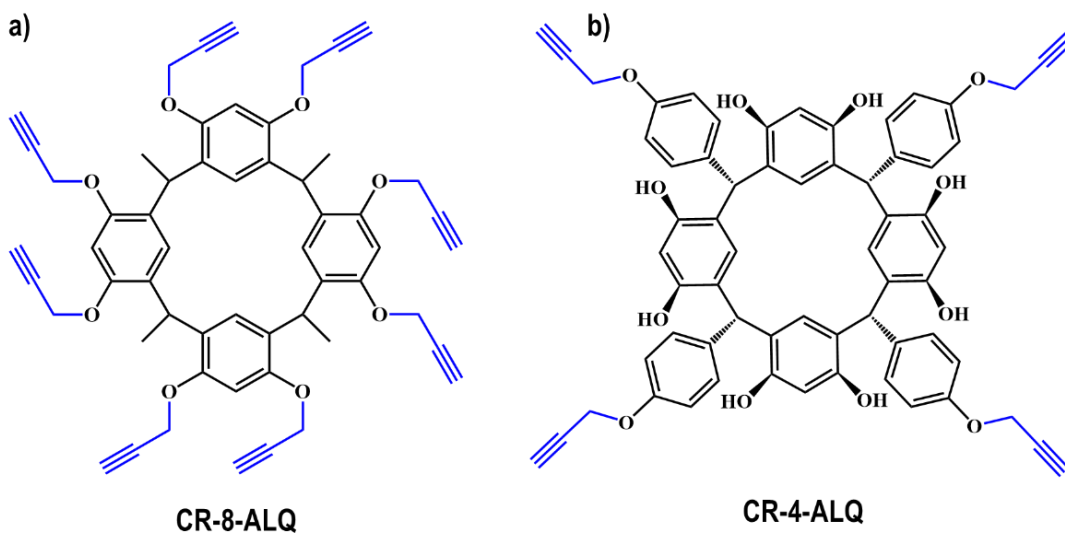


Figura 23. Derivados del calix[4]resorcinareno sintetizados en este estudio a) CR-8-ALQ modificado en su borde superior y b) CR-4-ALQ modificado en su borde inferior.

a) CR-8-ALQ (*rccc*)

Para la síntesis del precursor C-tetrametilcalix[4]resorcinareno, CR-8-ALQ, la conformación más estable reportada es la de tipo *rccc-corona*, esto se establece a partir de las cavidades profundas formadas y una estabilización de las mismas mediante puentes de hidrógeno mediados por los grupos hidroxilo presentes [20], [22], [23], [127]. Se han reportado otras conformaciones como *rcct-diamante*, que rara vez se observa [128], y *rccc-bote* para C-tetrametil-2-nitrocalix[4]resorcinareno [129].

Para la síntesis del derivado CR-8-ALQ, ver Figura 24.a, previamente se sintetizó el precursor C-tetrametilcalix[4]resorcinareno (compuesto 1). Para la obtención de esta molécula se proponen en la literatura [113], [130], [131], varios procedimientos de síntesis, que se pueden realizar entre el resorcinol y el acetaldehído. para este trabajo se propuso llevar a cabo la reacción entre acetaldehído y resorcinol utilizando el procedimiento descrito por A.G. Sverker, *et. al.* [113]. Como se muestra en la sección experimental, la síntesis de resorcinareno hizo mediante la ciclocondensación, catalizada por ácido, empleando reflujo durante 1 h. El producto sólido formado se filtró, lavó y secó de acuerdo con el proceso de purificación convencional. El análisis por cromatografía en capa delgada (CCD) preliminar mostró la formación de dos productos; sin embargo, el análisis de RMN-¹H mostró varias señales de resonancia para los protones aromáticos para la mezcla de confómeros a 6,08 a 6,79 ppm, los fragmentos de puentes de metileno a 4.37 y 4,45 ppm y grupos hidroxilo ($\delta = 8,41$ a 8,65 ppm). La complejidad de las señales observadas en el espectro RMN-¹H contrastaba con los resultados obtenidos previamente [113], [131], en los cuales se publicó que las reacciones de ciclocondensación permiten la formación de dos confómeros (*silla* y *corona*). Nuestros resultados evidenciaron la formación de un tercer producto como lo demuestra el número de señales en la región alifática, que puede considerarse como un tercer confómero. Para la ciclocondensación entre acetaldehído y resorcinol no se encontró en la literatura reportes sobre la caracterización de tres productos de reacción. Para establecer si la mezcla de reacción correspondía a tres isómeros estructurales (confómeros) o quizás uno de los productos correspondía a un intermedio tipo trioxano, se propuso purificar los productos de la reacción y analizarlos para así establecer cuál de los dos tipos de productos podría formarse. Por lo tanto, se analizó la mezcla de reacción mediante RP-HPLC con detector UV/vis (210 nm), y se ensayaron dos columnas C18, una empacada y una

monolítica. El método de separación optimizado (usando la columna monolítica) mostró un perfil cromatográfico con la presencia de tres picos a tiempos de retención bien diferenciados, t_R 6,7, 8,7 y 9,9 min (Figura 24.b).

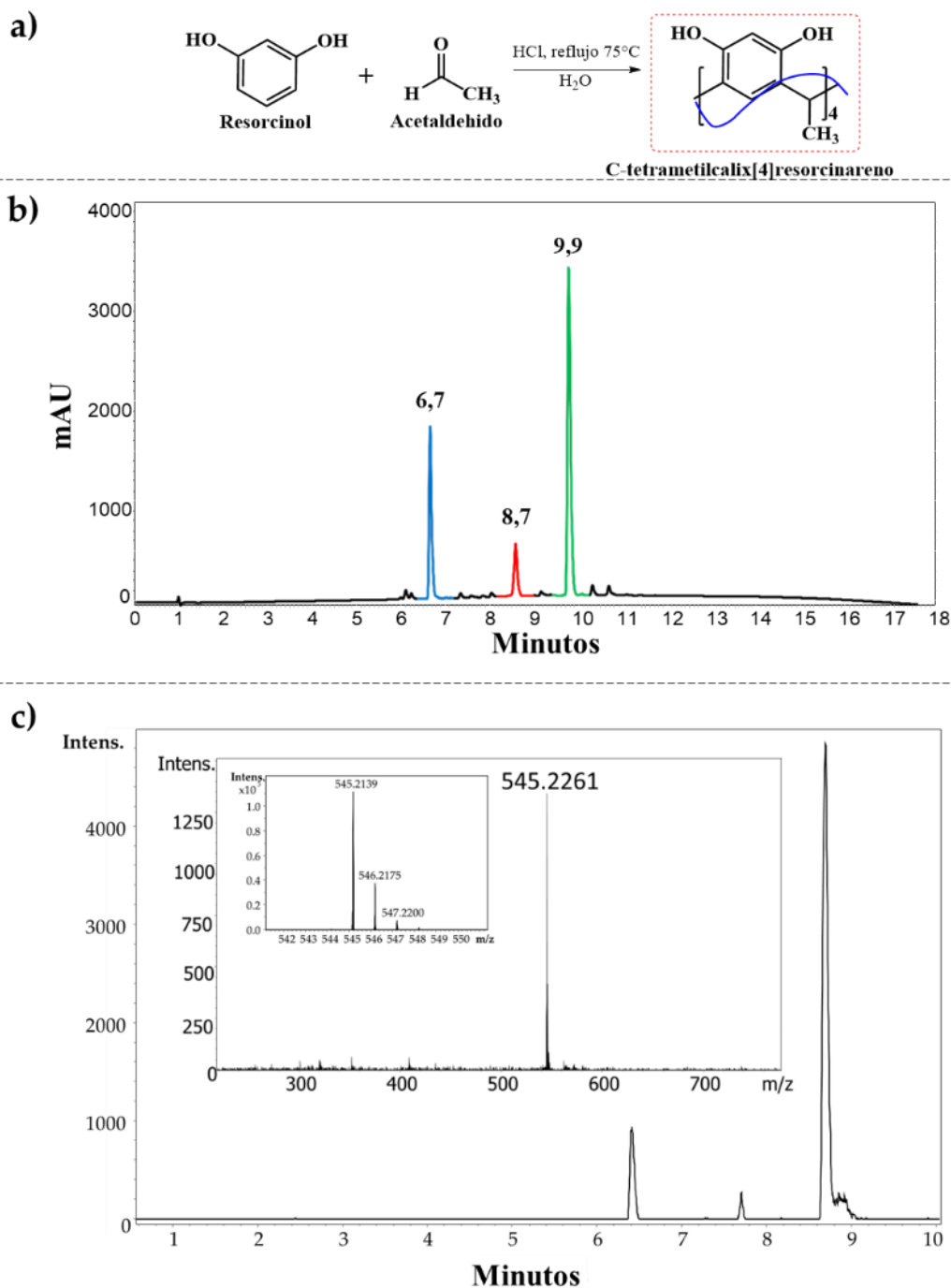


Figura 24. a) Reacción de cicloadición entre resorcinol y acetaldehído. Análisis de la mezcla de reacción por b) RP-HPLC/UV-Vis, análisis registrado a 210 nm y c) UHPLC-MS (ESI), TIC se presenta el espectro de masas del pico a los 8,7 min.

Luego, el método de análisis se transfirió a una columna de UHPLC, y la mezcla de reacción se analizó por LC-MS (ESI), en modo de iones positivos. El perfil cromatográfico también mostró tres picos principales, y todos ellos exhibieron un espectro de masas con una señal en m/z 545,21 correspondiente a la especie $[M+H]^+$ (Figura 24.c). De acuerdo con la información obtenida del análisis LC-MS, se confirmó la formación de tres productos. Y además, se pudo deducir que los tres productos son isómeros.

Una vez establecido que el producto sólido obtenido corresponde a una mezcla de tres isómeros (compuestos 1a, 1b y 1c), se decidió separarlos mediante la técnica RP-SPE descrita previamente [132], [133]. A partir del perfil de RP-HPLC se calculó el porcentaje de disolvente B (TFA 0,05% en acetonitrilo) en el que eluyó cada confórmero (%Be). Es importante aclarar que este cálculo toma en cuenta que: i) el gradiente utilizado varió de 5% a 100% de solvente B en solvente A (TFA 0,05% en agua), ii) el tiempo de gradiente fue de 17 minutos, iii) el tiempo de retardo para el programa de HPLC fue de 1,0 min, iv) el tiempo de residencia (dwell time) del equipo de HPLC fue de 0,9 min y (v) el tiempo muerto de la columna fue de 0,82 min. Específicamente, la especie con tiempo de retención de 6,7 minutos eluyó al 26,7%B, para las especies en 8,7 y 9,9 el %Be fue 37,8% y 44,6% , respectivamente. Esta información nos permitió diseñar un programa de elución en gradiente para separar los productos obtenidos mediante la técnica RP-SPE, se sembró la mezcla de confórmeros en el cartucho y la elución se realizó con soluciones (10 mL/fracción) en las que se fue aumentando el porcentaje de disolvente B en el eluyente. Las fracciones recolectadas se analizaron en línea, usando un equipo UV-VIS que tienen una celda de flujo, y luego también se analizaron por RP-HPLC para determinar la pureza cromatográfica. El compuesto correspondiente al pico con $t_R = 6,7$ min (Figura 25.b) eluyó en las fracciones que tenían un rango de disolvente B de 19–26% B, el segundo compuesto ($t_R = 8,7$ min, Figura 25.b) eluyó en un rango de 33–35% B, y finalmente la especie mayoritaria ($t_R = 9,9$ min) eluyó en un rango de 37–42% B . Las fracciones que contenían cada confórmero puro se mezclaron y luego se liofilizaron. Los productos purificados se cuantificaron y las conformaciones de los derivados del macrociclo se establecieron mediante espectroscopía de RMN- 1H en DMSO- d_6 a temperatura ambiente (Figura 25Figura 25.a).

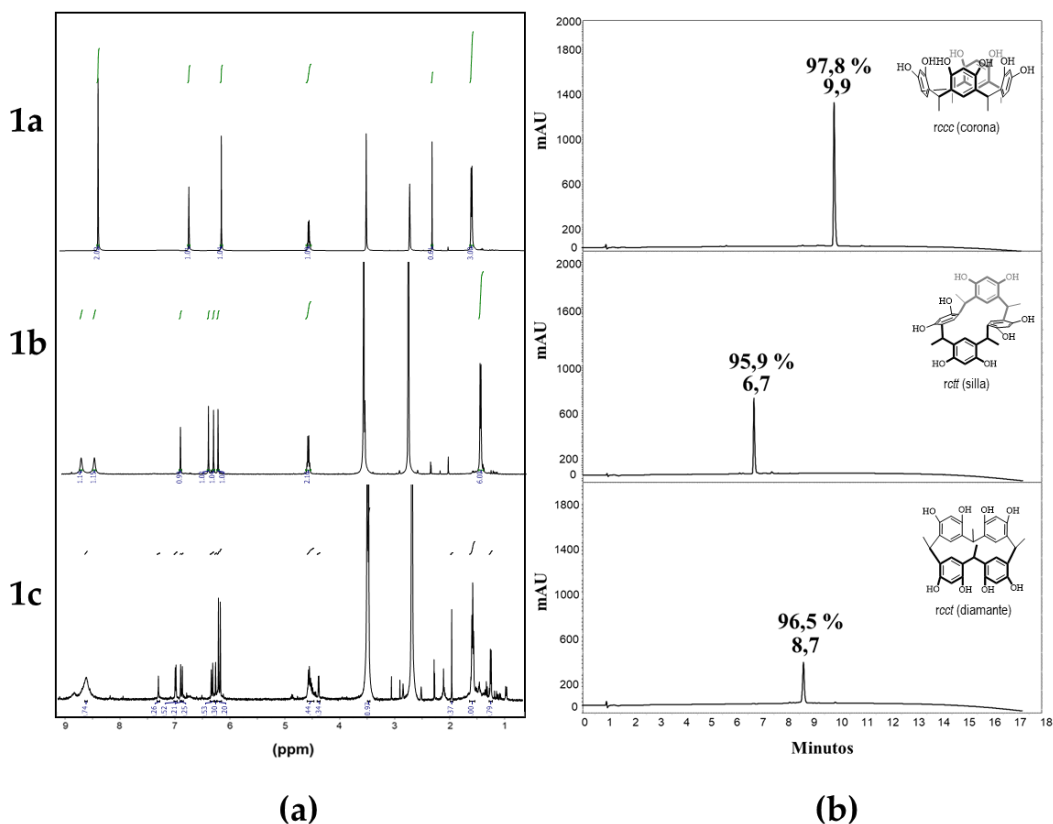


Figura 25. a) Espectros de RMN-¹H y b) Perfil cromatográfico de 1a, 1b y 1c.

El espectro de RMN-¹H del producto mayoritario (compuesto 1a, $t_R = 9,9$ min) presenta una señal a 8,53 ppm asignada a grupos hidroxilo unidos a residuos de resorcinol en el sistema macrocíclico. En la región aromática se aprecian dos señales en los residuos de resorcinol, una correspondiente a los protones en posición orto respecto al grupo hidroxilo a 6,15 ppm y la otra señal correspondiente a los protones en posición meta respecto al grupo hidroxilo. grupos a 6,77 ppm. En la región alifática, el compuesto presentó la señal característica de un puente metino a 4,45 ppm y la señal a 1,39 ppm correspondiente al grupo metilo. Todas las señales fueron consistentes con la estructura del conformero corona-*rccc*, producto esperado (Figura 25.a), que tiene menos señales en el espectro [131].

Por otro lado, el espectro de RMN-¹H del producto 1b (Figura 25.a) ($t_R = 6,7$ min) mostró dos señales, a 8,41 y 8,65 ppm, correspondientes a dos clases de grupos hidroxilo unidos a residuos de resorcinol en el sistema macrocíclico. En la región aromática se aprecian cuatro señales en los residuos de resorcinol, dos

correspondientes a los protones en posición orto respecto al grupo hidroxilo a 6,08 y 6,17 ppm, y las otras dos correspondientes a los protones en posición meta respecto a los grupos hidroxilo a 6,26 y 6,79 ppm. En la región alifática se observaron dos señales, a 4,37 y 1,15 ppm, correspondientes a los grupos metino y metilo, respectivamente. Por lo tanto, estos patrones son consistentes con la estructura del conformero silla esperado [131].

El producto 1c (Figura 25.a) ($t_R = 8,7$ min), mostró una fuerte tendencia a la descomposición; por tal motivo, su caracterización se realizó solo en solución. Como se muestra en la Figura 25.a, la ausencia total de simetría en el conformero 1c se refleja en los espectros de RMN- ^1H , por lo que el número de señales del producto contrasta con el número de señales de los conformeros corona y silla. El espectro de RMN- ^1H de 1c mostró las señales características de un sustituyente metilo a 1,35 y 1,40 ppm y en el rango de 4,38 a 4,46 ppm para el puente metino. Los protones aromáticos a 6,12, 6,16, 6,21 y 6,29 ppm se asignaron a los protones en la posición orto de los grupos hidroxilo del residuo de resorcinol. Además, en la región aromática, se observaron señales para protones meta del resto resorcinareno a 6,86, 6,90, 6,98 y 7,29 ppm. La señal de los grupos hidroxilo se observó en el rango de 8,50 a 8,90 ppm. Finalmente, la integración de las señales es consistente con un macrociclo tetamérico. La multiplicidad de señales para cada tipo de protón en el espectro de 1c sugiere diferentes ambientes químicos para cada uno de los anillos fenólicos, por lo que el patrón espectral es característico de la conformación de diamante.

El conformero más estable y con mayor rendimiento, *ccc-corona*, se seleccionó para ser funcionalizado en los grupos hidroxilos aromáticos para la generación del derivado CR-8-ALQ. Esta funcionalización se da bajo la reacción de sustitución nucleofílica, Figura 26.

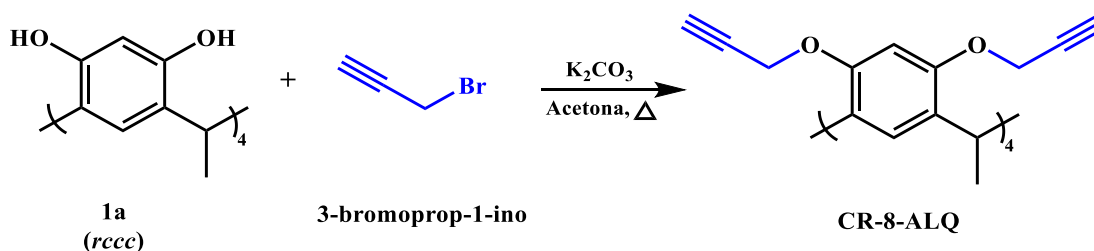


Figura 26. Esquema de reacción para la formación del macrociclo CR-8-ALQ.

El seguimiento de la reacción se llevó mediante RP-HPLC donde los precursores bromuro de propargilo ($t_R=3,9$ min) y el C-tetrametilcalix[4]resorcinareno (1a) ($t_R=9,3$ min) a 24 h de reacción disminuyeron su área relativa y se generó una nueva especie con t_R de 15,1 min, ver Figura 27. A pesar de los intentos por enriquecer la especie mayoritaria ($t_R=15,1$ min) esta se logró obtener solo con una pureza cromatográfica del 67,0%, este producto fue caracterizado mediante espectrometría de masas UHPLC-MS.

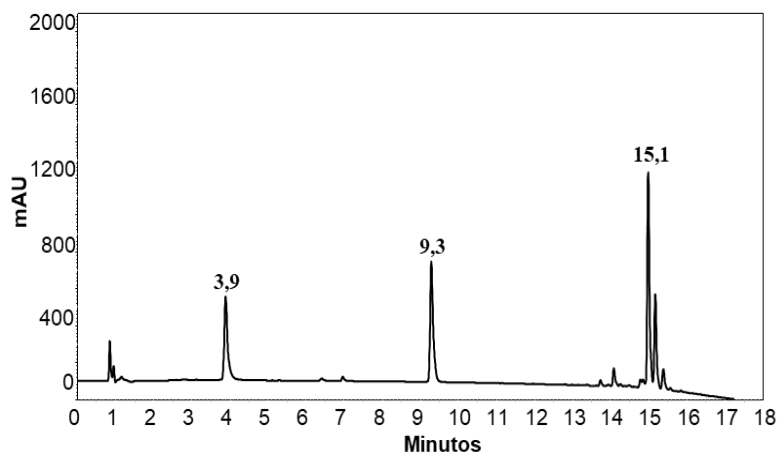


Figura 27. Seguimiento de la reacción de formación del macrociclo CR-8-ALQ ($t=24$ h). Bromuro de propargilo ($t_R=3,9$ min), C-tetrametilcalix[4]resorcinareno (1a) ($t_R=9,3$ min)

El análisis por masas registrado en el modo de iones positivos exhibió un espectro de masas con una señal en m/z 849,3285 correspondiente a las especies $[M+H]^+$ y cuya relación m/z teórica esperada para el producto CR-8-ALQ era de 849,33 u.m.a. Esto corrobora que se logró funcionalizar todos los grupos -OH fenólicos del resorcinareno, ver Figura 28.

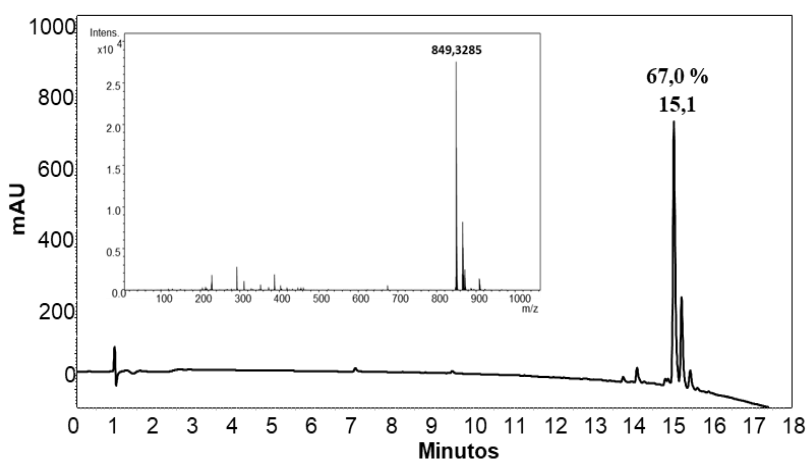
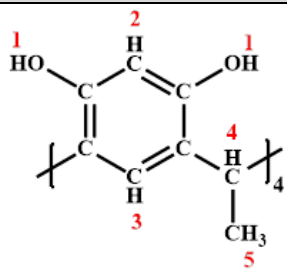
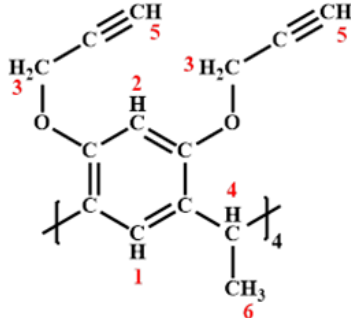


Figura 28. Perfil cromatográfico y espectro de masas ESI-Q/TOF del producto octa-funcionalizado puro confórmero rccc (CR-8-ALQ).

Para comprobar si la conformación *rccc-corona* del precursor C-tetrametilcalix[4]resorcinareno, se mantuvo luego de la funcionalización, el producto obtenido fue analizado mediante RMN-¹H, en la región aromática se aprecian una señal a 6,72 ppm correspondiente a los protones en posición orto o meta respecto al grupo hidroxilo, sin embargo, una de las señales faltantes fue solapada con el solvente usado (CDCl₃). En la región alifática se observaron dos señales, a 2,49 y 1,45 ppm, correspondientes a los grupos metilo y metino, respectivamente. Por lo tanto, estos patrones son consistentes con la estructura del conformero *rccc-corona* esperado, las señales obtenidas para RMN-¹H se resumen en la Tabla 11, (los espectros de RMN-¹H y RMN-¹³C se pueden observar en el Anexo A.1).

Tabla 11. Desplazamientos químicos RMN-¹H para el precursor 1a (*rccc*) y CR-8-ALQ (*rccc*).

	Estructura	Protón	Señales (ppm)
1 ^a		1	8,53
		2	6,77
		3	6,14
		4	4,45
		5	1,39
CR-8-ALQ		1	7,26
		2	6,72
		3	4,61
		4	4,42
		5	2,49
		6	1,45

b) CR-4-ALQ (*rccc* y *rctt*)

El derivado CR-4-ALQ, ver Figura 23, se sintetizó mediante ciclocondensación catalizada por ácido, utilizando resorcinol y un aldehído previamente funcionalizado con el grupo propargilo. El aldehído 4-(prop-2-in-1-iloxi)benzaldehído, fue sintetizado a partir de la reacción de sustitución nucleofílica entre el bromuro de propargilo y el hidroxilo aromático del *p*-hidroxibenzaldehído. En la Figura 29, se puede observar el perfil

cromatográfico de los precursores *p*-hidroxibenzaldehído y bromuro de propargilo (Figura 29.a y Figura 29.b, respectivamente), el seguimiento de la reacción se llevó a cabo mediante RP-HPLC a tiempo 0 h (Figura 29.c) y 4 h (Figura 29.d). Como se puede observar a un tiempo de reacción de 4 h, el precursor *p*-hidroxibenzaldehído con $t_R = 3,9$ min se consumió por completo y apareció una nueva especie en $t_R = 7,2$ min, este producto fue precipitado en frío y lavado con agua. El producto de reacción fue obtenido con una pureza cromatográfica de 99,7%, su caracterización por LC-MS mostró una señal en m/z de 161,0568, m/z teórica es de 161,06, Figura 30. El análisis por RMN- ^1H mostró una señal a 10,08 ppm característico del aldehído, las señales para los protones aromáticos a 8,05 y 7,28 ppm, para el protón de $-\text{CH}_2-$ se presenta una señal a 4,96 ppm y finalmente una señal a 2,76 ppm que integra para un protón característico para $-\text{C}\equiv\text{CH}$, esta última señal corrobora la funcionalización del $-\text{OH}$ del grupo hidroxilo del precursor *p*-hidroxibenzaldehído, el espectro RMN- ^1H y RMN- ^{13}C se pueden encontrar en el Anexo A.2.

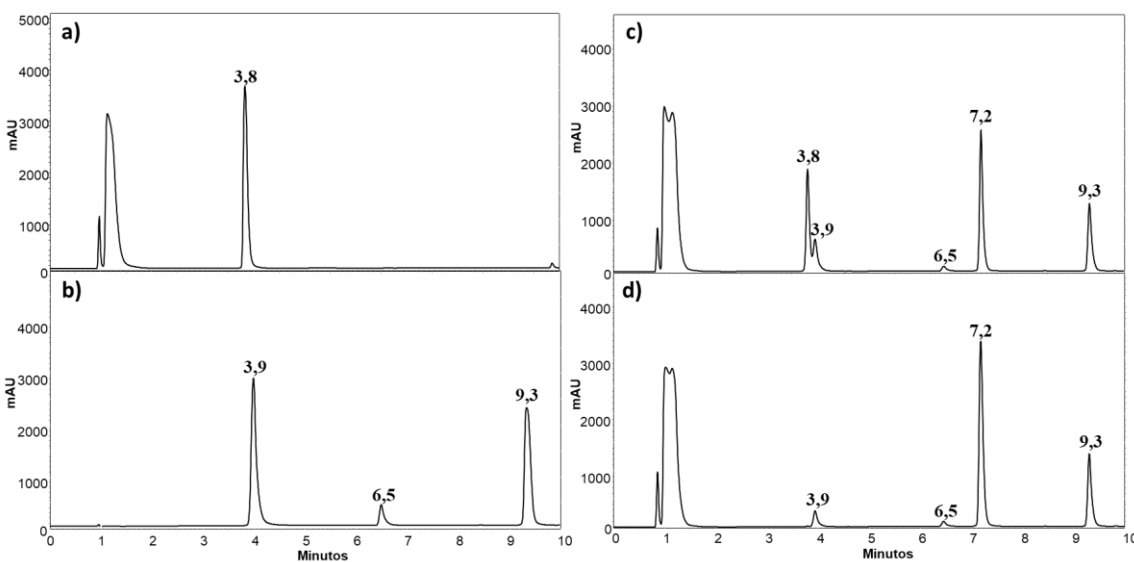


Figura 29. Seguimiento de la reacción para la síntesis del precursor 4-(prop-2-in-1-iloxi)benzaldehído (*p*-HF). Perfil cromatográfico de a) *p*-hidroxibenzaldehído, b) bromuro de propargilo a c) $t = 0$ h y d) $t = 4$ h.

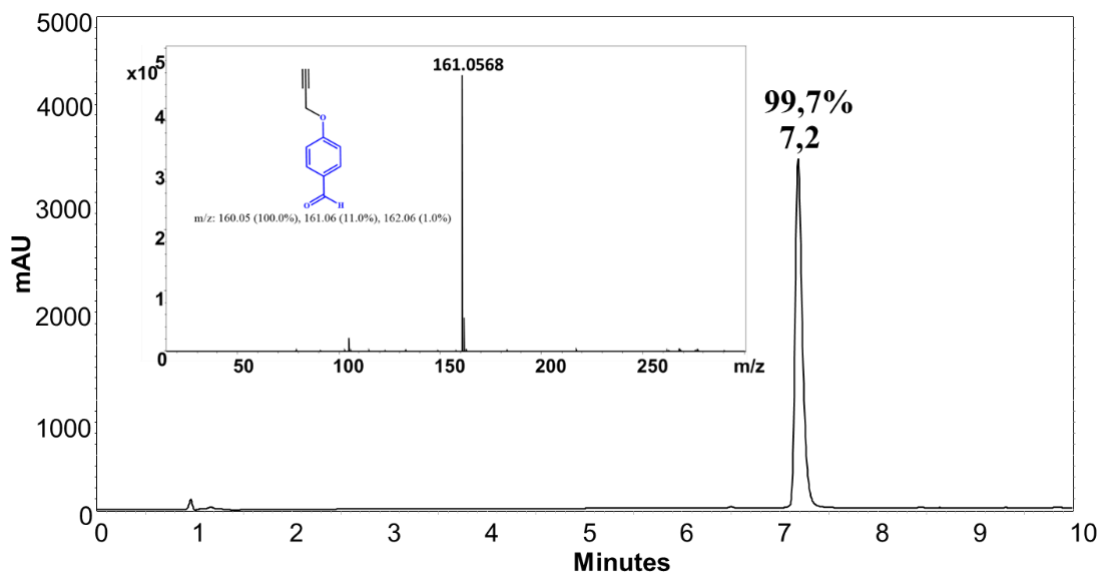


Figura 30. Caracterización mediante RP-HPLC y LC-MS de 4-(prop-2-in-1-iloxi)benzaldehído.

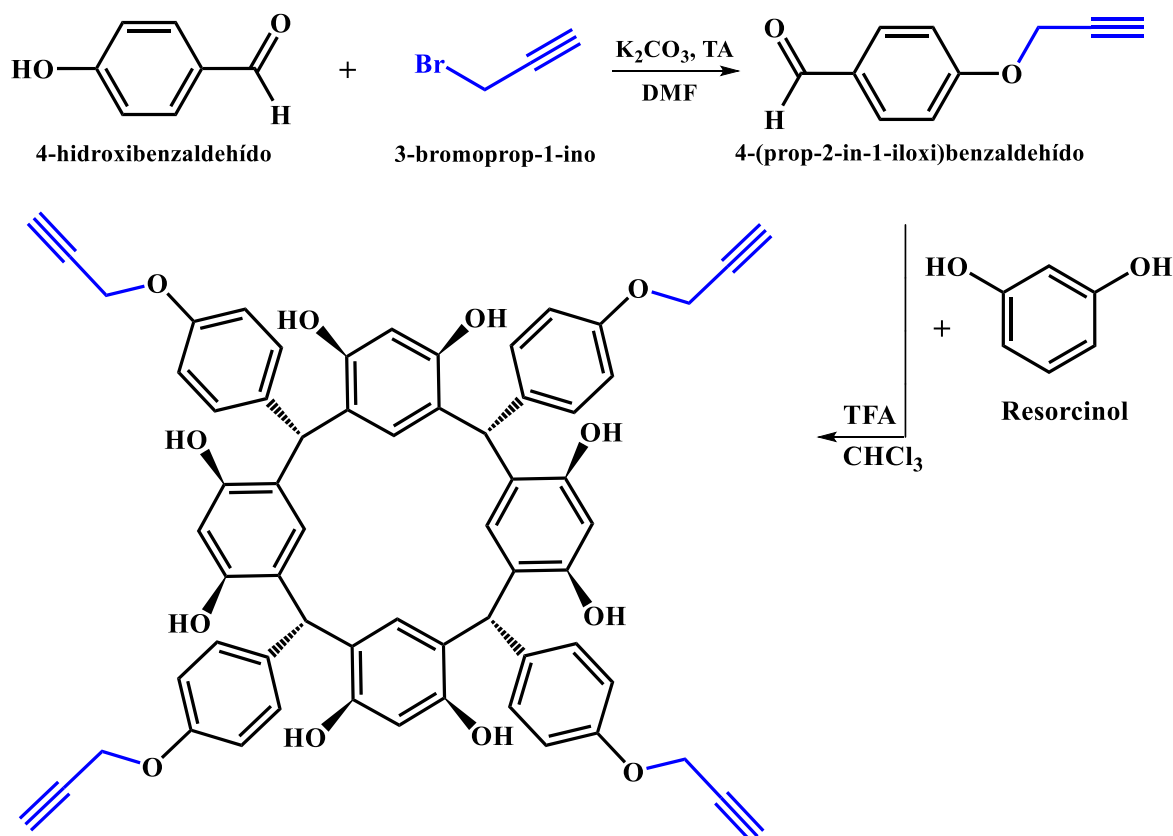


Figura 31. Esquema de la síntesis del macrocíclo CR-4-ALQ.

El C-Tetra(4-(prop-2-yn-1-iloxi)fenil)calix[4]resorcinareno (CR-4-ALQ) fue sintetizado como se describe detalladamente en la sección de metodologías, ver Figura 31. En la Figura 32 se presenta el perfil cromatográfico del producto de reacción entre el 4-(prop-2-in-1-iloxi)benzaldehído y el resorcinol; donde se observan dos señales principales a t_R de 9,6 min y 9,8 min. Se ha reportado que se puede obtener un solo conformero o una mezcla conformacional como producto de reacción en la síntesis de este tipo de derivados, de manera general hay una gran tendencia a formar mezclas si el aldehído usado es aromático [134], [135]. Para caracterizar los dos productos principales, se llevó a cabo un proceso de purificación/separación y recristalización [134], luego cada producto purificado se caracterizó por RP-HPLC, RMN- 1H y RMN- ^{13}C . El primer producto ($t_R=9,6$ min) se obtuvo como un sólido blanco, su perfil cromatográfico muestra una sola especie con una pureza de 96,4% (Figura 33.a), para este producto las asignaciones de las señales de RMN- 1H a campo bajo (8,51-8,46 ppm) sugieren la presencia de protones de los diferentes grupos -OH con una integración para cuatro protones, así como los protones que componen el anillo aromático del resorcinol con señales entre 6,50-6,12 ppm, la información fue confirmada por RMN- ^{13}C con señales a 101,7 y 101,6 ppm. La caracterización de este producto sugiere que corresponde al conformero *rctt-silla*, ver Anexo A.3. Por otro lado, el segundo producto se obtuvo como un sólido amarillo, que presentó una pureza cromatográfica de 77,9%, (Figura 33.b), y su espectro de RMN- 1H muestra una única señal singlete a campo bajo 8,54 ppm que integra para 8 protones, esto sugiere que todos los protones de los grupos -OH del resorcinol son equivalentes, y por tanto este producto debería corresponder al conformero *rccc-corona*, Tabla 12, (el espectro RMN- 1H y RMN- ^{13}C se pueden encontrar en el Anexo A.4). Los dos derivados de resorcinareno se caracterizaron por espectrometría de masas MALDI-TOF, la relación m/z teórica calculada para CR-4-ALQ fue de 1009,08 y las relaciones m/z obtenidas experimentalmente para el conformero *rctt* fue de 1009,03 y para el conformero *rccc* 1008,70, ver Figura 33.

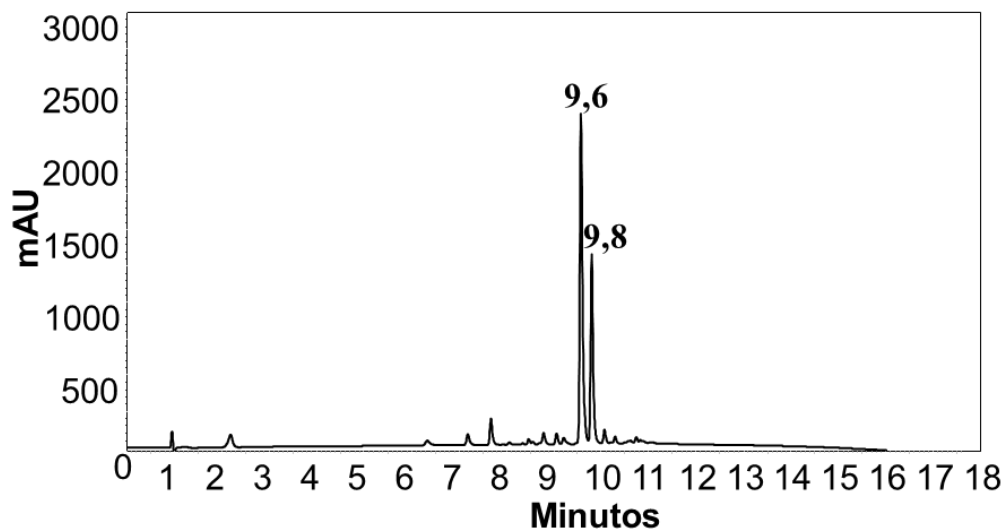


Figura 32. Confórmers obtenidos en la síntesis del CR-4-ALQ funcionalizado con el grupo alquino.

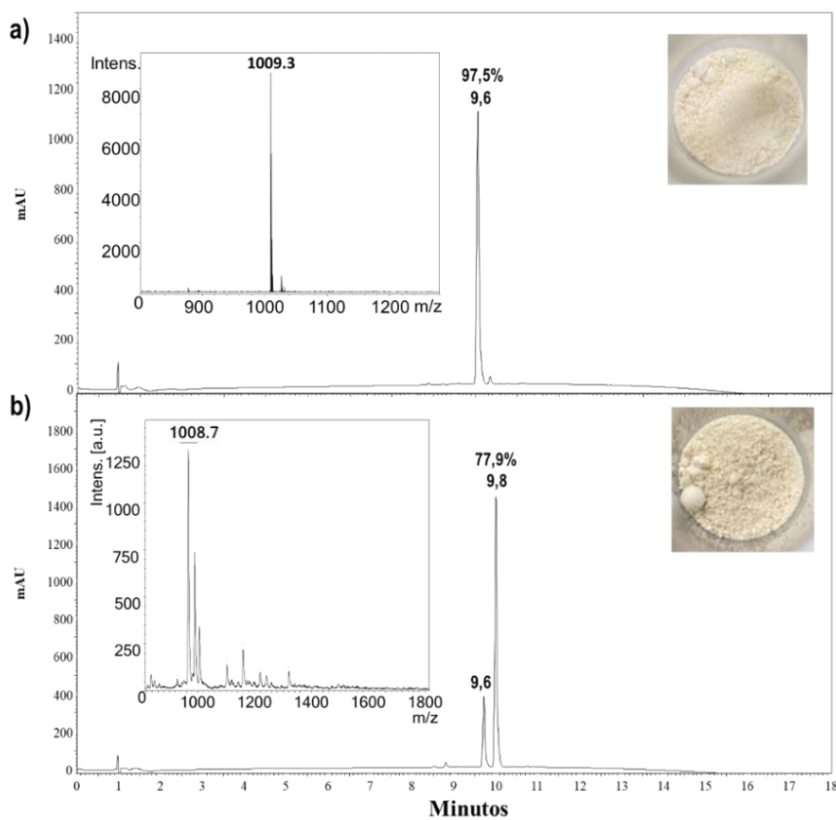
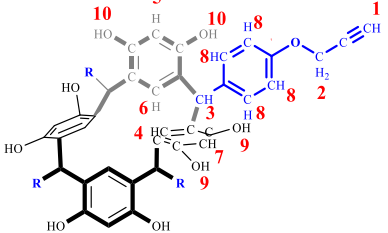
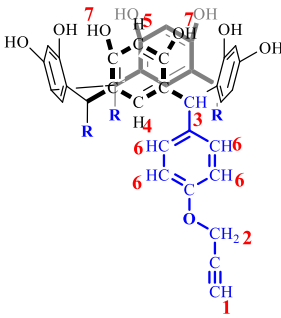


Figura 33. Perfil cromatográfico y espectro de masas (MALDI-TOF) del CR-4-ALQ: a) confómero *rctt-silla* y b) confómero *rccc-corona* purificados.

Tabla 12. Desplazamientos químicos RMN-¹H para los derivados CR-4-ALQ (*rctt*) y CR-4-ALQ (*rccc*).

CR-4-ALQ (<i>rctt</i>), silla			CR-4-ALQ (<i>rccc</i>) corona		
Estructura	Protón	Señales (ppm)	Estructura	Protón	Señales (ppm)
	1	3,55-3,57		1	3,55-3,57
	2	4,62		2	4,62
	3	5,47		3	5,56
	4	5,51		4	6,12
	5	6,12		5	6,50
	6	6,27		6	6,63
	7	6,30		7	8,54
	8	6,50			
	9	8,44			
	10	8,51			

A continuación, se resume la caracterización de cada uno de los precursores y derivados de resorcinareno sintetizados y descritos previamente, Tabla 13.

Tabla 13. Resumen de la caracterización de los precursores y derivados de calix[4]resorcinareno.

Familia	Código	Compuesto	RP-HPLC t_r (min)	Pureza (%)	MASA	
					Teórica [M]	m/z [M+H] ⁺
Precursores	1a	C-tetrametilcalix[4]resorcinareno	9,9	97,8	544,6	545,2
	<i>p</i> -HF	4-(prop-2-in-1-iloxi)benzaldehído)	7,2	99,7	160,1	161,1
Derivados	CR-8-ALQ (<i>rccc</i>)	Octa-2-(prop-2-in-1-iloxi)-C-tetrametilcalix[4]resorcinareno (<i>rccc</i>)	15,0	67,0	848,3	849,3
	CR-4-ALQ (<i>rctt</i>)	C-Tetra(4-(prop-2-in-1-iloxi)fenil)calix[4]resorcinareno (<i>rctt</i>)	9,6	87,2	1008,3	1009,3
	CR-4-ALQ (<i>rccc</i>)	C-Tetra(4-(prop-2-in-1-iloxi)fenil)calix[4]resorcinareno (<i>rccc</i>)	9,8	77,9	1008,3	1008,3

Con los resultados obtenidos de la síntesis de los derivados de calix[4]resorcinareno se cumple la totalidad del objetivo específico 1. Parte de los resultados y metodologías reportadas en este apartado fueron publicados en la revista Antibiotics y ACS Omega, (Para más información, ver Anexo B.1 y B.2).

4.1.2 Síntesis y caracterización de péptidos.

Para el desarrollo de este proyecto se obtuvieron once (11) péptidos derivados de los fragmentos 20-25 de la LfcinB, 32-35 de la BF y un péptido de poli-Alanina (ver Tabla 7). Las moléculas purificadas y caracterizadas, por cromatografía líquida (RP-HPLC) y espectrometría de masas MALDI-TOF, fueron empleadas para los ensayos de actividad biológica. Puntualmente, se sintetizaron, purificaron y caracterizaron: i) tres péptidos lineales que corresponden a las secuencias seleccionadas, estos se usaron como controles, y corresponden a los motivos mínimos de actividad de la LfcinB (20-25): RRWQWR (P1) y la BF (32-35): RLLR (P5) y un péptido palindrómico derivado de la LfcinB (20-25)_{pal}: RWQWRWQWR (P8). ii) seis azida-péptidos, que contenían en el extremo N-terminal un residuo del ácido (S)-6-azido-2-(Fmoc-amino)hexanoico derivado de cada una de las secuencias de los péptidos control, P3: K(N₃)-RRWQWR P7: K(N₃)-RLLR, P9: K(N₃)-RWQWRWQWR, dos azida-péptidos que contenían una molécula espaciadora, el ácido 6-aminohexanoico (Ahx), entre la secuencia peptídica y ácido (S)-6-azido-2-(Fmoc-amino)hexanoico, P4: K(N₃)-Ahx-RRWQWR y P10: K(N₃)-Ahx-RLLRLLR, y un péptido de poli Alaninas funcionalizado con azida, P11: K(N₃)-AAAA. Y iii) dos péptidos polivalentes (tetrámeros), en donde se empleó un núcleo o core de tipo proteico, P2: ((RRWQWR)₂K-Ahx-C)₂ y P6: ((RLLR)₂K-Ahx-C)₂. A continuación, se discutirán los resultados obtenidos de la síntesis de las secuencias involucradas en esta investigación junto con su caracterización.

Todos los péptidos anteriormente descritos, fueron obtenidos mediante síntesis de péptidos en fase sólida (SPPS) usando la estrategia Fmoc/tBu, ver Figura 34. En esta estrategia el grupo alfa amino de cada uno de los aminoácidos está protegido con el grupo 9-fluorenilmetoxicarbonilo (Fmoc) que es estable bajo condiciones ácidas, a su vez las cadenas laterales están protegidas por grupos como el tertbutilo o tritilo que son lábiles a ácidos y estables en medio básico. Este esquema de protección ortogonal permite la desprotección selectiva del grupo alfa amino de los aminoácidos mientras que los grupos protectores de las cadenas laterales permanecen estables. La SPPS-Fmoc/tBu se puede generalizar en tres etapas: i) remoción del grupo Fmoc, ii) activación y acople del aminoácido (formación de un éster reactivo y del enlace peptídico) y iii) desanclaje del péptido del soporte sólido (clivaje) y desprotección de las cadenas laterales, como se muestra en la Figura 34, [136]–[138].

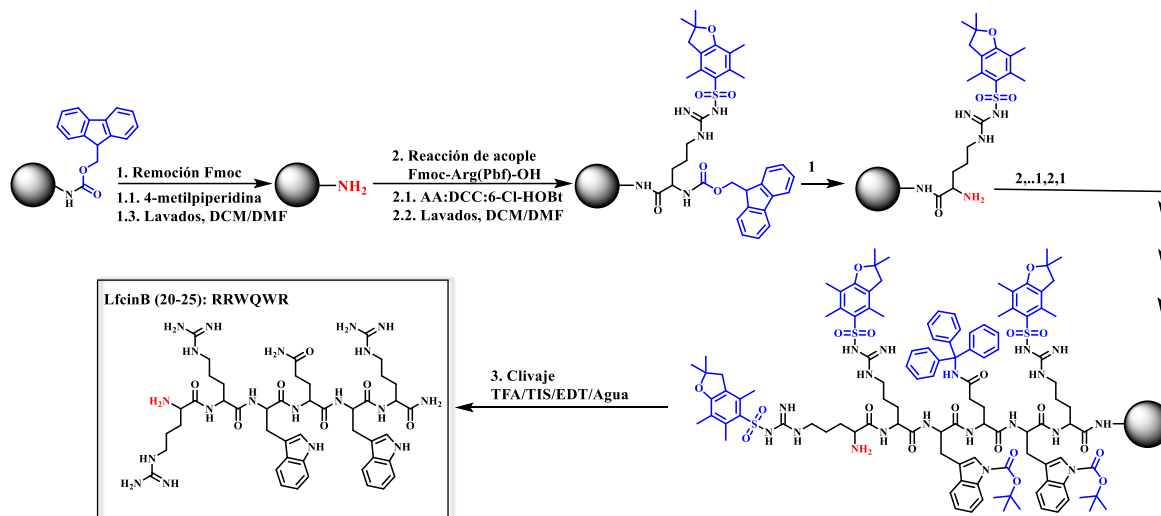


Figura 34. Esquema general de la síntesis de péptidos utilizando la metodología SPPS-Fmoc/tBu. Ejemplo secuencia RRWQWR

Los resultados de síntesis (Anexo A.5) de los péptidos indicaron que la estrategia usada fue adecuada para la obtención de las moléculas propuestas. Específicamente, en este trabajo se implementó la 4-metilpiperidina, a una concentración de 2,5% (%v/v) en DMF, como reactivo para la remoción del grupo Fmoc; cabe resaltar que esta concentración es diez veces menor a la comúnmente usada en los protocolos reportados para la SPPS [115]. Para la mayoría de los aminoácidos solo se requirió un ciclo de acople para su incorporación en la secuencia peptídica. El coctel de clivaje TFA/agua/TIS/EDT (93/2/2,5/2,5 %v/v/v/v) fue adecuado para los péptidos control y precursores diméricos de los tetrámeros, sin embargo, para los péptidos funcionalizados con azida (P3, P4, P7, P9, P10 y P11) se evidenció en su perfil cromatográfico la presencia de dos especies mayoritarias; a manera de ejemplo se presenta el perfil cromatográfico para el péptido P4: K(N₃)-Ahx-RRWQWR, donde se puede observar la presencia de especies con t_R entre 4,5-5,0 min, ver Figura 35.a. Con el fin de solventar esta dificultad en la etapa de clivaje se decidió modificar la solución utilizada, suprimiendo los capturadores (scavengers) y evaluando diferentes proporciones, además del coctel de clivaje mencionado inicialmente se probaron otras composiciones: i) TFA/agua/TIS (92/4/4 %v/v/v) y ii) TFA/agua (95/5 %v/v).

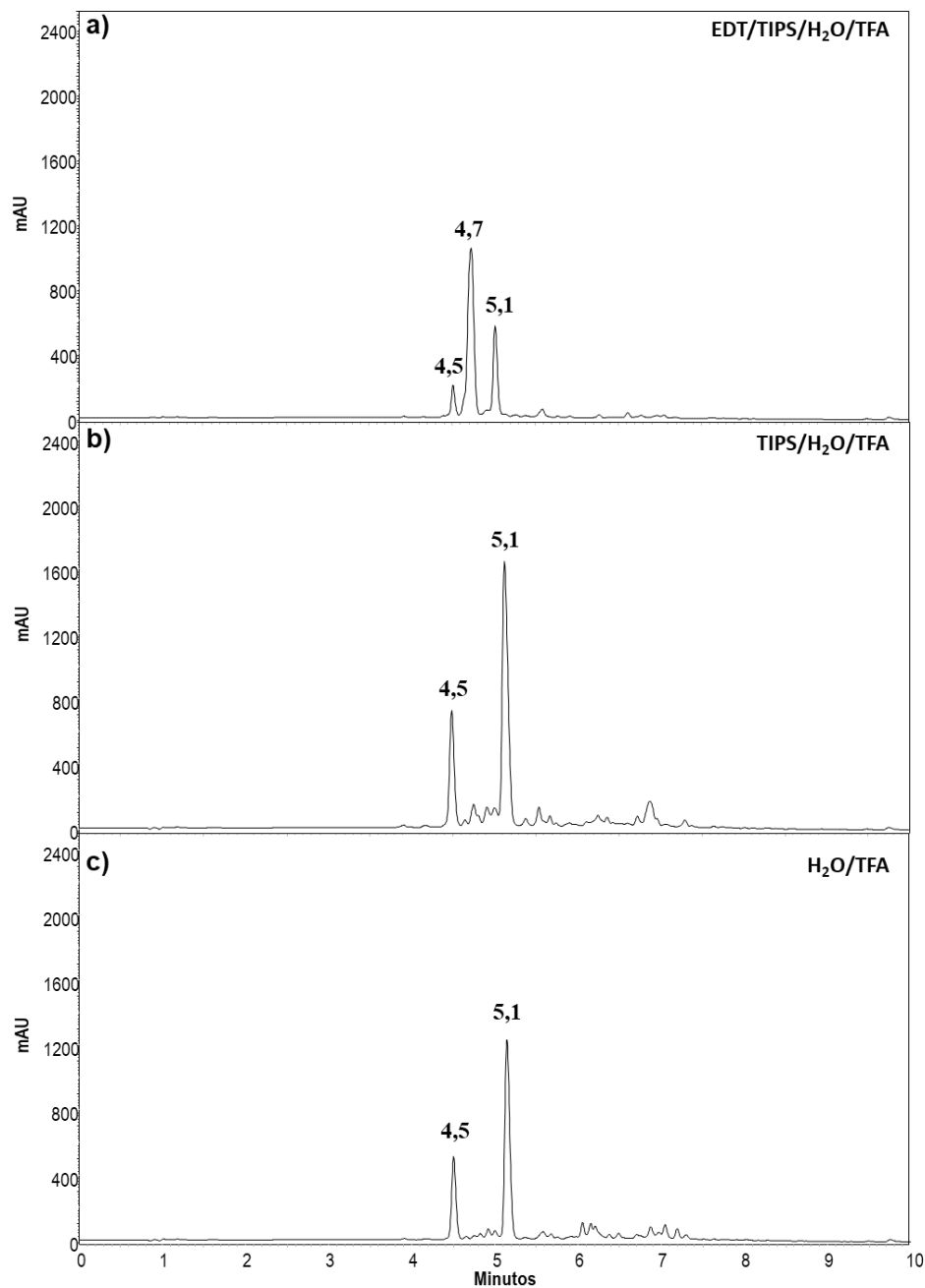


Figura 35. Perfiles cromatográficos para el péptido (K(N₃)-Ahx-RRWQWR) obtenido al usar diferentes condiciones de clivaje: a) EDT/TIPS/H₂O/TFA, b) TIPS/H₂O/TFA, c) H₂O/TFA.

Como se puede observar en la Figura 35.b y Figura 35.c. al suprimir el EDT (1,2-etanodiol) de la solución de clivaje el perfil cromatográfico mejoró evidenciando la presencia de dos especies mayoritarias con t_R de 4,5 y 5,1 min. Previamente Schneggenburger *et. al.*, ya habían reportado la dificultad en el proceso de clivaje de

diversos péptidos de ácidos nucleicos (PNA- peptide Nucleic Acid), donde al utilizar scavengers como el EDT y/o TIPS da como resultado la aparición de subproductos de la reacción, donde en algunos casos se obtenía la especie deseada el azida-péptido, pero a su vez ocurría un proceso de reducción del grupo azida ($-N_3$) a amina ($-NH_2$) [139]. El producto crudo, obtenido al utilizar TFA/agua (95/5 %v/v) como solución de clivaje, fue analizado mediante ESI-Q/TOF, donde, mediante deconvolución de las señales, se obtuvo un valor de masa experimental de 1252,6608 u.m.a para la especie con t_R : 5,1 min y 1226,6824 u.m.a para la especie con t_R : 4,5 min. Este resultado indicó que la especie con t_R : 5,1 min corresponde al producto esperado ($K(N_3)$ -Ahx-RRWQWR) cuyo valor de masa teórica esperada es 1252,72 u.m.a y la especie con t_R : 4,5 min corresponde al producto de la reducción del grupo azida a amina ($K(NH_2)$ -Ahx-RRWQWR) cuya masa esperada era 1226,73 u.m.a, ver Figura 36, Tabla 14. Para fines prácticos, estos péptidos no fueron sometidos al proceso de purificación por SPE dado que las condiciones de la reacción de química click son selectivas y la especie minoritaria (péptidos con amina) no es un problema en la reacción.

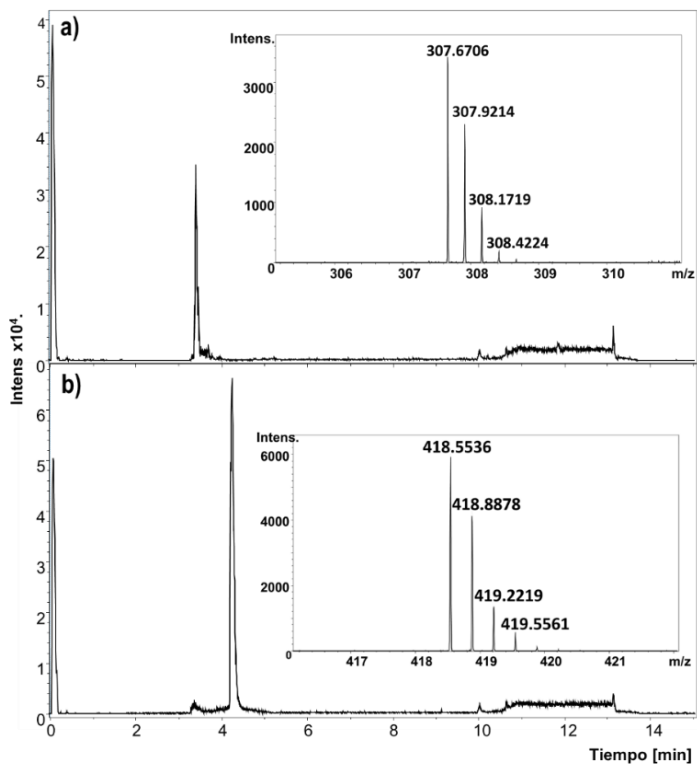


Figura 36. TIC y espectro de masas ESI-Q/TOF de a) $K(NH_2)$ -Ahx-RRWQWR y b) $K(N_3)$ -Ahx-RRWQWR.

Para los péptidos P2 y P6 que corresponden a péptidos polivalentes, tetraméricos, la estrategia usada fue la incorporación de una Cisteína (Cys) en el extremo C-terminal de la secuencia peptídica, para la posterior oxidación del grupo tiol de la cadena lateral con la subsecuente formación tetrámeros, (ver Figura 37), [140], [141]. Para el caso de la LfcinB, se han diseñado péptidos polivalentes que presentan el motivo mínimo LfcinB (20-25): RRWQWR, en su forma dimérica LfcinB (20-25)₂ y tetramérica LfcinB (20-25)₄. Se ha evaluado tanto su actividad antibacteriana como anticancerígena [77], [79], [142]. Se sintetizaron dos péptidos polivalentes correspondientes a las secuencias P2: ((RRWQWR)₂K-Ahx-C)₂ y P6: ((RLLR)₂K-Ahx-C)₂. Estas secuencias peptídicas se sintetizan con el fin de generar estructuras dendríméricas con un core o núcleo diferente a los derivados de calix[4]resorcinareno.

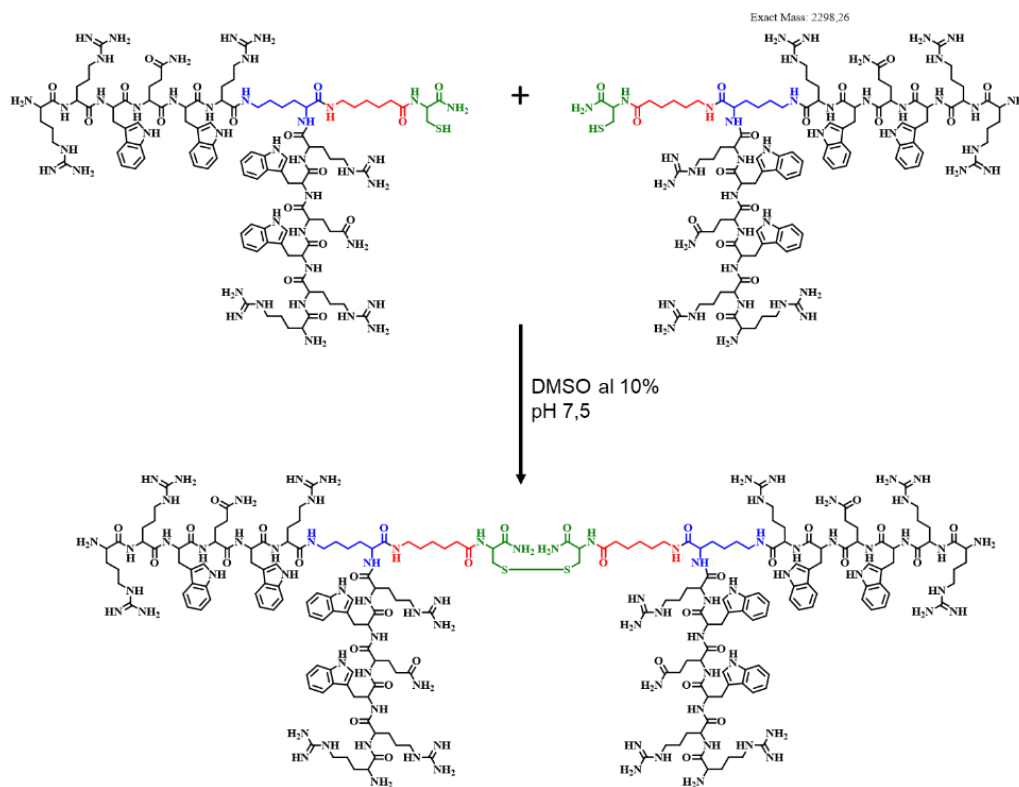


Figura 37. Esquema de reacción de la oxidación del grupo tiol presente en la Cys, para la obtención de péptidos tetraméricos a partir de dímeros.

Tabla 14. Resumen de la caracterización analítica de los péptidos control, azida-péptidos y tetrameros derivados de la LfcinB y BF obtenidos.

Familia	Código	Secuencia	RP-HPLC t_R (min)	Pureza (%)	MASA	
					Teórica [M]	m/z [M+H] ⁺
LfcinB (20-25)	P1	RRWQWR	4,1	92,5	985,5	986,5
	P2	((RRWQWR) ₂ K-Ahx-C) ₂	5,6	96,8	2295,1 [‡]	2295,1 [‡]
	P3	K(N ₃)-RRWQWR	5,1	83,7*	1139,6	1139,4
	P4	K(N ₃)-Ahx-RRWQWR	5,4	79,8*	1252,5	1252,5
BF (32-35)	P5	RLLR	2,8	97,2	555,4	556,2
	P6	((RLLR) ₂ K-Ahx-C) ₂	5,7	95,9	2873,9	2874,9
	P7	K(N ₃)-RLLR	5,3	82,6*	709,5	709,9
LfcinB (20-25) _{pal}	P8	RWQWRWQWR	6,5	94,2	1485,8	1484,6
	P9	K(N ₃)-RWQWRWQWR	7,2	70,4*	1639,9	1640,7
Otros	P10	K(N ₃)-Ahx-RLLRLLR	6,2	92,2*	1360,9	1360,3
	P11	K(N ₃)-AAAA	1,7	98,1*	455,3	456,3

* Péptido crudo, †Precursor dimérico

Con los resultados obtenidos de la síntesis de péptidos se cumple a totalidad el objetivo específico 2. La revisión bibliográfica de las metodologías y diseños implementados en la síntesis de los péptidos sintéticos (péptidos funcionalizados con azida, diméricos/tetraméricos y química click) fueron consolidados y publicados en un artículo de revisión en la revista Current Organic Chemistry. (Para más información, ver Anexo B.3).

4.2 Síntesis de dendrímeros mediante química click CuAAC

a) Optimización condiciones química click

Una vez obtenidos los resorcinarenos funcionalizados con el grupo alquino y los péptidos modificados con el aminoácido lisina azida (K(N₃)), se procedió a la optimización de las condiciones de química click, para la cicloadición azida-alquino catalizada por cobre (I) (CuAAC); esta optimización de la ruta sintética incluyó parámetros como, solvente, proporciones, temperatura, entre otros. Previamente se reportó la síntesis de una quimera peptídica entre la LfcinB (20-25): RRWQWR y BF (32-35): RLLR mediante cicloadición azida alquino catalizada por cobre [88], como punto de partida se probaron estas condiciones optimizadas para moléculas peptídicas. Para ello se utilizaron los precursores azida (Fmoc-Lys(N₃)-OH, P11: K(N₃)-AAAA, P10: K(N₃)-Ahx-

RLLRLLR) y precursores alquino (Fmoc-Pra-OH, *p*-HF). Los datos recopilados de la optimización de las diferentes reacciones se consolidan en la Tabla 15. Todos los productos fueron caracterizados mediante espectrometría de masas MALDI-TOF donde se corrobora la generación de los respectivos productos mediante la unión de los precursores azida-compuestos y alquino-compuestos mediante la comparación de su masa teórica y la relación *m/z* esperada.

Tabla 15. Optimización condiciones química click con precursores

Azida-compuesto	Alquino-Compuesto	Temperatura	Solvente	Tiempo de reacción	MASA	
					Teórica [M]	<i>m/z</i> [M+H] ⁺
Fmoc-Lys(N ₃)-OH	Fmoc-Pra-OH	80°C	MeOH:H ₂ O	15 min	732,3	729,3
	<i>p</i> -HF	TA	DMF	1,5 h	554,2	554,2
	CR-4-ALQ (<i>rctt</i>)	TA	DMF	3 h	2584,9	2583,3
P11	Fmoc-Pra-OH	TA	DMF	24 h	790,4	790,3
	<i>p</i> -HF	TA/40°C	DMF	24 h/6 h	615,3	614,3
	CR-4-ALQ (<i>rctt</i>)	TA/80°C	MeOH:H ₂ O	24 h (N/R)	2829,4	-
		TA/80°C	DMF	38 h (N/R)	2829,4	-
		TA/80°C	ACN	24 h (N/R)	2829,4	-
		TA	DMF:H ₂ O	2,5 h	2829,4	2831,5
	P10	<i>p</i> -HF	40°C	MeOH	8 h (N/R)	1520,9
40°C			DMF	6 h	1520,9	1519,4

P11: K(N₃)-AAAA, **P10:** K(N₃)-Ahx-RLLRLLR, ***p*-HF:** 4-(prop-2-in-1-iloxi)benzaldehído, **CR-4-ALQ (*rctt*):** C-tetra(4-(prop-2-in-1-iloxi)fenil)calix[4]resorcinareno. **N/R:** No Reacción.

La selección del solvente de reacción se realizó teniendo en cuenta lo reportado en literatura y basados en la solubilidad de cada una de las moléculas a evaluar. Inicialmente se probó la mezcla de solvente polares MeOH:H₂O, este solvente fue apto para la reacción entre los Fmoc-aminoácidos, Fmoc-Lys(N₃)-OH y Fmoc-Pra-OH, pero no fue útil con el derivado de calix[4]resorcinareno, CR-4-ALQ (*rctt*), dado que este no es soluble en la mezcla. Cabe resaltar que para la mayoría de las reacciones probadas, la reacción click (CuAAC) en N,N-Dimetilformamida (DMF) genera los productos esperados a tiempos de reacción que oscilaron en un rango de 15 min a 24 h, esta reacción se vio favorecida al aumentar la temperatura de reacción, sin embargo, se

encontró que el incremento de la temperatura generó una solución viscosa difícil de manejar, por esta razón se decidió trabajar a temperatura ambiente (TA) con tiempos de reacción mayores. Se probó entonces la DMF para la reacción del CR-4-ALQ (*rctt*) con el péptido P11, se empleó también como solvente la DMF, que había funcionado en las reacciones de este péptido con Fmoc-Pra-OH y con p-HF, sin embargo, la reacción no procedió, Figura 38, con el macrociclo. Para derivados de calix[4]resorcinareno han reportado el acetonitrilo como uno de los solventes donde se puede llevar a cabo la reacción click, aunque los dos precursores, P11 y CR-4-ALQ fueron solubles en el solvente de reacción, esta no generó los productos esperados después de 24 h de reacción, una de las principales causas de que no ocurriera la reacción en ACN se puede atribuir a que el catalizador generado *in situ* no es soluble en este disolvente, ver Figura 38.

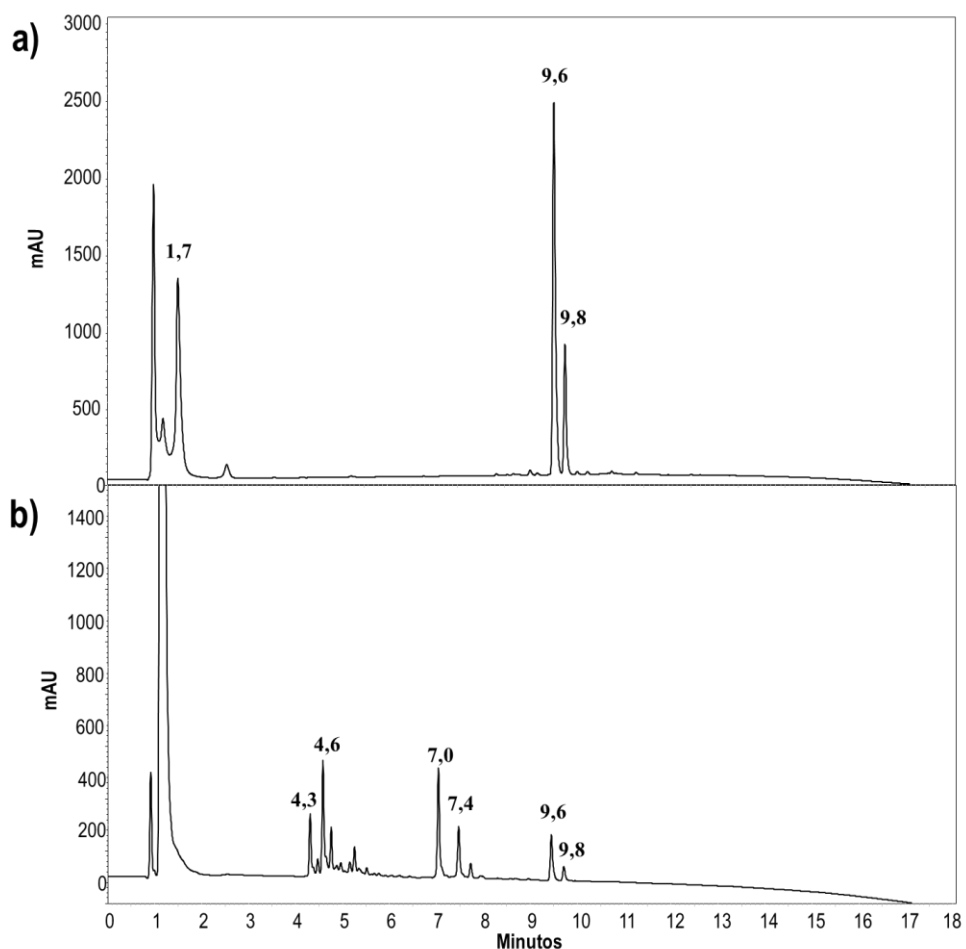


Figura 38. Perfil cromatográfico de la reacción de química click de P11: K(N₃)-AAAA (t_R : 1,7 min) y CR-4-ALQ (*rctt*) (t_R : 9,6 min), 24 h en a) ACN y b) DMF:H₂O (2:1).

Finalmente, para la reacción entre CR-4-ALQ (*rctt*) y P11 se empleó una mezcla DMF:H₂O (2:1), en la Figura 38.b. se puede evidenciar que el P11 con t_R : 1,7 min se consumió por completo y nuevas especies con t_R entre 4,3 min y 7,4 min aparecen, esta mezcla de reacción se analizó mediante espectrometría de masas en donde se encontró que uno de los productos correspondía al producto tetra-funcionalizado.

En resumen, con los resultados obtenidos, se lograron definir las condiciones más favorables para la síntesis de los dendrímeros péptido-resorcinareno mediante cicloadición azida-alquino: como solvente una mezcla DMF:H₂O (2:1), como catalizador la especie de cobre (I) generada *in situ* mediante la reacción de ascorbato de sodio (C₆H₇NaO₆) y sulfato de cobre penta-hidratado (CuSO₄·5H₂O), todas las reacciones se realizaron a temperatura ambiente.

b) Reacción click con CR-4-ALQ (*rccc* y *rctt*)

La síntesis de los dendrímeros procede de la reacción entre el alquino-derivado de resorcinareno y el azida-péptido. Para facilitar la lectura, a partir de este momento se nombran los dendrímeros (D) con la sigla del péptido correspondiente. Por ejemplo, el dendrímero entre CR-4-ALQ (*rctt*) y el P3, se llamará DP3. Optimizadas las condiciones de la reacción click (CuAAC) con los diferentes alquino- y azida-compuestos, se decidió sintetizar los dendrímeros DP3, DP7 y DP9, ver Tabla 8. Para ello inicialmente se partió del derivado de resorcinareno CR-4-ALQ (*rctt*), cuya sustitución es inferior al octa-funcionalizado, esto con el fin de evaluar si se puede llegar a presentar impedimento estérico en la incorporación de las secuencias peptídicas. Así se probaron las siguiente reacciones con péptidos funcionalizados con: i) una molécula espaciadora, el ácido 6-aminohexanoico (P4 y P10), ii) sin molécula espaciadora, y variando la longitud de la cadena entre 4 aminoácidos para el caso del derivado de BF (P7) y 8-11 aminoácidos para los derivados de LfcinB (P3 y P9, respectivamente), estas modificaciones nos permitieron evidenciar si la hidrofobicidad o la longitud de la cadena afectan la completa sustitución de los derivados de resorcinareno mediante química click. En la Tabla 16, se presentan las condiciones, así como la caracterización parcial de los productos de reacción obtenidos.

Tabla 16. Resumen de las condiciones y caracterización de la síntesis de los dendrímeros péptido-resorcinareno.

Dendrímero	Azida-compuesto	Alquino-compuesto	Tiempo de reacción	Pureza (%)	RP-HPLC t_R (min)	Funcionalización	MASA	
							Teórica [M]	m/z [M+H] ⁺
DP4	P4	CR-4-ALQ (<i>rctt</i>)	48 h	-	-	Mono	2262,6	-
				-	-	Di	3516,1	-
				-	-	Tri	4769,5	-
				-	-	Tetra	6023,0	-
DP10	P10	CR-4-ALQ (<i>rctt</i>)	48 h	-	-	Mono	2369,5	2373,6
				-	-	Di	3730,2	3732,3
				-	-	Tri	5091,1	5093,0
				-	-	Tetra	6452,1	-
DP3	P3	CR-4-ALQ (<i>rctt</i>)	2 h	74,6	6,4	Tetra	5566,8	5575,2
DP7 (<i>rctt</i>)	P7	CR-4-ALQ (<i>rctt</i>)	2 h	96,4	6,0	Tetra	3847,2	3847,5
DP7 (<i>rccc</i>)	P7	CR-4-ALQ (<i>rccc</i>)	2 h	96,4	6,0	Tetra	3847,2	3847,5
DP9	P9	CR-4-ALQ (<i>rctt</i>)	6 h	-	-	Mono	2648,2	2662,4
				-	-	Di	4288,0	4356,2
				-	-	Tri	5927,9	6042,8
				-	-	Tetra	7567,7	-

P4: K(N₃)-Ahx-RRWQWR, **P10:** K(N₃)-Ahx-RLLRLLR, **P3:** K(N₃)-RRWQWR, **P7:** K(N₃)-RLLR, **P9:** K(N₃)-RWQWRWQWR

Para el caso de la reacción de CuAAC entre CR-4-ALQ (*rctt*) y los péptidos P4 y P10, donde tenemos la presencia del espaciador, ácido 6-aminohexanoico, los tiempos de reacción fueron prolongados (48 h) y el perfil cromatográfico mostró la presencia de varias especies sin obtenerse una especie mayoritaria; el análisis mediante espectrometría de masas MALDI-TOF del producto obtenido nos sugiere que la funcionalización fue incompleta obteniéndose los productos mono, di, tri-funcionalizado y en ninguno de los casos tetra funcionalizado, ver Figura 39.

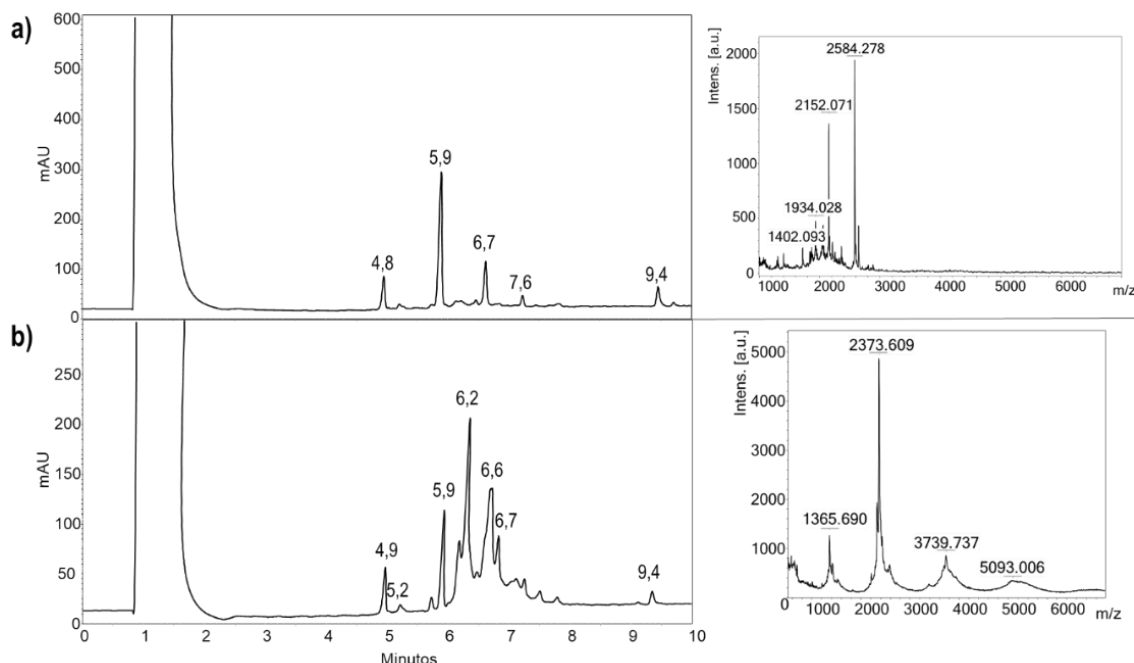


Figura 39. Perfil cromatográfico (izquierda) y espectro de masas (derecha) del producto de reacción entre el macrociclo CR-4-ALQ (*rcft*) y a) **P4:** K(N₃)-Ahx-RRWQWR o b) **P10:** K(N₃)-Ahx-RLLRLLR.

Al emplear para la reacción de química click las secuencias peptídicas sin espaciador (P3: K(N₃)-RRWQWR, P7: K(N₃)-RLLR), los tiempos de reacción fueron menores (hasta las 2 h), y adicionalmente se observó una especie mayoritaria. La reacción con P7 mostró un perfil cromatográfico más limpio con un mayor rendimiento (75,6%) en comparación a P3 (56,6%) lo que nos sugiere que la incorporación de secuencias cortas es más viable al momento de obtener producto con una funcionalización completa, ver Figura 40.a y Figura 40.b. Con el fin de corroborar que la longitud de la secuencia y que la presencia del ácido 6-aminohexanoico afecta la funcionalización completa del derivado de resorcinareno, se decidió evaluar la viabilidad sintética del dendrímero con el P9: K(N₃)-RWQWRWQWR, como se puede observar, aunque el tiempo de reacción disminuyó en comparación con P4 y P10, el producto presentó una mezcla de productos con funcionalizaciones incompletas; encontrando especies correspondientes al resorcinareno CR-4-ALQ (*rcft*) mono, di y tri sustituido con P9.

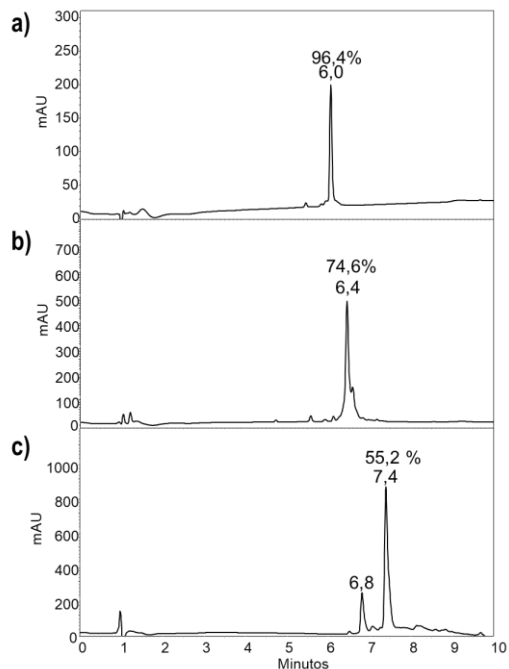


Figura 40. Perfil cromatográfico del producto de reacción de CuAAC entre a) CR-4-ALQ (*rctt*) y P7 y b) CR-4-ALQ (*rctt*) y P3 y c) CR-4-ALQ (*rctt*) y P9.

A continuación, se presentan los resultados obtenidos para el dendrímero DP7 (*rctt*): CR-4-ALQ(*rctt*)-(AAC-(K)-RLLR)₄. En la Figura 41 aparece el esquema de reacción de química click para la obtención de DP7.

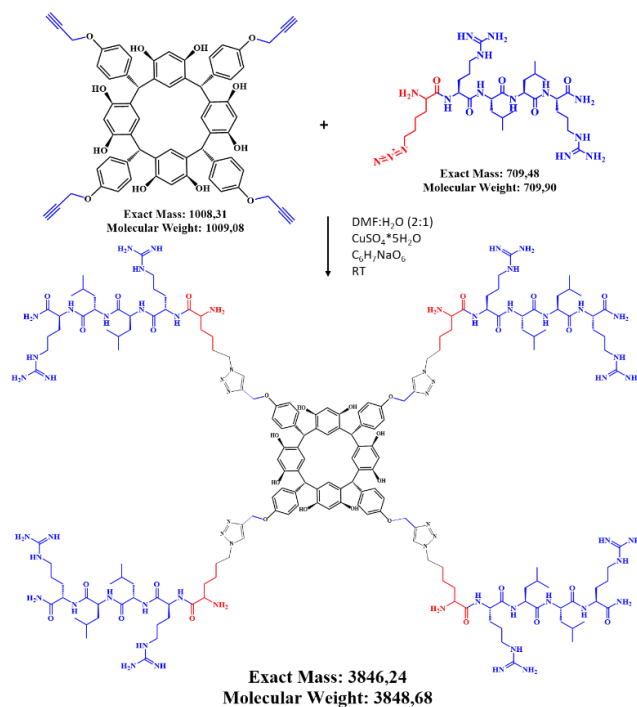


Figura 41. Esquema de la síntesis del dendrímero DP7: CR-4-ALQ(*rctt*)-(AAC-(K)-RLLR)₄

El seguimiento de la reacción de cicloadición entre CR-4-ALQ (*rctt*) y el péptido P7: K(N₃)-RLLR, se realizó a través del análisis por RP-HPLC, para lo que fueron tomadas alícuotas a diferentes tiempos de reacción (Figura 42). En el tiempo inicial de reacción (0 h) se observaron las señales correspondientes al péptido P7 (t_R : 5,3 min) y el resorcinareno funcionalizado CR-4-ALQ (*rctt*) (t_R : 9,6 min), se evidenció la aparición de nuevas especies con tiempos de retención intermedios. Después de una hora y media de reacción (1,5 h) se observó una especie mayoritaria con t_R de 6,0 min, se evidencia que la señal del CR-4-ALQ (*rctt*) se ha reducido a un 10% de la inicial y aún se observa péptido P7 (adicionado en exceso). Las señales que estaban a tiempos de retención de 6,3, 7,2 y 7,9 min desaparecieron, sugiriendo que son especies correspondientes a conjugación incompletas del péptido al resorcinareno, (mono, di o tri sustituido).

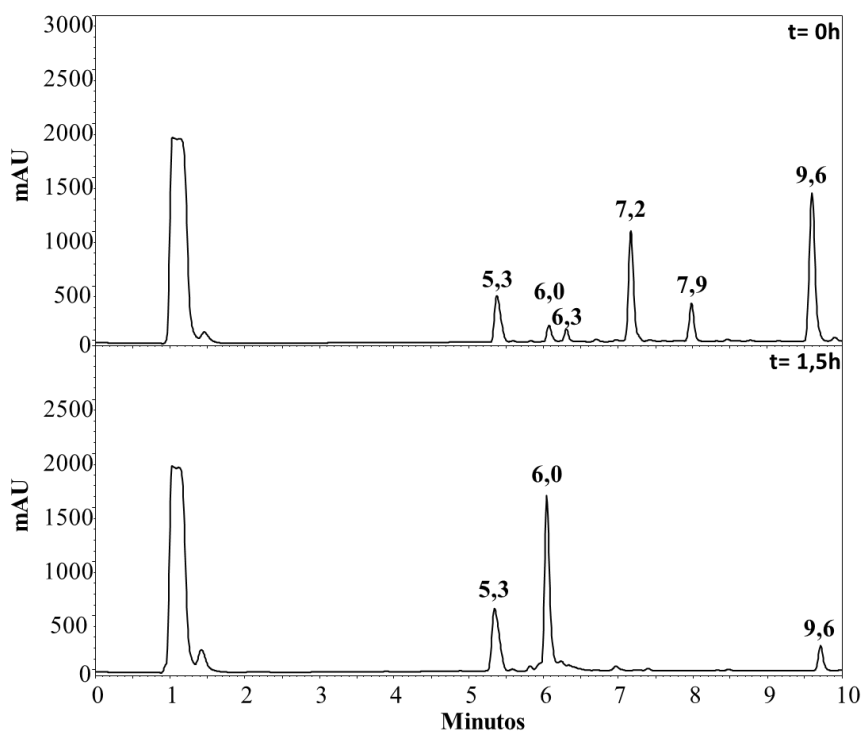


Figura 42. Seguimiento, mediante RP-HPLC, de la reacción de obtención del dendrímero DP7: CR-4-ALQ(*rctt*)-(AAC-(K)-RLLR)₄.

Los productos obtenidos fueron purificados mediante RP-SPE para retirar el exceso de catalizador, solvente y otras especies que no reaccionaron. El perfil cromatográfico del producto puro se muestra en la Figura 43, así como su caracterización mediante espectrometría de masas MALDI-TOF, donde se encontró la relación m/z 3847,5 correspondiente a la señal de la especie $[M+H]^+$ del dendrímero tetra funcionalizado (m/z monoisotópica

teórica: 3847,2 u.m.a). En la Tabla 17, se pueden encontrar los datos de caracterización, tanto para los precursores peptídicos como el núcleo de resorcinareno al igual que los dendrímeros sintetizados.

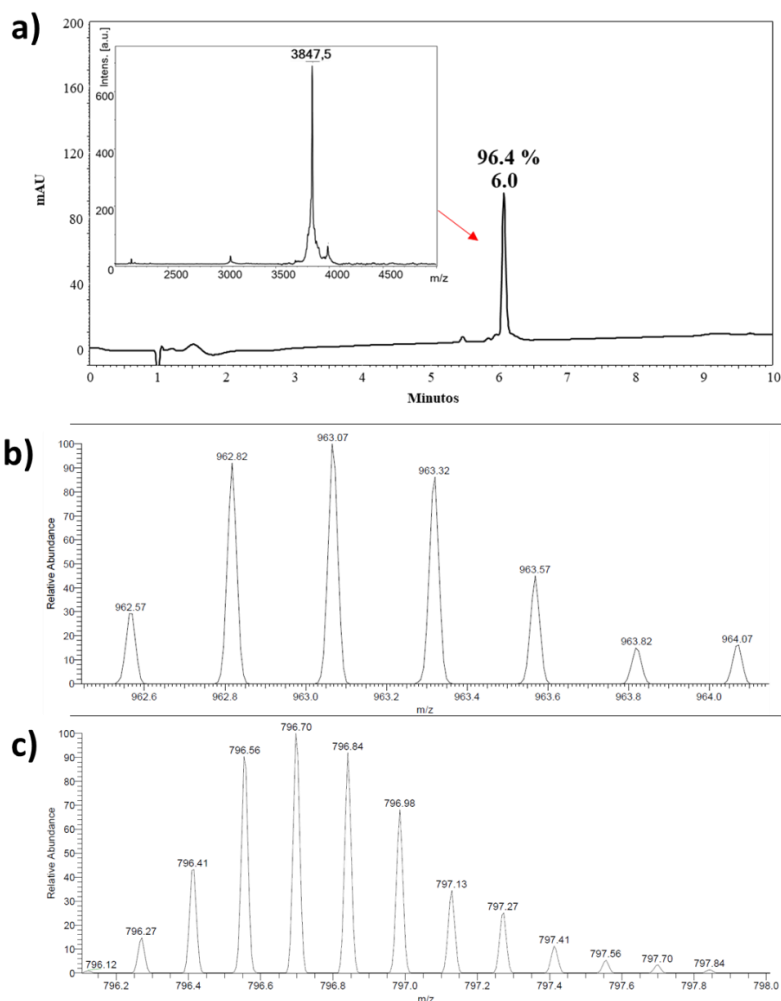


Figura 43. a) Perfil cromatográfico y espectro MALDI-TOF MS del dendrímero DP7 purificado: CR-4-ALQ_(rctt)-(AAC-(K)-RLLR)₄ y b) HR-MS del dendrímero DP7, se muestran las señales correspondientes a la distribución isotópica de la especie $[M+4H]^{4+}$; monoisotópico experimental M es 3846,28 u.m.a. c) HR-MS del dendrímero DP3, se muestran las señales correspondientes a la distribución isotópica de la especie $[M+7H]^{7+}$; monoisotópico experimental M es 5572,84 u.m.a.

Los resultados obtenidos en la optimización de las condiciones de reacción (ver Tabla 16) y de los dendrímeros sintetizados, ver Tabla 17, sugieren que: i) entre mayor sea la funcionalización del derivado de resorcinareno menos viable será la reacción, por esta razón se descartó el uso del derivado octa-funcionalizado CR-8-ALQ, ii) al incorporar la molécula espaciadora (Ahx) las secuencias peptídicas se hacen más apolares esto generó una funcionalización incompleta obteniéndose productos mono, di y tri sustituidos, iii) la reacción de secuencias

peptídicas cortas con el núcleo de resorcinareno se ve favorecida tal vez por reducción del impedimento estérico (resultados de los dendrímeros DP3 y DP9), iv) con los resultados de los dendrímeros DP7_(rctt) y DP7_(rccc) se evidencia que la conformación no es un parámetro determinante en la reacción click. Sin embargo, el rendimiento del conformero rccc fue inferior.

Tabla 17. Resumen de la caracterización de dendrímeros péptido-resorcinareno.

Código	Dendrímero	RP-HPLC		Rendimiento (%)	MASA	
		t _R (min)	Pureza (%)		Teórica [M]	Exp. [M+H] ⁺ m/z
DP3	CR-4-ALQ-(AAC-(K)-RRWQWR) ₄	6,4	74,6	56,6	5570,4	5575,2
DP7 (rctt)	CR-4-ALQ _(rctt) -(AAC-(K)-RLLR) ₄	6,0	96,4	75,6	3847,2	3847,5
DP7 (rccc)	CR-4-ALQ _(rccc) -(AAC-(K)-RLLR) ₄	6,0	88,7	60,1	3847,2	3844,2
DP9	CR-4-ALQ-(AAC-(K)-RWQWRWQWR) ₄	7,4	55,2	-	7567,71	-

Con los resultados obtenidos de la optimización de la ruta sintética vía química click y la síntesis de los dendrímeros péptido-resorcinareno se cumple la totalidad del objetivo específico 3. La revisión bibliográfica sobre condiciones de química click usada en derivados de calix[4]resorcinareno se consolidaron en un artículo de revisión publicado en la revista ACS Omega. Parte de los resultados de la funcionalización de los péptidos sintéticos y optimización de la reacción click CuAAC en secuencias derivadas de LfcinB y BF fueron publicados en la revista *ChemistrySelect*. (Para más información, ver Anexos B.4 y B.5).

4.3 Actividad Antimicrobiana

A los péptidos control y dendrímeros obtenidos con mayor rendimiento se les evaluó su actividad antimicrobiana. Con estos ensayos se pretendía determinar si los péptidos RRWQWR y RLLR unidos a un núcleo de resorcinareno (CR-4-ALQ (rctt)), mediante ciclación intramolecular con puente triazol, presentaba o no actividad antimicrobiana frente a cepas de referencia, *E. coli* ATCC 25922, *S. aureus* ATCC 25923, aislados clínicos de *E. coli* y *S. aureus* y cepas de *Candida spp.*

4.3.1 Concentración Mínima Inhibitoria (CMI) y Concentración Mínima Bactericida (CMB)

Inicialmente, los péptidos control lineales (P1 y P5) y tetraméricos (P2 y P6), el resorcinareno CR-4-ALQ_(rctf) y los dendrímeros sintetizados (DP3 y DP7) se probaron frente a una cepa de referencia de *E. coli* (American Type Culture Collection) sensible a ciprofloxacino (ATCC 25922), en la Tabla 18 se resumen los resultados encontrados: (i) Los péptidos lineales y el núcleo, CR-4-ALQ_(rctf), no fueron activos contra la cepa ensayada a las concentraciones estudiadas (CMI de 203 μ M para P1, >359 μ M para P5 y >198 para CR-4-ALQ_(rctf)). Mientras que, (ii) los dendrímeros DP3, DP7 (*rctf*) y DP7 (*rccc*) presentaron actividad antibacteriana con CMI de 36, 13 y 52 μ M, respectivamente. (iii) Al comparar la actividad de las secuencias polivalentes construidas sobre un núcleo proteico versus la presentada por las moléculas construidas sobre el núcleo de resorcinareno (DP7 vs P6 y DP3 vs P2), se observa que la actividad antibacteriana es similar; por ejemplo, DP7 (*rctf*) y P6 que presentan cuatro copias de la secuencia RLLR mostraron CMI de 13 y 18 μ M, respectivamente frente a *E. coli* ATCC 25922. (iv) Si comparamos la actividad del dendrímero DP7 (*rctf*) y DP7 (*rccc*) cuya conformación es diferente (silla y corona, respectivamente) se evidencia que la actividad frente a *E. coli* ATCC 25922 es dependiente de la conformación del dendrímero, para DP7 (*rctf*) se encontró una CMI de 13 μ M en comparación al dendrímero DP7 (*rccc*) que, aunque fue activo, presentó una CMI cuatro veces mayor (52 μ M).

Tabla 18. Actividad antibacteriana de los péptidos control y los dendrímeros péptido-resorcinareno. Los valores de MIC/MBC se expresan en μ M.

Actividad antibacteriana contra ATCC		<i>E. coli</i> 25922	<i>S. aureus</i> 25923
Familia	Secuencia	CMI/CMB μ M (μ g/mL)	CMI/CMB μ M (μ g/mL)
Controles	P1: RRWQWR	203/203 (200/200)	>203/>203 (200/200)
	P5: RLLR	>359/>359 (>200/>200)	>359/>359 (>200/>200)
	P2: ((RRWQWR) ₂ K-Ahx-C) ₂	22/44 (100/200)	22/44 (100/200)
	P6: ((RLLR) ₂ K-Ahx-C) ₂	18/36 (50/100)	36/36 (100/100)
	CR-4-ALQ _(rctf)	>198/>198 (>200/>200)	>198/>198 (>200/>200)
Dendrímeros	DP3: CR-4-ALQ _(rctf) -(AAC-(K)-RRWQWR) ₄	36/36 (200/200)	ND
	DP7 (<i>rctf</i>): CR-4-ALQ _(rctf) -(AAC-(K)-RLLR) ₄	13/26 (50/100)	13/>52 (50/>200)
	DP7 (<i>rccc</i>): CR-4-ALQ _(rccc) -(AAC-(K)-RLLR) ₄	52/>52 (200/>200)	ND

ND: No Determinado

Luego, se seleccionó el dendrímero DP7 (*rctt*), que presentó la mayor actividad antibacteriana contra *E. coli*, para ser evaluado frente a *S. aureus*. DP7 (*rctt*) presentó una CMI de 13 μM en comparación con la CMI del péptido de control P5 >359 μM , ver Tabla 18, este resultado es muy interesante ya que, para la mayoría de los casos, los péptidos sintéticos que son activos contra cepas Gram-negativas resultan ser poco activos en cepas Gram-positivas, esto debido en gran parte a la diferencia estructural de sus membranas. El dendrímero DP7 (*rctt*) fue activo tanto en la cepa Gram-negativa como Gram-positiva con valores de CMI iguales. Los controles usados presentaron en *S. aureus* (25923) el mismo comportamiento que el descrito para la cepa de referencia de *E. coli*. Una vez establecido que los dendrímeros presentaron actividad antibacteriana contra cepas de referencia, se procedió a evaluar su actividad contra aislados clínicos sensibles, resistentes y multirresistentes de *E. coli* y *S. aureus*. Se seleccionaron entonces para este análisis los dendrímeros DP7 (*rctt*) y DP7 (*rccc*), los resultados obtenidos se resumen en la Tabla 19.

Tabla 19. Actividad antibacteriana contra aislados clínicos de los dendrímeros DP7 (*rctt*): CR-4-ALQ_(*rctt*)-(AAC-(K)-RLLR)₄ y DP7 (*rccc*): CR-4-ALQ_(*rccc*)-(AAC-(K)-RLLR)₄. Los valores de CMI/CMB se expresan en concentración μM .

Actividad antibacteriana de los dendrímeros DP7 (<i>rctt</i>) y DP7 (<i>rccc</i>) frente a aislados clínicos					
Cepa	Código	Sensible (S) Resistente (R) Multirresistente (M)	Resistente a:	DP7 (<i>rctt</i>)	DP7 (<i>rccc</i>)
				CMI/CMB μM ($\mu\text{g}/\text{mL}$)	CMI/CMB μM ($\mu\text{g}/\text{mL}$)
<i>E. coli</i>	1004	S	-	26/>52 (100/>200)	52/>52 (200/>200)
	129797	R	AM, SAM, CEF	26/52 (100/200)	26/>52 (100/>200)
	301755	M	AM, SAM, CPE, CAZ, CAX, CIP, GEN, NIT, NOR, STX	13/26 (50/100)	26/52 (100/200)
<i>S. aureus</i>	109095	R	P	26/52 (100/200)	52/52 (200/200)
	117719	M	P, TET	52/52 (200/200)	52/>52 (200/>200)
	124653	M	P, ERY, TET	13/52 (50/200)	26/>52 (100/>200)

P: penicilina, **TET:** tetraciclina, **ERY:** eritrosina, **AM:** ampicilina, **SAM:** ampicilina/sulbactam, **CPE:** cefepima, **CAZ:** ceftazidima, **CAX:** ceftriaxona, **CIP:** ciprofloxacina, **GEN:** gentamicina, **NIT:** nitrofuranto-in, **NOR:** norfloxacina, **STX:** trimetoprima/sulfametoxazol.

La cepa multirresistente de *E. coli* (301755) fue la más sensible al efecto del dendrímero DP7 (*rctt*) con una CMI de 13 μM , esta cepa es resistente a diversos antibióticos convencionales como ampicilina, ciprofloxacino, entre otros. Para el caso de las cepas resistente y sensible (129797 y 1004) la CMI exhibida por DP7 (*rctt*) fue de 26 μM . Por otro lado, con las cepas de *S. aureus* DP7 (*rctt*) fue más activo contra la cepa 124653 (CMI 13

μM), que es resistente a penicilina, tetraciclina y eritrosina; con las otras dos cepas 109095 (resistente) y 117719 (multirresistente) también presentó actividad con CMI de 26 y 52 μM , respectivamente. En resumen, el dendrímero DP7 (*rctt*) presentó actividad contra cepas de *E. coli* y *S. aureus*, sensibles, resistentes y mutirresistentes, con CMI que variaron de 13 a 52 μM , Tabla 19. De manera general la actividad de DP7 (*rctt*) y DP7 (*rccc*) fueron similares, sin embargo, el valor de CMB para DP7 (*rccc*) en todos los casos fue superior a los exhibidos por DP7 (*rctt*).

4.3.2 Curvas de Letalidad-Muerte y Sinergia

La cinética de inhibición del crecimiento causada por el dendrímero DP7 (*rctt*): CR-4-ALQ_(*rctt*)-(AAC-(K)-RLLR)₄, se evaluó frente a todas las cepas estudiadas. Contra *E. coli* ATCC 25922, el dendrímero DP7 (*rctt*), presentó un efecto bactericida a concentraciones de 26 μM (CMI) y 52 μM (2×CMI), ver Figura 44.a. Y se observó un efecto bacteriostático a 13 μM (0,5×CMI), en esta concentración exhibió un efecto inhibitorio significativo en comparación con la curva de crecimiento normal. Por otro lado, el efecto de DP7 (*rctt*) en la cepa de *S. aureus* ATCC 23922, no se presentó prolongación de la fase de latencia (adaptación) para este caso, solo exhibió efecto bacteriostático a una concentración de 52 μM (2×CMI), Figura 44.b.

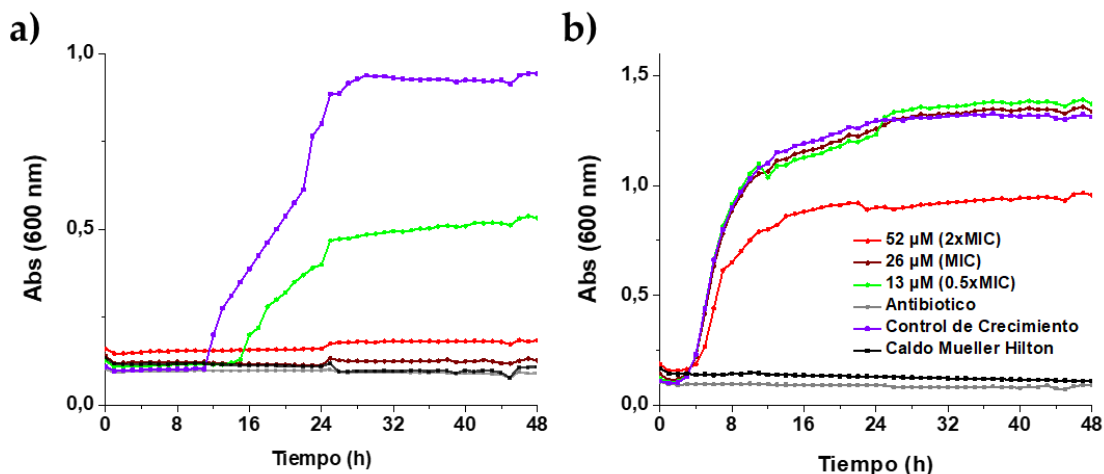


Figura 44. Curva de cinética de inhibición de crecimiento. a) Las cepas de *E. coli* ATCC 25922 y b) *S. aureus* ATCC 23922 se incubaron con dendrímero DP7 (*rctt*) durante 48 h utilizando concentraciones de dendrímero correspondientes a 0,5×CMI (línea verde), CMI (línea marrón) y 2×CMI (línea roja). Como antibiótico se empleó en a) Ciprofloxacino y en b) Vancomicina.

A las concentraciones evaluadas en la cinética de inhibición, el dendrímero no presentó actividad hemolítica significativa, para todos los casos fue menor al 4,3%, ver Tabla 20. Frente a la cepa de *E. coli* más sensible (ATCC 25922), se determinó si presenta un efecto sinérgico con CIP. Para todos los casos, el índice FIC calculado presenta una actividad indiferente (I), lo que sugiere que el dendrímero DP7 (*rctt*) actúa de manera más eficiente al ser usado de manera individual como tratamiento, ver Tabla 20.

Tabla 20. Actividad hemolítica, bacteriostática y bactericida del dendrímero DP7 (*rctt*): CR-4-ALQ_(*rctt*)-(AAC-(K)-RLLR)₄ y prueba de sinergia de mezclas de ciprofloxacina CIP (1) y dendrímero DP7 (*rctt*) (2).

Actividad Bacteriostática y Bactericida del dendrímero DP7 (<i>rctt</i>)				
Cepa	Código	Efecto μM ($\mu\text{g/mL}$)		$\mu\text{M}/\text{H}\%$
		Bacteriostático	Bactericida	
<i>E. coli</i>	ATCC 25922	13 (50)	26 (100)	13/3,7
	1004	>52 (>200)	>52 (>200)	52/4,3
	129797	>52 (>200)	>52 (>200)	52/4,3
	301755	>52 (>200)	>52 (>200)	52/4,3
<i>S. aureus</i>	ATCC 23922	26 (100)	>26 (>100)	26/4,0
	109095	52 (>200)	>52 (>200)	52/4,3
	117719	>104 (>400)	>104 (>400)	52/4,3
	124653	>26 (>100)	>26 (>100)	26/4,0
Ensayo de Sinergia contra <i>E. coli</i> ATCC 25922				
CIP (1) y Dendrímero (2) mixture (1/2 $\mu\text{g/mL}$)	FIC (MIC)		Índice FIC	Actividad
	1	2		
0,0058/3,125	2,00	0,0625	2,10	I
0,0058/6,25	2,00	0,125	2,10	I
0,0058/12,5	2,00	0,25	2,30	I
0,0058/25	2,00	0,5	2,50	I
0,0029/50	0,125	1,00	1,10	I
0,00018/100	0,0625	2,00	2,10	I
Promedio			2,00	I

Valores de CMI para (1) (0,0029 $\mu\text{g/mL}$) y (2) (50 $\mu\text{g/mL}$); Indiferencia (I) cuando FIC>1,00.

En general, los dendrímeros son moléculas que contienen cuatro secuencias anfipáticas, hidrofóbicas y cargadas positivamente. Estos resultados son consistentes con informes anteriores que sugieren que un aumento en la hidrofobicidad, la carga neta positiva y la anfipaticidad podrían mejorar la interacción e internalización de la membrana bacteriana de péptidos [143].

Con los resultados obtenidos en la evaluación de la actividad antibacteriana de los dendrímeros péptido-resorcinareno y péptidos control se cumple parcialmente el objetivo específico 4. Los resultados de actividad

de los péptidos control fueron publicados en la revista Chemistry & Biodiversity y RSC Advances. (Para más información, ver Anexos B.6 y B.7).

4.4 Actividad antifúngica

Para evaluar la actividad antifúngica se seleccionó el dendrímero que presentó mayor actividad antibacteriana y mejor rendimiento, DP7 (*rctt*): CR-4-ALQ_(*rctt*)-(AAC-(K)-RLLR)₄. El dendrímero fue evaluado frente a cepas de *C. albicans* y *C. auris*. En el caso de *C. albicans* se ensayó una cepa sensible (SC5314) y otra resistente a fluconazol (FLC), 256 HUSI-PUJ correspondiente a un aislado clínico. Para *C. auris* se empleó la cepa de referencia (435, sensible) y un aislado clínico resistente a FLC y a anfotericina B (537).

Tabla 21. Actividad antifúngica del dendrímero DP7 (*rctt*): CR-4-ALQ_(*rctt*)-(AAC-(K)-RLLR)₄.

Actividad antifúngica del dendrímero DP7 (<i>rctt</i>): CR-4-ALQ _(<i>rctt</i>) -(AAC-(K)-RLLR) ₄				
Cepa	Código	Sensible (S) Resistente (R)	Resistente a:	CMI/CMF μM (μg/mL)
<i>C. albicans</i>	SC5314	S	-	26/26 (100/100)
	256 HUSI-PUJ	R	FLC	13/13 (50/50)
<i>C. auris</i>	435 HUSI-PUJ	S	FLC	26/>26 (100/>100)
	537 HUSI-PUJ	R	FLC, AmB	>26/>26 (>100/>100)

FLC: Fluconazol, **AmB:** Anfotericina B.

Los estudios de actividad antifúngica de DP7 (*rctt*) mostraron valores de CMI y CMF de 26 μM para *C. albicans* ATCC SC5314 cepa sensible a fluconazol, interesantemente, el aislado de *C. albicans* 256 HUSI-PUJ resistente a fluconazol, fue más sensible al dendrímero, con valores de CMI y CMF de 13 μM. Las cepas de *C. auris* fueron menos sensibles al efecto de DP7 (*rctt*), ver Tabla 21. Previamente, se había evaluado la actividad antifúngica del péptido palindrómico BF(32-35)_{pal}: RLLRLLR, que presenta dos copias de BF (32-35) frente a *C. Albicans* ATCC SC5314 y el aislado de *C. Albicans* 256 HUSI-PUJ encontrándose valores de CMI >183 μM [144], [145], mientras que el dendrímero DP7 mostró una mayor actividad antifúngica con valores de CMI de 26 y 13 μM, respectivamente. Estos resultados sugieren que la presentación de la secuencia en el dendrímero puede ser la causa de que se potencie la actividad antifúngica.

Los ensayos de actividad antifúngica no estaban involucrados dentro de los objetivos de este trabajo por lo que son un logro adicional. Parte de los resultados y optimización de las metodologías fueron publicados en la revista *Antibiotics* (Para más información, ver Anexos B.8 y B.9).

4.5 Actividad citotóxica

La actividad citotóxica de los dendrímeros DP7 (*rctt*) y DP3, fue evaluada mediante el ensayo de hemólisis. El porcentaje de actividad hemolítica para los péptidos control había sido previamente reportado, en el caso del péptido LfcinB (20-25): RRWQWR (P1) presentó un porcentaje de hemólisis del 1%, mientras que el péptido BF(32-35): RLLR (P5) presentó una alta actividad hemolítica con un 63% a una concentración de 200 $\mu\text{g}/\text{mL}$ [11], [146]. Los dendrímeros DP3 y DP7 (*rctt*), fueron evaluados a diferentes concentraciones, ver Figura 45. Se puede observar que DP7 (*rctt*) presentó valores de hemólisis inferiores al 5% para todas las concentraciones evaluadas; lo cual contrasta con la secuencia original (P5) RLLR que es altamente hemolítica. Por otro lado, DP3 presentó valores inferiores al 10% de hemólisis a concentraciones inferiores a 100 $\mu\text{g}/\text{mL}$; pero causó un porcentaje de hemólisis cercano al 15% a una concentración de 200 $\mu\text{g}/\text{mL}$. Podemos inferir que la generación de dendrímeros promovió una disminución de la actividad hemolítica del péptido BF(32-35): RLLR y a su vez no genera un aumento considerable de la actividad hemolítica en secuencias como RRWQWR.

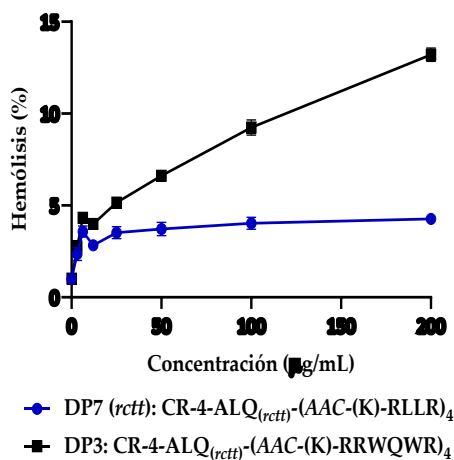


Figura 45. Actividad hemolítica de dendrímeros peptídicos de resorcinareno derivados de LfcinB (20-25) y BF (32-35).

Finalmente, se evaluó la actividad citotóxica de los dendrímeros péptido-resorcinareno, frente a diferentes líneas celulares tanto cancerosas como no cancerosas; estas fueron fibroblastos (cultivo primario normal) y dos líneas de cáncer la MCF-7 (cáncer de mama) y HeLa (cáncer de cervix), los resultados obtenidos (ver Figura 46), sugieren que no presentan ningún tipo de efecto en estos modelos. De igual manera, el péptido LfcinB (20-25): RRWQWR ha sido probado previamente y este al igual que su dendrímero no presenta ningún efecto contra las líneas celulares evaluadas, sin embargo, si se puede inferir que aunque la polivalencia en algunos casos potenciaron la actividad anticancerígena contra MCF-7 como lo fue para el péptido tetramérico LfcinB (20-25)₄: (RRWQWR)₄-K₂-C₂ [147], la polivalencia no es el único criterio que se debe considerar para que una molécula presente actividad anticancerígena, dado que los dendrímeros aquí sintetizados cumplieran con este criterio, aun así no presentaron ningún tipo de efecto contra esta línea celular. Este resultado, sugiere la acción selectiva de los dendrímeros como posibles agentes antimicrobianos en bacterias y/o hongos, generando una selectividad a estos patógenos y no a las células en un posible modelo *in vivo*.

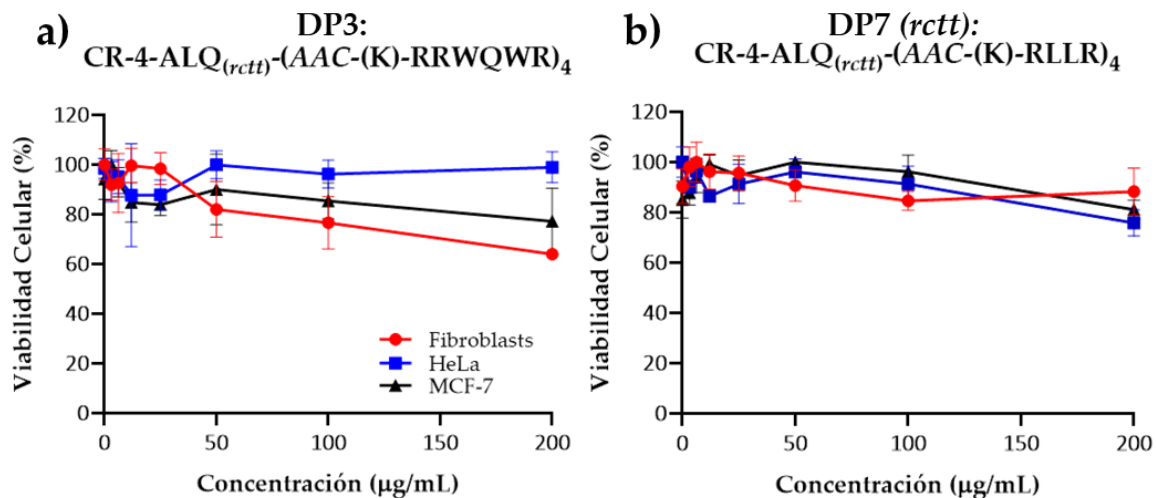


Figura 46. Actividad citotóxica sobre fibroblastos y líneas MCF-7 y HeLa de los dendrímeros a) DP3 y b) DP7 (*rctt*).

Los ensayos de actividad citotóxica no están involucrados dentro de los objetivos por lo que son un logro adicional. Los resultados de actividad antibacteriana, antifúngica y citotóxica fueron publicados en la publicación en la revista *Antibiotics* (Para más información, ver anexo B.1).

5. Conclusiones

Once péptidos derivados de las secuencias LfcinB(20-25): RRWQWR y BF(32-35): RLLR fueron sintetizados usando de la síntesis de péptidos en fase sólida (SPPS), y la estrategia Fmoc/tBu. Por familia se incluyeron análogos lineales, análogos polivalentes (tetrámeros) y cuatro péptidos funcionalizados con azida en el extremo N-terminal, para dos de ellos se incluyó en la secuencia una molécula espaciadora (Ahx). Se optimizó el reactivo empleado para la remoción del grupo Fmoc del alfa-amino de los aminoácidos; reduciendo la concentración de la 4-metilpiperidina a una décima parte de la concentración comúnmente empleada en SPPS-Fmoc/tBu. Se evidenció como subproducto del clivaje de los azida-péptidos un producto en el que la azida se redujo a grupo amino; el coctel de clivaje que mostró un menor porcentaje de este subproducto fue el que contenía el ácido trifluoroacético y como scavenger el agua.

Por otro lado, dos núcleos derivados de calix[4]resorcinareno fueron sintetizados mediante ciclocondensación catalizada por ácido entre un aldehído y resorcinol. Estas moléculas precursoras se obtuvieron con porcentajes de pureza cromatográficas superiores al 80% y su caracterización mediante masas corroboró que se obtuvieron las especies deseadas. Los resorcinarenos fueron funcionalizados con el grupo alquino en los grupos hidroxilos fenólicos y en el puente de metileno, para este último fue necesario usar en la reacción de formación del resorcinareno el 4-(prop-2-in-1-iloxi)benzaldehído. Para el caso de los derivados de alquino-resorcinareno se evidenció a formación de confórmeros, así, para el resorcinareno CR-8-ALQ se obtuvo la configuración corona-*rccc* de manera mayoritaria, mientras que para el resorcinareno CR-4-ALQ se lograron obtener y aislar los confórmeros silla-*rctt* y corona-*rccc*.

A partir de los azida-péptidos, P3: K(N₃)-RRWQWR y P7: K(N₃)-RLLR, y el macrociclo funcionalizado CR-4-ALQ con el grupo alquino, fue posible sintetizar tres dendrímeros tetra-funcionalizados obtenidos por la

reacción de cicloadición de azida-alquino catalizada por cobre, CuAAC (química click). Parámetros como solvente, proporciones, temperatura y catalizador, fueron optimizados uno a uno, encontrando que las mejores condiciones para llevar a cabo esta reacción click entre péptidos y derivados de resorcinareno son: solvente DMF:H₂O (2:1), temperatura ambiente, tiempos de reacción de 2 horas, catalizador CuSO₄·5H₂O y ascorbato de sodio. Se evidencio que secuencias largas necesitan mayores tiempos de reacción y se presentan mayores subproductos correspondientes a funcionalizaciones incompletas. Los dendrímeros DP3 y DP7 se obtuvieron con purzas cromatográficas superiores al 80%.

Estos nuevos dendrímeros presentaron actividad antimicrobiana contra *E. coli* ATCC 25922, *S. aureus* ATCC 23922 y aislados clínicos bacterianos y cepas de *Candida spp.* (con valores de CMI que variaron entre 13 y 52 µM), esta actividad fue superior a la presentada por los péptidos control y el núcleo de resorcinareno, sugiriendo que la estructura polivalente potencia la actividad antimicrobiana. Los dendrímeros péptido-resorcinareno no presentaron efecto citotóxico en sangre, fibroblastos o líneas celulares de cáncer, lo que significa que moléculas pueden ser consideradas como agentes antimicrobianos selectivos.

En este trabajo se estableció una nueva ruta para la síntesis de dendrímeros funcionalizados con secuencias peptídicas, en los que se incluyó un núcleo no proteico, es la primera vez que se reporta la síntesis de dendrímeros tetra-funcionalizados con secuencias derivadas de LfcinB y BF y se demostró que estas macromoléculas presentan actividad antimicrobiana contra cepas Gram-positivas y Gram-negativas, sensibles y resistentes a antibióticos; adicionalmente presentaron actividad antifúngica.

6. Productos Académicos

Parte de los resultados obtenidos en esta tesis doctoral fueron publicados en las siguientes modalidades: (i) nueve (9) publicaciones en revista científica indexada, (ii) cinco (5) presentaciones de póster en congreso científico internacional/nacional y (iii) una (1) presentación oral en congreso científico nacional.

Los artículos científicos y certificados de participación fueron consignados en el anexo B de la siguiente manera:

Artículos Científicos:

1. **Título del artículo:** Use of Click Chemistry for Obtaining an Antimicrobial Chimeric Peptide Containing the LfcinB and Buforin II Minimal Antimicrobial Motifs

Revista: ChemistrySelect

Estado: Publicado (2020)

Descripción: En este artículo se reportan los estudios preliminares de las condiciones de reacción de química click usadas en la síntesis de los dendrímeros péptido-resorcinareno.

2. **Título del artículo:** Short peptides conjugated to non-peptidic motifs exhibit antibacterial activity

Revista: RSC Advances

Estado: Publicado (2020)

Descripción: En este artículo se reportan la actividad antibacteriana contra *E. coli* ATCC 25922 y *S. aureus* ATCC 25923 de los péptidos control RRWQWR y RWQWRWQWR.

3. **Título del artículo:** Designing Short Peptides: A Sisyphean Task?

Revista: Current Organic Chemistry

Estado: Publicado (2020)

Descripción: Artículo de revisión como parte del estado del arte de esta investigación. En este, se plantean las posibles estrategias químicas que pueden ser empleadas para potenciar la actividad antimicrobiana de péptidos sintéticos.

4. **Título del artículo:** Designing Chimeric Peptides: A Powerful Tool for Enhancing Antibacterial Activity

Revista: Chemistry & Biodiversity

Estado: Publicado (2020)

Descripción: En este artículo se reportan la actividad antibacteriana contra *E. coli* ATCC 25922 y *S. aureus* ATCC 25923 de los péptidos control RLLR y RLLRLLR, así como la optimización del ensayo de sinergia que se realizó como un trabajo complementario a los objetivos propuestos.

5. **Título del artículo:** Efficient Separation of C-Tetramethylcalix[4]resorcinarene Conformers by Means of Reversed-Phase Solid-Phase Extraction

Revista: ACS Omega

Estado: Publicado (2022)

Descripción: En este artículo se reporta el nuevo método para purificación de derivados de C-tetrametilcalix[4]resorcinareno por RP-SPE que se desarrolló como parte de esta investigación y que fue empleado para la purificación de los derivados sintetizados.

6. **Título del artículo:** Chimeric Peptides Derived from Bovine Lactoferricin and Buforin II: Antifungal Activity against Reference Strains and Clinical Isolates of *Candida* spp.

Revista: Antibiotics

Estado: Publicado (2022)

Descripción: En este artículo se reportan los resultados de la actividad antifúngica de los péptidos control RLLR y RLLRLLR contra los aislados fúngicos clínicos usados en el actual proyecto como complemento al objetivo específico 4.

7. **Título del artículo:** In Vitro Antifungal Activity of Chimeric Peptides Derived from Bovine Lactoferricin and Buforin II against *Cryptococcus neoformans* var. *grubii*

Revista: Antibiotics

Estado: Publicado (2022)

Descripción: Investigación complementaria donde se reportan los resultados de la actividad antifúngica contra *Cryptococcus neoformans* var. *grubii* de los péptidos control RRWQWR y RLLRLLR. Así como la optimización del ensayo de concentración mínima fungicida.

8. **Título del artículo:** Copper(I)-Catalyzed Alkyne–Azide Cycloaddition (CuAAC) “Click” Reaction: A Powerful Tool for Functionalizing Polyhydroxylated Platforms

Revista: ACS OMEGA

Estado: Publicado (2023)

Descripción: Artículo de revisión como parte del estado del arte de esta investigación. En este, se plantean las condiciones click usadas en la actualidad para bases polihidroxiladas del tipo calixareno y resorcinareno.

9. **Título del artículo:** Peptide-Resorcinarene Conjugates Obtained via Click Chemistry: Synthesis and Antimicrobial Activity

Revista: Antibiotics

Estado: Publicado (2023)

Descripción: En este artículo se reportan los resultados de síntesis y de la actividad antimicrobiana y citotóxica de los dendrímeros péptidos-resorcinareno sintetizados en el actual proyecto.

Presentaciones orales:

1. **Título de la presentación Oral:** Uso de la cicloadición azida-alquino catalizada por cobre (química click) en la obtención de un péptido quimérico antibacteriano derivado de la Lactoferrina Bovina y la Buforina II.

Congreso: IX SIMPOSIO DE QUÍMICA APLICADA (IX SIQUIA) Y I CONGRESO INTERNACIONAL DE NANOQUÍMICA, NANOFÍSICA Y NANOMEDICINA (I CINNN)

Lugar y año: Armenia, Colombia, 2019.

Descripción:

Reconocimiento: Mención Honorífica – Como el mejor trabajo de investigación en la categoría oral, sesión Química orgánica y productos Naturales.

Posters:

1. **Título del poster:** Antimicrobial activity of peptide-resorcinarene dendrimers derived from the sequence BF (32-35): RLLR obtained by the CuAAC click chemical reaction

Congreso: XXXIX Reunión Bienal de Química

Lugar y año: Zaragoza, España 2023.

2. **Título del poster:** Evaluación del Efecto Bacteriostático/Bactericida de Péptidos Quiméricos Derivados de la Lactoferrina Bovina Y Buforina II.

Congreso: XVIII Congreso Colombiano de Química

Lugar y año: Popayán, Colombia, 2019.

3. **Título del video-poster:** Synthetic Lfcinb Derived Peptides: Antimicrobial Activity.

Congreso: III Workshop de “Péptidos terapéuticos para bioaplicaciones”

Lugar y año: Valparaíso, Chile, 2021.

Reconocimiento: 1 Lugar en la Sección “Video Póster”.

4. **Título del poster:** Reacción de Formación de C-Tetrametilcalix[4]resorcinareno: Estudio de la Formación de Confórmeros Mediante RP-HPLC.

Congreso: 34° Congreso Latinoamericano de Química CLAQ 2020, el XVIII COLACRO, el X COCOCRO, el II SPAE y el IV C2B2

Lugar y año: Cartagena, Colombia, 2021.

5. **Título del poster:** Antibacterial Activity of Peptide-Resorcinarene Dendrimers Synthesized Through Click Chemistry Azide-Alkyne Cycloaddition Reaction.

Congreso: 36th European and 12th International Peptide Symposium EPS 2022

Lugar y año: Sitges, España, 2022.

6. **Título del poster:** Clinical isolates multi drug-resistant of *Candida* spp., are susceptible to palindromic peptide: RWQWRWQWR, derived from Bovine Lactoferricin

Congreso: 36th European and 12th International Peptide Symposium EPS 2022

Lugar y año: Sitges, España, 2022.

Otros productos académicos

Tesis de Pregrado (Codirección):

1. **Título:** Evaluación De La Actividad Antibacteriana De Péptidos Sintéticos Análogos De La Buforina II Contra *Escherichia Coli*, *Pseudomonas aeruginosa* y *Staphylococcus aureus*.

Estudiante: Angie Katherine Hernández Cardona

Universidad: Universidad Colegio Mayor de Cundinamarca.

Lugar y año: Bogotá, Colombia, septiembre 2019.

Reconocimiento: Mención meritoria.

2. **Título:** Actividad Antibacteriana, Antifúngica y Otras Aplicaciones de Dendrímeros con Núcleos del Tipo Calixareno y/o Resorcinareno: Revisión del Estado del Arte.

Estudiante: Andrea Carolina Hernández Pardo

Universidad: Universidad Colegio Mayor de Cundinamarca.

Lugar y año: Bogotá, Colombia, noviembre 2021.

Reconocimiento: Mención meritoria.

3. **Título:** Determinación de Mecanismos de Acción de Péptidos Frente A Bacterias: Revisión del Estado del Arte de las Metodologías Empleadas.

Estudiante: Karen Tatiana Díaz Rodríguez

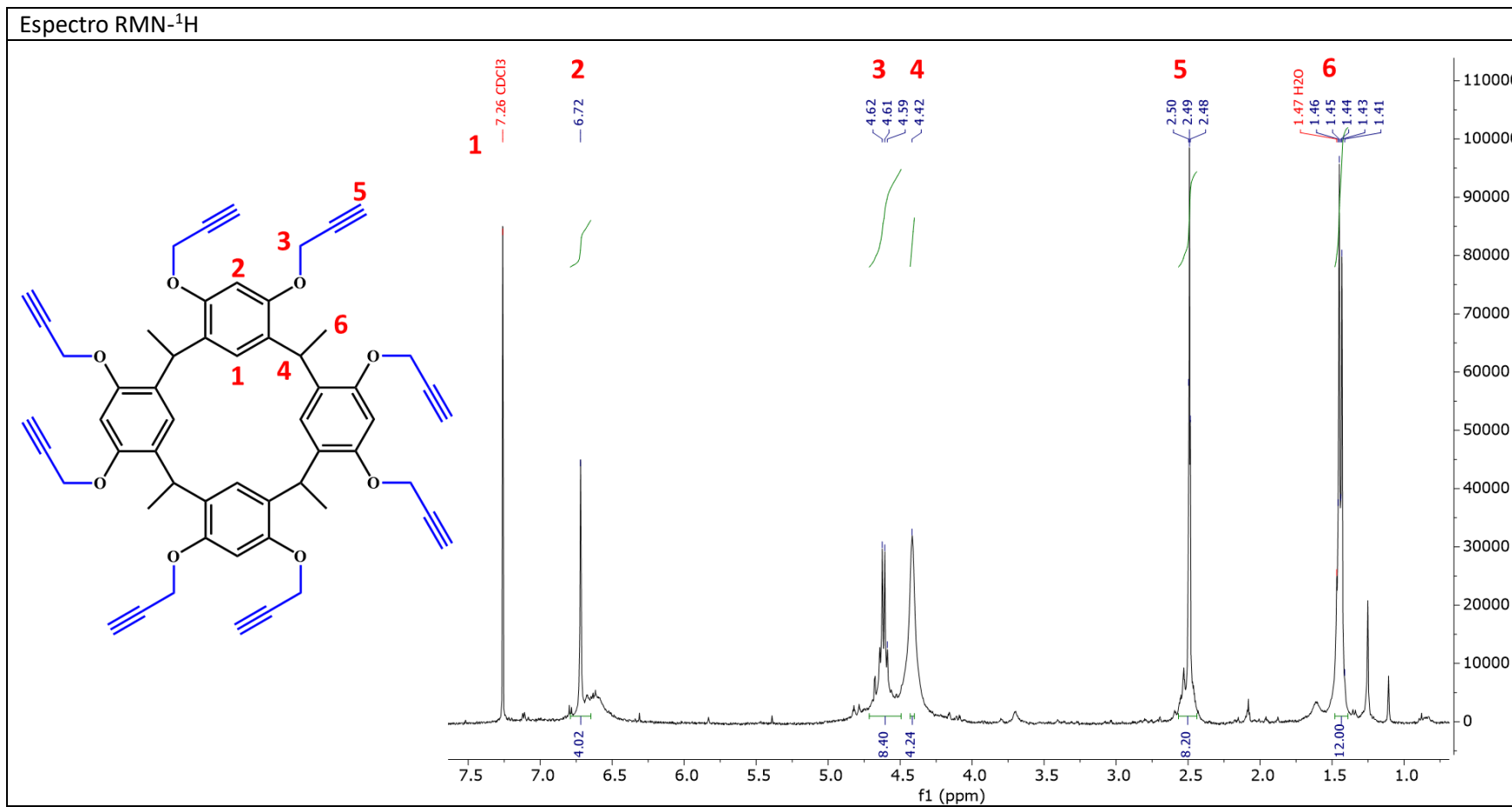
Universidad: Universidad Colegio Mayor de Cundinamarca.

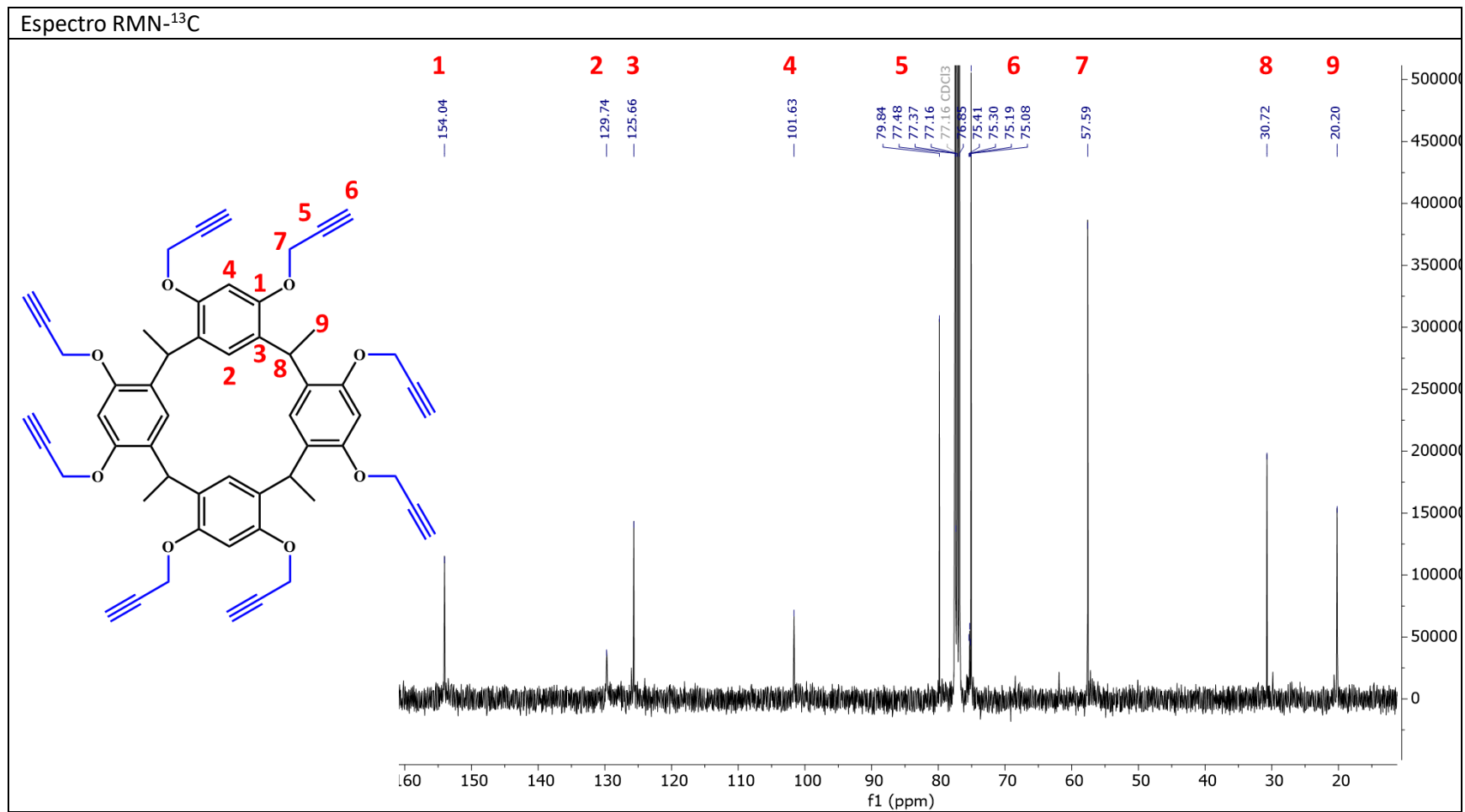
Lugar y año: Bogotá, Colombia, abril 2021.

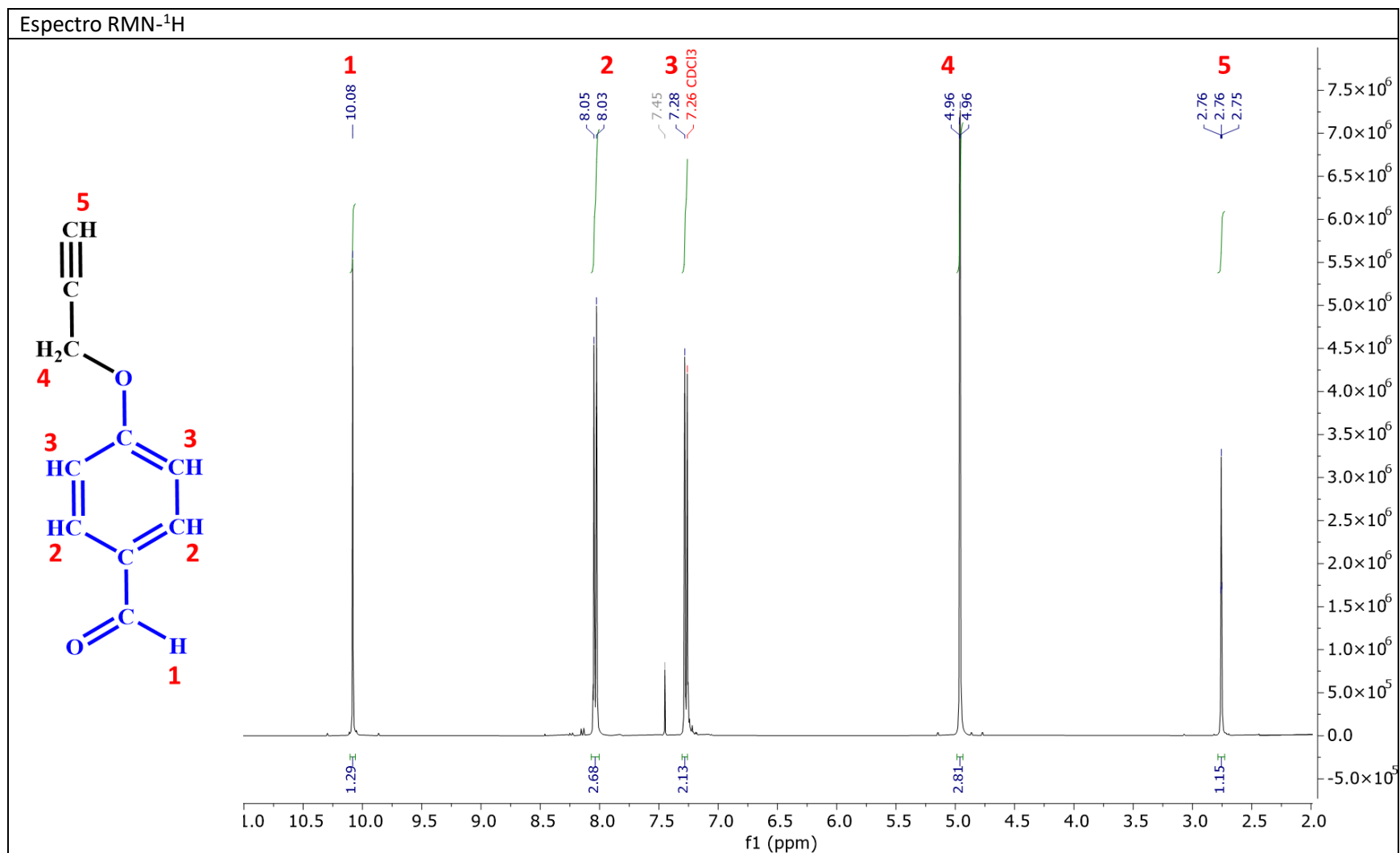
7. Anexo A: Espectros RMN ^1H y ^{13}C de derivados de resorcinareno y precursores. Reporte de síntesis de los péptidos sintéticos.

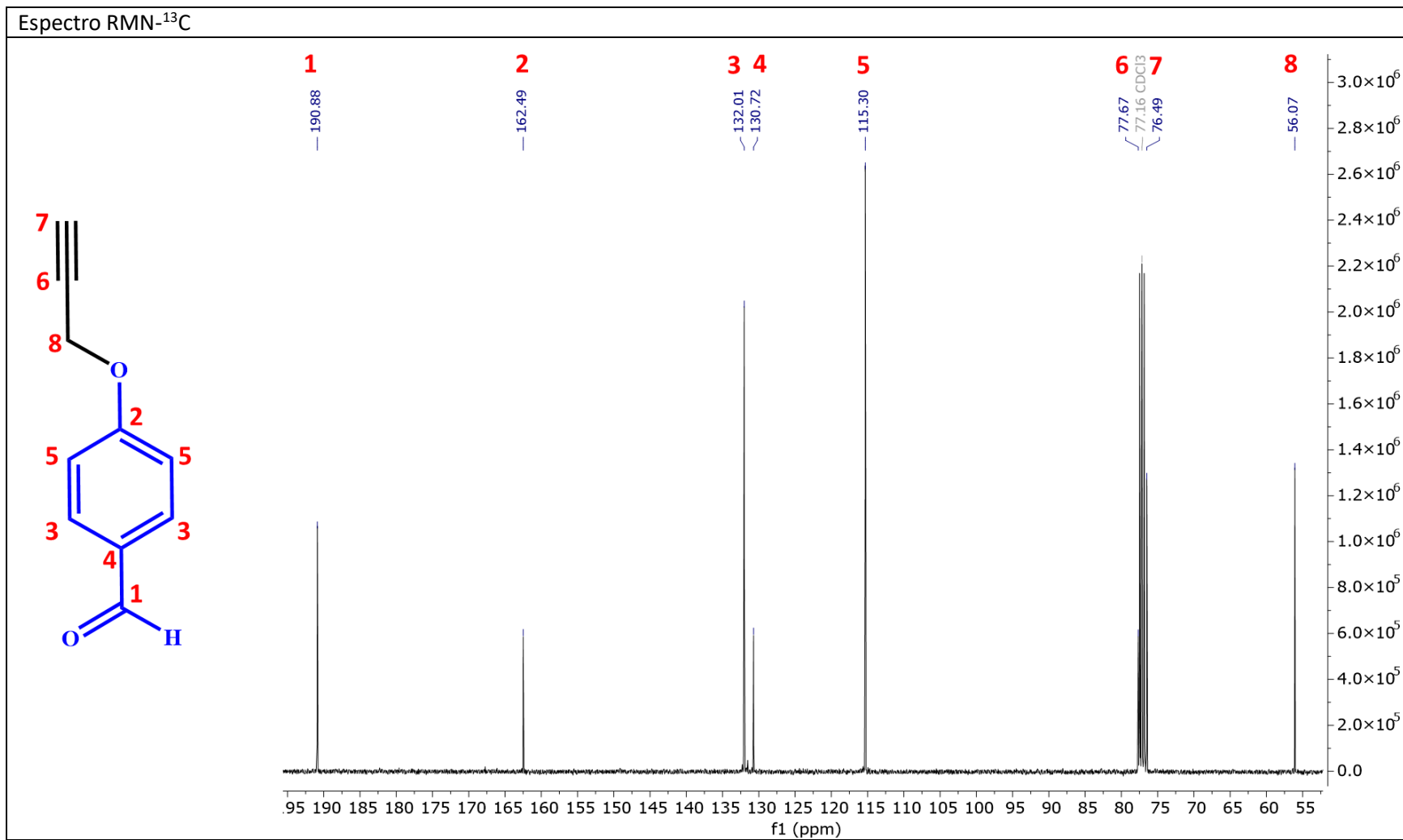
	Pag.
A.1. Espectros de RMN ^1H y ^{13}C para CR-8-ALQ (<i>rccc</i>)	92-93
A.2. Espectros de RMN ^1H y ^{13}C de 4-(prop-2-in-1-iloxi)benzaldehído	94-95
A.3. Espectros de RMN ^1H y ^{13}C para CR-4-ALQ (<i>rctf</i>)	96-97
A.4. Espectros de RMN ^1H y ^{13}C para CR-4-ALQ (<i>rccc</i>)	98-99
A.5. Reporte de síntesis de los péptidos sintéticos	100-113

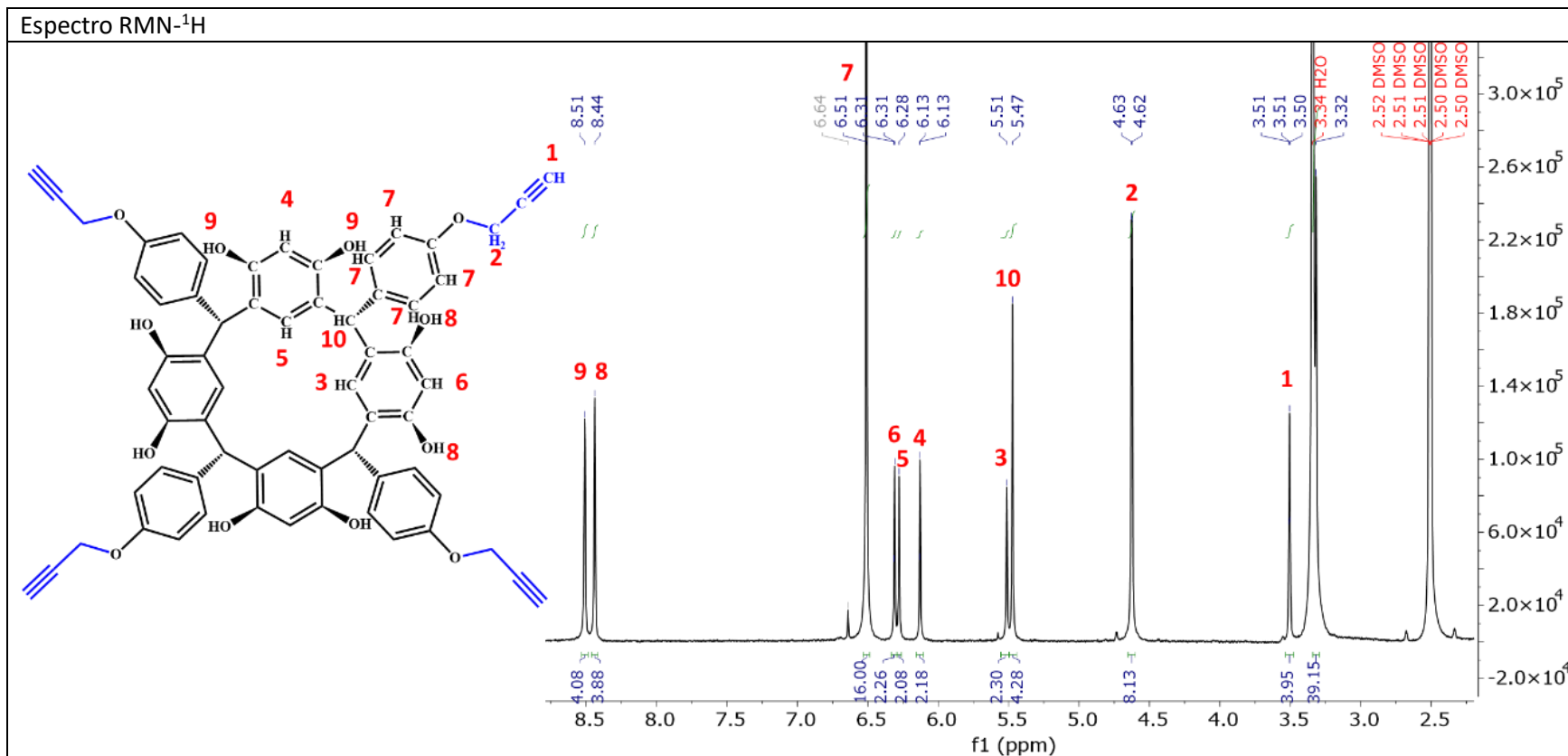
A.1. Espectros de RMN ^1H y ^{13}C para CR-8-ALQ (rccc)

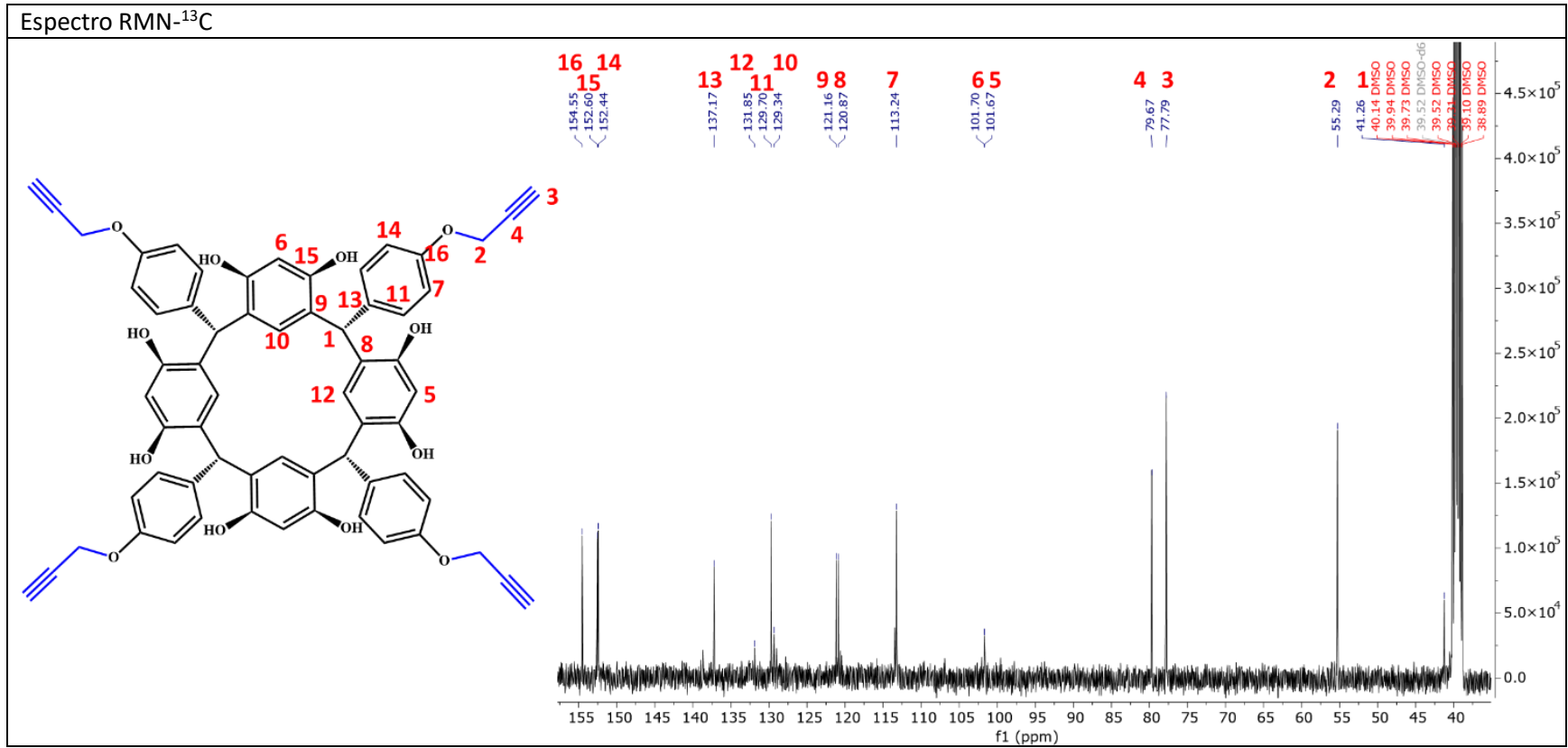


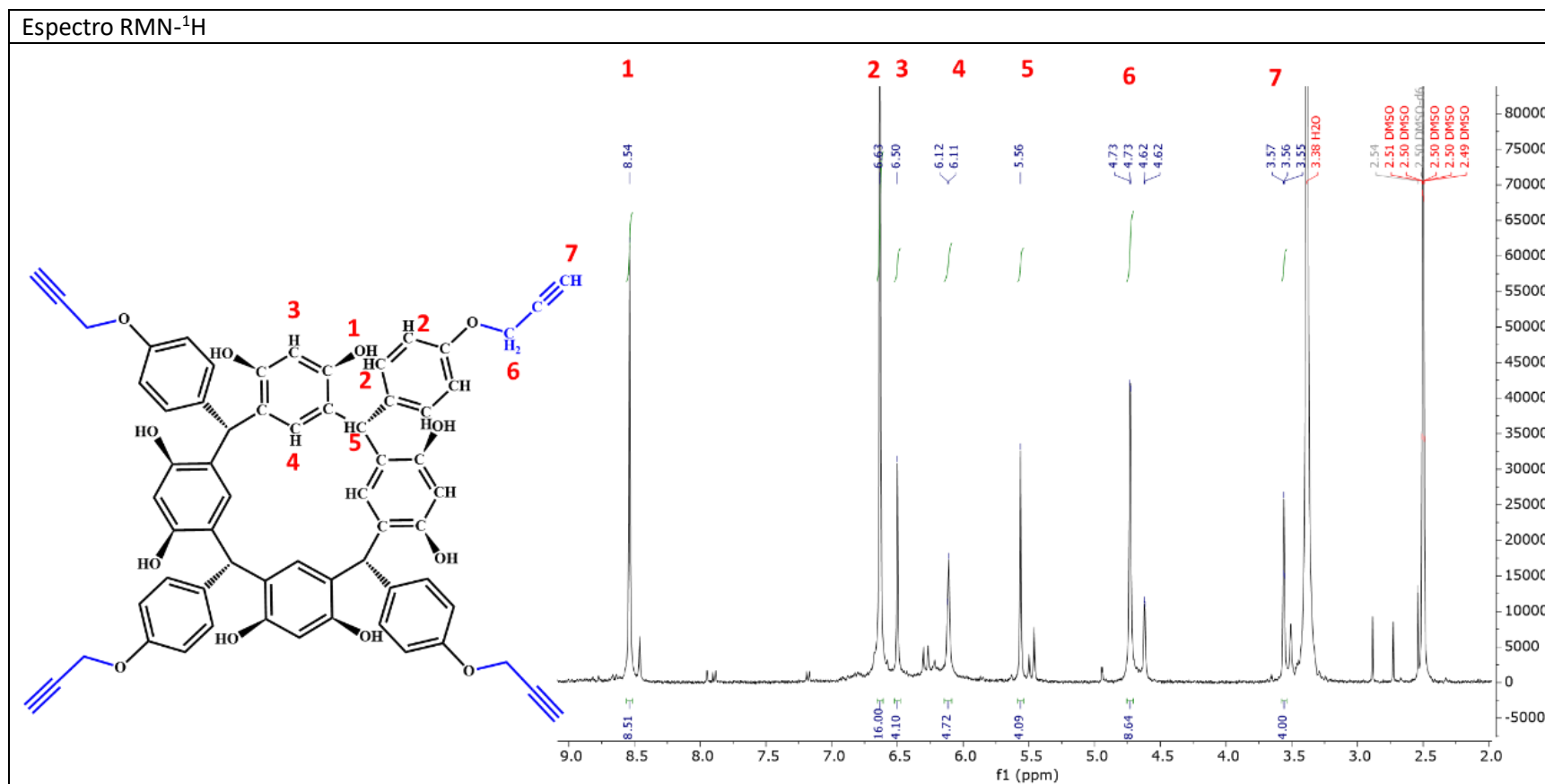


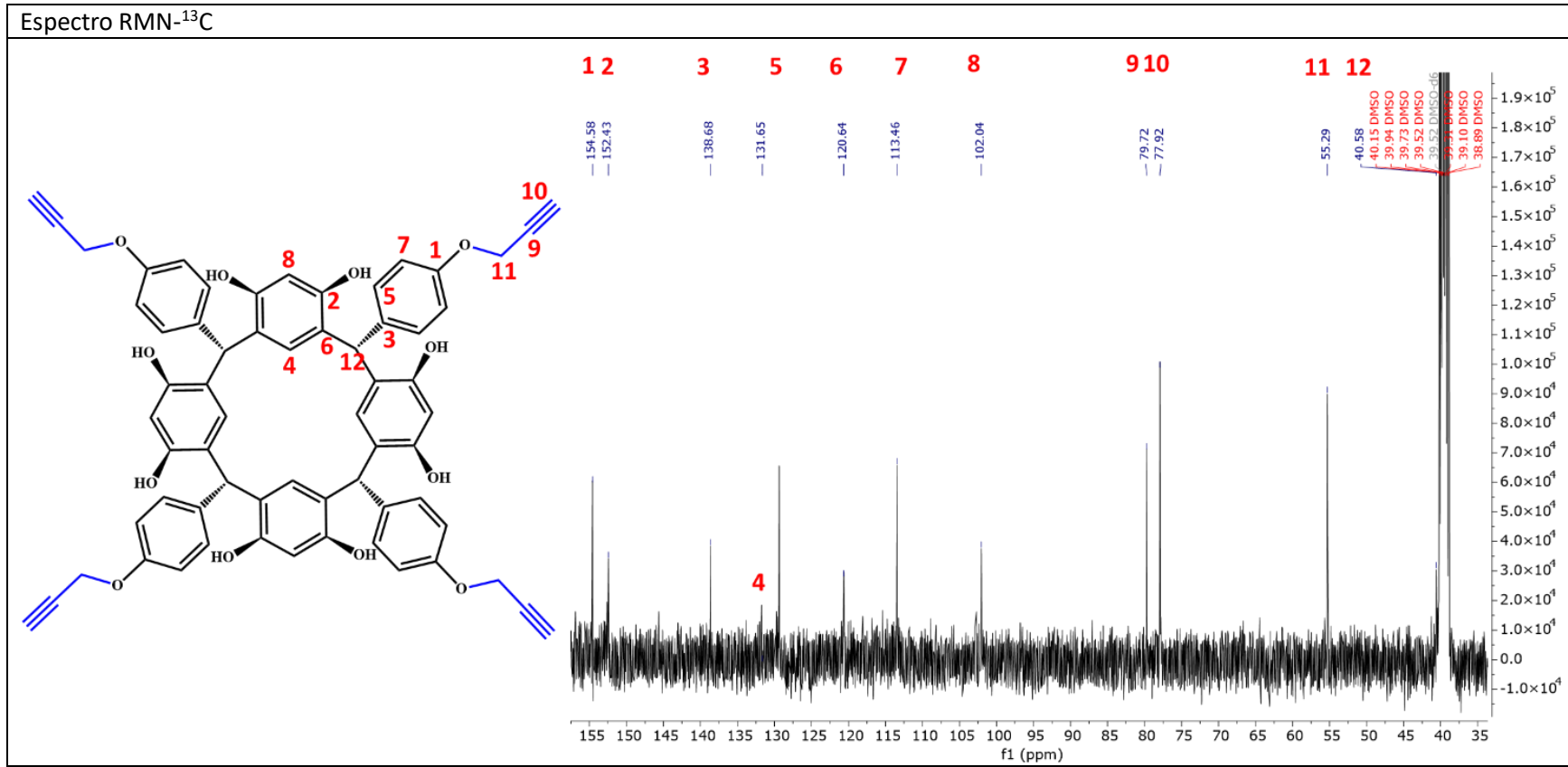
A.2. Espectros de RMN ^1H y ^{13}C de 4-(prop-2-in-1-iloxi)benzaldehído



A.3. Espectros de RMN ^1H y ^{13}C para CR-4-ALQ (*rcftt*)



A.4. Espectros de RMN ^1H y ^{13}C para CR-4-ALQ (rccc)



Síntesis y caracterización de los péptidos diseñados

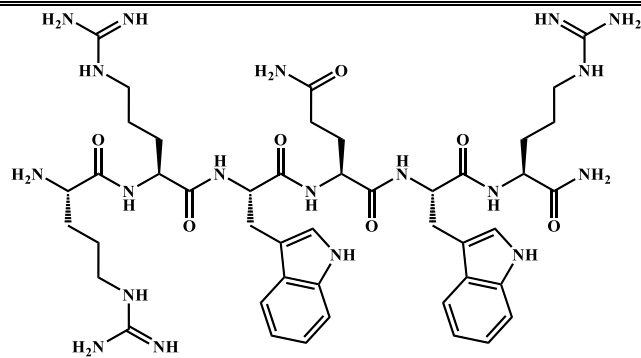
A continuación, se presentan los resultados obtenidos de la síntesis química de los péptidos sintéticos (Tabla A.3), en cada una de las figuras se encuentra reportada la siguiente información: Estructura (Panel A), comportamiento de síntesis (Panel B), caracterización del péptido puro por RP-HPLC (Panel C) y espectrometría de masas MALDI-TOF (Panel D).

Tabla A.3. Secuencias derivadas de LfcinB(20-25) y BFII(32-35) sintetizadas, purificadas y caracterizadas.

Familia	Código	Secuencia
LfcinB (20-25)	P1	RRWQWR
	P2	((RRWQWR) ₂ K-Ahx-C) ₂
	P3	K(N ₃)-RRWQWR
	P4	K(N ₃)-Ahx-RRWQWR
BF (32-35)	P5	RLLR
	P6	((RLLR) ₂ K-Ahx-C) ₂
	P7	K(N ₃)-RLLR
LfcinB (20-25)_{pal}	P8	RWQWRWQWR
	P9	K(N ₃)-RWQWRWQWR
Otros	P10	K(N ₃)-Ahx-RLLRRLLR
	P11	K(N ₃)-AAAA

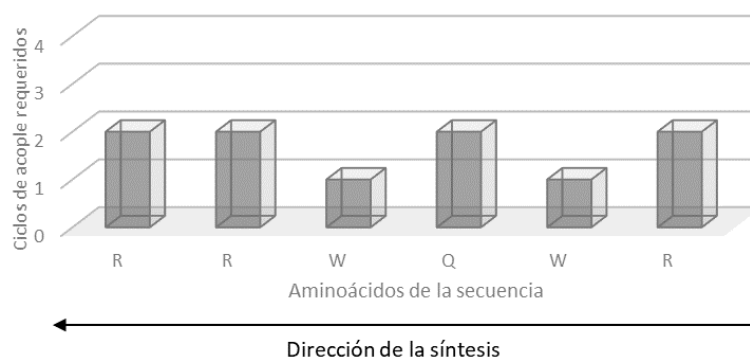
REPORTE DE SÍNTESIS (1) – LfcinB(20-25): RRWQWR

A

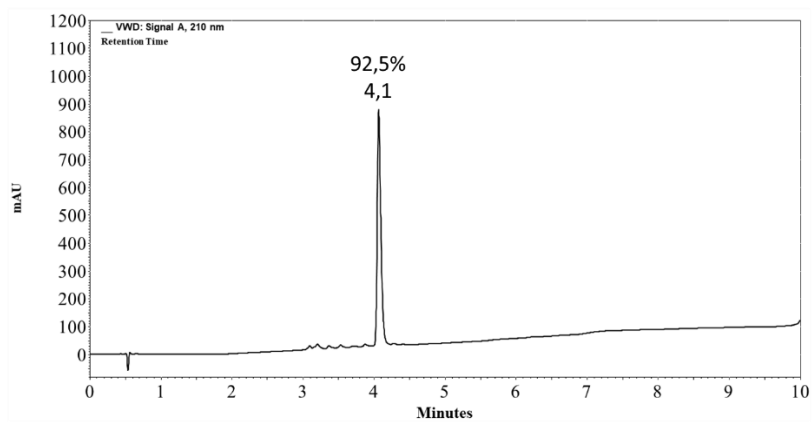


Exact Mass: 985.55

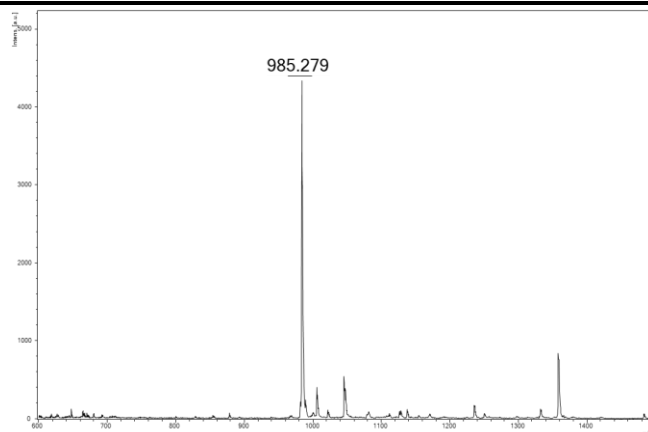
B



C

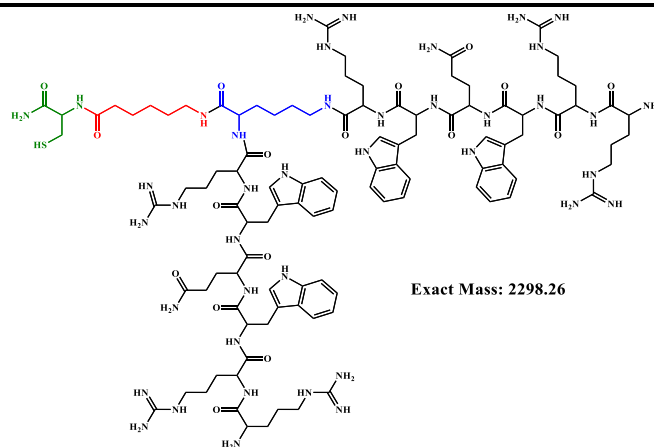


D

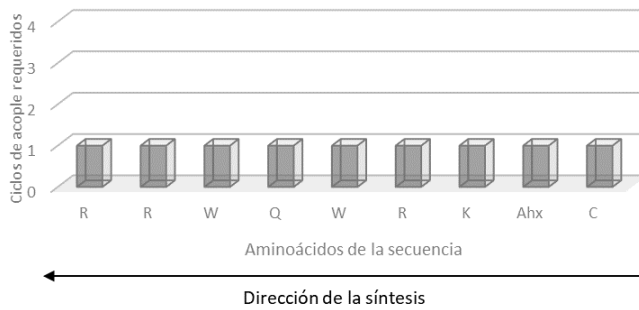


REPORTE DE SÍNTESIS (2) – Precursor dimérico (RRWQWR)₂K-Ahx-C

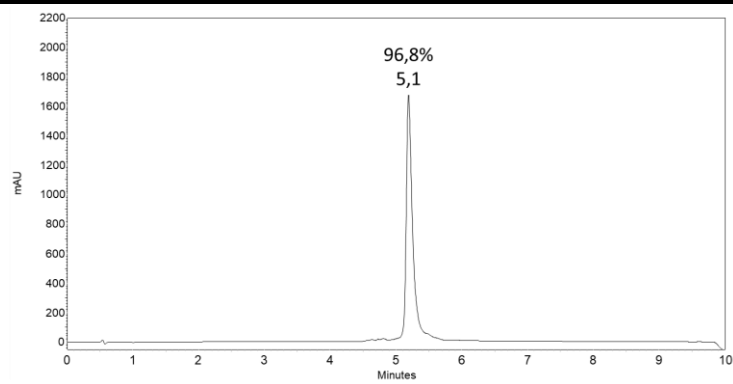
A



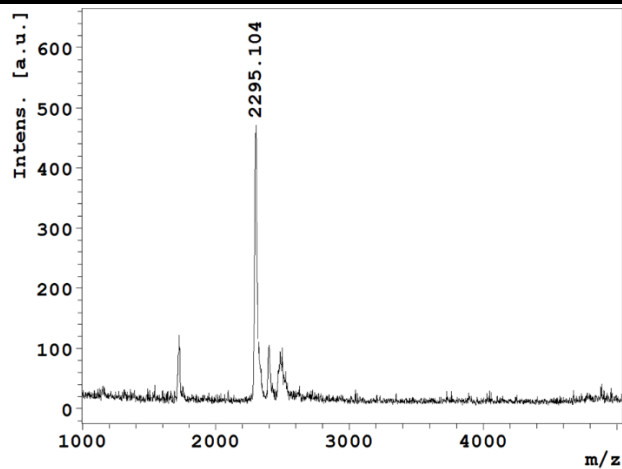
B



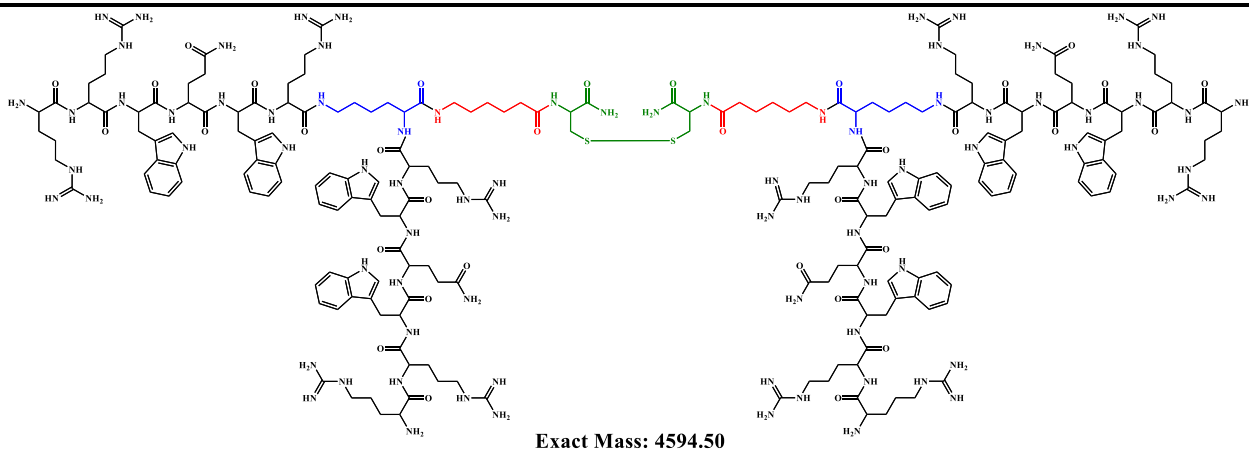
C



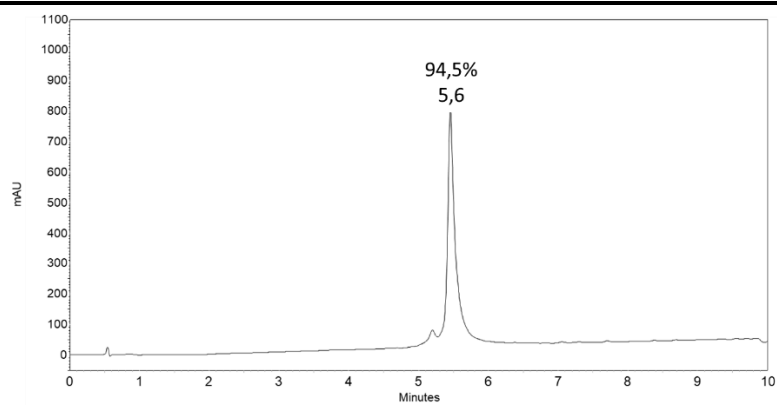
D

REPORTE DE SÍNTESIS (2.1) – ((RRWQWR)₂K-Ahx-C)₂

A

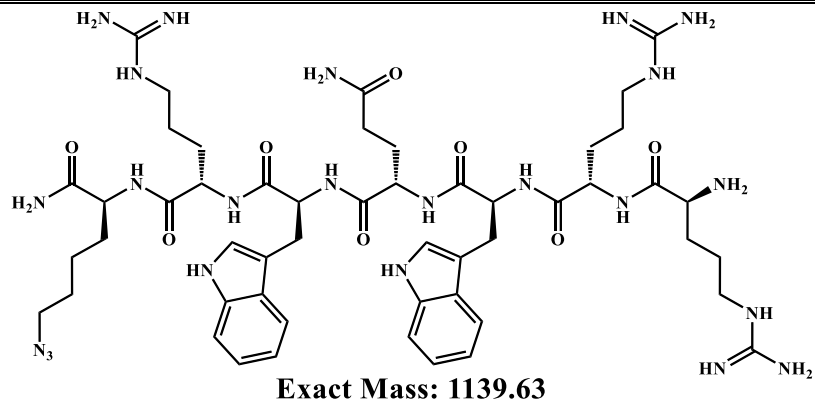


C

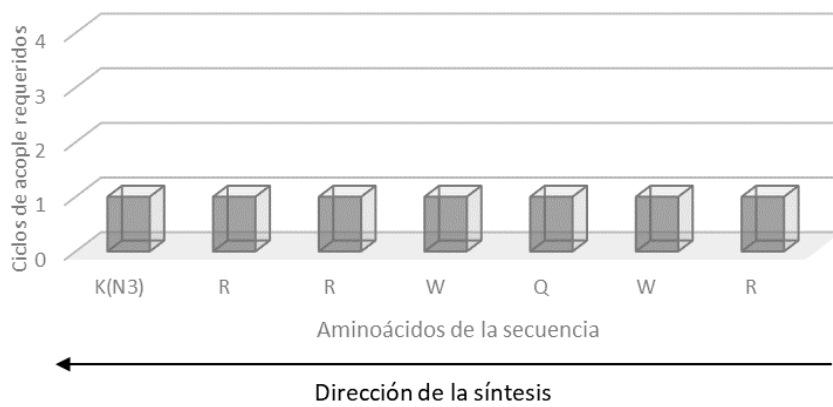


REPORTE DE SÍNTESIS (3) – K(N₃)-RRWQWR

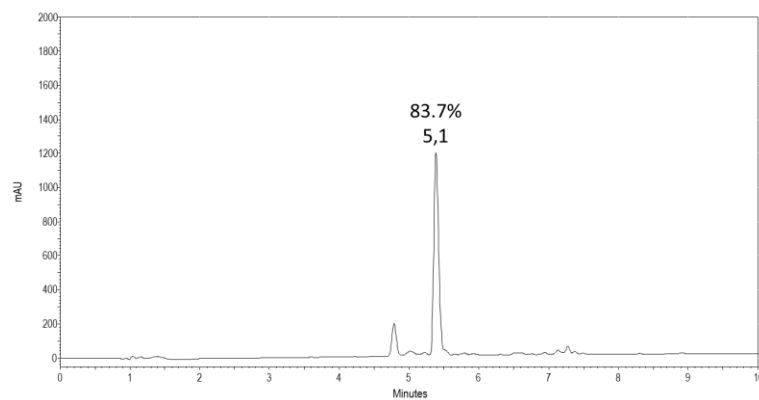
A



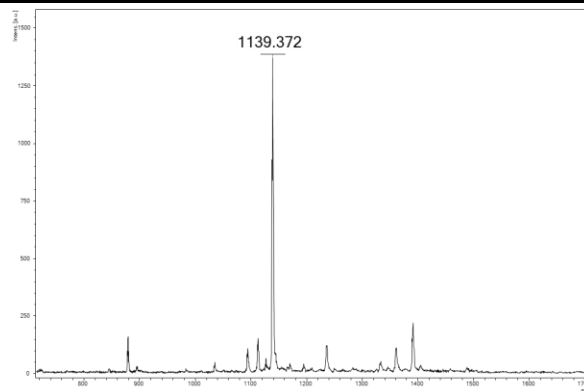
B



C

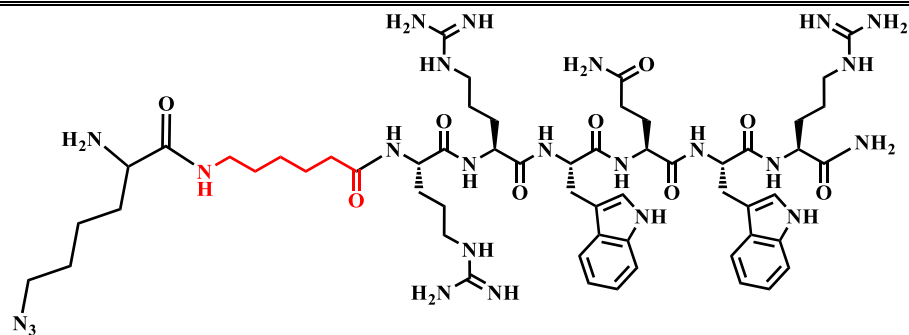


D



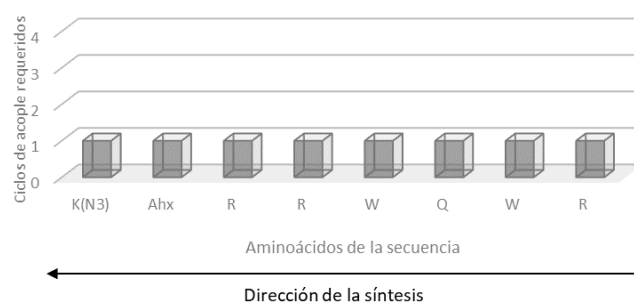
REPORTE DE SÍNTESIS (4) – K(N₃)-Ahx-RRWQWR

A

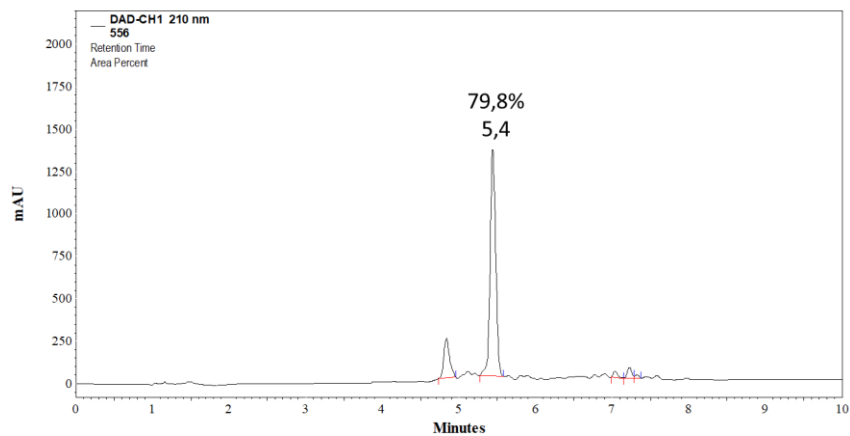


Exact Mass: 1252.72

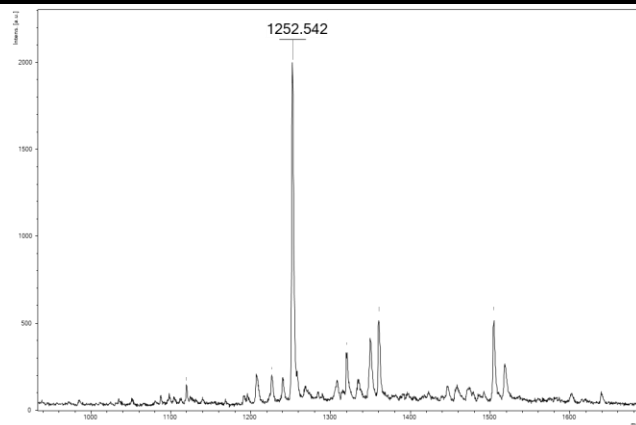
B



C

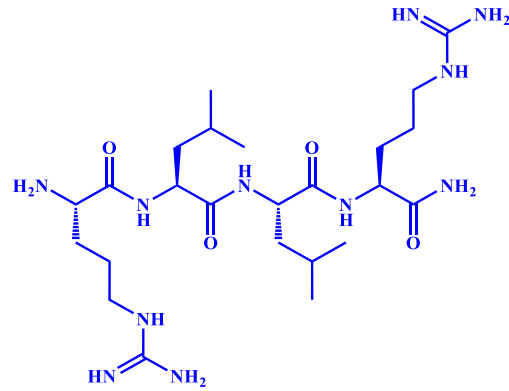


D



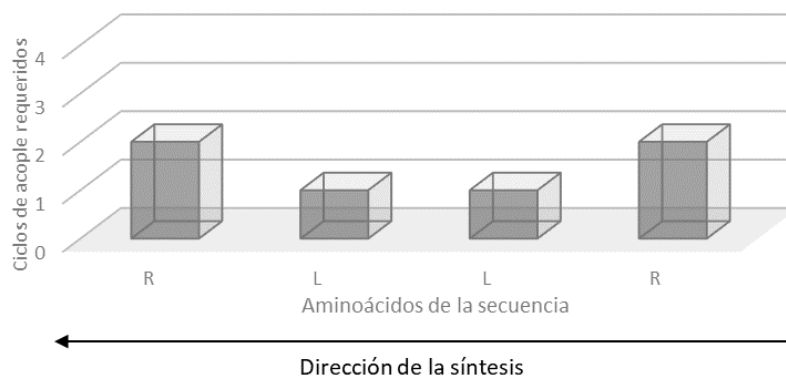
REPORTE DE SÍNTESIS (5) – BFII(32-35): RLLR

A

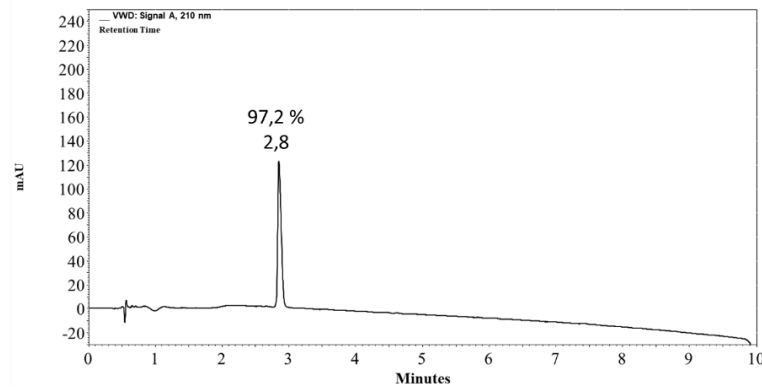


Exact Mass: 555.40

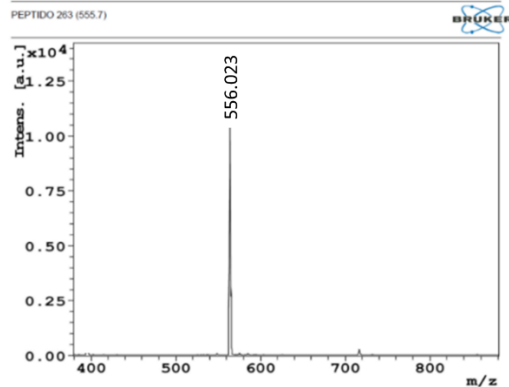
B



C

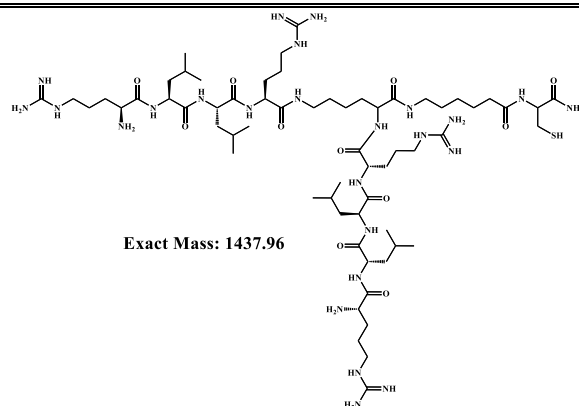


D

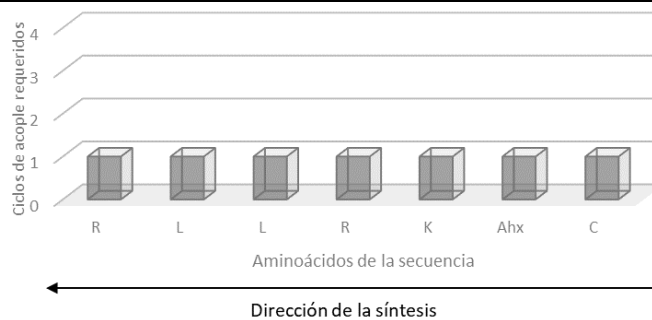


REPORTE DE SÍNTESIS (6) – Precursor dimerico (RLLR)₂K-Ahx-C

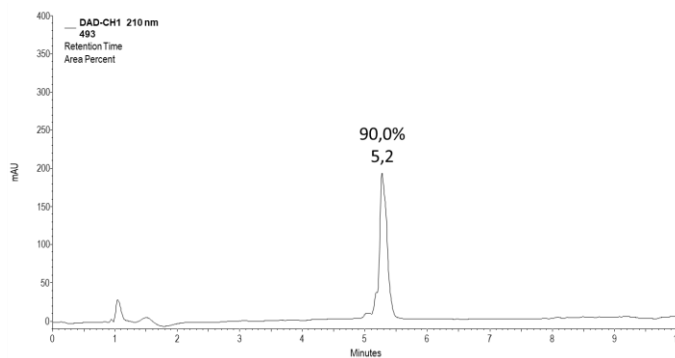
A



B

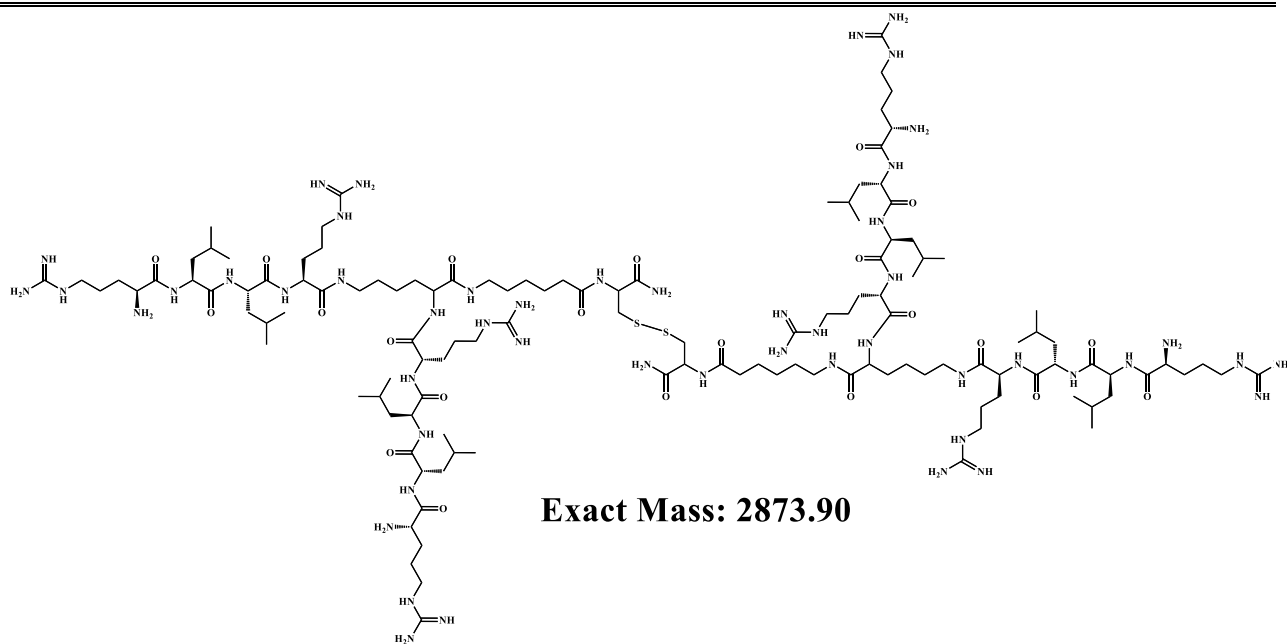


C

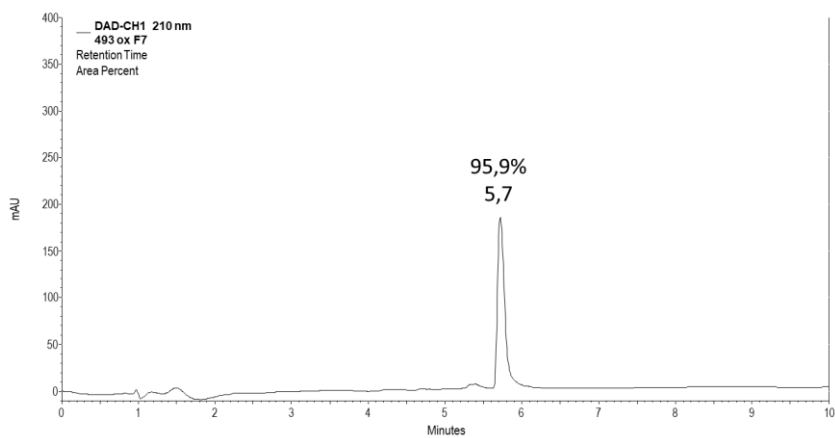


REPORTE DE SÍNTESIS (6.1) – ((RLLR)₂K-Ahx-C)₂

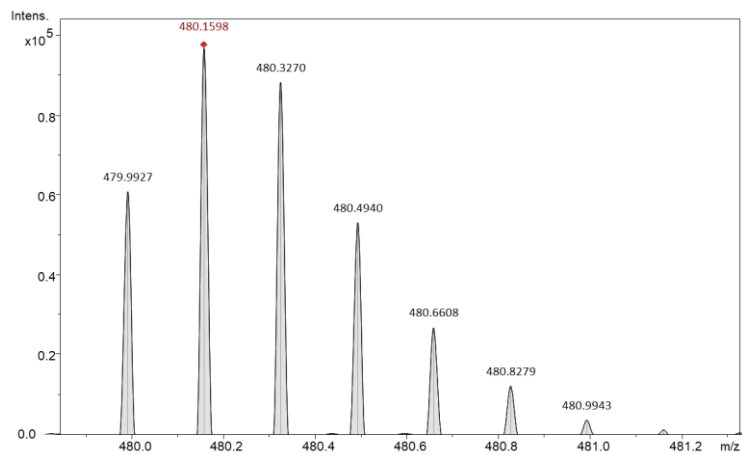
A



C

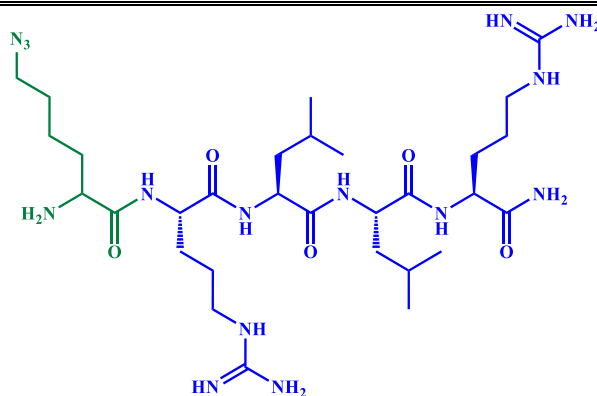


D



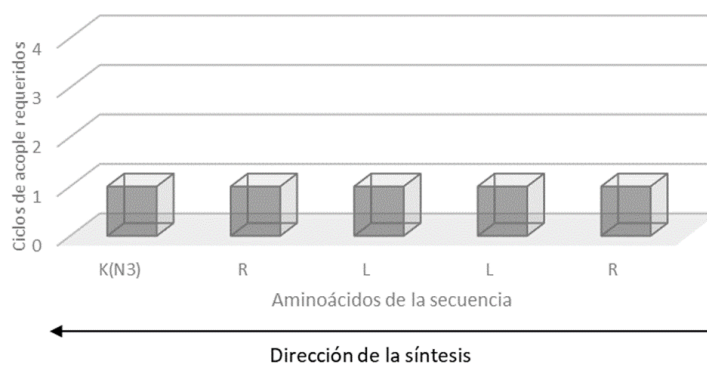
REPORTE DE SÍNTESIS (7) – P2 – Lys(N₃)-BFII(32-35): K(N₃)-RLLR

A

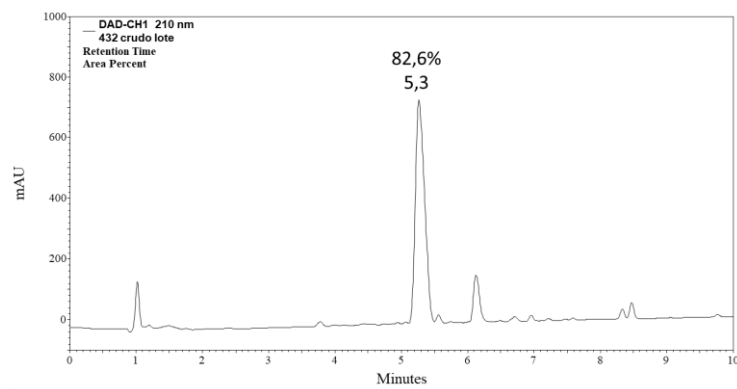


Exact Mass: 709.48

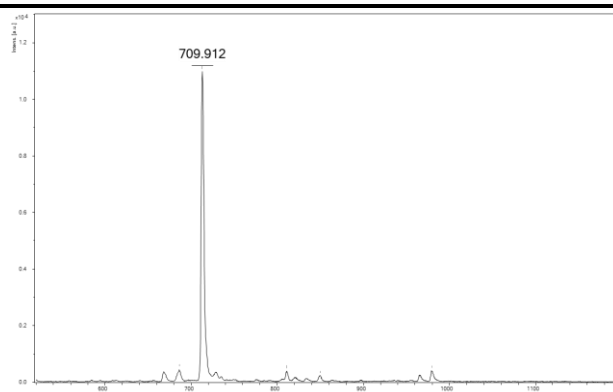
B



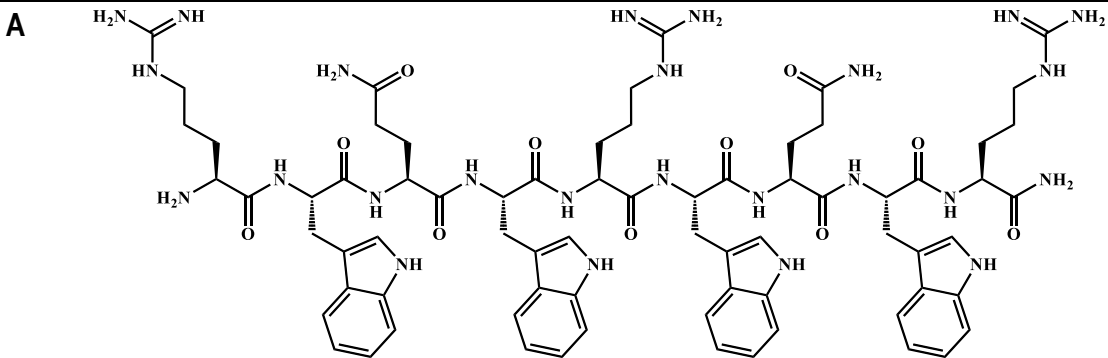
C



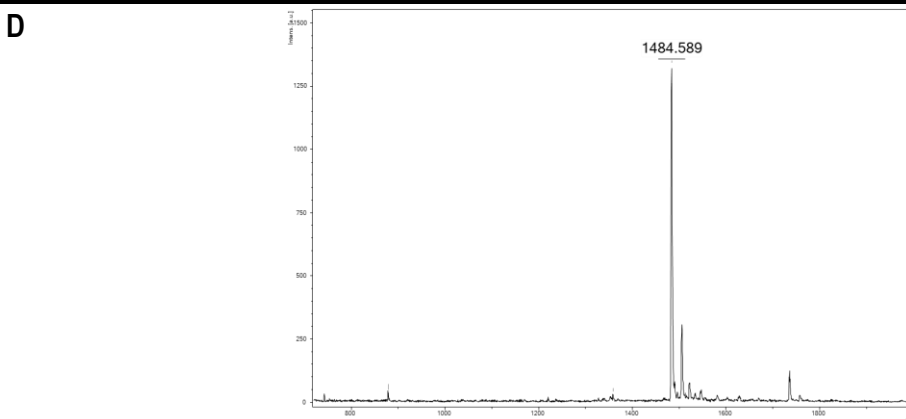
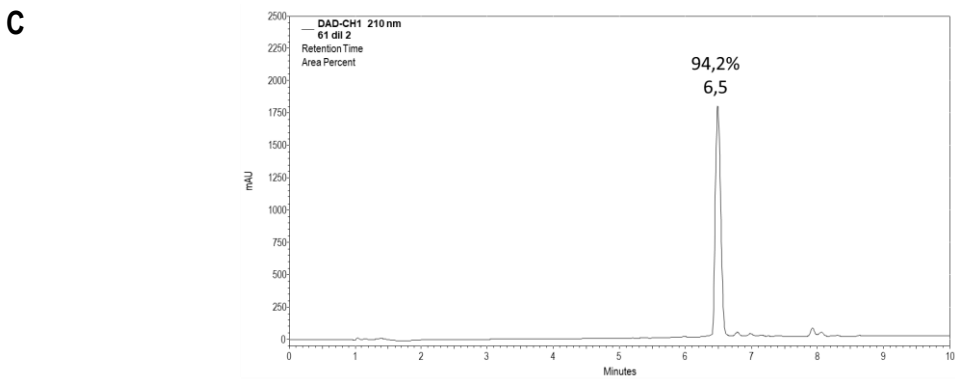
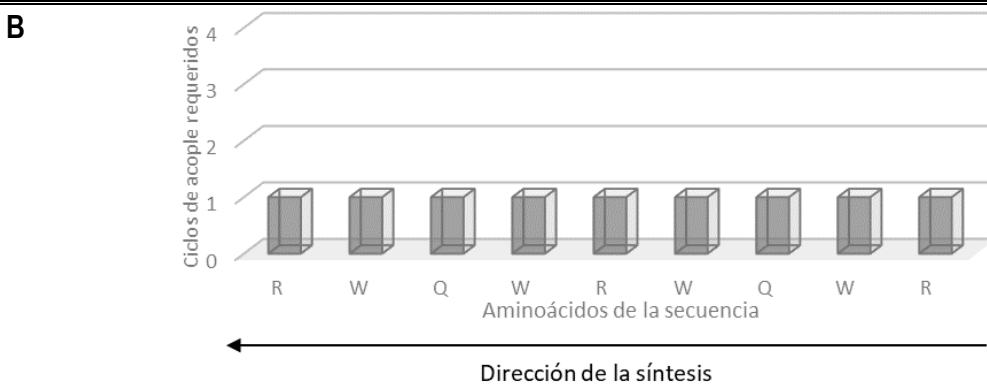
D



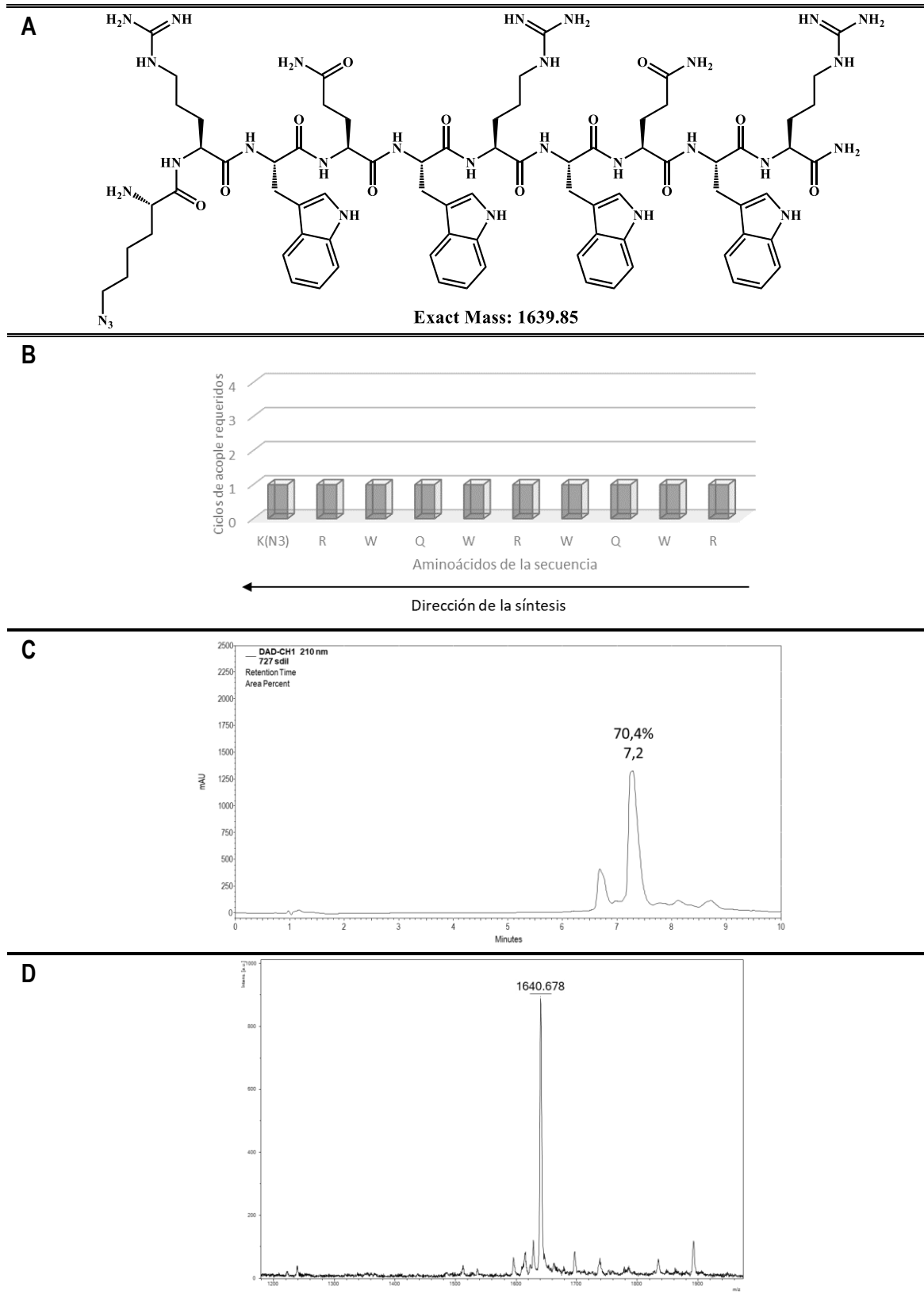
REPORTE DE SÍNTESIS (8) – RWQWRWQWR



Exact Mass: 1485.76

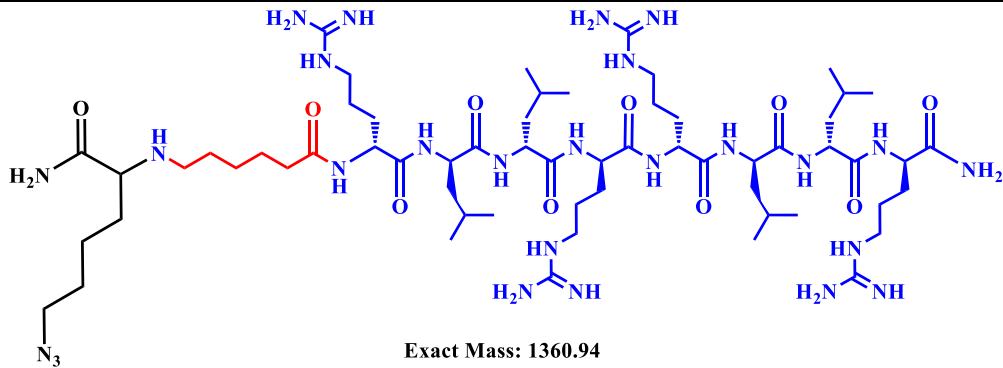


REPORTE DE SÍNTESIS (9) – K(N₃)-RWQWRWQWR

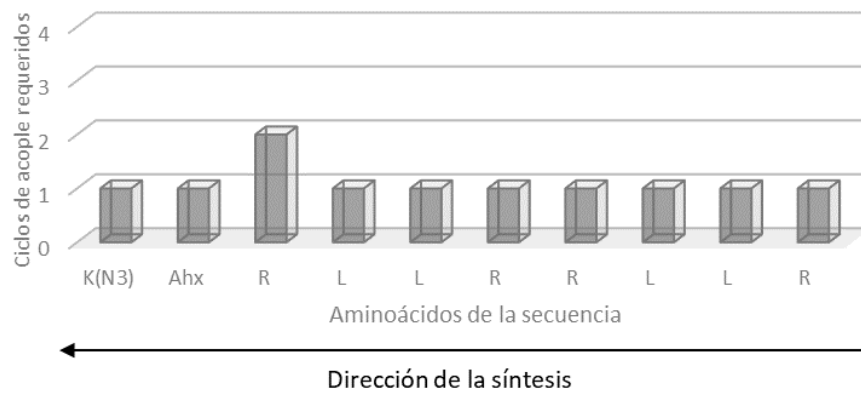


REPORTE DE SÍNTESIS (10) – K(N₃)-Ahx-RLLRLLL

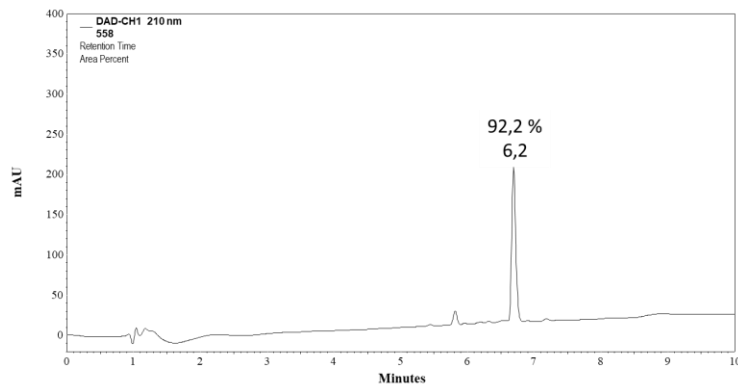
A



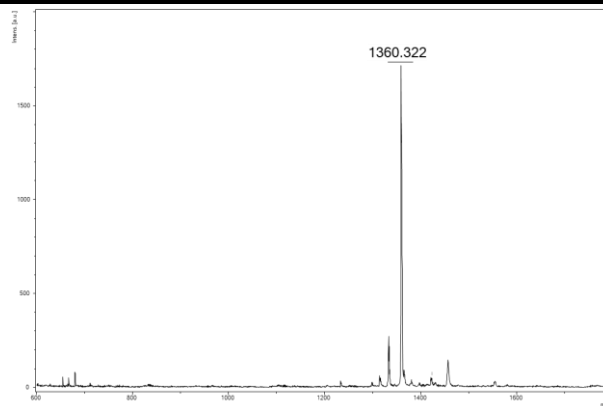
B



C

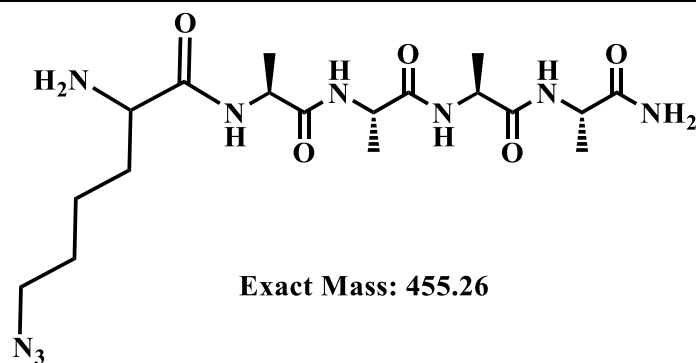


D

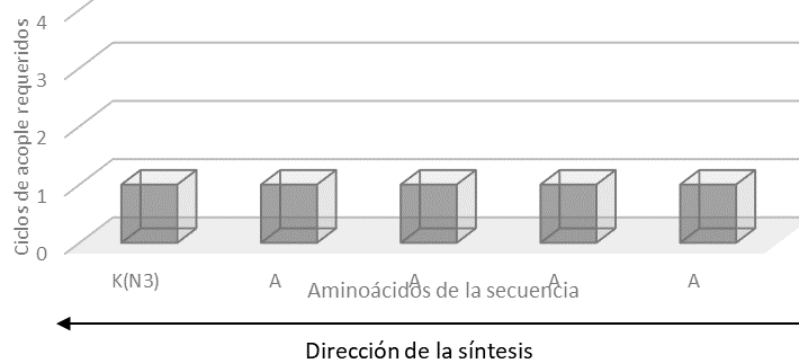


REPORTE DE SÍNTESIS (11) – K(N₃)-AAAA

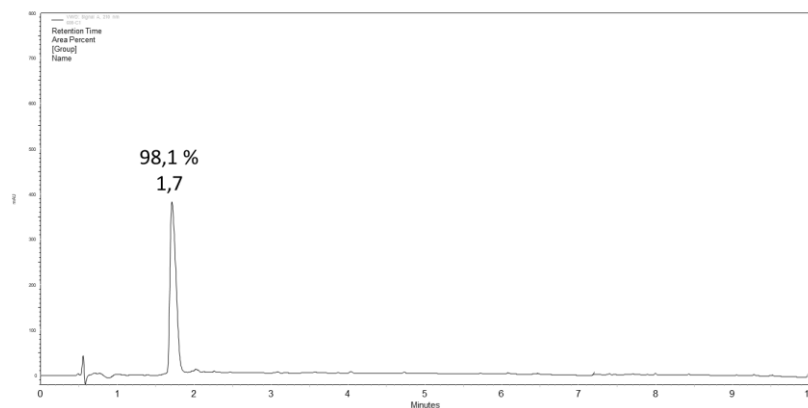
A



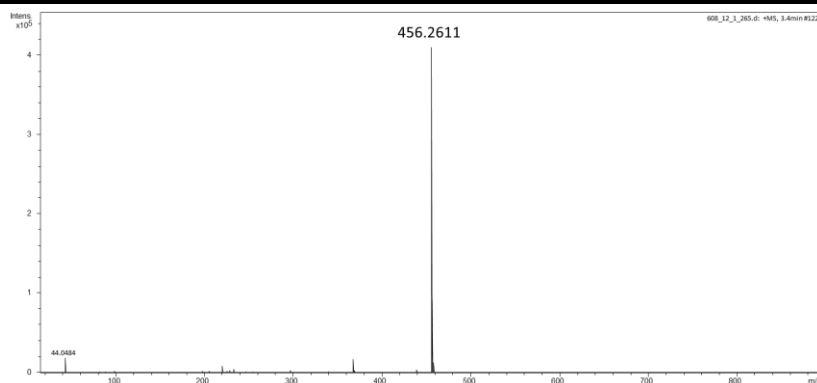
B



C



D







8. Anexo B: Productos Académicos (Artículos)

	Pag.
B.1. Peptide-Resorcinarene Conjugates Obtained via Click Chemistry: Synthesis and Antimicrobial Activity	115-131
B.2. Efficient Separation of C-Tetramethylcalix[4]resorcinarene Conformers by Means of Reversed-Phase Solid-Phase Extraction	132-138
B.3. Designing Short Peptides: A Sisyphean Task?	139-165
B.4. Copper(I)-Catalyzed Alkyne–Azide Cycloaddition (CuAAC) “Click” Reaction: A Powerful Tool for Functionalizing Polyhydroxylated Platforms	166-182
B.5. Use of Click Chemistry for Obtaining an Antimicrobial Chimeric Peptide Containing the LfcinB and Buforin II Minimal Antimicrobial Motifs	183-185
B.6. Designing Chimeric Peptides: A Powerful Tool for Enhancing Antibacterial Activity	186-197
B.7. Short peptides conjugated to non-peptidic motifs exhibit antibacterial activity	198-204
B.8. In Vitro Antifungal Activity of Chimeric Peptides Derived from Bovine Lactoferricin and Buforin II against <i>Cryptococcus neoformans</i> var. <i>grubii</i>	205-218
B.9. Chimeric Peptides Derived from Bovine Lactoferricin and Buforin II: Antifungal Activity Against Reference Strains and Clinical Isolates of <i>Candida</i> spp.	219-231

Article

Peptide-Resorcinarene Conjugates Obtained via Click Chemistry: Synthesis and Antimicrobial Activity

Héctor Manuel Pineda-Castañeda ¹, Mauricio Maldonado-Villamil ¹, Claudia Marcela Parra-Giraldo ², Aura Lucía Leal-Castro ¹, Ricardo Fierro-Medina ¹, Zuly Jenny Rivera-Monroy ¹, and Javier Eduardo García-Castañeda ^{1,*}

¹ Chemistry Department, Universidad Nacional de Colombia, Bogotá 111321, Colombia; hmpinedac@unal.edu.co (H.M.P.-C.); mmaldonadov@unal.edu.co (M.M.-V.); allealc@unal.edu.co (A.L.L.-C.); rfierrom@unal.edu.co (R.F.-M.); zriveram@unal.edu.co (Z.J.R.-M.)

² Human Proteomics and Mycosis Unit, Infectious Diseases Research Group, Department of Microbiology, Pontificia Universidad Javeriana, Bogotá 110231, Colombia; claudia.parra@javeriana.edu.co

* Correspondence: jaegarciaca@unal.edu.co



Citation: Pineda-Castañeda, H.M.; Maldonado-Villamil, M.; Parra-Giraldo, C.M.; Leal-Castro, A.L.; Fierro-Medina, R.; Rivera-Monroy, Z.J.; García-Castañeda, J.E. Peptide-Resorcinarene Conjugates Obtained via Click Chemistry: Synthesis and Antimicrobial Activity. *Antibiotics* **2023**, *12*, 773. <https://doi.org/10.3390/antibiotics12040773>

Academic Editor: Jean-Marc Sabatier

Received: 22 March 2023

Revised: 12 April 2023

Accepted: 14 April 2023

Published: 18 April 2023



Copyright: © 2023 by the authors. Licensee MDPI, Basel, Switzerland. This article is an open access article distributed under the terms and conditions of the Creative Commons Attribution (CC BY) license (<https://creativecommons.org/licenses/by/4.0/>).

Abstract: Antimicrobial resistance (AMR) is one of the top ten threats to public health, as reported by the World Health Organization (WHO). One of the causes of the growing AMR problem is the lack of new therapies and/or treatment agents; consequently, many infectious diseases could become uncontrollable. The need to discover new antimicrobial agents that are alternatives to the existing ones and that allow mitigating this problem has increased, due to the rapid and global expansion of AMR. Within this context, both antimicrobial peptides (AMPs) and cyclic macromolecules, such as resorcinarenes, have been proposed as alternatives to combat AMR. Resorcinarenes present multiple copies of antibacterial compounds in their structure. These conjugate molecules have exhibited antifungal and antibacterial properties and have also been used in anti-inflammatory, antineoplastic, and cardiovascular therapies, as well as being useful in drug and gene delivery systems. In this study, it was proposed to obtain conjugates that contain four copies of AMP sequences over a resorcinarene core. Specifically, obtaining (peptide)₄-resorcinarene conjugates derived from LfcinB (20–25): RRRQWR and BF (32–34): RLLR was explored. First, the synthesis routes that allowed obtaining: (a) alkynyl-resorcinarenes and (b) peptides functionalized with the azide group were established. These precursors were used to generate (c) (peptide)₄-resorcinarene conjugates by azide-alkyne cycloaddition CuAAC, a kind of click chemistry. Finally, the conjugates' biological activity was evaluated: antimicrobial activity against reference strains and clinical isolates of bacteria and fungi, and the cytotoxic activity over erythrocytes, fibroblast, MCF-7, and HeLa cell lines. Our results allowed establishing a new synthetic route, based on click chemistry, for obtaining macromolecules derived from resorcinarenes functionalized with peptides. Moreover, it was possible to identify promising antimicrobial chimeric molecules that may lead to advances in the development of new therapeutic agents.

Keywords: dendrimers; resorcinarene; click chemistry; CuAAC; antibacterial activity; antifungal activity; clinical isolate

1. Introduction

The indiscriminate use of antibiotics has generated an increase in antimicrobial resistance (AMR). Recent reports issued by the World Health Organization (WHO) describe the importance of finding new molecules that are able to counteract AMR; this problem is considered to be a growing threat to health worldwide [1,2]. As an example, the WHO has reported bacterial and fungal strains that exhibit greater resistance. Among these are found: *Acinetobacter*, *Pseudomonas*, and several *Enterobacteriaceae* (including *Klebsiella*, *Escherichia coli*, *Serratia*, and *Proteus*), followed by *Enterococcus faecium* and

Staphylococcus aureus, among others [3,4], as well as the appearance of drug-resistant fungi of *Candida* species (*Candida albicans*, *C. glabrata*, *C. tropicalis*, *C. parapsilosis*, and *C. Krusei*).

In recent decades, antimicrobial agents derived from protein sources have been developed, and peptides with greater antimicrobial potential against a wide variety of resistant microorganisms than their original proteins have been found. Antimicrobial peptides (AMPs) have been described as a primary defense barrier against infections caused by external pathogens [5]. Currently, AMPs are a source of the design and development of new antimicrobial molecules. To obtain therapeutic agents based on AMPs, modifications to the original sequences have been proposed, including (i) the incorporation of unnatural amino acids, (ii) sequences with conformational restriction, (iii) peptide chimeras, (iv) palindromic structures, and (v) structures with multiple presentation of the active motif; the latter may contain an antibacterial motif of peptide origin or an organic/inorganic core [6]. Obtaining polyvalent peptides can be associated with various forms synthesis pathways, e.g., the use of divergent or convergent strategies, the use of cores based on modified amino acids, or organic motifs as polyhydroxylated platforms, such as calixarenes and resorcinarenes. This latter has become a new source of molecules that are currently being studied for the generation of polyvalent molecules, thanks to its great versatility for synthesis and the reactivity provided by the hydroxyl groups and other reactive positions present in these structures.

In this way, resorcinarenes, also known as calix[4]resorcinarenes, are polyhydroxylated macrocyclic compounds derived from resorcinol, first synthesized by Baeyer et al. from aliphatic and aromatic aldehydes [7,8]. They are made up of four resorcinol rings joined by a bridging atom, usually carbon within a methylene group at positions 4 and 6, giving the formation of a cyclic structure typically represented as a truncated *cone* with an upper and lower rim. These bridging atoms are often replaced by aliphatic and/or aromatic chains, allowing the formation of conformational isomers (stereoisomerism) [9]. The versatility of these host systems stems from synthetically easy modifications either on the upper or lower rim of these macrocycles. However, core (unsubstituted) resorcinarene conformations are known to be modulated quite easily by reaction conditions when the host is synthesized [10]. Five possible conformers have been reported: (i) *crown*, (ii) *boat*, (iii) *saddle*, (iv) *chair*, and (v) *diamond* (Figure 1) [11]. Each of these conformations is possible, depending on aspects such as the position of the resorcinol units and the substituents in the methylene bridges; this gives rise to a library of molecules [11–16]. Thus, the versatility in the synthesis of polyhydroxylated platforms has allowed the incorporation of substituents, which allows the use of new strategies, such as click chemistry, for the synthesis of functionalized calixarenes/resorcinarenes.

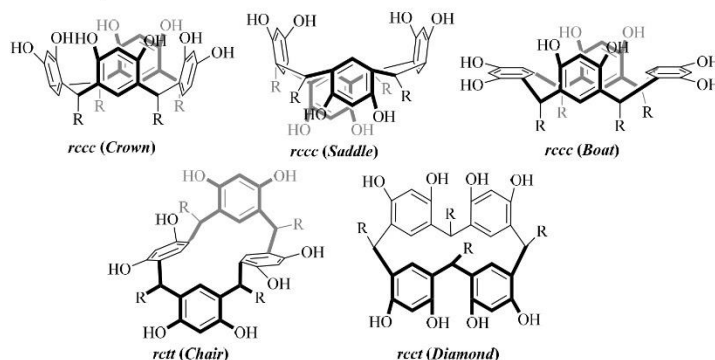


Figure 1. Reported conformational isomers, according to the relative configuration of the substituents in the methylene bridges.

Click chemistry is currently one of the most-used tools for the generation of complex organic molecules [17]. The advantages of using click chemistry in organic synthesis are remarkable: in many cases they occur under mild conditions, free of solvents, and with high yields and short reaction times, which makes this new strategy a viable alternative for obtaining conjugated molecules [18]. The present study highlights the use of click chemistry for the generation of functionalized resorcinarenes with several copies of an AMP, specifically the azide-alkyne cycloaddition catalyzed by copper (I) (CuAAC) on polyhydroxylated platforms of the resorcinarene type [19,20]. Although their development is still limited and they are in the exploratory phase, antimicrobial peptide-resorcinarene conjugates are promising candidates for treating infections caused by drug-resistant bacteria and fungi. The resorcinarenes have demonstrated broad antibacterial and antifungal activity and have also exhibited functions useful as diagnostic tools, therapeutic agents, molecular recognition, and transport vehicles for genes and drugs [21].

Even though at present no peptide-resorcinarene conjugates with antibacterial and/or antifungal activity have been reported in clinical trial phases, there are some agents derived from dendrimer structures with other types of applications in clinical trials; for example, DEP[®] docetaxel9 [22] is a drug used for solid tumors, including breast, prostate, and lung cancer, DEP[®] cabazitaxel is a non-detergent version of the leading cancer drug [23], MAG-Tn3 dendrimer vaccine is used for breast cancer [24], ImDendrim is used for inoperable liver cancer [25], and OP-101 is used for X-linked adrenoleukodystrophy [26].

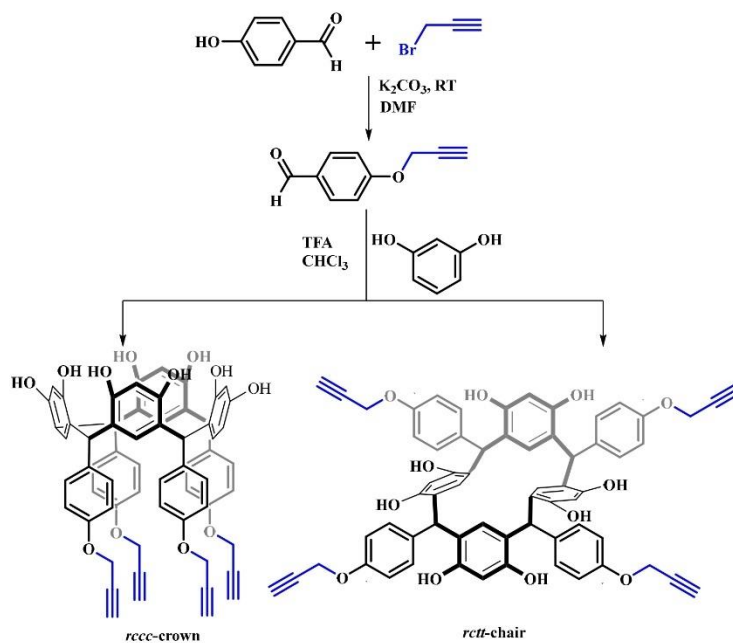
In this context, the present investigation studies the synthesis and characterization of peptide-resorcinarene conjugates derived from LfcinB and buforin, a strategy that will allow the generation of molecules that present several copies of the selected AMPs on an unprotected and polyhydroxylated nucleus.

2. Results and Discussion

For the synthesis of peptide-resorcinarene conjugates, we decided to evaluate three variables, so we divided our research into the following steps: step (1) evaluation of the synthetic routes that allow obtaining functionalized resorcinarenes with alkyne groups and the synthetic feasibility of peptides that contain an azide group in their structure; step (2) the synthetic parameters that allow the generation of the conjugated molecule peptide-resorcinarene by means of azide/alkyne cycloaddition; and step (3) the antibacterial activity of the conjugates obtained. These results will allow the identification of promising molecules that will generate advances in the development of new antimicrobial agents. The results obtained in step 1 to step 3 are shown below.

2.1. Synthesis and Characterization of Resorcinarene and Peptide Precursors

For generating the conjugates, first we had to obtain two precursors: (i) the resorcinarene core functionalized with alkyne groups, and (ii) peptides functionalized with azide motifs. It was proposed to attach the precursors via click chemistry. We selected the resorcinarenes as the core for the conjugates, because this kind of molecule has been the focus of great interest in the field of chemistry due to its low toxicity and the fact that it can be modified with a diversity of functional groups, generating a great variety of pharmacologically active derivatives, including compounds with antimicrobial activity against Gram-positive and Gram-negative bacteria, fungi, and parasites [27]. In this investigation, as a first step it was decided to carry out the synthesis of a nucleus derived from resorcinarene functionalized with alkyne groups on the lower rim. This nucleus was synthesized through acid-catalyzed cyclocondensation (see Scheme 1) using resorcinol and an aldehyde previously functionalized with the propargyl group (see Supplementary Material, Figure S1).



Scheme 1. Synthesis of the C-Tetra(4-(prop-2-yn-1-yloxy)phenyl)calix[4]resorcinarene.

We specifically synthesized the C-Tetra(4-(prop-2-yn-1-yloxy)phenyl)calix[4]resorcinarene (CTpH(F)), as is detailed in the methodology section. As can be seen in Figure 2a, the chromatographic profile of the reaction product shows two principal signals, at 9.6 min and 9.8 min. It has been reported that a single conformer or a conformational mixture can be obtained as a reaction product in the synthesis of this type of resorcinarene derivative [28,29]. To characterize the two principal products, a purification/separation and recrystallization process was carried out [30], and then each purified product was characterized via RP-HPLC, 1H -NMR, and ^{13}C -NMR. A white solid was obtained, and its chromatographic profile shows a single species at 9.6 min with a purity of 96.4% (Figure 2b). For this product, the assignments of the 1H -NMR signals at low field (8.51–8.46 ppm) suggest the presence of protons from the different OH groups with an integration of four for each one, as well as the protons that make up the aromatic ring of resorcinol with signals between 6.50 and 6.12 ppm. This information was confirmed by means of ^{13}C -NMR with signals at 101.7 and 101.6 ppm, Figure 3a. The characterization of this product suggests that it corresponds to the chair (*rctt*) conformer. The second product was obtained as a yellow solid; it exhibits 77.9% chromatographic purity, Figure 2c, and its 1H -NMR spectrum shows a single singlet signal at low field 8.54 ppm that integrates for 8 protons. This suggests that all of the protons of the OH groups of resorcinol are equivalent, and therefore this product should correspond to the *rrcc* conformer, Figure 3b. The two resorcinarene derivatives were characterized using MALDI-TOF mass spectrometry. Table 1 shows the MS data obtained (product characterization is presented in Supplementary Material, Figures S2–S4).

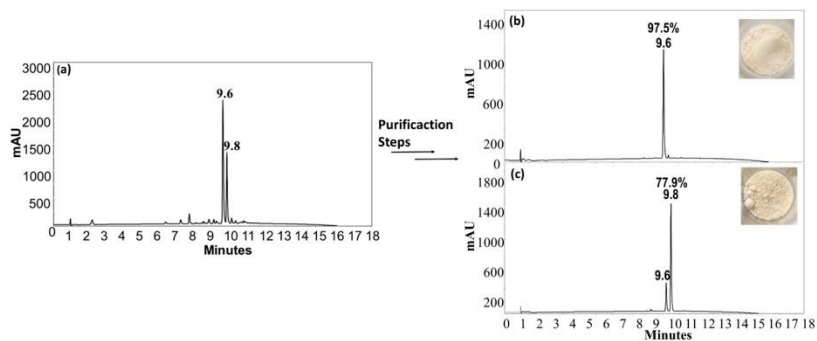


Figure 2. Chromatographic profile of crude reaction product (a) obtained in the synthesis of C-Tetra(4-(prop-2-yn-1-yloxy)phenyl)calix[4]resorcinarene. (b,c) show the profiles obtained for purified products.

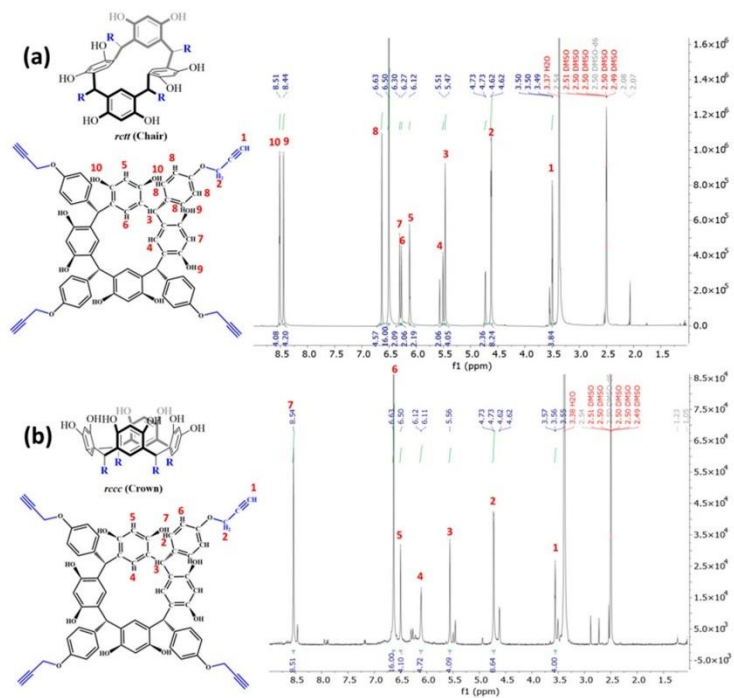


Figure 3. ¹H-RMN of (a) *rctt* conformer and (b) *rccc* conformer pure obtained in the synthesis of C-Tetra(4-(prop-2-yn-1-yloxy)phenyl)calix[4]resorcinarene.

Table 1. Peptide, alkynyl-resorcinarenes precursors, and synthesized conjugates. RP-HPLC and MS characterization summary.

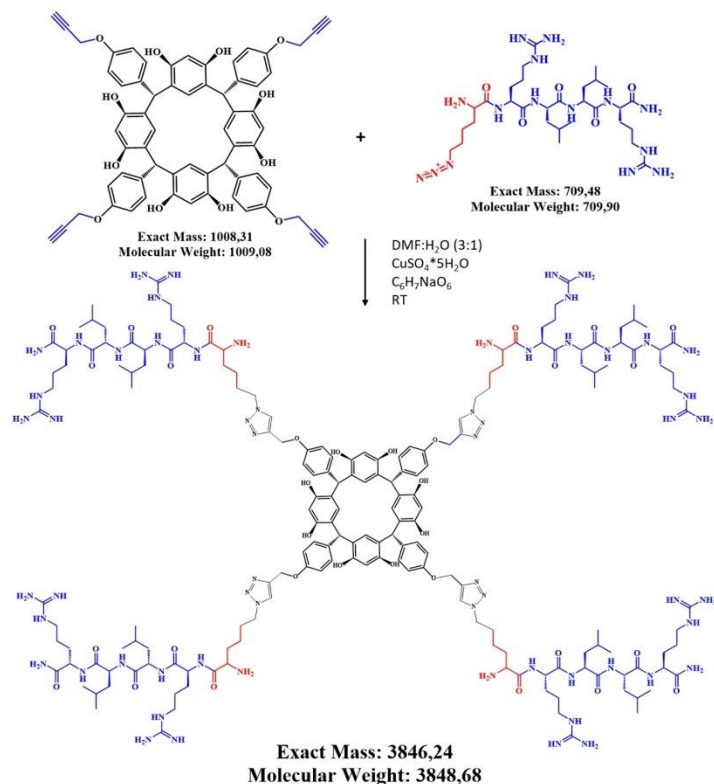
Peptides ^a	RP-HPLC		MS		
	t _R (min)	Purity ^b (%)	Theoretical ^c [M+H] ⁺	m/z [M+H] ⁺	
RLLR	2.4	97.2	556.0	556.2	
RRWQWR	4.1	92.5	986.5	986.5	
K(N ₃)-RLLR	5.3	98.2	710.5	709.9	
K(N ₃)-RRWQWR	5.4	83.7	1139.6	1139.4	
Alkynyl-resorcinarene	RP-HPLC			MS	
	t _R (min)	Purity ^b (%)	Yield (%)	Theoretical ^c [M+H] ⁺	m/z [M+H] ⁺
CTpH(F) (<i>rcft</i>)	9.6	97.5	58.9	1009.3	1009.3
CTpH(F) (<i>rccc</i>)	9.8	77.9	20.8	1009.3	1008.7
(Peptide) ₄ -resorcinarene conjugates	RP-HPLC			MS	
	t _R (min)	Purity ^b (%)	Yield (%)	Theoretical ^c [M+H] ⁺	m/z [M+H] ⁺
CTpH(F)-(AAC-(K)-RLLR) ₄ (<i>rcft</i>)	6.0	96.4	75.6	3847.2	3847.5
CTpH(F)-(AAC-(K)-RLLR) ₄ (<i>rccc</i>)	6.0	88.7	60.1	3847.2	3844.2
CTpH(F)-(AAC-(K)-RRWQWR) ₄ (<i>rcft</i>)	6.4	74.6	56.6	5570.4	5575.2

^a All peptides have amide group at C-terminal end; ^b Chromatographic purity; ^c M: monoisotopic mass.

We selected two AMPs motifs: specifically, the following molecules were synthesized, purified, and characterized: (i) two linear peptides that correspond to the peptide sequences selected, the minimal antibacterial motifs of the AMPs LfcinB, residues 20–25: RRWQWR, and buforin BF, residues 32–35: RLLR, which were obtained to be used as control; and (ii) two azide-peptides, in which the azide group was introduced at the N-terminal end using the residue Fmoc-azidolysine, i.e., the sequences obtained were: K(N₃)-RRWQWR-NH₂ and K(N₃)-RLLR-NH₂. All the peptides were obtained via solid-phase peptide synthesis (SPPS) over Rink amide resin, using the Fmoc/tBu strategy (in Supplementary Material, Figure S5 presents an azide-peptide synthesis diagram). Our results (Table 1) show that the implemented methodology was adequate for obtaining the proposed peptides. Specifically, in this investigation, an optimized methodology was used where the concentration of the Fmoc removal reagent, 4-methylpiperidine, was 2.5% *v/v* in DMF. It should be noted that this concentration is ten times lower than that commonly used in the reported protocols for SPPS. For most amino acids, only one coupling cycle was required for their incorporation into the peptide sequence. The TFA/water/TIPS/EDT cleavage cocktail (93/2/2.5/2.5 *v/v/v/v*) was adequate for control peptides; however, for azide-functionalized peptides, the EDT and TIPS scavengers were suppressed, in order to avoid the reduction of the azide motif to an amine group [31].

2.2. Synthesis and Characterization of Peptide-Resorcinarene Conjugates

Once the nucleus derived from resorcinarene and the peptide sequences had been successfully functionalized, the next step was to obtain the peptide-resorcinarene conjugates by means of copper-catalyzed azide-alkyne cycloaddition reaction, CuAAC. Our aim was to achieve a complete functionalization of the resorcinarene, thus generating a tetravalent molecule, i.e., (peptide)₄-resorcinarene, as is shown in Scheme 2.



Scheme 2. Synthesis of the conjugated CTpH(F)-(AAC-(K)-RLLR)₄ by copper-catalyzed azide-alkyne cycloaddition (CuAAC).

First, we optimized the CuAAC, azide-alkyne cycloaddition conditions. As an example, Scheme 2 shows the reaction between the alkynyl-resorcinarene, CTpH(F), and the azide-peptide, K(N₃)-RLLR. Parameters such as solvent, equivalent excess, and temperature, among others, were optimized one by one. The reaction was monitored through RP-HPLC, and aliquots at different reaction times were taken. As an example, in Figure 4, the chromatographic reaction profile is shown at times 0 and 1.5 h. At time 0 (Figure 4a, $t = 0$ h), signals corresponding to peptide K(N₃)-RLLR and the CTpH(F) were observed at t_R of 5.3 and 9.6 min, respectively. Additionally, four new signals were also observed, specifically at 6.0, 6.3, 7.2, and 7.9 min. After 1.5 h of reaction (Figure 4a, $t = 1.5$ h), the signal at t_R of 6.0 min is the major component. This result suggests that the signals between 6.3 and 7.9 min could correspond to incomplete functionalization, i.e., CTpH(F) conjugated with one, two, or three peptide chains.

The obtained products were purified by means of RP-SPE to remove the excess of catalyst, solvent, and starting reagents that did not react. The chromatographic profile of the pure CTpH(F)-(AAC-(K)-RLLR)₄ (*rctt*) conjugate is shown in Figure 4b, as well as its characterization by MALDI-TOF and HR mass spectrometry, where the m/z ratio corresponds to $[M+H]^+$ or $[M+4H]^{4+}$ of the tetra-functionalized conjugated, respectively. In general, in Table 1, a summary of the characterization data for precursors and the conjugates is presented. At supplementary material, Figures S6 and S7 present additional information about characterization of final conjugates.

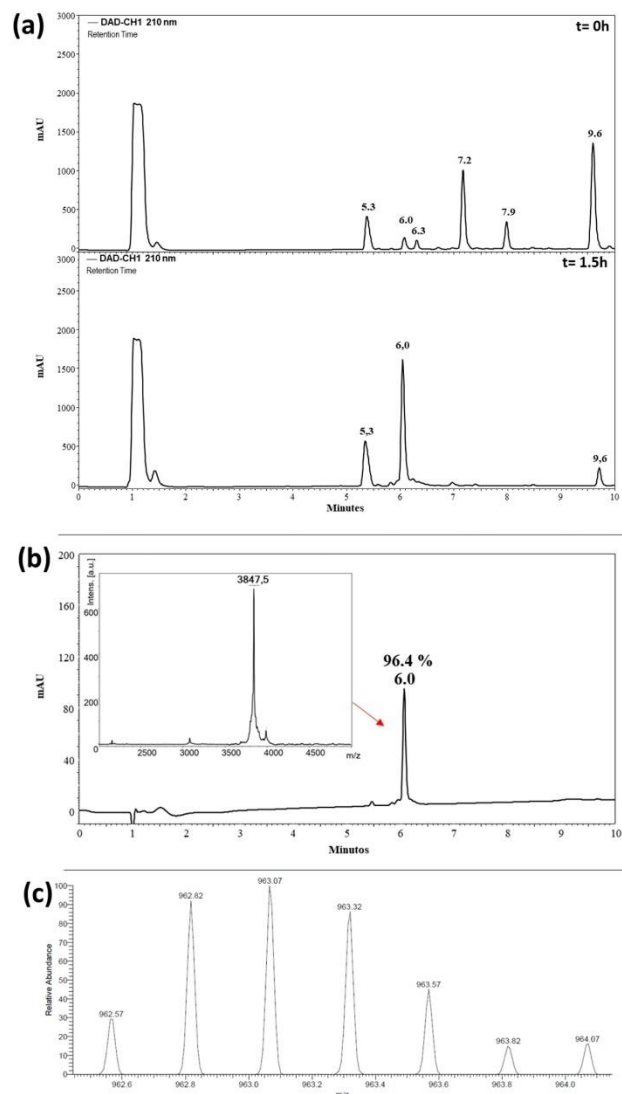


Figure 4. Click reaction between azide-peptide, $K(N_3)$ -RLLR (t_R : 5.3 min) and the alkynyl-resorcinarene CTPH(F), (*rectt*, t_R : 9.6 min). (a) Reaction monitoring by means of RP-HPLC at time 0 and 1.5 h. (b) Chromatographic profile, and MALDI-TOF MS spectrum of purified conjugate: CTPH(F)-(AAC-(K)-RLLR)₄ (*rectt*). (c) CTPH(F)-(AAC-(K)-RLLR)₄ (*rectt*) HR-MS, the signals corresponding to isotopic distribution of $[M+4H]^{4+}$ species are showed; monoisotopic experimental M is 3846.28 uma.

2.3. Antibacterial/Antifungal Activity against Reference Strains and Clinical Isolates

The antibacterial activity of tetravalent conjugates (resorcinarene-peptide) was evaluated against the reference strain *E. coli* ATCC 25922, susceptible to ciprofloxacin. Resorcinareno-

peptide conjugates exhibited greater antibacterial activity against the ATCC strain of *E. coli* 25922 (MICs ranging from 13 to 52 μ M) than control peptides RLLR and RRWQWR. Interestingly, conjugates that contained four copies of RLLR, CTpH(F)-(AAC-(K)-RLLR)₄ exhibited differences in their activity; specifically, the chair conformer (*rcft*) was four times more active than the crown conformer (*rccc*). These results suggest that the resorcinarene conformation directly influences the antibacterial activity. On the other hand, the conjugate that contained four copies of the sequence RRWQWR in chair conformation (*rcft*) was active against *E. coli* 25922, six times greater than the lineal sequence. The conjugate CTpH(F)-(AAC-(K)-RLLR)₄ (*rcft*) also exhibited antibacterial effect against *S. aureus* ATCC 25923 (MIC of 13 μ M). This strain is sensitive to vancomycin. Similarly, the control peptides exhibited no antibacterial effect against this strain at the concentrations tested (Table 2).

Table 2. Antimicrobial activity of tetravalent conjugates, (peptide)₄-resorcinarene.

Antibacterial activity against ATCC strains			
Molecule	Sequence	MIC/MBC (μ M)	
		<i>E. coli</i> 25922	<i>S. aureus</i> 25923
Control Peptide	RLLR	>359 / >359	>359 / >359
	RRWQWR	203 / 203	>203 / >203
Conjugate	CTpH(F)-(AAC-(K)-RLLR) ₄ (<i>rcft</i>)	13 / 26	13 / Nd
	CTpH(F)-(AAC-(K)-RLLR) ₄ (<i>rccc</i>)	52 / >52	Nd
	CTpH(F)-(AAC-(K)-RRWQWR) ₄ (<i>rcft</i>)	36 / 36	Nd
Conjugate CTpH(F)-(AAC-(K)-RLLR) ₄ (<i>rcft</i>) antimicrobial activity			
Strain (classification)	Resistant to	MIC/MBC (μ M)	
<i>E. coli</i> 1004 (S)	-	26 / >52	
<i>E. coli</i> 129797 (R)	AM, SAM, CEF	26 / 52	
<i>E. coli</i> 301755 (M)	AM, SAM, CPE, CAZ, CAX, CIP, GEN, NIT, NOR, STX	13 / 26	
<i>S. aureus</i> 109095 (R)	P	26 / 52	
<i>S. aureus</i> 117719 (M)	P, TET	52 / 52	
<i>S. aureus</i> 124653 (M)	P, ERY, TET	13 / 52	
Strain (classification)	Resistant to	MIC/MFC (μ M)	
<i>C. albicans</i> SC5314 (S)	-	26 / 26	
<i>C. albicans</i> 256 HUSI-PUJ (R)	FLC	13 / 13	
<i>C. auris</i> 435 (S)	FLC	26 / >26	

Classification: S: sensitive, R: resistant, M: multi-resistant strain. Nd: Not Determined. Antimicrobials: P: Penicillin, TET: Tetracycline, ERY: Erythrosine, AM: Ampicillin, SAM: Ampicillin/sulbactam, CPE: Cefepime, CAZ: Ceftazidime, CAX: Ceftriaxone, CIP: Ciprofloxacin, GEN: Gentamicin, NIT: Nitrofurantoin, NOR: Norfloxacin, STX: Trimethoprim/sulfamethoxazole, FLC: Fluconazole.

The antimicrobial activity of the conjugate CTpH(F)-(AAC-(K)-RLLR)₄ (*rcft*) against clinical isolates of *E. coli*, *S. aureus*, *C. albicans*, or *C. auris* (sensitive or resistant to different antibiotics) was evaluated (Table 2). Our result showed that all the clinical isolates evaluated were sensitive to the conjugate. The conjugate resorcinarene-peptide showed the highest antibacterial effect against clinical isolated multidrug-resistant *E. coli* 301755 and clinical isolated resistant *S. aureus* 124653 (MICs values of 13 μ M), the same MIC value observed for the ATCC strains. This conjugate also exhibited antibacterial activity against the other clinical isolates of *E. coli* and *S. aureus*, with MICs values ranging from 26 to 52 μ M. On the other hand, the antifungal activity of conjugate CTpH(F)-(AAC-(K)-RLLR)₄ (*rcft*) was tested

against clinical isolates of *C. albicans* and *C. auris*. The fluconazole-resistant clinical isolate, *C. albicans* 256 HUSI-PUJ, was more sensitive to the conjugate resorcinarene-peptide (MIC 13 μM). The conjugate also exhibited antifungal activity against sensitive strains *C. albicans* SC5314 and *C. auris* (MIC of 26 μM).

The antifungal activity of the peptide RLLRLLR, which contains two copies of the buforin minimal antibacterial motif, did not exhibit activity against the *C. albicans* strain ATCC SC5314 (sensitive to fluconazole) and clinical isolate *C. albicans* 256 HUSI-PUJ resistant to fluconazole (MIC value of >183 μM) [32], suggesting that the conjugation of the RLLR sequence with the resorcinarene motif increased the antifungal activity (Table 2). Our results suggest that the binding of the resorcinarene motif to the peptide sequence increased antifungal and antibacterial activity against reference strains and resistant and multiresistant clinical isolates. This suggests that functionalization of resorcinarene with a short cationic peptide (RLLR or RRWQWR) is a promising strategy for obtaining molecules with antibacterial potential. The incorporation of the peptide sequence into resorcinarene increased the solubility of the resorcinarene motif, allowing it to interact with the pathogenic cell. Additionally, the resorcinarene motif may increase the stability of the peptide sequence by facilitating the interaction of the cationic sequence with the cell surface.

The growth inhibition kinetics caused by CTpH(F)-(AAC-(K)-RLLR)₄ (*rctt*) was evaluated against *E. coli* ATCC 25922 (Figure 4a) for 48 h. At MIC value (13 μM), a bacteriostatic effect was observed (green line), while a bactericide effect was observed for conjugate concentrations of 26 and 52 μM (two and four times the MIC value, respectively, Figure 5). For *S. aureus* ATCC 25923, only a bacteriostatic effect was exhibited at a concentration of 52 μM (2 \times MIC). These results confirm the antibacterial effect of the CTpH(F)-(AAC-(K)-RLLR)₄ (*rctt*) conjugate.

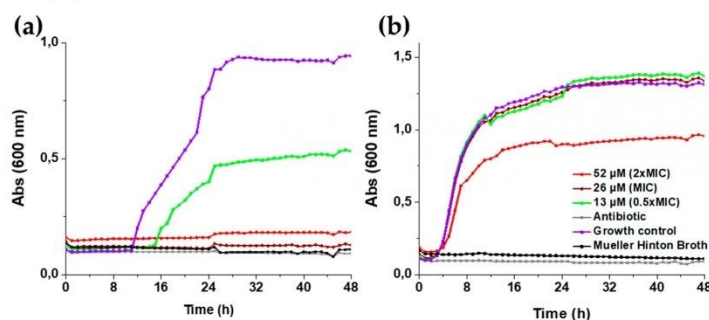


Figure 5. Time-kill curve plot. (a) *E. coli* ATCC 25922 and (b) *S. aureus* ATCC 25923 strains were incubated with CTpH(F)-(AAC-(K)-RLLR)₄ (*rctt*), for 48 h using conjugate concentrations corresponding to 0.5 \times MIC (green line), MIC (brown line), and 2 \times MIC (red line) values. Antibiotic (a) ciprofloxacin (b) vancomycin.

2.4. Cytotoxic/Hemolytic Activity

The hemolytic effect of the (peptide)₄-resorcinarene conjugates CTpH(F)-(AAC-(K)-RLLR)₄ (*rctt*) and CTpH(F)-(AAC-(K)-RRWQWR)₄ (*rctt*) was evaluated using concentrations from 3.1 to 200 $\mu\text{g}/\text{mL}$ (Figure 6). Neither of the two conjugates exhibited a significant hemolytic effect at the MIC values observed in the antifungal and antibacterial assays. The CTpH(F)-(AAC-(K)-RLLR)₄ (*rctt*) conjugate exhibited a low hemolytic effect (about 4% at all concentrations evaluated), suggesting that this molecule is selective for the fungal and bacterial strains evaluated. The hemolytic activity of the peptide RLLR was 63% at 200 $\mu\text{g}/\text{mL}$, while RRWQWR showed hemolysis of 1% [33]. We can infer that the generation of the tetravalent conjugates decreased the hemolytic activity of the RLLR sequence.

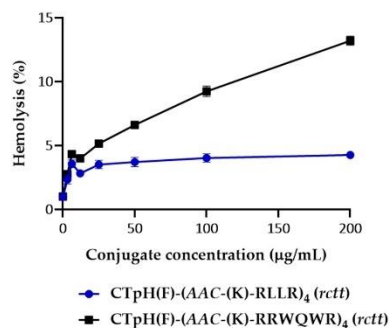


Figure 6. Hemolytic activity of (peptide)₄-resorcinarene derived from LfcinB (20–25) and BF (32–35).

Our results showed that the resorcinarene-peptide CTPH(F)-AAC-(K(N₃)-RLLR)₄ (rctt) exhibited a lower hemolytic effect and higher antibacterial activity than the LRLR peptide, suggesting that this synthetic strategy is useful for developing treatments against bacterial infections.

Finally, the cytotoxic effect of the conjugates over fibroblasts, MCF-7, and HeLa cell lines was evaluated (Figure 7). The results show that neither conjugate exhibits significant cytotoxic effect in these models, suggesting that they are selective for the fungal and bacterial strains evaluated. Conversely, the peptide ((RRWQWR)₄-K₂-C₂), which contains four copies of the RRWQWR sequence, exhibited cytotoxicity against these cancer cell lines, bacterial, and fungal strains, suggesting that the resorcinarene-peptide conjugates only affect the bacterial and fungal cells [34].

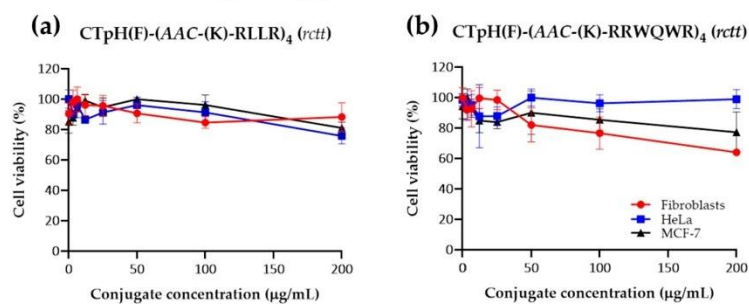


Figure 7. Cytotoxic activity on fibroblasts and MCF-7 and HeLa lines of the peptide-resorcinarene dendrimers obtained.

3. Materials and Methods

3.1. General Method

Reagents Rink amide resin, Fmoc-Leu-OH, Fmoc-Arg(Pbf)-OH, Fmoc-Trp(Boc)-OH, Fmoc-Gln(Trt)-OH, Dicyclohexylcarbodiimide (DCC), and 1-Hydroxy-6-chlorobenzotriazole (6-Cl-HOBt) were purchased from AAPPTec (Louisville, KY, USA). Reagents acetonitrile (ACN), trifluoroacetic acid (TFA), dichloromethane (DCM), diisopropylethylamine (DIPEA), N,N-dimethylformamide (DMF), ethanedithiol (EDT), isopropanol (IPA), methanol, and triisopropylsilane (TIS) were acquired from Merck (Darmstadt, Germany). SPE Supelclean™ LC-18 columns were purchased from Sigma-Aldrich (St. Louis, MO, USA). Trypticase Soy Agar (TSA), Mueller Hinton Agar (MHA), and Plate Count Agar (PCA) media were purchased from Scharlau. Mueller Hinton Broth medium was purchased from Merck. The *Escherichia coli* ATCC 25922 bacterial strain was purchased from the ATCC. The MCF-7 and

HeLa cell lines were obtained from ATCC[®] (Manassas, VA, USA). All the reagents were used directly, without previous purification.

¹H spectra were recorded at 400 MHz on a Bruker Advance 400 instrument. RP-HPLC analyzes were performed on a Chomolith C18 column (Merck, Kenilworth, NJ, USA, 50 mm), using an Agilent 1200 Liquid Chromatograph (Agilent, Omaha, NE, USA). The products were analyzed on a Bruker Impact 2 LC Q-TOF MS equipped with electrospray ionization (ESI) in positive mode and on a Bruker MicroFlex MALDI-TOF mass spectrometer.

3.2. Peptide Synthesis

Two azide-functionalized peptide sequences derived from LfcinB (20–25) and BF (32–35) were tested, as shown in Table 1. Additionally, control peptides corresponding to the LfcinB minimal motifs were synthesized and evaluated.

The designed peptides were obtained manually using the solid-phase peptide synthesis methodology, with the Fmoc/tBu strategy (SPPS-Fmoc/tBu). Rink Amida resin (200 mg, 0.46 meq/g) was used as a solid support, which was conditioned with DMF for 12 h. (i) Removal of the Fmoc group was performed by treatment with 5% 4-methylpiperidine in DMF, 10 min at room temperature (RT) ($\times 2$); then the resin was washed with DMF ($\times 5$), IPA (3), and DCM ($\times 3$). Thereupon, a fraction of the dry resin was subjected to the Kaiser test. (ii) The Fmoc-amino acid was mixed with DCC/6-Cl-HOBt in DMF to activate it by ester formation. This reaction was stirred for 15 min at room temperature. Then, the reaction mixture was added to the deprotected resin and left to react for 1 h at RT. The solution was then discarded, the resin was washed with DMF ($\times 3$; 1 min), DCM ($\times 3$; 1 min), and the Kaiser test was performed. When this test was positive, the resin was treated again with the Fmoc-activated amino acid until the test was negative. (iii) Deprotection of the side chains and cleavage of the peptide from the resin was performed by treating the dried resin-peptide with the cleavage solution containing TFA/water/TIS/EDT (93/2/2.5/2.5% v/v/v/v), for 4 h at RT. For azide-peptides, TIS and EDT were avoided. Then, the crude peptide was precipitated by treatment with cold ethyl ether, washings ($\times 5$) were carried out with this solvent, and the solid was dried at RT. Finally, the products were analyzed via RP-HPLC.

3.3. Synthesis of Resorcinarenes

3.3.1. Synthesis of Precursor 1

The synthesis of 4-(prop-2-yn-1-yloxy)benzaldehyde (precursor 1) was adapted from de Kivrak et al. [35]. 4-Hydroxybenzaldehyde (0.032 mmol) was dissolved in DMF. Then, 3-bromoprop-1-yne (0.042 mmol) and potassium carbonate (0.042 mmol) were added at room temperature. The resulting mixture was stirred constantly at room temperature for 4 h. After the completion of the reaction, the reaction mixture was cooled to 0 °C, filtered and washed with distilled water (yield 88.0%). Precursor 1 was characterized by means of ¹H and ¹³C NMR, RP-HPLC and mass spectrometry. 4-(prop-2-yn-1-yloxy)benzaldehyde: white solid in yield 88.0%. M.p. 76–78 °C. ¹H-NMR, δ (DMSO-d₆, room temperature, ppm): 10.08 (s, 1H, CHO), 8.05–8.03 (d, 2H aromatic CH), 7.45–7.28 (d, 2H aromatic CH), 4.96 (s, 2H, CH₂), 2.76 (s, 1H, HC \equiv C).

3.3.2. C-Tetra(4-(prop-2-yn-1-yloxy)phenyl)calix[4]resorcinarene

(10.0 mmol) of resorcinol was dissolved in (10.0 mmol) of the previously synthesized aldehyde (Precursor 1: 4-(prop-2-yn-1-yloxy)benzaldehyde). Subsequently, 25 mL of chloroform was added in a cold bath. Once the mixture was obtained, TFA (5.0 mL) was slowly added. This mixture was stirred at 60–65 °C for 32 h in an inert atmosphere. After the formation of a white precipitate, it was washed with successive washes of diethyl ether and acetone and dried with a drying gun (yield 58.9%). The solid obtained was characterized by means of ¹H and ¹³C NMR, RP-HPLC and mass spectrometry. C-Tetra(4-(prop-2-yn-1-yloxy)phenyl)calix[4]resorcinarene (crown-*rccc*): white solid in yield 20.8%. M.p. > 250 °C decomposition. ¹H NMR, δ (DMSO-d₆, room temperature, ppm): δ 3.57 (t, 4H, H⁷), 4.73 (d,

8H, H⁶), 5.56 (s, 4H, H⁵), 5.52 (s, 4H, H⁴), 6.50 (s, 4H, H³), 6.63 (br. m, 16H, H²), 8.54 (s, 8H, OH). ¹³C NMR (150.9 MHz, DMSO-d₆, 30 °C): δ 40.58 (s, C¹²), 55.29 (s, C¹¹), 77.92 (s, C¹⁰), 79.72 (s, C⁹), 102.04 (s, C⁸), 113.46 (s, C⁷), 120.64 (s, C⁶), 120.64 (s, C⁶), 131.65 (s, C⁵), 138.68 (s, C³), 152.43 (s, C²), 154.58 (s, C¹). C-Tetra(4-(prop-2-yn-1-yloxy)phenyl)calix[4]resorcinarene (chair-*rctt*): white solid in yield 58.9%. M.p. > 250 °C decomposition. ¹H NMR, δ (DMSO-d₆, room temperature, ppm): δ 3.50 (t, 4H, H¹), 4.62 (d, 8H, H²), 5.47 (s, 4H, H¹⁰), 5.51 (s, 2H, H³), 6.12 (s, 2H, H⁴), 6.27 (s, 2H, H⁵), 6.30 (s, 2H, H⁶), 6.50 (br. m, 16H, H⁷), 8.44 (s, 4H, OH⁸), 8.51 (s, 4H, OH⁹). ¹³C NMR (150.9 MHz, DMSO-d₆, 30 °C): δ 41.26 (s, C¹), 55.29 (s, C²), 77.79 (s, C³), 79.67 (s, C⁴), 101.67 (s, C⁵), 101.70 (s, C⁶), 113.24 (s, C⁷), 120.87 (s, C⁸), 121.16 (s, C⁹), 129.34 (s, C¹⁰), 129.70 (s, C¹¹), 131.85 (s, C¹²), 137.17 (s, C¹³), 152.44 (s, C¹⁴), 152.60 (s, C¹⁵), 154.55 (s, C¹⁶).

3.4. (Peptide)₄-Resorcinarene Conjugate Synthesis (Click Chemistry)

For the synthesis of the dendrimers, protocols from the literature [33,36–38] were adapted. Briefly, the crude peptide functionalized with azide (0.05 mmol) and the resorcinarene base (0.01 mmol) were dissolved and mixed in H₂O/DMF (1:3 v/v), and then the catalyst copper sulfate pentahydrate (CuSO₄·5H₂O) (0.00008 mmol) and sodium ascorbate (0.000016 mmol) were added to the reaction mixture. The mixture was maintained with constant stirring at RT, 30 °C, for 6 h. The progress of the reaction was monitored by RP-HPLC. Finally, the dendrimer was purified using RP-SPE and characterized via liquid chromatography (RP-HPLC) and mass spectrometry (MALDI-TOF).

3.5. Purification and Characterization

For RP-SPE, Supelclean ENVI-18 SPE cartridges (5 g bed weight, 20 mL volume) were used. SPE columns were activated before use with 30 mL methanol, 30 mL ACN (containing 0.1% TFA, solvent B) and equilibrated with 30 mL water (containing 0.1% TFA, solvent B), solvent A). Elution of the peptide or peptide-resorcinarene dendrimer was performed by increasing the percentage of solvent B in the eluent. The collected fractions were analyzed via RP-HPLC. Fractions containing the pure product were pooled and then lyophilized, and the pure product was analyzed via MALDI-TOF MS mass spectrometry. This analysis was performed on a Bruker MicroFlex MALDI-TOF mass spectrometer. RP-HPLC analyses were performed on a Chromolith C18 (50 × 4.6 mm) using an Agilent 1200 Liquid Chromatograph (Agilent, Omaha, NE, USA). Gradient elution from solvent B (0.05% TFA in acetonitrile) to solvent A (0.05% TFA in water) was performed as follows: 5/5/100/100/5/5% B at 01/01/18/21/21.1/24 min. Detection was performed at 210 nm, and the flow rate was 2 mL/min. The sample concentration was 1.0 mg/mL, and 10 µL was injected.

3.6. Activity Assays

3.6.1. Antibacterial Activity

The minimum inhibitory concentration (MIC) was determined using a broth microdilution assay. Specifically, 90 µL of Mueller Hinton broth and 90 µL of peptide (initial concentration 444 µg/mL) were added to a 96-well plate, with serial dilutions (200, 100, 50, 25, 12.5, and 6, 2 µg/mL). Then, 10 µL (5 × 10⁵ CFU/mL) of inoculum was added to each well, and the final volume in each well was 100 µL. They were incubated for 24 h at 37 °C, and absorbance at 620 nm was measured using the ELISA reader. To determine the minimum bactericidal concentration (MBC), an aliquot was taken from each well and placed on a Mueller Hinton Agar plate. After 24 h of incubation at 37 °C, the MBC was determined. Each of these tests was performed in duplicate [39].

3.6.2. Antifungal Activity

Antifungal susceptibility testing was performed using the broth microdilution (BMD) method, following CLSI M27-A3 guidelines with slight modifications [40]. Briefly, yeast suspension was prepared in 0.85% saline (SS) and adjusted to 1–5 × 10⁶ cells/mL (0.5 McFarland

standard). It was then diluted in RPMI 1640 liquid medium (Sigma-Aldrich, Saint Louis, MA, USA) (with MOPS, pH 7.2) and adjusted to 0.5×10^3 – 2.5×10^3 cells/mL. A measure of 100 μ L of yeast inoculum was added to a 96-well plate containing serial dilutions of the dendrimer. The final concentrations used were 200, 100, 50, 25, 12.5, and 6.2 μ g/mL. FLC drug was used as a control (0.125 to 128 μ g/mL). Minimal inhibitory concentrations (MICs) were visualized and densitometry (595 nm, microplate reader, iMarkTM, Bio-rad) was used to determine the lowest concentration that caused a significant decrease compared to the untreated growth control after 48 h of incubation. The MIC endpoint was defined as the lowest concentration capable of inhibiting 80% of cell growth compared to its respective positive control. Three independent trials were performed. To verify that the tested molecule could kill yeast cells, the plates were also tested for minimal fungicidal concentration (MFC). Briefly, aliquots from each well of the susceptibility test assays were transferred to plates containing Sabouraud Dextrose Agar (SDA), which were then incubated.

3.7. Time-Kill Curve

The time-kill curve was constructed using the CLSI protocol, with some modifications [41]. Before testing, the bacterial strains of *E. coli* ATCC 25922 and *S. aureus* ATCC were subcultured in Tryptic Soy Agar. The colonies of a 24 h culture were suspended in 9 mL of heart infusion broth and adjusted to the standard by means of a calibration curve. These procedures resulted in an initial inoculum of approximately 5×10^5 CFU/mL. The final working volumes in the peptide ($0.5 \times$ MIC, MIC, and $2 \times$ MIC final concentrations) and inoculum experiments were 270 μ L and 30 μ L, respectively. The samples were incubated on Bioscreen C equipment for 48 h at 37 °C, and absorbance readings (600 nm) were obtained at 0 h (before the addition of peptide) and then repeatedly every hour up to 48 h.

3.8. Cytotoxic Activity

3.8.1. Cell Culture

For all cell lines, the medium used was Dulbecco's Modified Eagle's Medium (DMEM)/Ham F-12 Nutrient Mix. For the MCF-7 line, the medium was supplemented with 10% fetal bovine serum (SFB), 1.5 g/L of NaHCO₃ and NaOH up to pH 7.4, amphotericin (200 μ g/mL), and 1% penicillin and streptomycin. For fibroblast cells, in addition to the above, hydrocortisone (250 μ g/mL) was added. All the media were filtered through a 0.22 μ m membrane.

3.8.2. MTT Assay

Briefly, cells were seeded with complete medium in 96-well plates at a rate of 10,000 cells and 100 μ L per well and allowed to adhere to the plates for 24 h. Subsequently, the complete medium was removed, and incomplete medium was added for synchronization for another 24 h. The cells were incubated at 37 °C for 2, 24, or 48 h with 100 μ L of peptide at the concentrations to be evaluated (200, 100, 50, 25, 12.5, 6.25, and 3.1 μ g/mL). Next, the peptide was removed from the box and 100 μ L of incomplete medium with 10% 3-(4,5-dimethylthiazol-2-yl)-2,5-diphenyltetrazole (MTT) bromide was added and incubated for 4 h. The medium was replaced with 100 μ L of isopropanol (IPA), and after 30 min of incubation at 37 °C, the absorbance at 575 nm was measured. Incomplete culture medium with 10% MTT was used as a negative control, and cells without MTT treatment were used as a positive control [34].

3.8.3. Hemolysis Assay

First, 5.0 mL of heparinized peripheral blood was centrifuged at 1000 rpm for 7 min. The erythrocyte fraction was suspended in 10 μ of saline solution (SS) and washed twice by centrifugation at 1000 rpm for 7 min. The erythrocytes (2% hematocrit) were incubated with peptide (ranging from 6.2 to 200 μ g/mL) for 2 h at 37 °C. SS was used as a negative control, while distilled water was used as a positive control. The mixtures were centrifuged, the supernatants were collected, and the absorbance was determined to be 540 nm [42].

4. Conclusions

Using solid phase peptide synthesis (SPPS), it was possible to obtain two azide-functionalized peptides derived from LfcinB and BF. Moreover, an alkyne-functionalized resorcinarene-derived core was synthesized. Through click chemistry, CuAAC, it was possible to obtain two tetra-functionalized dendrimers characterized using RP-HPLC, ESI-MS, and MALDI-TOF. These new conjugates showed enhanced antimicrobial activity against *E. coli* ATCC 25922, *S. aureus* ATCC 25923, and bacterial clinical isolates and strains of *Candida* spp. There was no evidence of any type of effect on the cytotoxic activity in blood, fibroblasts, or cancer cell lines, which means that these tetravalent (peptide)_n-resorcinarene conjugates are selective antimicrobial agents. In addition, a new route for the synthesis of functionalized conjugates with peptide sequences was established, since this is the first time that the synthesis of tetra-functionalized resorcinarenes with sequences derived from LfcinB and BF has been reported.

Supplementary Materials: The following supporting information can be downloaded at: <https://www.mdpi.com/article/10.3390/antibiotics12040773/s1>, Figure S1: Analysis of p-hydroxyphenyl functionalized with the alkyne group (4-(prop-2-yn-1-yloxy)benzaldehyde), chromatographic profile and mass spectra; Figure S2: Chromatographic profile and mass spectrum of purified (a) *rcct*-chair conformer and (b) *recc*-crown conformer; Figure S3: Analysis of C-tetra(p-hydroxyphenyl)calix[4]resorcinarene *rcct* functionalized with the alkyne group, ¹³C-NMR; Figure S4: C-tetra(p-hydroxyphenyl)calix[4]resorcinarene *recc* functionalized with the alkyne group, ¹³C-NMR; Figure S5: Azide-peptide synthesis diagram; Figure S6: Chromatographic profiles of the peptide-resorcinarene conjugates (a) CTpH(F)-(AAC-(K)-RLLR)₄ (*rcct*), (b) CTpH(F)-(AAC-(K)-RRWQWR)₄ (*rcct*); Figure S7: HR-MS of the peptide-resorcinarene conjugates (a) CTpH(F)-(AAC-(K)-RLLR)₄ (*rcct*), (b) CTpH(F)-(AAC-(K)-RRWQWR)₄ (*rcct*).

Author Contributions: Conceptualization, M.M.-V. and Z.J.R.-M.; funding acquisition, M.M.-V., Z.J.R.-M. and C.M.P.-G.; investigation, H.M.P.-C., M.M.-V. and Z.J.R.-M.; methodology, H.M.P.-C., A.L.L.-C., C.M.P.-G., R.F.-M. and J.E.G.-C.; project administration, M.M.-V. and Z.J.R.-M.; writing—original draft, H.M.P.-C., M.M.-V. and Z.J.R.-M.; writing—review and editing, A.L.L.-C., C.M.P.-G., R.F.-M. and J.E.G.-C. All authors have read and agreed to the published version of the manuscript.

Funding: This research was funded by COLCIENCIAS, Project contract RC No 846–2019.

Institutional Review Board Statement: Not applicable.

Informed Consent Statement: Not applicable.

Data Availability Statement: Not applicable.

Conflicts of Interest: The authors declare no conflict of interest.

References

1. WHO. Antibiotic Resistance. Available online: <http://www.who.int/mediacentre/factsheets/antibiotic-resistance/en/> (accessed on 15 February 2023).
2. WHO. Prevention & AMP. Available online: <http://www.who.int/antimicrobial-resistance/amr-aidememoire-may2016.pdf> (accessed on 15 February 2023).
3. WHO. Available online: http://www.who.int/antimicrobial-resistance/Microbes_and_Antimicrobials/en/ (accessed on 15 February 2023).
4. WHO. WHO Publishes List of Bacteria for Which New Antibiotics Are Urgently Needed. Available online: <http://www.who.int/mediacentre/news/releases/2017/bacteria-antibiotics-needed/en/> (accessed on 15 February 2023).
5. Castañeda-Casimiro, J.; Ortega-Roque, J.A.; Marcela, A.; Aquino-Andrade, A.; Serafin-López, J.; Estrada-Parra, S.; Estrada, I. Péptidos Antimicrobianos: Péptidos Con Múltiples Funciones. *Alerg. Asma Inmunol.* **2009**, *18*, 16–29.
6. Pineda-Castañeda, H.M.; Insuasty-Cepeda, D.S.; Niño-Ramírez, V.A.; Curtidor, H.; Rivera-Monroy, Z.J. Designing Short Peptides: A Sisyphean Task? *Curr. Org. Chem.* **2020**, *24*, 2448–2474. [CrossRef]
7. Agrawal, Y.K.; Patadia, R.N. Studies on Resorcinarenes and Their Analytical Applications. *Rev. Anal. Chem.* **2006**, *25*, 155–239. [CrossRef]
8. Shah, M.D.; Agrawal, Y. Calixarene: A New Architecture in the Analytical and Pharmaceutical Technology. *J. Sci. Ind. Res.* **2012**, *71*, 21–26.
9. Jain, V.K.; Kanaiya, P.H. Chemistry of calix[4]resorcinarenes. *Russ. Chem. Rev.* **2011**, *80*, 75–102. [CrossRef]

10. Puttreddy, R.; Beyeh, N.K.; Rissanen, K. Conformational changes in C_{methyl}-resorcinarene pyridine: N-oxide inclusion complexes in the solid state. *Cryst. Eng. Comm.* **2016**, *18*, 4971–4976. [[CrossRef](#)]
11. Moore, D.; Watson, G.W.; Gunnlaugsson, T.; Matthews, S.E. Selective formation of the *rcft* chair stereoisomers of octa-O-alkyl Resorcin[4]arenes using Brønsted acid catalysis. *New J. Chem.* **2008**, *32*, 994–1002. [[CrossRef](#)]
12. Ziaja, P.; Krogul, A.; TS, P.; Litwinienko, G. Structure and stoichiometry of resorcinarene solvates as host-guest complexes—NMR, X-ray and thermoanalytical studies. *Thermochim. Acta* **2016**, *623*, 112–119. [[CrossRef](#)]
13. Castillo-Aguirre, A.A.; Pérez-Redondo, A.; Maldonado, M. Influence of the hydrogen bond on the iteroselective O-alkylation of calix[4]resorcinarenes. *J. Mol. Struct.* **2020**, *1202*, 127402. [[CrossRef](#)]
14. Pedro-Hernández, L.D.; Martínez-Klimova, E.; Cortez-Maya, S.; Mendoza-Cardozo, S.; Ramírez-Ápan, T.; Martínez-García, M. Synthesis, Characterization, and Nanomedical Applications of Conjugates between Resorcinarene-Dendrimers and Ibuprofen. *Nanomaterials* **2017**, *7*, 163. [[CrossRef](#)]
15. Tang, H.; Guo, H.; Yang, F.; Zhu, S. Synthesis and mesomorphic properties of calix[4]resorcinarene-triphenylene oligomers. *Liq. Cryst.* **2017**, *44*, 1566–1574. [[CrossRef](#)]
16. Reynolds, M.R.; Pick, F.S.; Hayward, J.J.; Trant, J.F. A Concise Synthesis of a Methyl Ester 2-Resorcinarene: A Chair-Conformation Macrocyclic. *Symmetry* **2021**, *13*, 627. [[CrossRef](#)]
17. Rashad, A.A. Click Chemistry for Cyclic Peptide Drug Design. *Methods Mol. Biol.* **2019**, *2001*, 133–145. [[CrossRef](#)] [[PubMed](#)]
18. Ahmad Fuaad, A.A.H.; Azmi, F.; Skwarczynski, M.; Toth, I. Peptide Conjugation via CuAAC ‘click’ Chemistry. *Molecules* **2013**, *18*, 13148–13174. [[CrossRef](#)] [[PubMed](#)]
19. Singh, M.S.; Chowdhury, S.; Koley, S. Advances of Azide-Alkyne Cycloaddition-Click Chemistry over the Recent Decade. *Tetrahedron* **2016**, *72*, 5257–5282. [[CrossRef](#)]
20. Pineda-Castañeda, H.M.; Rivera-Monroy, Z.J.; Maldonado, M. Copper(I)-Catalyzed Alkyne–Azide Cycloaddition (CuAAC) “Click” Reaction: A Powerful Tool for Functionalizing Polyhydroxylated Platforms. *ACS Omega* **2023**, *8*, 3650–3666. [[CrossRef](#)] [[PubMed](#)]
21. Alfei, S.; Schito, A.M. From Nanobiotechnology, Positively Charged Biomimetic Dendrimers as Novel Antibacterial Agents: A Review. *Nanomaterials* **2020**, *10*, 2022. [[CrossRef](#)]
22. Baker, S.D.; Sparreboom, A.; Verweij, J. Clinical Pharmacokinetics of Docetaxel: Recent Developments. *Clin. Pharm.* **2006**, *45*, 235–252. [[CrossRef](#)]
23. Starpharma. *Starpharma to Commence DEP® Cabazitaxel Phase 1/2 Trial*; BioSpectrum: Singapore, 2018.
24. INSTITUT PASTEUR. *A Synthetic Glycopeptide for Anti-Tumor Immunotherapy: From Design to First Use in Human*; INSTITUT PASTEUR: Paris, France, 2015.
25. ClinicalTrials. *Treatment of Non-Responding to Conventional Therapy Inoperable Liver Cancers by In Situ Introduction of ImDendrim (ImDendrim)*; National Library of Medicine: Bethesda, MD, USA, 2017.
26. ClinicalTrials. *A Study to Evaluate the Safety, Tolerability, and Pharmacokinetics of OP-101 after Intravenous Administration in Healthy Volunteers*; National Library of Medicine: Bethesda, MD, USA, 2018.
27. Patel, P.; Patel, V.; Patel, P.M. Synthetic Strategy of Dendrimers: A Review. *J. Indian Chem. Soc.* **2022**, *99*, 100514. [[CrossRef](#)]
28. Soomro, Z.H.; Cecioni, S.; Blanchard, H.; Praly, J.P.; Imbert, A.; Vidal, S.; Matthews, S.E. CuAAC synthesis of resorcin[4]arene-based glycoclusters as multivalent ligands of lectins of lectins. *Org. Biomol. Chem.* **2011**, *9*, 6587–6597. [[CrossRef](#)]
29. Knyazeva, I.R.; Abdrafikova, D.K.; Mukhamedyanova, K.M.; Syakaev, V.V.; Gabidullin, B.M.; Gubaidullin, A.T.; Habicher, W.D.; Burirov, A.R.; Pudovik, M.A. Synthesis of novel highly functionalized triazole-linked calix[4]resorcinols via click reaction. *Mendeleev Commun.* **2017**, *27*, 556–558. [[CrossRef](#)]
30. Pineda-Castañeda, H.M.; Maldonado, M.; Rivera-Monroy, Z.J. Efficient Separation of C-Tetramethylcalix[4]resorcinarene Conformers by Means of Reversed-Phase Solid-Phase Extraction. *ACS Omega* **2023**, *8*, 231–237. [[CrossRef](#)] [[PubMed](#)]
31. Schneggenburger, P.E.; Worbs, B.; Diederichsen, U. Azide Reduction during Peptide Cleavage from Solid Support—The Choice of Thioscavenger? *J. Pept. Sci.* **2010**, *16*, 10–14. [[CrossRef](#)] [[PubMed](#)]
32. Aguirre-Guataqui, K.; Márquez-Torres, M.; Pineda-Castañeda, H.M.; Vargas-Casanova, Y.; Ceballos-Garzon, A.; Rivera-Monroy, Z.J.; García-Castañeda, J.E.; Parra-Giraldo, C.M. Chimeric Peptides Derived from Bovine Lactoferrin and Buforin II: Antifungal Activity against Reference Strains and Clinical Isolates of *Candida* spp. *Antibiotics* **2022**, *11*, 1561. [[CrossRef](#)]
33. Pineda-Castañeda, H.M.; Bonilla-Velásquez, L.D.; Leal-Castro, A.L.; Fierro-Medina, R.; García-Castañeda, J.E.; Rivera-Monroy, Z.J. Use of Click Chemistry for Obtaining an Antimicrobial Chimeric Peptide Containing the LfcinB and Buforin II Minimal Antimicrobial Motifs. *ChemistrySelect* **2020**, *5*, 1655–1657. [[CrossRef](#)]
34. Guerra, J.R.; Cárdenas, A.B.; Ochoa-Zarzosa, A.; Meza, J.L.; Pérez, A.U.; Fierro-Medina, R.; Monroy, Z.J.R.; Castañeda, J.E.G. The Tetrameric Peptide LfcinB (20–25)₄ Derived from Bovine Lactoferrin Induces Apoptosis in the MCF-7 Breast Cancer Cell Line. *RSC Adv.* **2019**, *9*, 20497–20504. [[CrossRef](#)] [[PubMed](#)]
35. Kivrak, A.; Yilmaz, C.; Konus, M.; Koca, H.; Aydemir, S.; Oagaz, J.A. Synthesis and biological properties of novel 1-methyl-2-(2-(prop-2-yn-1-yloxy)benzylidene)hydrazine analogues. *Turk. J. Chem.* **2018**, *42*, 306–316. [[CrossRef](#)]
36. Li, X. Click to Join Peptides/Proteins Together. *Chem. Asian J.* **2011**, *6*, 2606–2616. [[CrossRef](#)]
37. Avrutina, O.; Empting, M.; Fabritz, S.; Daneschdar, M.; Frauendorf, H.; Diederichsen, U.; Kolmar, H. Application of copper(I) catalyzed azide-alkyne[3+2] cycloaddition to the synthesis of template-assembled multivalent peptide conjugates. *Org. Biomol. Chem.* **2009**, *7*, 4177–4185. [[CrossRef](#)]

38. Suárez, A. Reacciones de cicloadición 1,3-dipolares a alquinos catalizadas por cobre. *An. Quím.* **2012**, *108*, 306–313.
39. Cockerill, F.; Clinical and Laboratory Standards Institute. *Methods for Dilution Antimicrobial Susceptibility Tests for Bacteria That Grow Aerobically: Approved Standard*; Clinical and Laboratory Standards Institute: Malvern, PA, USA, 2015.
40. Clinical and Laboratory Standards Institute. M27-A3. In *Reference Method for Broth Dilution Antifungal Susceptibility Testing of Yeasts Approved Standard—Third Edition*; Clinical and Laboratory Standards Institute: Wayne, PA, USA, 2008.
41. Barry, A.L.; Craig, W.A.; Nadler, L.H.; Reller, L.B. M26-A: Methods for Determining Bactericidal Activity of Antimicrobial Agents; Approved Guideline. *Clin. Lab. Stand. Inst.* **1999**, *19*, 56–78.
42. Langan, T.; Rodgers, K.; Chou, R. Synchronizaton of Mammalian Cell Cultures by Serum Deprivation. *Methods Cell Sci.* **2017**, *1524*, 97–105. [[CrossRef](#)]

Disclaimer/Publisher's Note: The statements, opinions and data contained in all publications are solely those of the individual author(s) and contributor(s) and not of MDPI and/or the editor(s). MDPI and/or the editor(s) disclaim responsibility for any injury to people or property resulting from any ideas, methods, instructions or products referred to in the content.

Efficient Separation of C-Tetramethylcalix[4]resorcinarene Conformers by Means of Reversed-Phase Solid-Phase Extraction

Héctor Manuel Pineda-Castañeda, Mauricio Maldonado, and Zuly Jenny Rivera-Monroy*

Cite This: *ACS Omega* 2023, 8, 231–237

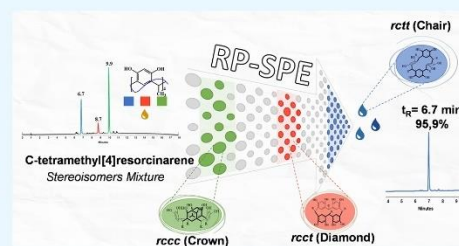
Read Online

ACCESS |

Metrics & More

Article Recommendations

ABSTRACT: A reversed-phase high-performance liquid chromatography (RP-HPLC) method was developed to study the conformer formation generated during the reaction for obtaining C-tetramethylcalix[4]resorcinarene. The chromatographic method was used to design a strategy for purifying the reaction products, using solid-phase extraction columns (RP-SPE) and gradient elution. The chromatographic profiles of the cyclocondensation reaction between resorcinol and acetaldehyde show the presence of three products under the different reaction and precipitation conditions studied. Using RP-SPE, it was possible to enrich the products, which were later characterized by means of RP-HPLC and ¹H nuclear magnetic resonance (NMR). This investigation explored and established a new method for RP-HPLC analysis and RP-SPE separation of conformational isomers obtained in the formation reaction of C-tetramethylcalix[4]resorcinarene.



1. INTRODUCTION

Currently, the synthesis and characterization of macrocycles have generated great interest since they have exhibited great versatility in their use in supramolecular chemistry, catalysis, and separation science, and they have also attracted much interest due to their potential use in designing drug delivery systems.^{1–5} Many receptors and host molecules adopt specific geometries and conformations.⁶ Among these compounds are resorcinarenes, also known as calix[4]resorcinarenes. These are polyhydroxylated macrocyclic compounds derived from resorcinol, first synthesized by Baeyer et al. from aliphatic and aromatic aldehydes.^{7,8} They are made up of four resorcinol rings joined by a bridging atom, usually carbon within a methylene group at positions 4 and 6, producing the formation of a cyclic structure typically represented as a truncated cone with an upper and lower edge (Figure 1a). These bridging atoms are often replaced by aliphatic and/or aromatic chains, allowing the formation of conformational isomers (stereoisomerism).⁹

The versatility of these host systems stems from easy synthetic modifications to either the upper or lower edge of these macrocycles. However, it is known that the resorcinarene conformations of the nucleus (unsubstituted) are quite easily modulated by the reaction conditions when the host is synthesized.⁶ Five possible conformers have been reported: (i) crown, (ii) boat, (iii) saddle, (iv) chair, and (v) diamond (Figure 1b).¹⁰ Each of these conformations is possible according to aspects such as the position of the resorcinol units and the substituents on the methylene bridges. For most

of the cases reported in the synthesis of C-tetramethylcalix[4]resorcinarene, the most stable conformation is the crown type. It is established from the deep cavities formed and their stabilization by means of hydrogen bonds mediated by the hydroxyl groups present.^{11–14} Other unusual conformations have been reported, such as *rccf*-diamond for C-tetramethylcalix[4]resorcinarene, which is rarely observed,¹⁵ and the *rccf*-boat for C-tetramethyl-2-nitrocalix[4]resorcinarene.¹⁶ In the C_{4v} conformation, intramolecular hydrogen bonds between adjacent phenolic hydroxyl groups preserve the crown structure.

The interconversion of conformational isomers has been reported from the synthesis of a triangular structural brick-wall framework based on C-tetramethylcalix[4]resorcinarene and 1,4-bis(pyridyl)ethylene (bpe) formed by converting a polymeric structure with a bowl-to-boat conformational change.¹⁷ When the conformation is converted from bowl to boat, the intramolecular hydrogen bonds within the upper edge break and change their orientation to the axial direction. This allows hydrogen bonding with the bpe dimers that are redirected into the cavity to facilitate bond formation.¹⁸

Received: May 23, 2022

Accepted: August 11, 2022

Published: December 21, 2022



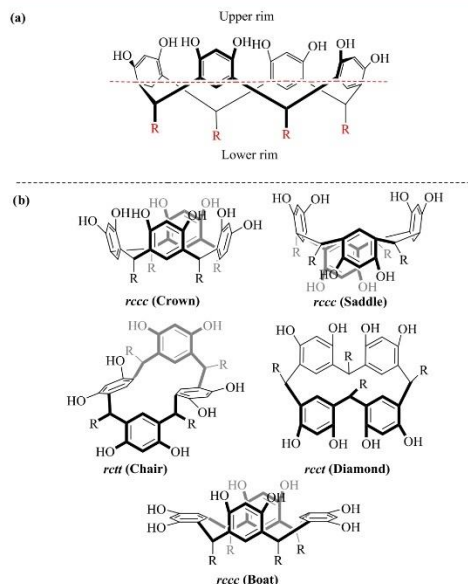


Figure 1. (a) Illustration of the structure of calix[4]resorcinarene crown conformer (upper ring and lower ring). (b) Reported conformational isomers and relative configuration of the substituents on the methylene bridge.

However, sometimes under different synthesis conditions, the presence of conformer mixtures is reported, which makes it difficult to properly characterize each of the products, and there are frequent difficulties for separation since the reaction product behaves as a single compound viewed through TLC and liquid chromatography (LC), but the ^1H NMR and ^{13}C NMR spectrum is consistent with there being two isomers. Alternatives have been sought on this subject, trying to recrystallize the material, but they did not change the relationship of the signals or enrich the conformers.¹⁹ In an effort to solve these difficulties, methods for separating mixtures of conformational isomers for C-tetra(*p*-hydroxyphenyl)calix[4]resorcinarene have been described, where through RP-HPLC two well-resolved signals corresponding to the crown and chair isomers were found, and through the application of an RP-SPE protocol, the separation of the two stereoisomers with high purity and their subsequent characterization using techniques such as FT-IR, ^1H NMR, and ^{13}C NMR were achieved, which confirmed their chemical identity.^{20,21} Although the derivatives of calix[4]resorcinarene are molecules that are of great interest in the chemical and pharmaceutical field given their wide range of applications, there is a limitation in their purification stages. To solve this difficulty, in the present investigation, a new method for RP-HPLC analysis and RP-SPE separation of conformational isomers obtained in the formation reaction of C-tetramethylcalix[4]resorcinarene were explored and established.

2. MATERIALS AND METHODS

2.1. General Method. ^1H spectra were recorded at 400 MHz on a Bruker Advance 400 instrument. Molar mass was determined with an Agilent 6470 triple quadrupole mass spectrometer. RP-HPLC analyses were performed on a Chromolith RP-18e column (Merck, Kenilworth, NJ, 50 mm), using an Agilent 1200 Liquid Chromatograph (Agilent, Omaha, NE). All products were analyzed on a Bruker Impact II LC Q-TOF MS equipped with electrospray ionization (ESI) in positive mode.

2.2. Synthesis of C-Tetramethylcalix[4]resorcinarene (Stereoisomers Mixture). We followed the method reported by Hoegberg et al.²² A 1,3-dihydroxybenzene solution (1 mmol) and acetaldehyde (1 mmol) in water (4.0 mL) was added drop by drop to hydrochloric acid (1.0 mL) and was heated at reflux with constant stirring for 1 h. A precipitate was rapidly formed. The precipitate was formed, cooled in an ice bath, and washed with water to remove traces of acid. The filtrate was dried under reduced pressure and characterized by means of ^1H NMR.

2.2.1. C-Tetramethylcalix[4]resorcinarene (Crown) 1a. White solid in yield 37.5%. M.P. >250 °C decomposition. ^1H NMR, δ (DMSO- d_6 , room temperature, ppm): CH_3 (1.39, d), CH (4.45, q), aromatic CH (6.14, s), aromatic CH (6.77, s), OH (8.53, s).

2.2.2. C-Tetramethylcalix[4]resorcinarene (Chair) 1b. Cream solid in yield 6.25%. M.P. >250 °C decomposition. ^1H NMR, δ (DMSO- d_6 , room temperature, ppm): CH_3 (1.15, d), CH (4.37, q), aromatic CH (6.08, 6.17, s), aromatic CH (6.26, 6.79, s), OH (8.41, 8.65, s).

2.2.3. C-Tetramethylcalix[4]resorcinarene (Diamond) 1c. Cream solid in yield 3.6%. M.P. >250 °C decomposition. ^1H NMR, δ (DMSO- d_6 , room temperature, ppm): CH_3 (1.15, 1.40), CH (4.38–4.46), aromatic CH (6.12, 6.16, 6.21, 6.29), aromatic CH (6.86, 6.90, 6.98, 7.29), OH (8.50–8.90).

2.3. LC Q-TOF MS. All products were analyzed on a Bruker Impact IILC Q-TOF MS equipped with electrospray ionization (ESI) in positive mode. Chromatographic conditions were: Intensity Solo C18 column (2.1 \times 100 mm, 1.8 μm) (Bruker Daltonik), at a temperature of 40 °C and a flow rate of 0.250 mL/min. Mobile phase water (A) and acetonitrile (B), each containing 0.1% formic acid. Gradient elution 5/5/95/95/5/5% B in 0/1/11/13/13.1/15 min. ESI source conditions: end plate offset 500 V, capillary 4500 V, nebulizer 1.8 bar, dry gas nitrogen 8.0 L/min, dry temperature 220 °C. Scan mode Auto MS/MS with spectral range 20–1000 m/z , spectra rate 2 Hz, and collision energy of 5.0 eV.

2.4. Separation of the Mixture by RP-HPLC. RP-HPLC analyses were performed on a Chromolith RP-18e (50 \times 4.6 mm) using an Agilent 1200 liquid chromatograph (Agilent, Omaha, NE). A gradient elution of solvent B (TFA 0.05% in acetonitrile) in solvent A (TFA 0.05% in water) was performed as follows: 5/5/100/100/5/5% B at 0/1/18/21/21.1/24 min. Detection was performed at 210 nm, and the flow rate was 2 mL/min. The sample concentration of C-tetramethylcalix[4]resorcinarene (conformational mixture) was 1.0 mg/mL, and 10 μL was injected.

2.5. Separation of the Mixture via SPE. Supelclean ENVI-18 SPE cartridges (bed wt. 5 g, volume 20 mL) were used. SPE columns were activated prior to use with 30 mL of methanol and 30 mL of ACN (containing 0.1% TFA, solvent B) and were equilibrated with 30 mL of water (containing

0.1% TFA, solvent A). C-Tetramethylcalix[4]resorcinarene (conformational mixture) (46 mg) was dissolved in 1000 μL of ACN/ H_2O (50:50), and the solution was added to the column. The conformational mixture elution was performed by increasing the percentage of solvent B in the eluent. The collected fractions were analyzed via RP-HPLC. The fractions containing the pure conformer were mixed and then lyophilized.

3. RESULTS AND DISCUSSION

As can be found in the literature,^{22–24} there are several synthesis procedures that can be carried out between resorcinol and acetaldehyde. These methods involve changing conditions such as pH and temperature, among others. Considering several of these published articles, we proposed to carry out a reaction between acetaldehyde and resorcinol using the procedure described by Hoegberg et al.²² As it is shown in the Material and Methods (section 2.2), the synthesis of resorcinarene was carried out through the acid-catalyzed cyclocondensation of resorcinol with acetaldehyde in water heated at reflux for 1 h. The solid product formed was filtered, washed, and dried in accordance with the conventional purification process. Preliminary TLC analysis of the solid showed the formation of two products; however, ^1H NMR analysis of the solid showed several resonance signals for the aromatic hydrogen atoms for the conformer mixture at 6.08–6.79 ppm, the methylene bridges fragments at 4.37 and 4.45 ppm, and hydroxyl moieties ($\delta = 8.41–8.65$ ppm). Due to the complexity of the signals observed in the ^1H NMR spectrum by means of the methodology adapted from the literature, this contrasts with the results obtained previously,^{22,24} in which it was reported that the cyclocondensation reactions allow the formation of two conformers (chair and crown). The formation of a third product was seen, as evidenced by the number of signals in the aliphatic region, which can be considered to be a third conformed, or the formation of trioxane ring (Figure 2), which can be formed even under the working reaction conditions.^{25,26}

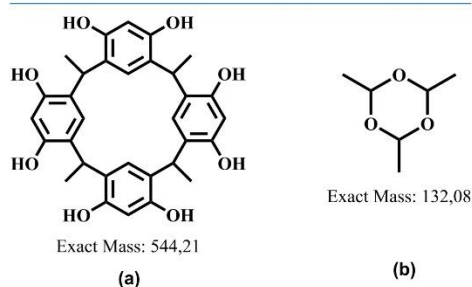


Figure 2. Possible products formed during the cyclocondensation reaction between acetaldehyde and resorcinol: (a) C-tetramethylcalix[4]resorcinarene conformers and (b) 2,4,6-trimethyl-1,3,5-trioxane.

As mentioned, these results were interesting since the characterization of three products from the cyclocondensation between acetaldehyde and resorcinol was not found in the consulted literature. To establish if the reaction mixture corresponded to three structural isomers or perhaps one of the products corresponded to a trioxane-type intermediate, we

proposed to establish which of the two product types could be formed. Therefore, first, the mixture was analyzed by means of RP-HPLC with a UV/vis detector (210 nm), and then two C18 columns were tested, a packed and a monolithic. The optimized separation method (using the monolithic column) showed a chromatographic profile in the presence of three well-resolved peaks at $t_R = 6.7, 8.7,$ and 9.9 min (Figure 3b). Then, the reaction mixture was analyzed via UPLC and electrospray ionization (ESI)-mass spectrometry (MS), recording in the positive-ion mode. The chromatographic profile also showed three principal peaks, and all of them exhibited an MS spectrum with a signal at m/z 545.21 corresponding to the $[\text{M} + \text{H}]^+$ species (Figure 3c). According to the information obtained from the UPLC-MS analysis, the formation of three products was confirmed. Additionally, it can be deduced that the three products are isomers.

Once it was established that the solid product obtained corresponds to a mixture of three isomers, it was decided to separate them using the previously described RP-SPE technique.^{20,21} From the RP-HPLC profile, using eq 1, the percentage of solvent B (TFA 0.05% in acetonitrile) was calculated, in which each conformer eluted ($\%B_e$).

$$\%B_e = \%B_i + (t_{R_i} - (t_D + t_{\text{delay}} + t_0)) \frac{\Delta\%B}{t_G} \quad (1)$$

Specifically, the RP-HPLC used elution program was: 5/5/100/100/5/5% B at 0/1/18/21/21.1/24 min, where $t_G = 17$ min, $t_{\text{delay}} = 1$ min, $\%B_i = 5\%$ and $\Delta\%B = 95\%$. Additionally, the HPLC dwell time (t_D) and column dead time (t_0) were previously measured and they correspond to 0.9 and 0.82 min. As an example, eq 2 shows the determination of $\%B_e$ for a peak at 6.7 min.

$$\begin{aligned} \%B_e &= 5\% + (6.7 - (0.9 + 1.0 + 0.82)) \text{min} \frac{95\%}{17 \text{ min}} \\ &= 27\%B \end{aligned} \quad (2)$$

Equation 1 allowed us to establish that the peak at retention times of 6.7, 8.7, and 9.9 min eluted at 27, 38, and 45% of solvent B, respectively. This information allowed us to design a gradient elution program for separating the conformers by means of the SPE technique. The planned program initiated with a 5% B fraction and increased then to 10, 15, 17, 19, 22, 24, 26, 28, 30, 33, 35, 36, 37, 40, 42, 50, and 100% B; 10 mL of each fraction were prepared.

Then, 45.6 mg of the conformational mixture was dissolved in 1000 μL of ACN/ H_2O (50:50) and loaded onto a 5 g RP-SPE cartridge. The elution was performed by increasing the percentage of solvent B in the eluent. The collected fractions were analyzed online, via UV-vis dispositive, and then by RP-HPLC, to determine the chromatographic purity. The compound corresponding to the peak with $t_R = 6.7$ min (Figure 3b) eluted in a range of solvent B of 19–26% B, the second compound ($t_R = 8.7$ min, Figure 3b) eluted in a range of 33–35% B, and finally the majority species, ($t_R = 9.9$ min) eluted in a $\%B$ range of 37–42. The fractions containing each pure conformer were mixed and then lyophilized. This method furnishes products with great purity; there is no need for sophisticated equipment, and the consumption of the mobile phase is minimal.

The purified products were quantified, and the conformations of the macrocycle derivatives were established via ^1H NMR spectroscopy in $\text{DMSO}-d_6$ at room temperature (Figure

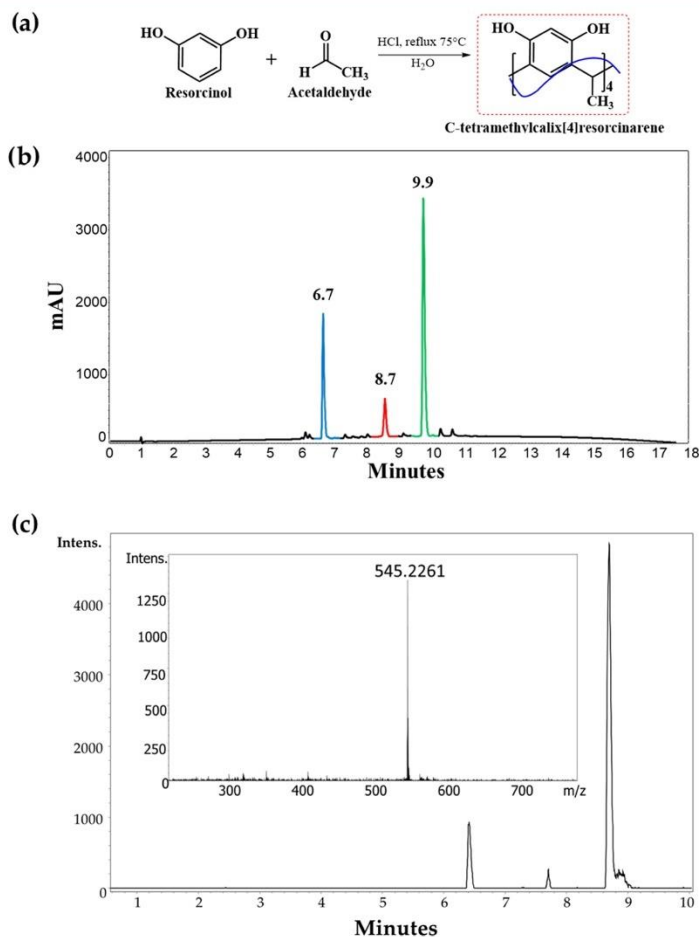


Figure 3. (a) Reaction of cycloaddition between resorcinol and acetaldehyde. Reaction mixture analysis by (b) RP-HPLC/UV-Vis, analysis recorded at 210 nm, and (c) UPLC-MS (ESI). TIC and MS spectra of the peak at 8.7 min.

4). The ¹H NMR spectra of the majority product ($t_R = 9.9$ min) showed a signal at 8.53 ppm assigned to hydroxyl groups attached to resorcinol residues in the macrocyclic system. In the aromatic region, two signals can be seen in the resorcinol residues, one corresponding to the protons in the ortho position with respect to the hydroxyl group at 6.15 ppm and the other signal corresponding to the protons in the meta position with respect to the hydroxyl groups at 6.77 ppm. In the aliphatic region, the compound displayed the characteristic signal of a methine bridge at 4.45 ppm and the signal at 1.39 ppm corresponding to the methyl group. So, all of the patterns were consistent with the structure of the expected crown conformer **1a**, which has fewer signals in the spectrum.²⁴ On the other hand, the ¹H NMR spectra of product **1b** ($t_R = 6.7$ min) showed two signals, at 8.41 and 8.65 ppm, corresponding

to two classes of hydroxyl groups attached to resorcinol residues in the macrocyclic system. In the aromatic region, four signals can be seen in the resorcinol residues, two corresponding to the protons in the ortho position with respect to the hydroxyl group at 6.08 and 6.17 ppm and the other two corresponding to the protons in the meta position with respect to the hydroxyl groups at 6.26 and 6.79 ppm. In the aliphatic region, two signals were observed, at 4.37 and 1.15 ppm, corresponding to the methine and methyl groups. Thus, these patterns were consistent with the structure of the expected chair conformer.²⁴

Product **1c** ($t_R = 8.7$ min) showed a strong tendency for decomposition; for this reason, its characterization was only carried out in solution. As shown in Figure 4, the complete absence of symmetry in conformer **1c** is reflected in the ¹H

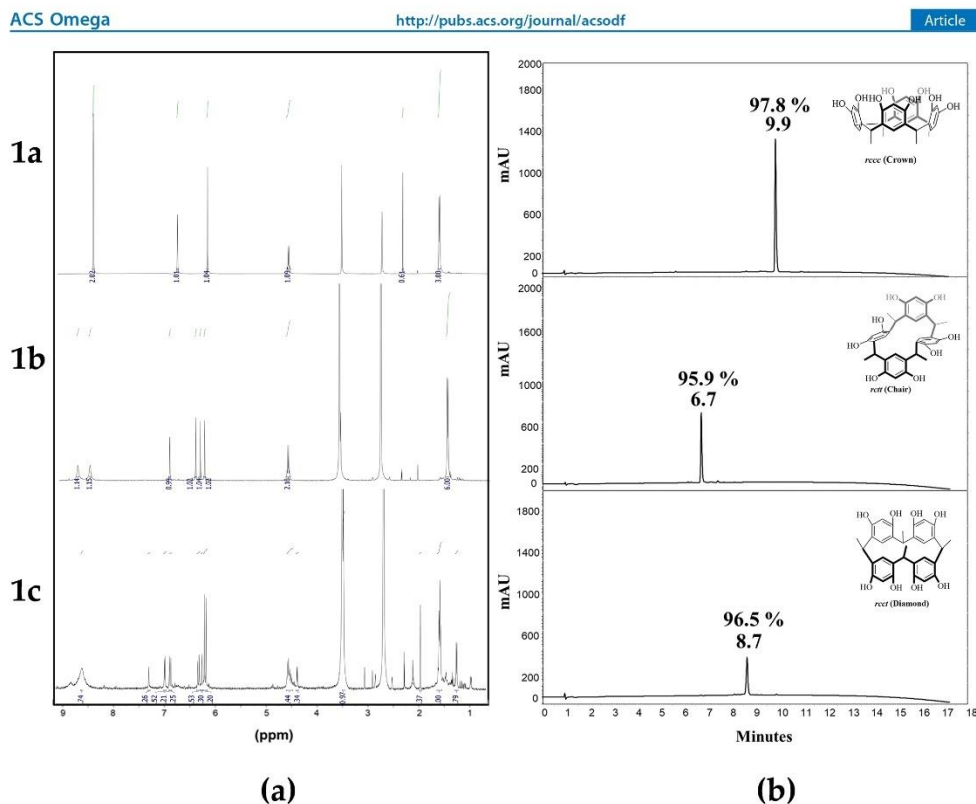


Figure 4. (a) ^1H NMR spectra and (b) chromatographic profile of **1a**, **1b**, and **1c**; for each peak, the chromatographic purity (%) obtained after the RP-SPE process is shown.

NMR spectra, so the number of signals for the product contrasts with the number of signals of crown and chair conformers. The ^1H NMR spectrum of **1c** displayed the characteristic signals of a methyl substituent at 1.35 and 1.40 ppm and in the range of 4.38–4.46 ppm for the methine bridge. The aromatic protons at 6.12, 6.16, 6.21, and 6.29 ppm were assigned to the protons in the ortho position of hydroxyl groups for the resorcinol residue. Also, in the aromatic region, signals for meta-protons of the resorcinarene moiety were observed at 6.86, 6.90, 6.98, and 7.29 ppm. The signal for the hydroxyl groups was observed in the range of 8.50–8.90 ppm; the full assignment can be seen in Table 1. Finally, the integration of the signals is consistent with a tetrameric macrocycle. The multiplicity of signals for each type of proton in the spectrum of **1c** suggests different chemical environments for each of the phenolic rings, so the spectral pattern is characteristic of the diamond conformation.

To understand the formation of **1a** during the cyclocondensation reaction between resorcinol and acetaldehyde, the chromatographic profile of the reaction solution was obtained from time 0 to 60 min (reaction time), obtaining the chromatogram every 10 min. As shown in Figure 5, during the first moments of the reaction, conformer **1c** is formed in good

Table 1. Chemical Shifts for Isomer **1c** in the ^1H NMR Spectrum

General structure	Proton	1c
	1	8.50–8.90
	2	6.86 6.90 6.98 7.29
	3	6.12 6.16 6.21 6.29
	4	4.38–4.46
	5	1.35 1.40

proportion; however, as the reaction progresses, the amount that is formed tends to decrease. Considering that the most stable conformer is the crown, in which both OH groups of the two opposite resorcinol units oriented toward the cavity act as hydrogen-bond donors, conformers **1b** and **1c** can be interconverted to the more stable conformer **1a** since the energy values are relatively low.²⁷ The composition of the reaction products reflects the balance between the rate of the

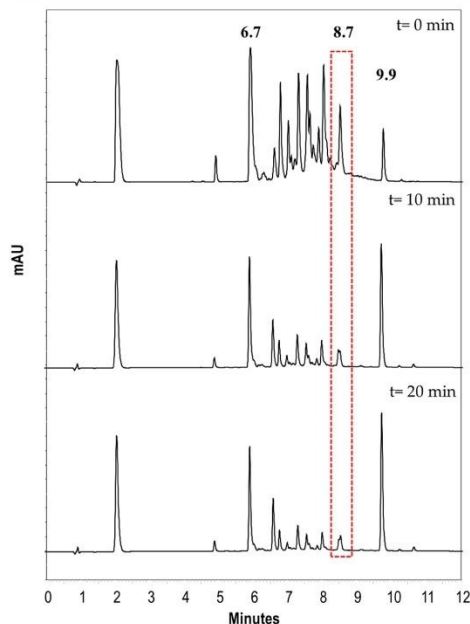


Figure 5. Chromatographic profile of the cyclocondensation reaction between resorcinol and acetaldehyde over time.

conformational and the annulus inversion in the reaction conditions.

4. CONCLUSIONS

Analysis by means of RP-HPLC and LCMS (positive-ESI) of the cyclocondensation of resorcinol with acetaldehyde in water showed the formation of three of the several possible C-tetramethylcalix[4]resorcinarene conformers. With the RP-HPLC information, it was possible to design a purification protocol using RP-SPE and gradient elution. The purified products were well characterized, i.e., conformational analysis of all of these compounds was done via NMR. The crown conformation was the main product obtained, but the chair and diamond conformers were also generated with acceptable yields. The method developed was applied, and it has the advantages of high sensitivity, low running cost, and simple operation. The analytical separation process used can be adapted to carry out studies on the formation of conformers of analogous systems.

AUTHOR INFORMATION

Corresponding Author

Zuly Jenny Rivera-Monroy – Chemistry Department, Universidad Nacional de Colombia, Bogotá 11321, Colombia; orcid.org/0000-0001-6915-8488; Email: zriveram@unal.edu.co

Authors

Héctor Manuel Pineda-Castañeda – Chemistry Department, Universidad Nacional de Colombia, Bogotá 11321, Colombia

Mauricio Maldonado – Chemistry Department, Universidad Nacional de Colombia, Bogotá 11321, Colombia

Complete contact information is available at:

<https://pubs.acs.org/10.1021/acsomega.2c03218>

Author Contributions

The manuscript was written through contributions of all authors. All authors have given approval to the final version of the manuscript.

Notes

The authors declare no competing financial interest.

ACKNOWLEDGMENTS

The authors are thankful to Minciencias for its financial support of the Project RC 846-2019: “Diseño y obtención de nuevos agentes antibacterianos basados en dendrímeros péptido-resorcinareno: Una alternativa para combatir la resistencia bacteriana” and to the Universidad Nacional de Colombia-Sede Bogotá for the doctoral scholarship “Asistente Docente”.

REFERENCES

- (1) Da Silva, E.; Lazar, A. N.; Coleman, A. W. Biopharmaceutical Applications of Calixarenes. *J. Drug Delivery Sci. Technol.* **2004**, *14*, 3–20.
- (2) Basilotta, R.; Mannino, D.; Filippone, A.; Casili, G.; Prestifilippo, A.; Colarossi, L.; Raciti, G.; Esposito, E.; Campolo, M. Role of Calixarene in Chemotherapy Delivery Strategies. *Molecules* **2021**, *26*, 3963.
- (3) Yuksel, N.; Köse, A.; Fellah, M. F. The Supramolecularly Complexes of Calix[4]Arene Derivatives toward Favipiravir Antiviral Drug (Used to Treatment of COVID-19): A DFT Study on the Geometry Optimization, Electronic Structure and Infrared Spectroscopy of Adsorption and Sensing. *J. Incl. Phenom. Macrocycl. Chem.* **2021**, *101*, 77–89.
- (4) Shurpik, D. N.; Padnya, P. L.; Stoikov, I. I.; Cragg, P. J. Antimicrobial Activity of Calixarenes and Related Macrocycles. *Molecules* **2020**, *25*, 5145.
- (5) Curtis, A. D. M. Simple Calix[n]Arenes and Calix[4]-Resorcinarenes as Drug Solubilizing Agents. *J. Nanomed. Res.* **2015**, *2*, 1–8.
- (6) Puttreddy, R.; Beyeh, N. K.; Rissanen, K. Conformational Changes in C-methyl-Resorcinarene Pyridine: N -Oxide Inclusion Complexes in the Solid State. *CrystEngComm* **2016**, *18*, 4971–4976.
- (7) Agrawal, Y. K.; Patadia, R. N. Studies on Resorcinarenes and Their Analytical Applications. *Rev. Anal. Chem.* **2006**, *25*, 155–239.
- (8) Shah, M. D.; Agrawal, Y. Calixarene: A New Architecture in the Analytical and Pharmaceutical Technology. *J. Sci. Ind. Res.* **2012**, *71*, 21–26.
- (9) Jain, V. K.; Kanaiya, P. H. Chemistry of Calix[4]Resorcinarenes. *Russ. Chem. Rev.* **2011**, *80*, 75–102.
- (10) Moore, D.; Watson, G. W.; Gunnlaugsson, T.; Matthews, S. E. Selective Formation of the R_{ctt} Chair Stereoisomers of Octa-O-Alkyl Resorcin[4]Arenes Using Bronsted Acid Catalysis. *New J. Chem.* **2008**, *32*, 994–1002.
- (11) Ziaja, P.; Krogul, A.; Pawlowski, T. S.; Litwinienko, G. Structure and stoichiometry of resorcinarene solvates as host-guest complexes - NMR, X-ray and thermoanalytical studies. *Thermochim. Acta* **2016**, *623*, 112–119.
- (12) Velásquez-Silva, A.; Cortés, B.; Rivera-Monroy, Z. J.; Pérez-Redondo, A.; Maldonado, M. Crystal Structure and Dynamic NMR

Studies of Octaacetyl-Tetra(Propyl)Calix[4]Resorcinarene. *J. Mol. Struct.* **2017**, *1137*, 380–386.

(13) Castillo-Aguirre, A. A.; Pérez-Redondo, A.; Maldonado, M. Influence of the Hydrogen Bond on the Itereoselective O-Alkylation of Calix[4]Resorcinarenes. *J. Mol. Struct.* **2020**, *1202*, No. 127402.

(14) Español, E.; Villamil, M. M. Calixarenes: Generalities and Their Role in Improving the Solubility, Biocompatibility, Stability, Bioavailability, Detection, and Transport of Biomolecules. *Biomolecules* **2019**, *9*, 90.

(15) He, M.; Johnson, R. J.; Escobedo, J. O.; Beck, P. A.; Melancon, B. J.; Treleaven, W. D.; Strongin, R. M.; Lewis, P. T.; Kim, K. K.; St Luce, N. N.; Mrse, A. A.; Davis, C. J.; Fronczek, F. R. Chromophore Formation in Resorcinarene Solutions and the Visual Detection of Mono- and Oligosaccharides. *J. Am. Chem. Soc.* **2002**, *124*, 5000–5009.

(16) Beyeh, N. K.; Rissanen, K. Tetranitroresorcin[4]Arene: Synthesis and Structure of a New Stereoisomer. *Tetrahedron Lett.* **2009**, *50*, 7369–7373.

(17) Forero, R. A. S. *Reacción de Sulfometilación de Resorcinarenos Alquilados En El Borde Inferior y Estudio Del Efecto de Estos Sustituyentes En El Proceso de Reconocimiento Molecular de Colina*; Universidad Nacional de Colombia: Sede Bogotá, 2018.

(18) Ma, B. Q.; Coppens, P. Transformation of a C-Methylcalix[4]-Resorcinarene-Based Host-Guest Complex from a Wave-like to a Novel Triangular Brick-Wall Architecture. *Chem. Commun.* **2003**, *3*, 504–505.

(19) Reynolds, M. R.; Pick, F. S.; Hayward, J. J.; Trant, J. F. A Concise Synthesis of a Methyl Ester 2-Resorcinarene: A Chair-Conformation Macrocyclic. *Symmetry* **2021**, *13*, 627.

(20) Castillo-Aguirre, A. A.; Rivera Monroy, Z. J.; Maldonado, M. Analysis by RP-HPLC and Purification by RP-SPE of the C-Tetra(p-Hydroxyphenyl)Resorcinolarene Crown and Chair Stereoisomers. *J. Anal. Methods Chem.* **2019**, *2019*, 1–6.

(21) Cepeda, D. I.; Pineda Castañeda, H.; Rodríguez Mayor, A.; García Castañeda, J.; Maldonado Villamil, M.; Fierro Medina, R.; Rivera Monroy, Z. Synthetic Peptide Purification via Solid-Phase Extraction with Gradient Elution: A Simple, Economical, Fast, and Efficient Methodology. *Molecules* **2019**, *24*, 1215.

(22) Hoegberg, A. G. S. Two Stereoisomeric Macrocyclic Resorcinol-Acetaldehyde Condensation Products. *J. Org. Chem.* **2002**, *45*, 4498–4500.

(23) Mu, H.; Zhou, R.; Sun, J.; Yan, C. Syntheses and Crystal Structures of Functionalized Tetramethyl Resorcinarenes. *Chem. Res. Chin. Univ.* **2015**, *31*, 925–929.

(24) Ito, H.; Nakayama, T.; Sherwood, M.; Miller, D.; Ueda, M. Characterization and Lithographic Application of Calix[4]-Resorcinarene Derivatives. *Chem. Mater.* **2008**, *20*, 341–356.

(25) Fehling, H. Ueber Zwei Dem Aldehyd Isomere Verbindungen. *Ann. Pharm.* **1838**, *27*, 319–322.

(26) Wankhede, N. N.; Wankhede, D. S.; Lande, M. K.; Arbad, B. R. Densities and Ultrasonic Velocities of Binary Mixtures of 2,4,6-Trimethyl-1,3,5-Trioxane + n-Alcohols at 298.15, 303.15 and 308.15 K. *Indian J. Chem. Technol.* **2006**, *13*, 149155, <http://nopr.niscpr.res.in/handle/123456789/7015>

(27) Thondorf, I.; Brenn, J.; Böhmer, V. Conformational Properties of Methylene Bridged Resorcinarenes. *Tetrahedron* **1998**, *54*, 12823–12828.

Recommended by ACS

Electrochromic Performance of Sputtered NbTi-Based Mixed Metal Oxide Thin Films with a Metallic Seed Layer

Karunanithi Balamurugan, Balasubramanian Subramanian, *et al.*

DECEMBER 28, 2022

ACS OMEGA

READ 

Fe₃O₄ Composite Superparticles with RGD/Magnetic Dual-Targeting Capabilities for the Imaging and Treatment of Non-Small Cell Lung Cancer

Nan Zhao, Hua Xin, *et al.*

FEBRUARY 14, 2023

ACS OMEGA

READ 

Effect of Nitrogen in Combination with Different Levels of Sulfur on Wheat Growth and Yield

Khadij Dawar, Subhan Danish, *et al.*

DECEMBER 25, 2022

ACS OMEGA

READ 

Synergistic Mechanism of Ultrasonic-Chemical Effects on the CH₄ Adsorption-Desorption and Physicochemical Properties of Jincheng Anthracite

Xiaomin Liang, Wenqing Zhu, *et al.*

DECEMBER 20, 2022

ACS OMEGA

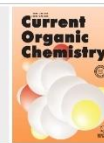
READ 

Get More Suggestions >



REVIEW ARTICLE

Designing Short Peptides: A Sisyphean Task?



Héctor M. Pineda-Castañeda¹, Diego S. Insuasty-Cepeda¹, Víctor A. Niño-Ramírez¹, Hernando Curtidor² and Zuly J. Rivera-Monroy^{1,*}

¹Chemistry Department, Sciences Faculty, Universidad Nacional de Colombia, Bogotá, Colombia; ²Universidad ECCI, Bogotá, Colombia

Abstract: Over the last few years, short peptides have become a powerful tool in basic and applied research, with different uses like diagnostic, antimicrobial peptides, human health promoters or bioactive peptides, therapeutic treatments, templates for peptidomimetic design, and peptide-based vaccines. In this endeavor, different approaches and technologies have been explored, such as bioinformatics, large-scale peptide synthesis, omics sciences, structure-activity relationship studies, and a biophysical approach, among others, seeking to obtain the shortest sequence with the best activity. The advantage of short peptides lies in their stability, ease of production, safety, and low cost. There are many strategies for designing short peptides with biomedical and industrial applications (targeting the structure, length, charge, or polarity) or as a starting point for improving their properties (sequence data base, de novo sequences, templates, or organic scaffolds). In peptide design, it is necessary to keep in mind factors such as the application (peptidomimetic, immunogen, antimicrobial, bioactive, or protein-protein interaction inhibitor), the expected target (membrane cell, nucleus, receptor proteins, or immune system), and particular characteristics (shorter, conformationally constrained, cyclic, charged, flexible, polymerized, or pseudopeptides). This review summarizes the different synthetic approaches and strategies used to design new peptide analogs, highlighting the achievements, constraints, and advantages of each.



Zuly J. Rivera-Monroy

ARTICLE HISTORY

Received: June 15, 2020
Revised: July 30, 2020
Accepted: August 05, 2020

DOI:
10.2174/138527282499200910094034



Keywords: Short peptides, non-natural amino acid, click chemistry, cyclic peptide, tetrameric peptide, dimeric peptide.

1. INTRODUCTION

Peptides are smaller versions of proteins. Many of them exhibit important biological activities (antibacterial, antifungal, and anticancer). Currently, the miniaturization of everything is sought, and the field of peptides is not an exception. This is why the design of short peptides that exhibit activity has been an undertaking that develops daily. The present review will guide the reader with respect to different synthetic strategies implemented for short peptide synthesis, which involves the incorporation of non-natural molecules (organic or inorganic moieties), carbohydrates, lipids, proteins, D-amino acids, *etc.*, allowing improvement in the activity and/or stability of the peptide. The incorporation of these molecules into a peptide sequence requires expanding the chemical strategies for obtaining promising molecules for biomedical applications. Another approach consists of increasing the number of chains in order to obtain polyvalent peptides (dimers, trimers, tetramers, octamers, polymers, *etc.*). The polyvalence of short sequences could enhance the peptide's bioavailability, making it more resistant to proteases and reducing elimination from the body, thus ensuring effective peptide concentration on the target cell. The multiple antigen peptide (MAP) strategy allows the design and synthesis of dimeric, tetrameric, and octameric peptides with enhanced

polyvalent activity. The bright disulfide formation involves diverse synthetic strategies in order to obtain dimeric, tetrameric, polymeric, and cyclic peptides, which are used as carriers and/or immunogens. Cyclic peptides often show improvements in binding affinity, specificity, or stability compared to their linear analogues, due to the imposition of restricted geometries. The synthesis of chimeric peptides is a promising approach that uses diverse synthetic routes in the solid and solution phases. Click chemistry has emerged and has broadened the spectrum of chemical reactions that can be implemented in the design and synthesis of short peptides.

2. NON-NATURAL AMINO ACIDS

2.1. Silaproline

Cell-penetrating peptides have become a valuable tool for transporting vectors into the cell. They usually have amphipathic and hydrophobic characteristics that facilitate the translocation of the peptide through the membrane [1]. Within this context, proline-rich amphipathic peptides have been evaluated, and the incorporation of Silaproline (Sip) favors amphipathic interaction with the cell membrane [2]. Therefore, a large number of pseudo peptides have been reported into which the unnatural amino acid, Sip, was incorporated in order to significantly enhance its cell membrane penetration capacity.

Sip is an amino acid analogous to proline, in which γ -carbon is replaced by a dimethylsilyl group. The carbon-silicon bond measures approximately 0.35 angstroms, which makes it longer than the

*Address correspondence to this author at the Chemistry Department, Sciences Faculty, Universidad Nacional de Colombia, Bogotá, Colombia; ^bUniversidad ECCI, Bogotá, Colombia; Tel: +57-1-316 5000; E-mail: zriveram@unal.edu.co

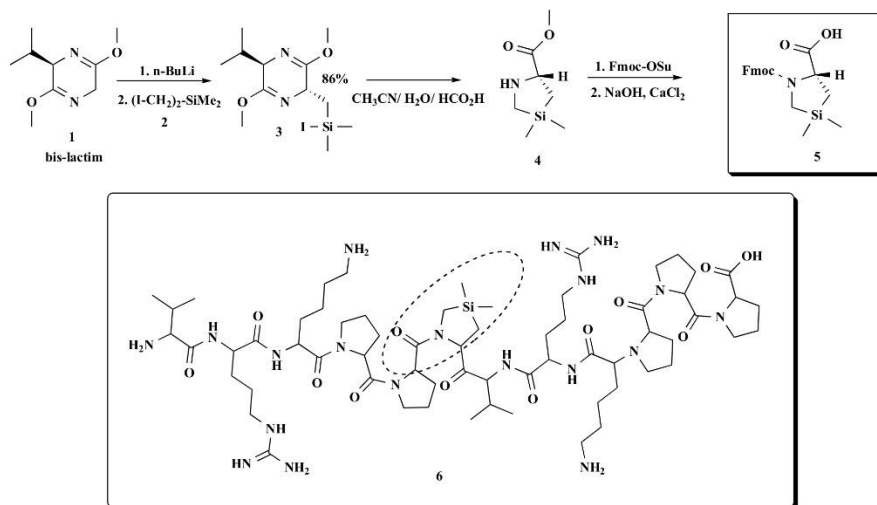


Fig. (1). A synthetic route for obtaining silaneproline and cell-penetrating peptide VRKPP-Syp-VRKPPP [5, 6].

C-C bond, plus the C-Si-C angle is significantly less (90°) than the C-C-C one (105°) [3]. These characteristics give it fourteen times more lipophilicity than the original amino acid Fmoc-Pro-OH, which explains its superiority with respect to the ability to cross cell membranes [4]. In Sip synthesis, it is necessary to use an alkylating agent with two halogens (Bis(iodomethyl)-(dimethyl)silane) (2), which allow the nitrogen cyclization and then the C-alkylation of (3). Compound (1) is a starting reagent commonly used in the synthesis of amino acids. The synthesis starts with the deprotonation of (1), using *n*-BuLi as a strong base for the subsequent alkylation of (2) (Fig. 1), which generates a planar cyclic intermediate that allows the diastereoselective alkylation, obtaining the *trans* product (3) at 86% yields (Fig. 1). Once this diastereoisomer has been purified *via* flash column chromatography, a mixture of acetonitrile/water/formic acid (49:49:2 v/v) is added. Under these conditions, the nucleophilic attack of nitrogen on the carbon adjacent to the silicon proceeds, which is facilitated by the iodide ion as a good leaving group, to finally generate a 5-membered cycle (4). Finally, the amino group is protected using Fmoc-OSu and demethylation in the presence of NaOH and CaCl₂, in order to get (5). This Fmoc-amino acid was used in a conventional manner in the solid-phase peptide synthesis (SPPS) and Fmoc/tBu strategy, where (5) is incorporated at position 6 to get peptide (6) [5, 6]. Replacing the proline with Sip residue on the hydrophobic side of this cell-penetrating peptide improves its activity, and the peptide internalization in HeLa cells is increased and its toxicity is reduced [7].

2.2. γ -AApeptide

Another interesting approach to peptide design is γ -peptides. These are oligomers of γ -substituted-N-acylated-N-aminoethyl-amino acids [8]. This strategy has been shown to increase resistance to enzymatic hydrolysis, chemo-diversity, and bioavailability [9]. The main way to obtain γ -peptides is through building block synthesis and conventional SPPS. The γ -amino acid building block is synthesized and then incorporated by means of SPPS, leading to a

γ -AApeptide (Fig. 2). The starting reagent is Fmoc-aminoaldehyde (1), which reacts with the benzyl-2-aminoacetate (2) by reductive amination in the presence of NaCNBH₃, effecting the substitution of the hydrogen of the amine group of (2), producing (3) without compromising the carboxyl group. This reaction is carried out in the presence of a protic polar solvent such as methanol (reductive Borch amination). Product (3) is treated with hydrogen on Pd/C to remove the benzyl group, and then the α -amine group is acylated to obtain (4) (Fig. 2). Then (4) is coupled to a solid support using DIC/HOBt as a coupling reagent, obtaining (5). Then a substituent R is joined to the α -amine group, and the Fmoc group is removed while the side chain remains in the γ position of (6) [10].

2.3. Asymmetric Epoxidation

A rather particular application of peptides containing unnatural amino acids is as catalysts in organic reactions such as the Friedel-Crafts-type, hydrogen transfer, asymmetric epoxidation, and oxyaminations. It has been reported that using small quantities of peptide anchored to a polymeric resin, under aqueous rather than organic conditions, allows accelerating the chemical reactions, thus increasing the efficiency and selectivity [12]. The asymmetric epoxidation catalyzed by peptides allows obtaining optically active compounds, high stereoselectivity being the most important aspect [13]. There are several ways to perform asymmetric epoxidations; however, the most common way is using hydrogen peroxide as an oxidizing agent. A limitation of this oxidizing agent is its difficulty in inducing enantioselective reactions, since these reactions largely depend on a high steric hindrance, which facilitates a single product formation, a property that hydrogen peroxide lacks, due to its small size. To solve this enantioselectivity problem, some authors have described the use of peptides with non-natural amino acids as catalysts for asymmetric epoxidation using hydrogen peroxide. Peptides anchored to polymeric resin are incorporated into the reaction in catalytic amounts, which allows them to be added as heterogeneous catalysts so they can be reused. These peptides usually have a hy-

drophobic region of poly-Leu, with α -helix conformation, followed by a small β -turn fragment of two to five amino acids as Pro that generate conformational changes in the secondary structure. This β -turn region has been described as being related to the catalytic capacity of the peptide in asymmetric epoxidation. Analogous sequences have been described in which modifications are made in the catalytic region, changing proline to non-natural amino acids of a different chemical nature as compounds (1 to 4, Fig. 3), giving improvements in terms of yields and enantioselectivity. Additionally, it has been found that using peptides as catalysts allows the reaction to be carried out in an aqueous medium instead of an organic medium, which has been described as increasing the yield by up to 50%. Akawaga *et al.* reported the use of a Pro-D-Pro-Aib-Trp-Trp-(Leu)₂₄ peptide anchored to PEG-PS amphiphilic resin as a catalyst in the asymmetric epoxidation in the aqueous medium (H₂O₂-TFA-H₂O) (1:1:1 v/v), at RT for 3 h with 57% yield and enantioselectivity of -73% (Fig. 3, condition 1). When the hydrophobic region was modified, changing the poly-Leu to poly-Ile, the yields decreased to 24% and the enantioselectivity was considerably reduced (Fig. 3, condition 2), suggesting that the alpha-helix structure generated by the poly-Leu is relevant to the catalytic activity of the peptide. When a proline residue was removed from the β -turn catalytic region and the α -aminoisobutyric acid (Aib) was replaced by acetylcholine (Ach), the yield increased by 20% and the enantioselectivity was -76% (Fig. 3, condition 3). And finally, when three Ala(1-pyn) residues were incorporated after Ach, the best catalytic conditions were obtained, with yields of 80% and enantioselectivity of 90%, and the trans/cis ratio was 99 to 1 (condition 4) (Fig. 3) [14].

2.4. Aminoalkyl Radicals

Dehydroalanine (Dha) is an amino acid commonly used as an intermediate to obtain unnatural amino acids with side chains of diverse natures [15]. The reactivity of the alkene group of the Dha side chain allows photocatalytic reactions through a free radical pathway. The modification of the Dha side chain using tertiary amines was recently reported. An electron was removed through photolytic catalysis to form the alpha-amino radical, which reacts specifically with the alkene group through nucleophilic addition, allowing the generation of a new side chain, which depends on the moiety bonded to the tertiary amine. This synthesis strategy is a very powerful and versatile tool, since it allows: (i) the incorporation of the natural amino acid in any position of the sequence, through the traditional coupling reaction to incorporate Dha, to later (ii) modify the side chain with an amine tertiary containing symmetric and asymmetric radicals (Fig. 4) [16].

3. PEPTIDES WITH THIOL AND DISULPHIDE BONDS

The peptide secondary structure affects the peptide stability against external agents such as hydrolytic enzymes, and also its therapeutic potency. Synthetic strategies have been developed to introduce S-S linkers or mimics such as: metabolically stable disulfide bond substitutes, peptide cyclization using a disulfide-bridge, introduction of one or more regioselective disulfide bonds into the peptide chain, and disulfide bonds between peptide binding motifs.

3.1. Disulfide Bond Substitution

Since disulfide bonds are unstable to reducing agents and disulfide isomerase activity, when the disulfide bridge is reduced, the peptide chain opens and the peptide loses its secondary/tertiary structure and its activity. Synthetic strategies have been developed in which these disulfide bonds are replaced with analogue substi-

tutes, allowing the preservation of the structural conformation and the biochemical or bactericidal activity, since these analogs are more stable in the presence of reducing agents. Within the arsenal of metabolically stable disulfide bond substitutes or mimics are: diamino acids, thioethers, diselenides, triazoles, and hydrocarbon bridges [17].

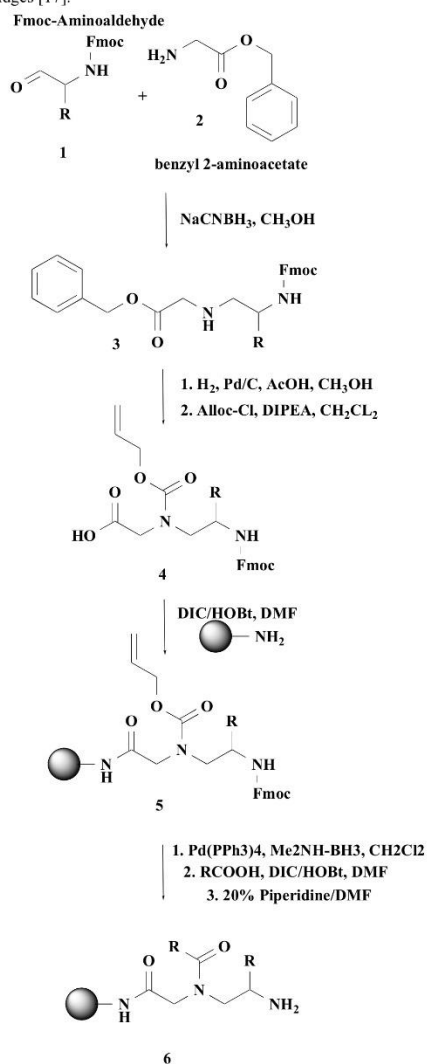


Fig. (2). γ -A-peptide synthesis [11].

Diaminodiacids are molecules derived from L-asparagine, L-glutamine, L-glycine, and L-homoserine, and have protective groups compatible with SPPS Fmoc/tBu methodology. As is shown

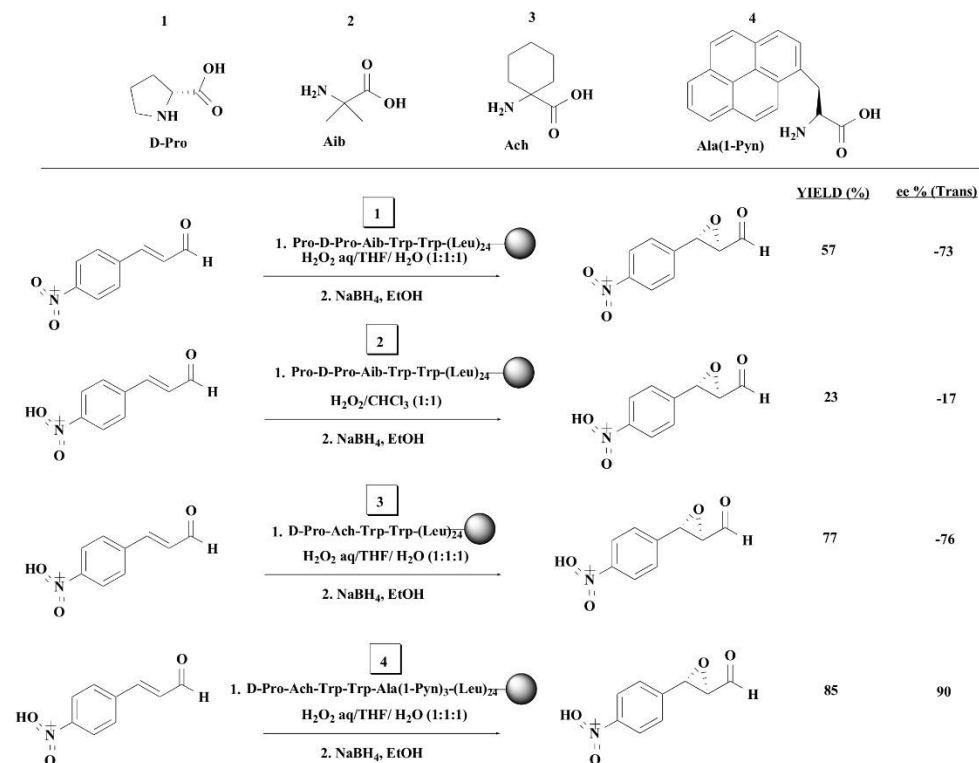


Fig. (3). Non-natural amino acids are commonly used in the development of peptide catalysts. Asymmetric epoxidation conditions using modified catalytic peptides [14].

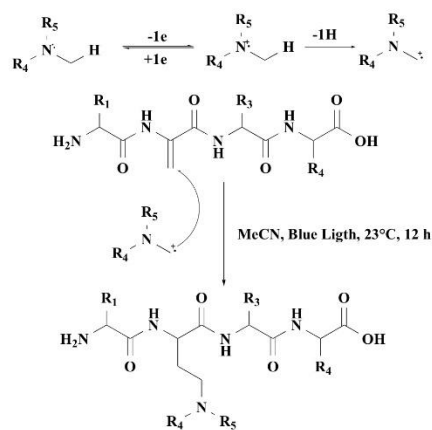


Fig. (4). Peptide synthesis using aminoalkylated non-natural amino acids using Dha as an intermediate [16].

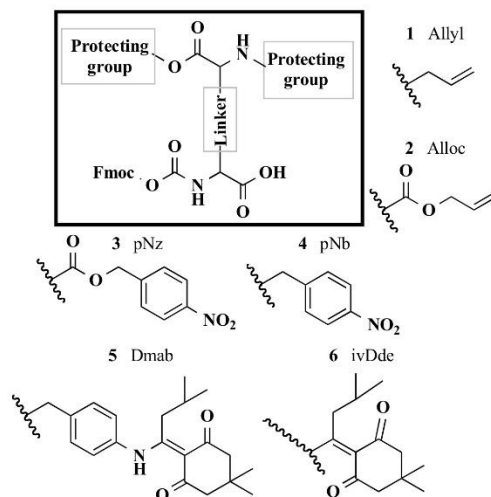


Fig. (5). Protecting groups for diaminodiacids.

in Fig. (5), the protecting groups used are: allyl (1), allyloxycarbonyl (Alloc) (2), nitrobenzyl (pNz) (3) and p-nitrobenzyl (pNb) (4), which can be removed by treatment with $[\text{Pd}(\text{PPh}_3)_4]/\text{PhSiH}_3$ or SnCl_2/HCl . Preparation of disulfide bond substitutes containing protecting group 4-(N-[1-(4,4-dimethyl-2,6-dioxocyclohexylidene)-3-methyl-butyl]amino)-benzyl (Dmab) (5) and 1-(4,4-dimethyl-2,6-dioxo-cyclohex-1-ylidene)-3-methylbutyl (ivDde) (6) has also been reported.

Sun *et al.* [18], reported the synthesis of the Fmoc-homocysteine using homoserine as the starting material. The Fmoc-homocysteine is the starting material for efficient synthesis of a diaminodiacid introducing the C-C-S-C-C bridge. The Fmoc-homocysteine unit was synthesized as follows (Fig. 6): homoserine (1) reacted with Fmoc-OSu in aqueous 1,4-dioxane solution, protecting the α -amino group, and then it reacted with tert-butyl 2,2,2-trichloroacetimidate to protect the α -acid group, obtaining (2). In the third step, (2) reacted with methane sulfonyl chloride in a TEA/DCM mixture, leading to an intermediate (3). Then (3) was efficiently converted into (4) by substitution reaction with thioacetic acid to form the thioester on the γ -carbon. Finally, (4) was treated with sodium hydroxide solution, causing thioester hydrolysis and forming the thiol group in the γ -carbon, obtaining the protected homocysteine (5) with 11% yield (Fig. 6a). The second homocysteine unit, containing Allyl/Alloc protecting groups, was synthesized from L-homoserine (1) (Fig. 6b), which was reacted first with allyl chloroformate and then with allyl bromide to form intermediate (6), which has the α -amino protected by the Alloc group and the α -carboxyl protected by the Allyl group. Finally, the hydroxy group of the γ carbon was replaced by bromination with tetrabromomethane and triphenylphosphine, obtaining (7), with a 40% yield. From amino acids (5) and (7) (Fig. 6c), the intermediate diaminodiacid (8) was synthesized by thioalkylation with an efficiency of 80%, followed by removal of the tBu group in an acid medium, obtaining the Allyl/Alloc diaminodiacid (9), with a thioether bridge of five atoms (C-C-S-C-C), with synthetic efficiency of 74%.

Using the diaminodiacid 9 (Fig. 6c), the oxytocin analog was synthesized *via* SPPS-Fmoc, as shown in Fig. (7), sequentially coupling amino acid (1) and introducing the diaminodiacid into the chain using PyBOP ((benzotriazol-1-yloxy) tripyrrolidinophosphonium-hexafluorophosphate), HOAT (3-hydroxytriazolo[4,5-b]pyridine) and NMM (N-methylmorpholine), obtaining the linear peptide intermediate (2). The other amino acids were sequentially coupled in the standard way until the complete linear peptide sequence was obtained, and the Fmoc group was removed from the Tyr with 20% of 2-methyl piperidine/DMF, obtaining intermediate (3). The Ally/Alloc protecting groups were removed by treatment with $\text{Pd}(\text{PPh}_3)_4$, obtaining intermediate (4), where the free carboxyl group of the diaminodiacid side chain underwent cyclization by intramolecular amidation with the amino group of the Tyr using PyAOP, HOAT and NMM, obtaining the resin-anchored oxytocin analog peptide (5). As a final step, cleavage was performed, obtaining the oxytocin analog with a five-atom thioether bridge (6) to replace the four-atom disulfide bridge of the natural hormone (Fig. 7) [18].

Xu *et al.* [19], introduced a combination of the protecting groups Dmab and ivDde into the diaminodiacid structure [19] (Fig. 8), which is compatible with the Fmoc-SPPS strategy, generating a four-atom thioether bridge.

The synthesis of diaminodiacid (6) was carried out from L-homoserine (1) and S-(triphenylmethyl)-L-cysteine (3). (1) was reacted with Fmoc-OSu and in a second stage with tert-butyl bromide (tBuBr) in the presence of N, N, N'-triethyl-benzene-methanaminiochloride (TEBAC) to protect the carboxyl group. The bromination of the resulting intermediate protected with Fmoc- and tert-butyl in the third stage was achieved in the presence of tetrabromomethane (CBr_4) and triphenylphosphine (PPh_3), obtaining (2), with a yield of 27%. On the other hand, S-(triphenylmethyl)-L-cysteine (3) was reacted with ivDde-OH and Dmab-OH, obtaining the fully protected amino acid. In the third stage, the triphenylme-

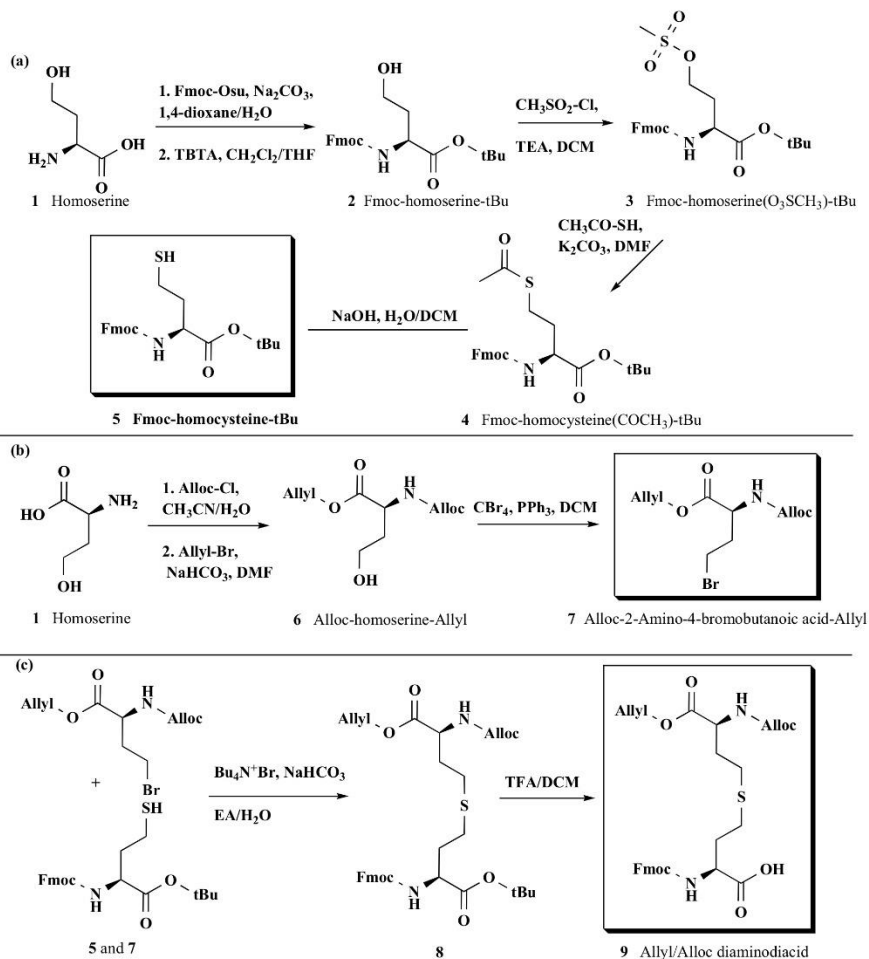


Fig. (6). Synthesis of the intermediate amino acids and the diaminodiacid Allyl/Alloc with a five atoms thioether bridge.

thyl protecting group was cleaved with TFA, producing compound (4), with a final yield of 36% (Fig. 8a and 8b). Fully protected diaminodiacid intermediate Dmb/ivDde of (5) was obtained by thioalkylation reaction between compounds (2) and (4) (yield 45%). The tert-butyl group was cleaved with TFA to obtain the final product Dmb/ivDde diaminodiacid (6), with an overall yield of 12% from (1) (Fig. 8c).

By inserting the previously synthesized diaminodiacid (6) (Fig. 8), it was possible to carry out the synthesis of the linear chain corresponding to the analog of oxytocin (1), as shown in Fig. (9). The removal of the Dmb/ivDde protecting groups was carried out with 2% NH₂NH₂ and 20% piperidine, obtaining synthetic intermediate

(2), which underwent a cyclization step by lactamization using PyBOP, HOBT, and NMM to obtain (3). Finally, cleavage was performed with TFA allowing the production of the four-atom thioether-bridged oxytocin analog, a four-atom disulfide-linker mimic (4) (Fig. 9) [19]. It should be noted that this last procedure with Dmb/ivDde groups has the advantage of no requirement of using compounds with heavy metals for the selective removal of the protecting groups on the diaminodiacid residue. In this analog oxytocin synthesis, using the SPPS-Fmoc-tBu method, piperidine was used at a concentration of 20%. Recently, it was demonstrated that Fmoc group removal could be performed under more environmentally friendly conditions and at a lower cost [20] using 2.5% 4-methyl-

piperidine (efficiency >99%). Fig. (10) shows oxytocin analogues with thioether bridges of four (1) and five (2) carbons synthesized using the above-mentioned strategies.

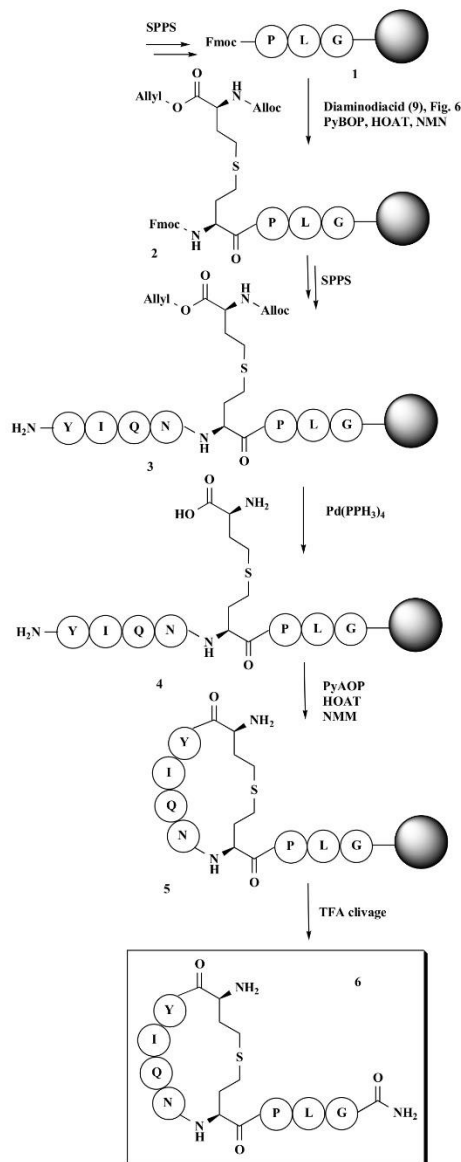


Fig. (7). SPPS Synthesis of an oxytocin analogue with a five-atom thioether bridge.

3.2. Cyclization of Peptides using the Thiolactone Strategy

Within the cyclization of peptides by disulfide bridges, there are at least two approaches: normal disulfide bridge formation and chain-to-tail disulfide bridge formation. The first one consists of the formation of disulfide bridges from two cysteines positioned within the peptide sequence, which will be more vulnerable to enzymatic degradation or reducing agents. The second approach seeks the formation of chain-to-tail disulfide bridges from a thiolactone residue, introduced at the N-terminus of a peptide synthesized *via* SPPS, which after an aminolysis process, leaves a free thiol, thanks to the nucleophilic attack of an amine on the thiolactone, resulting in an N-terminal homocysteine residue. Free thiol can then form a disulfide bond with the C-terminal thiol resulting from the use of a cysteamine 2-chlorotrityl resin, generating a cyclic peptide, as is shown in Fig. (11). The advantage of this strategy is that the N-terminus is blocked, and thus the action of exoproteases is reduced [21].

Van Lysebetten *et al.* reported the synthesis of peptide sequences between three and six residues in length and cyclization using the thiolactone strategy [21]. Fig. (12) shows the synthesis of a short six-residue peptide, synthesized *via* SPPS-Fmoc from a cysteamine 2-chlorotrityl resin (1), which allows the peptide released from the solid support to have free C-terminal thiol functionality. After completion of the target peptide (2), thiolactone block (3) is introduced at the N-terminus under standard coupling conditions (HBTU, DIPEA, DMF), obtaining the intermediate 4 anchored to the solid support. (3) was previously synthesized in a one-step reaction from DL-homocysteine hydrochloride and glutaric anhydride. The cleavage was carried out in an acid medium, 95% TFA, allowing the peptide to be separated from the resin and the removal of the labile protecting groups, obtaining (5). Finally, (5) was cyclized *via* aminolysis in DMF. (5) was pretreated with TCEP with the addition of propylamine, allowing two-step cyclization, aminolysis, and disulfide bridge formation, obtaining the cyclic peptide (6). Note that thiolactones are reactive to the nucleophilic attack of primary amines. The thiol released after thiolactone aminolysis can form a disulfide bond with the C-terminal thiol (Fig. 11). Since the thiolactone derivative has a chiral carbon, a racemized product can be obtained unless one of the enantiomers is isolated and used in the synthesis of the peptide-thiolactone [21].

3.3. Regioselective Synthesis of Peptides Rich in Disulfide Bridges

In the chemical synthesis of natural and non-natural peptides that contain more than one disulfide bridge, it is necessary to use strategies that allow regioselective disulfide bond formation. Orthogonal strategy, using cysteines with different protective groups that can be removed under specific conditions or oxidative folding strategies, has been described. Among the protecting groups for the thiol group in cysteines, there are groups that are removed using: (i) basic medium, (ii) acid medium, (iii) heavy metal ions, (iv) reducing agents, or (v) hydrazine, which must be chosen depending on the different disulfide bonds to be incorporated within the structure of the peptide. Table I [22-31] summarizes the reported protective groups for cysteines, the types of SPPS strategy in which they are used, and the chemical conditions for the protecting group removal.

Dekan *et al.* used cysteines with their side-chain protected with Meb, Acn, Msbh, or Trt for regioselective construction of disulfide bridges in the two native and vicinal hepcidin isomer syntheses. Hepcidin is a small peptide hormone of 25 residues containing four disulfide bridges, between residues 7-23, 10-22, 11-19 and 13-14,

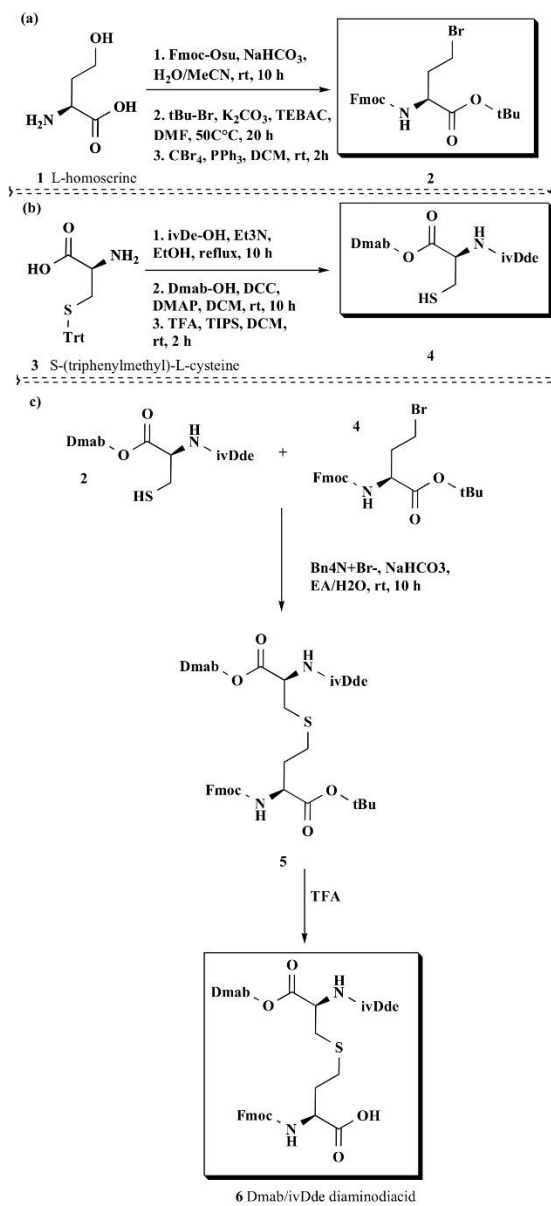


Fig. (8). Synthesis of the intermediate amino acids and the diaminoacid Dmab/ivDde with a four-atom thioether bridge.

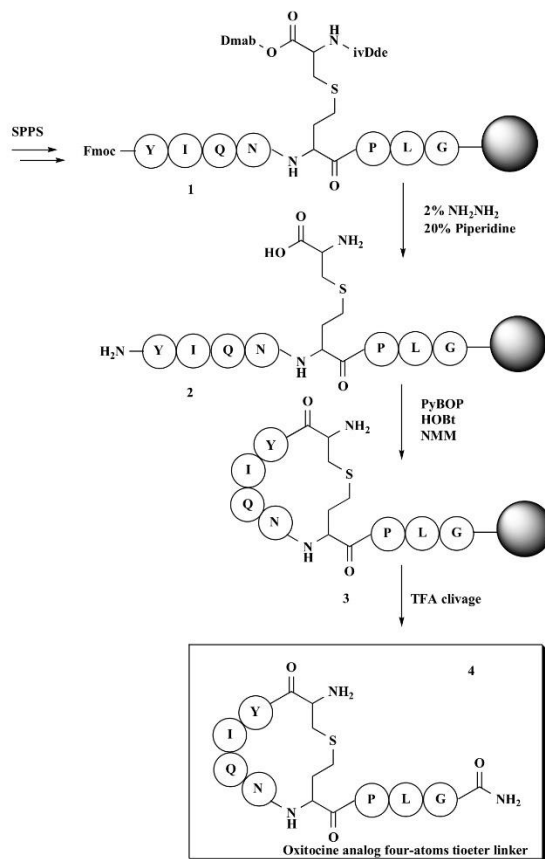


Fig. (9). Cyclization step in the synthesis of four-carbon oxytocin analogue with diamino acid Dmab/ivDde. Disulfide bridge in red.

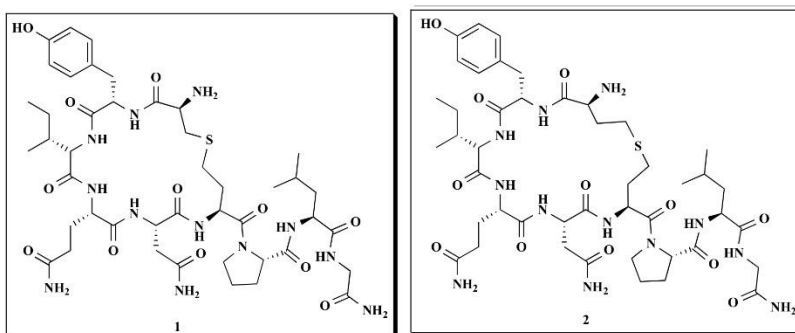


Fig. (10). Oxytocin analogs with thioether bridge of four atoms (1) and five atoms (2).

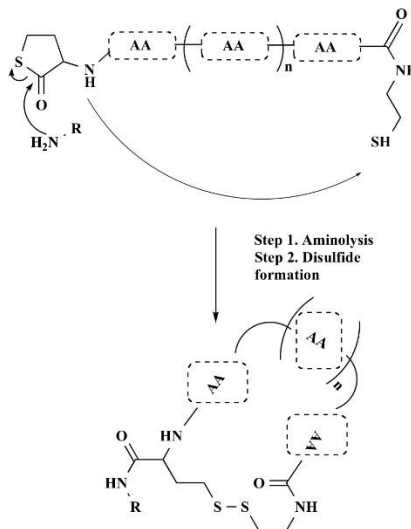


Fig. (11). Cyclization of thiolactone from side chain to tail. Cyclization of thiolactone occurs in two steps: aminolysis, which releases thiol from the ring and introduces an N-terminal modification; the free thiol then forms a disulfide bond with the C-terminal thiol, generating the cyclic peptide.

so the regioselective orthogonal synthesis approach is the most appropriate way to build the target molecule. Therefore, the synthesis was performed using the SPPS-Fmoc/tBu strategy, and the same protecting group was used in each cysteine pair required for obtaining the regioselective disulfide bridge. Fig. (13) shows the vicinal hepcidin synthesis. First, the corresponding amino acid sequence was built on Fmoc-Thr(OtBu)-Wang resin using HBTU/DIPEA activation for the coupling reactions, obtaining (1), which was treated with TFA/TIPS/H₂O solution in order to separate the peptide from the solid support and remove the side protecting groups (step 1). The Trt group, labile in acid medium, was removed from the vicinal cysteine side chains, and the disulfide bridge was formed by means of the action of DMSO (step 2), obtaining intermediate (2), which contained the first regioselective disulfide bridge. The Acn groups joined to side chains of ¹¹Cys and ¹⁹Cys were oxidized with I₂ (step 3), allowing the formation of (3). The side-chain protecting group Meb of the ⁷Cys and ²³Cys was removed by treating (3) with HF/p-cresol (9:1), leaving the thiol groups free (step 4), which were oxidized by the addition of I₂, forming the third disulfide bond and obtaining (4). The Msbh groups remained intact during the previous oxidation and acid treatments. To form the last disulfide bond, (4) was treated with NH₄I, 1% DMS/TFA, selectively removing the Msbh groups. Then the oxidation allowed the formation of fourth disulfide bond regioselective, obtaining the vicinal hepcidin (5) as the final product. This process shows the success of the SPPS-Fmoc/tBu strategy for the synthesis of short peptides with regioselective disulfide bridges, as well as the possibility of chemically synthesizing peptides and hormones with complex structures or even obtaining peptides with various cysteine residues with oxidized and/or reduced side chains [32]. Thalluri *et al.* indicate the preventive measures that must be taken when using I₂ as an oxidant for the formation of disulfide bonds, since it can oxidize residues of Met and Trp [33].

4. BRANCHED PEPTIDES: DIMERIC, TETRAMERIC, AND DENDRIMER PEPTIDES

Dimeric and tetrameric peptides are branched macromolecules that may exhibit symmetry. All dendrimers and dimeric and tetrameric peptides are composed of a core containing reactive points, allowing the joining of amino acids, peptide sequences, and branched units [34]. Additionally, the incorporation of a functionalized organic and inorganic core to anchored peptide chains by means of specific reactions allows the construction of peptide dendrimers. Next, three-branched peptide synthesis strategies are described: a) based on protecting groups, b) strategies based on chemical ligation [23], and c) peptide dendrimers [35].

4.1. Strategy Based on Protecting Groups

The strategy based on protecting groups corresponds to the selective use of amino acids with orthogonal protecting groups that can only be removed under specific chemical conditions, allowing the selective removal of the protecting group in the side chain of Lys, Glu, and Asp residues. In this way, side chains containing free amino or carboxyl groups can react with protected residues, elongating two or more chains simultaneously, obtaining the branched peptide. Polyvalent peptide synthesis following this strategy allows obtaining dimeric peptides (RWQWRWQWR)₂K-Ahx, (FKARRWQWRMKKLG)₂K-Ahx and the tetramer ((RWQWRWQWR)₂K-Ahx-C)₂. The synthesis of the dimers was achieved by incorporation of Fmoc-Lys(Fmoc)-OH into a peptide chain to form the core Fmoc-Lys(Fmoc)-Ahx-Cys-resin. Then, under basic conditions, the Fmoc groups of both α-amino and ε-amino were removed simultaneously, obtaining H₂N-Lys(NH₂)-Ahx-Cys-resin, which contains two free amine groups that are used to simultaneously grow the two chains *via* the SPPS-Fmoc/tBu method. For the construction of the tetramer, the dimer (RRWQWR)₂-

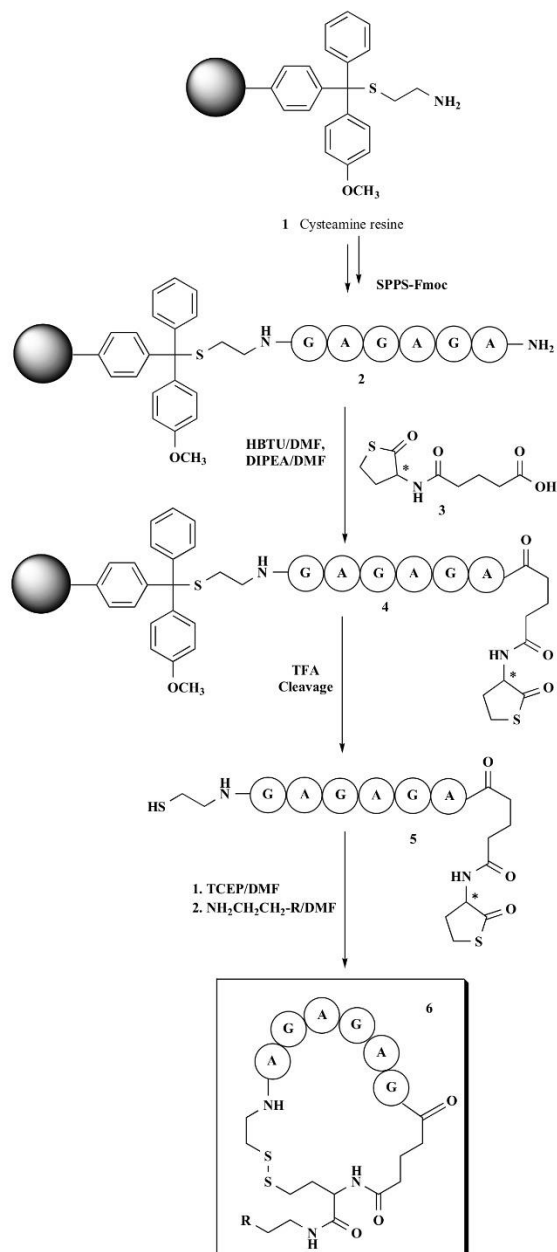


Fig. (12). Synthetic route for thiolactone cyclised peptides.

Table 1. Protecting groups for cysteine and its removal conditions.

Protecting Group	SPPS	Removal Conditions
Trt	Fmoc	At least 25% TFA [22]
Mob	Boc	TFMSA [22]; HF, anisole; Hg(II) acetate or trifluoroacetate in TFA or AcOH; Ag(I) trifluoromethane sulfonate in TFA [23]
Meb	Boc	TFMSA; HF, anisole; trichloromethylsilane or silicon Tetrachloride [22]
Dpm	Fmoc	It can only be cleaved below 60% TFA. It can be used to replace group Trt to avoid unwanted checkout problem [22].
Mmt	Fmoc	1% TFA [22]
Hmb	Fmoc	When placed on the side chain of Cys, Cys (Hmb _α) is stable to TFA in SPPS. When is treated with neutral aqueous buffers, it is cleanly converted to acid-labile Cys (Hmb _β), which can be treated with TFA to generate free Cys [24].
Fmoc	-	2.5 % 4-methylpiperidine [20]
TiAcM	-	Hydrolysis at pH 11 [25]
AcM, PhacM	-	Labile Ions to Metals: AgOAc or Hg(OAc) ₂ , Pd (II) complexes in aqueous medium (low toxicity) [26, 27]
StBu	-	NMM (0.1 M) and β-mercaptoethanol (20%) [28]
Tmp	Fmoc	DTT (Dithiothreitol) in less than 10 min [28].
Npys	Boc	Is cleaved under neutral conditions using a stoichiometric amount of tri-n-butylphosphine in water at RT or with an excess of 2-mercaptoethanol [29].
pNB, Pac, Pocam	Boc	Zn/AcOH or SnCl ₄ /HCl [30, 31]
Msbh	Fmoc	NH ₄ I/Dymethylsulfide/TFA [31]

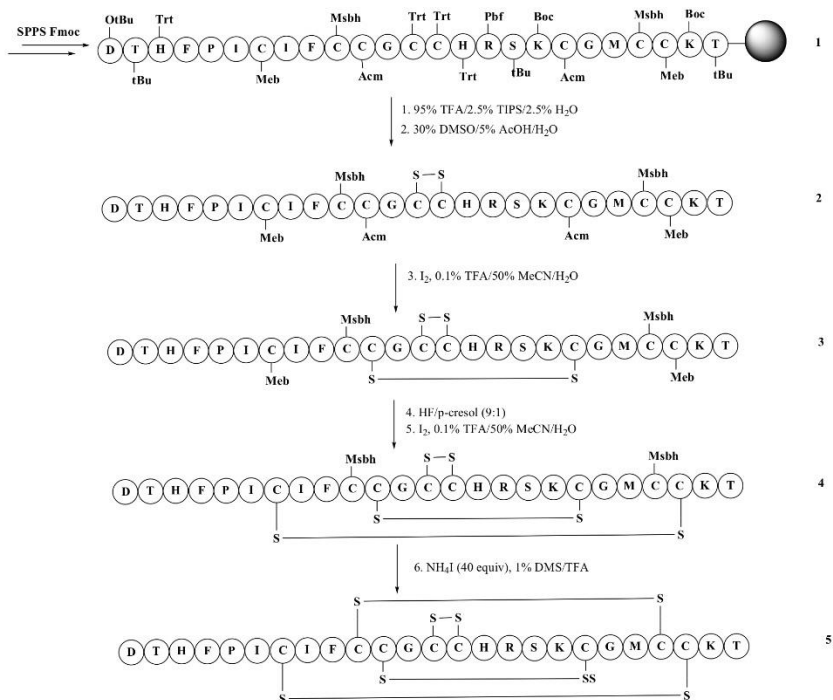


Fig. (13). Regiospecific synthesis of vicinal hepsidin containing four disulfide bonds.

K-Ahx-C was used as a starting point, which incorporates a cysteine residue at its C-terminal end, which allows the formation of a unique disulfide bridge by oxidation with DMSO 10% in a buffer of pH 7.5 [36]. The dimeric peptide oxidation to obtain the tetrameric peptide was monitored by means of RP-HPLC [37]. Polyvalent peptides derived from bovine lactoferricin sequences exhibited greater activity than their monomeric analogs, specifically with respect to their antibacterial effect against both Gram-positive and Gram-negative bacteria strains, and also their selective cytotoxic effect against breast cancer cells lines increased [38, 39].

4.2. Strategies based on Chemical Ligation

These strategies consist of synthesizing peptide blocks, which, by ligation reaction, are linked, obtaining a branched peptide. Pasumoti *et al.*, reported the synthesis of a functionalized core of 4-mercapto-L-lysine starting from L-aspartic acid by the stereoselective introduction of thiol and amino groups. The 4-mercapto-L-lysine allows the formation of dendrimers, to which three peptide sequences can be joined through cysteine-mediated ligation. As shown in Fig. (14), this core, like lysine, has two protecting groups, Cbz and Boc, attached to the α and ϵ amino, with the availability of cysteine-mediated ligation. In step 1, the carboxy-terminal end of the modified lysine reacts with the terminal amine group of the first peptide, allowing the formation of an amide bond. Then the selective removal of Cbz or Boc groups and the combination of the amine group with a C-terminal thioester are carried out under chemical ligation conditions in order to form the amide bond, allowing the attachment of two additional peptides [40, 41].

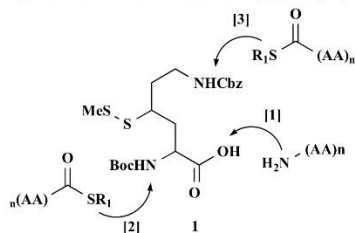


Fig. (14). 4-Mercapto-L-lysine mediated sequential native chemical ligation that provides branched peptides [41].

4.3. Peptide Dendrimers

The constituent parts of three-dimensional peptide dendrimers are (a) a core, which can be of organic or inorganic nature, a macrocyclic, inorganic or organic polyhedron, or nanoparticles, (b) branch points or bifurcations, which in the case of peptide-dendrimers, can be formed using Lys, Glu or Asp, and (c) the branches, which will correspond to a certain peptide sequence. Dendrimer peptide synthesis based on the nuclei of polyhedral oligomeric silsesquioxane (POSS) has been reported. The three-dimensional siloxane molecule, a highly functionalizable inorganic molecule with a relatively rigid cubic structure, possesses 8 positions that can react and that extend outwards in three dimensions. Pu *et al.*, reported the synthesis of derivatives of this nucleus with reaction times of 16 h, with good yields. Starting from 3-aminopropyl triethoxysilane in methanol, concentrated HCl and reaction at 90 °C for 16 h, POSS-NH₂ was formed. The amino group present in each of the eight vertices of the inorganic nucleus was chemically modified until an alkyne functionalization at the

ends in two stages was obtained, first using succinic acid and then with 2-propynylamine, obtaining the POSS-(alkyne)₈. The azido-functionalized dendritic peptides were synthesized using Boc-L-Lys(Boc)-OH by divergent approximation. The azide-functionalized poly (L-lysine) dendrimers were obtained by means of aminolysis, mesylation, and finally azidation until two poly (L-lysine) dendrimers end-functionalized by the azide group were obtained. The azide group within the end of the poly (L-lysine) dendrimer enables binding with the core of POSS-(alkyne)₈ through the Cu-catalyzed azide-alkyne addition cycle (CuAAC) [42].

The use of the POSS core to obtain peptide dendrimers functionalized with poly-L-glutamic [43], poly L-lysine, and poly L-glutamic acid modified with magnetic nanoparticles (MNP) of iron oxide (II, III), Fe₃O₄, using the ligand exchange method, has been reported [44]. There are reports on the divergent and convergent methods for poly-lysine and poly-glutamic synthesis in solution and/or solid-phase synthesis [35].

5. CYCLIC SHORT PEPTIDES

The synthesis of cyclic peptides through the conversion of linear peptides has become one of the most profitable strategies in the design of peptides. Since then, it has been shown that cyclization improves the biological stability and the selectivity in *in vivo* systems, and in some cases, it enhanced the antibacterial, antiviral, antifungal and anticancer activity [45-48]. The strategies of conversion of linear peptides into cyclic peptides are based on reactions between groups present in the peptide sequence, such as the α -amine group of the N-terminal end, the α -carboxylic group of the C-terminal end, reactive groups of amino acid side chains such as Lys, Cys, and Asp, and even functional groups of non-peptide origin such as azide or alkyne [49]. The methods used for the generation of cyclic peptides can be grouped into four general categories, as shown in Fig. (15): *i*) head-to-tail (homodetic): the peptide bond is formed between the N-terminal α -amine group and the C-terminal α -carboxyl group [50, 51]; *ii*) side chain-to-tail: the peptide bond is formed between the N-terminal α -amine group and the functional amino acid group of the side chain; *iii*) head-to-side chain (heterodetic): the peptide bond is formed between the C-terminal α -carboxyl group and functional amino acid groups of the side chain (heterodetic); and *iv*) side chain-to-side chain: the bond is formed between two amino acid side chains [52-54].

Cyclic peptides that contain only peptide-type linkages are called homodesics, while cyclic peptides containing other functional groups that connect their amino acids are called heterodetics. Such modifications may include esters, thioamides, reduced amide bonds, ethers, thioethers, sulfoxides, or heterocycles, among others (Fig. 16). These modifications directly interfere with the peptide activity, and in many cases, it has been observed that it leads to greater metabolic stability, since the peptide bond incision enzymes (proteases) cannot act correctly. These modifications have also been found in natural products. Examples of them are oxasols and thiazoles, which have been found in ribosomally synthesized peptides. When these modifications are incorporated into cyclic peptides, the entire backbone is influenced, as compared to a linear peptide, where only one region is affected [55].

5.1. Oxime Ligation-mediated Peptide Cycling

The oxime ligation method consists of joining an aminoxy group (-O-NH₂) to an aldehyde motif. This reaction has been implemented in the synthesis of cyclic peptides, incorporating these

functional groups into the peptide sequence, either at its N- or C-terminal, as shown in Fig. (17).

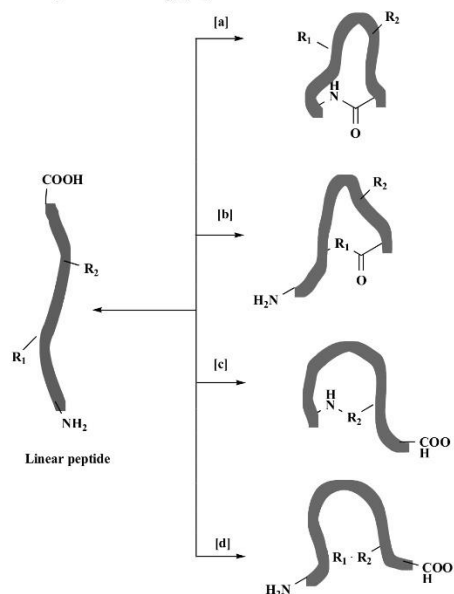


Fig. (15). Types of peptide cyclization. a) head-to-tail, b) head-to-side chain, c) side chain-to-tail and d) side chain-to-side chain.

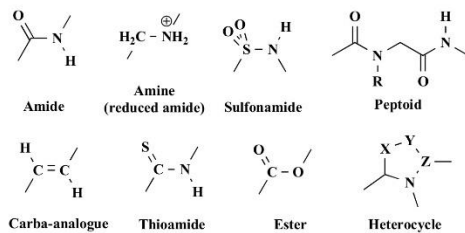


Fig. (16). Chemical modifications to the peptide bond.

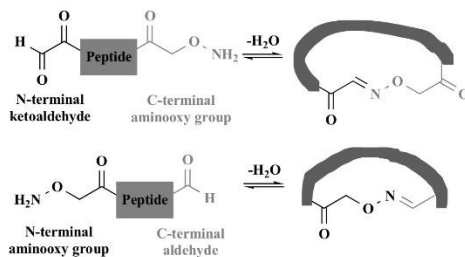


Fig. (17). (a) hydrazone-based cyclization, (b) oxime-based cyclization.

This type of chemical cyclization has been used to a greater extent for the synthesis of cyclic peptides that involve the binding of side chains. Bérubé *et al.* [56] implemented an oxime-type resin for the generation of two anabaenopeptins (APs) by means of the cyclic peptide head-to-side chain approach (Fig. 18). These APs were synthesized using the cyclization/incision reaction based on oxime resin, under retrosynthetic parameters. Compound (6) was obtained *via* concomitant acid-catalyzed cyclization/cleavage in resin using oxime resin using the epsilon-amino group of a Lys as a nucleophile (Fig. 18). The linear peptide sequence (4) was synthesized using DIC/6-Cl-HOBT, the protected linear peptide (4) was cyclized and cleaved in the presence of DIPEA acetic acid in DCM to get the precursor (5), which was obtained with a yield of 74%. The removal of the carboxybenzyl group (Cbz) had to be carried out by means of palladium-catalyzed hydrogenation, where the expected unprotected cyclic peptide (6) was obtained with 60% yield. Secondary products such as symmetric cyclic dimers were reported. They originated from the amino group that attacks a neighboring monomer in the resin as the initial step. This is a strategy that combines a solid-phase method, a solution-phase method, and the use of an endocyclic lysine, which represents a novel way of synthesizing cyclic peptides using oxime-type resins [56].

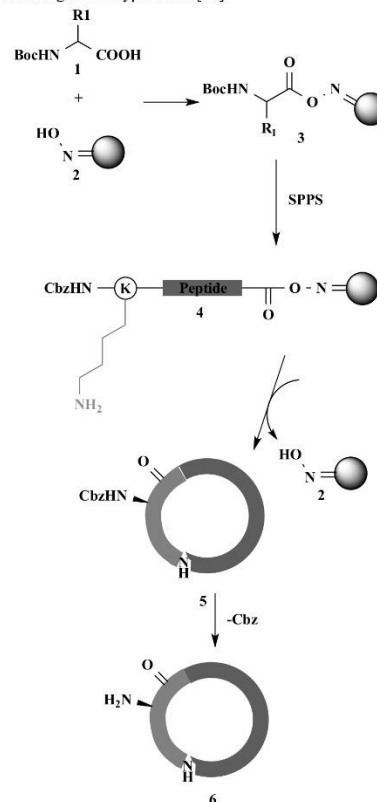


Fig. (18). Synthesis of APs cyclic peptides.

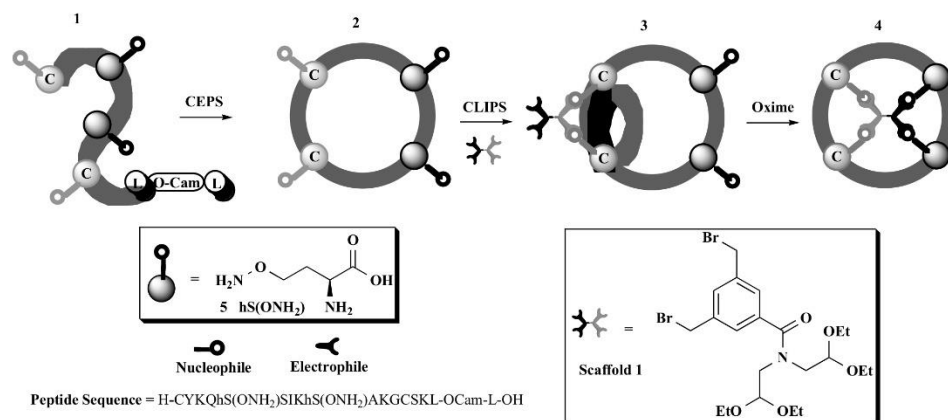


Fig. (19). Schematic representation of the CEPS/CLIPS/oxime cyclizations and the evaluated scaffold and peptides.

Streefkerk *et al.* [57] synthesized multicyclic peptides that are common in nature and have received great attention due to their great biological potential. The synthetic process of tetracyclic peptides involves chemo-enzymatic peptide synthesis (CEPS), chemical linkage of peptides onto scaffolds (CLIPS), and oxime ligation (Fig. 19). It was necessary to develop a new type of small-molecule scaffold, comprising two reactive primary bromides (CLIPS) in combination with an aldehyde moiety (scaffold 1). The aldehyde was chemically protected with diethyl acetal groups, and they were released after the initial CLIPS reaction to ensure controlled and regioselective cyclization. Cyclization of CEPS followed by CLIPS and subsequently, oxime ligation was considered the most direct approach. The aminoxy residue was introduced using aminoxy-homoserine (hS(OH₂)). For this type of cyclization, the yields were low, due to side reactions, including the formation of isopropylidene, the incomplete coupling of Fmoc-hS(OH₂Boc)-OH, and elimination of the aminoxy motif. In general, the CLIPS reactions were carried out under standard reaction conditions (0.5 mM peptide solution, ~0.9 equiv. of Scaffold (1), aqueous NH₄HCO₃ solution (pH > 8.0) at room temperature (RT), to give the corresponding bicyclic product (3). This was followed by the deprotection of (1) with TFA, for the ligation of the oxime. Then peptide 3 was dried in a vacuum, and the oxime was again ligated in aqueous dimethyl sulfoxide in order to finally obtain the multicyclic form (4) [57]. Oxime ligation is highly chemoselective since aminoxy and aldehyde are bio-orthogonal with the side chain functionalities. It has been reported that undesired reactions to unprotected nucleophilic side chains can be suppressed by an adjustment of the pH when implementing acidic buffer systems; however, this type of methodology in the synthesis of cyclic peptides is unusual and likely is largely due to the possibility of hydrolysis of the oxime bond, the formation of a mixture of E/Z isomers, and possible side reactions [58].

5.2. Peptide Cyclization Mediated by Azide-alkyne Cycloaddition

Angell *et al.* [59], reported cyclic peptide synthesis by incorporating non-peptidic fragments into the peptidomimetics, since it presents an alternative way of incorporating new functional groups

such as azide and alkyne. The synthesis of conjugated peptides by means of click chemistry can be applied to the synthesis of cyclic peptides, as described in Fig. (20). The precursor linear (1) was recrystallized and isolated with an overall yield of 70%, and linear precursor cyclization gave the "monomeric" (2) and "dimeric" (3) products. The formation of the 5-member ring product was carried out as follows: Precursor (1) was dissolved in THF and a copper catalyst was added, and the reaction mixture was stirred for 10-14 h, maintaining the final concentration lower than 0.001 M, the dimeric product (3) being obtained with 12% yields. This is mainly due to the limited solubility of products in organic and aqueous solvents [59].

A new approach to CuAAC reactions in the generation of cyclic peptides has been reported. White *et al.* reported the application and structural analysis of cyclic peptides obtained by CuAAC and ruthenium-catalyzed cycloaddition between an azide group and alkyne (RuAAC). These linkages were evaluated in four serine protease inhibitors based on the sunflower trypsin inhibitor-1 framework (Fig. 21). The use of CuAAC leads to the generation of 1,4 triazoles, while the ruthenium catalyst favors the generation of 1,5 triazoles. However, the use of RuAAC on the peptide containing unprotected side chains is not recommended because side reactions may appear. In order to avoid this inconvenience, the RuAAC reaction should be carried out by dissolving the protected peptide (2) in DMF and adding chlorine (pentamethylcyclopentadienyl) (cyclooctadiene)ruthenium (II) catalyst under anhydrous conditions at 80 °C for up to 18 h. After removing the protecting groups, the peptides were purified *via* RP-HPLC in order to isolate product (3), with 10% yields [60].

5.3. Imine-mediated Macro cycling and Aziridine Aldehyde-based Multicomponent Macro cycling

In 2017, Malins *et al.* [61] reported a macro cycling method applied to peptides using the amino group from the N-terminal end and an aldehyde moiety at the C-terminal end (Fig. 22A). The peptide cyclization was carried out by the formation of an intramolecular imine (2) in an aqueous medium in highly diluted solutions, followed by a nucleophilic attack to the cycle, allowing the incorporation of a substituent in order to obtain the cyclic peptide (3).

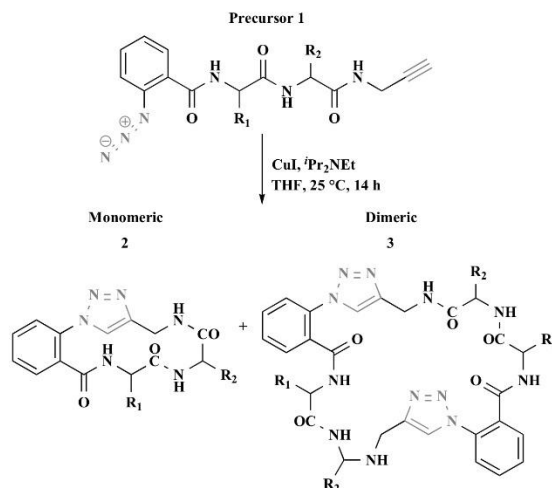


Fig. (20). Copper-catalyzed cyclization reaction.

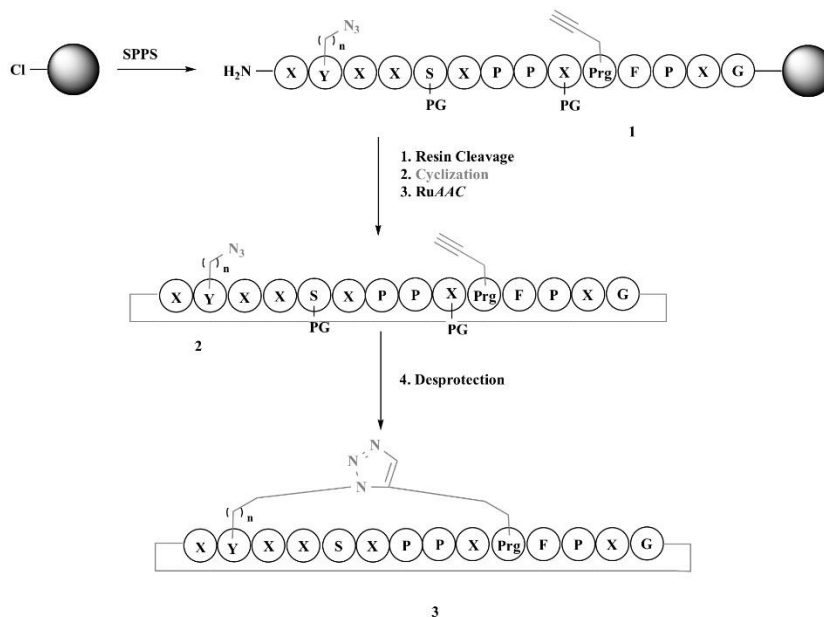


Fig. (21). Overview of the synthesis of 1,4 and 1,5 triazole-bridged disulfide mimetics in cyclic protease inhibitors. PG: Protecting group. X: amino acid corresponding to a specific sequence. Y: Aza (n = 1) or hAza (n = 2).

The choice of nucleophile is essential at this stage, since external nucleophiles such as KCN and NaBH₃CN generate α-aminonitriles or secondary amines, respectively, while internal nucleophiles adjacent to the N-terminal amino group, including

indole, imidazole, and thiol, generate heterocycles at the cyclization site [61]. The versatility of this cyclization technique lies in its ability to introduce various modifications after cyclization. Macrocyclic systems of five to ten amino acids in length have been reported,

allowing the generation of analogs derived from the same linear precursors. Hill *et al.* [62] reported another macrocyclization system based on four components: N-terminal amine and C-terminal carboxyl groups (4), isocyanide 5, and aziridine aldehyde 6 (Fig. 22B). This reaction proceeds through a concerted mechanism, generating products with great stereoselectivity. The cyclization process was mediated by an intermediate imidoanhydride, which was formed in a concerted manner from aziridine aldehyde, isocyanide, the amine of the N-terminal region, and the adjacent amide. The imidoanhydride is then attacked by the carboxylate group, inducing the O to N-acyl transfer to aziridine, producing cyclic peptide (7) (Fig. 22B). The peptide fragment was obtained *via* SPPS using the Fmoc/tBu method, while the isocyanides are commercially available or can be easily synthesized [62]. These peptide cyclization methods gave high yields, and the multi-component cyclic peptides could be a synthetic alternative for cyclizing peptides and discovering cyclic peptide-based drugs.

5.4. Cyclization Mediated by Native Chemical Ligation and Derivatives

Native chemical ligation (NCL) involves the reaction between the N-terminal Cys and a C-terminal thioester of unprotected peptides in an aqueous solution at pH 7.0. Advances in NCL and its derived methodologies have improved the scope of cyclic peptide synthesis. Macmillan *et al.* [63], reported the synthesis of cyclic analogs derived from the β -defensin family using reverse native chemical ligation followed by intramolecular trans-thioesterification and acyl transfer to convert linear peptides into biologically active cyclic products. They described a new, simple route for obtaining cyclic peptides from linear precursor peptides (Fig. 23). Compound (1) was treated under NCL standard conditions (2% w/v MESNa, pH 7.0), and 24 h time was required to complete the reaction. When the reaction was carried out using pH 5.8, compound (2) was obtained with higher yields [63]. Acosta *et al.* [64], implemented a variant of the NCL methodology using a solid support, specifically the "safe capture" Fmoc-MeDbz/MeNbz-resin in the Tyr-cyclodepsipeptides synthesis by "head-to-side chain" through cyclative cleavage. The peptide was built using the SPPS-Fmoc/tBu method on a FmocMeDbz-Gly-Rink-ChemMatrix resin, and the Fmoc-amino acids were coupled using DIC and OxymaPure in

DMF. Fmoc-Tyr(CITrt)-OH was incorporated into the N-terminal of the sequence, and the Fmoc was removed with 20% piperidine in DMF. Then the α -amino group was acylated with hexanoic acid. The Hx-Tyr(CITrt)-peptidyl-MeDbzGly-Rink-ChemMatrix resin was activated with *p*-nitrophenyl chloroformate in anhydrous DCM, followed by cyclization with DIPEA in DMF for 45 min to render Hx-Tyr(CITrt)-peptidylMeNbz-resin. The peptide-resin was then treated with TFA/DCM to remove the CITrt protecting group, and the final cyclative cleavage was carried out by treating the peptide-resin with DIPEA/DCM. This technology represents a user-friendly method for the preparation of these cyclic peptides [64].

5.5. Other Strategies

Other strategies have emerged for cyclic peptide synthesis. Nefzi *et al.* [65], described the synthesis of integrin ligands containing the RGD sequence by means of an efficient solid-phase intramolecular thioalkylation reaction (Fig. 24). The parallel synthesis of RGD cyclic peptides containing thiazolyl groups was carried out. They started from *p*-methylbenzhydramine hydrochloride (MBHA-HCl) resin functionalized with Fmoc-Cys-(Trt)-OH (1). Linear RGD peptides (2) were synthesized *via* the SPPS-Fmoc/tBu method, and the free α -amine of the N-terminal end was treated with Fmoc-isothiocyanate. Then the Fmoc group was removed in order to obtain (3). Subsequently, the thiourea was treated with 1,3-dichloroacetone (Hantzsch cyclocondensation) to obtain α -chloromethyl thiazolyl resin-peptide (4). The Trt group was removed by treatment with 5% TFA/DCM, and the resin-peptide was treated with Cs_2CO_3 /DMF in order to induce an $\text{S}_{\text{N}}2$ intramolecular thioalkylation reaction. Then the resin-peptide was treated with HF/anisole, and the macrocyclic peptidomimetics thio-methylthiazolyl (5) was obtained with a good yield (>30%) and high purity (>70%) [65]. Rivera *et al.* [66], reported peptide macrocyclization strategies by transition metal catalysis. This report provides a complete description of metal-catalyzed peptide macrocyclization as a special class of the late-stage peptide derivatization method, which also includes new trends in decarboxylative radical macrocyclizations and the interaction between photo-redox and transition-metal catalysis [66]. LeValley *et al.* [67], reported the synthesis of cyclic peptides based on orthogonal click chemistry reactions, specifically photoinitiated thiol-ene and strain-promoted azide-alkyne

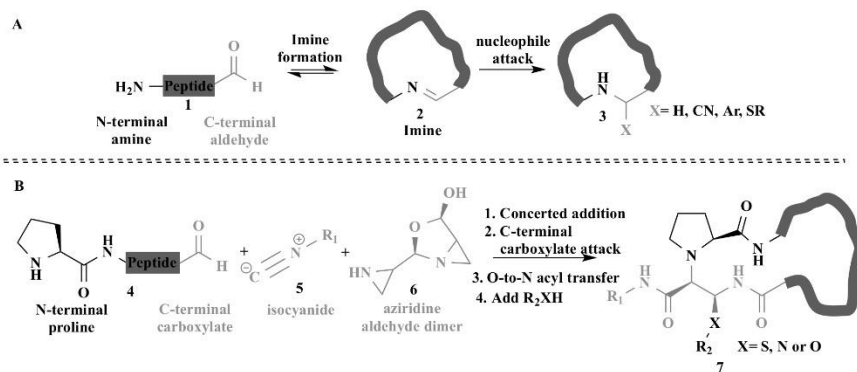


Fig. (22). (A) Cyclization mediated by imine formation between the N-terminal amine and the C-terminal aldehyde and (B) Multicomponent peptide macrocyclization.

cycloaddition (SPAAC), demonstrating that it is a useful method for synthesizing cyclic RGD peptides using orthogonal click chemistry reactions with a chemically active point. A photoinitiated thiol-ene reaction was used for cyclization in solution, producing an azide-functionalized cyclic peptide. The utility of azide-functionalized cyclic RGD for conjugation with hydrogels and fluorophores has been demonstrated [67]. Kogon *et al.* [68], reported the synthesis of the imidazopyrrolopyrazine ring system, suggesting that cyclisation of the tripeptide produces the expected cyclic endiamino peptide *via* enol-tosylate. The high ring-strain of the nine-member cyclic peptide triggers the trans-annular nucleophilic attack of the endiamino amine group on the proline amide carbonyl group, producing the azacyclol, and then dehydration allows obtaining the imidazopyrrolopyrazine derivative [68]. Cyclic peptides often show improvements in binding affinity, specificity, or stability compared to their linear analogs, due to the imposition of restricted geometries. It is important to note that cyclization does not necessarily lead to improvements at all, even in some of these properties. In addition, it was demonstrated that the cyclization of peptides sometimes decreases the degree of penetration of the cell membrane. The absence of charges at the N- and C-terminal can reduce the effectiveness of the proteomic sequencing techniques, such as mass spectrometry and Edman degradation, making quality control and characterization efforts more complicated than with linear peptides [69].

6. CONJUGATED SHORT PEPTIDES VIA “CLICK” CHEMISTRY

Peptide conjugates are of particular interest because improvements in their activity have been found, since they decrease side effects in the host, thus generating greater specificity to the target. The development of techniques for obtaining peptide-peptide chimeric conjugates such as that reported by Pineda *et al.* [70] or Liu *et al.* [73], peptide-sugar such as that reported by Collet *et al.* [71] or peptide-polymer reported by Kumar *et al.* [72], among others, has largely been possible due to the great progress that has been made in the incorporation of click chemical reactions into peptide synthesis (Fig. 25) [70-73]. The term “click chemistry” was introduced by Fokin and Sharpless and describes a specific type of chemistry, the chemical union of small fragments in a simple “click”. These reactions have characteristics such as (i) high efficiency, (ii) stereospecific reactions, (iii) easy isolation of the product, (iv) low-cost reagents (catalysts), and (v) the use of non-toxic solvents such as water. Over time, the great importance of one of the first click chemistry reactions has been reported, the copper-catalyzed variant of the Huisgen azide-alkyne cycloaddition (CuAAC). However, with the great advance in the field of organic chemistry, new variants and reactions have been described and applied in the synthesis of peptide conjugates. This is how thiolene, Diels-Alder reactions, ligation of oximes, and a variant of CuAAC known as a strain-promoter of azide-alkyne cycloaddition (SPAAC), among others, have become a focus of great importance in the development of new peptide-based agents (Fig. 25)

6.1. Cu(I)-Catalyzed Azide-alkyne Cycloaddition (CuAAC)

CuAAC was first reported by Huisgen. Years later, thanks to Sharpless, who defined it under the click reaction term, it became part of a special category of organic reactions known as click chemical reactions. This reaction (Fig. 26) involves the formation of the copper acetylide complex (2), which will lead to the formation of the 6-member triazole-copper cycle (5). This intermediate undergoes a rearrangement under an acid-base process that involves sol-

vent molecules to give the formation of the cycle 1,2,3-triazole (7), and the release of the catalyst starts the cycle again. The use of copper (I) species as a catalyst is essential for this reaction. It has been reported that changing the reaction conditions, such as the solvent, the temperature (heating or microwave), and the presence of reducing agents, can improve the obtention of the desired product. A wide variety of compounds derived from copper have been evaluated as catalysts for CuAAC reaction, such as copper (I) iodide (CuI), copper (I) bromide (CuBr), copper (II) sulfate pentahydrate (CuSO₄·5H₂O), and copper (0) itself in filing form [74, 75]. Bock *et al.* [76] used CuBr and reflux in toluene for the generation of 1,2,3-triazole ring-linked cyclic peptides [76]. On the other hand, Pineda *et al.* [70] used CuSO₄·5H₂O together with a reducing agent (ascorbic acid) in EtOH: H₂O at 80 °C to produce a 1,2,3-triazole ring-linked chimeric peptide. In this approach, the copper (I) species were generated *in situ*.

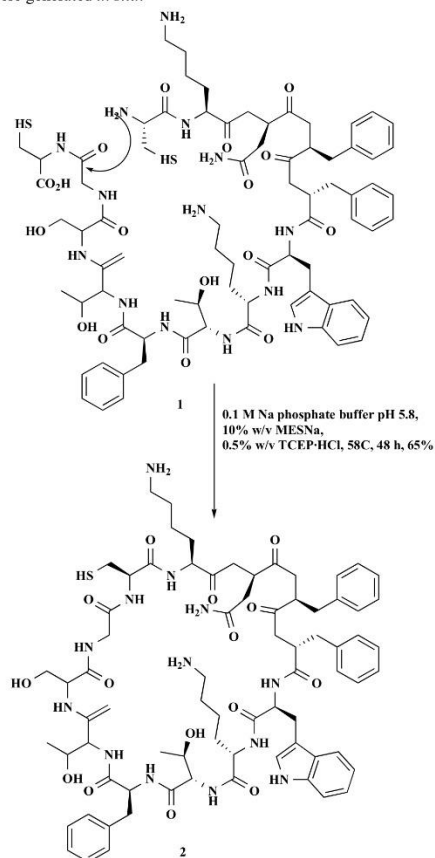


Fig. (23). Head-to-tail cyclization route to somatostatin analog from latent thioester.

The CuAAC reaction has been implemented for the conjugation of peptide-peptide and/or peptide-organic molecules, such as

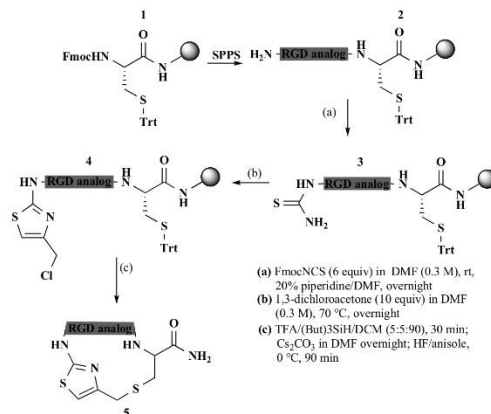


Fig. (24). Parallel synthesis of different thiazolyl containing RGD cyclic peptides.

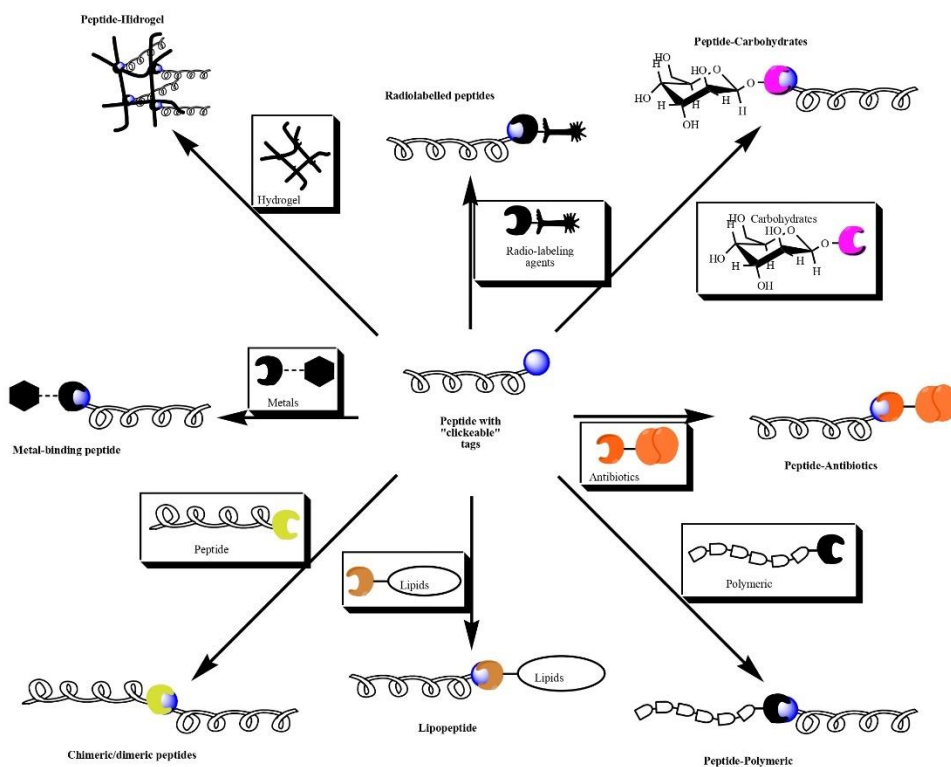


Fig. (25). Types of peptides conjugated with antibiotic biomolecules, polymers, carbohydrates, hydrogels, complexed metals, and chimeric/dimeric peptides synthesized by click chemical reactions.

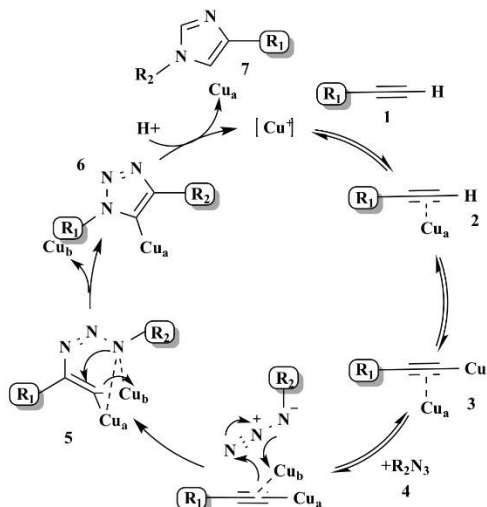


Fig. (26). CuAAC mechanism for the formation of the triazole ring.

antibiotics [77], radiolabels [78, 79], polymers [80], terpenes [81], carbohydrates [71], phosphonates [82], fluorinated α -hydroxy acids [83], and metal-chelating scaffolds [84, 85]. All of these have taken advantage of the principle of azide-alkyne cycloaddition and have modified this strategy in order to adapt it to their needs. Examples of conjugated peptides using this type of click chemistry are presented in Fig. (27).

6.2. Strain-Promoted Azide-alkyne Cycloaddition (SPAAC)

Variants of the Huisgen reaction have been developed, one of which is known as strain-promoted azide-alkyne cycloaddition (SPAAC). This reaction is characterized by getting rid of the copper (I) catalyst used in CuAAC since several drawbacks have been reported when using peptides, proteins, and metal-organic derivatives together. This reaction is described in Fig. (28A). The cyclooctyne (2) has a highly reactive alkyne group, which reacts with azide moiety (1) to produce (3). However, several drawbacks have been reported for this azide-alkyne cycloaddition, such as *i*) the high reactivity of the cyclic system, *ii*) non-regioselective reactions, *iii*) the possibility that the cyclic system can react with thiol groups (-SH) present in Cys *via* thiol-yne reaction, and *iv*) high cost, limiting the use of this reaction. This type of click reaction has been used to obtain short peptides conjugated with polymers, radiolabels, metals, and other peptide sequences [86-88]. One of the great advantages of using this reaction over its counterpart, CuAAC, is that the reaction product is generated in a short time with minimal reaction conditions, and in most cases, product (3) is obtained with high yields, without the need for a purification stage. An example of obtaining SPAAC-based peptide conjugates is that reported by Slagle *et al.* [89], generating a system of functionalized microbubbles on its surface with peptide sequences. The SPAAC conjugation is described in Fig. (28B). The surface-embedded dibenzocyclooctin-functionalized PEGylated phosphatidylethanolamine (5) reacts with the peptide RGD functionalized with the azide group (4) to form the

bioconjugate lipid (6). This peptide-lipid conjugate system associated with the generation of microbubbles is of utmost importance for the diagnosis of tumor angiogenesis [89].

6.3. Thiol-ene Reaction

Another alternative to click chemistry reactions is the reaction between a thiol group (-SH) and an alkene. This reaction is characterized by the liberation of copper metallic catalysts in CuAAC and the high cost of the cyclic system in SPAAC. This reaction is carried out in aqueous solution, and in most cases, occurs under physiological conditions (pH 7.0), and is photo-initiated by UV radiation. However, secondary reactions can occur associated with UV radiation, such as oxidation of the thiol group to generate disulfides and alkene polymerization [90-93]. Wang *et al.* [94] reported the generation of stapled macrocyclic systems where they took an advantage of cysteines present in the peptide sequence to generate higher stability in the structure. Fig. (29) shows the peptide-stapling reaction carried out in organic solvents, because hydrocarbon dienes and 2,2-dimethoxy-2-phenylacetophenone radical initiator (DMPA) are not soluble in water. In order to overcome these difficulties, they used 1,3-diallylurea (2) and the photo-inducible radical initiator 2,2'-Azobis [2-(2-imidazolin-2-yl)propane] dihydrochloride (VA044, 3), both soluble in water. By reacting (1), (2) and (3) by irradiation at 365 nm and pH 4.0, product 5 was generated, with 53% yields. When the reaction was improved by adding a reducing agent such as tris (2-carboxy ethyl) phosphine hydrochloride (TCEP, 4), the yield increased to 95% [94].

6.4. Other Reactions

The Thiol-Michael reaction, the Diels-Alder reaction, Staudinger ligation, oxime ligation, and native chemical ligation have been of great interest for obtaining new analogues derived from short peptides. The thiol-maleimide reaction is one of the thiol-Michael type reactions. It is characterized by being a highly

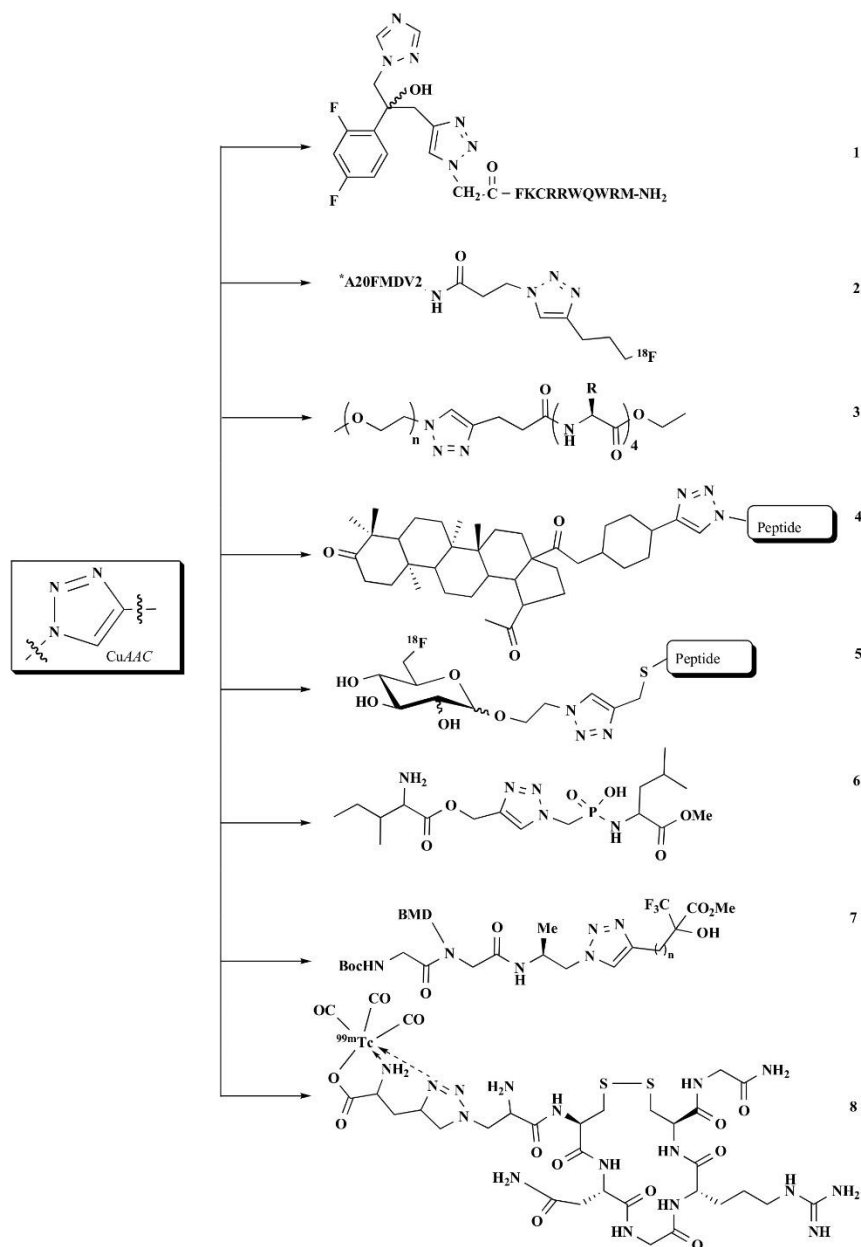


Fig. (27). Peptides conjugated via CuAAC alkyne-azide cycloaddition reaction. Antibiotics (1), radio markers (2), polymers (3), terpenes (4), sugars (5), phosphonates (6), fluorinated α -hydroxy acids (7), and metal-chelating scaffold (8). *A20FMDV2: NAVPNLRGDLQVLAQKVART-C(O)NH₂.

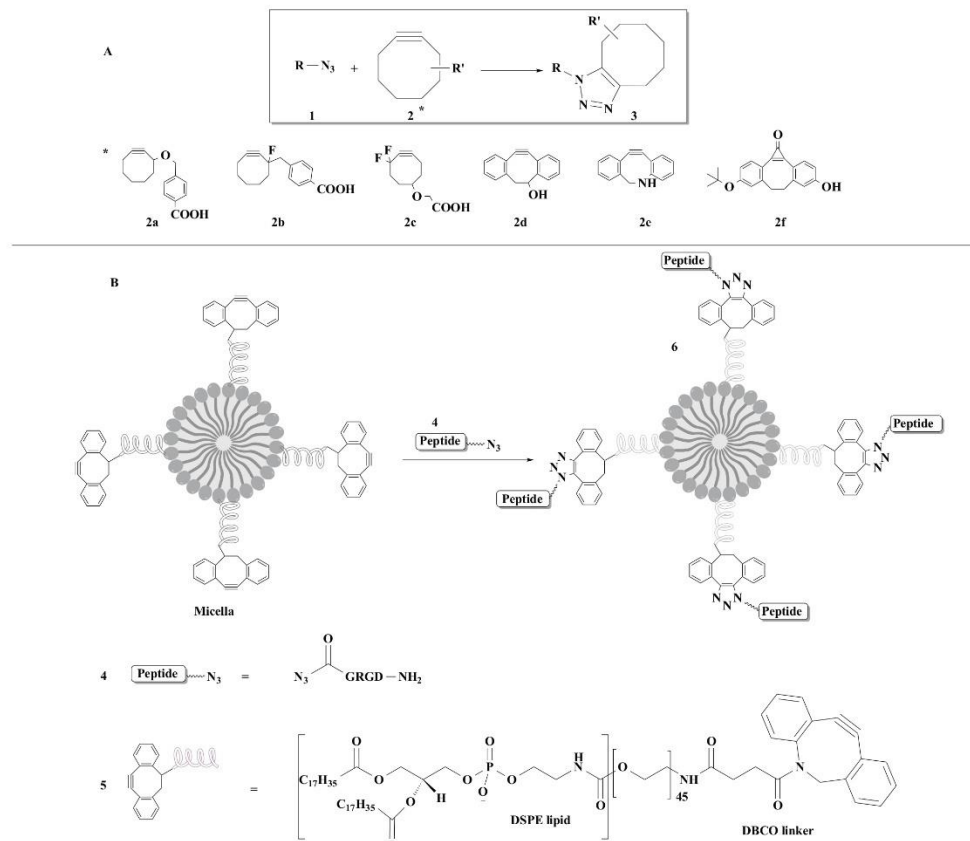


Fig. (28). SPAAC cycle formation and general reaction (A). Mechanism for generating functionalized microbubbles using SPAAC (B).

effective addition reaction and proceeds with rapid kinetics under physiological conditions. It is the most efficient "click" reaction for synthesizing large peptide conjugates with high yields. Wangler *et al.* [95] synthesized a high molecular weight dendron functionalized with short peptides, and Sun *et al.* [96], reported the importance of the thiol-acrylate reaction, which is a thiol-Michael reaction for the generation of peptide conjugates with polymers, stating that the most relevant facts are *i)* the thiol pKa, *ii)* the catalyst nucleophilicity, *iii)* solvent, and *iv)* reaction medium basicity could affect the reaction rate (Fig. 30A). Elbert and Hubbell [97] synthesized acrylate and acrylamide modified polyethylene glycol (PEG) and explored its reactions with peptides containing thiol moieties. It was found that using dilute PEG diacrylate concentration (2% w/v PEG diacrylate, molecular weight 8,000), the Michael addition reaction of thiol-acrylate at pH 8.0 proceeds rapidly. The resulting PEG-peptide conjugate (3) exhibited low cytotoxicity and transfection efficiencies similar to PEL, indicating that this peptide-PEG-based vehicle can be used for gene delivery [95-97].

The Diels-Alder reaction is another reaction used to obtain peptide conjugates [98]. It is defined in a general way as a cycloaddition [4 + 2] between a diene and a substituted alkene. It has been reported that this reaction in many cases requires high temperatures, which can be seen as a disadvantage when applied to peptides, since many sequences have been reported as unstable at high temperatures. For this reason, the reaction for the generation of peptide derivatives is usually carried out at RT. Montgomery *et al.* [99] mentioned the importance of the Diels-Alder reaction in peptides, since it represents a versatile approach to stabilizing proteins. The Diels-Alder cyclization is a versatile tool for stabilizing protein structural motifs in a wide variety of chemical environments (Fig. 30B). Diels-Alder cyclized (DAC) peptides containing the RGD motif (4) are undergoing clinical testing in oncology. The diene-dienophile functional groups span a wide range of structures and reactivity. Diene 2,4-hexadiene and maleimide dienophiles were used. Peptides of various lengths and sequences were synthesized, containing orthogonally protected Cys(tBuS-) and Lys(Mmt-) side chains. Sequential deprotection of cysteine residue on resin and

alkylation of hexadiene with 1-bromo-2,4-hexadiene proceeded quantitatively. The diene-containing amino acid Fmoc-Cys(2,4-hexadiene)-OH (**5**) can be incorporated *via* SPPS using the Fmoc/tBu strategy. Subsequent deprotection of Lys in resin and acylation with *N*-maleimide-glycine in an RGD-model peptide resulted in the formation of (**8**), with high conversion yields of ~85-95%. Heating of the resin in DMSO was an optimal condition for maximizing cyclic conversion, but it also resulted in a higher proportion of isomeric products, which may be due to the disaggregation of the protected peptide into the resin, confirming the compatibility of Diels-Alder peptide cyclization in various organic and aqueous environments [99].

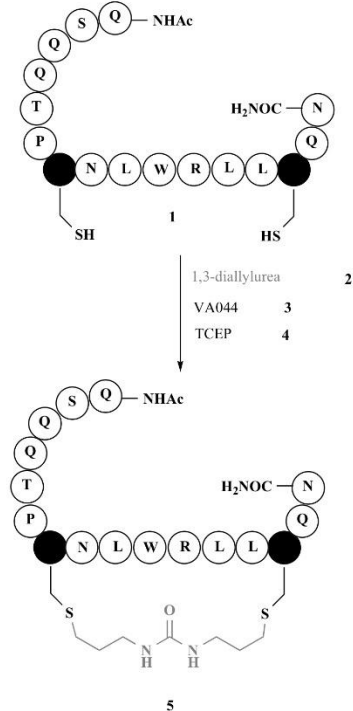


Fig. (29). Peptide-based thiol-ene reaction in aqueous solution.

Staudinger's ligation is the reaction between an azide group and a phosphine moiety to form a native amide bond, and as by-products, phosphine oxide and a nitrogen molecule were described [100, 101]. This chemical linkage has been implemented for obtaining carbohydrate-conjugated peptides and the ligation between a peptide-resin with another peptide in the solution. Kim *et al.* [102], (Fig. 30C) reported Staudinger ligation using as a starting point Fmoc-Phe-Phe-OH, which was assembled to (**9**) by means of SPPS and the Fmoc/tBu strategy, followed by solid-phase Staudinger ligatures between (**9**) and the azido acid (**11**). In order to minimize contamination of the released peptides, they added <1 equivalent of azido acid to (**10**), and the reaction was followed by TLC. All the

reactions were completed within 24 and 40 h in THF/H₂O (3:1) at RT, and tripeptides were obtained in quantitative yields. Product (**14**) was obtained with high purity, thus dispensing with the need for any purification step. Another notable advantage of solid-phase Staudinger ligation is the reuse of resin-bound phosphinothiol (up to five times). The phosphine oxide (**15**) attached to resin can easily be recovered from the ligation product by simple filtration and reduced with an excess of trichlorosilane [102].

Another chemical linkage is oxime ligation, a condensation reaction between a carbonyl group (-aldehyde/-ketone) with an aminoxy group that results in a conjugated molecule linked by an oxime bond. This reaction, in addition to exhibiting the basic characteristics of a "click" reaction, has advantages such as *i*) it does not require any metallic catalyst, and *ii*) the oxime bond formed is sensitive to pH, which is highly useful for the generation of biomaterials sensitive to pH. Guthrie *et al.* [105] reported the use of oxime ligation for the generation of peptide-peptide conjugates, showing that this reaction is highly dependent on the solvent and the buffer concentration (Fig. 30D) [103-105].

NCL is a reaction that occurs between a thioester and an N-terminal cysteine, generating the formation of an amide bond with a cysteine in the junction. The reaction proceeds through a reversible transthioesterification step, followed by intramolecular displacement S → N-acyl, which generates an amide bond. This reaction gives high yields at room temperature conditions and neutral pH in aqueous solution, one NCL variant involves the use of modified amino acids in which a thiol group has been introduced. In this context, β-thiol-valine (penicillamine) and γ-thiol-valine, have been reported. These thiol-valine molecules at N-terminal end react with the thioester by transthioesterification. The resulting thioester-bound intermediate undergoes rapid intramolecular acyl transfer there creating an amide bond. Then desulfurization provides a valine residue into the peptide at the ligation site [64, 106, 107]. Ingale *et al.* [108] reported multiple uses of this reaction for the parallel ligation of peptide conjugate with lipid and a sugar (Fig. 30E). The results demonstrated the optimal conjugation of lipophilic peptide thioester (**19**), peptide thioester (**20**), and N-terminal cysteine glycopeptide (**21**) to obtain the peptide complex (**22**). Furthermore, 2-mercaptoethane sulfonate was found to be a more effective catalyst compared to thiophenol. In this regard, it was observed that the liposome-mediated NCLs were formed in 2 h, which is remarkably fast. The high reaction rate can probably be attributed to a concentration effect on liposomes [108].

CONCLUSION

Short peptides have become a valuable tool, given their versatility and diversity in different applications at the chemical and biological levels. However, over the years, researchers have had to face great challenges in terms of the stability and potentiation of the peptides' activity. The design of short peptides could resemble a Sisyphean task, given its high complexity. However, the significant potential of these molecules has spurred the development of a large number of studies and investigations, which have had an impact on the development of a lot of strategies in the design of short peptides, which require difficult synthetic and experimental work, in order to obtain promising molecules in a wide variety of applications, from biological activity to even organic synthesis, which necessitates the continuation of investing efforts in the development of strategies to obtain new short peptides, which are increasingly promising. This review describes some of the most widely available

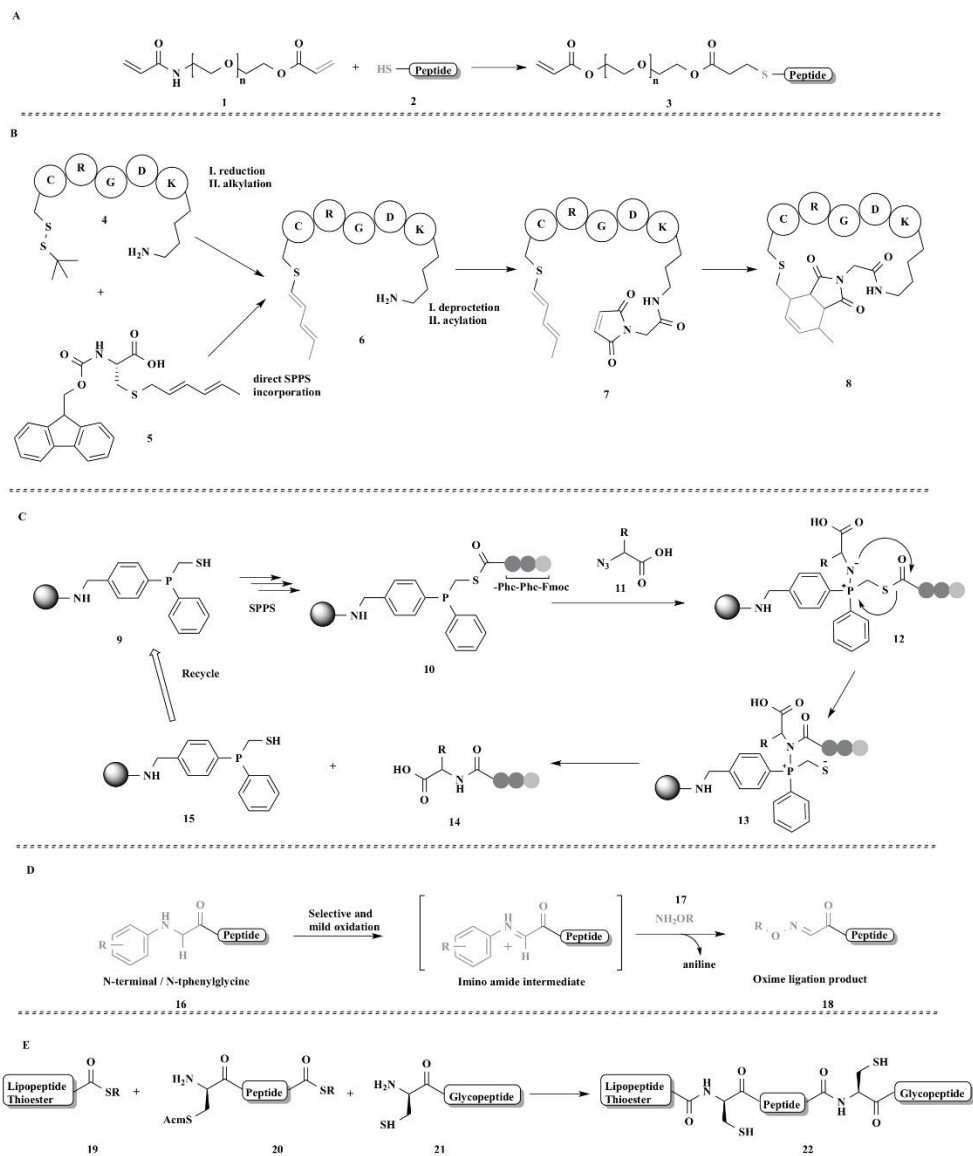


Fig. (30). (A) Thiol-Michael containing peptide to PEG-diacrylate, (B) Diels-Alder, (C) Staudinger ligation, (D) ligation with oximes and (E) native ligation.

strategies used in the design and development of short peptides, mainly covering the incorporation of unnatural amino acids, obtaining polyvalent structures, formation of cycles, generation of disulfide bridges, and the design of peptides conjugated by click chemis-

try. All these strategies open up a world of possibilities since thanks to them, it is possible to obtain promising molecules with greatly improved stability and highly potent biological or synthetic activity with respect to the original unmodified sequences.

CONSENT FOR PUBLICATION

Not applicable.

FUNDING

This research was funded by COLCIENCIAS grant numbers: RC N° 706-2018 and RC N° 846-2019.

CONFLICT OF INTEREST

The authors declare no conflict of interest, financial or otherwise.

ACKNOWLEDGEMENTS

Authors are thankful to COLCIENCIAS for the financial support of the projects 110180762973 and 110184467183 with contract RC N° 706-2018 and RC N° 846-2019, respectively.

REFERENCES

- Derakhshankhah, H.; Jafari, S. Cell penetrating peptides: a concise review with emphasis on biomedical applications. *Biomed. Pharmacother.*, **2018**, *108*, 1090-1096. <https://doi.org/10.1016/j.biopha.2018.09.097> PMID: 30372809
- Ball, L.J.; Kühne, R.; Schneider-Mergener, J.; Oeschkin, H. Recognition of proline-rich motifs by protein-protein-interaction domains. *Angew. Chem. Int. Ed. Engl.*, **2005**, *44*(19), 2852-2869. <https://doi.org/10.1002/anie.200400618> PMID: 15880548
- Vivet, B.; Cavelier, F.; Martinez, J.; Aubry, A. A silaprolin-containing dipeptide. *Acta Cryst. C*, **2000**, *56*, 1452-1454. <https://doi.org/10.1107/s0108270100012294>
- Cavelier, F.; Vivet, B.; Martinez, J.; Aubry, A.; Didierjean, C.; Vicherat, A.; Marraud, M. Influence of silaprolin on peptide conformation and bioactivity. *J. Am. Chem. Soc.*, **2002**, *124*(12), 2917-2923. <https://doi.org/10.1021/ja017440q> PMID: 11902882
- Vivet, B.; Cavelier, F.; Martinez, J. Synthesis of silaprolin, a new proline surrogate. *Eur. J. Org. Chem.*, **2000**, *2000*, 807-11. [https://doi.org/10.1002/\(SICI\)1099-0690\(200003\)2000:5<807::AID-EJOC807>3.0.CO;2-E](https://doi.org/10.1002/(SICI)1099-0690(200003)2000:5<807::AID-EJOC807>3.0.CO;2-E)
- Rémond, E.; Martin, C.; Martinez, J.; Cavelier, F. Silicon-containing amino acids: synthetic aspects, conformational studies, and applications to bioactive peptides. *Chem. Rev.*, **2016**, *116*(19), 11654-11684. <https://doi.org/10.1021/acs.chemrev.6b00122> PMID: 27529497
- Pujals, S.; Sabido, E.; Tarragó, T.; Giralt, E. all-D proline-rich cell-penetrating peptides: a preliminary *in vivo* internalization study. *Biochem. Soc. Trans.*, **2007**, *35*(Pt 4), 794-796. <https://doi.org/10.1042/BST0350794> PMID: 17635150
- Debuene, F.; Da Silva, J.A.; Pianowski, Z.; Duran, F.J.; Winssinger, N. Expanding the scope of PNA-encoded libraries: divergent synthesis of libraries targeting cysteine, serine and metallo-proteases as well as tyrosine phosphatases. *Tetrahedron*, **2007**, *63*, 6577-6586. <https://doi.org/10.1016/j.tet.2007.03.033>
- Patch, J.A.; Barron, A.F. Mimicry of bioactive peptides via non-natural, sequence-specific peptidomimetic oligomers. *Curr. Opin. Chem. Biol.*, **2002**, *6*(6), 872-877. [https://doi.org/10.1016/S1367-5931\(02\)00385-X](https://doi.org/10.1016/S1367-5931(02)00385-X) PMID: 12470744
- Niu, Y.; Hu, Y.; Li, X.; Chen, J.; Cai, J. γ -AApeptides: design, synthesis and evaluation. *New J. Chem.*, **2011**, *35*, 542-545. <https://doi.org/10.1039/C0NJ00943A>
- Shi, Y.; Teng, P.; Sang, P.; She, F.; Wei, L.; Cai, J. γ -AApeptides: design, structure, and applications. *Acc. Chem. Res.*, **2016**, *49*(3), 428-441. <https://doi.org/10.1021/acs.accounts.5b00492> PMID: 26990964
- Davie, E.A.C.; Mennen, S.M.; Xu, Y.; Miller, S.J. Asymmetric catalysis mediated by synthetic peptides. *Chem. Rev.*, **2007**, *107*(12), 5759-5812. <https://doi.org/10.1021/cr068377w> PMID: 18072809
- Wang, X.; Reisinger, C.M.; List, B. Catalytic asymmetric epoxidation of cyclic enones. *J. Am. Chem. Soc.*, **2008**, *130*(19), 6070-6071. <https://doi.org/10.1021/ja801181u> PMID: 18422314
- Akagawa, K.; Kudo, K. Asymmetric epoxidation of α,β -unsaturated aldehydes in aqueous media catalyzed by resin-supported peptide-containing unnatural amino acids. *Adv. Synth. Catal.*, **2011**, *353*, 843-847. <https://doi.org/10.1002/adsc.201000805>
- Navo, C.D.; Mazon, N.; Oroz, P.; Gutiérrez-Jiménez, M.L.; Marín, J.; Asenjo, J.; Avenozza, A.; Busio, J.H.; Corzana, F.; Zurbano, M.M.; Jiménez-Osés, G.; Peregrina, J.M. Synthesis of N_α -substituted α,β -diamino acids via stereoselective *N*-Michael additions to a chiral bicyclic dehydroalanine. *J. Org. Chem.*, **2020**, *85*(5), 3134-3145. <https://doi.org/10.1021/acs.joc.9b03020> PMID: 32040912
- Aycock, R.A.; Pratt, C.J.; Jui, N.T. Aminoalkyl radicals as powerful intermediates for the synthesis of unnatural amino acids and peptides. *ACS Catal.*, **2018**, *8*, 9115-9119. <https://doi.org/10.1021/acscatal.8b03031>
- Cui, H.K.; Guo, Y.; He, Y.; Wang, F.L.; Chang, H.N.; Wang, Y.J.; Wu, F.M.; Tian, C.L.; Liu, L. Diaminodiacid-based solid-phase synthesis of peptide disulfide bond mimics. *Angew. Chem. Int. Ed. Engl.*, **2013**, *52*(36), 9558-9562. <https://doi.org/10.1002/anie.201302197> PMID: 23804284
- Sun, S.S.; Chen, J.; Zhao, R.; Bierer, D.; Wang, J.; Fang, G.M. Efficient synthesis of a side-chain extended diaminodiacid for solid-phase synthesis of peptide disulfide bond mimics. *Tetrahedron Lett.*, **2019**, *60*, 1197-1201. <https://doi.org/10.1016/j.tetlet.2019.03.061>
- Xu, Y.; Wang, T.; Guan, C.J.; Li, Y.M.; Liu, L.; Shi, J. Dmab/ivDde protected diaminodiacids for solid-phase synthesis of peptide disulfide-bond mimics. *Tetrahedron Lett.*, **2017**, *58*, 1677-1680. <https://doi.org/10.1016/j.tetlet.2017.03.024>
- Rodríguez, V.; Pineda, H.; Ardila, N.; Insuasty, D.; Cárdenas, K.; Román, J. Efficient Fmoc group removal using diluted 4-methylpiperidine: an alternative for a less-polluting SPPS-Fmoc/tBu protocol. *Int. J. Pept. Res. Ther.*, **2019**, *26*, 585-587. <https://doi.org/10.1007/s10989-019-09865-9>
- Van Lysebetten, D.; Felissati, S.; Antonatou, E.; Carrette, L.L.G.; Espeel, P.; Focquet, E.; Du Prez, F.E.; Madder, A. A thiolactone strategy for straightforward synthesis of disulfide-linked side-chain-to-tail cyclic peptides featuring an *N*-terminal modification handle. *ChemBioChem*, **2018**, *19*(6), 641-646. <https://doi.org/10.1002/cbic.201700323> PMID: 29314620
- Fang, G.M.; Chen, X.X.; Yang, Q.Q.; Zhu, L.J.; Li, N.N.; Yu, H.Z. Discovery, structure, and chemical synthesis of disulfide-rich peptide toxins and their analogs. *Chin. Chem. Lett.*, **2018**, *29*, 1033-1042. <https://doi.org/10.1016/j.ccl.2018.02.002>
- Hussain, W.; Skwarczynski, M.; Tot, H.I. *Peptide Synthesis Methods and Protocols*; Springer Science, **2020**.
- Qi, Y.K.; Tang, S.; Huang, Y.C.; Pan, M.; Zheng, J.S.; Liu, L. Hmb(off/on) as a switchable thiol protecting group for native chemical ligation. *Org. Biomol. Chem.*, **2016**, *14*(18), 4194-4198. <https://doi.org/10.1039/C6OB00450D> PMID: 27102373
- Tang, S.; Si, Y.Y.; Wang, Z.P.; Mei, K.R.; Chen, X.; Cheng, J.Y.; Zheng, J.S.; Liu, L. An efficient one-pot four-segment condensation method for protein chemical synthesis. *Angew. Chem. Int. Ed. Engl.*, **2015**, *54*(19), 5713-5717. <https://doi.org/10.1002/anie.201500051> PMID: 25772600
- Pentelute, B.L.; Kent, S.B.H. Selective desulfurization of cysteine in the presence of Cys(Acm) in polypeptides obtained by native chemical ligation. *Org. Lett.*, **2007**, *9*(4), 687-690. <https://doi.org/10.1021/ol0630144> PMID: 17286375
- Jbara, M.; Maity, S.K.; Brik, A. Palladium in the chemical synthesis and modification of proteins. *Angew. Chem. Int. Ed. Engl.*, **2017**, *56*(36), 10644-10655. <https://doi.org/10.1002/anie.201702370> PMID: 28383786
- Postma, T.M.; Giraud, M.; Albericio, F. Trimethoxyphenylthio as a highly labile replacement for tert-butylthio cysteine protection in Fmoc solid phase synthesis. *Org. Lett.*, **2012**, *14*(21), 5468-5471. <https://doi.org/10.1021/ol3025499> PMID: 23075145
- Rei, M.; Takahide, K.; Thomas, K.E.; Gary, M.R. 3-Nitro-2-pyridinesulfonyl group for protection and activation of the thiol function of cysteine. *Chem. Lett.*, **1981**, *10*, 737-740. <https://doi.org/10.1246/cl.1981.737>
- Muttenthaler, M.; Ramos, Y.G.; Feytens, D.; de Araujo, A.D.; Alewood, P.F. p-Nitrobenzyl protection for cysteine and selenocysteine: a more stable alternative to the acetylaminomethyl group. *Biopolymers*, **2010**, *94*(4), 423-432. <https://doi.org/10.1002/bip.21502> PMID: 20593464
- Postma, T.M.; Albericio, F. Disulfide formation strategies in peptide synthesis. *Eur. J. Org. Chem.*, **2014**, *2014*, 3519-3530. <https://doi.org/10.1002/ejoc.201402149>
- Dekan, Z.; Mobli, M.; Pennington, M.W.; Fung, E.; Nemeth, E.; Alewood, P.F. Total synthesis of human hepcidin through regioselective disulfide-bond formation by using the safety-catch cysteine protecting group 4,4'-dimethylsulfonylbenzhydryl. *Angew. Chem. Int. Ed. Engl.*, **2014**, *53*(11), 2931-2934. <https://doi.org/10.1002/anie.201310103> PMID: 24604812
- Thalluri, K.; Kou, B.; Yang, X.; Zaykov, A.N.; Mayer, J.P.; Gelfanov, V.M.; Liu, F.; DiMarchi, R.D. Synthesis of relaxin-2 and insulin-like peptide 5 enabled by novel tethering and traceless chemical excision. *J. Pept. Sci.*, **2017**, *23*(6), 455-465. <https://doi.org/10.1002/psc.3010> PMID: 28466571
- Sadler, K.; Tam, J.P. Peptide dendrimers: applications and synthesis. *J. Biotechnol.*, **2002**, *90*(3-4), 195-229. [https://doi.org/10.1016/S1389-0352\(01\)00061-7](https://doi.org/10.1016/S1389-0352(01)00061-7) PMID: 12071226
- Crespo, L.; Sanclimens, G.; Pons, M.; Giralt, E.; Royo, M.; Albericio, F. Peptide and amide bond-containing dendrimers. *Chem. Rev.*, **2005**, *105*(5), 1663-1681. <https://doi.org/10.1021/cr0304491> PMID: 15884786

Designing Short Peptides

Current Organic Chemistry, 2020, Vol. 24, No. 21 2473

- [36] León-Calvijo, M.A.; Leal-Castro, A.L.; Almanzar-Reina, G.A.; Rosas-Pérez, J.E.; García-Castañeda, J.E.; Rivera-Monroy, Z.J. Antibacterial activity of synthetic peptides derived from lactoferricin against *Escherichia coli* ATCC 25922 and *Enterococcus faecalis* ATCC 29212. *BioMed Res. Int.*, **2015**, *2015*, 453826.
<http://dx.doi.org/10.1155/2015/453826> PMID: 25815317
- [37] Huertas, N.J.; Monroy, Z.J.R.; Medina, R.F.; Castañeda, J.E.G. Antimicrobial activity of truncated and polyvalent peptides derived from the FKCRRWQWRMKKGLA sequence against *Escherichia coli* ATCC 25922 and *Staphylococcus aureus* ATCC 25923. *Molecules*, **2017**, *22*(6), e987.
<http://dx.doi.org/10.3390/molecules22060987> PMID: 28613262
- [38] Casanova, Y.V.; Guerra, J.A.R.; Pérez, Y.A.U.; Castro, A.L.L.; Reina, G.A.; Castañeda, J.E.G.; Monroy, Z.J.R. Antibacterial synthetic peptides derived from bovine lactoferricin exhibit cytotoxic effect against MDA-MB-468 and MDA-MB-231 breast cancer cell lines. *Molecules*, **2017**, *22*(10), 1-11.
<http://dx.doi.org/10.3390/molecules22101641> PMID: 28961215
- [39] Solarte, V.A.; Rosas, J.E.; Rivera, Z.J.; Arango-Rodríguez, M.L.; García, J.E.; Vermot, J.P. A tetrameric peptide derived from bovine lactoferricin exhibits specific cytotoxic effects against oral squamous-cell carcinoma cell lines. *BioMed Res. Int.*, **2015**, *2015*, 630179.
<http://dx.doi.org/10.1155/2015/630179> PMID: 26609531
- [40] Dawson, P.E.; Muir, T.W.; Clark-Lewis, I.; Kent, S.B. Synthesis of proteins by native chemical ligation. *Science*, **1994**, *266*, 776-779.
<http://dx.doi.org/10.1126/science.7973629>
- [41] Pasunooti, K.K.; Yang, R.; Vedachalam, S.; Gorityala, B.K.; Liu, C.F.; Liu, X.W. Synthesis of 4-mercapto-L-lysine derivatives: potential building blocks for sequential native chemical ligation. *Bioorg. Med. Chem. Lett.*, **2009**, *19*(22), 6268-6271.
<http://dx.doi.org/10.1016/j.bmcl.2009.09.107> PMID: 19833511
- [42] Pu, Y.J.; Yuan, H.; Yang, M.; He, B.; Gu, Z.W. Synthesis of peptide dendrimers with polyhedral oligomeric silsesquioxane cores via Click chemistry. *Chin. Chem. Lett.*, **2013**, *24*, 917-920.
<http://dx.doi.org/10.1016/j.ccl.2013.06.015>
- [43] Yuan, H.; Luo, K.; Lai, Y.; Pu, Y.; He, B.; Wang, G.; Wu, Y.; Gu, Z. A novel poly(L-glutamic acid) dendrimer based drug delivery system with both pH-sensitive and targeting functions. *Mol. Pharm.*, **2010**, *7*(4), 953-962.
<http://dx.doi.org/10.1021/mp1000923> PMID: 20481567
- [44] Zhu, R.; Jiang, W.; Pu, Y.; Luo, K.; Wu, Y.; He, B. Functionalization of magnetic nanoparticles with peptide dendrimers. *J. Mater. Chem.*, **2011**, *21*, 5464-5474.
<http://dx.doi.org/10.1039/c0jm02752a>
- [45] Feni, L.; Jütten, L.; Parente, S.; Piarulli, U.; Neundorff, I.; Diaz, D. Cell-penetrating peptides containing 2,5-diketopiperazine (DKP) scaffolds as shuttles for anti-cancer drugs: conformational studies and biological activity. *Chem. Commun. (Camb.)*, **2020**, 56642, 5685-5688.
<http://dx.doi.org/10.1039/D0CC01490G> PMID: 32319458
- [46] Jing, X.; Jin, K. A gold mine for drug discovery: Strategies to develop cyclic peptides into therapies. *Med. Res. Rev.*, **2020**, *40*(2), 753-810.
<http://dx.doi.org/10.1002/med.21639> PMID: 31599007
- [47] Zorzi, A.; Deyle, K.; Heimis, C. Cyclic peptide therapeutics: past, present and future. *Curr. Opin. Chem. Biol.*, **2017**, *38*, 24-29.
<http://dx.doi.org/10.1016/j.cbpa.2017.02.006> PMID: 28249193
- [48] Ramesh, S.; Govender, T.; Kruger, H.G.; de la Torre, B.G.; Albericio, F. Short Anti-Microbial Peptides (SAMPs) as a class of extraordinary promising therapeutic agents. *J. Pept. Sci.*, **2016**, *22*(7), 438-451.
<http://dx.doi.org/10.1002/psc.2894> PMID: 27352996
- [49] Ermer, P.; Luther, A.; Zbinden, P.; Obrecht, D. Frontier between cyclic peptides and macrocycles. *Methods Mol. Biol.*, **2019**, *2001*, 147-202.
http://dx.doi.org/10.1007/978-1-4939-9504-2_9 PMID: 31134572
- [50] D'Amato, A.; Della Sala, G.; Izzo, I.; Costabile, C.; Masuda, Y.; De Riccardis, F. Cyclic octamer peptoids: simplified isomers of bioactive fungal cyclopeptides. *Molecules*, **2018**, *23*(7), 20-23.
<http://dx.doi.org/10.3390/molecules23071779> PMID: 30029532
- [51] Butler, S.J.; Jolliffe, K.A.; Lee, W.Y.G.; McDonough, M.J.; Reynolds, A.J. Synthesis of backbone modified cyclic peptides bearing dipicolylamino sidearms. *Tetrahedron*, **2011**, *67*, 1019-1029.
<http://dx.doi.org/10.1016/j.tet.2010.11.100>
- [52] Tonelli, A.E. *Cyclic Peptides*; Royal Society of Chemistry: Cambridge, **2017**.
- [53] Gang, D.; Kim, D.W.; Park, H.S. Cyclic peptides: promising scaffolds for biopharmaceuticals. *Genes (Basel)*, **2018**, *9*(11), e557.
<http://dx.doi.org/10.3390/genes9110557> PMID: 30453533
- [54] Joo, S.H. Cyclic peptides as therapeutic agents and biochemical tools. *Biomol. Ther. (Seoul)*, **2012**, *20*(1), 19-26.
<http://dx.doi.org/10.4062/biomolther.2012.20.1.019> PMID: 24116270
- [55] Demmer, O.; Frank, A.O.; Kessler, H. Design of cyclic peptides In: *Peptide and Protein Design for Biopharmaceutical Applications*; John Wiley and Sons, **2009**.
<http://dx.doi.org/10.1002/978047049708.ch4>
- [56] Berubé, C.; Borgia, A.; Voyer, N. A novel route towards cycle-tail peptides using oxime resin: teaching an old dog a new trick. *Org. Biomol. Chem.*, **2018**, *16*(47), 9117-9123.
<http://dx.doi.org/10.1039/C8OB01868E> PMID: 30270392
- [57] Streefkerk, D.E.; Schmidt, M.; Ippel, J.H.; Hackeng, T.M.; Nuijens, T.; Timmerman, P.; van Maarseveen, J.H. Synthesis of constrained tetracyclic peptides by consecutive CEPS, CLIPS, and oxime ligation. *Org. Lett.*, **2019**, *21*(7), 2095-2100.
<http://dx.doi.org/10.1021/acs.orglett.9b00378> PMID: 30912446
- [58] Chow, H.Y.; Zhang, Y.; Matheson, E.; Li, X. Ligation technologies for the synthesis of cyclic peptides. *Chem. Rev.*, **2019**, *119*, 9971-10001.
<http://dx.doi.org/10.1021/acs.chemrev.8b00657> PMID: 31318534
- [59] Angell, Y.; Burgess, K. Ring closure to β -turn mimics via copper-catalyzed azide/alkyne cycloadditions. *J. Org. Chem.*, **2005**, *70*(23), 9595-9598.
<http://dx.doi.org/10.1021/jo0516180> PMID: 16268639
- [60] White, A.M.; de Veer, S.J.; Wu, G.; Harvey, P.J.; Yap, K.; King, G.J.; Swanberg, J.E.; Wang, C.K.; Law, R.H.P.; Durek, T.; Craik, D.J. Application and structural analysis of triazole-bridged disulfide mimetics in cyclic peptides. *Angew. Chem. Int. Ed. Engl.*, **2020**, *59*(28), 11273-11277.
<http://dx.doi.org/10.1002/anie.202003435> PMID: 32270580
- [61] Malins, L.R.; deGruyter, J.N.; Robbins, K.J.; Scola, P.M.; Eastgate, M.D.; Ghadiri, M.R.; Baran, P.S. Peptide macrocyclization inspired by non-ribosomal imine natural products. *J. Am. Chem. Soc.*, **2017**, *139*(14), 5233-5241.
<http://dx.doi.org/10.1021/jacs.7b01624> PMID: 28326777
- [62] Hhi, R.; Rai, V.; Yudin, A.K. Macrocyclization of linear peptides enabled by amphoteric molecules. *J. Am. Chem. Soc.*, **2010**, *132*(9), 2889-2891.
<http://dx.doi.org/10.1021/ja910544p> PMID: 20155938
- [63] Macmillan, D.; De Cecco, M.; Reynolds, N.L.; Santos, L.F.A.; Barran, P.E.; Dorin, J.R. Synthesis of cyclic peptides through an intramolecular amide bond rearrangement. *ChemBioChem*, **2011**, *12*(14), 2133-2136.
<http://dx.doi.org/10.1002/cbic.201100364> PMID: 21805553
- [64] Acosta, G.A.; Murray, L.; Royo, M.; de la Torre, B.G.; Albericio, F. Solid-phase synthesis of head to side-chain tyr-cyclopeptides through a cyclative cleavage from Fmoc-McDbz/McNbz-resins. *Front. Chem.*, **2020**, *8*, 298.
<http://dx.doi.org/10.3389/fchem.2020.00298> PMID: 32391324
- [65] Nefzi, A.; Fenwick, J.E. N-terminus 4-chloromethyl thiazole peptide as a macrocyclization tool in the synthesis of cyclic peptides: application to the synthesis of conformationally constrained RGD-containing integrin ligands. *Tetrahedron Lett.*, **2011**, *52*(7), 817-819.
<http://dx.doi.org/10.1016/j.tetlet.2010.12.043> PMID: 21423849
- [66] Rivera, D.G.; Ojeda-Carralero, G.M.; Reguera, L.; Van der Eycken, E.V. Peptide macrocyclization by transition metal catalysis. *Chem. Soc. Rev.*, **2020**, *49*(7), 2039-2059.
<http://dx.doi.org/10.1039/C9CS00366E> PMID: 32142086
- [67] LeValley, P.J.; Ovadia, E.; Bresette, C.A.; Sawicki, L.A.; Mavarakis, E.; Bai, S.; Kloxin, A.M. Design of functionalized cyclic peptides through orthogonal Click reactions for cell culture and targeting applications. *Chem. Commun. (Camb.)*, **2018**, *54*(50), 6923-6926.
<http://dx.doi.org/10.1039/C8CC03218A> PMID: 29863200
- [68] Kogon, Y.; Goren, L.; Pappo, D.; Rudi, A.; Kashman, Y. Cyclic endiamino peptides: A new synthesis of imidazopyrazines. *Eur. J. Org. Chem.*, **2009**, *2009*, 1852-1854.
<http://dx.doi.org/10.1002/ejoc.200900008>
- [69] Claro, B.; Bastos, M.; Garcia-Fandino, R. *Design and Applications of Cyclic Peptides*; Elsevier Ltd., **2018**.
<http://dx.doi.org/10.1016/B978-0-08-100736-5.00004-1>
- [70] Pineda-Castañeda, H.M.; Bonilla-Velásquez, L.D.; Castro, A.L.L.; Fierro-Medina, R.; García-Castañeda, J.E.; Rivera-Monroy, Z.J. Use of Click chemistry for obtaining an antimicrobial chimeric peptide containing the LfcinB and Buforin II minimal antimicrobial motifs. *ChemistrySelect*, **2020**, *5*, 1655-1657.
<http://dx.doi.org/10.1002/slct.201903834>
- [71] Collet, C.; Maskali, F.; Clément, A.; Chrétien, F.; Poussier, S.; Karcher, G.; Marie, P.Y.; Chapleur, Y.; Lamandé-Langle, S. Development of 6-[(18F)]fluoro-carbohydrate-based prosthetic groups and their conjugation to peptides via Click chemistry. *J. Labelled Comp. Radiopharm.*, **2016**, *59*(2), 54-62.
<http://dx.doi.org/10.1002/jlcr.3362> PMID: 26780055
- [72] Kumar, S.; Hause, G.; Binder, W.H. Thio-bromo "Click" reaction derived polymer-peptide conjugates for their self-assembled fibrillar nanostructures. *Macromol. Biosci.*, **2020**, *20*(6), e2000048.
<http://dx.doi.org/10.1002/mabi.202000048> PMID: 32285651
- [73] Liu, B.; Huang, H.; Yang, Z.; Liu, B.; Gou, S.; Zhong, C.; Han, X.; Zhang, Y.; Ni, J.; Wang, R. Design of novel antimicrobial peptide dimer analogues with enhanced antimicrobial activity *in vitro* and *in vivo* by intermolecular triazole bridge strategy. *Peptides*, **2017**, *88*, 115-125.
<http://dx.doi.org/10.1016/j.peptides.2016.12.016> PMID: 28040477
- [74] Masri, E.; Ahsanullah; Accorsi, M.; Rademann, J. Side-chain modification of peptides using a phosphoranylidene amino acid. *Org. Lett.*, **2020**, *22*(8), 2976-2980.
<http://dx.doi.org/10.1021/acs.orglett.0c00713> PMID: 32223201
- [75] Quigley, N.G.; Tomassi, S.; Di Leva, F.S.; Di Maro, S.; Richter, F.; Steiger, K. Click-chemistry (CuAAC) trimerization of an $\alpha\beta\beta$ -integrin targeting Ga-68-peptide: enhanced contrast for *in-vivo* PET imaging of human lung adenocarcinoma xenografts. *ChemBioChem*, **2020**, *20*(20), 2836-2843.
<http://dx.doi.org/10.1002/cbic.202000200>

- [76] Bock, V.D.; Spejler, D.; Hiemstra, H.; van Maarseveen, J.H. 1,2,3-Triazoles as peptide bond isosteres: synthesis and biological evaluation of cyclo-tetrapeptide mimics. *Org. Biomol. Chem.*, **2007**, *5*(6), 971-975. <http://dx.doi.org/10.1039/b616751a> PMID: 17340013
- [77] Ptaszyńska, N.; Olkiewicz, K.; Okońska, J.; Gucwa, K.; Łęgoska, A.; Gitiń-Domagalska, A.; Dębowski, D.; Lica, J.; Heldt, M.; Milewski, S.; Ng, T.B.; Rolka, K. Peptide conjugates of lactoferricin analogues and antimicrobials-Design, chemical synthesis, and evaluation of antimicrobial activity and mammalian cytotoxicity. *Peptides*, **2019**, *117*, 170079. <http://dx.doi.org/10.1016/j.peptides.2019.04.006> PMID: 30959143
- [78] Kluba, C.A.; Bauman, A.; Valverde, I.E.; Vomstein, S.; Mindl, T.L. Dual-targeting conjugates designed to improve the efficacy of radiolabeled peptides. *Org. Biomol. Chem.*, **2012**, *10*(37), 7594-7602. <http://dx.doi.org/10.1039/c2ob26127h> PMID: 22898743
- [79] Hausner, S.H.; Marik, J.; Gagnon, M.K.J.; Sutcliffe, J.L. *In vivo* positron emission tomography (PET) imaging with an alphavbeta6 specific peptide radiolabeled using 18F-Click chemistry: evaluation and comparison with the corresponding 4-[18F]fluorobenzoyl- and 2-[18F]fluoropropionyl-peptides. *J. Med. Chem.*, **2008**, *51*(19), 5901-5904. <http://dx.doi.org/10.1021/jm800608s> PMID: 18785727
- [80] Topkova, N.; Fornyhough, C.M.; Butler, M.F.; Armes, S.P.; Ryan, A.J.; Zopham, P.D.; Adams, D.J. The effect of PEO length on the self-assembly of poly(ethylene oxide)-tetrapeptide conjugates prepared by "Click" chemistry. *Langmuir*, **2009**, *25*(18), 11082-11089. <http://dx.doi.org/10.1021/la901413n> PMID: 19685857
- [81] Govdi, A.I.; Vasilevsky, S.F.; Nenajdenko, V.G.; Sokolova, N.V.; Tolstikov, G.A. 1,3-Cycloaddition synthesis of 1,2,3-triazole conjugates of benzoic acid with peptides. *Russ. Chem. Bull.*, **2011**, *60*, 2401-2405. <http://dx.doi.org/10.1007/s11172-011-0369-3>
- [82] Artysushin, O.I.; Sharova, E.V.; Yarkovich, A.N.; Genkina, G.K.; Vinogradova, N.V.; Brel, V.K. Design of phosphonate analogs of short peptides by "Click" chemistry. *Russ. Chem. Bull.*, **2015**, *64*, 2172-2177. <http://dx.doi.org/10.1007/s11172-015-1134-9>
- [83] Sokolova, N.V.; Vorobyeva, D.V.; Osipov, S.N.; Vasilyeva, T.P.; Nenajdenko, V.G. Synthesis of α -trifluoromethyl- α -hydroxy acid-peptide conjugates via Click chemistry. *Synthesis (Stuttg.)*, **2012**, *44*, 130-136. <http://dx.doi.org/10.1055/s-0031-1289609>
- [84] Vats, K.; Sharma, R.; Kameswaran, M.; Sarma, H.D.; Satpati, D.; Dash, A. Design, synthesis, and comparative evaluation of ^{99m}Tc(CO)₃-labeled N-terminal and C-terminal modified asparagine-glycine-arginine peptide constructs. *J. Pept. Sci.*, **2019**, *25*(7), e3192. <http://dx.doi.org/10.1002/psc.3192> PMID: 31309677
- [85] Zhang, W.Y.; Banerjee, S.; Imberti, C.; Clarkson, G.J.; Wang, Q.; Zhong, Q. Strategies for conjugating iridium(III) anticancer complexes to targeting peptides via copper-free Click chemistry. *Inorg. Chim. Acta*, **2020**, *503*, 119396. <http://dx.doi.org/10.1016/j.ica.2019.119396>
- [86] Wang, X.; Gobbo, P.; Suchy, M.; Workentin, M.S.; Hudson, R.H.E. Peptide-decorated gold nanoparticles via strain-promoted azide-alkyne cycloaddition and post assembly deprotection. *RSC Adv.*, **2014**, *4*, 43087-43091. <http://dx.doi.org/10.1039/C4RA07574A>
- [87] Sachin, K.; Jadhav, V.H.; Kim, E.M.; Kim, H.L.; Lee, S.B.; Jeong, H.J.; Lim, S.T.; Sohn, M.H.; Kim, D.W. F-18 labeling protocol of peptides based on chemically orthogonal strain-promoted cycloaddition under physiologically friendly reaction conditions. *Bioconjug. Chem.*, **2012**, *23*(8), 1680-1686. <http://dx.doi.org/10.1021/bc3002425> PMID: 22770524
- [88] DeForest, C.A.; Polizzotti, B.D.; Anselth, K.S. Sequential Click reactions for synthesizing and patterning three-dimensional cell microenvironments. *Nat. Mater.*, **2009**, *8*(8), 659-664. <http://dx.doi.org/10.1038/nmat2473> PMID: 19543279
- [89] Slagle, C.J.; Thamm, D.H.; Randall, E.K.; Borden, M.A. Click conjugation of cloaked peptide ligands to microbubbles. *Bioconjug. Chem.*, **2018**, *29*(5), 1534-1543. <http://dx.doi.org/10.1021/acs.bioconjchem.8b00084> PMID: 29614859
- [90] Hoyle, C.E.; Bowman, C.N. Thiol-ene Click chemistry. *Angew. Chem. Int. Ed. Engl.*, **2010**, *49*(9), 1540-1573. <http://dx.doi.org/10.1002/anie.200903924> PMID: 20166107
- [91] Williams, E.T.; Harris, P.W.R.; Jamaluddin, M.A.; Loomes, K.M.; Hay, D.L.; Brimble, M.A. Solid-phase thiol-ene lipidation of peptides for the synthesis of a potent CGRP receptor antagonist. *Angew. Chem. Int. Ed. Engl.*, **2018**, *57*(36), 11640-11643. <http://dx.doi.org/10.1002/anie.201805208> PMID: 29978532
- [92] Stewart, J.M. *Peptide Synthesis*; Springer: New York, **2020**.
- [93] Forner, M.; DeLafus, S.; Androu, D. Peptide-based multi-epitopic vaccine platforms via Click reactions. *J. Org. Chem.*, **2020**, *85*(3), 1626-1634. <http://dx.doi.org/10.1021/acs.joc.9b02798> PMID: 31782300
- [94] Wang, Y.; Bruno, B.J.; Cornillie, S.; Nogueira, J.M.; Chen, D.; Cheatham, T.E., III; Lim, C.S.; Chou, D.H. Application of thiol-yne/thiol-ene reactions for peptide and protein macrocyclizations. *Chemistry*, **2017**, *23*(29), 7087-7092. <http://dx.doi.org/10.1002/chem.201700572> PMID: 28345248
- [95] Wängler, C.; Maschauer, S.; Prante, O.; Schäfer, M.; Schirmacher, R.; Bartenstein, P.; Eisenhut, M.; Wängler, B. Multimerization of cRGD peptides by Click chemistry: synthetic strategies, chemical limitations, and influence on biological properties. *ChemBioChem*, **2010**, *11*(15), 2168-2181. <http://dx.doi.org/10.1002/cbic.201000386> PMID: 20827791
- [96] Sun, Y.; Liu, H.; Cheng, L.; Zhu, S.; Cai, C.; Yang, T. Thiol Michael addition reaction: a facile tool for introducing peptides into polymer-based gene delivery systems. *Polym. Int.*, **2018**, *67*, 25-31. <http://dx.doi.org/10.1002/pi.5490>
- [97] Elbert, D.L.; Hubbell, J.A. Conjugate addition reactions combined with free-radical cross-linking for the design of materials for tissue engineering. *Biomacromolecules*, **2001**, *2*(2), 430-441. <http://dx.doi.org/10.1021/bm0056299> PMID: 11749203
- [98] de Araújo, A.D.; Palomo, J.M.; Cramer, J.; Seitz, O.; Alexandrov, K.; Waldmann, H. Diels-Alder ligation of peptides and proteins. *Chemistry*, **2006**, *12*(23), 6095-6109. <http://dx.doi.org/10.1002/chem.200600148> PMID: 16807971
- [99] Montgomery, J.E.; Donnelly, J.A.; Fanning, S.W.; Speltz, T.E.; Shangguan, X.; Coukos, J.S.; Greene, G.L.; Moellering, R.E. Versatile peptide macrocyclization with Diels-Alder cycloadditions. *J. Am. Chem. Soc.*, **2019**, *141*(41), 16374-16381. <http://dx.doi.org/10.1021/jacs.9b07578> PMID: 31523967
- [100] Schilling, C.I.; Jung, N.; Biskup, M.; Schepers, U.; Bräse, S. Bioconjugation via azide-Staudinger ligation: an overview. *Chem. Soc. Rev.*, **2011**, *40*(9), 4840-4871. <http://dx.doi.org/10.1039/c0cs00123f> PMID: 21687844
- [101] Soellner, M.B.; Tam, A.; Raines, R.T. Staudinger ligation of peptides at non-glycyl residues. *J. Org. Chem.*, **2006**, *71*(26), 9824-9830. <http://dx.doi.org/10.1021/jo0620056> PMID: 17168602
- [102] Kim, H.; Cho, J.K.; Aimoto, S.; Lee, Y.S. Solid-phase staudinger ligation from a novel core-shell-type resin: a tool for facile condensation of small peptide fragments. *Org. Lett.*, **2006**, *8*(6), 1149-1151. <http://dx.doi.org/10.1021/ol0530629> PMID: 16524290
- [103] Guthrie, Q.A.E.; Proulx, C. Oxime ligation via *in situ* oxidation of *N*-phenylglycyl peptides. *Org. Lett.*, **2018**, *20*(9), 2564-2567. <http://dx.doi.org/10.1021/acs.orglett.8b00713> PMID: 29694052
- [104] Decostaire, I.E.; Lelièvre, D.; Aucagne, V.; Delmas, A.F. Solid phase oxime ligations for the iterative synthesis of polypeptide conjugates. *Org. Biomol. Chem.*, **2014**, *12*(22), 5536-5543. <http://dx.doi.org/10.1039/C4OB00760C> PMID: 24953534
- [105] Guthrie, Q.A.E.; Young, H.A.; Proulx, C. Ketoxime peptide ligations: oxidative couplings of alkoxyamines to *N*-aryl peptides. *Chem. Sci. (Camb.)*, **2019**, *10*(41), 9506-9512. <http://dx.doi.org/10.1039/C9SC04028E> PMID: 32110307
- [106] Agouridas, V.; El Mahdi, O.; Diemer, V.; Cargnoli, M.; Monbaliu, J.M.; Melnyk, O. Native chemical ligation and extended methods: mechanisms, catalysis, scope, and limitations. *Chem. Rev.*, **2019**, *119*(12), 7328-7443. <http://dx.doi.org/10.1021/acs.chemrev.8b00712> PMID: 31050890
- [107] Chen, J.; Wan, Q.; Yuan, Y.; Zhu, J.; Danishefsky, S.J. Native chemical ligation at valine: a contribution to peptide and glycopeptide synthesis. *Angew. Chem. Int. Ed. Engl.*, **2008**, *47*(44), 8521-8524. <http://dx.doi.org/10.1002/anie.200803523> PMID: 18833563
- [108] Ingale, S.; Buskas, T.; Booms, G.J. Synthesis of glyco(lipo)peptides by liposome-mediated native chemical ligation. *Org. Lett.*, **2006**, *8*(25), 5785-5788. <http://dx.doi.org/10.1021/ol062423x> PMID: 17134272

Copper(I)-Catalyzed Alkyne–Azide Cycloaddition (CuAAC) “Click” Reaction: A Powerful Tool for Functionalizing Polyhydroxylated Platforms

Héctor Manuel Pineda-Castañeda, Zuly Jenny Rivera-Monroy, and Mauricio Maldonado*

Cite This: *ACS Omega* 2023, 8, 3650–3666

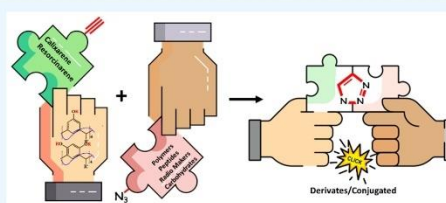
Read Online

ACCESS |

Metrics & More

Article Recommendations

ABSTRACT: Click chemistry is currently one of the most used tools for the generation of complex organic molecules. The advantages of using click chemistry in organic synthesis are remarkable; in many cases, the reactions occur under mild conditions and are free of solvents, with high yields and short reaction times. This makes it an extraordinarily effective and viable alternative for obtaining complex/conjugated molecules. In this review, the use of click chemistry CuAAC is especially emphasized for polyhydroxylated platforms such as resorcinarenes or calixarenes, focusing mainly on aspects of synthesis, specifically conditions, reagents, and methodologies.



1. INTRODUCTION

Polyhydroxylated platforms such as calixarenes and resorcinarenes (Figure 1) have become new sources of molecules that

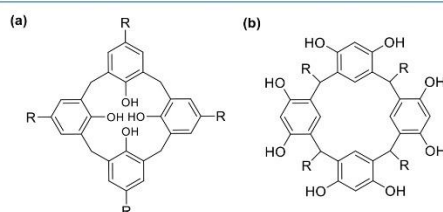


Figure 1. Representation of (a) calix[4]arene and (b) calix[4]-resorcinarene.

are currently being studied for the generation of polyvalent molecules, given their great versatility for synthesis and the reactivity provided by the hydroxyl groups and other reactive positions present in these structures. These polyhydroxylated platforms exhibit great host–host inclusion affinity with a great variety of molecules of organic and inorganic origin. Some examples are in the report by Da Silva et al. in 2003, where they studied their noncovalent inclusion with steroids such as testosterone¹ and their interaction with antibacterial drugs such as those reported by Dawn et al. in 2017.² They also have a high affinity for different metal ions such as Cu²⁺, Fe²⁺, Co²⁺, Ni²⁺, and Zn²⁺,^{3–6} and the interaction of these ligands with proteins have allowed the recognition, detection, modification/

modulation, and separation of proteins, as reported by Oshima et al. in 2012.⁷ Additionally, polyhydroxylated platforms have been found to have several pharmaceutical applications due to their potential for encapsulating drugs, increasing their solubility, bioavailability, oral absorption, and stability under heat, light, and acidic conditions.⁸

In this way, the exploration of the reactivity of the hydroxyl groups and the versatility in the synthesis of the polyhydroxylated platforms have allowed new synthesis techniques such as click chemistry to be incorporated into the synthesis of derivatives of calixarenes or resorcinarenes (Figure 2). This has allowed new derivatives to emerge, such as carbohydrate binding, reported in 2006 by Dondoni et al.,⁹ the incorporation of short peptides, the generation of photoactive complexes,¹⁰ the affinity and chemical binding to gold surfaces in the generation of biosensors reported by Feng et al.,¹¹ and the inclusion of photoreactive chromophores such as those synthesized by Liu et al.,¹² among others. The use of these polyhydroxylated bases also allows obtaining dendrimers with improved pharmaceutical applications, such as for selective delivery in specific drug regions, as reported by Li et al. in 2016, where the affinity of this type of platform to Fe³⁺ ions was found, which generated a targeting vector and a selective

Received: September 28, 2022

Accepted: December 23, 2022

Published: January 18, 2023



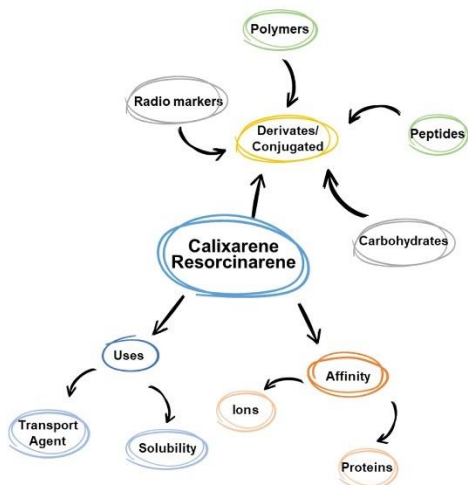


Figure 2. Use and applications of polyhydroxylated platforms of the calixarene/resorcinarene type.

delivery of Dauricin in the treatment of primary intercerebral hemorrhage,⁵ or the improvement of the solubility of some anti-inflammatory drugs such as ibuprofen and naproxen in an aqueous medium, as reported by Khan et al. in 2017.¹³

In this review, the actual and potential applications of click chemistry in the modification of polyhydroxylated platforms via copper-catalyzed alkyne–azide cycloaddition will be discussed, including chemical conditions for the reactions and reagents, among other aspects in the processes described in the specialized literature.

2. POLYHYDROXYLATED PLATFORMS (CALIXARENES/RESORCINARENES)

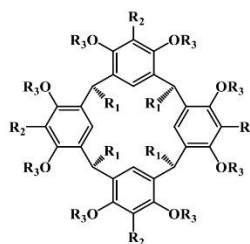
The calix[*n*]arenes are macrocycles or cyclic oligomers mainly based on the condensation product between para-substituted phenols and formaldehyde. One of the characteristics of this type of compound is the great variety of conformations that can be formed. Specifically, the term calixarene is derived from the term calix, or cup, since geometrically these types of compounds are expressed in this way. Given this characteristic of spatial geometry that they may have, it has been directly correlated with the uptake of ions in the small cavities formed between the different units; these cavities depend on the size of the different units. This is why they have been reported with units of 4, 6, and 8, among the most common ones.^{8,14}

On the other hand, resorcinarenes, also known as calix[4]-resorcinarenes, are polyhydroxylated macrocyclic compounds derived from resorcinol, which were synthesized and reported for the first time by Baeyer et al. in the year 1872 from aliphatic or aromatic aldehydes.^{15,16} They are made up of four resorcinol rings linked together at positions 4 and 6 by a methine bond. These are often functionalized, allowing for a wide spectrum of conformational isomers (stereoisomerism).^{17–19} Five possible conformers have been reported for resorcinarene: (i) crown, (ii) boat, (iii) saddle, (iv) chair, and (v) diamond.²⁰ Any of these conformations are possible

depending on aspects such as the position of the resorcinol units and the substituents on the methine bridges. For most of the cases reported in the synthesis of resorcinarene derivatives, the most stable conformation has been shown to be the crown type, established from the deep cavities formed and a stabilization by hydrogen bonds mediated by the hydroxyl groups present.^{8,21–23}

The functionalization at the macrocycle methylene bridge arises from the aldehyde used in the preparation of resorcinarene derivatives, since the group attached to the aldehyde forms the lower edge. A wide variety of aldehydes have been used in the preparation of resorcinarenes, including saturated alkyl aldehydes, unsaturated alkyl aldehydes, and sulfur-containing aldehydes (Table 1). These functionalized aldehydes lead to the construction of resorcinarenes that have various bottom edge functionalities.²⁴

Table 1. Calix[4]resorcinarene Functionalization at R1, R2, and R3 Positions



R ₁	R ₂	R ₃	Ref.
	H	Ac	25
	H	Me	26
	H	CH ₂ C(O)NEt ₂	27
		H	28
	H	Me	29
	H	PPh ₂	30
	H	Me	29
	H	Me	31
	H	H	32
	CH ₃ SO ₃ Na	H	33

Calixarenes can be functionalized in the aromatic ring from the starting materials by varying the nature of the substituent group on the phenol or in the hydroxyl group,^{34–36} while the reactivity of the resorcin[4]arenes is mainly located at three points: on the hydroxyl groups, at position 2 of the hydroxyl group, and by modification through the introduction of

functionalized aldehyde.^{23,37–39} Functionalizing substances such as diazonium salts,^{40–43} methyl sulfonates,^{44,45} ammonium groups,^{46,47} acylation,^{22,48} formylation,^{49,50} and aminomethylation,⁵¹ among others,^{52,53} can be introduced into the hydroxylated platform by means of easily accessible reactions selectively, with good yields (Figure 3).

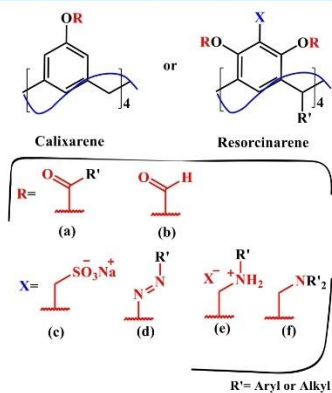
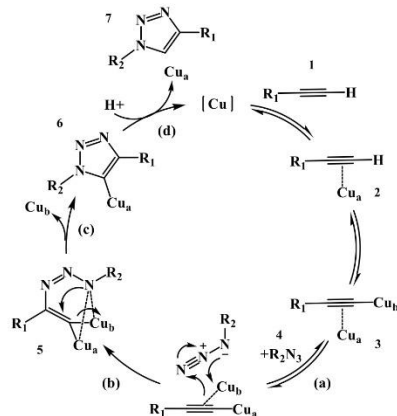


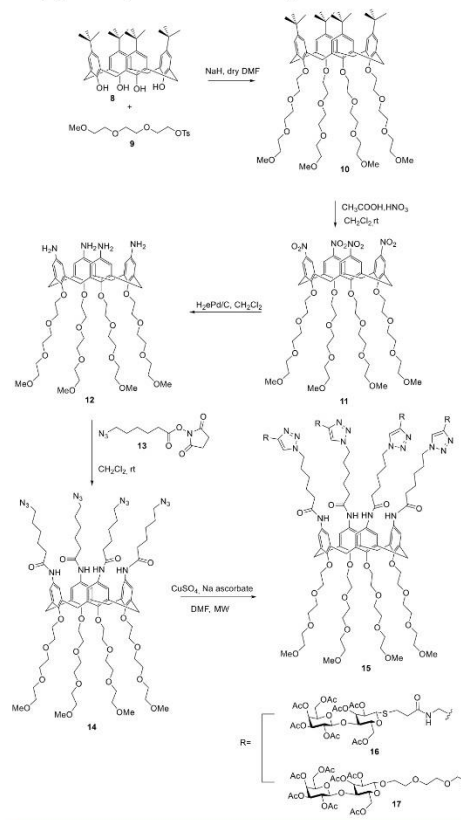
Figure 3. Modification of calixarenes or resorcinarenes with (a) diazonium salts, (b) methyl sulfonates, (c), ammonium groups, (d), acylation, (e) formylation, and (f) aminomethylation among others.

Scheme 1. CuAAC Mechanism for Triazole Ring Formation⁵⁷



These modifications allow interaction with other types of more specific reactions, such as click chemistry. The application of these types of compounds is limited, due to their hydrophobic properties, making them poorly soluble in aqueous media; however, by introducing substitutions in their methylene bridges, a great variety of functional groups can be obtained, with which the original molecule can partially modify its hydrophobicity, allowing its applications to be expanded.⁵⁴

Scheme 2. Synthesis of Water-Soluble Calix[4]arene Conjugated Glycocluster Containing Lactose⁵⁷



3. CLICK CHEMISTRY

Click chemistry is an efficient and modern technique applied to the synthesis of complex molecules. The 2022 Nobel Prize in Chemistry recognized its importance and its applications; it sought to make easier some difficult processes. Barry Sharpless and Morten Meldal have laid the groundwork for a functional form of chemistry, click chemistry, in which molecular building blocks come together quickly and efficiently. Carolyn Bertozzi has taken click chemistry to a new dimension and has begun to use it in living organisms.⁵⁵ The concept of click chemistry was incorporated by Sharpless, where the assembly of small building blocks to form more complex structures is simplified.^{56,57} Many of the criteria in click chemistry are subjective, and although measurable and objective criteria could be agreed upon, it is unlikely that any one reaction will be perfect for every situation and application. Characteristics have been mentioned for a reaction to be considered within the click concept, for example: (i) stereospecificity, (ii) ease of product purification, (iii) use of low-cost reagents and catalysts, (iv) high efficiency, and (v) mild reaction conditions (it is possible to carry out this type of reaction in polar and

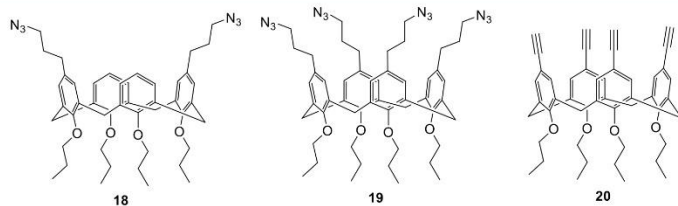


Figure 4. Functionalized calixarene bases, di- and tetrasubstituted and another tetrasubstituted with available alkyne groups.

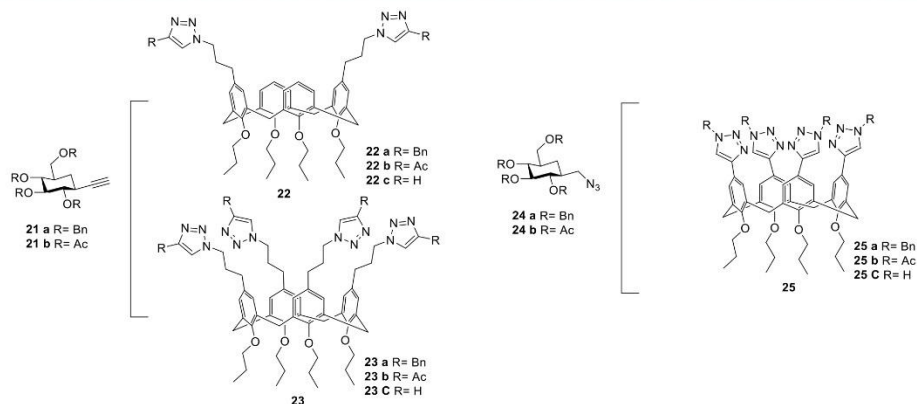
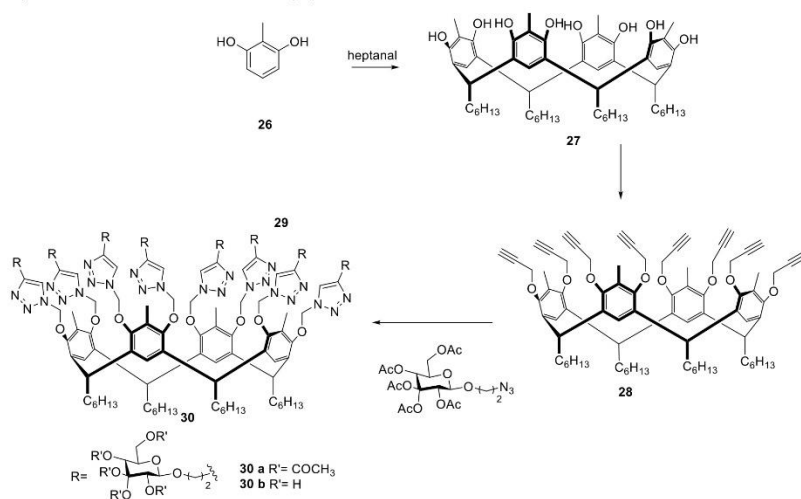


Figure 5. Synthesis of calixarene derivatives with ethynyl tetra-*O*-benzyl- β -D-glucopyranoside or tetra-*O*-acetyl- β -D-glucopyranoside.

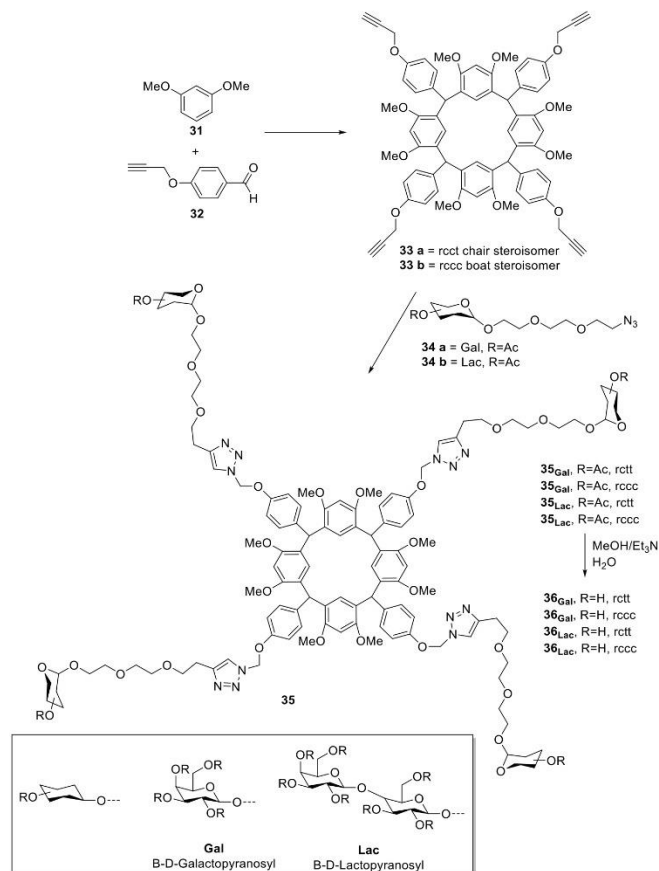
Scheme 3. Synthesis of Derivatives of Tetraethynylcalix[4]resorcinarenes⁶⁶



environmentally friendly solvents such as water and methanol).^{58–60}

3.1. Copper-Catalyzed Azide–Alkyne Cycloaddition (CuAAC) Reaction. The copper-catalyzed azide–alkyne cycloaddition reaction (CuAAC) was introduced by Meldal

Scheme 4. Synthesis of a Family of Tetravalent Macrocycles Functionalized with Galactose and Lactose Based on a Nucleus of Resorcin[4]arene³¹

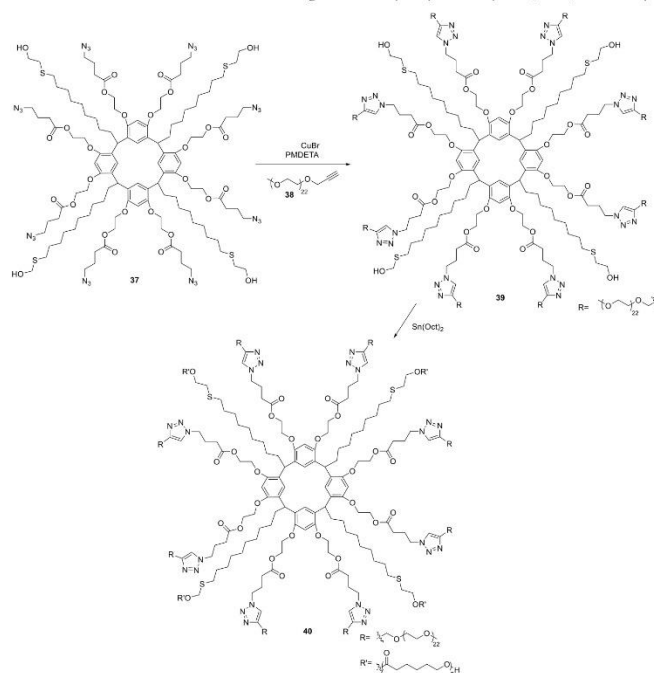


et al. in 2001,⁶¹ it is based on a 1,3-dipolar Huisgen cycloaddition, which is a nonconcerted reaction where copper(I) acetylides react with azides and nitrile oxides, resulting in 1,4-disubstituted 2,3-triazoles and 3,4-disubstituted isoxazoles.⁶² Later on, this reaction began to form part of a special group of organic chemistry known as click chemistry reactions.⁶³ The CuAAC reaction mechanism is explained in Scheme 1. First, the copper acetylide complex **2** is formed between the alkyne **1** and the copper(I) species. Then, **2** coordinates a second Cu, generating complex **3**. An important feature of this mechanism is that the azide **4** cycloaddition to the resulting dicopper species is a stepwise process: in the first place, (a) azide **4** coordination to the dicopper **3** core yielding the first C–N bond, and this leads to a subsequent formation of the six-membered methacycle **5**, followed by (b) intramolecular C–N bond formation yielding the triazolyl-Cu(I) intermediate **6** and dissociating one of the two coppers. This intermediate, which is not very stable, undergoes a final step, a

proton transfer from the alkyne to the triazolyl ligand that allows the regeneration of the alkynyl-Cu(I) complex and the release of the 1,4-triazole product **7**.⁵⁷

The importance of the copper(I) species used as a catalyst has been reported. Variations in reaction conditions have been reported, such as (i) temperature (rt or MW),³¹ (ii) solvents (DMF, THF, and H₂O),^{64,65} (iii) generation of copper(I) in situ through the use of reducing agents from copper(II),^{64,66–69} and (iv) use of solvent-free copper nanoparticles (CuNPs).¹⁰

A wide variety of copper-derived compounds have been evaluated as effective catalysts in the reaction of CuAAC copper(I) species, such as copper(I) iodide (CuI)^{66,70} and copper(I) bromide (CuBr),^{12,71} copper(II), such as copper(II) sulfate pentahydrate (CuSO₄·5H₂O),⁷² or the same copper(0) using copper nanoparticles (CuNPs).¹⁰ In 2020, for example, Pineda-Castañeda et al. used CuSO₄·5H₂O together with a reducing agent (ascorbic acid) in EtOH/H₂O at 80 °C to

Scheme 5. Synthesis of a Derivative of a Resorcinarene Coupled to Polyethylene Glycol (PEG) and Polycaprolactone (PCL)⁷¹

produce a chimeric peptide linked by a 1,2,3-triazole ring.⁷³ This same reaction has been used in the synthesis of calixarene derivatives by Tang et al. by controlling the molar ratios of the alkyne and azide precursors. They were able to design and synthesize novel calix[4]resorcinarene-triphenylene with monomeric, dimeric, and tetrameric designs with yields of 50–60% using copper(I) as a catalyst in situ using CuSO₄·5H₂O and sodium ascorbate reducing agent in DMF. On the other hand, in 2013 Gao et al. used CuBr at reflux in DMF for the generation of Miktoarm A8B4 amphiphilic star copolymers centered on resorcinarene, based on poly(ϵ -caprolactone) and poly(ethylene glycol) by means of a controlled ring-opening polymerization (CROP) combination.⁷¹

The CuAAC reactions have been implemented for obtaining a wide variety of conjugates of calixarenes or resorcinarenes, in which organic and inorganic motifs have been incorporated into them, for example, radiomarkers,⁷⁴ polymers,⁷¹ carbohydrates,^{70,66,75} gold supports,¹¹ cyclodextrins,⁷⁶ and peptides,¹⁰ among others. All these derivatives will be described later in detail.

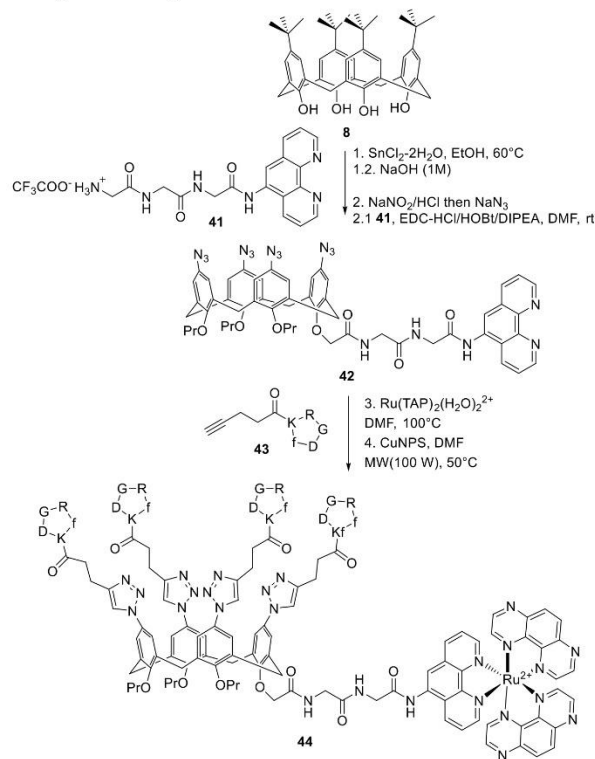
3.1.1. Calixarene/Resorcinarene Functionalized via CuAAC. In 2011, derivatives of calixarenes conjugated to carbohydrates through CuAAC were reported by Galante et al. They reported the synthesis of a water-soluble calix[4]arene conjugated glycocluster containing lactose (Scheme 2).⁷⁷

The tetraazide derivative calix[4]arene **14** was generated from *p*-*tert*-butylcalix[4]arene **8** in its cone form, which was guaranteed by functionalizing its lower rim with methyl-capped triethylene glycol chains **9**. The alkylation of calix[4]arene **8**

with tosylate **9** was carried out under standard conditions (NaH in DMF) to provide **10**, which was subjected to ipso-nitration, resulting in the substitution of *tert*-butyl groups with nitro groups in compound **10**, generating derivative **11**, which was hydrogenated in the presence of a Pd–C catalyst to give tetraamino derivative **12**. The reaction of **12** with four molecules of *N*-succinimidoyl ester **13** led to the derivative of tetraazide calix[4]arene **14**. This molecule presented an overall yield of 43%. On the other hand, lactose derivatives functionalized with an alkyne group **16** and **17** reacted give to the calixarene nucleus **14** under conditions suitable for the generation of carbohydrate derivatives; thus, the synthesis was carried out in a microwave reactor in DMF solution at 70 °C in the presence of 0.2 equiv of CuSO₄ and 0.4 equiv of sodium ascorbate. The product was purified by chromatography on silica gel, giving the tetralactosyl derivative **15** in a yield of 80%.⁷⁷

In 2006, Dondoni et al. reported the synthesis of C-glycoside clustering on calix[4]arene. Three functionalized calixarene bases were reported, two of which have the azide group **18** and **19** and another replacement with alkyne groups **20** (Figure 4). In the synthesis of calixarene derivatives **22** and **23** with ethynyl tetra-*O*-benzyl- β -D-glucopyranoside **21** or tetra-*O*-acetyl- β -D-glucopyranoside **24** in the presence of CuI and *i*-Pr₂-EtN in toluene at room temperature generated the desired 1,4-disubstituted 1,2,3-triazole rings **22** and **23**, each one carrying β -C-glucosyl residues (Figure 5). These reactions occurred with a high degree of efficiency. This was corroborated by the yield between **21a** and **18** of 73% and a

Scheme 6. Synthesis of a Ruthenium(II) Photoreactive Complex Bound to a Calix[4]arene Platform with Multiple Cyclopeptides Containing the RGD Sequence¹⁰



similar yield between **21a** and the tetraazide derivative **19** of 63%. Even higher degrees of efficiency were recorded in the stoichiometric reactions of tetra-*O*-acetyl- β -D-glucopyranoside **21b** with the same polyazide calixarene **18** and **19**, which in fact produced the corresponding C-glycosyl-calix[4]arenes **22b** and **23b** in 96% and 86% yields, respectively.⁹

Thus, in both cases each triazole-forming cycloaddition reaction appeared to have occurred in an almost quantitative manner. The authors suggested that the higher reactivity of **21b** with respect to **21a** is due to steric factors, because the *O*-acetyl groups are less bulky than the *O*-benzyl groups and thus result in a less hindered matrix. For the case of the derivative tetraethynylcalix[4]arene **20**, the same conditions were used previously; this process exhibited a high degree of efficiency, corroborated by overall yields of 61% and 83% for **25a** and **25b**, respectively. The spatial arrangement of the four sugar-containing arms in the calix[4]arene derivative **23** and **25** may vary due to some flexibility of the macrocycle ring.⁹

In the same way, derivatives of tetraethynylcalix[4]-resorcinarenes have been reported. In 2019, Husain et al. reported the synthesis of a resorcin[4]arene glycoconjugate consisting of eight β -D-glucopyranoside residues constructed in the phenolic parts of the upper edge of resorcin[4]arene by

multiple 1,2,3-triazole bonds, 1,4-disubstituted **30** (Scheme 3).⁶⁶

For the synthesis of **30** (Scheme 3), resorcin[4]arene **27** was first synthesized after the acid-catalyzed cyclocondensation reaction of methyl resorcinol **26** with heptanal. Compound **27** was then treated with propargyl bromide in the presence of potassium carbonate in refluxing acetone to achieve the octapropargyl resorcin[4]arene intermediate **28**. This was reacted with 2-azidoethyl β -D-glucopyranoside tetraacetate **29a**, and the reaction was carried out under chloroform reflux in the presence of CuI and DIPEA to produce the octaacetoxy derivative **30a** in 91% yield. Overall deacetylation using a NaOMe solution resulted in **30b** with an overall yield of 92%. This new eight-armed resorcin[4]arene glycoconjugate **30b** offers an enlarged flexible pseudosaccharide cavity that can act as a molecular container for water-insoluble azide and/or alkyne substrates, presented as an effective catalyst in the reaction of CuAAC species poorly soluble in water with only 1 mol %, with excellent yields and short reaction times.⁶⁶

The versatility in the synthesis of polyhydroxylated bases makes it possible to select the point reactive group's incorporation. For example, in 2011 Soomro et al. reported the synthesis of a family of tetravalent macrocycles function-

Scheme 7. Formation of the Nucleobase Calix[4]arenes Using the Nitrogenous Bases Cytosine (C), Thymine (T), Adenine (A), and Guanine (G)⁷⁸

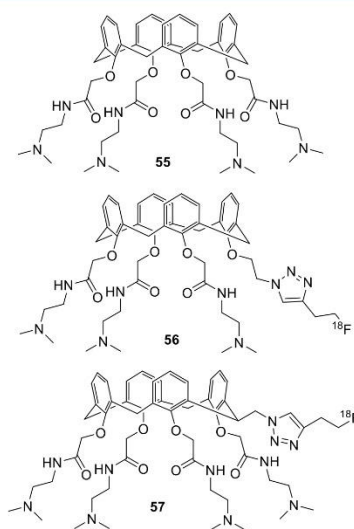
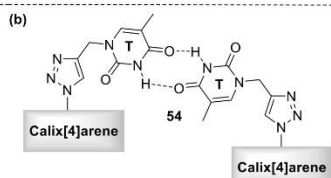
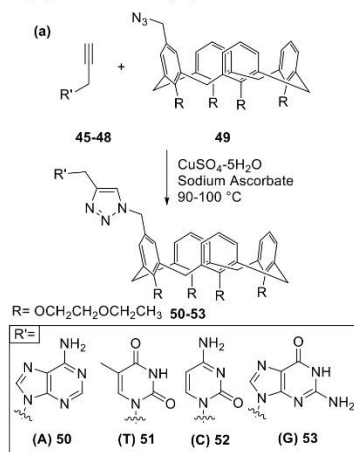


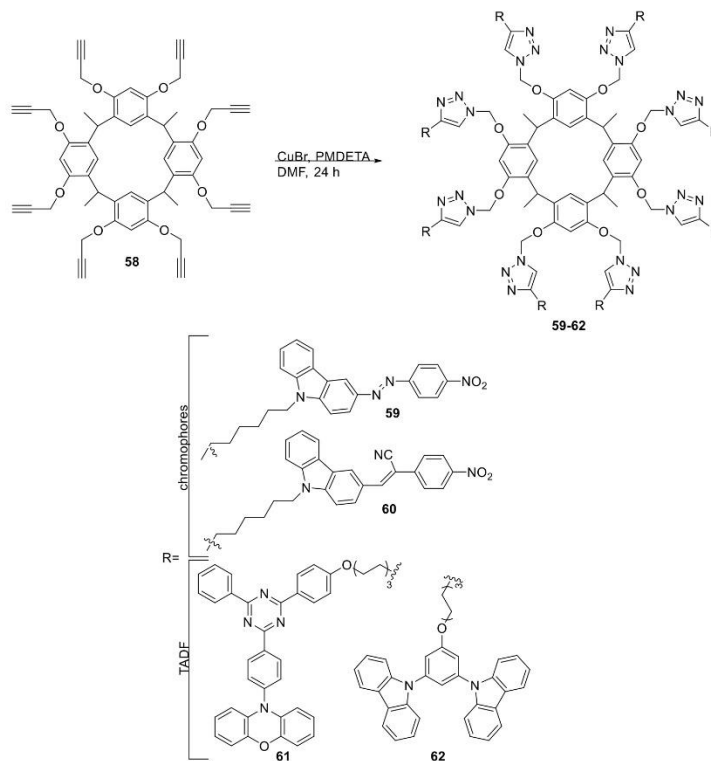
Figure 6. Synthesis of two close calixarene mimetics derivatives of calixarene.

alized with galactose and lactose based on a nucleus of resorcin[4]arene. They described the development of diastereoselective synthetic pathways for the formation of lower border propargylated resorcin[4]arenes and their functionalization through copper-catalyzed azide-alkyne click chemistry. Its lower rim was functionalized with specifically prefunctionalized aldehydes 4-(propargyloxy)benzaldehyde **32** (Scheme 4). This direct acid-catalyzed synthesis resulted in products of the form *rcft* (chair) **33a** and *recc* (boat) **33b**. Glycoconjugate **35** was obtained from **33**, which was reacted with galactoside **34a** and azidofunctionalized lactoside **34b** by means of CuAAC using CuI/DIPEA in DMF, assisted by MW with a total reaction time of 15 min to produce acetylated glucoclusters **35Gal** and **35Lac**. They exhibited yields of between 58% and 85%. Deacetylation was carried out under mild solvolysis conditions in order to obtain the hydroxylated glucoclusters **36Gal** and **36Lac**. The *recc* stereochemistry of propargylated resorcin[4]arene was conserved in the conjugated macromolecules.³¹

In 2013, Gao et al. reported the synthesis of a derivative of a resorcinarene coupled to polyethylene glycol (PEG) and polycaprolactone (PCL). This amphiphilic star copolymer was synthesized by a click chemistry reaction and controlled ring-opening polymerization (CROP). The azide group was incorporated at its upper edge by means of a nucleophilic substitution reaction of a halide derivative with sodium azide to give the formation of functionalized resorcin[4]arene **37** (Scheme 5). In the first instance, PEG-functionalized alkyne **38** was incorporated via CuAAC at **37** using PMDETA in DMF as a CuBr catalyst, with a reaction time of 48 h at 40 °C. Product **39** was recovered with column chromatography and a subsequent lyophilization with a yield of 84%. The synthesis of copolymer **40** was carried out by means of the controlled ring-opening polymerization of *ε*-CL as a tetrafunctional macromolecular initiator and Sn(Oct)₂ as a catalyst in dry ethanol at 100 °C for 24 h. The crude product was dissolved in THF and poured into cold diethyl ether to precipitate the final product, which was dried under vacuum to constant weight. Finally, **40** was obtained with a yield of 95%. The importance of these new derivatives of resorcinarene polymers is because both PCL and PEG are biocompatible and nontoxic polymers, so that the resorcinarene-PEG-PCL **40** copolymer synthesized via CuAAC in this article would have potential application in biomedical areas, in addition to the importance of the reactivity provided by the hydroxyl at the end of the PCL chains, which provides the possibility of conjugating them with drugs, making them a viable strategy for drug administration.⁷¹

Peptide sequences and nitrogenous bases have been incorporated into polyhydroxylated structures to generate multivalent systems that can provide selective selectivity for cells or ions.^{10,78} Ruthenium-based photoactive complexes have been actively studied for their biological applications as potential diagnostic agents against cancer. To provide selective cell selection, Kajouji et al. developed a multivalent system composed of a ruthenium(II) photoreactive complex bound to a calix[4]arene platform with multiple cyclopentapeptides containing the RGD sequence (Scheme 6).¹⁰

They started from a derivative of *p*-*tert*-butylcalix[4]arene **8**, which was functionalized on its upper border with azide groups **42**. This was reacted with C-[RGDfK]-alkyne **43**, a peptide sequence functionalized with an alkyne group. The copper(I) species used as a catalyst was generated in situ from a mixture of CuSO₄·5H₂O and sodium ascorbate. Unfortunately, this

Scheme 8. Derived Resorcinarene with Chromophores and Compounds with Thermally Activated Delayed Fluorescence (TADF)⁷⁹

methodology led to low yields and a lack of reproducibility in the case of derivative **44**, even when MW heating was used. They thereupon decided to switch to the use of copper nanoparticles (CuNPs), since it is known that nanomaterials efficiently catalyze a wide range of organic reactions and especially azide–alkyne cycloaddition. They brought the mixture to 50 °C with the assistance of MW (100 W) for 1 h, where they obtained product **44** with a yield of 31% after a purification step in semipreparative RP-HPLC.¹⁰

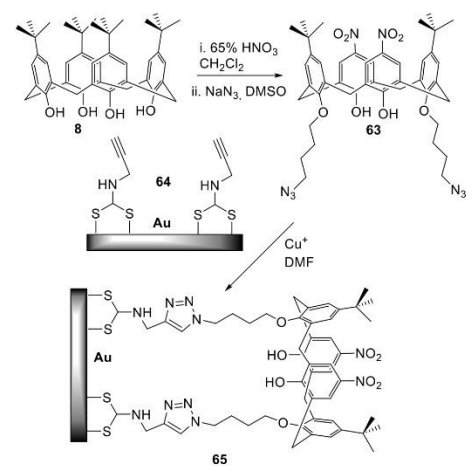
On the other hand, nitrogenous bases (cytosine (C), thymine (T), adenine (A), and guanine (G)) were incorporated into structures of the calixarene type by means of click chemistry CuAAC (Scheme 7a). The nitrogenous bases were functionalized with an alkyne group, **45–48**, which reacted under click chemistry conditions, generating the copper(I) species in situ by means of the reduction of Cu²⁺; **45–48** react with functionalized calixarene with an azide group on its upper edge 5-methylazidocalix[4]arene **49**, thus giving the formation of the nucleobase calix[4]arenes corresponding to **50–53**, with yields that ranged from 66% to 85%. The four derivatives of calix[4]arene efficiently complexed with alkali-metal ions. The presence of nitrogenous bases on the upper border did not alter the selectivity to this type of ion but allowed understanding the recognition between nucleic bases

in the assembly of derivatives in CDCl₃ in the construction of high-order molecular structures **54**, as shown in Scheme 7b.⁷⁸

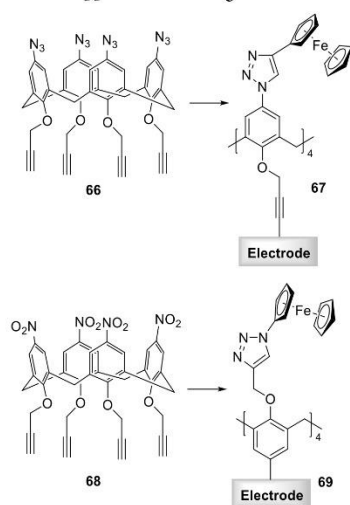
The incorporation of radiomarkers into calixarene-type platforms has been reported as possible additional evaluation agents in antiangiogenic cancer therapy. In 2015, Lämpchen et al. reported the design of two close calixarene mimetics derivatives of calixarene **0118 55** (Figure 6), containing a terminal alkynyl functional group, developed through a semiautomated procedure optimized for radiolabeling with 2-[¹⁸F]-fluoroethylazide using click chemistry. For this, they generated the copper(I) species in situ using CuSO₄·5H₂O and sodium ascorbate as a reducing agent. This was carried out in a DMF/H₂O solution at rt overnight. After purification and formulation by semipreparative HPLC, the [¹⁸F] lower rim tagged [¹⁸F] analogue **56** and the [¹⁸F] equatorially tagged **57** were obtained with a radiochemical purity of >97%.⁷⁴

In platforms of the resorcinarene type, chromophores and compounds with thermally activated delayed fluorescence (TADF) were incorporated (Scheme 8). Liu et al.¹² in 2016 and Wang et al. in 2020⁷⁹ reported resorcinarene conjugates obtained with click chemistry (CuAAC) using as a functionalized platform octaalkylcalix[4]resorcinarene **58**. In both syntheses, the copper(I) species was used directly, using CuBr and PMDETA stabilizer in DMF for 24 h. For the case

Scheme 9. Design and Development of an Electrode Using a Functionalized Gold Surface¹¹



Scheme 10. Synthesis of Calixarene Derivatives Suitable for Their Attachment to a Vitreous Carbon Electrode (GCE) Surface on the Upper or Lower Edge⁸⁰



of compound **59**, it was obtained with a yield of 40% compared to compound **60**, which exhibited a yield of 75%. This type of compound can have applications in the generation of new photosensitive materials.

Applications such as the generation of diagnostic electrodes have also been the focus of research in recent years using these type of polyhydroxylated platforms conjugated by click chemistry. In 2013, Feng et al. reported the design and development of an electrode using a functionalized gold

Scheme 11. Synthesis of a New Macrocycle of Calix[4]resorcinarene Functionalized with Tetra-triazole⁸¹

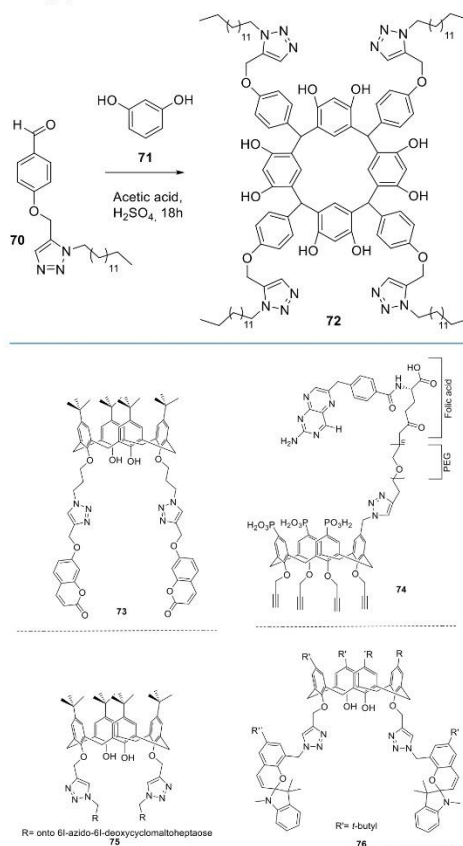
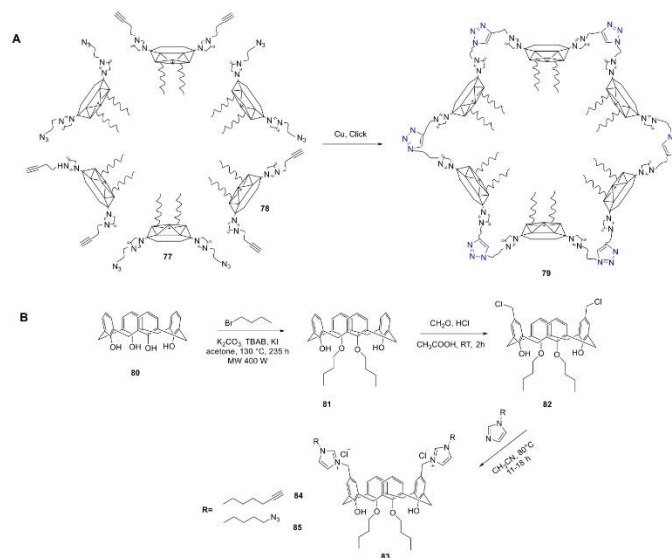


Figure 7. Biologically active molecules such as coumarin **73, folic acid **74**, cyclodextrins **75**, and spiroindoline **76** have also been incorporated in functionalized calixarene/resorcinarene platforms.**

surface (Scheme 9); the amino alkylene groups were first assembled on a gold surface by S–Au bonds after CS₂ was added, and then the end azide of **63** reacted with alkyne groups of **64** with a Cu⁺ catalyst.¹¹

Simultaneously, the two steps in the gold surface modification process were successfully observed via X-ray photoelectron spectroscopy (XPS). This type of electrode exhibited selectivity in the detection of *o*-phenylenediamine compared to its *m*- and *p*-isomers.¹¹ On the other hand, in 2016 Buttress et al. reported the synthesis of calixarene derivatives **66** and **68** suitable for attachment to a vitreous carbon electrode (GCE) surface on the upper or lower rim (Scheme 10). Once attached to the GCE surface, the exposed face of calixarene was designed for easy modification, using the copper-catalyzed alkyne azide cycloaddition reaction

Scheme 12. (A) Representation of the Formation of the Polymeric Nanoparticles Using a Supramolecular Approach and (B) Synthetic Pathway for Macrocycles 84 and 85 Containing Azidoalkylimidazolium/Alkynylimidazolium Groups on the Upper Rim^{83,84}



(CuAAC), where they obtained functionalized electrodes 67 and 69.⁸⁰

In 2020, Qadri et al. reported the synthesis of a new macrocycle of calix[4]resorcinarene functionalized with tetra-triazole 72 used for the detection of copper ions in an aqueous medium (Scheme 11). The photophysical potential of compound 72 can be determined by a variety of cations (Ba^{2+} , Ca^{2+} , Co^{2+} , Hg^{2+} , K^+ , Mg^{2+} , Mn^{2+} , Na^+ , NH_4^+ , and Pd^{2+}). The macrocycle of calix[4]resorcinarene based on triazole 68 interacts with the Cu^{2+} ion in preference to other cations. This new tetra-triazole compound 72 was synthesized from an aldehyde functionalized with an aliphatic chain 70 via click chemistry for a subsequent reaction with resorcinol 71 in an acid medium.⁸¹

Biologically active molecules such as coumarin,⁷² folic acid,⁸² cyclodextrins,⁷⁶ and spiroindoline³ have also been incorporated by means of click chemistry to these functionalized calixarene/resorcinarene-type platforms (Figure 7). These four derivatives were obtained under the same synthetic route of click chemistry, using Cu(I) generated in situ as a catalyst through the reaction of $\text{CuSO}_4 \cdot 5\text{H}_2\text{O}$ and sodium ascorbate, with rt temperature variation for 73, 74, and 76 assisted by MW for 75, all in a mixture of polar solvents.

The generation of macrocycles of calixarene derivatives linked together through CuAAC click chemistry has already been reported. In 2020/2021, Butilov et al. reported that a new imidazolium amphiphilic calix[4]arene with terminal acetylene fragments in the polar region was synthesized according to a two-step scheme including regioselective chloromethylation of distal di-O-butyl calix[4]arene and subsequent interaction with 1-(hex-5-yn-1-yl)-1*H*-imidazole. The aggregation properties (CAC and the size and ζ potential of aggregates) of alkynyl

calix[4]arene 78, as well as of previously synthesized azidopropyl calix[4]arene 77 and their 1/1 mixture, were announced. Macrocycles with azide and alkyne fragments in the polar region were covalently cross-linked under CuAAC conditions in water (Scheme 12A). For the synthesis of target macrocycles containing azidoalkylimidazolium/alkynylimidazolium groups, it was carried out through the alkylation of the corresponding N-substituted imidazoles with dichloromethyl calix[4]arene derivative 82 (Scheme 12B). The foregoing synthetic strategy allows introducing any alkyl/imidazolium fragments into the lower/upper rims of a calix[4]arene macrocyclic platform in just three steps with high yields. *p*-H-calix[4]arene 80, presynthesized from *p*-butyl-calix[4]arene using *de-tert*-butylation with AlCl_3 in the presence of phenol, was treated by butyl bromide to give bis-O-butyl derivative 81, which was then incorporated into a Blanc chloromethylation to give calix[4]arene 82 with a nearly qualitative yield (Scheme 12B). The final step was the reaction of calix[4]arene 83 with 1-(3-azidopropyl)-1*H*-imidazole or 1-(hex-5-yn-1-yl)-1*H*-imidazole.^{83,84}

Finally, Table 2^{85–93} shows examples of the incorporation of other organic molecules, such as cationic, ionic, nonionic, allyl, benzyl, triphenylene, thiazole acetate, dimethyl acetylenedicarboxylate, and polyammonium, along with their required conditions. This comparative table allows us to show the great versatility that the copper-catalyzed cycloaddition reaction can have between an alkyne group and an azide group (CuAAC) in the generation of new calixarene/resorcinarene derivatives.

4. CONCLUSIONS

In summary, this review has shown the most significant advances in copper-catalyzed azide–alkyne cycloaddition

Table 2. Examples of the Incorporation of Other Organic Molecules

Alkyl/Azide substituent	Platform	Derivative	Conditions/ yield	Ref.	
			CuSO ₄ , sodium ascorbate; 24 h at 60 °C in THF/EtOH/H ₂ O (1/2/2) Yield: 80 %	85	
			Not reported	86	
			i) CuI, Et ₃ N, toluene, 4h, 40 °C ii) HCl, dioxane, rt	70	
					Yield: 86-92 %
			phenyl propargyl ether (excess), CuI-P(OEt) ₃ , toluene, 100 °C Yield: 86-87 %	87	
					phenyl propargyl ether, CuSO ₄ ·5H ₂ O, sodium ascorbate, THF/H ₂ O, 60 °C. Yield: 68-92 %
					phenyl propargyl ether, CuSO ₄ ·5H ₂ O, sodium ascorbate, THF/H ₂ O, 60 °C. Yield: 70-84 %

Table 2. continued

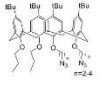
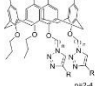
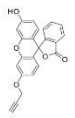
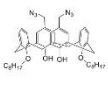
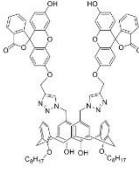
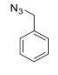
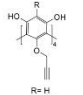
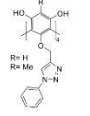
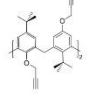
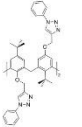
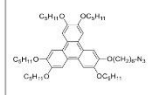
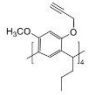
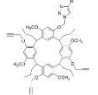
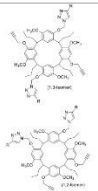
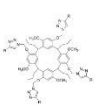
Alkyl/Azide substituent	Platform	Derivative	Conditions/ yield	Ref.
			phenyl propargyl ether (excess), CuI-P(OEt) ₃ , toluene, 100 °C Yield: 60-86 %	
			CuI, NEt ₃ , THF- H ₂ O, reflux, 12h Yield: 67 %	53
			Sodium ascorbate, CuSO ₄ ·5H ₂ O, THF-H ₂ O, reflux Yield: 67-72 %	54
			CuI, 110 °C or CuI, MW, 110 °C Yield: 77 %	59
				CuSO ₄ , DMF sodium ascorbate 1:1 (mol ratio of reactants)
			Yield: 60 %	
			CuSO ₄ , DMF sodium ascorbate 2:1 (mol ratio of reactants) Yield: 58 %	
			CuSO ₄ , DMF sodium ascorbate 4:1 (mol ratio of reactants) Yield: 51 %	

Table 2. continued

Alkyl/Azide substituent	Platform	Derivative	Conditions/ yield	Ref.
			CuSO ₄ , DMF sodium ascorbate, 70 °C, 12 h Yield: 65 %	90
			CuI, CH ₃ CN, MW, 80 °C, 90 min Yield: 22-28 %	91
H ₂₅ C ₁₂ N ₃			[Cu(CH ₃ CN) ₂][PF ₆], TBTA, DMF Yield: 62 %	92
			CuI, Et ₃ N, Toluene, RT, 24 h Yield: 29 %	93

(CuAAC) used in the generation of new calixarenes/resorcinarenes. The reaction between alkynes and azide derivatives using copper(I) as a catalyst for the functionalization of polyhydroxylated platforms is a powerful tool in molecular design. This review opens up a new opportunity for researchers from all areas who want to synthesize macromolecules with calixarene/resorcinarene-type nuclei using click chemistry for its functionalization. Thus, we consolidated synthetic conditions and routes that will allow the advancement of complex molecule synthesis in a more efficient and faster way. These new molecules generated from triazole rings will allow extending the applications of polyhydroxylated compounds by incorporating organic and/or inorganic molecules with potential pharmaceutical applications.

■ AUTHOR INFORMATION

Corresponding Author

Mauricio Maldonado – Chemistry Department, Universidad Nacional de Colombia, Bogotá, Bogotá 11321, Colombia; orcid.org/0000-0001-9695-878X; Email: mmaldonadov@unal.edu.co

Authors

Héctor Manuel Pineda-Castañeda – Chemistry Department, Universidad Nacional de Colombia, Bogotá, Bogotá 11321, Colombia

Zuly Jenny Rivera-Monroy – Chemistry Department, Universidad Nacional de Colombia, Bogotá, Bogotá 11321, Colombia; orcid.org/0000-0001-6915-8488

Complete contact information is available at: <https://pubs.acs.org/10.1021/acsomega.2c06269>

Author Contributions

The manuscript was written through contributions of all authors. All authors have given approval to the final version of the manuscript.

Notes

The authors declare no competing financial interest.

■ ACKNOWLEDGMENTS

This research was conducted with the financial support of COLCIENCIAS, Project “Diseño y obtención de nuevos agentes antibacterianos basados en dendrímeros péptido-

resorcinarreno: Una alternativa para combatir la resistencia bacteriana. RC-846 2019. HERMES Code 45746".

REFERENCES

- (1) Da Silva, E.; Valmalle, C.; Becchi, M.; Cuilleron, C. Y.; Coleman, A. W. The Use of Electrospray Mass Spectrometry (ES/MS) for the Differential Detection of Some Steroids as Calix-[n]-arene Sulphonate Complexes. *J. Incl. Phenom.* **2003**, *46*, 65–69.
- (2) Dawn, A.; Chandra, H.; Ade-Browne, C.; Yadav, J.; Kumari, H. Multifaceted Supramolecular Interactions from C-Methylresorcin[4]-arene Lead to an Enhancement in In Vitro Antibacterial Activity of Gatifloxacin. *Chem. - A Eur. J.* **2017**, *23*, 18171–18179.
- (3) Nag, R.; Polepalli, S.; Althaf Hussain, M.; Rao, C. P. Ratiometric Cu²⁺ Binding, Cell Imaging, Mitochondrial Targeting, and Anticancer Activity with Nanomolar IC₅₀ by Spiro-Indoline-Conjugated Calix[4]arene. *ACS Omega* **2019**, *4*, 13231–13240.
- (4) Jeerupan, J.; Konishi, G. I.; Nemoto, T.; Shin, D. M.; Nakamoto, Y. Synthesis of multifunctional poly(calix[4]resorcinarreno). *Polym. J.* **2007**, *39*, 762–763.
- (5) Li, M.; Liu, G.; Wang, K.; Wang, L.; Fu, X.; Lim, L. Y.; Chen, W.; Mo, J. Metal ion-responsive nanocarrier derived from phosphonated calix[4]arenes for delivering dauricine specifically to sites of brain injury in a mouse model of intracerebral hemorrhage. *J. Nanobiotechnology* **2020**, *18*, 1–19.
- (6) Bahojb Noruzi, E.; Kheirkhahi, M.; Shaabani, B.; Geremia, S.; Hickey, N.; Asaro, F.; Nitti, P.; Kafil, H. S. Design of a Thiosemicarbazide-Functionalized Calix[4]arene Ligand and Related Transition Metal Complexes: Synthesis, Characterization, and Biological Studies. *Front. Chem.* **2019**.
- (7) Oshima, T.; Baba, Y. Recognition of exterior protein surfaces using artificial ligands based on calixarenes, crown ethers, and tetraphenylporphyrins. *J. Incl. Phenom. Macrocycl. Chem.* **2012**, *73*, 17–32.
- (8) Español, E. S.; Villamil, M. M. Calixarenes: Generalities and their role in improving the solubility, biocompatibility, stability, bioavailability, detection, and transport of biomolecules. *Biomolecules* **2019**, *9*, 90.
- (9) Dondoni, A.; Marra, A. C-glycoside clustering on calix[4]arene, adamantane, and benzene scaffolds through 1,2,3-triazole linkers. *J. Org. Chem.* **2006**, *71*, 7546–7557.
- (10) Kajouji, S.; Marcellis, L.; Mattiuzzi, A.; Grassin, A.; Dufour, D.; Van Antwerpen, P.; Boturyn, D.; Defrancq, E.; Surin, M.; De Winter, J.; et al. Synthesis and photophysical studies of a multivalent photoreactive Ru II -calix[4]arene complex bearing RGD-containing cyclopeptide. *Beilstein J. Org. Chem.* **2018**, *14*, 1758–1768.
- (11) Feng, N.; Luo, L.; Zhang, G.; Miao, F.; Wang, C.; Tian, D.; Li, H. Wettability recognition for isomeric phenylenediamine by nitro-calix[4]arene click chemistry. *RSC Adv.* **2013**, *3*, 19278–19281.
- (12) Liu, W.; Yang, H.; Wu, W.; Gao, H.; Xu, S.; Guo, Q.; Liu, Y.; Xu, S.; Cao, S. Calix[4]resorcinarreno-based branched macromolecules for all-optical photorefractive applications. *J. Mater. Chem. C* **2016**, *4*, 10684–10690.
- (13) Khan, K.; Lal Badshah, S.; Ahmad, N.; Rashid, H. U.; Mabkhot, Y. Inclusion complexes of a new family of non-ionic amphiphilic dendrocalix[4]arene and poorly water-soluble drugs naproxen and ibuprofen. *Molecules* **2017**, *22*, 783.
- (14) Kumar, R.; Sharma, A.; Singh, H.; Suating, P.; Kim, H. S.; Sunwoo, K.; Shim, I.; Gibb, B. C.; Kim, J. S. Revisiting Fluorescent Calixarenes: From Molecular Sensors to Smart Materials. *Chem. Rev.* **2019**, *119*, 9657–9721.
- (15) Agrawal, Y. K.; Patadia, R. N. Studies on Resorcinarrenes and their Analytical Applications. *Rev. Anal. Chem.* **2006**, *25*, 155–239.
- (16) Shah, M. D.; Agrawal, Y. Calixarene: A new architecture in the analytical and pharmaceutical technology. *J. Sci. Ind. Res. (India)* **2012**, *71*, 21–26.
- (17) Jain, V. K.; Kanaiya, P. H. Chemistry of calix[4]resorcinarrenes. *Russ. Chem. Rev.* **2011**, *80*, 75–102.
- (18) Tian, H. W.; Liu, Y. C.; Guo, D. S. Assembling features of calixarene-based amphiphiles and supra-amphiphiles. *Mater. Chem. Front.* **2020**, *4*, 46–98.
- (19) Georghiou, P. E. Calixarenes and fullerenes. *Calixarenes and Beyond* **2016**, 879–919.
- (20) Moore, D.; Watson, G. W.; Gunnlaugsson, T.; Matthews, S. E. Selective formation of the rctt chair stereoisomers of octa-O-alkyl resorcin[4]arenes using Bronsted acid catalysis. *New J. Chem.* **2008**, *32*, 994–1002.
- (21) Ziąja, P.; Krogul, A.; Pawłowski, T. S.; Litwinienko, G. Structure and stoichiometry of resorcinarreno solvates as host-guest complexes - NMR, X-ray and thermoanalytical studies. *Thermochim. Acta* **2016**, *623*, 112–119.
- (22) Velásquez-Silva, A.; Cortés, B.; Rivera-Monroy, Z. J.; Pérez-Redondo, A.; Maldonado, M. Crystal structure and dynamic NMR studies of octaacetyl-tetra(propyl)calix[4]resorcinarreno. *J. Mol. Struct.* **2017**, *1137*, 380–386.
- (23) Castillo-Aguirre, A. A.; Pérez-Redondo, A.; Maldonado, M. Influence of the hydrogen bond on the iteroselective O-alkylation of calix[4]resorcinarrenes. *J. Mol. Struct.* **2020**, *1202*, 127402.
- (24) Das, S.; Das, M. K. *Surface Modification of Nanoparticles for Targeted Drug Delivery*; Pathak, Y. V., Ed.; Springer International Publishing: 2019.
- (25) Palmer, K. J.; Wong, R. Y.; Jurd, L.; Stevens, K. The Structures of the Octaacetate Esters of Two Condensation Tetramers of Resoreinol with. *Acta Crystallogr. B* **1976**, *B32*, 847–852.
- (26) Iwanek, W. The synthesis of octamethoxyresorcin[4]arenes catalysed by Lewis acids. *Tetrahedron* **1998**, *S4*, 14089–14094.
- (27) Han, J.; Yan, C. G. Synthesis, crystal structure and configuration of resorcinarreno amides. *J. Incl. Phenom. Macrocycl. Chem.* **2008**, *61*, 119–126.
- (28) O'Farrell, C. M.; Chudomel, J. M.; Collins, J. M.; Dignam, C. F.; Wenzel, T. J. Water-soluble calix[4]resorcinarrenes with hydroxyproline groups as chiral NMR solvating agents. *J. Org. Chem.* **2008**, *73*, 2843–2851.
- (29) Botta, B.; Pierini, M.; Monache, G. D.; Subissati, D.; Subrizi, F.; Zappia, G. Synthesis of amino and ammonium resorcin[4]arenes as potential receptors. *Synthesis (Stuttg)* **2008**, *2008*, 2110–2116.
- (30) Xu, W.; Rourke, J. P.; Vittal, J. J.; Puddephatt, R. J. Transition Metal Rimmed-Calixresorcinarreno Complexes. *Inorg. Chem.* **1995**, *34*, 323–329.
- (31) Soomro, Z. H.; Cecioni, S.; Blanchard, H.; Praly, J. P.; Imberty, A.; Vidal, S.; Matthews, S. E. CuAAC synthesis of resorcin[4]arene-based glycoclusters as multivalent ligands of lectins. *Org. Biomol. Chem.* **2011**, *9*, 6587–6597.
- (32) Sardjono, R. E.; Kadarohman, A.; Mardhiyah, A. Green Synthesis of Some Calix[4]Resorcinarreno Under Microwave Irradiation. *Procedia Chem.* **2012**, *4*, 224–231.
- (33) Han, X.; Park, J.; Wu, W.; Malagon, A.; Wang, L.; Vargas, E.; Wikramanayake, A.; Houk, K. N.; Leblanc, R. M. A resorcinarreno for inhibition of Aβ fibrillation. *Chem. Sci.* **2017**, *8*, 2003–2009.
- (34) Morales, A.; Santana, A.; Althoff, G.; Melendez, E. Host-guest interactions between calixarenes and Cp₂NbCl₂. *J. Organomet. Chem.* **2011**, *696*, 2519–2527.
- (35) Liška, A.; Ludvík, J. Stereoelectrochemistry of calixarenes – Molecules with multiple redox centers. *Curr. Opin. Electrochem.* **2018**, *8*, 45–51.
- (36) Bakas, I.; Hayat, A.; Piletsky, S.; Piletska, E.; Chehimi, M. M.; Nogue, T.; Rouillon, R. Electrochemical impedimetric sensor based on molecularly imprinted polymers/sol-gel chemistry for methadone organophosphorous insecticide recognition. *Talanta* **2014**, *130*, 294–298.
- (37) Castillo-Aguirre; Maldonado. Preparation of Methacrylate-based Polymers Modified with Chiral Resorcinarrenes and Their Evaluation as Sorbents in Norepinephrine Microextraction. *Polymers (Basel)* **2019**, *11*, 1428.
- (38) Velásquez-Silva, B. A.; Castillo-Aguirre, A.; Rivera-Monroy, Z. J.; Maldonado, M. Aminomethylated calix[4]resorcinarrenes as

- modifying agents for glycidyl methacrylate (GMA) rigid copolymers surface. *Polymers (Basel)* **2019**, *11*, 1147.
- (39) Castillo-Aguirre, A.; Rivera-Monroy, Z.; Maldonado, M. Selective o-alkylation of the crown conformer of tetra(4-hydroxyphenyl)calix[4]resorcinarene to the corresponding tetraalkyl ether. *Molecules* **2017**, *22*, 1660.
- (40) Maldonado, M.; Sanabria, E.; Batanero, B.; Esteso, M.Á. Apparent molar volume and viscosity values for a new synthesized diazoted resorcin[4]arene in DMSO at several temperatures. *J. Mol. Liq.* **2017**, *231*, 142–148.
- (41) Jain, V. K.; Kanaiya, P. H.; Bhojak, N. Synthesis, spectral characterization of azo dyes derived from calix[4]resorcinarene and their application in dyeing of fibers. *Fibers Polym.* **2008**, *9*, 720–726.
- (42) Elçin, S.; İlhan, M. M.; Deligöz, H. Synthesis and spectral characterization of azo dyes derived from calix[4]arene and their application in dyeing of fibers. *J. Incl. Phenom. Macrocycl. Chem.* **2013**, *77*, 259–267.
- (43) Maldonado, M.; Sanabria, E.; Velasquez-Silva, A.; Casas-Hinestroza, J. L.; Esteso, M. A. Comparative study of the volumetric properties of three regioisomers of diazoted C-tetra(propyl)-resorcin[4]arene in DMSO at various temperatures. *J. Mol. Liq.* **2021**, *325*, 115252.
- (44) Sanabria, E.; Esteso, M.; Pérez-Redondo, A.; Vargas, E.; Maldonado, M. Synthesis and Characterization of Two Sulfonated Resorcinarenes: A New Example of a Linear Array of Sodium Centers and Macrocycles. *Molecules* **2015**, *20*, 9915–9928.
- (45) Bartenstein, J. E.; Lucas, N. T. Reduced symmetry triflate-resorcin[4]arenes. *Supramol. Chem.* **2012**, *24*, 618–626.
- (46) Utomo, S. B.; Saputro, A. N. C.; Rinanto, Y. Functionalization of C-4-methoxyphenylcalix[4]resorcinarene with several ammonium compounds. In *Proceedings of the IOP Conference Series: Materials Science and Engineering*; Institute of Physics Publishing: 2016; Vol. 107, p 012042.
- (47) Hong, M.; Zhang, Y. M.; Liu, Y. Selective binding affinity between quaternary ammonium cations and water-soluble calix[4]-resorcinarene. *J. Org. Chem.* **2015**, *80*, 1849–1855.
- (48) Casas-Hinestroza, J.; Maldonado, M. Conformational Aspects of the O-acetylation of C-tetra(phenyl)calixpyrogallol[4]arene. *Molecules* **2018**, *23*, 1225.
- (49) Ballistreri, F. P.; Pappalardo, A.; Tomaselli, G. A.; Sfrassetto, G. T.; Vittorino, E.; Sortino, S. Synthesis and photophysics of a fullerene-triquinoxaline ensemble. *New J. Chem.* **2010**, *34*, 2828–2834.
- (50) Pappalardo, A.; Amato, M. E.; Ballistreri, F. P.; Notti, A.; Tomaselli, G. A.; Toscano, R. M.; Sfrassetto, G. T. Synthesis and topology of [2 + 2] calix[4]resorcinarene-based chiral cavitand-salen macrocycles. *Tetrahedron Lett.* **2012**, *53*, 7150–7153.
- (51) Castillo-Aguirre, A.; Esteso, M. A.; Maldonado, M. Resorcin[4]arenes: Generalities and Their Role in the Modification and Detection of Amino Acids. *Curr. Org. Chem.* **2020**, *24*, 2412–2425.
- (52) Han, J.; Cai, Y. H.; Liu, L.; Yan, C. G.; Li, Q. Syntheses, crystal structures, and electrochemical properties of multi-ferrocenyl resorcinarenes. *Tetrahedron* **2007**, *63*, 2275–2282.
- (53) Yang, Q.; Yan, C.; Zhu, X. A fluorescent chemosensor for paeonol based on tetramethoxy resorcinarene tetraoxyacetic acid. *Sensors Actuators, B Chem.* **2014**, *191*, 53–59.
- (54) Chamley, M.; Fairfull-Smith, K.; Williams, N. H.; Haycock, J. W. Evaluation of anti-inflammatory calixarene-peptides for biomaterial modification. *Eur. Cells Mater.* **2006**, *11*, 26.
- (55) Press release: The Nobel Prize in Chemistry 2022 - NobelPrize.org Available online: <https://www.nobelprize.org/prizes/chemistry/2022/press-release/> (accessed on Oct 28, 2022).
- (56) Kolb, H. C.; Sharpless, K. B. The growing impact of click chemistry on drug discovery. *Drug Discovery Today* **2003**, *8*, 1128–37.
- (57) Bock, V. D.; Hiemstra, H.; Van Maarseveen, J. H. Cu I-catalyzed alkyne-azide “click” cycloadditions from a mechanistic and synthetic perspective. *Eur. J. Org. Chem.* **2006**, *2006*, 51–68.
- (58) Kaur, J.; Saxena, M.; Rishi, N. An Overview of Recent Advances in Biomedical Applications of Click Chemistry. *Bioconjugate Chem.* **2021**, *32* (8), 1455–1471.
- (59) Shin, J. A.; Lim, Y. G.; Lee, K. H. Copper-catalyzed azide-alkyne cycloaddition reaction in water using cyclodextrin as a phase transfer catalyst. *J. Org. Chem.* **2012**, *77*, 4117–4122.
- (60) Buckley, B. R.; Figueres, M. M. P.; Khan, A. N.; Heaney, H. A. New Simplified Protocol for Copper(I) Alkyne-Azide Cycloaddition Reactions Using Low Substoichiometric Amounts of Copper(II) Precatalysts in Methanol. *Synlett* **2015**, *27*, 51–56.
- (61) Meldal, M.; Diness, F. Recent Fascinating Aspects of the CuAAC Click Reaction. *Trends Chem.* **2020**, *2*, 569–584.
- (62) Himo, F.; Lovell, T.; Hilgraf, R.; Rostovtsev, V. V.; Noodleman, L.; Sharpless, K. B.; Fokin, V. V. Copper(I)-catalyzed synthesis of azoles. DFT study predicts unprecedented reactivity and intermediates. *J. Am. Chem. Soc.* **2005**, *127*, 210–216.
- (63) Huisgen, R. *Proc. Chem. Soc.* **1961**, 357–396.
- (64) Knyazeva, I. R.; Abdrafikova, D. K.; Mukhamedyanova, K. M.; Syakaev, V. V.; Gabidullin, B. M.; Gabidullin, A. T.; Habicher, W. D.; Burilov, A. R.; Pudovik, M. A. Synthesis of novel highly functionalized triazole-linked calix[4]resorcinols via click reaction. *Mendeleev Commun.* **2017**, *27*, 556–558.
- (65) Tang, H.; Guo, H.; Yang, F.; Zhu, S. Synthesis and mesomorphic properties of calix[4]resorcinarene–triphenylene oligomers. *Liq. Cryst.* **2017**, *44*, 1566–1574.
- (66) Husain, A. A.; Bisht, K. S. Synthesis of a novel resorcin[4]-arene-glucose conjugate and its catalysis of the CuAAC reaction for the synthesis of 1,4-disubstituted 1,2,3-triazoles in water. *RSC Adv.* **2019**, *9*, 10109–10116.
- (67) Kamata, K.; Nakagawa, Y.; Yamaguchi, K.; Mizuno, N. 1,3-Dipolar cycloaddition of organic azides to alkynes by a dicopper-substituted silicotungstate. *J. Am. Chem. Soc.* **2008**, *130*, 15304–15310.
- (68) Brotherton, W. S.; Michaels, H. A.; Tyler Simmons, J.; Clark, R. J.; Dalai, N. S.; Zhu, L. Apparent copper(II)-accelerated azide-alkyne cycloaddition. *Org. Lett.* **2009**, *11*, 4954–4957.
- (69) Gonzalez-Silva, K.; Rendon-Nava, D.; Alvarez-Hernández, A.; Mendoza-Espinosa, D. Copper(II) accelerated azide-alkyne cycloaddition reaction using mercaptopyrindine-based triazole ligands. *New J. Chem.* **2019**, *43*, 16538–16545.
- (70) Burilov, V. A.; Fatikhova, G. A.; Dokuchaeva, M. N.; Nugmanov, R. I.; Mironova, D. A.; Dorovatovskii, P. V.; Khrustalev, V. N.; Solovieva, S. E.; Antipin, I. S. Synthesis of new p-tert-butylcalix[4]arene-based polyammonium triazolyl amphiphiles and their binding with nucleoside phosphates. *Beilstein J. Org. Chem.* **2018**, *14*, 1980–1993.
- (71) Gao, C.; Wang, Y.; Gou, P.; Cai, X.; Li, X.; Zhu, W.; Shen, Z. Synthesis and characterization of resorcinarene-centered amphiphilic A 8B4 miktoarm star copolymers based on poly(ϵ -caprolactone) and poly(ethylene glycol) by combination of CROP and “click” chemistry. *J. Polym. Sci. Part A Polym. Chem.* **2013**, *51*, 2824–2833.
- (72) Hosseinzadeh, R.; Domehri, E.; Tajbakhsh, M.; Bekhradnia, A. New fluorescent sensor based on a calix[4]arene bearing two triazole-coumarin units for copper ions: application for Cu²⁺ detection in human blood serum. *J. Incl. Phenom. Macrocycl. Chem.* **2019**, *93*, 245–252.
- (73) Pineda-Castañeda, H. M.; Bonilla-Velásquez, L. D.; Leal-Castro, A. L.; Fierro-Medina, R.; García-Castañeda, J. E.; Rivera-Monroy, Z. J. Use of Click Chemistry for Obtaining an Antimicrobial Chimeric Peptide Containing the LfcinB and Buforin II Minimal Antimicrobial Motifs. *ChemistrySelect* **2020**, *5*, 1655–1657.
- (74) Lappchen, T.; Dings, R. P. M.; Rossin, R.; Simon, J. F.; Visser, T. J.; Bakker, M.; Walhe, P.; Van Mourik, T.; Donato, K.; Van Beijnum, J. R.; et al. Novel analogs of antitumor agent calixarene 0118: Synthesis, cytotoxicity, click labeling with 2-[18F]-fluoroethylazide, and in vivo evaluation. *Eur. J. Med. Chem.* **2015**, *89*, 279–295.
- (75) Gajjar, J. A.; Vekariya, R. H.; Parekh, H. M. Recent advances in upper rim functionalization of resorcin[4]arene derivatives: Synthesis and applications. *Synth. Commun.* **2020**, *50*, 2545–2571.
- (76) Garska, B.; Tabatabai, M.; Ritter, H. Calix[4]arene-click-cyclodextrin and supramolecular structures with watersoluble

NIPAAm-copolymers bearing adamantyl units: "Rings on ring on chain. *Beilstein J. Org. Chem.* **2010**, *6*, 784–788.

(77) Galante, E.; Geraci, C.; Sciuto, S.; Campo, V. L.; Carvalho, I.; Sesti-Costa, R.; Guedes, P. M. M.; Silva, J. S.; Hill, L.; Nepogodiev, S. A.; et al. Glycoclusters presenting lactose on calix[4]arene cores display trypanocidal activity. *Tetrahedron* **2011**, *67*, 5902–5912.

(78) Liu, W.; Minier, M. A.; Franz, A. H.; Curtis, M.; Xue, L. Synthesis of nucleobase-calix[4]arenes via click chemistry and evaluation of their complexation with alkali metal ions and molecular assembly. *Supramol. Chem.* **2011**, *23*, 806–818.

(79) Wang, F.; Qiu, W.; Zeng, J.; Yuan, P.; Zong, W.; Wu, W.; Liu, Y.; Xu, S.; Su, S. J.; Cao, S. Calix[4]resorcinarene-based hyperstructured molecular thermally activated delayed fluorescence yellow-green emitters for non-doped OLEDs. *J. Mater. Chem. C* **2020**, *8*, 4469–4476.

(80) Buttress, J. P.; Day, D. P.; Courtney, J. M.; Lawrence, E. J.; Hughes, D. L.; Blegg, R. J.; Crossley, A.; Matthews, S. E.; Redshaw, C.; Bulman Page, P. C.; et al. Janus' Calixarenes: Double-Sided Molecular Linkers for Facile, Multianchor Point, Multifunctional, Surface Modification. *Langmuir* **2016**, *32*, 7806–7813.

(81) Qadri, T.; Ali, I.; Hussain, M.; Ahmed, F.; Shah, M. R.; Hussain, Z. Synthesis of New Tetra Triazole Functionalized Calix[4]resorcinarene and Chemosensing of Copper Ions in Aqueous Medium. *Curr. Org. Chem.* **2020**, *24*, 332–337.

(82) Mo, J.; Eggers, P. K.; Yuan, Z. X.; Raston, C. L.; Lim, L. Y. Paclitaxel-loaded phosphonated calixarene nanovesicles as a modular drug delivery platform. *Sci. Rep.* **2016**, *6*, 1–12.

(83) Burirov, V.; Garipova, R.; Mironova, D.; Sultanova, E.; Bogdanov, I.; Ocherednyuk, E.; Evtugyn, V.; Osin, Y.; Rizvanov, I.; Solovieva, S.; et al. New poly-imidazolium-triazole particles by CuAAC cross-linking of calix[4]arene bis-azide/alkyne amphiphiles - a prospective support for Pd in the Mizoroki-Heck reaction. *RSC Adv.* **2021**, *11*, 584–591.

(84) Burirov, V.; Mironova, D.; Sultanova, E.; Garipova, R.; Evtugyn, V.; Solovieva, S.; Antipin, I. Nhc polymeric particles obtained by self-assembly and click approach of calix[4]arene amphiphiles as support for catalytically active Pd nanoclusters. *Molecules* **2021**, *26*, 6864.

(85) Ryu, E. H.; Zhao, Y. Efficient synthesis of water-soluble calixarenes using click chemistry. *Org. Lett.* **2005**, *7*, 1035–1037.

(86) Sliwa, W.; Deska, M. Syntheses and reactivity of calixarenes functionalized at meso positions. *Arkivoc* **2012**, *2012*, 173–210.

(87) Gorbunov, A.; Kuznetsova, J.; Deltsov, I.; Molokanova, A.; Cheshkov, D.; Bezzubov, S.; Kovalev, V.; Vatsouro, I. Selective azide-alkyne cycloaddition reactions of azidoalkylated calixarenes. *Org. Chem. Front.* **2020**, *7*, 2432–2441.

(88) Burirov, V. A.; Artemenko, A. A.; Garipova, R. I.; Amirova, R. R.; Fatykhova, A. M.; Borisova, J. A.; Mironova, D. A.; Sultanova, E. D.; Evtugyn, V. G.; Solovieva, S. E.; et al. New Calix[4]arene-Fluorescein Conjugate by Click Approach-Synthesis and Preparation of Photocatalytically Active Solid Lipid Nanoparticles. *Molecules* **2022**, *27*, 2436–2436.

(89) Matthews, S. E.; Cecioni, S.; O'Brien, J. E.; MacDonald, C. J.; Hughes, D. L.; Jones, G. A.; Ashworth, S. H.; Vidal, S. Fixing the Conformation of Calix[4]arenes: When Are Three Carbons Not Enough? *Chem. - A Eur. J.* **2018**, *24*, 4436–4444.

(90) Ahmed, F.; Perveen, S.; Shah, K.; Shah, M. R.; Ahmed, S. Synthesis and characterization of triazole based supramolecule for interaction with cefuroxime in tap water and blood plasma. *Ecotoxicol. Environ. Saf.* **2018**, *147*, 49–54.

(91) Zhang, H.; Ippel, H.; Miller, M. C.; Wong, T. J.; Griffioen, A. W.; Mayo, K. H.; Pieters, R. J. Hybrid ligands with calixarene and thiodigalactoside groups: galectin binding and cytotoxicity. *Org. Chem. Front. an Int. J. Org. Chem.* **2019**, *6*, 2981–2990.

(92) Schlüter, D.; Korsching, K. R.; Azov, V. A. Lower-Rim-Modified Calix[4]arene-Pyrrolotetrahydrofulvalene Molecular Tweezers. *Eur. J. Org. Chem.* **2021**, *2021*, 4469–4476.

(93) Malakhova, M.; Gorbunov, A.; Ozerov, N.; Korniltsev, I.; Ermolov, K.; Bezzubov, S.; Kovalev, V.; Vatsouro, I. Triazolated

calix[4]semitubes: assembling strategies towards long multicalixarene architectures. *Org. Chem. Front.* **2022**, *9*, 3084–3092.

Recommended by ACS

Effects of Vegetal Extracts and Metabolites against Oxidative Stress and Associated Diseases: Studies in *Caenorhabditis elegans*

Estefani Yaqueclin Hernández-Cruz, José Pedraza-Chaverri, et al.
FEBRUARY 27, 2023
ACS OMEGA

READ 

Moisture Property and Thermal Behavior of Two Novel Synthesized Polyol Pyrrole Esters in Tobacco

Wenpeng Fan, Miao Lai, et al.
JANUARY 27, 2023
ACS OMEGA

READ 

Directional Conversion of Volatiles from Low-Rank Coal to BTX-Rich Tar by Combined *In Situ* and *Ex Situ* Catalytic Pyrolyses

Tao Liu, Xiaodong Zhang, et al.
JANUARY 17, 2023
ACS OMEGA

READ 

Efficacious Removal of Trace Mercury from Honeysuckle Water Decoction Using Multifunctional Mesoporous Carbon

Wenjie Lu, Ming Yu, et al.
DECEMBER 05, 2022
ACS OMEGA

READ 

Get More Suggestions >

Biological Chemistry & Chemical Biology

Use of Click Chemistry for Obtaining an Antimicrobial Chimeric Peptide Containing the LfcinB and Buforin II Minimal Antimicrobial Motifs

 Hector M. Pineda-Castañeda,^[a] Laura D. Bonilla-Velásquez,^[b] Aura Lucía Leal-Castro,^[c]
 Ricardo Fierro-Medina,^[a] Javier E. García-Castañeda,^[d] and Zuly J. Rivera-Monroy^{*,[a]}

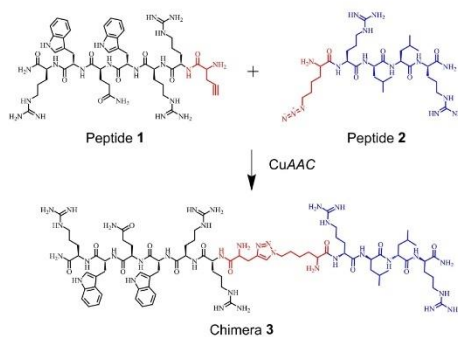
A chimeric peptide derived from Lactoferricin B (LfcinB) and Buforin II (BFII) was designed. It specifically contains the reported antimicrobial minimal motif sequences LfcinB (20–25): RRWQWR and BFII (32–35): RLLR. The chimeric peptide was synthesized by intramolecular cyclization with a triazole bridge. The Chimera 3 exhibited higher antimicrobial activity against *E. coli* ATCC 25922 (MIC 93 μ M) and *S. aureus* ATCC 25923 (93 μ M) than the original sequences. Furthermore, it did not exhibit a significant hemolytic effect.

The concept of click chemistry was introduced by Sharpless et al., and it is a modern, efficient method used in the synthesis of complex molecules by assembling (click) small blocks.^[1] It has been reported that the Huisgen reaction is a cycloaddition between an azide and an alkyne that proceeds in the presence of a copper (I) catalyst under mild conditions. This process is known as CuAAC (copper-catalyzed variant of azide-alkyne Huisgen cycloaddition), which is a click chemistry reaction. CuAAC is characterized by stereospecificity and a high degree of efficiency, the products are easily purified, requiring mild reaction conditions, and it takes place in water and is therefore economical.^[2] CuAAC has been implemented in solid-phase peptide synthesis (SPPS), where peptides derived from anoplin were synthesized and linked through a triazole bridge. These

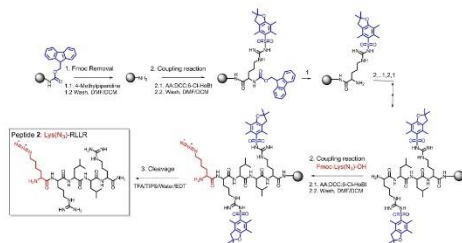
peptides exhibited an increase in antibacterial activity against different bacterial strains.^[3] The modified amino acids in their side chains with azide and alkyne groups allow obtaining precursor peptides that are bound by the CuAAC reaction. The CuAAC reaction can be performed with Fmoc-Lys(N₃)-OH ((S)-2-(Fmoc-amino)-6-azidoheptanoic), which has an azide group in the ϵ -amino group of lysine and the (S)-2-(Fmoc-amino)-4-pentynoic acid (Pra) containing an alkyne group.^[3] The aim of the present investigation was to obtain a chimeric peptide containing the minimal motifs with antibacterial activity derived from LfcinB (RRWQWR) and Buforin II (RLLR). For this purpose, the peptides Pra-RRWQWR and Lys(N₃)-RLLR were synthesized using the SPPS and Fmoc/tBu strategy (Scheme 1). The Pra and Fmoc-Lys(N₃)-OH amino acids were incorporated at the N-terminal extreme of the sequences. Then the products were linked by means of the CuAAC reaction (Scheme 1). The antimicrobial activity of the purified chimeric peptide against *E. coli* ATCC 25922 and *S. aureus* ATCC 25923 was evaluated.

In order to establish the optimal experimental conditions for the CuAAC reaction, it was necessary to standardize (i) amounts of precursors and catalysts, (ii) solvents and their proportions, (iii) reaction time, and (iv) temperature. It has been reported that polar solvents favor the generation of the triazole ring^[4–7]. In attempting to carry out this reaction in polar aprotic solvents such as DMF, ring generation was not observed.^[8] It

- [a] H. M. Pineda-Castañeda, Prof. R. Fierro-Medina, Prof. Z. J. Rivera-Monroy
 Chemistry Department
 Universidad Nacional de Colombia
 Carrera 45 No 26–85, Building 451, Office 334, Bogotá Zip Code 11321,
 Colombia
 E-mail: hmpinedac@unal.edu.co
 zriveram@unal.edu.co
- [b] L. D. Bonilla-Velásquez
 Biotechnology Institute
 Universidad Nacional de Colombia
 Carrera 45 No 26–85, Building 451, Office 334, Bogotá Zip Code 11321,
 Colombia
- [c] Prof. A. L. Leal-Castro
 Medicine Faculty
 Universidad Nacional de Colombia
 Carrera 45 No 26–85, Building 451, Office 334, Bogotá Zip Code 11321,
 Colombia
- [d] Prof. J. E. García-Castañeda
 Pharmacy Department
 Universidad Nacional de Colombia
 Carrera 45 No 26–85, Building 451, Office 334, Bogotá Zip Code 11321,
 Colombia



Scheme 1. Copper-catalyzed azide-alkyne cycloaddition of Pra-RRWQWR (1) with Lys(N₃)-RLLR (2) for obtaining the chimeric peptide (3)



Scheme 2. Precursor Peptide (P2) (Lys(N₃)-RLLR) Synthesis. SPPS-Fmoc/tBu methodology was used, at N-terminal end it was incorporated the (S)-2-(Fmoc-amino)-6-azidohexanoic acid (in red).

was established that the CuAAC reaction proceeds in protic polar solvents such as water:methanol (1:1 v/v), using the minimum volumes needed to dissolve the precursors and catalysts.^[9] It has been reported that azide and alkyne species in an equimolar ratio (0.012 mmol) are required, while the catalyst (0.031 mmol) will have an excess, to guarantee the reaction at short times.^[4] The temperature parameter was adopted from Arnusch et al. This reaction was carried out at 80 °C.^[8] Finally, the reaction time was established by monitoring the reaction via RP-HPLC.

Chimera 3 was synthesized using the methodology reported by Liu et al., with some modifications. As first step, precursor peptides P1 and P2 corresponding to (S)-2-(Fmoc-amino)-4-pentynoic acid (NH₂-Pra-RRWQR-CONH₂) and (S)-2-(Fmoc-amino)-6-azidohexanoic acid (NH₂-K(εN₃)-RLLR-CONH₂) respectively, were synthesized via SPPS-Fmoc/tBu methodology. A mixture containing crude peptides P1 (0.012 mmol) and P2 (0.012 mmol) was prepared in Water/MeOH (1:1, v/v), and then copper sulphate pentahydrate (0.031 mmol) and ascorbic acid (0.035 mmol) were added. The reaction mixture was gently stirred at 80 °C for 10 min. The reaction progress was monitored by RP-HPLC. Finally, the Chimera 3 was purified using RP-SPE and characterized by RP-HPLC and mass spectrometry (MALDI-TOF).^[3]

Peptides were purified by solid phase extraction (RP-SPE) according to Insuasty et al. procedure. Briefly, a SupelcleanTM SPE column (5 g, 45 μm, 60 Å) was activated using 30 mL of methanol, 30 mL of Solvent B (Acetonitrile/TFA 0.05%) and equilibrated with 30 mL of Solvent A (Water/TFA 0.05%). Then, crude peptide (150 mg) was dissolved in Solvent A (1.0 mL), load to the activated column and eluted using solutions with increasing percentage of Solvent B. Each fraction had a total volume of 12 mL, fractions containing pure peptide were identified via RP-HPLC and they were lyophilized. Final purified products were analyzed by MALDI-TOF mass spectrometry.^[10]

Figure 1 shows the chromatographic profile of the CuAAC reaction at time zero (*t*₀); peptides Pra-RRWQR and Lys(N₃)-RLLR coelute at *t*_R=4.1 min (Figure 1.a). After ascorbic acid (antioxidant agent) was added and the reaction mixture was gently shaken at 80 °C for 10 min, an aliquot of the reaction

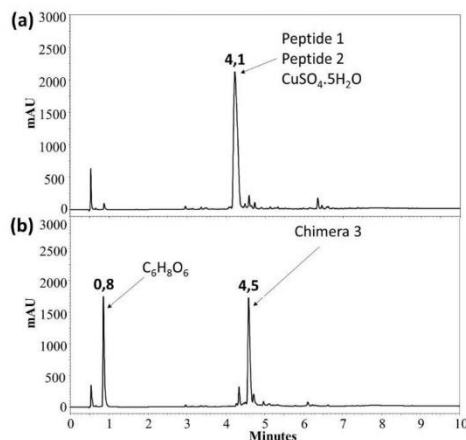


Figure 1. Monitoring the CuAAC reaction. (a) Time zero; it can be observed that precursor peptides co-elute (*t*_R = 4.1 min.), and (b) formation of the chimeric peptide 3, *t*_R = 4.5 min, after 10 min reaction

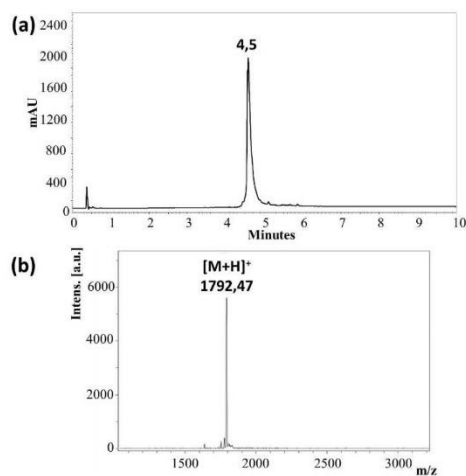


Figure 2. (a) Chromatographic profile and (b) MALDI-TOF mass spectrum of the purified chimeric peptide 3.

mixture was analyzed via RP-HPLC. The chromatographic profile shows that the peak area of the precursor peptide decreased and a new peak at *t*_R=4.5 min, which corresponds to chimeric peptide 3, was observed (Figure 1.b).

The crude product was purified via RP-SPE using an elution gradient, which increases the acetonitrile concentration,^[10] and the fractions were analyzed via RP-HPLC and those containing the chimeric peptide were collected, obtaining a product with

Table 1. Synthetic peptides derived from Bovine Lactoferricin and Buforin. Summary of characterization (RP-HPLC and MALDI-TOF MS) and antibacterial activity of purified products.

Peptide	RP-HPLC t_R (min)	Purity (%)	Mass		Hemolytic Activity % hemolysis	Antimicrobial Activity MIC (μ M)	
			Theoretical	Experimental m/z		<i>E. coli</i> ATCC 25922	<i>S. aureus</i> ATCC 25923
Chimera 3	4.5	90.7	1790.1	1792.5	3.3	93	93
RRWQWR	4.0	92.5	985.5	988.2	1.1	203	>200
RLLR	2.8	97.2	555.4	564.0	12.2	>200	>200

a chromatographic purity of 90.7%. The overall yield of the CuAAC reaction was 15.5%. The chimeric peptide was characterized via MALDI-TOF MS, where the m/z ratio is in accordance with the theoretical molecular weight (Figure 2 and Table 1).

Then in order to determine if the joining of the RRWQWR and RLLR sequences through intramolecular cyclization with a triazole bridge increases the antimicrobial activity against *E. coli* ATCC 25922 and *S. aureus* ATCC 25923, the antibacterial activity of Chimera 3, LfcinB (20–25), and BFII (32–35) was evaluated. Chimera 3 exhibited higher antibacterial activity against the evaluated strains than the control peptides, RRWQWR and RLLR. The chimeric peptide is a molecule containing two sequences that are positively charged, hydrophobic, and amphipatic. These results are consistent with previous reports that suggest that an increase in the hydrophobicity, positive net charge, and amphipaticity could improve interaction with the bacterial membrane and peptide internalization.^[11] The mechanism, associated with the RRWQWR sequence, implies possible electrostatic interaction with the membranes, causing their disruption and/or peptide internalization, which leads to intracellular targets.^[12,13] On the other hand, the motif RLLR is present in the Buforin sequence, which internalizes into bacteria and interacts with the DNA.^[14,15] The antibacterial activity of the chimeric peptide could be due to a dual mechanism that involves membrane affectation and targets in the cytoplasmic and the nucleus. Additionally, Chimera 3 has a hemolytic effect of 3.3% at MIC, while peptide BFII (32–35) exhibited 12.2% hemolysis at 200 μ M, suggesting that chimeric peptide exhibited a therapeutically index higher than the precursor peptides. The triazole joining reduces the high hemolytic effect of RLLR sequence while potency the antibacterial activity of the chimeric peptide.

In this paper we reported the synthesis of the Chimera 3 using click chemistry and its significant antibacterial activity against *S. aureus* and *E. coli* strains, suggesting that chimeric peptides containing sequences derived from LfcinB and Buforin are a versatile strategy for obtaining molecules with therapeutic potential.

Acknowledgment

This research was conducted with the financial support of the División de Investigación y Extensión sede Bogotá (DIEB), Universidad Nacional de Colombia through the project coded 41569: "Péptidos Quiméricos Derivados de la Lactoferricina Bovina Y la Buforina: Diseño, Síntesis y Evaluación de su Actividad Antibacteriana".

Keywords: Antimicrobial peptides · azide-alkyne cycloaddition · Bovine Lactoferricin · Buforin · chimeric peptide · click chemistry

- [1] H. C. Kolb, K. B. Sharpless, *Drug Discovery Today* **2003**, *8*, 1128–37.
- [2] J. Thundimadathil, *Chem. Informationsdienst* **2013**, *44*, 34–37.
- [3] B. Liu, H. Huang, Z. Yang, B. Liu, S. Gou, C. Zhong, X. Han, Y. Zhang, J. Ni, R. Wang, *Peptides* **2017**, *88*, 115–125.
- [4] X. Li, *Chem. Asian J.* **2011**, *6*, 2606–2616.
- [5] L. D. Pachón, J. H. Van Maarseveen, G. Rothenberg, *Adv. Synth. Catal.* **2005**, *347*, 811–815.
- [6] A. Suárez, *An. Quim.* **2012**, *108*, 306–313.
- [7] O. Avrutina, M. Empting, S. Fabritz, M. Daneschdar, H. Frauendorf, U. Diederichsen, H. Kolmar, *Org. Biomol. Chem.* **2009**, *7*, 4177–4185.
- [8] C. J. Arnusch, H. Branderhorst, B. De Kruijff, R. M. J. Liskamp, E. Breukink, R. J. Pieters, *Society*, **2007**, 13437–13442.
- [9] Y. L. Angell, K. Burgess, *Chem. Soc. Rev.* **2007**, *36*, 1674–1689.
- [10] D. S. Insuasty, H. M. Pineda, A. V. Rodríguez, J. E. García, M. Maldonado, R. Fierro, Z. J. Rivera, *Molecules* **2019**, *24*, 1215.
- [11] Z. Jiang, A. I. Vasil, J. D. Hale, R. E. W. Hancock, M. L. Vasil, R. S. Hodges, *Biopolymers*, **2008**, *90*, 369–383.
- [12] J. L. Gifford, H. N. Hunter, H. J. Vogel, *Cell. Mol. Life Sci.* **2005**, *62*, 2588–2598.
- [13] S. Farnaud, C. Spiller, L. C. Moriarty, A. Patel, V. Gant, E. W. Odell, R. W. Evans, *FEMS Microbiol. Lett.* **2004**, *233*, 193–199.
- [14] C. B. Park, H. S. Kim, S. C. Kim, *Biochem. Biophys. Res. Commun.* **1998**, *244*, 253–257.
- [15] S. A. Jang, H. Kim, J. Y. Lee, J. R. Shin, D. J. Kim, J. H. Cho, S. C. Kim, *Peptides*, **2012**, *34*, 283–289.

Submitted: October 11, 2019

Accepted: January 17, 2020



DOI: 10.1002/cbdv.202000885

FULL PAPER



Designing Chimeric Peptides: A Powerful Tool for Enhancing Antibacterial Activity

Héctor Manuel Pineda-Castañeda,^a Kevin Andrey Huertas-Ortiz,^a Aura Lucía Leal-Castro,^b Yerly Vargas-Casanova,^c Claudia Marcela Parra-Giraldo,^c Javier Eduardo García-Castañeda,^d and Zuly Jenny Rivera-Monroy^{*a}

^a Chemistry Department, Universidad Nacional de Colombia, Carrera 45 No. 26–85, Building 451, Office 409, Bogotá, Zip Code 11321, Colombia, e-mail: zjriveram@unal.edu.co

^b Medicine Faculty, Universidad Nacional de Colombia, Carrera 45 No. 26–85, Building 451, Office 409, Bogotá, Zip Code 11321, Colombia

^c Microbiology Department, Pontificia Universidad Javeriana, Carrera 7 No. 40–62, Bogotá, Zip Code 110231, Colombia

^d Pharmacy Department, Universidad Nacional de Colombia, Carrera 45 No. 26–85, Building 450, Office 213, Bogotá, Zip Code 11321, Colombia

Chimeric peptides containing short sequences derived from bovine Lactoferricin (LfcinB) and Buforin II (BFII) were synthesized using solid-phase peptide synthesis (SPPS) and characterized via reversed-phase liquid chromatography and mass spectrometry. The chimeras were obtained with high purity, demonstrating their synthetic viability. The chimeras' antibacterial activity against Gram-positive and Gram-negative strains was evaluated. Our results showed that all the chimeras exhibited greater antibacterial activity against the evaluated strains than the individual sequences, suggesting that chemical binding of short sequences derived from AMPs significantly increased the antibacterial activity. For each strain, the chimera with the best antibacterial activity exerted a bacteriostatic and/or bactericidal effect, which was dependent on the concentration. It was found that: (i) the antibacterial activity of a chimera is mainly influenced by the linked sequences, the palindromic motif RLLRRLLR being the most relevant one; (ii) the inclusion of a spacer between the short sequences did not significantly affect the chimera's synthesis process; however, it enhanced its antibacterial activity against Gram-negative and Gram-positive strains; on the other hand, (iii) the replacement of Arg with Lys in the LfcinB or BFII sequences improved the chimeras' synthesis process without significantly affecting their antibacterial activity. These results illustrate the great importance of the synthesis of chimeric peptides for the generation of promising antibacterial peptides.

Keywords: chimeric peptide, LfcinB, Buforin, antibacterial activity, chimera.

Introduction

The increasing emergence of antibiotic-resistant bacterial strains reduces the effectiveness of the drugs used to treat infections. In many regions of the world, inappropriate use of medicines in humans and animals can lead to people's dying from common infections or

minor injuries. According to the World Health Organization (WHO), the most resistant bacterial strains are *Acinetobacter*, *Pseudomonas*, and several *Enterobacteriaceae* (including *Klebsiella*, *Escherichia coli*, *Serratia* and *Proteus*), followed by *Enterococcus faecium* and *Staphylococcus aureus*, among others.^[1,2]

Within this context, a new challenge in the field of health is posed: the search for new molecules with therapeutic potential capable of fighting infections caused by resistant strains and whose activity is based on mechanisms of action different from those that

Supporting information for this article is available on the WWW under <https://doi.org/10.1002/cbdv.202000885>

conventional antibiotics exhibit. Antimicrobial peptides (AMPs) have been described as being part of the innate immune system, being the first defense barrier against infections caused by external pathogens.^[3] Currently, AMPs are used as templates for designing and developing new antimicrobial molecules. In order to obtain new therapeutic agents, the AMP sequences could be modified using synthetic strategies such as (i) incorporation of non-natural amino acids to increase the resistance to peptide proteolytic degradation, (ii) disulfide bond formation to obtain peptides with conformational restriction, (iii) synthesis of peptides containing multiple chains with the same sequence, (iv) peptides containing palindromic sequences, and (v) chimeric peptides that contain two or more peptide fragments derived from AMP motifs.^[4] Chimera design and synthesis is considered one of the most promising alternatives for identifying peptides with potent antibacterial activity.^[5–7] Chimeras are formed by sequences derived from several AMPs, where each of these acts under a specific mechanism of action. Bacteria are eliminated through the dual mechanism of the chimera and are less prone to induce resistance.^[5]

Bovine lactoferricin (LfcinB) is an AMP that was identified in hydrolyzed lactoferrin protein (LF) caused by gastric pepsin. This peptide has shown antibacterial, antiviral, antifungal and antiparasitic activity. The positive side chains of LfcinB interact electrostatically with the negatively-charged molecules expressed on the bacterial membrane, and then, the hydrophobic residues bind to the bilipid layer, destabilizing the plasma membrane and causing cell lysis or peptide internalization,^[8–14] while buforin II (BFII) is an antimicrobial peptide with extensive activity against Gram-positive and Gram-negative bacteria as well as fungi. BFII is internalized in the cytoplasm without causing cell lysis and interacts with DNA and RNA by inhibiting cell functions that lead to cell death.^[15–19]

In the present investigation, chimeric peptides containing short sequences derived from both LfcinB and BFII were designed, synthesized, and characterized. The LfcinB-derived sequence selected for this research was LfcinB (20–25): RRWQWR (**1**), which is the minimum motif with antibacterial, antifungal, and anticarcinogenic activity. The BFII-derived sequences used were the palindromic motifs RLLR (**2**) and RLLRLLR (**3**) (Figure 1). Additionally, it was also included the **4** and **5** motifs in which for RRWQWR and RLLRLLR sequences the Arg residues were replaced by Lys residues. Our results showed that the chimeras can be obtained with high purity, demonstrating their synthetic viability. The antibacterial activity of chimeric

peptides against Gram-positive and Gram-negative strains was evaluated, and the results showed that all the chimeric peptides exhibited greater antibacterial activity than their precursor peptides. The design and synthesis of chimera containing antibacterial sequences could be a promising tool for the development of drugs for the treatment of bacterial infections.

Results and Discussion

The objective of this study was to establish if chimeras that contain short sequences derived from LfcinB, **1** and **4**, which are linked to the short palindromic sequences derived from BFII, **2**, **3** or **5**, exhibit greater antibacterial activity than their precursor peptides. The designed chimeras can be classified as follows: Group I (Figure 2) includes chimeric peptides **6**, **7**, and **8**, containing precursor **1** in the N-terminal region attached to precursor **2** or **3** in the C-terminal region. Group II (Figure 3) consists of peptides **9**, **10**, and **11**, containing precursor peptide **1** in the C-terminal region, while precursor peptide **2** or **3** is located in the N-terminal region. Group III (Figure 4) consists of chimeras **12**, **13**, and **14**, containing precursor peptides **4** or **5**, in which Arg was changed to Lys, attached to precursor peptides **1** and **3** (Table 1). The precursor sequences derived from LfcinB and BFII were alternated in the N- or C-terminal region to establish if the precursor sequence position at the chimera affects their synthesis and/or antibacterial activity. 6-Aminohexanoic acid (Ahx) was included in some chimeras as a spacer in order to i) determine if the spacer incorporation facilitates synthesis of the chimera and ii) establish if it influences the antibacterial activity.

The designed chimeras were synthesized through SPPS, using the Fmoc/Bu strategy. All the chimeras were obtained without synthetic difficulties and were purified via solid-phase extraction (RP-SPE), obtaining products with chromatographic purities between 85% and 99%. The MS spectra of the purified products showed a main signal at m/z , corresponding to the $[M + H]^+$ specie. The chimeras' characterization indicated that it was possible to obtain all the designed peptides (Table 1, Figure S1).

The synthesis of the chimeras showed that in most cases the incorporation of Arg residues into the peptide-resin required the highest number of coupling reactions compared to the other residues. It was established that the incorporation of Arg residue in position 1 (the last amino acid attached to peptide-resin) into the sequence of the chimeras **6**, **7**, and **8**

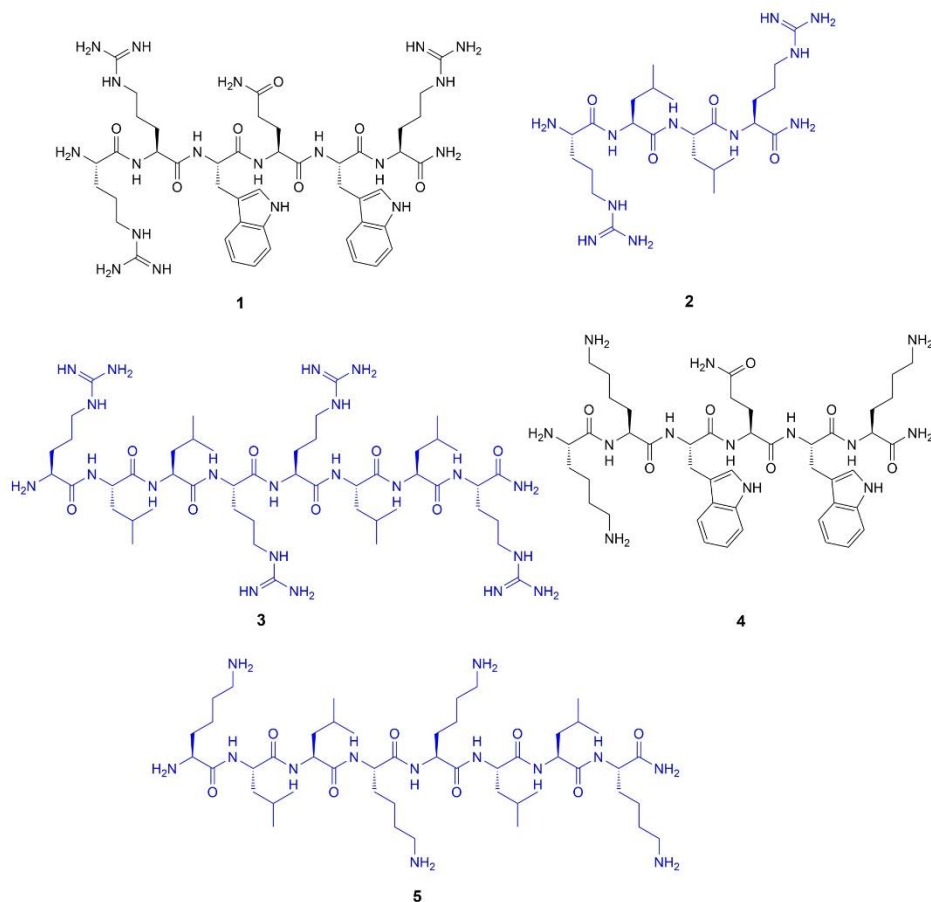


Figure 1. Chemical structures of precursor peptides: RRWQWR-NH₂ (1), RLLR-NH₂ (2), RLLRRLR-NH₂ (3), KKWQWK-NH₂ (4), and KLLKLLK-NH₂ (5). Sequences derived from LfcinB (in black) and from BFII (in blue).

required three cycles of the coupling reaction to complete the reaction. These results show that the inclusion of the spacer among the precursor sequences did not affect the synthesis process. Similarly, the alternation of LfcinB- or BFII-derived precursor sequences in the N- or C-terminal region of the chimeras did not influence the synthesis viability. On the other hand, when all Arg residues were changed to Lys, as in chimera **14**, the synthesis was friendly, because all the amino acids only required a coupling reaction, this being the peptide with the highest synthetic viability.

It was determined that when Arg was switched to Lys in the LfcinB- or BFII-derived precursor sequences, the synthesis process was facilitated because of requiring fewer coupling reactions, suggesting that regardless of the sequence, the replacement of Arg with Lys improved the peptide's synthesis (Table 1).

The antibacterial activity of the chimeric and precursor peptides was evaluated against Gram-negative bacterial strains of *E. coli* (ATCC 11775, ATCC 25922), and *P. aeruginosa* ATCC 27853, and Gram-positive bacteria strains *S. aureus* ATCC 25923, and

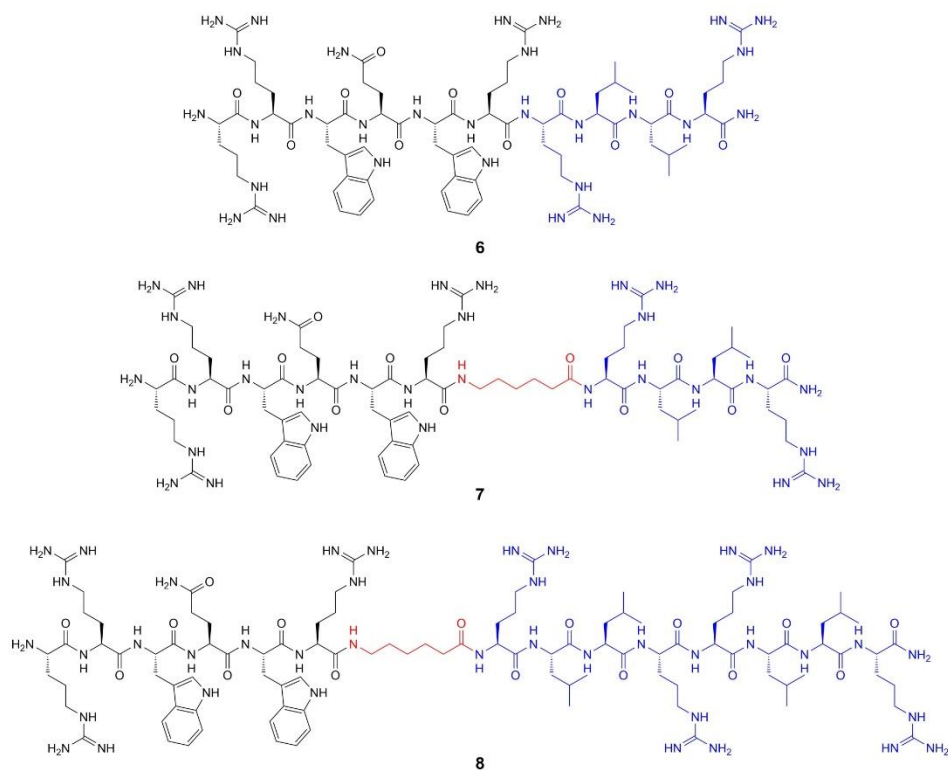


Figure 2. Chemical structures of designed chimeras. Group I: RRWQWRLLR-NH₂ (**6**), RRWQWR-Ahx-RLLR-NH₂ (**7**), and RRWQWR-Ahx-RLLRLLR-NH₂ (**8**).

E. faecalis ATCC 29212. The results showed that all the precursor peptides exhibited low antibacterial activity against the strains evaluated (Table 2). All the chimeras exhibited greater antibacterial activity against a majority of the strains evaluated than their precursor peptides. Chimeras **6** and **7** exhibited similar antibacterial activity against *E. coli* 25922, while **7** exhibited greater antibacterial activity against *E. coli* 11775 and *P. aeruginosa* 27853 than **6**. By contrast, **7** exhibited greater antibacterial activity against *S. aureus* 25923 and *E. faecalis* 29212 than **6**. These results indicate that chimera **6** exhibits better antibacterial activity against Gram-positive strains than **7**, and **7** exhibits greater antibacterial activity against Gram-negative strains than **6**. Interestingly, similar behavior was observed for chimeras **9** and **10**, suggesting that

the inclusion of the spacer (Ahx) modulates the antibacterial activity, favoring the antibacterial activity on Gram-negative strains. When the antibacterial activity of the chimeras of group I is compared, it can be seen that **8** exhibited higher antibacterial activity against the strains evaluated than **6** and **7**, suggesting that the palindromic motif RLLRLLR significantly increased the antibacterial activity. Similarly, for group II, chimera **11** exhibited the greatest antibacterial activity against the strains evaluated. On the other hand, on comparing antibacterial activity the chimeras of group I with those group II, it can be seen that the position of LfcinB or BFII sequences in the C- or N-terminal region did not significantly affect the antibacterial activity.

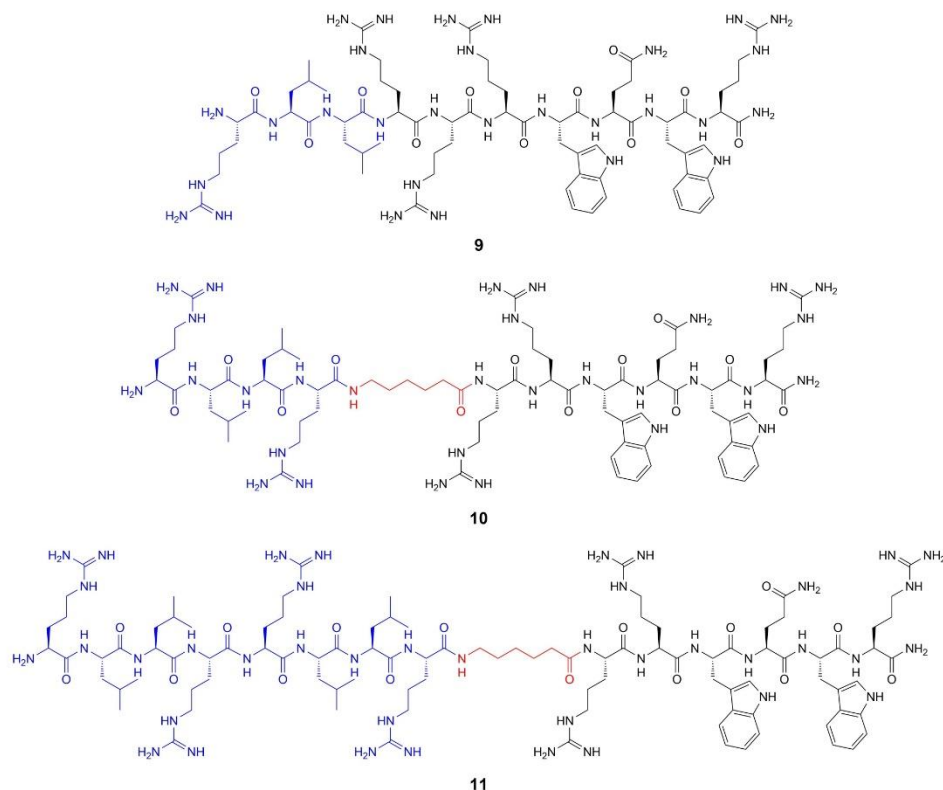


Figure 3. Chemical structures of designed chimeras. Group II: RLLRRRWQWR-NH₂ (**9**), RLLR-Ahx-RRWQWR-NH₂ (**10**), and RLLRRLLR-Ahx-RRWQWR-NH₂ (**11**).

Chimeras in groups I and II exhibited greater antibacterial activity against Gram-negative strains compared to that observed in Gram-positive strains. Chimeras **12** and **8** exhibited similar antibacterial activity against *E. coli* strains, suggesting that the substitution of Arg with Lys in the palindromic sequence RLLRRLLR did not affect the antibacterial activity in these strains. However, **12** exhibited lower antibacterial activity against *P. aeruginosa*, *S. aureus*, and *E. faecalis* strains than **8**, indicating that the substitution of Arg with Lys diminished the antibacterial activity in these strains. Chimera **13** exhibited a small decrease in antibacterial activity against the strains evaluated compared to chimera **8**. These results suggest that the substitution of Arg with Lys in one of

the LfcinB or BfII sequences does not significantly affect the antibacterial activity. It has been established that amino acids containing positively-charged side chains, such as arginine, are of great importance in antibacterial activity, due to their ability to interact electrostatically with the negative charges present in the bacterial membrane. In addition, the difficulty of incorporating Arg, Met, Cys or Trp residues into the peptide-resin in SPPS methodology has been established, leading to increased consumption of solvents and reagents and decreased efficiency of the purification process.^[20] Our results agree with previous reports, which indicated that one of the alternatives for carrying out the synthesis of AMPs rich in cationic residues is the substitution of residues such as Arg

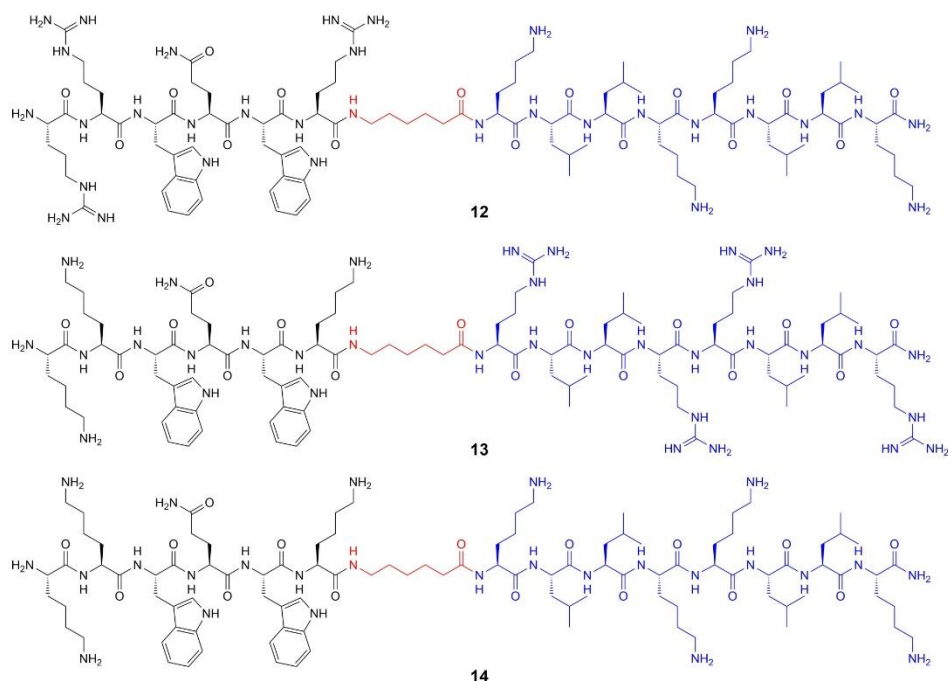


Figure 4. Chemical structures of designed chimeras. Group III: RRWQWR-Ahx-KLLKLLK-NH₂ (**12**), KKWQWK-Ahx-RLRRLLR-NH₂ (**13**), and KKWQWK-Ahx-KLLKLLK-NH₂ (**14**).

with Lys. This strategy produces high coupling yields at low reaction times. The activity that results for peptides where the Arg residues have been replaced with Lys have maintained the activity, and in very few cases is activity lost.^[21–28]

The chimeras synthesized here contain one sequence that disrupts the cell membrane (LfcinB) and another that internalizes into the cell (BFII). This design is in accordance with a previous report that indicates that to design chimeras, the binding of an AMP to a sequence with the capacity to internalize (CPPs) could be a promising approach for enhancing the antimicrobial activity.^[29] CPPs have a great diversity of sequences and structures, with the ability to cross the cytoplasmic membrane, reaching the interior of the cell, giving these structures several advantages over other transporters; in this sense, the BFII sequence can be considered to be a CPP.^[4,30] Our results showed that the chimeras increased their antibacterial activity compared with their peptide precursors. This behavior

has also been observed with other chimeras derived from the LfcinB sequence.

The antibacterial activity against *E. coli* ATCC 25922 of a chimera containing LfcinB and LfcinH sequences FKCRRWQWRMRKVRGPPVSCIKRDS was evaluated. This chimera exhibited a MIC value of 32 μ M, compared to LfcinH (18–42), which has a MIC higher than 128 μ M, indicating a considerable increase in its antibacterial activity.^[5] Another example of a chimera was the one reported by Xu et al., where they demonstrated that the LFchimera FKCRRWQW(WKLLSKAQEKFGKKNKSR)RMKKLGK, derived from LFcin (17–30) FKCRRWQWRMKKLG and LFampin (268–284) WKLLSKAQEKFGKKNKSR, exhibited increased elastase activity and avoided the formation of biofilms of *P. aeruginosa*. They found that the antibacterial activity is concentration-dependent, which regulates the inhibition of elastase and the formation of biofilm. The LFchimera activity was significantly stronger than those of LF, LFcin, LFampin, or LFcin plus LFampin.^[31]

Table 1. Precursor and chimeric peptides analysis by RP-HPLC and MALDI-TOF MS.^[a]

Code	Sequence	RP-HPLC		MALDI-TOF MS
		t _R (min)	Purity (%)	m/z [M + H] ⁺
Precursor peptides				
1	RRWQWR	4.1	92.5	988.2
2	RLLR	2.8	97.2	564.0
3	RLLRRLLR	4.4	98.2	1096.2
4	KKWQWK	3.7	97.0	903.9
5	KLLKLLK	4.0	99.0	984.3
Chimeric peptides				
6	RRWQWRLLR	5.0	96.0	1523.1
7	RRWQWR-Ahx-RLLR	5.1	94.3	1640.2
8	RRWQWR-Ahx-RLLRRLLR	6.1	90.0	2179.1
9	RLLRRRWQWR	4.7	95.5	1523.6
10	RLLR-Ahx-RRWQWR	5.4	85.5	1638.6
11	RLLRRLLR-Ahx-RRWQWR	5.9	90.0	2179.6
12	RRWQWR-Ahx-KLLKLLK	5.9	85.2	2067.4
13	KKWQWK-Ahx-RLLRRLLR	5.8	99.4	2089.0
14	KKWQWK-Ahx-KLLKLLK	5.7	86.6	1983.7

^[a] All peptides contain an amide group at the C-terminal end.

Table 2. Antibacterial activity of the precursor and chimeric peptides. MIC values are expressed in μM concentration.

Code	Minimal Inhibitory Concentration (MIC), μM				
		<i>E. coli</i>	<i>P. aeruginosa</i>	<i>S. aureus</i>	<i>E. faecalis</i>
	25922	11775	27853	25923	29212
Precursor peptides					
1	200	203	203	> 200	> 200
2	> 200	> 200	> 200	> 200	> 200
3	91	183	183	> 200	> 200
4	> 222	> 222	> 222	> 222	–
5	204	–	204	> 204	–
Chimeric peptides					
6	16	66	131	66	131
7	15	31	31	122	> 200
8	11	23	11	23	46
9	33	33	131	131	> 200
10	15	15	61	122	> 200
11	6	11	23	46	46
12	12	24	48	48	97
13	24	24	24	48	48
14	25	51	101	101	101

On the other hand, when all Arg residues were substituted with Lys in both precursor sequences in order to obtain chimera **14**, their antibacterial activity diminished considerably. These results suggest that if the Arg residues are partially replaced, the antibacterial activity is conserved, suggesting that for the design of peptide chimeras it is necessary to conserve some Arg residues, which could be involved in the

mechanism of action. Chimeras **8**, **9**, and **11** exhibited the greatest antibacterial activity against the *E. coli* strains evaluated, and chimeras **8** and **11** exhibited the greatest antibacterial activity against the Gram-negative strains evaluated, while chimera **8** exhibited the greatest antibacterial activity against the Gram-positive strains evaluated. Furthermore, chimeras **8** and **11** exhibited the best results, being considered by us

as promising for drug development for treating bacterial infections. Our results demonstrated that the design of chimeras from short sequences derived from AMPs is a strategy that allows obtaining peptides with enhanced antibacterial activity.

The antibacterial effect of chimeras **8** and **11** was evaluated against *E. coli*, *S. aureus*, and *E. faecalis* strains for 48 h, using three chimeric peptide concentrations, corresponding to 0.5×MIC, MIC, and 2×MIC values (time-kill curves, Table 3). The curves obtained showed that chimera **8** exhibited both bacteriostatic and bactericidal effect against all strains evaluated, being higher in *E. coli* (ATCC 25922 and ATCC 11775) strains. Chimera **8** exhibited the greatest bactericidal and bacteriostatic effect against *E. coli* 25922 strains. On the contrary, chimeric peptide **11** only exhibited a bacteriostatic effect in all the strains evaluated, being higher against *E. coli* strains (Table 3). As an example, the time-kill curves plot for *E. coli* ATCC 11775 and *E. coli* ATCC 25922 strains incubated with chimera **8** are presented in Figure 5. For the time-kill curves of **8** against *E. coli* ATCC 11775; the strain was treated with the chimera at 11, 23, and 46 μM for 48 h. When the chimera concentration was 11 μM (0.5×MIC) and 23 μM (MIC), the adaptation phase was prolonged up to 7 h and 15 h, respectively, while for the control (strain without treatment), the adaptation phase

started after 2 h of treatment, and **8** at 11 μM (MIC) only prolonged the adaptation phase of the *E. coli* ATCC 25922 strain up to 7 h. These results suggest that chimeras containing short sequences derived from LfcinB and BfII increase their antibacterial activity against the strains evaluated, generating bacteriostatic and/or bactericidal effects.

All the chimeras synthesized exhibited a low hemolytic effect at the evaluated chimera concentrations, indicating that the chemical binding of the precursors confers selectivity for bacterial strains. Chimera **8** had MIC values ranging from 11 to 56 μM for the evaluated strains, and their hemolytic effect percentage at these same concentrations was 2% and 9%, respectively. Similarly, chimera **11** showed MIC values from 5.8 to 46 μM, and the hemolytic effect percentage at these same concentrations was 3.8% to 7.1%, respectively.

In order to establish if the mixture of precursor peptides **1** and **2** exhibits the same antibacterial activity as chimeras **6**, **7**, **9**, or **10**, synergy assays were carried out. Precursor peptides **1** and **2** were combined in various concentration ratios, in accordance with the checkerboard methodology. The results indicated that the antibacterial effect of the peptide mixture could be classified as indifferent (FIC > 1.0) in all evaluated ratios, except that when the peptides

Table 3. Hemolytic, bacteriostatic, and bactericide activity of chimeric peptides and synergy test of peptide **1** and **2** mixtures.^[a]

Chimera	Strain	Effect (μM)		μM/H%
		Bacteriostatic	Bactericide	
8	<i>E. coli</i> 11775	23	46	11/5.2
	<i>E. coli</i> 25922	11	23	23/4.5
	<i>S. aureus</i>	46	> 46	46/7.1
	<i>E. faecalis</i>	46	92	92/17.4
11	<i>E. coli</i> 11775	11	> 23	6/3.8
	<i>E. coli</i> 25922	11	> 11	11/4.0
	<i>S. aureus</i>	46	92	46/1
	<i>E. faecalis</i>	46	92	92/15.4

Synergy test in <i>E. coli</i> ATCC 25922					
Peptide 1 and 2 mixture		FIC (MIC)		Index FIC	Activity
(1/2 μg/mL)	1	2			
100/6.25	1.00	0.03		1.03	I
100/12.5	1.00	0.06		1.06	I
100/25	1.00	0.13		1.13	I
50/50	0.50	0.25		0.75	I
50/100	0.50	0.50		1.00	I
25/200	0.25	1.00		1.25	I
Average				1.04	I

^[a] MIC values for **1** (100 μg/mL) and **2** (200 μg/mL); Indifference (I) when FIC > 1.

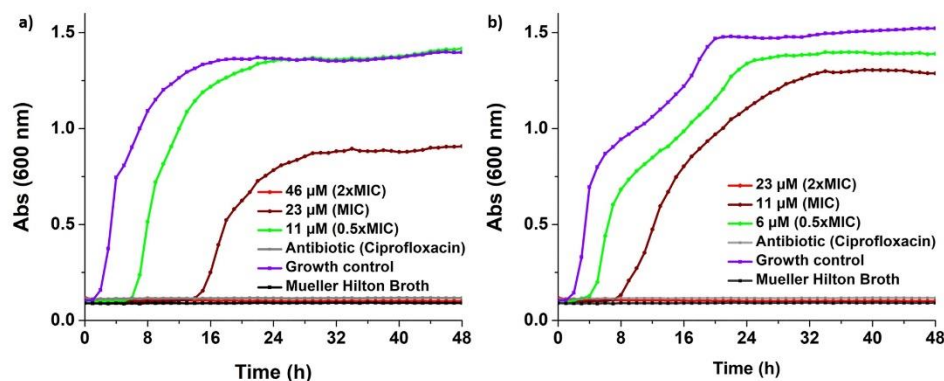


Figure 5. Time-kill curve plot. (a) *E. coli* ATCC 11775 and (b) *E. coli* ATCC 25922 strains were incubated with chimera **8**: RRWQWR-Ahx-RLLRLLR, for 48 h using chimera concentrations corresponding to 0.5×MIC (green line), MIC (brown line), and 2×MIC (red line) values.

ratio was 50/50, the effect was additivity ($FIC > 0.5 < 1$). The mixture of precursor peptides 1 and 2 did not have a synergistic effect on the antibacterial activity at the concentration ratios evaluated. On the other hand, when these sequences were chemically joined, the antibacterial activity increased significantly compared with that of the precursor peptides. In this context, our results confirmed that the chimeras containing short sequences derived from LfcinB and BfII exhibited significant antibacterial activity. Also, it was shown that the antibacterial activity depends on the precursor sequences joined chemically and the use of Ahx as a spacer.

Conclusions

Using the SPPS-Fmoc/^tBu strategy, it was possible to obtain chimeric peptides containing short sequences derived from LfcinB and BfII, which has not been previously reported. The antibacterial activity of chimeras containing the RRWQWR, RLLR, and RLLRLLR sequences was higher compared with the precursor peptides. Chimeras RRWQWR-Ahx-RLLRLLR (**8**) and RLLRLLR-Ahx-RRWQWR (**11**), exhibited the greatest antibacterial activity against the strains evaluated. These chimeras exhibited a bactericidal and bacteriostatic effect, depending on the chimera concentration as well the evaluated strain. The mixture of precursor peptides RRWQWR (**1**) and RLLR (**2**) did not exhibit a synergistic antibacterial effect against the *E.*

coli 25922 strain. The relationship between the design of the studied chimeras in this article and their biological activity allows us to conclude that: (i) incorporation of the spacer molecule (Ahx) modulates the antibacterial activity, increasing the chimera's activity against Gram-negative strains; (ii) chimeras containing two copies of the palindromic minimal motif (RLLR (**2**)) exhibit the greatest antibacterial activity; and (iii) partial replacement of the Arg residues with Lys does not severely affect the MIC values of the chimeric peptides and improves the synthetic process.

Experimental Section

Reagents and Materials

Müller-Hinton, Agar SPC, Müller-Hinton Broth (MHB), *E. coli* ATCC 11775, *E. coli* ATCC 25922, *P. aeruginosa* ATCC 27853, *S. aureus* ATCC 25923 and *E. faecalis* ATCC 29212 were obtained from ATCC (Manassas, VA, USA). *N,N*-Diisopropylethylamine (DIPEA), triisopropylsilane (TIPS), 1,2-ethanedithiol (EDT), 4-methylpiperidine, pyridine, and ninhydrin were obtained from Sigma-Aldrich (St. Louis, MO, USA). Rink amide resin, Fmoc-amino acids, 6-chloro-1-hydroxy-benzotriazole (6-Cl-HOBt), and *N,N*-dicyclohexylcarbodiimide (DCC) were purchased from AAPPTec (Louisville, KY, USA). Methanol, diethyl ether, *N,N*-dimethylformamide (DMF), absolute ethanol, dichloromethane (DCM), acetonitrile (ACN), isopropyl alcohol (IPA), and tri-

fluoroacetic acid (TFA) were obtained from Honeywell Burdick & Jackson (Muskegon, MI, USA). All reagents were used without further purification.

Solid-Phase Peptide Synthesis (SPPS)

Peptides were synthesized using manual solid-phase peptide synthesis with the Fmoc/Bu strategy (SPPS-Fmoc/Bu).^[32] Briefly, Rink amide resin (100 mg, 0.46 meq/g) was used as solid support. (i) Fmoc group removal was carried out through treatment with 2.5% 4-methylpiperidine in *N,N*-dimethylformamide (DMF). (ii) For the coupling reaction, Fmoc-amino acids were pre-activated with DCC/6-Cl-HOBt in DMF at room temperature (iii) Side-chain deprotection reactions and peptide separation from the resin were carried out with a cleavage cocktail containing TFA/water/TIPS/EDT (92.5:2.5:2.5:2.5% v/v). (iv) The crude peptides were precipitated by treatment with cool diethyl ether, dried at r.t., and analyzed using RP-HPLC analytical chromatography.

Purification of Molecules via RP-SPE

The peptides were purified using solid-phase extraction (SPE) on columns of two commercial houses (Silicycle® SiliaPrep™ C18 17%, 5 g, 45 μm, 60 Å and Supelclean™ SPE Tube 17%, 5 g, 45 μm, 60 Å). SPE columns were activated prior to use with 30 mL methanol, 30 mL ACN (containing 0.1% TFA), and were equilibrated with 30 mL water (containing 0.1% TFA). Up to 150 mg of crude peptide was dissolved in 1 to 2 mL of solvent A, and the solution was added to the column. The peptide elution was performed by increasing the percentage of solvent B in the eluent. The collected fractions were analyzed via RP-HPLC and MALDI-TOF MS. The fractions containing the pure peptide were mixed and then lyophilized.^[33]

Reversed-Phase High-Performance Liquid Chromatography (RP-HPLC) Analysis

RP-HPLC analysis was performed on a Chromolith® C-18 (50×4.6 mm) column using an Agilent 1200 liquid chromatograph (Omaha, NE, USA) with UV detector. For the analysis of crude peptides (10 μL, 1 mg/mL), a linear gradient was applied from 5% to 50% solvent B (0.05% TFA in acetonitrile (ACN)) in solvent A (0.05% TFA in water) with a gradient time of 8 min. A delay time of 1.00 min was applied. The flow rate was 2.0 mL/min at r.t. Detection was at 210 nm.

MALDI-TOF MS

This analysis was performed on an Ultraflex III MALDI-TOF mass spectrometer (Bruker Daltonics, Bremen, Germany) in reflectron mode, using an MTP384 polished steel target (Bruker Daltonics), α-cyano-4-hydroxycinnamic acid as a matrix; laser: 500 shots and 25–30% power.

Antibacterial Activity Assays

The minimal inhibitory concentration (MIC) was determined using a microdilution assay.^[13] In brief, bacterial strains (*E. coli* ATCC 11775, *E. coli* ATCC 25922, *P. aeruginosa* ATCC 27853, *S. aureus* ATCC 25923 and *E. faecalis* ATCC 29212) were incubated for 18 to 24 h at 37 °C in Müller-Hinton broth (MHB) until an optical density of 0.15 to 0.30 (620 nm) was obtained. 90 μL of MHB was mixed with 90 μL of peptide (440 μg/mL), and using a 96-well microtiter plate peptide, serial dilution (200, 100, 50, 25, 12.5, and 6.2 μg/mL) was performed. 10 μL of inoculum (2×10^6 CFU/mL) was added to each well. Final volume in each well was 100 μL. Then, they were incubated for 24 h at 37 °C, and the absorbance at 620 nm was measured using an Asys Expert Plus plate reader. For determining the minimum bactericidal concentration (MBC), a small sample was taken from each well using an inoculation loop, which was then spread on Müller-Hinton Agar (MHA) plates and incubated overnight at 37 °C. MBC was considered to be the plate which exhibited no bacterial growth. Each of these tests was performed twice ($n = 2$).

Time-Kill Curve

The time-kill curve was constructed using the CLSI protocol, with some modifications.^[34,35] Before testing, the bacterial strains of *E. coli* ATCC 11775, *E. coli* ATCC 25922, *P. aeruginosa* ATCC 27853, *S. aureus* ATCC 25923 and *E. faecalis* ATCC 29212 were subcultured in Tryptic Soy Agar. The colonies of a 24 h culture were suspended in 9 mL of Heart Infusion Broth and adjusted to a standard by means of a calibration curve, these procedures resulted in an initial inoculum of approximately 5×10^5 CFU/mL. The final working volumes in the peptide (0.25×MIC, MIC, and 2×MIC final concentrations) and inoculum experiments were 270 μL and 30 μL, respectively. The samples were incubated on a Bioscreen C equipment for 48 h at 37 °C and absorbance readings (600 nm) were ob-

tained at 0 h (before the addition of peptide) and then repeatedly every hour until the completion of 48 h.

Synergy Test

The synergy test was performed according to the checkerboard method.^[34] 25 μ L of peptide 1 and 25 μ L of peptide 2 were mixed (final concentrations: 0; 0.06; 0.12; 0.25; 0.50; 1 and 2 times the MIC) in order to obtain all possible combinations between them. Then, 50 μ L of inoculum of *E. coli* ATCC 25922 (5×10^5 CFU/mL) was added and incubated at 37°C for 16–20 h, and the new MIC was established. The fractional inhibitory concentration (FIC) index was calculated as follows:

$$\frac{(1)}{\text{MIC}(1)} + \frac{(2)}{\text{MIC}(2)} = \text{FIC}$$

Where MIC(1) and MIC(2) are the MICs of the two peptides. The MICs of the peptides determined in combination correspond to **1** and **2**, respectively. Combinations were classified as synergistic (FIC = 0.5), indifferent ($0.5 < \text{FIC} < 4$), and antagonist (FIC > 4).

Hemolysis Assay

5.0 mL of heparinized peripheral blood was centrifuged at 1000 rpm for 7 min. All experiments were approved by the Universidad Nacional de Colombia ethical committee (code number 04-19 2019). Informed consent of all participating subjects was obtained. The erythrocyte fraction was suspended in 10 μ L of saline solution (SS) and washed twice by centrifugation at 1000 rpm for 7 min. The erythrocytes (2% hematocrit) were incubated with peptide (ranging from 6.2 to 200 μ g/mL), for 2 h at 37°C. SS was used as negative control, while distilled water was used as positive control. The mixtures were centrifuged, the supernatants were collected, and the absorbance was determined to be 540 nm.^[34,36]

Acknowledgements

This research was conducted with the financial support of COLCIENCIAS 844-2019, Project: 'Diseño y obtención de nuevos agentes antibacterianos basados en dendrímeros péptido-resorcinareno: Una alternativa para combatir la resistencia bacteriana', Code 45746, RC 846-2019.

Author Contribution Statement

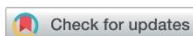
Héctor Manuel Pineda-Castañeda and Zuly Jenny Rivera-Monroy designed the chimeric peptides. Héctor Manuel Pineda-Castañeda synthesized these peptides. Héctor Manuel Pineda-Castañeda and Yerly Vargas-Casanova performed the antibacterial assays. Héctor Manuel Pineda-Castañeda, Kevin Andrey Huertas-Ortiz, Aura Lucía Leal-Castro, Claudia Marcela Parra-Giraldo, Javier Eduardo García-Castañeda and Zuly Jenny Rivera-Monroy participated in writing the article.

References

- [1] 'WHO | WHO publishes list of bacteria for which new antibiotics are urgently needed', can be found under <http://www.who.int/mediacentre/news/releases/2017/bacteria-antibiotics-needed/en/>, 2017.
- [2] 'WHO | World Health Organization', can be found under http://www.who.int/antimicrobial-resistance/Microbes_and_Antimicrobials/en/, 2016.
- [3] J. Castañeda-Casimiro, J. A. Ortega-Roque, A. Marcela, A. Aquino-Andrade, J. Serafín-López, S. Estrada-Parra, I. Estrada, 'Péptidos antimicrobianos: péptidos con múltiples funciones', *Alergia, asma e Inmunol.* **2009**, *18*, 16–29.
- [4] Z. Guo, H. Peng, J. Kang, D. Sun, 'Cell-penetrating peptides: Possible transduction mechanisms and therapeutic applications', *Biomed. Rep.* **2016**, *4*, 528–534.
- [5] M. Arias, L. J. McDonald, E. F. Haney, K. Nazmi, J. G. M. Bolscher, H. J. Vogel, 'Bovine and human lactoferricin peptides: Chimeras and new cyclic analogs', *BioMetals* **2014**, *27*, 935–948.
- [6] Y. F. Liu, X. Xia, L. Xu, Y. Z. Wang, 'Design of hybrid β -hairpin peptides with enhanced cell specificity and potent anti-inflammatory activity', *Biomaterials* **2013**, *34*, 237–250.
- [7] M. Arias, A. L. Hilchie, E. F. Haney, J. G. M. Bolscher, M. E. Hyndman, R. E. W. Hancock, H. J. Vogel, 'Anticancer activities of bovine and human lactoferricin-derived peptides', *Biochem. Cell Biol.* **2017**, *95*, 91–98.
- [8] J. L. Gifford, H. N. Hunter, H. J. Vogel, 'Lactoferricin: A lactoferrin-derived peptide with antimicrobial, antiviral, antitumor and immunological properties', *Cell. Mol. Life Sci.* **2005**, *62*, 2588–2598.
- [9] S. Farnaud, R. W. Evans, 'Lactoferrin – A multifunctional protein with antimicrobial properties', *Mol. Immunol.* **2003**, *40*, 395–405.
- [10] S. Farnaud, C. Spiller, L. C. Moriarty, A. Patel, V. Gant, E. W. Odell, R. W. Evans, 'Interactions of lactoferricin-derived peptides with LPS and antimicrobial activity', *FEMS Microbiol. Lett.* **2004**, *233*, 193–199.
- [11] N. D. J. Huertas Méndez, Y. Vargas Casanova, A. K. Gómez Chimbi, E. Hernández, A. L. Leal Castro, J. M. Meló Díaz, Z. J. Rivera Monroy, J. E. García Castañeda, 'Synthetic Peptides Derived from Bovine Lactoferricin Exhibit Antimicrobial Activity against *E. coli* ATCC 11775, *S. maltophilia* ATCC 13636 and *S. enteritidis* ATCC 13076', *Molecules* **2017**, *22*, 1–10.

- [12] N. de J. Huertas, Z. J. R. Monroy, R. F. Medina, J. E. G. Castañeda, 'Antimicrobial Activity of Truncated and Poly-valent Peptides Derived from the FKRRQWQWRMKKGLA Sequence against *Escherichia coli* ATCC 25922 and *Staphylococcus aureus* ATCC 25923', *Molecules* **2017**, *22*, DOI: 10.3390/molecules22060987.
- [13] Y. Vargas Casanova, J. A. Rodríguez Guerra, Y. A. Umaña Pérez, A. L. Leal Castro, G. Almanzar Reina, J. E. García Castañeda, Z. J. Rivera Monroy, 'Antibacterial Synthetic Peptides Derived from Bovine Lactoferricin Exhibit Cytotoxic Effect against MDA-MB-468 and MDA-MB-231 Breast Cancer Cell Lines', *Molecules* **2017**, *22*, 1–11.
- [14] S. C. Vega, D. A. Martínez, M. del S. Chala, H. A. Vargas, J. E. Rosas, 'Design, Synthesis and Evaluation of Branched RRWQWR-Based Peptides as Antibacterial Agents Against Clinically Relevant Gram-Positive and Gram-Negative Pathogens', *Front. Microbiol.* **2018**, *9*, 329.
- [15] C. B. Park, H. S. Kim, S. C. Kim, 'Mechanism of action of the antimicrobial peptide buforin II: Buforin II kills microorganisms by penetrating the cell membrane and inhibiting cellular functions', *Biochem. Biophys. Res. Commun.* **1998**, *244*, 253–257.
- [16] C. B. Park, K. Yi, K. Matsuzaki, M. S. Kim, S. C. Kim, 'Structure-activity analysis of buforin II, a histone H2A-derived antimicrobial peptide: The proline hinge is responsible for the cell-penetrating ability of buforin II', *Proc. Natl. Acad. Sci. USA* **2000**, *97*, 1–6.
- [17] J. Hyun, B. Hyun, S. Chang, 'Buforins: Histone H2 A-derived antimicrobial peptides from toad stomach', *BBA-Biomembranes* **2009**, *1788*, 1–9.
- [18] S. A. Jang, H. Kim, J. Y. Lee, J. R. Shin, D. J. Kim, J. H. Cho, S. C. Kim, 'Mechanism of action and specificity of antimicrobial peptides designed based on buforin IIb', *Peptides* **2012**, *34*, 283–289.
- [19] H. M. Pineda-Castañeda, L. D. Bonilla-Velásquez, A. L. Leal-Castro, R. Fierro-Medina, J. E. García-Castañeda, Z. J. Rivera-Monroy, 'Use of Click Chemistry for Obtaining an Antimicrobial Chimeric Peptide Containing the LfcinB and Buforin II Minimal Antimicrobial Motifs', *ChemistrySelect* **2020**, *5*, 1655–1657.
- [20] P. Lloyd-Williams, F. Albericio, E. Giralt, 'Chemical Approaches to the Synthesis of Peptides and Proteins', CRC Press, 1997.
- [21] M. Arias, K. Piga, M. Hyndman, H. Vogel, 'Improving the Activity of Trp-Rich Antimicrobial Peptides by Arg/Lys Substitutions and Changing the Length of Cationic Residues', *Biomol. Eng.* **2018**, *8*, 19.
- [22] L. Li, I. Vorobyov, T. W. Allen, 'The different interactions of lysine and arginine side chains with lipid membranes', *J. Phys. Chem. B* **2013**, *117*, 11906–11920.
- [23] S. Bouchet, R. Tang, F. Fava, O. Legrand, B. Bauvois, 'The CNGRC-GG_D(KLAKLAK)₂ peptide induces a caspase-independent, Ca²⁺-dependent death in human leukemic myeloid cells by targeting surface aminopeptidase N/CD13', *Oncotarget* **2016**, *7*, 19445–19467.
- [24] K. E. Burns, T. P. McCleerey, D. Thévenin, 'PH-Selective Cytotoxicity of pHLLP-Antimicrobial Peptide Conjugates', *Sci. Rep.* **2016**, *6*, 1–10.
- [25] E. H. Ryu, E. J. Yang, E. R. Woo, H. C. Chang, 'Purification and characterization of antifungal compounds from *Lactobacillus plantarum* HD1 isolated from kimchi', *Food Microbiol.* **2014**, *41*, 19–26.
- [26] J. Y. Kim, J. H. Han, G. Park, Y. W. Seo, C. W. Yun, B. C. Lee, J. Bae, A. R. Moon, T. H. Kim, 'Necrosis-inducing peptide has the beneficial effect on killing tumor cells through neuropilin (NRP-1) targeting', *Oncotarget* **2016**, *7*, 10.
- [27] K. A. Camillo, Ø. Rekdal, B. Sveinbjörnsson, 'LTX-315 (Oncopore™): A short synthetic anticancer peptide and novel immunotherapeutic agent', *Oncoimmunology* **2014**, *3*, 7–9.
- [28] M. A. León-Calvijo, Z. J. Rivera-Monroy, A. L. Leal-Castro, J. E. García-Castañeda, G. A. Almanzar-Reina, J. E. Rosas-Pérez, 'Antibacterial Activity of Synthetic Peptides Derived from Lactoferricin against *Escherichia coli* ATCC 25922 and *Enterococcus faecalis* ATCC 29212', *BioMed Res. Int.* **2015**, *2015*, 1–8.
- [29] X. Carolina Pulido, M. Royo, F. Albericio, H. Rodríguez, 'Péptidos que atraviesan la membrana celular como potenciales transportadores de fármacos', *Bionatura* **2016**, *1*, 208–216.
- [30] J. Regberg, A. Srimanee, Ü. Langel, 'Applications of Cell-Penetrating Peptides for Tumor Targeting and Future Cancer Therapies', *Pharmaceuticals* **2012**, *5*, 991–1007.
- [31] G. Xu, W. Xiong, Q. Hu, P. Zuo, B. Shao, F. Lan, X. Lu, Y. Xu, S. Xiong, 'Lactoferrin-derived peptides and Lactoferricin chimera inhibit virulence factor production and biofilm formation in *Pseudomonas aeruginosa*', *J. Appl. Microbiol.* **2010**, *109*, 1311–1318.
- [32] V. Rodríguez, H. Pineda, N. Ardila, D. Insuasty, K. Cárdenas, J. Román, M. Urea, D. Ramírez, R. Fierro, Z. Rivera, J. García, 'Efficient Fmoc Group Removal Using Diluted 4-Methylpiperidine: An Alternative for a Less-Polluting SPPS-Fmoc/Bu Protocol', *Int. J. Pept. Res. Ther.* **2020**, *26*, 585–587.
- [33] D. Insuasty Cepeda, H. Pineda Castañeda, A. Rodríguez Mayor, J. García Castañeda, M. Maldonado Villamil, R. Fierro Medina, Z. Rivera Monroy, 'Synthetic Peptide Purification via Solid-Phase Extraction with Gradient Elution: A Simple, Economical, Fast, and Efficient Methodology', *Molecules* **2019**, *24*, 1215.
- [34] Y. Vargas-Casanova, A. V. Rodríguez-Mayor, K. J. Cardenas, A. L. Leal-Castro, L. C. Muñoz-Molina, R. Fierro-Medina, Z. J. Rivera-Monroy, J. E. García-Castañeda, 'Synergistic bactericide and antibiotic effects of dimeric, tetrameric, or palindromic peptides containing the RWQWR motif against Gram-positive and Gram-negative strains', *RSC Adv.* **2019**, *9*, 7239–7245.
- [35] M. D. C. S. Arthur L. Barry, P. D. William A. Craig, M. D. Harriette Nadler, P. D. L. Barth Reller, 'M26-A: Methods for Determining Bactericidal Activity of Antimicrobial Agents; Approved Guideline', *Clin. Lab. Stand. Inst.* **1999**, *19*, 56–78.
- [36] V. Solarte, J. Rosas, Z. Rivera, J. E. García, M. Arango, J.-P. Vernot, 'A tetrameric peptide derived from bovine lactoferricin exhibits specific cytotoxic effects against Oral Squamous-Cell Carcinoma Cell Line', *BioMed Res. Int.* **2015**, *13*.

Received October 29, 2020
 Accepted December 21, 2020

Cite this: *RSC Adv.*, 2020, 10, 29580

Short peptides conjugated to non-peptidic motifs exhibit antibacterial activity

Natalia Ardila-Chantré,^a Angie Katherine Hernández-Cardona,^b Hector Manuel Pineda-Castañeda,^b Sandra Mónica Estupiñán-Torres,^b Aura Lucía Leal-Castro,^c Ricardo Fierro-Medina,^d Zuly Jenny Rivera-Monroy^b and Javier Eduardo García-Castañeda^{b,*a}

Short peptides derived from buforin and lactoferricin B were conjugated with other antimicrobial molecules of different chemical natures. The sequences RLLR, RLLRLLR, RWQWRWQWR, and RRWQWR were conjugated at their N-terminal end with non-peptidic molecules such as 6-aminohexanoic acid, ferrocene, caffeic acid, ferulic acid, and oxolinic acid. Peptide conjugates and unmodified peptides were synthesized by means of solid-phase peptide synthesis using the Fmoc/tBu strategy (SPPS-Fmoc/tBu), purified via RP-SPE, and characterized via RP-HPLC and MS. The peptides' antibacterial activity against bacterial strains *E. coli* ATCC 25922 and *S. aureus* ATCC 25923 was evaluated, and the results showed that the peptide conjugates exhibited higher antibacterial activity than the original unconjugated peptides. Conjugation of AMPs is a promising strategy for designing and identifying new drugs for treating bacterial infections.

Received 7th July 2020
Accepted 30th July 2020

DOI: 10.1039/d0ra05937d

rsc.li/rsc-advances

Introduction

The increase in the resistance of pathogens to conventional antibiotics and the lack of therapeutic options for treating infections has led the World Health Organization (WHO) to consider the promotion of the development of new antibacterial drugs to be a priority.¹ The identification and development of new antibacterial agents based on antimicrobial peptides (AMPs) has emerged as a novel alternative that can replace and/or complement conventional treatments. AMPs have been identified in prokaryotes and eukaryotes, they exhibit a broad activity spectrum against bacteria, fungi, viruses, and parasites, and they exhibit multiple action mechanisms and have a low potential for inducing resistance.^{2–4}

The AMP buforin (¹AGRGKQGGKVRAKAKTRSSRAGLQFPVGRVHRLLRKGNK³⁹) is a 39-amino acid peptide isolated from the stomach tissue of the toad *Bufo garzizans*. Buforin II (¹⁶TRSSRAGLQFPVGRVHRLLRK³⁷) is a 21-amino acid peptide, and its sequence is identical to the N-terminal region of histone H2A. This peptide exhibited antimicrobial activity similar to buforin.⁵ It can be translocated across the bacterial membranes and can bind to DNA and RNA

without damaging the cell membrane.^{6,7} Buforin IIb (RAGLQFPVGRLLRLLRLLRLLR) is an analogue peptide of buforin II that contains three times the RLLR motif, and it has exhibited significant antimicrobial activity.⁵

Lactoferricin B (¹⁷FKRRWQWRMCKLGLGAPSTCVRRAF⁴¹) is a 25-amino acid peptide located in the N-terminal region of bovine lactoferrin protein (BLF).^{8,9} LfcinB was identified in the hydrolysate of BLF caused by the gastric pepsin, and the antibacterial activity of LfcinB is greater than that of the native protein.^{8,10–12} LfcinB exhibited antibacterial, antifungal, antiviral, antiparasitic, and anticancerigenic activity in *in vitro* and *in vivo* assays.^{8,13–15} It has been suggested that the antibacterial activity of LfcinB is mediated by the electrostatic interaction between the positively-charged amino acid side chains (Arg and Lys) and the negative charges of the bacterial surface molecules of Gram-positive (teichoic acid) and Gram-negative (LPS) strains. So there is an interaction between the side chains of hydrophobic residues (Trp) and the lipid bilayer, causing membrane disruption and cellular lysis.^{8,16,17} Also, it has been reported that LfcinB can internalize into the cell, suggesting intracellular targets.^{18,19} On the other hand, previous studies have shown that short peptides derived from LfcinB exhibited significant antibacterial activity, a characteristic similar to that of LFB and LfcinB. The RRWQWR sequence has been reported to be the minimal motif with antibacterial, antifungal, and anticancerigenic activity.^{9,20,21} Peptide Rh-RRWQWR which containing rhodamine at its N-terminal end showed greater activity against *E. coli* JM-109 than the unmodified peptide. The peptide can be translocated through the plasma membrane of

^aDepartamento de Ciencias, Universidad Nacional de Colombia, Carrera 45 No. 26-85, Building 450, Office 203, Bogotá, Zip Code 11321, Colombia. E-mail: jaegarciaca@unal.edu.co

^bDepartamento de Bacteriología, Universidad Colegio Mayor de Cundinamarca, Bogotá Calle 28 No. 5B-02, Bogotá 110311, Colombia

^cFacultad de Medicina, Universidad Nacional de Colombia, Carrera 45 No. 26-85, Building 471, Bogotá, Zip Code 11321, Colombia



Paper

E. coli without affecting the integrity of the membrane and the translocation depends of peptide concentration. In addition, this peptide binds to the DNA suggesting that this molecule could be a possible target.²² The palindromic peptide LfcinB (20–25)_{pal} RWQWRWQWR exhibited greater antimicrobial activity against Gram-negative and Gram-positive strains than the minimal motif, LFB and LfcinB.^{21,23–25}

The development of new drugs based on the improvement of existing AMPs through the modification of their structure is a promising strategy. Also, the aim is to reduce manufacturing costs by obtaining short sequences with greater antibacterial activity.²⁶ Through the strategy called conjugation, it is possible to obtain new entities from the union of sequences derived from AMPs such as buforin and LfcinB with other antimicrobial molecules, with the aim of enhancing their antibacterial activity.^{27,28} In the present investigation, sequences derived from buforin (RLLR, RLLRLLR) and LfcinB (RRWQWR, RWQWRWQWR) were synthesized by means of SPPS Fmoc/*t*Bu and conjugated with non-peptidic organic molecules such as 6-aminohexanoic acid (Ahx), ferrocene (Fc), caffeic acid (CA), ferulic acid (FA), and oxolinic acid (OA) (Fig. 1). We evaluated the synthetic viability and established if the incorporation of these molecules into peptidic sequences enhanced the antibacterial activity against *E. coli* ATCC 25922 and *S. aureus* ATCC 25923.

Fc is a metallocene that exhibits antimalarial, antitumor, and antibacterial properties. This compound has been incorporated into a variety of molecules in order to improve their biological activity.²⁹ Metzler-Nolte *et al.* synthesized OM-AMPs by conjugating Fc during SPPS. They found that the incorporation of Fc in some cases improved the antibacterial activity compared to the peptides used as a control. For example, the Fc-

WRWRW peptide exhibited antibacterial activity against *S. aureus* with a minimum inhibitory concentration (MIC) of 7 μ M, while the WRWRW sequence had an MIC of 16 μ M against the same strain.^{30,31} Other studies suggest that the antibacterial activity of peptides is affected by the metallocene conjugated to AMPs, as well as the position in the sequence.³²

CA and FA are phenolic acids derived from the secondary metabolism of plants and have antibacterial and antioxidant properties.³³ These molecules exhibit a broad spectrum of antimicrobial activity against Gram-positive and Gram-negative bacteria such as *E. coli*, *S. aureus*, *L. monocytogenes*, and *B. cereus*, as well as against fungi such as *C. albicans*.^{34,35}

OA is a first-generation synthetic quinolone; it has been used as an antibacterial drug. It exhibits restricted antibacterial activity against Gram-negative aerobic bacteria, particularly Enterobacteriaceae such as *E. coli*. Because of its narrow spectrum of activity and the emergence of resistance, it has been replaced by third- and fourth-generation quinolones.^{36,37}

In the present investigation, peptide conjugates derived from LfcinB and Buforin containing 6-aminohexanoic acid (Ahx), ferrocene (Fc), caffeic acid (CA), ferulic acid (FA), and oxolinic acid (OA) were synthesized by employing the SPPS method. The antibacterial activity of these peptide conjugates against *S. aureus* and *E. coli* strains was evaluated, and the results showed that the incorporation of these non-peptidic molecules can increase the antibacterial activity, suggesting that conjugation of AMPs is a viable strategy for identifying promising peptides for the treatment of bacterial infections.

Experimental details

Solid-phase peptide synthesis

The peptides were synthesized using the manual solid-phase peptide synthesis (SPPS) Fmoc/*t*Bu strategy. 100 mg of Rink amide resin (0.46 meq. g^{-1}) was treated with DCM for 2 h at room temperature (RT), and the mixture was gently stirred. The Fmoc group removal was carried out through treatment of resin or resin-peptide with 2.5% 4-methylpiperidine in DMF (2×10 min). Then the resin was washed with DMF (5×1 min), and DCM (5×1 min).³⁸ The coupling reaction was performed by mixing Fmoc-amino acid (0.21 mmol) with DCC/6-Cl-HOBt (0.20/0.21 mmol) in DMF at RT for 15 min. Then the reaction mixture was added to the resin or resin-peptide and stirred for 2 h at RT. After that, the resin was washed with DMF (3×1 min) and DCM (2×1 min). Fmoc group removal and the incorporation of each amino acid was confirmed by the Kaiser test. Amino acid side chain deprotection and peptide separation from the resin were carried out by treatment with resin-peptide dried with solution containing TFA/water/TIPS/EDT (92.5/2.5/2.5/2.5; v/v) for 6–8 h at RT and shaking. The crude peptides were precipitated by treatment with cool ethyl ether and washed with ethyl ether (5 \times), after which they were dried at RT.

Peptide conjugates

All peptides were obtained simultaneously, to guaranty that the products were homogeneous, each reactor was initially loaded with

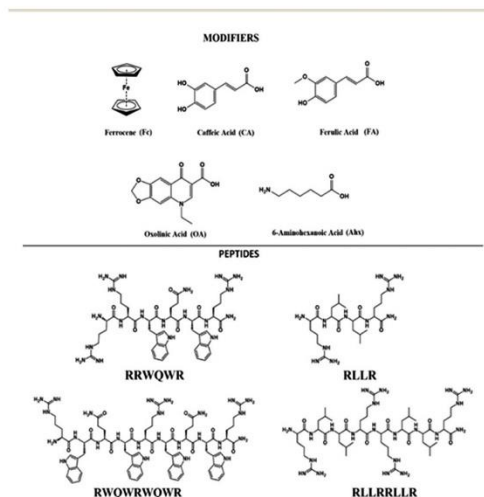


Fig. 1 Chemical structure of peptide sequences and non-peptidic molecules bound to peptides.



500 mg of resin, after incorporating the last amino acid of the sequence, the resin was divided into five parts, and they were loaded into five new reactors. In each reactor a non-peptidic molecule was incorporated to the peptide-resin, those reactions were monitored by Kaiser test, in all cases the test indicated complete reaction. The peptide conjugation was performed during the SPPS. The modifier was incorporated at the N-terminal position of the peptide using uronium salts as activators. The non-peptidic molecule (0.21 mmol) was pre-activated with DIPEA/TBTU (0.60/0.21 mmol) in DMF at RT for 5 min. Then, the activated modifier was mixed with resin-peptide and the reaction mixture was gently stirred for 4 h at RT (Scheme 1).³⁵ After that, the resin was washed with DMF (3 × 1 min) and DCM (2 × 1 min), and the reaction was monitored by means of the Kaiser test. Side chain deprotection reactions and peptide conjugate separation from the resin were carried out by treatment with a cleavage cocktail containing TFA/water/TIPS/EDT (92.5/2.5/2.5/2.5; v/v) for 6–8 h at RT and shaking. Then, crude peptides were precipitated by treatment with cool ethyl ether, dried at RT, and analysed using RP-HPLC analytical chromatography.

Reverse-phase HPLC

The peptides (10 μL , 1 mg mL^{-1}) were analyzed on a Merck Chromolith® C18 (50 × 4.6 mm) column, using an Agilent 1200 liquid chromatograph (Omaha, NE, USA) with UV-Vis detector (210 nm). A linear gradient was employed, from 5% to 70% solvent B (0.05% TFA in ACN) in solvent A (0.05% TFA in water) for 10 min at a flow rate of 2.0 mL min^{-1} at RT.

Peptide purification

All the peptides were purified *via* RP-SPE chromatography, using the method reported by Insuasty *et al.*³⁹ Briefly, solid-phase extraction columns (SUPELCO LC-18; 2.0 g) were activated with methanol, solvent B (acetonitrile containing 0.05% TFA), and solvent A (water containing 0.05% TFA) in accordance with the supplier's recommendations. The crude peptide was injected into the column and eluted using a gradient of solvent B (5–50%). The collected fractions were analyzed *via* RP-HPLC chromatography, and those that contained the pure peptide were collected and lyophilized.

MALDI-TOF MS

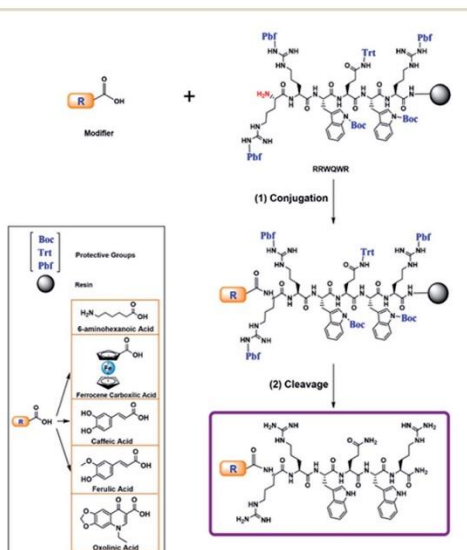
The purified peptides were analyzed following the method described by Roman *et al.* Briefly, the peptide (1 mg mL^{-1}) was mixed with the matrix (1.0 mg mL^{-1} of 2,5-dihydroxybenzoic acid, or sinapinic acid) (2 : 18, v/v), and then 1 μL of this mixture was seeded on a steel target. The experiment was carried out on an Ultraflex III TOF-TOF mass spectrometer (Bruker Daltonics, Bremen, Germany) in reflectron mode, using an MTP384 polished steel target (Bruker Daltonics). Laser: 500 shots and 25–30% power.

Minimum inhibitory concentration (MIC) assay

The minimum inhibitory concentration (MIC) was determined using the broth microdilution protocol from the Clinical and Laboratory Standards Institute guidelines,⁴⁰ in accordance with Vargas *et al.* Briefly, in a 96-well microtiter plate, 90 μL of peptide (200, 100, 50, 25, 12.5 and 6.2 $\mu\text{g mL}^{-1}$) and 10 μL of inoculum (5×10^6 CFU mL^{-1}) were added. After the mixture was incubated at 37 °C for 24 h, the absorbance was measured at 620 nm using an ELISA Human Reader. The MIC was defined as the lowest peptide concentration (μM) required to inhibit visible microbial growth. The MICs were the average values obtained in duplicate in two independent experiments. To determine the minimum bactericidal concentration (MBC), a small sample was taken from each well where there was no visible growth, using an inoculation loop, which was then spread on MHA plates and incubated overnight at 37 °C.⁴⁰ The MBC was considered to be the peptide concentration corresponding to the plate that showed no bacterial growth. Each of these tests was performed twice ($n = 2$).

Results and discussion

The development of new, effective, and safe antibacterial drugs is a priority for the treatment of infections caused by resistant bacterial strains. The conjugation of peptides has allowed modifying the properties of peptides and increasing their antibacterial activity and has become an alternative to the development of new antibiotic drugs. In the present investigation, sequences derived from buforin (RLLR and RLLRLLR) and LfcinB (RRWQWR and RWQWRWQWR) were functionalized with non-peptidic molecules containing carboxyl groups such as 6-aminohexanoic acid (Ahx), ferrocene, caffeic acid (CA), ferulic acid (FA), and oxolinic acid (OA), which have



Scheme 1 Conjugation of peptides during SPPS with different modifiers.

antioxidant and antibacterial properties (Fig. 1). These non-peptidic organic molecules have diverse chemical structures and different physicochemical properties. However, they contain a carboxyl group in their structure that allows them to attach to the amine group at the N-terminal end of the sequence through an amide bond during SPPS (Scheme 1). The peptides and peptide conjugates were obtained in similar way and the synthesis had no difficulties. The non-peptidic molecules incorporation into peptide chain was completed as Kaiser test indicated. All peptides were synthesized simultaneously, each reactor contained initially 500 mg of resin, after the last amino acid was incorporated, the peptide-resin was dried, weighted and divided in five new reactors, and then each non-peptidic molecule was incorporated. The sequences used in this investigation are: (i) LfcinB (20–25): RRWQWR, (ii) LfcinB (21–25)_{Pal}: RWQWRWQWR, BFII (32–35): RLLR, and BFII (32–35)_{Pal}: RLLRLLR (Fig. 1). These peptide sequences are derived from two AMPs that exert their antibacterial activity in different ways: LfcinB disrupts bacterial cell membranes, and Buforin is a cell-penetrating peptide that doesn't affect the membrane. Peptide conjugates were designed containing an Ahx residue at the N-terminal, which is a spacer for facilitating the incorporation of non-peptidic molecules (Fig. 2).

The coupling of non-peptidic molecules to the growing chain during the SPPS method was carried out using TBTU/DIPEA reagents, this being an efficient strategy. The conjugation reactions were carried out using a 3 molar excess of reagents with respect to the resin equivalents to guarantee complete reaction. The conjugated and control peptides were obtained using the SPPS-Fmoc/*t*Bu method, with high chromatographic purity in most cases (Fig. 3). The unmodified peptides and those that contained Ahx, Fc, and CA exhibited chromatographic purity higher than 90%, suggesting that the incorporation of the Ahx, FC, and CA does not affect the synthesis efficiency independently of the amino acid sequence. Incorporating Ahx

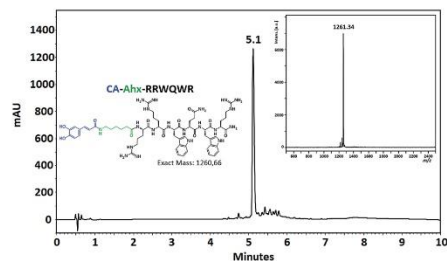


Fig. 3 Chromatographic profile and MALDI-TOF mass spectrum of the conjugated peptide CA-Ahx-RRWQWR.

residue confers hydrophobicity to the peptide sequence, which agrees with the t_R observed in the chromatographic profiles (Table 1). In the same way, the incorporation of the non-peptidic molecule into a sequence increased its hydrophobicity, since the t_R for each conjugate peptide was higher than that of the t_R of the analogous unconjugated. MALDI-TOF MS of the conjugate peptides showed that the purified products had the expected mass in all cases. In the mass spectra of the peptides containing Fc, a signal with 120 mass units less than the expected mass was observed. This signal can be attributed to the molecule with no cyclopentadienyl ring. The loss of this ring could occur during sample ionization. This behavior concurs with that found in previous papers that have reported this phenomenon.⁴¹

In the present study, 24 peptides (4 peptide controls and 20 peptide conjugates) were obtained, and it was possible to establish the experimental conditions for the conjugation of linear peptides derived from LfcinB and buforin at the N-terminus using the SPPS Fmoc/*t*Bu method. The antibacterial

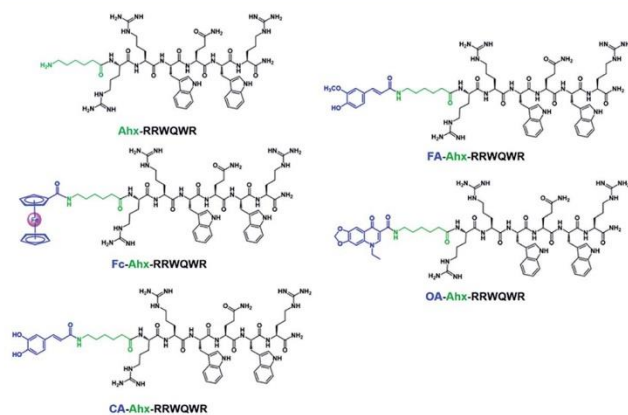


Fig. 2 Peptide conjugates with sequence RRWQWR and different modifiers. Ahx: 6-aminohexanoic acid, Fc: ferrocene, CA: caffeic acid, FA: ferulic acid, OA: oxolinic acid.



Table 1 Analytical characterization and antibacterial activity of peptide conjugates derived from buforin and bovine lactoferricin

Peptide sequence	RP-HPLC		MALDI TOF MS	Antibacterial activity MIC (MBC) in μM	
	t_{R} (min)	Purity (%)	m/z [M + H] ⁺	<i>E. coli</i> ATCC 25922	<i>S. aureus</i> ATCC 25923
RRWQWR	4.0	98	986.5	203 (203)	203 (>203)
Ahx-RRWQWR	4.3	98	1099.6	182 (182)	>182 (>182)
Fc-Ahx-RRWQWR	6.0	92	1311.9	76 (76)	153 (153)
CA-Ahx-RRWQWR	5.1	71	1261.3	79 (159)	159 (159)
FA-Ahx-RRWQWR	5.5	93	1275.7	157 (157)	39 (78)
OA-Ahx-RRWQWR	5.8	81	1343.5	75 (149)	37 (149)
RWQWRWQWR	5.8	99	1485.1	17 (34)	135 (>135)
Ahx-RWQWRWQWR	5.8	97	1600.3	63 (63)	16 (16)
Fc-Ahx-RWQWRWQWR	6.8	91	1812.2	>110 (>110)	55 (>110)
CA-Ahx-RWQWRWQWR	6.3	73	1762.8	57 (57)	28 (114)
FA-Ahx-RWQWRWQWR	6.5	81	1773.4	113 (113)	56 (113)
OA-Ahx-RWQWRWQWR	6.9	78	1843.6	7 (7)	54 (109)
RLLR	2.9	97	556.2	>360 (>360)	>360 (>360)
Ahx-RLLR	3.1	98	670.4	>299 (>299)	>299 (>299)
Fc-Ahx-RLLR	6.2	96	882.3	227 (227)	>227 (>227)
CA-Ahx-RLLR	5.1	95	832.5	>241 (>241)	60 (241)
FA-Ahx-RLLR	5.5	70	846.4	>237 (237)	237 (>237)
OA-Ahx-RLLR	6.0	87	912.9	110 (110)	27 (27)
RLLRLLR	4.3	96	1094.5	91 (183)	>183 (>183)
Ahx-RLLRLLR	5.2	97	1207.3	166 (166)	166 (166)
Fc-Ahx-RLLRLLR	7.2	97	1419.5	70 (141)	35 (70)
CA-Ahx-RLLRLLR	6.4	92	1370.0	37 (73)	73 (146)
FA-Ahx-RLLRLLR	6.7	87	1383.5	36 (72)	36 (72)
OA-Ahx-RLLRLLR	7.2	66	1451.5	34 (69)	17 (17)
Fc-COOH	—	—	—	>869 (>869)	>869 (>869)
CA	—	—	—	>1111 (>1111)	>1111 (>1111)
FA	—	—	—	>1031 (>1031)	>1031 (>1031)
OA	—	—	—	3/6	383 (>766)

activity of the unmodified peptides and peptide conjugates against *E. coli* ATCC 25922 and *S. aureus* ATCC 25923 strains was evaluated (Table 1). In *E. coli* ATCC 25922, peptide conjugates containing the motif RRWQWR exhibited lower values of MIC/MBC than the unmodified peptide (203 μM). Peptides OA-Ahx-RRWQWR, CA-Ahx-RRWQWR, and Fc-Ahx-RRWQWR, with MIC values of 75, 76, and 79 μM , respectively, exhibited the highest antibacterial activity against this strain. These results suggest that the inclusion of OA-Ahx, CA-Ahx, or Fc-Ahx at the N-terminal end of the sequence RRWQWR enhances its antibacterial activity against *E. coli* ATCC 25922. Similarly, peptide conjugates containing the RRWQWR sequence exhibited greater antibacterial activity against *S. aureus* ATCC 25923 than the unmodified peptide (MIC = 203 μM). Conjugate peptides OA-Ahx-RRWQWR and FA-Ahx-RRWQWR, with MIC values of 39 and 37 μM , respectively, exhibited the greatest activity against this strain. The antibacterial activity of peptide conjugates containing RRWQWR sequence could be due to the antibacterial activity additive effect of both the peptide and the non-peptidic molecule. Our results are in accordance with Moniruzzaman *et al.*²² report, since they found that the rhodamine incorporation at the RRWQWR sequence N-terminus end increases the antimicrobial activity against *E. coli* (JM-109). This suggests that the antibacterial activity of the conjugated peptides

may be associated with damage to the bacterial plasma membrane which leads to cellular lysis in according with the mechanism proposed for LfcinB.^{10,11} In addition, peptide conjugates may act on intracellular targets, which is in agreement with previous studies that showed that LfcinB is internalized in the bacteria *E. coli* 25922 and *S. aureus* 25923 as well as that the Rh-RRWQWR peptide can be translocated through the *E. coli* strain membrane.²²

Regarding the peptides that contain the RWQWRWQWR sequence, it is observed that several of the conjugates showed less antibacterial activity against *E. coli*, with the exception of the conjugated peptide OA-Ahx-RWQWRWQWR. This could be explained by the fact that the peptide sequence is longer and by including a non-peptide molecule of considerable size, it leads to the loss of amphipathicity causing that the activity decreases. Furthermore, as they are larger peptide conjugates, they can be added making difficult the interaction of the peptide with the membranes of Gram-negative bacteria. Furthermore, as observed, the unconjugated peptide has great antibacterial activity against *E. coli* with a MIC value of 17 μM , so in this case it is not necessary to conjugate with Ahx, Fc, FA or CA.

The peptide RWQWRWQWR exhibited no antibacterial activity against the *S. aureus* ATCC 25923 strain at the concentrations tested, while all peptide conjugates containing the



Paper

palindromic motif exhibited greater antibacterial activity against the *S. aureus* ATCC 25923 strain, especially the antibacterial activity of peptides Ahx-RWQWRWQWR and CA-Ahx-RWQWRWQWR, with MIC values of 16 and 28 μM , respectively. Therefore, we can establish that the incorporation of non-peptidic molecules into the palindromic sequence at the N-terminal end enhances the antibacterial activity against *S. aureus* ATCC 25923. In these cases, the increase in antibacterial activity against *S. aureus* can also be explained by the damage to the bacterial plasma membrane caused by the interaction between the conjugated peptide with teichoic acids and lipoteichoic acids of the plasma membrane.

It is interesting that the peptide OA-Ahx-RRWQWR and exhibited the greatest antibacterial activity against the strains evaluated and also the conjugated peptide OA-Ahx-RWQWRWQWR exhibited greater antibacterial activity against the *E. coli* ATCC 25922 strain than the palindromic sequence unconjugated and all the synthesized peptides. The above is explained because OA is an antibiotic agent and when conjugated to peptides it is possible to enhance antibacterial activity through a synergistic effect.³⁶ In this case, a mechanism of action is suggested that involves the entry of the conjugated peptide into the bacteria by the peptide fragment and the subsequent inhibition of bacterial DNA synthesis OA associated.³⁶ It highlights that OA-conjugated peptides exhibited significant antibacterial activity against *S. aureus* strain, taking into account that OA has no antibacterial activity against this Gram-positive strain, suggesting that the antibacterial activity of these conjugated peptides can be attributed to peptide sequence. It is possible that the mechanism of action for these peptides conjugates could be associated with the membrane translocation and/or disruption on the membrane. This is important since it allows suggesting that the peptide conjugation with antibiotics is an alternative to improve antibacterial action and avoid the development of resistance that has been reported for antibiotics such as OA. The OA-conjugated peptides could be considered to develop therapeutically agents against resistant strains.^{4,10,11,22}

Conjugated peptides containing the sequence RLLR exhibited antibacterial activity against *E. coli* ATCC 25922 similar to that of the unmodified peptide, except for the peptide OA-Ahx-RLLR, which exhibited the greatest antibacterial activity against this strain. On the other hand, peptides CA-Ahx-RLLR and OA-Ahx-RLLR and exhibited significant antibacterial activity against *S. aureus* ATCC 25923. Peptides conjugated with Fc, CA, FA, and OA containing the palindromic sequence RLLRRLLR exhibited greater antibacterial activity against both strains. Importantly, the peptides OA-Ahx-RLLRRLLR and FA-Ahx-RLLRRLLR exhibited the greatest activity against both strains. These results suggest that the antibacterial activity of the conjugated peptides is dependent on both the sequence and the non-peptidic molecule attached at the N-terminal end. It should further be noted that in some cases the conjugation increased the antibacterial activity against a specific strain, while for other conjugate peptides the antibacterial activity increased against both strains. It has been reported that the proline hinge in buforin is indispensable for the cell

penetrating activity, but the sequences RLLR and RLLRRLLR don't have it. For this reasons, they are noncell-penetrating peptides and they are as membrane acting peptides.⁶ For these conjugated peptides a mechanism of action is suggested where they attack the bacterial membrane leading to disruption of the cell membrane.

The antibacterial activity of the non-peptidic molecules Fc, CA and FA was significantly lower than the peptides and peptides conjugates and it was not possible to determine their MIC values at the concentrations evaluated.

Fc-conjugated peptides also show increased activity against Gram-positive and Gram-negative bacteria, suggesting that the joined Fc motif improves antibacterial activity as reported by other authors.^{31,42} Fc destabilizes cell membranes through lipid peroxidation and leads to cell lysis, therefore, for these conjugated peptides, a mechanism of action similar to that reported by altering membrane synthesis is suggested³² and pore formation, which was also evidenced with the Fc-RP1 peptide on vesicles. It may also be due to the increase of plasma membrane permeation that leads to an increase of peptide concentration at the cytosol and thus to better antibacterial activity.⁴² Furthermore, the antibacterial activity of these peptides was not caused by the redox action of the organometallic compound bound to the peptide, as reported.³²

Our results are in agreement with previous reports showing that the inclusion of organometallic compounds or antibiotics into peptides confers greater antibacterial activity against this bacterial strain.^{31,32,43} This results also suggest that the antibacterial activity of peptide conjugates depends on the physicochemical properties of the peptides, such as the length, sequence, charge, and structure, which are affected by the conjugation. Thus it can be concluded that the peptide conjugates identified in this study can be considered to be promising for inclusion in studies for the development of new antibacterial drug molecules. The results indicate that the conjugation of AMPs with non-peptidic molecules is a versatile and novel strategy that allows us to identify promising molecules with potent antibacterial activity against Gram-positive and/or Gram-negative strains. Finally, the synthesis of conjugated peptides is viable and opens up the possibility of introducing other molecules into the peptide sequences in order to improve their antibacterial activity.

Conclusions

We designed, synthesized, and characterized short peptide conjugates derived from buforin and lactoferrin B using different non-peptidic modifiers. The non-peptidic molecules as 6-aminohexanoic acid (Ahx), ferrocene (Fc), caffeic acid (CA) and ferulic acid (FA) have no antibacterial activity but being conjugated with peptides exhibited significantly activity against Gram-positive and Gram-negative bacteria. Also, it was shown that the peptide conjugates with the antibiotic agent OA had the lowest values of MIC due to a possible synergistic effect between sequence and OA. These studies demonstrated the antibacterial activity can be enhanced by conjugation of short sequences with non-peptidic motifs. The results reported here showed that the



peptide conjugation of short peptides derived from AMPs is viable and allows the design of synthetic peptides with enhanced antibacterial activity, which will be useful for developing new antibacterial agents.

Conflicts of interest

The authors declare no conflicts of interest.

Acknowledgements

This research was conducted with the financial support of COLCIENCIAS, Project: "Obtención de un prototipo peptídico promisorio para el desarrollo de un medicamento de amplio espectro para el tratamiento del cáncer de colon, cuello uterino y próstata". Code 110184466986, contract RC No. 845-2019.

References

- World Health Organization (WHO), *Antibacterial Agents in Clinical Development*, 2017.
- C. Cézard, V. Silva-pires, C. Mullié and P. Sonnet, *Sci. against Microb. Pathog. Commun. Curr. Res. Technol. Adv.*, Formatex Res. Center., 2011, pp. 926–937.
- J. Wang, X. Dou, J. Song, Y. Lyu, X. Zhu, L. Xu, W. Li and A. Shan, *Med. Res. Rev.*, 2019, **39**, 831–859.
- A. Giuliani, G. Pirri and S. F. Nicoletto, *Cent. Eur. J. Biol.*, 2007, **2**, 1–33.
- J. H. Cho, B. H. Sung and S. C. Kim, *Biochim. Biophys. Acta, Biomembr.*, 2009, **1788**, 1564–1569.
- C. B. Park, K.-S. Yi, K. Matsuzaki, M. S. Kim and S. C. Kim, *Proc. Natl. Acad. Sci. U. S. A.*, 2000, **97**, 8245–8250.
- S. A. Jang, H. Kim, J. Y. Lee, J. R. Shin, D. J. Kim, J. H. Cho and S. C. Kim, *Peptides*, 2012, **34**, 283–289.
- W. Bellamy, M. Takase, H. Wakabayashi, K. Kawase and M. Tomita, *J. Appl. Bacteriol.*, 1992, **73**, 472–479.
- M. Tomita, M. Takase, W. Bellamy and S. Shimamura, *Acta Paediatr. Jpn.*, 1994, **36**, 585–591.
- I. A. García-Montoya, T. S. Cendón, S. Arévalo-Gallegos and Q. Rascón-Cruz, *Biochim. Biophys. Acta, Gen. Subj.*, 2012, **1820**, 226–236.
- S. Farnaud and R. W. Evans, *Mol. Immunol.*, 2003, **40**, 395–405.
- K. S. Hoek, J. M. Milne, P. A. Grieve, D. A. Dionysius and R. Smith, *Antimicrob. Agents Chemother.*, 1997, **41**, 54–59.
- J. L. Gifford, H. N. Hunter and H. J. Vogel, *Cell. Mol. Life Sci.*, 2005, **62**, 2588–2598.
- J. H. Andersen, H. Jenssen and T. J. Gutteberg, *Antiviral Res.*, 2003, **58**, 209–215.
- W. Bellamy, K. Yamauchi, H. Wakabayashi, M. Takase, N. Takakura, S. Shimamura and M. Tomita, *Lett. Appl. Microbiol.*, 1994, **18**, 230–233.
- D. I. Chan, E. J. Prenner and H. J. Vogel, *Biochim. Biophys. Acta, Biomembr.*, 2006, **1758**, 1184–1202.
- S. Tomita, N. Shirasaki, H. Hayashizaki, J. Matsutama, Y. Benno and I. Kiyosawa, *Biosci., Biotechnol., Biochem.*, 1998, 1476–1482.
- H. H. Haukland, H. Ulvatne, K. Sandvik and L. H. Vorland, *FEBS Lett.*, 2001, **508**, 389–393.
- Y. H. Tu, Y. H. Ho, Y. C. Chuang, P. C. Chen and C. S. Chen, *PLoS One*, 2011, **6**, e28197.
- A. Richardson, R. de Antueno, R. Duncan and D. W. Hoskin, *Biochem. Biophys. Res. Commun.*, 2009, **388**, 736–741.
- N. d. J. Huertas, Z. J. R. Monroy, R. F. Medina and J. E. G. Castañeda, *Molecules*, 2017, **22**, 987.
- M. Moniruzzaman, M. Z. Islam, S. Sharmin, H. Dohra and M. Yamazaki, *Biochemistry*, 2017, **56**, 4419–4431.
- M. A. León-Calvijo, A. L. Leal-Castro, G. A. Almanzar-Reina, J. E. Rosas-Pérez, J. E. García-Castañeda and Z. J. Rivera-Monroy, *BioMed Res. Int.*, 2015, **2015**, 1–8.
- N. D. J. Huertas Méndez, Y. Vargas Casanova, A. K. Gómez Chimbí, E. Hernández, A. L. Leal Castro, J. M. Melo Diaz, Z. J. Rivera Monroy and J. E. García Castañeda, *Molecules*, 2017, **22**, 1–10.
- Y. Vargas-casanova, K. J. Cardenas, A. Luc and J. E. Garc, *RSC Adv.*, 2019, 7239–7245.
- A. Reinhardt and I. Neundorf, *Int. J. Mol. Sci.*, 2016, **17**, 701.
- N. Ptaszynska, K. Olkiewicz, J. Okonska, A. Legowska, K. Gucwa, A. Gitlin-Domagalska, D. Debowski, S. Milewski and K. Rolka, *Peptides*, 2019, 306–308.
- W. Aoki and M. Ueda, *Pharmaceuticals*, 2013, **6**, 1055–1081.
- U. Schatzschneider, in *Advances in Bioorganometallic Chemistry*, Elsevier Inc., 2019, pp. 173–192.
- G. Dirscherl and B. König, *Eur. J. Org. Chem.*, 2008, 597–634.
- J. T. Chantson, M. V. V. Falzacappa, S. Crovella and N. Metzler-Nolte, *ChemMedChem*, 2006, **1**, 1268–1274.
- B. Albada and N. Metzler-Nolte, *Acc. Chem. Res.*, 2017, **50**, 2510–2518.
- C. Magnani, V. L. B. Isaac, M. A. Correa and H. R. N. Salgado, *Anal. Methods*, 2014, **6**, 3203–3210.
- P. J. Herald and P. M. Davidson, *J. Food Sci.*, 1983, **48**, 1378–1379.
- M. Sova, *Mini-Rev. Med. Chem.*, 2012, **12**, 749–767.
- A. M. Emmerson, *J. Antimicrob. Chemother.*, 2003, **51**, 13–20.
- M. J. Kershaw and D. A. Leigh, *J. Antimicrob. Chemother.*, 1975, **1**, 311–315.
- V. Rodríguez, H. Pineda, N. Ardila, D. Insuasty, K. Cárdenas, J. Román, M. Urrea, D. Ramírez, R. Fierro, Z. Rivera and J. García, *Int. J. Pept. Res. Ther.*, 2020, **26**, 585–587.
- D. S. Insuasty Cepeda, H. M. Pineda Castañeda, A. V. Rodríguez Mayor, J. E. García Castañeda, M. Maldonado Villamil, R. Fierro Medina and Z. J. Rivera Monroy, *Molecules*, 2019, **24**, 1215.
- Clinical and Laboratory Standards Institute (CLSI), *CLSI Doc. M07-A9*, 2012, vol. 32, p. 18.
- D. P. Valencia, L. M. F. Dantas, A. Lara, J. García, Z. Rivera, J. Rosas and M. Bertotti, *J. Electroanal. Chem.*, 2016, **770**, 50–55.
- N. C. S. Costa, J. P. Piccoli, N. A. S. Id, C. Clementino, A. M. Fusco-almeida, S. R. De Annunzio, C. R. Fontana, J. B. M. Verga, S. F. E. Id, J. M. Pizauro-junior, M. A. S. Graminha and E. M. C. Id, *PLoS One*, 2020, 1–22.
- K. A. Ghaffar, W. M. Hussein, Z. G. Khalil and R. J. Capon, *Curr. Drug Delivery*, 2015, **12**, 108–114.



Article

In Vitro Antifungal Activity of Chimeric Peptides Derived from Bovine Lactoferricin and Buforin II against *Cryptococcus neoformans* var. *grubii*

Silvia Katherine Carvajal ¹, Yerly Vargas-Casanova ¹, Héctor Manuel Pineda-Castañeda ²,
 Javier Eduardo García-Castañeda ³, Zuly Jenny Rivera-Monroy ² and Claudia Marcela Parra-Giraldo ^{1,*}

¹ Unidad de Proteómica y Micosis Humanas, Grupo de Enfermedades Infecciosas, Departamento de Microbiología, Facultad de Ciencias, Pontificia Universidad Javeriana, Bogotá D.C. 110231, Colombia

² Chemistry Department, Universidad Nacional de Colombia, Carrera 45 No. 26–85, Building 451, Office 409, Bogotá D.C. 111321, Colombia

³ Pharmacy Department, Universidad Nacional de Colombia, Bogotá Carrera 45 No. 26–85, Building 450, Bogotá D.C. 111321, Colombia

* Correspondence: claudia.parra@javeriana.edu.co; Tel.: +57-1-3208320 (ext. 4305)



Citation: Carvajal, S.K.; Vargas-Casanova, Y.; Pineda-Castañeda, H.M.; García-Castañeda, J.E.; Rivera-Monroy, Z.J.; Parra-Giraldo, C.M. In Vitro Antifungal Activity of Chimeric Peptides Derived from Bovine Lactoferricin and Buforin II against *Cryptococcus neoformans* var. *grubii*. *Antibiotics* **2022**, *11*, 1819. <https://doi.org/10.3390/antibiotics11121819>

Academic Editor: Jean-Marc Sabatier

Received: 11 November 2022

Accepted: 13 December 2022

Published: 15 December 2022

Publisher's Note: MDPI stays neutral with regard to jurisdictional claims in published maps and institutional affiliations.



Copyright: © 2022 by the authors. Licensee MDPI, Basel, Switzerland. This article is an open access article distributed under the terms and conditions of the Creative Commons Attribution (CC BY) license (<https://creativecommons.org/licenses/by/4.0/>).

Abstract: Cryptococcosis is associated with high rates of morbidity and mortality. The limited number of antifungal agents, their toxicity, and the difficulty of these molecules in crossing the blood–brain barrier have made the exploration of new therapeutic candidates against *Cryptococcus neoformans* a priority task. To optimize the antimicrobial functionality and improve the physicochemical properties of AMPs, chemical strategies include combinations of peptide fragments into one. This study aimed to evaluate the binding of the minimum activity motif of bovine lactoferricin (LfcinB) and buforin II (BFII) against *C. neoformans* var. *grubii*. The antifungal activity against these chimeras was evaluated against (i) the reference strain H99, (ii) three Colombian clinical strains, and (iii) eleven mutant strains, with the aim of evaluating the possible antifungal target. We found high activity against these strains, with a MIC between 6.25 and 12.5 µg/mL. Studies were carried out to evaluate the effect of the combination of fluconazole treatments, finding a synergistic effect. Finally, when fibroblast cells were treated with 12.5 µg/mL of the chimeras, a viability of more than 65% was found. The results obtained in this study identify these chimeras as potential antifungal molecules for future therapeutic applications against cryptococcosis.

Keywords: *Cryptococcus neoformans*; cryptococcosis; antimicrobial peptides; chimeric peptides; antifungals; buforin II; bovine lactoferricin

1. Introduction

Invasive fungal infections are on the rise, causing high morbidity and mortality rates in immunocompromised individuals, especially those with lymphocytes below 200 cells/mm³, including HIV patients, cancer patients receiving chemotherapy, individuals who have undergone solid organs transplants, and those with hematopoietic stem cell transplantations [1–4].

Cryptococcus neoformans is an opportunistic basidiomycete encapsulated fungus that can cause cryptococcosis, especially in pulmonary regions or even in the meninges [5]. There are two varieties of *C. neoformans*: *grubii* (serotype A), which is ubiquitous worldwide, and *neoformans* (serotype D), found mainly in Europe [6]. The most prevalent species is *C. neoformans*, *grubii* being the most frequent variety. Therefore, the present study focuses on *C. neoformans* var. *grubii* [7].

Cryptococcosis is a potentially fatal opportunistic mycosis of global incidence. The global incidence of cryptococcal meningitis is estimated to be 223,100 cases per year, with 73% of the cases in sub-Saharan Africa. Worldwide, cryptococcal meningitis accounts for

181,100 deaths per year and is responsible for approximately 15% of AIDS-related deaths [8]. The incidence of cryptococcosis in Colombia in the period 1997–2016 was one case per 434,782 people. The departments with the highest incidence were Norte de Santander (1 case per 178,571 people) and Valle (1 case per 212,766 people) [9].

Despite established recommendations for the treatment of cryptococcosis, there are several limitations related to the antifungals that currently are clinically available: their global access remains restricted; there are few therapeutic alternatives; security profiles impose limitations; and drug penetration and distribution to the site of infection is challenging [10–13]. In addition, it has been described that *C. neoformans* can develop heteroresistance to fluconazole [14].

As a result of the problems described above, a demand for the development of new antifungal molecules has been triggered. Antimicrobial peptides (AMPs) have emerged as pharmaceutical candidates with promising antifungal activity. AMPs are molecules that are widely distributed in nature and play an important role in the innate immune system of various organisms. These peptides exhibit broad-spectrum antimicrobial and immunomodulatory activities against various microorganisms, including yeasts and molds. Most AMPs are cationic and amphipathic. Cationic AMPs are often helical, with short amino acid sequences (less than 100 amino acid residues) [15].

Antimicrobial peptides derived from bovine lactoferricin (LfcinB) and buforin II (BFII) have been shown to exhibit strong antimicrobial activity not only against bacteria but also against yeasts such as *C. neoformans* [16,17]. Synthetic chimeric peptides have emerged as a strategy for improving and enhancing the antimicrobial effects of AMPs. In a 2021 study, these chimerical peptides demonstrated a high degree of activity against both Gram-negative and Gram-positive bacteria [18]. Another recently published study tested these chimeras on *Candida* spp. [19]. The antifungal effect of these chimeras against *C. neoformans* has not been reported.

In light of the above, the present study evaluated the in vitro antifungal activity of chimeric peptides containing LfcinB (20–25): RRWQWR and BFII (32–35): RLLR sequences; specifically, the effect of chimeras on *C. neoformans* var. *grubii* strains.

2. Results

2.1. Antifungal Activity of Chimeric Peptides Derived from Bovine Lactoferricin and Buforin II against *Cryptococcus neoformans* var. *grubii*

The designed and synthesized peptides used for the purpose of this study were: C5: RRWQWR-Ahx-KLLKLLK, C6: KKWQWK-Ahx-RLLRLLR, and precursor peptides LfcinB (20–25): RRWQWR, BFII (32–35)_{Pal}: RLLRLLR, [K]-LfcinB (20–25): KKWQWK, and [K]-BFII (32–35)_{Pal}: KLLKLLK [18,19]. In both chimeras, 6-aminohexanoic acid (Ahx) was used as the spacer molecule. The H99 strain and one clinical isolate were sensitive to fluconazole (FLC), and two clinical isolates were considered dose-dependent sensitive (DDS) to this antifungal (Table 1). All mutants were sensitive to FLC (Table 2). For peptide C5, activity was found with a MIC of 12.5 µg/mL and an MFC of 12.5 µg/mL, depending on the strain; peptide C6 exhibited activity against the strains evaluated with a MIC of 6.25 µg/mL and an MFC of 6.25 µg/mL. No antifungal activity of the precursor peptides was observed at the concentrations tested against *C. neoformans* var. *grubii*.

The antifungal activity of chimeras and their precursor sequences in mutants involved in the TOR signaling pathway, ergosterol biogenesis, efflux pump mechanisms, and cell cycle control was evaluated. Mutants exposed to the C5 chimera exhibited a MIC between ≤3.125 and 12.5 µg/mL; when the mutants were incubated with the C6 chimera, they exhibited a MIC of 3.125 to 6.25 µg/mL. On the other hand, when treating the mutants with the precursor peptides of LfcinB (20–25) and BFII (32–35)_{Pal}, the MIC was >25 and >50 µg/mL, respectively (Table 2).

Table 1. Antifungal activity of fluconazole and peptides against *C. neoformans* var. *grubii*.

Code	Sequence	MIC/MFC µg/mL (µM)					
		H99		2807		2643	
		MIC	MFC	MIC	MFC	MIC	MFC
C5	RRWQWR-Ahx-KLLKLLK	12.5 (6)	12.5 (6)	12.5 (6)	12.5 (6)	12.5 (6)	12.5 (6)
C6	KKWQWK-Ahx-RLRRLLR	6.25 (3)	6.25 (3)	6.25 (3)	6.25 (3)	6.25 (3)	6.25 (3)
LfcinB (20–25)	RRWQWR	>25 (>25)	>25 (>25)	>25 (>25)	>25 (>25)	>25 (>25)	>25 (>25)
BFI (32–35) _{Pal}	RLRRLLR	>50 (>46)	>50 (>46)	>50 (>46)	>50 (>46)	>50 (>46)	>50 (>46)
[K]-LfcinB (20–25)	KKWQWK	>100 (111)	>100 (111)	>100 (111)	>100 (111)	ND	ND
[K]-BFI (32–35) _{Pal}	KLLKLLK	>100 (114)	>100 (114)	>100 (114)	>100 (114)	ND	ND
FLC	-	4	-	16	-	8	-

ND: not determined. FLC: fluconazole.

Table 2. Antifungal activity of fluconazole and peptides against mutants of *C. neoformans* var. *grubii*.

Code	Sequence	MIC/MFC µg/mL (µM)																					
		CNAG_04693		CNAG_01580		CNAG_04804		CNAG_06925		CNAG_02050		CNAG_02430		CNAG_06348		CNAG_00730		CNAG_05150		CNAG_02341		CNAG_02915	
		MIC	MFC	MIC	MFC	MIC	MFC	MIC	MFC	MIC	MFC	MIC	MFC	MIC	MFC	MIC	MFC	MIC	MFC	MIC	MFC	MIC	MFC
C5	RRWQWR-Ahx-KLLKLLK	6.25 (3)	25 (12)	3.125 (2)	3.125 (2)	6.25 (3)	6.25 (3)	6.25 (3)	6.25 (3)	6.25 (3)	6.25 (3)	6.25 (3)	6.25 (3)	6.25 (3)	6.25 (3)	6.25 (3)	6.25 (3)	12.5 (6)	12.5 (6)	12.5 (6)	12.5 (6)	<3.125 (≤2)	3.125 (2)
C6	KKWQWK-Ahx-RLRRLLR	6.25 (3)	12.5 (6)	6.25 (3)	6.25 (3)	6.25 (3)	6.25 (3)	6.25 (3)	6.25 (3)	6.25 (3)	6.25 (3)	6.25 (3)	6.25 (3)	6.25 (3)	6.25 (3)	6.25 (3)	6.25 (3)	6.25 (3)	6.25 (3)	6.25 (3)	6.25 (3)	6.25 (3)	6.25 (3)
LfcinB (20–25)	RRWQWR	>50 (>25)	>25 (>25)	>25 (>25)	>25 (>25)	>50 (>51)	>50 (>51)	>50 (>51)	>50 (>51)	>50 (>51)	>50 (>51)	>50 (>51)	>50 (>51)	>50 (>51)	>50 (>51)	>50 (>51)	>50 (>51)	>50 (>51)	>50 (>51)	>50 (>51)	>50 (>51)	>25 (>25)	>25 (>25)
BFI (32–35) _{Pal}	RLRRLLR	>50 (>46)	>50 (>46)	>50 (>46)	>50 (>46)	>50 (>46)	>50 (>46)	>50 (>46)	>50 (>46)	>50 (>46)	>50 (>46)	>50 (>46)	>50 (>46)	>50 (>46)	>50 (>46)	>50 (>46)	>50 (>46)	>50 (>46)	>50 (>46)	>50 (>46)	>50 (>46)	>50 (>46)	>50 (>46)
FLC	-	1	0.25	1	1	1	1	1	1	1	1	1	1	1	1	1	1	0.75	2	2	8	8	1.5

FLC: fluconazole.

2.2. Growth Inhibition and Killing Kinetics

The growth inhibition kinetics of the chimeras were evaluated against *C. neoformans* at different time intervals. The inhibitory effect of chimeras began 14 h after the start of incubation. With increasing time, the inhibitory effect of low concentrations of both chimeras on the fungal growth curve weakened. However, they still exhibited a significant inhibitory effect when compared with the precursor peptides. When the concentration of peptide C5 was 12.5 µg/mL, an ~30% decrease in growth was observed at 68–72 h (Figure 1a), while the fungicidal effect was observed at 25 µg/mL. The H99 strain was incubated with chimera C6 at 3.125 µg/mL and exhibited a prolongation of the lag phase (adaptation) with a growth reduction of ~27%. With ≥ 6.25 µg/mL, C6 exhibited a fungicidal effect at 68–72 h (Figure 1b). The 2807 clinical isolate incubated with peptide C5 at a concentration of 3.125 µg/mL exhibited a growth reduction of ~34%. When the peptide concentration was 6.25 to 12.5 µg/mL, a fungistatic effect was observed (reduced growth by 66% and 73%, respectively) (Figure 1c). When the 2807 was incubated with chimera C6 at a concentration of 1.56 µg/mL, it exhibited a growth reduction of ~24%, and when the peptide concentration was 3.125 to 6.25 µg/mL, a fungistatic effect was observed (reduced growth of 70% and 74%, respectively) (Figure 1d). The 3279 strain incubated with C5 at concentrations of 12.5 µg/mL exhibited a growth reduction of almost 18%, and the fungicidal effect was observed at 25 µg/mL (Figure 1e). When it was incubated with chimera C6 at a concentration of 6.25 µg/mL, it exhibited a growth reduction between ~18% and at a concentration of 12.5 µg/mL, a fungistatic effect was observed at 68–72 h (growth reduction ~76%) Table 3 (Figure 1f).

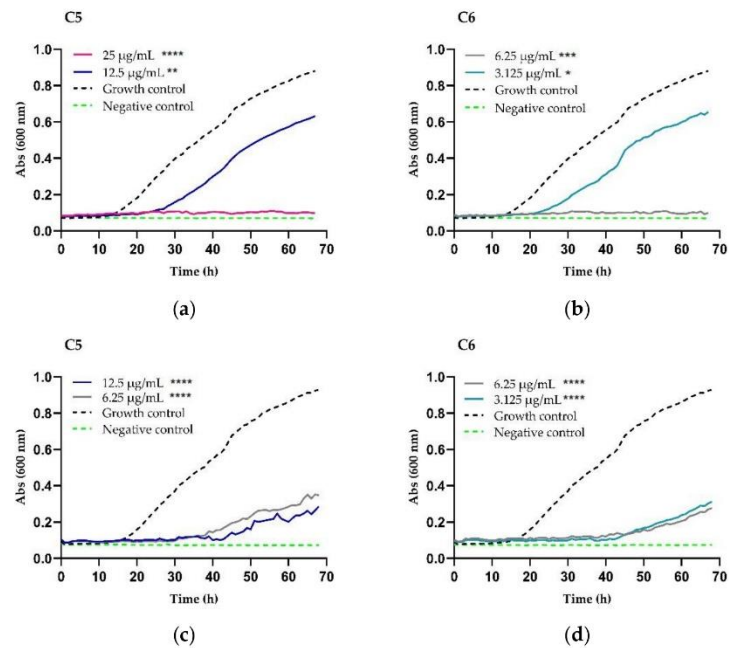


Figure 1. Cont.

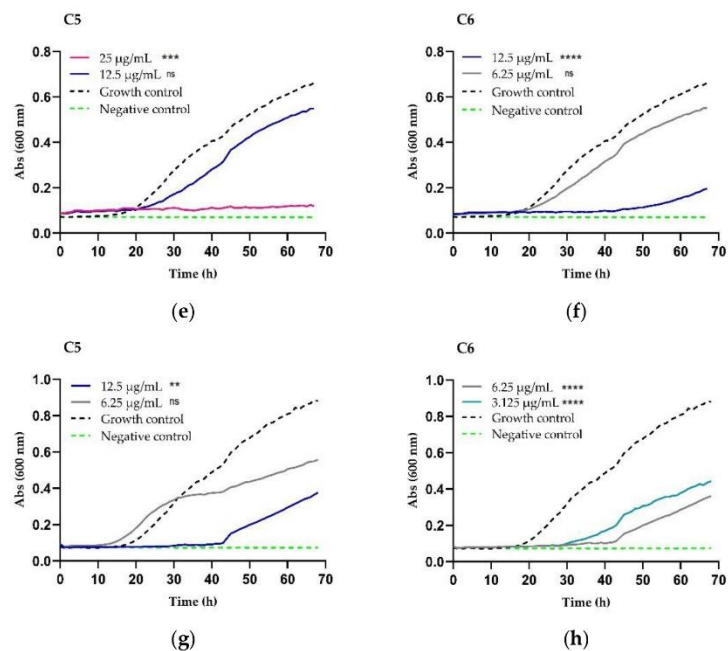


Figure 1. Chimeric peptides time-kill curve against *C. neoformans* var. *grubii*. (a,b) H99 strain; (c,d) clinical isolate 2807; (e,f) clinical isolate 3279; and (g,h) clinical isolate 2643. The asterisks represent the significance (* $p < 0.05$, ** $p < 0.01$, *** $p < 0.001$, **** $p < 0.0001$) among the strains exposed to the different concentrations and the strains without treatment (growth control or positive control); not significant (ns). RPMI medium without yeast and peptide (sterility control or negative).

Table 3. Growth inhibition test. Antifungal activity of chimeras against *C. neoformans* var. *grubii*.

Chimera	Strain	MIC µg/mL (µM)	Effect µg/mL (µM)	
			Fungistatic	Fungicide
C5 RRWQWR-Ahx-KLLKLLK	H99	12.5 (6)	12.5 (6)	25 (12)
	2807	12.5 (6)	6.25 (3)	>12.5 (>6)
	3279	12.5 (6)	12.5 (6)	25 (12)
	2643	12.5 (6)	6.25 (3)	>12.5 (>6)
C6 KKWQWK-Ahx-RLLRLLR	H99	6.25 (3)	3.125 (1.5)	6.25 (3)
	2807	6.25 (3)	3.125 (1.5)	>6.25 (>3)
	3279	6.25 (3)	6.25 (3)	>12.5 (>6)
	2643	6.25 (3)	6.25 (3)	>12.5 (>6)

The 2643 clinical isolate incubated with C5 at concentrations of 3.125 and 6.25 µg/mL exhibited a growth reduction of ~35%; when the concentration was increased to 12.5 µg/mL, a growth reduction of 61% was observed (fungistatic effect) (Figure 1g). When this clinical isolate was incubated with chimera C6 at 1.56 µg/mL, it exhibited a growth reduction of ~20%; at concentrations of 3.125 and 6.25 µg/mL, a fungistatic effect was observed at 68–72 h (Figure 1h).

2.3. Fluorescent Staining for Yeast Viability

The antifungal effect of chimera C6 was evaluated at concentrations between 3.125 and 25 $\mu\text{g}/\text{mL}$. A live control without treatment and a control of dead yeast cells treated with hypochlorite were used (results not shown). Live control cells were labeled with a blue fluorescence (calcofluor white M2R), highlighting cell wall chitin regardless of the metabolic state. Yeasts were also labeled with FUN1, using two different excitation filters (488 and 532 nm), revealing a yeast with a diffusely distributed green and red color, indicating plasma membrane integrity and the yeast cells' metabolic capability to convert this intracellular staining to a red-orange fluorescence (Figure 2).

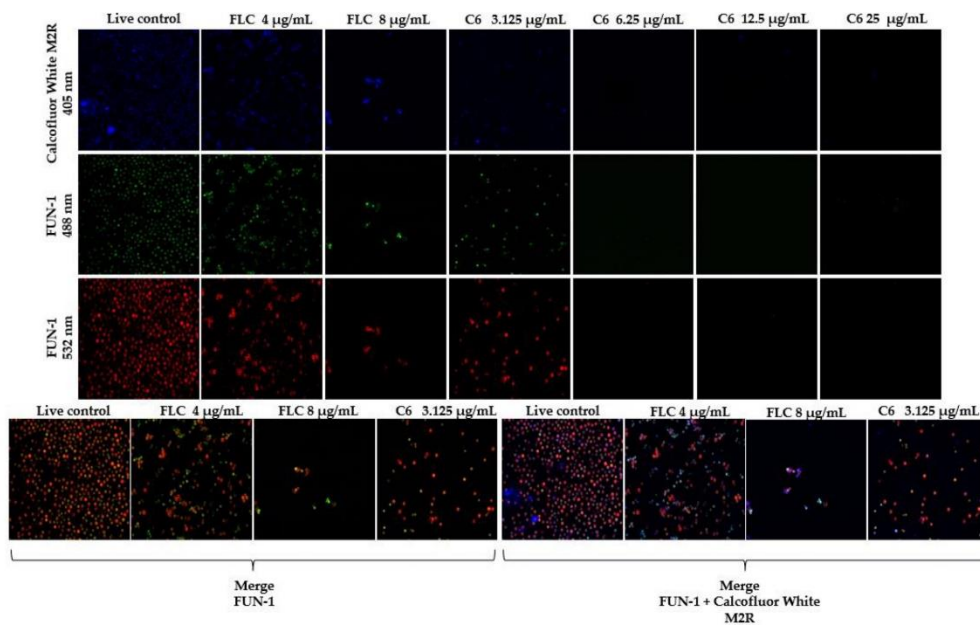


Figure 2. Cell viability assay of *C. neoformans* var. *grubii* after treatment (72 h) with C6 at 3.125 $\mu\text{g}/\text{mL}$, 6.25 $\mu\text{g}/\text{mL}$, 12.5 $\mu\text{g}/\text{mL}$, and 25 $\mu\text{g}/\text{mL}$.

Although metabolically active structures were observed, after 72 h of incubation with the chimera at concentrations of 6.25, 12.5, and 25 $\mu\text{g}/\text{mL}$, there was a >99% decrease in cell population. When the cells were treated with the peptide at a concentration of 3.125 $\mu\text{g}/\text{mL}$, a cellular decrease was visually observed in relation to the metabolism pattern of the living control. Similarly, a morphological variation was shown compared with the live control. When the cells were treated with fluconazole at 4 $\mu\text{g}/\text{mL}$ (corresponding to the MIC), a decrease in the cell population was observed with respect to the live control. When the cells were treated with 8 $\mu\text{g}/\text{mL}$ of fluconazole, a cell decrease of >80% was observed.

2.4. Checkerboard Assay

Considering that both peptide chimeras showed promising in vitro antifungal activity because the strains evaluated exhibited hypersensitivity to them, we proceeded to study the effect of the combination of each chimera with FLC via the checkerboard method, using the H99 reference strain and clinical isolate 2807. The results showed that the combination of C5 and FLC exhibited an additive effect (ΣFIC 1.0) in H99, while the combination of chimera and FLC in clinical isolate 2807 exhibited a synergistic effect, with an ΣFIC

index between 0.3 and 0.5 at two concentrations below the MIC of FLC and up to four concentrations below the MIC of this chimera. The combined effect of peptide C6 and FLC in reference strain H99 exhibited additivity, with decreased growth $\geq 90\%$, in two concentrations below the MIC of this chimera and one of FLC. For clinical isolate 2807, the analysis showed synergy, with an Σ FICI index between 0.3 and 0.5 up to four concentrations below the MIC of C5 and up to two concentrations below the MIC of FLC (Table 4).

Table 4. Effect of combining the chimeric peptides and FLC against *C. neoformans* H99 and 2807 clinical isolate.

Synergistic Effect of Chimera/FLC Combination against <i>C. neoformans</i> var. <i>grubii</i>								
Strain	Mixture	MIC _a	MIC _b	A	B	FICI	MIC _a /A	MIC _b /B
H99	C5 + FLC	12.5	4	6.25	2	1	2	2
2807		12.5	16	0.8	4	0.3	16	4
H99	C6 + FLC	6.25	4	1.56	2	0.8	4	2
2807		6.25	16	0.4	4	0.3	16	4

FLC: Fluconazole. MIC_a and MIC_b correspond to the MIC ($\mu\text{g}/\text{mL}$) of the chimeric peptide and FLC, respectively; A and B are the MIC values of peptide and fluconazole mixture, respectively. Minimum fractional concentration index (FICI); MIC_a/A and MIC_b/B indicate how peptide or FLC are potentiated after being evaluated in combination.

The precursor peptides LfcinB (20–25): RRWQWR, BFII (32–35)_{Pal}: RLLRLLR, [K]-LfcinB (20–25): KKWQWK, and [K]-BFII (32–35)_{Pal}: KLLKLLK did not show a synergistic effect when they were physically mixed, and no significant inhibitory activity was observed at the concentrations tested. When peptides [K]-LfcinB (20–25) (50 to 200 $\mu\text{g}/\text{mL}$) and BFII (32–35)_{Pal} (50 to 100 $\mu\text{g}/\text{mL}$) were combined, an inhibitory effect of approximately 90% was observed (Figure S1).

2.5. Cytotoxicity: MTT Assay

The viability of L929 murine fibroblast cells was determined after treatments with chimeric peptides at concentrations between 3.125 and 200 $\mu\text{g}/\text{mL}$. The results indicated that the fibroblasts' viability decreases depending on the concentration of the chimera, with an IC₅₀ value of 93.35 $\mu\text{g}/\text{mL}$ for chimera C5 and 67.44 $\mu\text{g}/\text{mL}$ for chimera C6. The viability was almost 10% when the cells were treated with the maximum concentration of chimera C6 (Figure 3).

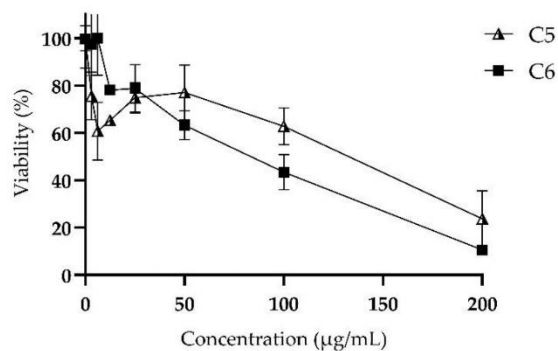


Figure 3. Cytotoxic effect of peptides on the mouse fibroblast cell line L929. Chimera C5: RRWQWR-Ahx-KLLKLLK (black and white triangle shape) and chimera C6: KKWQWK-Ahx-RLLRLLR (black box shape).

3. Discussion

This is the first study testing chimeric peptides derived from LfcinB and BFII in *C. neoformans*. Our results showed that both chimeras exhibited fungicidal and fungistatic antifungal activity against these yeasts. Pineda, H., et al. evaluated the potential of these molecules (sequences with partial substitution of Arg with Lys) in Gram-negative and Gram-positive bacteria, where the average MICs were 1297 μM and 24–48 μM , respectively [18]. Furthermore, they evaluated a chimera derived from LfcinB and BFII with total substitution of Arg with Lys and found a decrease in antimicrobial activity in the bacteria evaluated (MIC: 25–101 μM) [18]. They showed that chimeras with partial substitution of Arg with Lys maintained antimicrobial activity. In addition, it has been proven that the partial substitution of amino acids favors peptide synthesis and reduces costs [20,21].

For the design and synthesis of the peptide chimeras, the minimal antimicrobial motifs reported for each Lfcin B (RRWQWR) or BFII (RLLR) were used. These motifs are the shortest sequence of the original PAM that presents activity in various microorganisms. Park, C.B., et al. synthesized a series of buforin II analogues and evaluated their antifungal activity, showing that the RLLR motif had potent antimicrobial activity [17]. Furthermore, studies have shown that the lactoferricin B active site and minimal motif includes the RRWQWR sequence [22,23].

Our chimeras were designed as follows: (a) contains a partial substitution of Arg with Lys; (b) the LfcinB motif is in the N-terminal position and BFII in the C-terminal position; (c) the chimeras are separated by the spacer Ahx; and (d) a palindromic sequence derived from BFII (RLLRRLLR) was included. Our results indicate that these chimeras exhibit greater activity against all *C. neoformans* strains (≤ 3.125 to 12.5 $\mu\text{g}/\text{mL}$) compared with the precursor sequences (>25 $\mu\text{g}/\text{mL}$).

Positively-charged amino acid residues, such as Arg and Lys, have been described as playing an important role in antimicrobial activity because they promote electrostatic interactions between peptides and the membranes of microorganisms [24]. Despite this, the chemical differences in the side chain groups for Arg (guanidine group) and Lys (amine group) confer different properties on the peptides, affecting their antimicrobial activity. In most cases, the presence of Lys has been associated with a reduction in the antimicrobial activity of peptides. This behavior can be explained by the higher number of hydrogen bonds that the guanidine group can form in contrast to the amine group [25].

The chimeras contain a sequence that has been associated with membrane destabilization and cell lysis (LfcinB (20–25)) and another that can translocate within the cell without membrane damage (BFII (32–35)_{pal}) [26,27]. According to reports, for the design of chimeras, it could be considered that one of the sequences has the capacity for cellular internalization; this approach proposes a strategy to improve antimicrobial activity [28]. The results of this research showed that the chimeras increased the antifungal activity against *C. neoformans* var. *grubii* compared with the precursor peptides.

6-Aminohexanoic acid (Ahx) is a non-peptidic molecule. It exhibits hydrophobic behavior and has a flexible structure and adequate space between its terminal amino and carboxyl groups that give this molecule the possibility of being used as a spacer and linker of fragments of active molecules. Ahx does not necessarily generate antimicrobial activity by itself, but when conjugated with peptides, it can significantly improve antimicrobial activity [29,30].

Our findings show antifungal activity of chimeras in mutants with defects in proteins involved in the TOR signaling pathway, ergosterol biogenesis, efflux pump mechanisms, and cell cycle control (see Table S1 in the Supplemental Material). Using strains with the specific mutations described above, it was proposed that possible cellular mechanisms (modes of action or resistance) that were affected by the action of chimeric peptides could be detected, but this was not possible because resistance to chimeras was not found in mutants. However, other mutants—for example, those that are related to pathways involved in capsule biosynthesis—should be explored [31]. The antifungal activity of the chimeras against the mutants was similar to that of those observed in the reference and clinical

strains. All mutants were sensitive to the ergosterol biosynthesis inhibitor used for this study, fluconazole, especially one mutant, *sre1Δ* (CNAG_04804). Sre1 plays a central role in adaptation to low-oxygen growth. Under low-oxygen conditions, oxygen-dependent sterol synthesis is inhibited, leading to Sre1 activation. In *C. neoformans*, Sre1 and Scp1 mediate the adaptation necessary for the growth of this yeast in the host and the progression of cryptococcal infection [32,33]. In our study, we did not test hypoxic or anaerobic conditions. The correlation between chimera antifungal activity and ergosterol synthesis should be evaluated, possibly using mutants directly related to this process, such as *ERG11* (the target of azole antifungal agent mutants) [34,35].

According to the criteria of fungicidal activity (molecules that decrease fungal growth $\geq 99\%$) and fungistatic activity (molecules that decrease fungal growth $< 99\%$) in the results of the growth kinetics, we determined that these chimeras exhibit fungistatic activity and concentration-dependent fungicide in all of the strains and isolates evaluated. This approach was carried out using two different methodologies, broth microdilution and automated growth kinetics. Upon comparing the results of these two methodologies, few differences were seen. Despite this, it was observed that at concentrations of $> 12.5 \mu\text{g/mL}$, no growth was evidenced in most of the strains when they were treated with the chimeras.

Since the antifungal activity of the two chimeras was similar, it was decided to evaluate cell viability in the reference strain using one of the two chimeras by means of confocal microscopy. For this reason, the C6 chimera was evaluated in the H99 strain by staining with FUN1 and calcofluor white. Interestingly, the analyzed peptide exhibited antifungal activity with total inhibition, in visual terms, at 72 h, when treated with 6.25, 12.5, and 25 $\mu\text{g/mL}$. On the basis of these results, we were able to corroborate the fungicidal effect exerted by this chimera on yeast cells at concentrations greater than 6.25 $\mu\text{g/mL}$ for the H99 strain.

Combination therapy can be a therapeutic alternative for increasing the antimicrobial effect of drugs. The synergistic effect of the chimeras with FLC was evaluated against strain H99 and a clinical isolate DDS to FLC. The results showed that for H99, the combination chimera/FLC exhibited an effect of additivity and indifference ($\Sigma\text{FIC} = 1$) and indifference ($\Sigma\text{FIC} = 0.8$).

In clinical isolation, both chimeras with FLC showed a strong synergistic effect (ΣFIC 0.4 and 0.3, respectively). These findings emphasize the importance of reducing the concentrations of the treatments in order to enhance the activity against *C. neoformans* var. *grubii*. In the H99 strain, both chimera antifungal activities increased by a factor of 2 (MIC_a/A) when it was combined with 2 $\mu\text{g/mL}$ of FLC. In the 2807 isolate, the antifungal activity of both chimeras increased by a factor of 4 (MIC_a/A) when they were combined with 4 $\mu\text{g/mL}$ of FLC. In this case, its being a clinical isolate, this increase in activity is interesting because the amount of azole antifungal and the peptide required to kill the yeast decreased.

Due to the high antifungal activity observed for the chimeras, it was decided to evaluate whether the minimal motifs they contained (precursors), that is, the peptides with and without substitution of Arg with Lys, could have a synergistic effect through physical mixing. No activity was observed at the concentrations tested (3.125–100 $\mu\text{g/mL}$) nor were synergistic effects observed, particularly when mixing the RRWQWR and KLLKLLK sequences. Regarding the combination of KKWQWK and RLLRLLR, $> 90\%$ inhibition of yeast cells was observed when combining peptide KKWQWK at a concentration of 50, 100, and 200 $\mu\text{g/mL}$ with RLLRLLR at 50 and 100 $\mu\text{g/mL}$. Although these combinations exhibited an inhibitory effect, it was not comparable to the activity achieved by chimeras. In this context, these results confirm that chimera arrays are necessary for antifungal activity, since they exhibit a strong effect against *C. neoformans* var. *grubii* [18,36].

One of the main concerns about the use of antimicrobial peptides in systemic treatments is their toxicity. With antifungal and broad-spectrum capabilities, the new molecules must exhibit low toxicity to cells before considering medical use. These chimeras exhibited a low hemolytic effect, indicating that the chemical binding of the precursors confers selectivity for bacterial and *C. neoformans* var. *grubii* strains [18]. In a study in 2005, the effect

of LfcinB at 200 µg/mL on normal human T lymphocytes, fibroblasts, and endothelial cells was analyzed, demonstrating that this molecule was not toxic for these cultures [37]. Takeshima, K., et al. measured the cytotoxic activity of a BFII derivative against human fibroblast cells and found that it was practically non-toxic, at least up to 100 µM [38]. In our study, an IC₅₀ of 93.35 and 67.44 µg/mL was detected for peptides C5 and C6, respectively, and a viability of >65% was observed when cells were treated with 12.5 µg/mL of each chimera.

4. Materials and Methods

4.1. Fungal Isolates and Culture Conditions

A total of 15 *C. neoformans* strains were used in this study: (i) H99 reference strain, (ii) 3 Colombian clinical isolates, (iv) 11 mutants (associated with a target protein of subunit 2 of rapamycin complex, enzymes involved in ergosterol biogenesis, proteins with action in efflux pump mechanisms, and cell cycle control) (see Table S1 in the Supplemental Material). The majority of them were chosen on the basis of resistance-related phenotypes and antifungal targets using the FungiDB web interface and the strains' availability in the collection (Madhani, 2007).

4.2. Compounds

The research group Síntesis y Aplicación de Moléculas Peptídicas (SAMP) synthesized the chimeric and precursor peptides using the solid phase peptide synthesis methodology (SPPS) (Table 1) [18]. The characterization of the pure peptide via RP-HPLC and MALDI-TOF mass spectrometry is presented in the supplementary material (Figure S2). For this study, we used fluconazole (FLC) as a conventional antifungal.

4.3. Minimum Inhibitory and Fungicidal Concentration Assays

The in vitro susceptibility of chimeric, precursor peptides and FLC was evaluated by determining the minimal inhibitory concentration (MIC) on the basis of the broth microdilution method, according to document M27-A3 of the Clinical Laboratory Standards Institute (CLSI) [39]. It was diluted in RPMI-1640 medium (Sigma-Aldrich) at concentrations ranging from 1.6 to 100 µg/mL. The initial suspension (0.5 McFarland) was mixed into saline solution. Subsequently, a 1:50 dilution in saline solution and a 1:20 dilution in RPMI-1640 were tested ($0.5\text{--}2.5 \times 10^3$ cells/mL). The negative control was the medium only without inoculum, and the positive control was the medium plus inoculum. The incubation time was 72 h at 30 °C at 110 rpm. The MIC values were determined by measuring the absorbance at 595 nm in a microplate reader and were defined as the lowest concentration of peptides capable of inhibiting growth equal to or higher than 50% in relation to the positive control. The MIC for fluconazole (FLC; 0.125–64 µg/mL; Pfizer, Brazil) was also determined according to M27-A3. The lowest concentration of the antifungal agent that was able to inhibit growth by 50% with respect to the positive control was considered the MIC.

The minimal fungicidal concentration (MFC) was evaluated after the yeast's exposure to the chimeras (1.6 to 100 µg/mL), as described above. Aliquots (3 µL) from each well of the MIC microplates were transferred to Sabouraud dextrose agar (SDA) plates and incubated at 30 °C for 74 h. The MFC was defined as the lowest peptide concentration at which ≤1 colony was visible on the agar plate.

4.4. Growth Inhibition and Killing Kinetics

This was evaluated for the reference strain and the clinical isolates. The inoculum was adjusted to $0.5\text{--}2.5 \times 10^3$ cells/mL in RPMI-1640 medium and treated with three concentrations of each chimera (0.5 MIC, MIC, and 2 MIC). Untreated yeast cells were used as the drug-free control method. FLC was used as a conventional drug control. The suspensions were incubated in 100-well plates at 30 °C for 72 h in Bioscreen C MBR equipment, with absorbance (600 nm) automated readings taken every hour [40].

4.5. Fluorescent Staining for Yeast Viability

A commercial LIVE/DEAD™ yeast viability kit (Invitrogen, US) was used to analyze yeast viability after treatment with one of the chimeric peptides and FLC for 72 h at concentrations of 3.125, 6.25, 12.5, and 25 µg/mL and 4 and 8 µg/mL, respectively. In the dead control, the yeasts were treated with 5% hypochlorite for 10 min. Untreated yeast cells were used as a live control. Yeast cells were suspended in phosphate buffered saline (PBS). FUN-1 cell stains (10 µM) and calcofluor white (25 µM) were added to the yeast cell suspensions. After incubation in the dark at 30 °C for 30 min, the stained yeast was analyzed under a fluorescence microscope (Olympus FV1000) using filters set to excitation at approximately 488, 532, and 405 nm at 60× magnification [41]. Fungal cell viability was determined by means of fluorescence analysis in at least 10 fields. Staining and interpretation of fluorescence were performed according to the manufacturer's instructions.

4.6. Checkerboard Assay

The combined effect of FLC with the chimeric peptides was evaluated for the reference strain and one clinical isolate. The amounts of 50 µL of the chimeric peptide and 50 µL of antifungal (FLC) were added to the plates at final concentrations of: 2xMIC, MIC, 1/2xMIC, 1/4xMIC, 1/6xMIC, and 1/8xMIC. A yeast cell suspension was added at $0.5\text{--}2.5 \times 10^3$ cells/mL in 96-well plates. It was incubated for 72 h with shaking at 110 rpm and at 30 °C.

The effect of the combination of the two drugs was determined by calculating the fractional inhibitory concentration index (Σ FIC), which was calculated as follows: Σ FIC = (MIC_{combined}/MIC_{alone}) FLC + (MIC_{combined}/MIC_{alone}) peptide.

FIC values ≤ 0.5 was considered as synergistic effect, $0.5 < \text{FIC} < 1$ an additive effect, $1 < \text{FIC} < 4$ indifference, and $\text{FIC} \geq 4$ an antagonistic effect [42].

4.7. Cytotoxicity: MTT Assay

The cell line used for this approach was the mouse fibroblast L929. The cells were washed with saline solution, trypsinized, and incubated for 5 min at 37 °C with a 5% CO₂ atmosphere. The fibroblast cell suspension was prepared at a concentration of 1×10^6 cells in 7 mL of RPMI medium supplemented with fetal bovine serum (the number of cells needed for one plate) and dispensed into 96-well plates. Then, 70 µL of cells was added per well and incubated overnight at 37 °C and 5% CO₂. Dilutions of each peptide chimera (3.125–200 µg/mL) were formulated, and 50 µL of each were added to the plate in quadruplicate and incubated for 2 h at 37 °C and 5% CO₂. Control wells consisted of untreated cell cultures. In addition, 10 µL of MTT was added to each of the wells, and the plate was incubated for 4 h at 37 °C with a 5% CO₂ atmosphere. Following that, the total volume of each well was withdrawn, 100 L of DMSO was added, and it was incubated for 40 min at 37 °C with 5% CO₂.

Plates were read with an iMark™ microplate reader (Bio-rad, Hercules, CA, USA) measuring the absorbance at 595 nm. Wells of untreated fibroblast cells were considered to be the negative control.

4.8. Statistical Analysis

Curves were constructed using absorbance values and analyzed using GraphPad Prism 8.0.1 (GraphPad Software Inc., San Diego, CA, USA). Normalization of data was carried out (Shapiro–Wilk). Statistical differences were determined using analysis of variance (two-way ANOVA) followed by a Tukey–Kramer *post hoc* test. *p*-values ≤ 0.05 were considered statistically significant.

5. Conclusions

The results of the present study indicate that peptide chimeras derived from LfcinB and BFII exhibit significant antifungal activity against *C. neoformans* var. *grubii*. It was established that the chemical bonding of two short sequences with low activity allows

obtaining chimera with a greater antifungal effect against this yeast. The two chimeras exhibit similar antifungal activity against the tested strains, although each chimera contains a different precursor sequence with Arg substituted with Lys. No high MIC values or differences in antifungal activity of the chimeras in the mutants were found. Therefore, more studies are required to detect these chimeric peptides' possible mechanisms of action. Furthermore, both a concentration-dependent fungistatic and fungicidal activity and a synergistic and additive effect with fluconazole were observed. Chimera cytotoxicity on murine fibroblasts showed that more than seven times the MIC is needed to kill 50% of the fibroblast cells. Therefore, these chimeras present a relevant and promising antifungal effect and can be considered to be an alternative, novel prototype with potential for future research.

Supplementary Materials: The following supporting information can be downloaded at: <https://www.mdpi.com/article/10.3390/antibiotics11121819/s1>. Table S1: Strains used in the study; Figure S1: Effect of the physical combination between: [K]-BFII (32–35)_{pal}: (KLLKKLLK) and LfcinB (20–25): (RRWQWR); [K]-LfcinB (20–25): (KKWQWK) and BFII (32–35)_{pal}: (RLLRRLLR); Figure S2: Chemical characteristics of peptides.

Author Contributions: S.K.C. designed and performed experiments, analyzed data, and wrote the manuscript; Y.V.-C. designed experiments and revised the manuscript; H.M.P.-C. designed peptides and revised the manuscript; J.E.G.-C. designed peptides and revised the manuscript; Z.J.R.-M. designed peptides and revised the manuscript; C.M.P.-G. designed and supervised experiments and coordinated the manuscript. All authors have read and agreed to the published version of the manuscript.

Funding: This research received no external funding.

Institutional Review Board Statement: Not applicable.

Informed Consent Statement: Not applicable.

Data Availability Statement: Not applicable.

Acknowledgments: This research was conducted with the financial support of COLCIENCIAS 807–2018, Project: “Diseño de una formulación para el tratamiento de la candidiasis invasiva multihidroresistente, basada en péptidos de LfcinB libres o nanoencapsulados”. Code 120380763646, contract RC N° 715–2018.

Conflicts of Interest: The authors declare no conflict of interest.

References

1. He, Q.; Ding, Y.; Zhou, W.; Li, H.; Zhang, M.; Shi, Y.; Su, X. Clinical features of pulmonary cryptococcosis among patients with different levels of peripheral blood CD4+ T lymphocyte counts. *BMC Infect. Dis.* **2017**, *17*, 768. [CrossRef] [PubMed]
2. Lin, Y.Y.; Shiau, S.; Fang, C.T. Risk factors for invasive *Cryptococcus neoformans* diseases: A case-control study. *PLoS ONE* **2015**, *10*, e0119090. [CrossRef] [PubMed]
3. Schmiedel, Y.; Zimmerli, S. Common invasive fungal diseases: An overview of invasive candidiasis, aspergillosis, cryptococcosis, and *Pneumocystis pneumonia*. *Swiss Med. Wkly.* **2016**, *146*, w14281. [CrossRef]
4. Park, B.J.; Wannemuehler, K.A.; Marston, B.J.; Govender, N.; Pappas, P.G.; Chiller, T.M. Estimation of the current global burden of cryptococcal meningitis among persons living with HIV/AIDS. *Aids* **2009**, *23*, 525–530. [CrossRef] [PubMed]
5. May, R.C.; Stone, N.R.H.; Wiesner, D.L.; Bicanic, T.; Nielsen, K. *Cryptococcus*: From environmental saprophyte to global pathogen. *Nat. Rev. Microbiol.* **2016**, *14*, 106–117. [CrossRef] [PubMed]
6. Firacative, C.; Trilles, L.; Meyer, W. Recent advances in cryptococcus and cryptococcosis. *Microorganisms* **2022**, *10*, 13. [CrossRef]
7. Cogliati, M. Global Molecular Epidemiology of *Cryptococcus neoformans* and *Cryptococcus gattii*: An Atlas of the Molecular Types. *Scientifica* **2013**, *2013*, 675213. [CrossRef]
8. Rajasingham, R.; Smith, R.M.; Park, B.J.; Jarvis, J.N.; Govender, N.P.; Chiller, T.M.; Denning, D.W.; Loyse, A.; Boulware, D.R. Global burden of disease of HIV-associated cryptococcal meningitis: An updated analysis. *Lancet Infect. Dis.* **2017**, *17*, 873–881. [CrossRef]
9. Escandón, P.; Lizarazo, J.; Agudelo, C.I.; Castañeda, E. Cryptococcosis in Colombia: Compilation and analysis of data from laboratory-based surveillance. *J. Fungi.* **2018**, *4*, 32. [CrossRef]
10. Yang, Y.L.; Xiang, Z.J.; Yang, J.H.; Wang, W.J.; Xu, Z.C.; Xiang, R.L. Adverse Effects Associated With Currently Commonly Used Antifungal Agents: A Network Meta-Analysis and Systematic Review. *Front. Pharmacol.* **2021**, *12*, 697330. [CrossRef]

11. Felton, T.; Troke, P.F.; Hope, W.W. Tissue penetration of antifungal agents. *Clin. Microbiol. Rev.* **2014**, *27*, 68–88. [[CrossRef](#)] [[PubMed](#)]
12. Ashley, E.D. Antifungal drugs: Special problems treating central nervous system infections. *J. Fungi.* **2019**, *5*, 97. [[CrossRef](#)] [[PubMed](#)]
13. Loyse, A.; Thangaraj, H.; Easterbrook, P.; Ford, N.; Roy, M.; Chiller, T.; Govender, N.; Harrison, T.S.; Bicanic, T. Cryptococcal meningitis: Improving access to essential antifungal medicines in resource-poor countries. *Lancet Infect. Dis.* **2013**, *13*, 629–637. [[CrossRef](#)] [[PubMed](#)]
14. Mondon, P.; Petter, R.; Amalfitano, G.; Luzzati, R.; Concia, E.; Polacheck, I.; Kwon-Chung, K.J. Heteroresistance to fluconazole and voriconazole in *Cryptococcus neoformans*. *Antimicrob. Agents Chemother.* **1999**, *43*, 1856–1861. [[CrossRef](#)] [[PubMed](#)]
15. Nayab, S.; Aslam, M.A.; Rahman, S.U.; Sindhu, Z.U.D.; Sajid, S.; Zafar, N.; Razaq, M.; Kanwar, R. Amanullah. A Review of Antimicrobial Peptides: Its Function, Mode of Action and Therapeutic Potential. *Int. J. Pept. Res. Ther.* **2022**, *28*, 46. [[CrossRef](#)]
16. Vorland, L.H.; Ulvatne, H.; Andersen, J.; Haukland, H.H.; Rekdal, Ø.; Svendsen, J.S.; Gutteberg, T.J. Lactoferricin of bovine origin is more active than lactoferricins of human, murine and caprine origin. *Scand. J. Infect. Dis.* **1998**, *30*, 513–517.
17. Park, C.B.; Yi, K.S.; Matsuzaki, K.; Kim, M.S.; Kim, S.C. Structure-activity analysis of buforin II, a histone H2A-derived antimicrobial peptide: The proline hinge is responsible for the cell-penetrating ability of buforin II. *Proc. Natl. Acad. Sci. USA* **2000**, *97*, 8245–8250. [[CrossRef](#)]
18. Pineda-Castañeda, H.M.; Huertas-Ortiz, K.A.; Leal-Castro, A.L.; Vargas-Casanova, Y.; Parra-Giraldo, C.M.; García-Castañeda, J.E.; Rivera-Monroy, Z.J. Designing Chimeric Peptides: A Powerful Tool for Enhancing Antibacterial Activity. *Chem. Biodivers.* **2021**, *18*, e2000885. [[CrossRef](#)]
19. Aguirre-Guataqui, K.; Márquez-Torres, M.; Pineda-Castañeda, H.M.; Vargas-Casanova, Y.; Ceballos-Garzon, A.; Rivera-Monroy, Z.J.; García-Castañeda, J.E.; Parra-Giraldo, C.M. Chimeric Peptides Derived from Bovine Lactoferricin and Buforin II: Antifungal Activity against Reference Strains and Clinical Isolates of *Candida* spp. *Antibiotics* **2022**, *11*, 1561. [[CrossRef](#)]
20. Yang, S.T.; Shin, S.Y.; Lee, C.W.; Kim, Y.C.; Hahn, K.S.; Kim, J.I. Selective cytotoxicity following Arg-to-Lys substitution in tritrypticin adopting a unique amphipathic turn structure. *FEBS Lett.* **2003**, *540*, 229–233. [[CrossRef](#)]
21. Cárdenas-Martínez, K.J.; Grueso-Mariaca, D.; Vargas-Casanova, Y.; Bonilla-Velásquez, L.; Estupiñán, S.M.; Parra-Giraldo, C.M.; Leal, A.L.; Rivera-Monroy, Z.J.; García-Castañeda, J.E. Effects of Substituting Arginine by Lysine in Bovine Lactoferricin Derived Peptides: Pursuing Production Lower Costs, Lower Hemolysis, and Sustained Antimicrobial Activity. *Int. J. Pept. Res. Ther.* **2021**, *27*, 1751–1762. [[CrossRef](#)]
22. Sun, C.; Li, Y.; Cao, S.; Wang, H.; Jiang, C.; Pang, S.; Hussain, M.A.; Hou, J. Antibacterial Activity and Mechanism of Action of Bovine Lactoferricin Derivatives with Symmetrical Amino Acid Sequences. *Int. J. Mol. Sci.* **2018**, *19*, 2951. [[CrossRef](#)]
23. Tomita, M.; Takase, M.; Bellamy, W.; Shimamura, S. A review: The active peptide of lactoferrin. *Acta Paediatr. Jpn.* **1994**, *36*, 585–591. [[CrossRef](#)] [[PubMed](#)]
24. Arias, M.; Piga, K.B.; Hyndman, M.E.; Vogel, H.J. Improving the activity of trp-rich antimicrobial peptides by Arg/Lys substitutions and changing the length of cationic residues. *Biomolecules* **2018**, *8*, 19. [[CrossRef](#)] [[PubMed](#)]
25. Li, L.; Vorobyov, I.; Allen, T.W. The different interactions of lysine and arginine side chains with lipid membranes. *J. Phys. Chem.* **2003**, *117*, 11906–11920. [[CrossRef](#)] [[PubMed](#)]
26. Scocchi, M.; Mardirossian, M.; Runti, G.; Benincasa, M. Non-Membrane Permeabilizing Modes of Action of Antimicrobial Peptides on Bacteria. *Curr. Top. Med. Chem.* **2015**, *16*, 76–88. [[CrossRef](#)]
27. Park, C.B.; Kim, H.S.; Kim, S.C. Mechanism of action of the antimicrobial peptide buforin II: Buforin II kills microorganisms by penetrating the cell membrane and inhibiting cellular functions. *Biochem. Biophys. Res. Commun.* **1998**, *244*, 253–257. [[CrossRef](#)]
28. Pulido, X.C.; Royo, M.; Albericio, F.; Rodríguez, H. Cell Penetrating Peptides as potential drug carriers. *Bionatura* **2016**, *1*, 208–216.
29. Markowska, A.; Markowski, A.R.; Jarocka-Karpowicz, I. The importance of 6-aminohexanoic acid as a hydrophobic, flexible structural element. *Int. J. Mol. Sci.* **2021**, *22*, 12122. [[CrossRef](#)]
30. Ardila-Chantré, N.; Hernández-Cardona, A.K.; Pineda-Castañeda, H.M.; Estupiñán-Torres, S.M.; Leal-Castro, A.L.; Fierro-Medina, R.; Rivera-Monroy, Z.J.; García-Castaneda, J.E. Short peptides conjugated to non-peptidic motifs exhibit antibacterial activity. *RSC Adv.* **2020**, *10*, 29580–29586. [[CrossRef](#)]
31. Arastehfar, A.; Gabaldón, T.; García-Rubio, R.; Jenks, J.D.; Hoenigl, M.; Salzer, H.J.F.; Ilkit, M.; Lass-Flörl, C.; Perlin, D.S. Drug-resistant fungi: An emerging challenge threatening our limited antifungal armamentarium. *Antibiotics* **2020**, *9*, 877. [[CrossRef](#)] [[PubMed](#)]
32. Chang, Y.C.; Ingavale, S.S.; Bien, C.; Espenshade, P.; Kwon-Chung, K.J. Conservation of the sterol regulatory element-binding protein pathway and its pathobiological importance in *Cryptococcus neoformans*. *Eukaryot. Cell* **2009**, *8*, 1770–1779. [[CrossRef](#)] [[PubMed](#)]
33. Chang, Y.C.; Bien, C.M.; Lee, H.; Espenshade, P.J.; Kwon-Chung, K.J. Sre1p, a regulator of oxygen sensing and sterol homeostasis, is required for virulence in *Cryptococcus neoformans*. *Mol. Microbiol.* **2007**, *64*, 614–629. [[CrossRef](#)] [[PubMed](#)]
34. Jordá, T.; Puig, S. Regulation of Ergosterol Biosynthesis in *Saccharomyces cerevisiae*. *Genes* **2020**, *11*, 795. [[CrossRef](#)]
35. Sionov, E.; Chang, Y.C.; Garraffo, H.M.; Dolan, M.A.; Ghannoum, M.A.; Kwon-Chung, K.J. Identification of a *Cryptococcus neoformans* cytochrome P450 lanosterol 14 α -demethylase (Erg11) residue critical for differential susceptibility between fluconazole/voriconazole and itraconazole/posaconazole. *Antimicrob. Agents Chemother.* **2012**, *56*, 1162–1169. [[CrossRef](#)]

36. Kim, J.Y.; Park, S.C.; Noh, G.; Kim, H.; Yoo, S.H.; Kim, I.R.; Lee, J.R.; Jang, M.K. Antifungal effect of a chimeric peptide HN-MC against pathogenic fungal strains. *Antibiotics* **2020**, *9*, 454. [[CrossRef](#)]
37. Mader, J.S.; Salsman, J.; Conrad, D.M.; Hoskin, D.W. Bovine lactoferricin selectively induces apoptosis in human leukemia and carcinoma cell lines. *Mol. Cancer Ther.* **2005**, *4*, 612–624. [[CrossRef](#)]
38. Takeshima, K.; Chikushi, A.; Lee, K.K.; Yonehara, S.; Matsuzaki, K. Translocation of analogues of the antimicrobial peptides magainin and buforin across human cell membranes. *J. Biol. Chem.* **2003**, *278*, 1310–1315. [[CrossRef](#)]
39. Clinical and Laboratory Standards Institute (CLSI). *Reference Method for Broth Dilution. Ref Method Broth Dilution Antifung Susceptibility Test Yeasts Approv Stand*, 3rd ed.; M27-A3; Clinical and Laboratory Standards Institute (CLSI): Wayne, PA, USA, 2008.
40. Gil-Alonso, S.; Jauregizar, N.; Cantón, E.; Eraso, E.; Quindós, G. Comparison of the in vitro activity of echinocandins against *Candida albicans*, *Candida dubliniensis*, and *Candida africana* by time-kill curves. *Diagn. Microbiol. Infect. Dis.* **2015**, *82*, 57–61. [[CrossRef](#)]
41. Kwolek-Mirek, M.; Zadrąg-Tecza, R. Comparison of methods used for assessing the viability and vitality of yeast cells. *FEMS Yeast Res.* **2014**, *14*, 1068–1079. [[CrossRef](#)]
42. Mor, V.; Rella, A.; Farnoud, A.M.; Singh, A.; Munshi, M.; Bryan, A.; Naseem, S.; Konopka, J.B.; Ojima, I.; Bullesbach, E.; et al. Identification of a New Class of Antifungals Targeting the Synthesis of fungal sphingolipids. *mBio* **2015**, *6*, e00647. [[CrossRef](#)] [[PubMed](#)]



Article

Chimeric Peptides Derived from Bovine Lactoferricin and Buforin II: Antifungal Activity against Reference Strains and Clinical Isolates of *Candida* spp.

Katherine Aguirre-Guataqui ¹, Mateo Márquez-Torres ², Héctor Manuel Pineda-Castañeda ³,
Yerly Vargas-Casanova ¹, Andrés Ceballos-Garzon ⁴, Zuly Jenny Rivera-Monroy ^{3,*},
Javier Eduardo García-Castañeda ³ and Claudia Marcela Parra-Giraldo ^{1,*}

- ¹ Human Proteomics and Mycosis Unit, Infectious Diseases Research Group, Department of Microbiology, Carrera 7 # 43-82 Lab 404 Building 52, Pontificia Universidad Javeriana, Bogotá 111321, Colombia
² Bacteriology Department, Universidad Colegio Mayor de Cundinamarca, Bogotá 111321, Colombia
³ Synthesis and Application of Peptide Molecules Faculty of Sciences, Universidad Nacional of Colombia, Bogotá 111321, Colombia
⁴ MEDiS, INRAE, Université Clermont Auvergne, 63000 Clermont-Ferrand, France
* Correspondence: zriveram@unal.edu.co (Z.J.R.-M.); claudia.parra@javeriana.edu.co (C.M.P.-G.)



Citation: Aguirre-Guataqui, K.; Márquez-Torres, M.; Pineda-Castañeda, H.M.; Vargas-Casanova, Y.; Ceballos-Garzon, A.; Rivera-Monroy, Z.J.; García-Castañeda, J.E.; Parra-Giraldo, C.M. Chimeric Peptides Derived from Bovine Lactoferricin and Buforin II: Antifungal Activity against Reference Strains and Clinical Isolates of *Candida* spp. *Antibiotics* **2022**, *11*, 1561. <https://doi.org/10.3390/antibiotics11111561>

Academic Editor: Jean-Marc Sabatier

Received: 21 September 2022

Accepted: 27 October 2022

Published: 5 November 2022

Publisher's Note: MDPI stays neutral with regard to jurisdictional claims in published maps and institutional affiliations.



Copyright: © 2022 by the authors. Licensee MDPI, Basel, Switzerland. This article is an open access article distributed under the terms and conditions of the Creative Commons Attribution (CC BY) license (<https://creativecommons.org/licenses/by/4.0/>).

Abstract: Antimicrobial peptides (AMPs) are considered to be a valuable source for the identification and/or design of promising candidates for the development of antifungal treatments, since they have advantages such as lower tendency to induce resistance, ease of production, and high purity and safety. Bovine lactoferricin (LfcinB) and Buforin II (BFII) are AMPs to which great antimicrobial potential has been attributed. The minimum motives with antimicrobial activity derived from LfcinB and BFII are RRWQWR and RLLR, respectively. Nine chimeras containing the minimum motives of both peptides were synthesized and their antifungal activity against fluconazole (FLC)-sensitive and resistant *C. albicans*, *C. glabrata*, and *C. auris* strains was evaluated. The results showed that peptides C9: (RRWQWR)₂K-Ahx-RLLRRLLR and C6: KKWQWK-Ahx-RLLRRLLR exhibited the greatest antifungal activity against two strains of *C. albicans*, a FLC-sensitive reference strain and a FLC-resistant clinical isolate; no medically significant results were observed with the other chimeras evaluated (MIC ~200 µg/mL). The chimera C6 was also active against sensitive and resistant strains of *C. glabrata* and *C. auris*. The combination of branched polyvalent chimeras together with FLC showed a synergistic effect against *C. albicans*. In addition to exhibiting antifungal activity against reference strains and clinical isolates of *Candida* spp., they also showed antibacterial activity against both Gram-positive and Gram-negative bacteria, suggesting that these chimeras exhibit a broad antimicrobial spectrum and can be considered to be promising molecules for therapeutic applications.

Keywords: *Candida albicans*; bovine lactoferricin; Buforin II; antimicrobial peptides; chimeras

1. Introduction

Invasive candidiasis (IC) is the most prevalent fungal disease in intensive care unit (ICU) patients, accounting for 75% of all fungal infections. IC affects about 250,000 people each year, and its mortality rate is estimated to be 70% [1,2]. In the United States, candidemia is the third leading cause of bloodstream infections in ICU patients [3].

In these scenarios, the most frequently isolated yeast is *Candida albicans*, causing about 60% of all genital, oral, and cutaneous candidiasis infections [4]. *C. albicans* has been described as an innocuous commensal microorganism that is part of the microbiota of the gastrointestinal tract, genitourinary tract, oral cavities, and conjunctiva. When the host is immunosuppressed and/or has microbiota imbalance, this yeast can cause superficial infections (skin, mucous membranes of the mouth, and vagina). The hematogenous spread of the fungus can lead to invasive infections in almost all organs, which without effective treatment are life-threatening [5].

On the other hand, in recent years, other non-albicans species have been gaining importance; for example, in the United States and Europe, the second most isolated yeast is *C. glabrata*, whose incidence varies between 7% and 15% and commonly affects neoplastic and elderly patients [1,6,7]. Furthermore, the emerging yeast *C. auris* is clinically relevant, because it presents mortality rates ranging from 30% to 60% in immunocompromised patients and can additionally exhibit multidrug-resistance profiles [8,9].

The increase in fungal infections caused by *Candida* is mainly due to an increase in patients with neoplastic disease and/or who are HIV positive, and to prolonged use of medical devices (tubes, catheters, prostheses, and valves) and resistance caused by overuse of antibiotics [10]. Conventional antifungal agents have some disadvantages, such as toxicity and low efficacy against resistant strains, among others. For instance, amphotericin B (AmB) causes acute renal toxicity after prolonged administration, and FLC and itraconazole have low efficacy against some yeasts and cause hepatotoxicity [11,12].

AMPs are considered to be an important source of promising molecules for the development of new antifungal treatments. AMPs are part of the innate immune response, are less likely to induce adverse effects, are safe, and have a broad spectrum of activity [13,14]. On the other hand, AMPs have pharmacokinetic limitations, such as low bioavailability, due primarily to factors such as susceptibility to proteases, difficulty crossing membranes, rapid elimination from the body, etc. [15]. To overcome these limits and improve the antimicrobial activity, the native sequence of AMPs has been modified. Some of the optimization strategies of AMPs include reducing the amino acid chain, inserting non-natural amino acids, increasing the polyvalence of the sequence, and combining sequences of two or more AMPs (chimeras), among others [16–20]. LfcinB is a peptide fragment of 25 residues in length located in the N-terminal region of bovine lactoferrin (LfB) and is generated during hydrolysis of this protein with gastric pepsin [21,22]. It has been found that LfcinB possesses antimicrobial activity against fungi, bacteria, and viruses, among others [23–25]. The mechanism of action described for LfcinB is related to its electrostatic interaction between the cationic side chains and the negatively charged components of the cell surface of microorganisms, so the side chain of hydrophobic residues, such as tryptophan, interact with the lipid bilayer, destabilizing the cell membrane and causing lysis [21]. Buforin II (BFII) is a 21-residue peptide that is generated by the treatment of BFI with Lys-C endoproteinase. BFII causes permeability of the cell membrane, producing transient toroidal pores without generating lysis of the microorganism. After its internalization, it interacts with nucleic acids (DNA and RNA), inducing cell death [26,27].

LfcinB (20–25): RRWQWR is the shortest sequence derived from LfcinB with antibacterial, antifungal, and anticancer activity. In similar way, Buforin II (BFII) is an antimicrobial peptide with activity against Gram-positive and Gram-negative bacteria as well as fungi. Palindromic sequences have been designed from the 4-residue motif (RLLR) of Buforin II, and their antibacterial activity has been evaluated against Gram-negative and Gram-positive strains. The palindrome [RLLR]₅: RLLRLLRLLRLLRLLRLLR was reported to have an MIC of 0.7 µM against *E. coli*. Chimeras containing the minimum motif RRWQWR attached to RLLR or RLLRLLRLLR showed greater antibacterial activity than individual sequences [18,20,27–30].

In the present study, the antifungal activity of chimeric peptides containing the minimal motifs of both LfcinB (RRWQWR) [28,29] and BFII (RLLR) [27,30] against reference strains and clinical isolates of *C. albicans*, *C. glabrata*, and *C. auris*, sensitive and resistant to FLC, was evaluated. Three chimeric peptides with antifungal activity against these strains were identified. The synergistic effect on the antifungal activity of mixing some chimera with FLC was also established.

2. Results and Discussion

The chimeras used in this work contain sequences derived from LfcinB, an AMP that affects the integrity of the cell membrane, and from BFII, an AMP that is internalized into the cell and causes DNA damage. The antifungal activity of the chimeras was initially

evaluated against the reference strain *C. albicans* ATCC SC5314, sensitive to FLC and the clinical isolate of *C. albicans* 256 HUSI-PUJ, which is resistant to FLC. Considering their primary structure and polyvalence, the chimeras evaluated in this study were classified into three groups (Table 1):

- (I) The C1 and C3 peptides were synthesized and evaluated in order to establish whether the antifungal activity is affected by the position of the RRWQWR or RLLR sequences in the chimera. Chimeras C2 and C4 contained Ahx (6-aminoheptanoic acid residue) as a spacer for the two motifs. This is intended to establish whether the inclusion of the Ahx spacer between the two motifs affects the antifungal activity. The inclusion of the Ahx spacer facilitates the synthesis of the chimera and separates the two motifs so that each of them can interact independently with the cell surface of the pathogen.
- (II) Chimeras C5, C6, and C7 were synthesized and their antifungal activity was evaluated in order to determine whether partial or total replacement of Arg residues with Lys in RRWQWR and/or RLLR sequences affects their antifungal activity. Replacing Arg residues with Lys has been shown to facilitate and reduce the cost of chimeric synthesis [18].
- (III) Chimeras C8 and C9 were synthesized in order to establish whether the polyvalence of the RRWQWR motif increased the antifungal activity. Previous reports have shown that the polyvalence of the RRWQWR sequence increases antibacterial and anticancer activity [20,31].

Table 1. MIC and MFC values for each branched chimeric in the two *C. albicans* strains.

Antifungal Activity Against <i>C. albicans</i> Strains. µg/mL (µM)						
Group	Code	Sequence	ATCC SC5314		256 HUSI-PUJ	
			MIC	MFC	MIC	MFC
Control	LfcinB (20–25)	RRWQWR	200 (203)	200 (203)	200 (203)	200 (203)
	BFII (32–35) _{Pal}	RLLRLLR	>200 (>183)	>200 (>183)	>200 (>183)	>200 (>183)
I	C1	RRWQWRLLR	200 (131)	>200 (>131)	100 (66)	>200 (>131)
	C2	RRWQWR-Ahx-RLLR	200 (122)	>200 (>122)	200 (122)	>200 (>122)
	C3	RLLRRRQWR	100 (66)	200 (131)	100 (66)	200 (131)
	C4	RLLR-Ahx-RRWQWR	>200 (>122)	>200 (>122)	200 (122)	>200 (>122)
II	C5	RRWQWR-Ahx-KLLKKLLK	100 (48)	200 (97)	100 (48)	200 (97)
	C6	KKWQWK-Ahx-RLLRLLR	50 (24)	100 (48)	50 (24)	100 (48)
	C7	KKWQWK-Ahx-KLLKKLLK	200 (101)	>200 (>101)	200 (101)	>200 (>101)
III	C8	(RRWQWR) ₂ K-Ahx-RLLR	100 (37)	100 (37)	100 (37)	100 (37)
	C9	(RRWQWR) ₂ K-Ahx-RLLRLLR	50 (15)	50 (15)	50 (15)	50 (15)

2.1. Minimum Inhibitory and Fungicidal Concentration

In this investigation, chimeric peptides containing the precursor sequences LfcinB (20–25): RRWQWR and BFII (32–35)_{Pal}: RLLRLLR were synthesized and purified, and their antifungal activity against reference strain *C. albicans* ATCC SC5314 sensitive to FLC (MIC = 1 µg/mL) and a clinical isolate of *C. albicans* 256 HUSI-PUJ resistant to FLC (MIC = 64 µg/mL) was evaluated. Antifungal activity of the peptides RLLR or RLLR-RLLR has not been reported in the literature consulted to date.

The precursor peptides (controls) exhibited the lowest antifungal activity against *C. albicans* SC5314 and *C. albicans* 256 (Table 1). Peptide LfcinB (20–25) showed MIC and MFC values of 200 µg/mL (203 µM), while peptide BFII (32–35)_{Pal} had MIC and MFC values > 200 µg/mL, (>183 µM) greater than the maximum concentration of the peptide evaluated, indicating that these peptides do not exert significant antifungal activity against these strains. This is consistent with the results obtained by Muñoz et al. [32] and Pineda et al. [18] when they evaluated the peptide RRWQWR against the yeast *Saccharomyces cerevisiae* FY1679 and the peptide RLLRLLR against the gram-positive bacteria *Staphylococcus aureus* ATCC 25923 and *Enterococcus faecalis* ATCC 29212, where they did not find any antimicrobial activity at the concentrations evaluated (48–200 µg/mL).

In group I, the C1 (RRWQWRLLR) and C3 (RLLRRWQWR) chimeras lacked the Ahx spacer and the RRWQWR and RLLR motifs were alternatively bound in the N-terminal or C-terminal region of the sequence (Table 1). Moreover, the C1 and C3 chimeras showed higher antifungal activity against *C. albicans* strain SC5314 and the FLC-resistant clinical isolate *C. albicans* 256 than the precursor peptides and the C2 and C4 chimeras, suggesting that the inclusion of Ahx affects the antifungal activity against this strain. It was previously reported that the C1 and C3 chimeras showed antibacterial activity against Gram-positive and Gram-negative ATCC bacterial strains [18], suggesting that these chimeric peptides exhibit a broad spectrum of antimicrobial action. The C3 chimera showed higher antifungal activity (MIC ~100 µg/mL) against *C. albicans* SC5314 and the clinical isolate *C. albicans* 256 than the C1 peptide, suggesting that the position of the LfcinB (20–25) and BFII (32–35) motifs in the sequence might be relevant for antifungal activity against *C. albicans*. These results suggest that chemical linkage of the two precursor sequences in the C3 chimera enhances antifungal activity against the two *C. albicans* strains tested.

In group II, peptides C5 (RRWQWR-Ahx-KLLKLLK) and C6 (KKWQWK-Ahx-RLLRLLR) exhibited greater antifungal activity against the two strains evaluated than peptides C1, C2, C3, C4, and C7 (Table 1). These results indicate that the substitution of Arg with Lys in the RRWQWR sequence significantly increased the antifungal activity, and the substitution of the Arg residues with Lys residues in the RLLRLLR motif also increased the antifungal activity against both strains. On the other hand, the substitution of all Arg residues with Lys in chimera C7 did not increase the antifungal activity (MIC 200 µg/mL, 101 µM). Moreover, the results reported for C5 and C6 are similar to those obtained by Pineda et al.: C5 (MIC 100 µg/mL, 48 µM) and C6 (MIC 50 µg/mL, 24 µM) showed greater antibacterial activity than chimera C2 (MIC 200 µg/mL, 122 µM) [18,33]. According to the above, although for chimera C5 and C7 the MIC values can be considered similar to those of the precursors (controls), the C6 chimera exhibited greater activity, obtaining a MIC value up to 4 times lower than RRWQWR and RLLRLLR peptides.

In group III, peptides C8 ((RRWQWR)₂K-Ahx-RLLR) and C9 ((RRWQWR)₂K-Ahx-RLLRLLR) exhibited antifungal activity against the strains evaluated. Peptide C9 exhibited the greatest antifungal activity against both strains of *C. albicans*. These results suggest that the polyvalence of the motif RRWQWR plus the lineal dimer of the sequence RLLR increased the antifungal activity (Table 1).

Peptides C3, C5, C6, C8, and C9 showed moderate antifungal activity against the reference strain *C. albicans* SC5314 and the clinically isolated *C. albicans* 256, resistant to FLC. According to the categories proposed by Alves et al., synthetic antifungal molecules with MIC values between 26–100 µg/mL are considered to have moderate antifungal activity [34].

The results suggest that the partial replacement of Arg with Lys in one of the two motifs or the polyvalence of the RRWQWR motif enhances the antifungal activity. Peptides C6 and C9 showed the best results; both peptides exhibited the highest antifungal activity against the strains evaluated. Peptide C6 has more advantages for synthesis than peptide C9, due to the fact that peptide C6 has lesser residues than peptide C9; however, peptide C9 had the lowest MIC value against the clinically isolated *C. albicans* 256 resistant to FLC.

The results above described are in agreement with previous reports, in which peptides containing the minimal motif of LfcinB presented MICs between 0.8 and 400 µg/mL for *C. albicans* [35]. In addition, Chang et al. [36] reported that the viability of cells treated with LfcinB decreased as the concentration of LfcinB increased; similarly, the antifungal activity of the chimera was concentration dependent. Furthermore, Jang et al. [37] reported that peptides containing the minimum motif of BFII showed antifungal activity, with MIC values of 32 to >64 µg/mL in strains of *C. albicans* and *Cryptococcus neoformans*. This is the first report describing the antifungal activity of chimeras containing sequences of two AMPs (LfcinB and Buforin II). It is possible that chimeras composed of two AMP sequences exert their antifungal activity through the combination of their mechanisms of action. It has been suggested that LfcinB acts by permeating the cell membrane [21]. On the other hand,

BFII is internalized and interacts with nucleic acids by inhibiting processes of replication of genetic material and protein translation, leading to cell death [38]. The branched chimeric peptide C9 (MIC = 50 µg/mL/15 µM) exhibited greater antifungal effect compared to linear chimeras C2 (MIC = 200 µg/mL/122 µM) and C5 (MIC = 100 µg/mL/48 µM), possessing the same linker as the branched chimeras.

Taking into account the definition of fungistatic activity (decrease in the growth of a fungus by <99%) and fungicidal activity (decrease in the growth of a fungus by ≥99%) [39], our results show that chimeras C5, C6, C8, and C9 exhibited fungistatic and fungicidal activity in *C. albicans* SC5314 and *C. albicans* 256 (Figure 1). When a molecule exhibits fungicidal and/or fungistatic activity, therapeutic and prophylactic options, which can be monitored clinically, increase. It is important to highlight that chimeras C5, C6, C8, and C9 inhibited the growth of the *C. albicans* strains evaluated by more than 90%, being that these strains belong to the species most frequently involved in invasive candidiasis forms. The effect generated by the chimeric peptides depends on the concentration used; thus, it can be seen that higher concentrations are required to achieve the fungicidal effect compared to the concentrations that cause fungistatic activity (Table 2).

Table 2. Fungistatic and fungicide effect values for chimeras with higher activity against *C. albicans*.

Peptide	Time-Kill Result against <i>C. albicans</i> Strains—µg/mL (µM)			
	ATCC SC5314		256 HUSI-PUJ	
	Fungistatic *	Fungicide *	Fungistatic *	Fungicide *
C5	50 (24)	100 (48)	100 (48)	200 (97)
C6	25 (12)	50 (24)	50 (24)	100 (48)
C8	100 (37)	200 (73)	100 (37)	200 (73)
C9	13 (4)	25 (8)	13 (4)	25 (8)

* The values correspond to the fungistatic and fungicidal activity after 48 h of incubation.

Chimeras C5 and C6 showed fungicidal and fungistatic effects on *C. albicans* SC5314 and *C. albicans* 256 strains. Chimera C5 at 100 µg/mL (48 µM) showed a fungicidal effect against the *C. albicans* SC5314 strain during 48 h of incubation and a fungistatic effect at a chimera concentration of 50 µg/mL (24 µM) (Figure 1a). When the FLC-resistant clinically isolated *C. albicans* 256 was incubated for 48 h with chimera C5 at 200 µg/mL (97 µM), a fungicidal effect was observed, while chimera C5 at 100 µg/mL (48 µM) induced a fungistatic effect, inhibiting yeast growth up to approximately 30 h of incubation (Figure 1b).

Chimera C6 at 50 µg/mL (24 µM) exhibited a fungicidal effect against *C. albicans* SC5314, while at 25 µg/mL (12 µM), the effect was fungistatic, a decrease in the exponential phase being observed (Figure 1c). Similarly, this chimera at 100 µg/mL (48 µM) completely inhibited the growth of *C. albicans* 256 for 48 h. When this strain was incubated with chimera C6 at 50 µg/mL (24 µM), a fungistatic effect was observed (Figure 1d).

Chimera C8 generated a fungicidal effect on *C. albicans* SC5314 at 200 µg/mL (73 µM) during 48 h of treatment, while at 100 µg/mL (37 µM), a fungistatic effect was observed, and yeast growth was completely inhibited up to about 23 h (Figure 1e). Similarly, chimera C8 at 200 µg/mL (73 µM) also showed a fungicidal effect against *C. albicans* 256 after 48 h of treatment, while at 100 µg/mL (37 µM), it completely inhibited the yeast growth up to nearly 40 h of incubation (Figure 1f).

Chimera C9 exhibited fungicidal activity at 25 µg/mL (8 µM) on both *C. albicans* strains during 48 h of incubation, while at 12.5 µg/mL (4 µM) it exerted a fungistatic effect on the strains evaluated; the strain growth was completely inhibited up to approximately 20 h of treatment (Figure 1g,h). These results suggest that the antifungal activity is enhanced by the joining of two polyvalent motifs, the linear dimer of the RLLR sequence and the branched dimer of the RRWQWR.

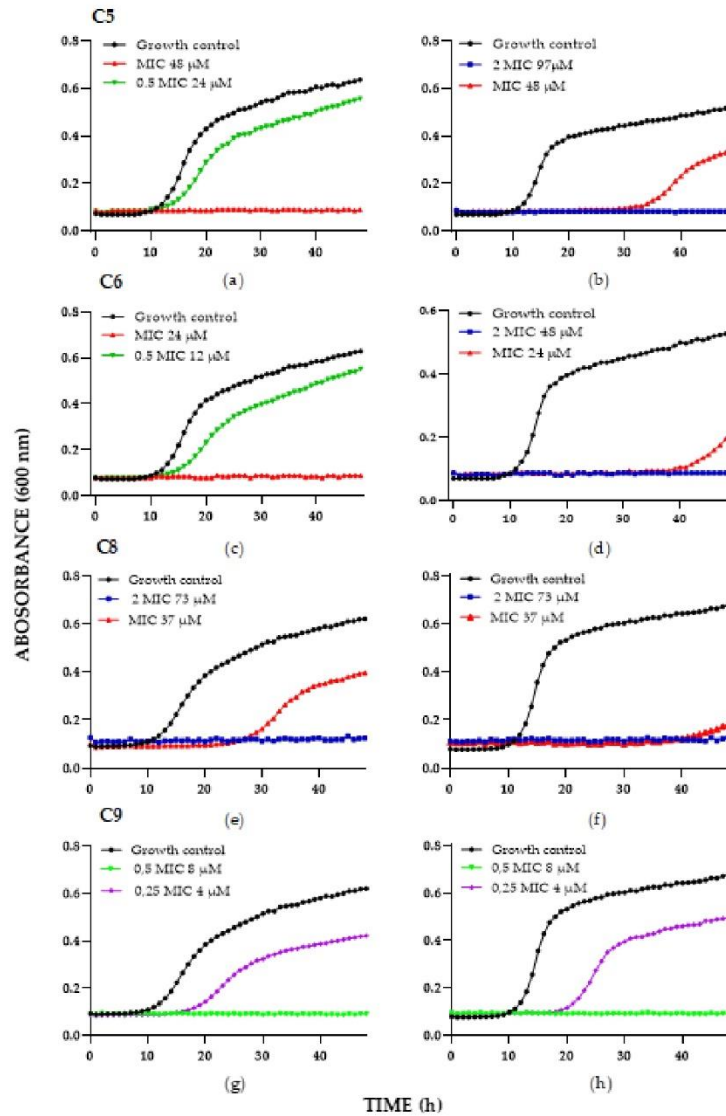


Figure 1. Time-kill curve of chimeras against reference and clinical isolates *Candida* species: (a,c,e,g) *C. albicans* SC5314, (b,d,f,h) *C. albicans* 256. The MIC value corresponds to the concentration obtained by the broth concentration method.

However, *C. albicans* 256 (resistant to FLC) and *C. albicans* SC5314 (sensitive to FLC) exhibited susceptibility to chimeras C3, C5, C6, C8, and C9, suggesting that the antifungal activity of both peptide chimeras is not affected by the resistance mechanisms that the isolated strains employ against FLC, a conventional antifungal. This particularity is of great

relevance, since these chimeras could be considered promising candidates for developing potential treatments against even resistant yeasts.

Additionally, the antifungal activity of C6 was assessed against other clinically relevant species, i.e., *C. glabrata* and *C. auris* [40–42] (Figure 2). Two sensitive (*C. glabrata* ATCC2001 and *C. auris* 0001) and two resistant (*C. glabrata* 1875 caspofungin-resistant and *C. auris* 537 AmB- FLC-resistant) isolates were included. Regarding the *C. glabrata* results, interestingly, in the reference strain, at 24 μM (50 $\mu\text{g}/\text{mL}$), C6 exerted a fungicidal effect, whereas the caspofungin-resistant isolate, at a concentration of 192 μM (400 $\mu\text{g}/\text{mL}$), exerted a fungistatic effect. For *C. auris*, the C6 chimera at 192 μM (400 $\mu\text{g}/\text{mL}$) showed a fungistatic effect on both isolates.

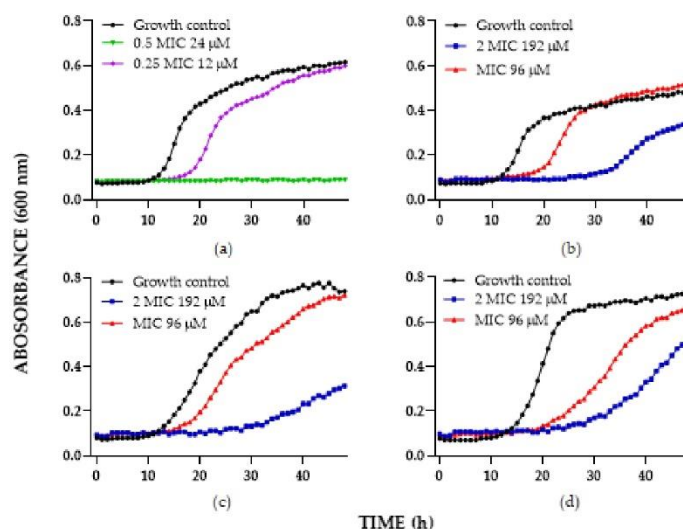


Figure 2. Time-kill curve of chimera C6 against: (a) *C. glabrata* 2001, (b) *C. glabrata* 1875, (c) *C. auris* 001, (d) *C. auris* 537. The MIC value corresponds to the concentration obtained by the broth concentration method.

2.2. Hemolytic Effect

Chimeras C3, C5, and C6 did not show a significant hemolytic effect (2–4%) at MIC concentrations, indicating that these peptides are not toxic to normal erythrocytes. The precursor peptide RLLR (200 $\mu\text{g}/\text{mL}$) exhibited a hemolytic effect of 63%, and the peptides RRWQWR (200 $\mu\text{g}/\text{mL}$) and RLLRLLR (200 $\mu\text{g}/\text{mL}$) exerted a hemolytic effect of 1% and 2%, respectively, while chimeras containing the motif RLLR or RLLRLLR did not show a significant hemolytic effect at MIC concentrations (hemolytic activity data of chimeras C1 to C7 were previously published by [18]). Similarly, the C8 chimera did not show a hemolytic effect on erythrocytes at any peptide concentration evaluated, even at concentrations where a fungicidal effect occurs (200 $\mu\text{g}/\text{mL}$), indicating that this peptide is not toxic to human red blood cells at the concentrations evaluated. Chimera C9, at 12.5 $\mu\text{g}/\text{mL}$ (4 μM) and 25 $\mu\text{g}/\text{mL}$ (8 μM), did not show hemolysis; at these chimeric concentrations, fungistatic and fungicidal effects, respectively, were observed (Table 3). Our results suggest that the inclusion of sequences with hemolytic activity in chimeras improves antifungal activity and decreases the hemolytic effect.

Table 3. Hemolysis percentage for control peptides and peptide chimeras.

Peptide	Hemolytic Activity	
	Concentration ($\mu\text{g/mL}$) *	% Hemolysis
RLLR	200	63
BFII (32–35) _{Pal}	200	2
LfcinB (20–25)	200	1
C1	100–200	5
C2	200	3
C3	100–200	4
C4	200	5
C5	50–200	2
C6	25–100	2
C7	200	6
C8	100	2
C9	13–50	2–11

* The values correspond to the concentrations where antifungal activity was evidenced.

2.3. Antifungal Activity of Chimeric Peptides Mixed with FLC

The mixture of chimera C6 (25 $\mu\text{g/mL}$) and FLC (0.5 $\mu\text{g/mL}$) showed an additive effect on antifungal activity (FICI = 1) in *C. albicans* SC5314, showing a twofold reduction in the MIC values of the peptide and the FLC. In the FLC-resistant clinical isolate *C. albicans* 256, the combination of peptide C6 and FLC induced an indifferent effect (FICI = 1.03). These results suggest that the combination of the C6 chimera with FLC, although it did not exhibit a synergistic effect against *C. albicans* SC5314, can increase the activity of FLC by a factor of two when mixed with a C6 chimera, while no significant antifungal activity was evidenced for the FLC-resistant strain *C. albicans* 256 (Table 4).

Table 4. Effect of combining the chimeric peptides with FLC on *C. albicans* SC5314 and 256 HUSI/PUJ strains.

<i>C. albicans</i> Strain	Peptide	Synergistic Result <i>C. albicans</i>						
		MIC _a	MIC _b	A	B	FICI	MIC _a /A	MIC _b /B
ATCC SC5314	C6	50	1	25	0.5	1	2	2
	C8	200	0.5	25	0.13	0.38	8	4
	C9	100	0.5	25	0.13	0.5	4	4
256 HUSI-PUJ	C6	100	32	3.1	32	1.03	32	1
	C8	100	32	50	32	1.5	2	1
	C9	50	32	25	16	1	2	2

MIC_a and MIC_b correspond to the MIC ($\mu\text{g/mL}$) of the chimeric peptide and fluconazole, respectively, and A and B are the MIC values when combining the peptides and fluconazole. Minimum fractional concentration index (FICI), MIC_a/A, and MIC_b/B represent the factor by which the chimera or FLC are potentiated after being evaluated in combination, respectively.

In contrast, a synergistic relationship was observed when both branched chimeric peptides (C8 and C9) were evaluated in combination with FLC in *C. albicans* SC5314, decreasing the MIC by a factor of between four and eight for the peptides and four for FLC (Table 4); this feature makes it possible to potentiate the antifungal activity of both molecules. The FLC-sensitive and -resistant *C. albicans* SC5314 and 256 strains, respectively, show equal susceptibility to each of the branched chimeras, evidence that the antifungal activity of the evaluated peptides is not affected by conventional antifungal resistance mechanisms.

The C8 peptide combined with FLC showed synergy for the antifungal activity against *C. albicans* SC5314, decreasing the MIC of the peptide by a factor of eight and a factor of four for FLC; however, the combination of the C8 peptide with FLC induces an indifferent effect.

C. albicans 256 (Table 4). These results suggest that the synthesis of chimeras containing MAP sequences is a promising strategy for combating resistant fungal mycoses, in order to extend the shelf life and efficacy of currently used drugs through the use of combination therapy. The results suggest that FLC-combined chimeras have the advantage of producing antifungal activity against resistant strains and may also alter the fungistatic activity of many compounds [43].

The emergence of the multidrug-resistant yeast *C. auris* and the circulation of resistant clones *C. glabrata* make it imperative to search for new therapeutic alternatives [44–46]. The C6 chimera was evaluated in combination with FLC against *C. glabrata* ATCC 2001 and 1875 and *C. auris* 001 and 537, obtaining an additive effect in three of them. For the reference strain *C. glabrata* 2001, an additive effect (FICI: 0.6) was observed, decreasing the MIC of the peptide by half and the FLC up to 10 times, in a way similar to what occurred in clinical isolates *C. auris* 001 and *C. auris* 537. In both cases, the MIC of FLC decreased by a factor of 2. Finally, for *C. glabrata*, an indifferent effect was obtained (Table 5).

Table 5. Effect of combining the C6 chimeric with FLC on *C. glabrata* and *C. auris* strain.

Synergistic Result <i>C. glabrata</i> and <i>C. Auris</i>							
Strain	MIC _a	MIC _b	A	B	FICI	MIC _a /A	MIC _b /B
<i>C. glabrata</i> ATCC 2001	100	0.3	50	0.03	0.6	2	10
<i>C. glabrata</i> 1875 CHU-PUJ	400	4	12.5	4	1.03	32	1
<i>C. auris</i> 001 HUSI-PUJ	400	32	12.5	16	0.53	32	2
<i>C. auris</i> 537 HUSI-PUJ	400	64	200	32	1	2	2

The results obtained by combining AMPs with FLC are consistent with the effect found by Vargas et al. [47], who also observed an additive effect against *C. albicans* and *C. auris* by the combination of a palindromic peptide derived from LfcinB with FLC, achieving an 8-fold enhancement of the activity of the AMPs through this mixture.

3. Materials and Methods

3.1. Reagents and Materials

The strain *C. albicans* SC5314 was purchased from ATCC (Manassas, VA, USA), and the clinical isolate *C. albicans* 256 HUSI-PUJ was obtained from the oral mucosa of a patient in the San Ignacio Hospital and deposited in the strain bank of the MICOH-P group of the PUJ (Pontificia Universidad Javeriana). Sabouraud dextrose agar (SDA), Roswell Park Memorial Institute 1640 Medium (RPMI 1640), saline, sterile distilled water (H₂O_d), seeding loop, O+ human red blood cells, 5 mL tubes with EDTA anticoagulant, Tween 20, Saline 0.85% saline, NEST Petri dishes, 96-well flat bottom and U-bottom test plates, fluconazole, red blood cells 50 mL Falcon tubes, 10 mL Falcon tubes, multichannel pipettes, 20–200 µL pipettes, 2–20 µL pipettes, 200 µL yellow tips, 200 µL yellow tips, 2–20 µL yellow tips, 200 µL yellow tips, 100–1000 µL blue tips, 0.1–10 µL white tips, 2 mL Eppendorf tubes, laminar flow chamber, ELISA reader (Expert Plus ASYS), spectrophotometer, Bioscreen C. 100-well honey comb plates specific for Bioscreen C. Fmoc-Arg(Pbf)-OH, Fmoc-Trp(Boc)-OH, Fmoc-Gln(Trt)-OH, Fmoc-Leu-OH, Fmoc-Lys(Fmoc)-OH, Fmoc-6-Ahx-OH, Rink amide resin, dicyclohexylcarbodiimide (DCC), and 1-hydroxy-6-Chlorobenzotriazole were purchased from AAPPTec (Louisville, KY, USA). Trifluoroacetic acid (TFA), acetonitrile (ACN), dichloromethane (DCM), N,N-dimethylformamide, ethanodithiol, triisopropylsilane, methanol, acetonitrile, and isopropanol were obtained from Merck (Darmstadt, Germany). SPE SupelcleanTM columns were purchased from Sigma-Aldrich (St. Louis, MO, USA).

3.2. Peptides

Chimeric peptides containing the LfcinB and BFII motifs were (i) synthesized using solid-phase peptide synthesis using Fmoc/tBu strategy, (ii) purified using RP-SPE chromatography, and (iii) characterized by RP-HPLC and MS (Supplementary material), following the protocol reported by [19].

3.3. *In Vitro* Antifungal Susceptibility Test

Antifungal susceptibility testing was carried out using the broth microdilution (BMD) method, following the CLSI M27-A3 guidelines with slight modifications [48]. Briefly, cells ($0.5\text{--}2.5 \times 10^3$ CFU/mL) were incubated with peptides (200, 100, 50, 25, 12.5, and 6.25 $\mu\text{g/mL}$) at 37 °C for 48 h. MICs were visualized and densitometry (595 nm, microplate reader, Bio-Rad, iMark™) was used to determine the lowest concentration of peptide that caused a significant decrease (MIC/2 or $\geq 50\%$) compared with the growth control (cells incubated in absence of peptide) ($n = 3$). In order to verify that the peptides were able to kill the yeast cells, the plates were also evaluated for minimum fungicidal concentration (MFC). Briefly, aliquots from each well from susceptibility testing assays were transferred to plates containing Sabouraud dextrose agar (SDA), which were then incubated at 37 °C for 24 h. The highest dilution with no growth on the agar plate was considered to be the MFC.

3.4. Time-Kill Curves

A time-kill kinetic assay was carried out according to the method previously described by Pfaller and coworkers [49] with minor modifications. The peptides (C5, C6, C8, and C9) diluted in RPMI were tested at a range of concentrations: 0 (control), 0.2, 0.5, 1, and 2 times the MIC value for each strain. The isolates were subcultured on SBD, and then an inoculum was adjusted to a $0.5\text{--}2.5 \times 10^3$ CFU/mL in an RPMI 1640 medium. Yeast inoculum (150 μL) was added to a 100-well plate containing serial dilutions of the peptides. The plates were incubated with agitation at 37 °C in a plate reader (Bioscreen C MBR automated turbidometric analyzer, Growth Curves Ltd., Helsinki, Finland), which takes hourly absorbance readings. Moreover, fluconazole MICs were used as a control. The readings were analyzed with Bioscreen software (Growth Curves USA, Piscataway, NJ, USA) and GraphPad Prism 8.0.1 (GraphPad Software, San Diego, CA, USA). Statistical comparisons were made using an analysis of variance (two-way ANOVA) followed by a Tukey–Kramer post hoc test. P values less than 0.005 were considered significant. To determine the fungistatic and fungicidal effects, a growth inhibition of $>70\%$ for 48 h was considered fungistatic, and a yeast kill of $\geq 99\%$ for 72 h was considered fungicidal. Moreover, previously determined FLC MICs (data not shown) were used as a control.

3.5. Hemolysis Assays

The hemolysis assays were carried out following the methodology reported by Vargas et al. [20] with some modifications, as follows. First, 5 mL of heparinized peripheral blood was centrifuged at 1000 g for 7 min. The erythrocyte fraction was suspended in 10 mL of saline solution (SS) and washed twice by centrifugation at 1000 g for 7 min. The erythrocytes (4% hematocrit) were incubated with peptide (ranging from 6.2 to 200 $\mu\text{g/mL}$), for 2 h at 37 °C. SS was used as negative control, while distilled water was used as a positive control. The mixtures were centrifuged, the supernatants were collected, and the absorbance was determined to be 450 nm.

3.6. Checkerboard Test

The *in vitro* interactions between the peptides (C6, C8, and C9) and the FLC drug were evaluated in a checkerboard assay, as previously described by Cokol et al. [50]. Briefly, each isolate was prepared by picking colonies from an overnight culture in SBD at 37 °C and suspended in a sterile normal saline PBS buffer. The fungal inoculum was adjusted to 0.5 MacFarland and the inoculum was adjusted to $0.5\text{--}2.5 \times 10^3$ CFU/mL. The drug-peptide combinations were formed over a range of concentrations: 0 (control) and 0.06 to

2 times the MIC [51]. The fractional inhibitory concentration index (FICI) was calculated as follows:

$$FICI = \frac{\text{CMI peptide in combination}}{\text{CMI peptide alone}} + \frac{\text{CMI FLC in combination}}{\text{CMI FLC alone}}$$

The calculated FICI was reported as synergy with values $FICI \leq 0.5$, additive $FICI > 0.5-1$, indifference $FICI > 1-4$, and antagonism $FICI \geq 4$ [52].

A synergistic effect was considered to be when the effect of the combination exceeded the effects of the individual components. An additive effect was when the effect of the combination was equal to the sum of the effects of the individual components. An indifferent effect was one in which the activity was equal to the effects of the most active component. Finally, an antagonism was a reduced effect of a drug combination observed compared to the effect of the single most effective substance [52].

4. Conclusions

In this study, we report for the first time the antifungal activity of nine chimeras containing the LfcinB and BfII minimal motifs. The chimeras C9: (RRWQWR)₂K-Ahx-RLLRRLLR and C6: KKWQWK-Ahx-RLLRRLLR exhibited the highest antifungal activity (MIC 50 µg/mL) than the precursors, no medically significant results were observed (MIC ~200 µg/mL) for the other chimeras evaluated. The peptide C9 showed promising antifungal properties being both fungistatic and fungicidal (25–12.5 µg/mL) against *C. albicans*. We also observed that the inclusion of Ahx as a spacer affects the antifungal activity against this strain. Furthermore, changing Arg to Lys in the LfcinB or BfII motifs enhanced the antifungal activity of the chimeras against the reference strain *C. albicans* SC5314 and the clinically isolated FLC-resistant *C. albicans* 256. The chimera containing the dimeric peptide LfcinB showed the highest antifungal activity against the tested strains, suggesting that this chimera design could be a successful strategy to enhance antifungal activity against reference strains or clinical isolates of *Candida* spp. It was also observed that these modifications help to reduce the toxicity of the peptides against mammalian cells, such as erythrocytes. Finally, it could be demonstrated that the chimeric peptides could be considered as a therapeutic alternative that acts individually, but also when combined with antifungals such as fluconazole.

Author Contributions: Conceptualization, Z.J.R.-M., J.E.G.-C. and C.M.P.-G.; Funding acquisition, Z.J.R.-M. and C.M.P.-G.; Investigation, K.A.-G., M.M.-T., H.M.P.-C., Y.V.-C., A.C.-G., Z.J.R.-M., J.E.G.-C. and C.M.P.-G.; Methodology, K.A.-G., M.M.-T., H.M.P.-C., Y.V.-C. and J.E.G.-C.; Project administration, C.M.P.-G.; Writing—original draft, K.A.-G., M.M.-T., H.M.P.-C., Y.V.-C. and A.C.-G.; Writing—review & editing, Z.J.R.-M., J.E.G.-C. and C.M.P.-G. All authors have read and agreed to the published version of the manuscript.

Funding: This research was funded by COLCIENCIAS 807–2018, Project: “Diseño de una formulación para el tratamiento de la candidiasis invasiva multidrogoresistente, basada en péptidos de LfcinB libres o nanoencapsulados”. Code 120380763646, contract RC N° 715–2018.

Institutional Review Board Statement: Not applicable.

Informed Consent Statement: Not applicable.

Data Availability Statement: Not applicable.

Conflicts of Interest: The authors declare no conflict of interest.

References

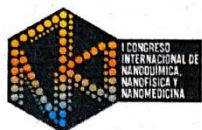
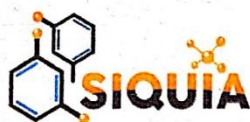
1. Pappas, P.G.; Lionakis, M.S.; Arendrup, M.C.; Ostrosky-Zeichner, L.; Kullberg, B.J. Invasive candidiasis. *Nat. Rev. Dis. Prim.* **2018**, *4*, 18026. [[CrossRef](#)]
2. Lai, C.C.; Tan, C.K.; Huang, Y.T.; Shao, P.L.; Hsueh, P.R. Current challenges in the management of invasive fungal infections. *J. Infect. Chemother.* **2008**, *14*, 77–85. [[CrossRef](#)]

3. de Bedout, C.; Gómez, B.L. Candida y candidiasis invasora: Un reto continuo para su diagnóstico temprano. *Infectio* **2010**, *14*, 159–171. [[CrossRef](#)]
4. Ch, G.; De Tema, R.; Gómez Quintero, C.H. Resistencia de levaduras del género *Candida* al fluconazol *Candida* yeast's resistance to fluconazol. *Infectio* **2010**, *14*, 172–180.
5. Basmacıyan, L.; Bon, F.; Paradis, T.; Lapaquette, P.; Dalle, F. *Candida Albicans* Interactions with the Host: Crossing the Intestinal Epithelial Barrier. *Tissue Barriers* **2019**, *7*, 1612661. [[CrossRef](#)]
6. Pfaller, M.A.; Pappas, P.G.; Wingard, J.R. Invasive Fungal Pathogens: Current Epidemiological Trends. *Clin. Infect. Dis.* **2006**, *43* (Suppl. 1), S3–S14. [[CrossRef](#)]
7. Logan, C.; Martin-Loeches, I.; Bicanic, T. Invasive candidiasis in critical care: Challenges and future directions. *Intensive Care Med.* **2020**, *46*, 2001–2014. [[CrossRef](#)]
8. de Jong, A.W.; Hagen, F. Attack, Defend and Persist: How the Fungal Pathogen *Candida auris* was Able to Emerge Globally in Healthcare Environments. *Mycopathologia* **2019**, *184*, 353–365. [[CrossRef](#)]
9. Černáková, L.; Roudbary, M.; Brás, S.; Tafaj, S.; Rodrigues, C.F. *Candida auris*: A quick review on identification, current treatments, and challenges. *Int. J. Mol. Sci.* **2021**, *22*, 4470. [[CrossRef](#)]
10. Yapar, N. Epidemiology and risk factors for invasive candidiasis. *Ther. Clin. Risk Manag.* **2014**, *10*, 95–105. [[CrossRef](#)]
11. Morio, F.; Jensen, R.H.; Le Pape, P.; Arendrup, M.C. Molecular basis of antifungal drug resistance in yeasts. *Int. J. Antimicrob. Agents* **2017**, *50*, 599–606. [[CrossRef](#)]
12. Cortés, J.A.; Ruiz, J.F.; Melgarejo-Moreno, L.N.; Lemos, E.V. Candidemia en Colombia. *Biomédica* **2020**, *40*, 195–207. [[CrossRef](#)]
13. Torres, M.D.T.; Sothiselvam, S.; Lu, T.K.; de la Fuente-Nunez, C. Peptide Design Principles for Antimicrobial Applications. *J. Mol. Biol.* **2019**, *431*, 3547–3567. [[CrossRef](#)]
14. Huan, Y.; Kong, Q.; Mou, H.; Yi, H. Antimicrobial Peptides: Classification, Design, Application and Research Progress in Multiple Fields. *Front. Microbiol.* **2020**, *11*, 582779. [[CrossRef](#)]
15. Bellotti, D.; Remelli, M. Lights and Shadows on the Therapeutic Use of Antimicrobial Peptides. *Molecules* **2022**, *27*, 4584. [[CrossRef](#)]
16. Vanzolini, T.; Bruschi, M.; Rinaldi, A.C.; Magnani, M.; Fraternali, A. Multitalented Synthetic Antimicrobial Peptides and Their Antibacterial, Antifungal and Antiviral Mechanisms. *Int. J. Mol. Sci.* **2022**, *23*, 545. [[CrossRef](#)]
17. Jiang, Y.; Chen, Y.; Song, Z.; Tan, Z.; Cheng, J. Recent advances in design of antimicrobial peptides and polypeptides toward clinical translation. *Adv. Drug Deliv. Rev.* **2021**, *170*, 261–280. [[CrossRef](#)]
18. Pineda-Castañeda, H.M.; Huertas-Ortiz, K.A.; Leal-Castro, A.L.; Vargas-Casanova, Y.; Parra-Giraldo, C.M.; García-Castañeda, J.E.; Rivera-Monroy, Z.J. Designing Chimeric Peptides: A Powerful Tool for Enhancing Antibacterial Activity. *Chem. Biodivers.* **2021**, *18*, e2000885. [[CrossRef](#)]
19. Barragán-Cárdenas, A.C.; Insuasty-Cepeda, D.S.; Cárdenas-Martínez, K.J.; López-Meza, J.; Ochoa-Zarzosa, A.; Umaña-Pérez, A.; Rivera-Monroy, Z.J.; García-Castañeda, J.E. LfcinB-Derived Peptides: Specific and punctual change of an amino acid in monomeric and dimeric sequences increase selective cytotoxicity in colon cancer cell lines. *Arab. J. Chem.* **2022**, *15*, 103998. [[CrossRef](#)]
20. Vargas-Casanova, Y.; Rodríguez-Mayor, A.V.; Cardenas, K.J.; Leal-Castro, A.L.; Muñoz-Molina, L.C.; Fierro-Medina, R.; Rivera-Monroy, Z.J.; García-Castañeda, J.E. Synergistic bactericide and antibiotic effects of dimeric, tetrameric, or palindromic peptides containing the RWQWR motif against Gram-positive and Gram-negative strains. *RSC Adv.* **2019**, *9*, 7239–7245. [[CrossRef](#)]
21. Sebastien Farnaud, R.W.E. Lactoferrin—A multifunctional protein with antimicrobial properties. *Mol. Immunol.* **2003**, *40*, 395–405. [[CrossRef](#)]
22. Gifford, J.L.; Hunter, H.N.; Vogel, H.J. Lactoferricin: A lactoferrin-derived peptide with antimicrobial, antiviral, antitumor and immunological properties. *Cell. Mol. Life Sci.* **2005**, *62*, 2588–2598. [[CrossRef](#)]
23. Yen, C.C.; Shen, C.J.; Hsu, W.H.; Chang, Y.H.; Lin, H.T.; Chen, H.L.; Chen, C.M. Lactoferrin: An iron-binding antimicrobial protein against *Escherichia coli* infection. *BioMetals* **2011**, *24*, 585–594. [[CrossRef](#)]
24. Fernandes, K.E.; Carter, D.A. The antifungal activity of lactoferrin and its derived peptides: Mechanisms of action and synergy with drugs against fungal pathogens. *Front. Microbiol.* **2017**, *8*, 2. [[CrossRef](#)]
25. Romo, T.D.; Bradney, L.A.; Greathouse, D.V.; Grossfield, A. Membrane binding of an acyl-lactoferricin B antimicrobial peptide from solid-state NMR experiments and molecular dynamics simulations. *Biochim. Biophys. Acta—Biomembr.* **2011**, *1808*, 2019–2030. [[CrossRef](#)]
26. Cho, J.H.; Sung, B.H.; Kim, S.C. Buforins: Histone H2A-derived antimicrobial peptides from toad stomach. In *Biochimica et Biophysica Acta—Biomembranes*; Elsevier B.V.: Amsterdam, The Netherlands, 2009; Volume 1788, pp. 1564–1569.
27. Park, C.B.; Yi, K.S.; Matsuzaki, K.; Kim, M.S.; Kim, S.C. Structure-activity analysis of buforin II, a histone H2A-derived antimicrobial peptide: The proline hinge is responsible for the cell-penetrating ability of buforin II. *Proc. Natl. Acad. Sci. USA* **2000**, *97*, 8245–8250. [[CrossRef](#)]
28. Tomita, M.; Takase, M.; Bellamy, W.; Shimamura, S. A review: The active peptide of lactoferrin. *Pediatr. Int.* **1994**, *36*, 585–591. [[CrossRef](#)]
29. Schibli, D.J.; Hwang, P.M.; Vogel, H.J. The structure of the antimicrobial active center of lactoferricin B bound to sodium dodecyl sulfate micelles. *FEBS Lett.* **1999**, *446*, 213–217. [[CrossRef](#)]
30. Jang, S.A.; Kim, H.; Lee, J.Y.; Shin, J.R.; Kim, D.J.; Cho, J.H.; Kim, S.C. Mechanism of action and specificity of antimicrobial peptides designed based on buforin IIb. *Peptides* **2012**, *34*, 283–289. [[CrossRef](#)]

31. Vargas Casanova, Y.; Rodríguez Guerra, J.A.; Umaña Pérez, Y.A.; Leal Castro, A.L.; Almanzar Reina, G.; García Castañeda, J.E.; Rivera Monroy, Z.J. Antibacterial Synthetic Peptides Derived from Bovine Lactoferricin Exhibit Cytotoxic Effect against MDA-MB-468 and MDA-MB-231 Breast Cancer Cell Lines. *Molecules* **2017**, *22*, 1641. [[CrossRef](#)]
32. Muñoz, A.; Marcos, J.F. Activity and mode of action against fungal phytopathogens of bovine lactoferricin-derived peptides. *J. Appl. Microbiol.* **2006**, *101*, 1199–1207. [[CrossRef](#)] [[PubMed](#)]
33. Cárdenas-Martínez, K.J.; Grueso-Mariaca, D.; Vargas-Casanova, Y.; Bonilla-Velásquez, L.; Estupiñán, S.M.; Parra-Giraldo, C.M.; Leal, A.L.; Rivera-Monroy, Z.J.; García-Castañeda, J.E. Effects of Substituting Arginine by Lysine in Bovine Lactoferricin Derived Peptides: Pursuing Production Lower Costs, Lower Hemolysis, and Sustained Antimicrobial Activity. *Int. J. Pept. Res. Ther.* **2021**, *27*, 1751–1762. [[CrossRef](#)]
34. Alves, D.D.N.; Ferreira, A.R.; Duarte, A.B.S.; Melo, A.K.V.; De Sousa, D.P.; Castro, R.D. De Breakpoints for the Classification of Anti- Candida Compounds in Antifungal Screening. *Biomed Res. Int.* **2021**, *2021*, 6653311. [[CrossRef](#)] [[PubMed](#)]
35. Fernandes, K.E.; Weeks, K.; Carter, D.A. Lactoferrin is broadly active against yeasts and highly synergistic with amphotericin B. *Antimicrob. Agents Chemother.* **2020**, *64*, e02284-19. [[CrossRef](#)]
36. Chang, C.K.; Kao, M.C.; Lan, C.Y. Antimicrobial activity of the peptide lfcinB15 against candida albicans. *J. Fungi* **2021**, *7*, 519. [[CrossRef](#)] [[PubMed](#)]
37. Jang, W.S.; Kim, H.K.; Lee, K.Y.; Kim, S.A.; Han, Y.S.; Lee, I.H. Antifungal activity of synthetic peptide derived from halocidin, antimicrobial peptide from the tunicate, *Halocynthia aurantium*. *FEBS Lett.* **2006**, *580*, 1490–1496. [[CrossRef](#)]
38. Pavia, K.E.; Spinella, S.A.; Elmore, D.E. Novel Histone-Derived Antimicrobial Peptides Use Different Antimicrobial Mechanisms. *Biochim. Biophys. Acta* **2012**, *1818*, 869. [[CrossRef](#)]
39. Lemos, A.S.O.; Florêncio, J.R.; Pinto, N.C.C.; Campos, L.M.; Silva, T.P.; Grazul, R.M.; Pinto, P.F.; Tavares, G.D.; Scio, E.; Apolônio, A.C.M.; et al. Antifungal Activity of the Natural Coumarin Scopoletin Against Planktonic Cells and Biofilms from a Multidrug-Resistant *Candida tropicalis* Strain. *Front. Microbiol.* **2020**, *11*, 1525. [[CrossRef](#)]
40. Hassan, Y.; Chew, S.Y.; Than, L.T.L. *Candida glabrata*: Pathogenicity and resistance mechanisms for adaptation and survival. *J. Fungi* **2021**, *7*, 667. [[CrossRef](#)]
41. Pfaller, M.A.; Diekema, D.J.; Turnidge, J.D.; Castanheira, M.; Jones, R.N. Twenty Years of the SENTRY Antifungal Surveillance Program: Results for *Candida* Species From 1997–2016. *Open Forum Infect. Dis.* **2019**, *6*, S79–S94. [[CrossRef](#)]
42. Ademe, M.; Girma, F. *Candida auris*: From Multidrug Resistance to Pan-Resistant Strains. *Infect. Drug Resist.* **2020**, *13*, 1287. [[CrossRef](#)] [[PubMed](#)]
43. Ježíková, Z.; Pagáč, T.; Viglaš, J.; Pfeiferová, B.; Šoltys, K.; Bujdáková, H.; Černáková, L.; Olejníková, P. Synergy Over Monotherapy. *Curr. Microbiol.* **2019**, *76*, 673–677. [[CrossRef](#)]
44. Pfaller, M.A.; Messer, S.A.; Woosley, L.N.; Jones, R.N.; Castanheira, M. Echinocandin and triazole antifungal susceptibility profiles for clinical opportunistic yeast and mold isolates collected from 2010 to 2011: Application of new CLSI clinical breakpoints and epidemiological cutoff values for characterization of geographic. *J. Clin. Microbiol.* **2013**, *51*, 2571–2581. [[CrossRef](#)] [[PubMed](#)]
45. Calvo, B.; Melo, A.S.A.; Perozo-Mena, A.; Hernandez, M.; Francisco, E.C.; Hagen, F.; Meis, J.F.; Colombo, A.L.; Satoh, K.; Makimura, K.; et al. First report of *Candida auris* in America: Clinical and microbiological aspects of 18 episodes of candidemia. *J. Infect.* **2016**, *73*, 369–374. [[CrossRef](#)] [[PubMed](#)]
46. Morales-López, S.E.; Parra-Giraldo, C.M.; Ceballos-Garzón, A.; Martínez, H.P.; Rodríguez, G.J.; Álvarez-Moreno, C.A.; Rodríguez, J.Y. Invasive Infections with Multidrug-Resistant Yeast *Candida auris*, Colombia. *Emerg. Infect. Dis.* **2017**, *23*, 162–164. [[CrossRef](#)]
47. Vargas-Casanova, Y.; Carlos Villamil Poveda, J.; Jenny Rivera-Monroy, Z.; Ceballos Garzón, A.; Fierro-Medina, R.; Le Pape, P.; Eduardo García-Castañeda, J.; Marcela Parra Giraldo, C. Palindromic Peptide lfcinB (21–25)Pal Exhibited Antifungal Activity against Multidrug-Resistant *Candida*. *ChemistrySelect* **2020**, *5*, 7236–7242. [[CrossRef](#)]
48. Clinical and Laboratory Standards Institute. *Reference Method for Broth Dilution Antifungal Susceptibility Testing of Yeasts. Approved Standard Third Edition; M27-A3*; Clinical and Laboratory Standards Institute: Wayne, PA, USA, 2008.
49. Pfaller, M.A.; Sheehan, D.J.; Rex, J.H. Determination of Fungicidal Activities against Yeasts and Molds: Lessons Learned from Bactericidal Testing and the Need for Standardization. *Clin. Microbiol. Rev.* **2004**, *17*, 268–280. [[CrossRef](#)]
50. Cokol-Cakmak, M.; Bakan, F.; Cetiner, S.; Cokol, M. Diagonal method to measure synergy among any number of drugs. *J. Vis. Exp.* **2018**, *2018*, 57713. [[CrossRef](#)]
51. Wei, G.-X.; Campagna, A.N.; Bobek, L.A. Factors affecting antimicrobial activity of MUC7 12-mer, a human salivary mucin-derived peptide. *Ann. Clin. Microbiol. Antimicrob.* **2007**, *6*, 14. [[CrossRef](#)]
52. European Committee for Antimicrobial Susceptibility Testing (EUCAST) of the European Society of Clinical Microbiology and Infectious Diseases (ESCMID). Terminology relating to methods for the determination of susceptibility of bacteria to antimicrobial agents. *Clin. Microbiol. Infect.* **2000**, *6*, 503–508. [[CrossRef](#)]

9. Anexo C: Certificados

	Pag.
C.1. IX Simposio de Química Aplicada (IX SIQUIA) y I Congreso Internacional de Nanoquímica, Nanofísica y Nanomedicina (I CINNN). <i>Uso de la cicloadición azida-alquino catalizada por cobre (química click) en la obtención de un péptido quimérico antibacteriano derivado de la Lactoferrina Bovina y la Buforina II.</i>	248
C.2. XVIII Congreso Colombiano de Química. <i>Evaluación del Efecto Bacteriostático/Bactericida de Péptidos Quiméricos Derivados de la Lactoferrina Bovina Y Buforina II.</i>	249
C.3. III Workshop de "Péptidos terapéuticos para bioaplicaciones". <i>Synthetic Lfcinb Derived Peptides: Antimicrobial Activity.</i>	250
C.4. 34° Congreso Latinoamericano de Química CLAQ 2020, el XVIII COLACRO, el X COCOCRO, el II SPAE y el IV C2B2. <i>Reacción de Formación de C-Tetrametilcalix[4]resorcinareno: Estudio de la Formación de Confórmeros Mediante RP-HPLC.</i>	251
C.5. 36th European and 12th International Peptide Symposium EPS 2022. <i>Antibacterial Activity of Peptide-Resorcinarene Dendrimers Synthesized Through Click Chemistry Azide-Alkyne Cycloaddition Reaction.</i>	252
C.6. 36th European and 12th International Peptide Symposium EPS 2022. <i>Clinical isolates multi drug-resistant of Candida spp., are susceptible to palindromic peptide: RWQWRWQWR, derived from Bovine Lactoferricin</i>	253
C.7. XXXIX RÉUNION BIENAL DE QUÍMICA. <i>Antimicrobial activity of peptide-resorcinarene dendrimers derived from the sequence BF (32-35): RLLR obtained by the CuAAC click chemical reaction.</i>	254



PROGRAMA DE QUÍMICA
FACULTAD DE CIENCIAS BÁSICAS Y TECNOLOGÍAS

**IX SIMPOSIO DE QUÍMICA APLICADA (IX SIQUIA) Y
I CONGRESO INTERNACIONAL DE NANOQUÍMICA, NANOFÍSICA Y
NANOMEDICINA (I CINNN)**

21, 22 Y 23 DE AGOSTO 2019
ARMENIA, COLOMBIA

Concede
MENCIÓN HONORIFICA

Al trabajo de Investigación

**USO DE LA CICLOADICIÓN AZIDA-ALQUINO CATALIZADA POR
COBRE (QUÍMICA CLICK) EN LA OBTENCIÓN DE UN PÉPTIDO
QUIMÉRICO ANTIBACTERIANO DERIVADO DE LA LACTOFERRICINA
BOVINA Y LA BUFORINA II.**

Autores:

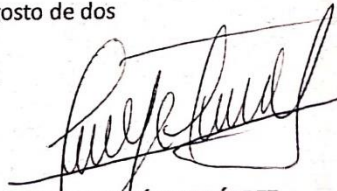
Hector M. Pineda, Javier E. García, Zuly J. Rivera.

Como el mejor trabajo de investigación en la categoría de
presentación oral, sesión Química Orgánica y productos
Naturales.

Dado en Armenia a los veintitrés (23) días del mes de agosto de dos
mil diecinueve (2019)


Dr. CRISTIÁN CAMILO VILLA


Dra. DIANA BLACH


Dr. JORGE ANDRÉS GUTIÉRREZ



XVIII
CONGRESO COLOMBIANO
de **Química**
Sostenibilidad e Innovación: Compromiso de Paz

CERTIFICA QUE:

Héctor Manuel Pineda Castañeda
Participó como ponente con el trabajo titulado:

Evaluación del efecto bacteriostático/bactericida de péptidos quiméricos derivados de la lactoferricina bovina y buforina II

En el XVIII Congreso Colombiano de Química, realizado en Popayán - Colombia, del 6 al 8 de Noviembre de 2019



Fernando Hernández
Presidente Comité Organizador




Andrea Carolina Cabaño
Presidente (E) ASQUIMCO-SUR







Constancia

La comisión organizadora del III Workshop de “Péptidos terapéuticos para bioaplicaciones” certifica que:

“Sr. Héctor Pineda”
“Obtuvo el 1° Lugar en la Sección “Video Póster”.

En el workshop, desarrollado el 17, 18 y 19 de Noviembre del 2021.

Atentamente,

Dra. Fanny Guzmán
Organizadora workshop

Dr. Fernando Albericio
Organizador workshop



El comité científico del 34° Congreso Latinoamericano de Química CLAQ 2020, el XVIII COLACRO, el X COCOCRO, el II SPAE y el IV C2B2.

Certifican que el trabajo titulado:

“REACCIÓN DE FORMACIÓN DE C-TETRAMETILCALIX[4]RESORCINARENO: ESTUDIO DE LA FORMACIÓN DE CONFÓRMEROS MEDIANTE RP-HPLC”

Fue presentado por: HECTOR MANUEL PINEDA-CASTAÑEDA, ZULY JENNY RIVERA-MONROY, MAURICIO MALDONADO-VILLAMIL.

Presentado en modalidad póster

En el marco del 34° Congreso Latinoamericano de Química CLAQ 2020.

Llevado a cabo en la ciudad de Cartagena, Colombia del 11 al 15 de octubre de 2021.

Dr. Harold Ardila
Presidente Comité organizador

Dra. Elena Stashenko
Presidente Comité Científico
CLAQ 2020, XVIII COLACRO, X COCOCRO, II SPAE

Dra. Maricela Viola
Presidente Comité Científico IV C2B2

36th EPS
European Peptide Symposium

12th IPS
International Peptide Symposium

Sitges
Barcelona
August 28 - September 2
2022



CERTIFICATE OF POSTER PRESENTATION

The Organising Committee is delighted to certify that the work:

**ANTIBACTERIAL ACTIVITY OF PEPTIDE-RESORCINARENE
DENDRIMERS SYNTHESIZED THROUGH CLICK CHEMISTRY
AZIDE-ALKYNE CYCLOADDITION REACTION**

and authors:

Sr. Héctor Pineda Castañeda
Prof. Mauricio Maldonado-Villamil
Prof. Zuly Rivera-Monroy

has been presented as poster during

**36th European and 12th International Peptide Symposium
EPS 2022**

held in Sitges, Spain on 28th August to 2nd September 2022

A handwritten signature in black ink, which appears to read 'Meritxell Teixidó', is written over a faint background image of the town of Sitges.

Dr. Meritxell Teixidó

36th EPS & 12th IPS Symposium Chair

36th EPS
European Peptide Symposium
12th IPS
International Peptide Symposium

Sitges

Barcelona
August 28 - September 2
2022



CERTIFICATE OF POSTER PRESENTATION

The Organising Committee is delighted to certify that the work:

Clinical isolates multi drug-resistant of *Candida* spp., are susceptible to palindromic peptide: RWQWRWQWR, derived from Bovine Lactoferricin

and authors:

MSc. Yerly Vargas Casanova

PhD Claudia Marcela Parra Giraldo

PhD Zuly Jenny Rivera Monroy

PhD Javier Eduardo García Castañeda

Sr. Héctor Pineda Castañeda

has been presented as poster during

**36th European and 12th International Peptide Symposium
EPS 2022**

held in Sitges, Spain on 28th August to 2nd September 2022

A handwritten signature in black ink, appearing to read 'Meritxell Teixidó', is written over a faint background image of the town of Sitges.

Dr. Meritxell Teixidó

36th EPS & 12th IPS Symposium Chair



CERTIFICATE OF PARTICIPATION

The President of the Organising Committee of the
**XXXIX REUNIÓN BIENAL DE LA SOCIEDAD ESPAÑOLA DE
 QUÍMICA**

CERTIFIES THAT:

**M. Maldonado, H.M. Pineda-Castañeda, Z. Rivera-
 Monroy**

contributed with the Poster entitled

**ANTIMICROBIAL ACTIVITY OF PEPTIDE-
 RESORCINARENE DENDRIMERS DERIVED FROM
 THE SEQUENCE BF (32-35): RLLR OBTAINED BY THE
 CuAAC CLICK CHEMICAL REACTION**

in the **XXXIX Reunión Bienal de la Sociedad Española de
 Química**, held in **Zaragoza** from 25th to 29th June, 2023.

And as evidence thereof, we hereby issue this certificate.

Prof. Fernando J. Lahoz
 President of the Organizing Committee

Abstracts published in Abstract Book with ISBN 978-84-09-52207-1 (S14-PP05)

Bibliografía

- [1] J. M. Sierra, E. Fusté, F. Rabanal, T. Vinuesa, and M. Viñas, “An overview of antimicrobial peptides and the latest advances in their development,” *Expert Opin Biol Ther*, vol. 17, no. 6, pp. 663–676, 2017, doi: 10.1080/14712598.2017.1315402.
- [2] “WHO | Antibiotic resistance,” *WHO*, 2017. <http://www.who.int/mediacentre/factsheets/antibiotic-resistance/en/> (accessed Dec. 24, 2017).
- [3] WHO, “Prevention & AMP,” 2016. <http://www.who.int/antimicrobial-resistance/amr-aidememoire-may2016.pdf> (accessed Dec. 24, 2017).
- [4] “WHO | WHO publishes list of bacteria for which new antibiotics are urgently needed,” *WHO*, 2017. <http://www.who.int/mediacentre/news/releases/2017/bacteria-antibiotics-needed/en/> (accessed Dec. 24, 2017).
- [5] “WHO | World Health Organization,” *WHO*, 2016. http://www.who.int/antimicrobial-resistance/Microbes_and_Antimicrobials/en/ (accessed Dec. 24, 2017).
- [6] M. A. León-Calvijo, A. L. Leal-Castro, G. A. Almanzar-Reina, J. E. Rosas-Pérez, J. E. García-Castañeda, and Z. J. Rivera-Monroy, “Antibacterial Activity of Synthetic Peptides Derived from Lactoferricin against *Escherichia coli* ATCC 25922 and *Enterococcus faecalis* ATCC 29212,” *Biomed Res Int*, vol. 2015, pp. 1–8, 2015, doi: 10.1155/2015/453826.
- [7] M. Dathe, H. Nikolenko, J. Klose, and M. Bienert, “Cyclization increases the antimicrobial activity and selectivity of arginine- and tryptophan-containing hexapeptides,” *Biochemistry*, vol. 43, no. 28, pp. 9140–9150, 2004, doi: 10.1021/bi035948v.
- [8] S. C. Vega, D. A. Martínez, M. del S. Chalá, H. A. Vargas, and J. E. Rosas, “Design, Synthesis and Evaluation of Branched RRWQWR-Based Peptides as Antibacterial Agents Against Clinically Relevant Gram-Positive and Gram-Negative Pathogens,” *Front Microbiol*, vol. 9, p. 329, Mar. 2018, doi: 10.3389/fmicb.2018.00329.

- [9] N. Dong *et al.*, "Short symmetric-end antimicrobial peptides centered on β -turn amino acids unit improve selectivity and stability," *Front Microbiol*, vol. 9, no. NOV, 2018, doi: 10.3389/fmicb.2018.02832.
- [10] B. Y. Jia *et al.*, "High cell selectivity and bactericidal mechanism of symmetric peptides centered on d-pro-gly pairs," *Int J Mol Sci*, vol. 21, no. 3, 2020, doi: 10.3390/ijms21031140.
- [11] H. M. Pineda-Castañeda, L. D. Bonilla-Velásquez, A. L. Leal-Castro, R. Fierro-Medina, J. E. García-Castañeda, and Z. J. Rivera-Monroy, "Use of Click Chemistry for Obtaining an Antimicrobial Chimeric Peptide Containing the LfcinB and Buforin II Minimal Antimicrobial Motifs," *ChemistrySelect*, vol. 5, no. 5, 2020, doi: 10.1002/slct.201903834.
- [12] Y.K. Agrawal and R.N. Patadia, "Studies on Resorcinarenes and their Analytical Applications," *Rev Anal Chem*, vol. 25, no. 3, pp. 155–239, 2006, doi: <https://doi.org/10.1515/REVAC.2006.25.3.155>.
- [13] M. D. Shah and Y. Agrawal, "Calixarene: A new architecture in the analytical and pharmaceutical technology," *J Sci Ind Res (India)*, vol. 71, pp. 21–26, Jan. 2012.
- [14] V. K. Jain and P. H. Kanaiya, "Chemistry of calix[4]resorcinarenes," *Russian Chemical Reviews*, vol. 80, no. 1, pp. 75–102, 2011, doi: 10.1070/rc2011v080n01abeh004127.
- [15] L. M. Tunstad *et al.*, "Host-Guest Complexation. 48. Octol Building Blocks for Cavitands and Carcerands," *Journal of Organic Chemistry*, vol. 54, no. 6, pp. 1305–1312, 1989, doi: 10.1021/jo00267a015.
- [16] H. Konishi, K. Ohata, O. Morikawa, and K. Kobayashi, "Calix[6]resorcinarenes: The first examples of [16] metacyclophanes derived from resorcinols," *J Chem Soc Chem Commun*, no. 3, pp. 309–310, 1995, doi: 10.1039/C39950000309.
- [17] K. Deleersnyder, H. Mehdi, I. T. Horváth, K. Binnemans, and T. N. Parac-Vogt, "Lanthanide(III) nitrobenzenesulfonates and p-toluenesulfonate complexes of lanthanide(III), iron(III), and copper(II) as novel catalysts for the formation of calix[4]resorcinarene," *Tetrahedron*, vol. 63, no. 37, pp. 9063–9070, 2007, doi: 10.1016/j.tet.2007.06.090.
- [18] M. Hedidi *et al.*, "Microwave-assisted synthesis of calix[4]resorcinarenes," *Tetrahedron*, vol. 62, no. 24, pp. 5652–5655, 2006, doi: 10.1016/j.tet.2006.03.095.
- [19] D. Moore, G. W. Watson, T. Gunnlaugsson, and S. E. Matthews, "Selective formation of the rctt chair stereoisomers of octa-O-alkyl resorcin[4]arenes using Brønsted acid catalysis," *New Journal of Chemistry*, vol. 32, no. 6, pp. 994–1002, 2008, doi: 10.1039/b714735j.

- [20] P. Ziaja, A. Krogul, P. TS, and G. Litwinienko, "Structure and stoichiometry of resorcinarene solvates as host-guest complexes - NMR, X-ray and thermoanalytical studies," *Thermochim Acta*, vol. 623, pp. 112–119, 2016, doi: 10.1016/j.tca.2015.10.018.
- [21] A. Velásquez-Silva, B. Cortés, Z. J. Rivera-Monroy, A. Pérez-Redondo, and M. Maldonado, "Crystal structure and dynamic NMR studies of octaacetyl-tetra(propyl)calix[4]resorcinarene," *J Mol Struct*, vol. 1137, pp. 380–386, Jun. 2017, doi: 10.1016/j.molstruc.2017.02.059.
- [22] A. A. Castillo-Aguirre, A. Pérez-Redondo, and M. Maldonado, "Influence of the hydrogen bond on the iteroselective O-alkylation of calix[4]resorcinarenes," *J Mol Struct*, vol. 1202, p. 127402, 2020, doi: 10.1016/j.molstruc.2019.127402.
- [23] E. S. Español and M. M. Villamil, "Calixarenes: Generalities and their role in improving the solubility, biocompatibility, stability, bioavailability, detection, and transport of biomolecules," *Biomolecules*, vol. 9, no. 3, 2019, doi: 10.3390/biom9030090.
- [24] R. A. Sarmiento Forero, "Reacción de sulfometilación de resorcinarenos alquilados en el borde inferior y estudio del efecto de estos sustituyentes en el proceso de reconocimiento molecular de Colina," Universidad Nacional de Colombia - Sede Bogotá, Jul. 2018.
- [25] A. Castillo-Aguirre, Z. Rivera-Monroy, and M. Maldonado, "Selective o-alkylation of the crown conformer of tetra(4-hydroxyphenyl)calix[4]resorcinarene to the corresponding tetraalkyl ether," *Molecules*, vol. 22, no. 10, Oct. 2017, doi: 10.3390/molecules22101660.
- [26] I. Victorovna-Lijanova, M. I. Reyes-Valderrama, J. L. Maldonado, G. Ramos-Ortiz, K. Tatiana, and M. Martínez-García, "Synthesis and cubic nonlinear optical behavior of phenyl and ferrocenyl-ended resorcinarene-based dendrimers," *Tetrahedron*, vol. 64, no. 19, pp. 4460–4467, 2008, doi: 10.1016/j.tet.2008.02.050.
- [27] D. Eisler, W. Hong, M. C. Jennings, and R. J. Puddephatt, "An organometallic octopus complex: Structure and properties of a resorcinarene with 16 cobalt centers," *Organometallics*, vol. 21, no. 19, pp. 3955–3960, 2002, doi: 10.1021/om020394y.
- [28] B. A. Velásquez-Silva, A. Castillo-Aguirre, Z. J. Rivera-Monroy, and M. Maldonado, "Aminomethylated calix[4]resorcinarenes as modifying agents for glycidyl methacrylate (GMA) rigid copolymers surface," *Polymers (Basel)*, vol. 11, no. 7, 2019, doi: 10.3390/polym11071147.

- [29] A. Shivanyuk, C. Schmidt, V. Böhmer, E. F. Paulus, O. Lukin, and W. Vogt, "Selective derivatization of resorcarenes. 3. C₂-symmetrical and transcavity bridged bis-benzoxazines derived from C(2v)-symmetrical tetratosylates," *J Am Chem Soc*, vol. 120, no. 18, pp. 4319–4326, 1998, doi: 10.1021/ja9729286.
- [30] B. Kuberski, M. Pecul, and A. Szumna, "A chiral 'frozen' hydrogen bonding in C₄-symmetric inherently chiral resorcin[4]arenes: NMR, X-ray, circular dichroism, and theoretical study," *European J Org Chem*, no. 18, pp. 3069–3078, 2008, doi: 10.1002/ejoc.200800247.
- [31] E. Sanabria, M. A. Estes, A. Pérez-Redondo, E. Vargas, and M. Maldonado, "Synthesis and characterization of two sulfonated resorcinarenes: A new example of a linear array of sodium centers and macrocycles," *Molecules*, vol. 20, no. 6, pp. 9915–9928, 2015, doi: 10.3390/molecules20069915.
- [32] H. Konishi, H. Yamaguchi, M. Miyashiro, K. Kobayashi, and O. Morikawa, "Functionalization at the extraannular positions of calix[4]resorcinarene using a Mannich-type thiomethylation," *Tetrahedron Lett*, vol. 37, no. 47, pp. 8547–8548, 1996, doi: 10.1016/0040-4039(96)01988-0.
- [33] M. P. Scott and M. S. Sherburn, *Resorcinarenes and Pyrogallolarenes*, Second Edi., vol. 1. Elsevier, 2017. doi: 10.1016/b978-0-12-409547-2.12475-8.
- [34] B. Astrid and V. Silva, "Funcionalización de materiales monolíticos con derivados de calix[4]resorcinareno y evaluación de su aplicación en el desarrollo de columnas para el análisis de péptidos por HPLC," 2018.
- [35] M. Urbaniak, J. Mattay, and W. Iwanek, "Synthesis of resorcinarene derivatives by the catalyzed mannich reaction, Part 2: Resorcinarene derivatives with unsaturated bonds," *Synth Commun*, vol. 38, no. 24, pp. 4345–4351, 2008, doi: 10.1080/00397910802326588.
- [36] S. Das and M. K. Das, *Surface Modification of Nanoparticles for Targeted Drug Delivery*. Cham: Springer International Publishing, 2019. doi: 10.1007/978-3-030-06115-9.
- [37] K. J. Palmer, R. Y. Wong, L. Jurd, and K. Stevens, "The Structures of the Octaacetate Esters of Two Condensation Tetramers of Resoreinol with," *Acta Crystallographica B*, vol. B32, pp. 847–852, 1976.
- [38] W. Iwanek, "The synthesis of octamethoxyresorc[4]arenes catalysed by Lewis acids," *Tetrahedron*, vol. 54, no. 46, pp. 14089–14094, 1998, doi: 10.1016/S0040-4020(98)00859-X.
- [39] J. Han and C. G. Yan, "Synthesis, crystal structure and configuration of resorcinarene amides," *J Incl Phenom Macrocycl Chem*, vol. 61, no. 1–2, pp. 119–126, 2008, doi: 10.1007/s10847-007-9403-3.

- [40] C. M. O'Farrell, J. M. Chudomel, J. M. Collins, C. F. Dignam, and T. J. Wenzel, "Water-soluble calix[4]resorcinarenes with hydroxyproline groups as chiral NMR solvating agents," *Journal of Organic Chemistry*, vol. 73, no. 7, pp. 2843–2851, Apr. 2008, doi: 10.1021/jo702751z.
- [41] B. Botta, M. Pierini, G. D. Monache, D. Subissati, F. Subrizi, and G. Zappia, "Synthesis of amino and ammonium resorcin[4]arenes as potential receptors," *Synthesis (Stuttg)*, no. 13, pp. 2110–2116, 2008, doi: 10.1055/s-2008-1067111.
- [42] W. Xu, J. P. Rourke, J. J. Vittal, and R. J. Puddephatt, "Transition Metal Rimmed-Calixresorcinarene Complexes," *Inorg Chem*, vol. 34, no. 1, pp. 323–329, Jan. 1995, doi: 10.1021/ic00105a050.
- [43] Z. H. Soomro *et al.*, "CuAAC synthesis of resorcin[4]arene-based glycoclusters as multivalent ligands of lectins," *Org Biomol Chem*, vol. 9, no. 19, pp. 6587–6597, 2011, doi: 10.1039/c1ob05676j.
- [44] R. E. Sardjono, A. Kadarohman, and A. Mardiyah, "Green Synthesis of Some Calix[4]Resorcinarene Under Microwave Irradiation," *Procedia Chem*, vol. 4, pp. 224–231, 2012, doi: 10.1016/j.proche.2012.06.031.
- [45] X. Han *et al.*, "A resorcinarene for inhibition of A β fibrillation," *Chem Sci*, vol. 8, no. 3, pp. 2003–2009, 2017, doi: 10.1039/c6sc04854d.
- [46] J. Han, Y. H. Cai, L. Liu, C. G. Yan, and Q. Li, "Syntheses, crystal structures, and electrochemical properties of multi-ferrocenyl resorcinarenes," *Tetrahedron*, vol. 63, no. 10, pp. 2275–2282, 2007, doi: 10.1016/j.tet.2006.12.073.
- [47] H. C. Kolb and K. B. Sharpless, "The growing impact of click chemistry on drug discovery.," *Drug Discov Today*, vol. 8, no. 24, pp. 1128–37, Dec. 2003.
- [48] J. Thundimadathil, "ChemInform Abstract: Click Chemistry in Peptide Science: A Mini-Review: Synthesis of Clickable Peptides and Applications," *ChemInform*, vol. 44, no. 45, pp. 34–37, 2013, doi: 10.1002/chin.201345215.
- [49] H. M. Pineda-Castañeda, Z. J. Rivera-Monroy, and M. Maldonado, "Copper(I)-Catalyzed Alkyne–Azide Cycloaddition (CuAAC) 'Click' Reaction: A Powerful Tool for Functionalizing Polyhydroxylated Platforms," *ACS Omega*, Jan. 2023, doi: 10.1021/ACSOMEGA.2C06269.
- [50] C. J. H. D. Díaz Díaz, M.G. Finn, K.B. Sharpless, V.V. Fokin, "Cicloaddición 1,3-dipolar de azidas y alquinos. I: principales aspectos sintéticos," *Anales de Química*, vol. 104, no. 3, pp. 173–180, Jul. 2008.
- [51] V. V. Rostovtsev, L. G. Green, V. V. Fokin, and K. B. Sharpless, "A stepwise Huisgen cycloaddition process: Copper(I)-catalyzed regioselective 'ligation' of azides and

- terminal alkynes,” *Angewandte Chemie - International Edition*, vol. 41, no. 14, pp. 2596–2599, Jul. 2002, doi: 10.1002/1521-3773(20020715)41:14<2596::AID-ANIE2596>3.0.CO;2-4.
- [52] H. M. Pineda Castañeda, “Péptidos quiméricos derivados de la lactoferricina bovina y la buforina: síntesis, caracterización y evaluación de su actividad antibacteriana,” Universidad Nacional de Colombia - Sede Bogotá, 2019. [Online]. Available: <http://bdigital.unal.edu.co/73364/>
- [53] T. Qadri, I. Ali, M. Hussain, F. Ahmed, M. R. Shah, and Z. Hussain, “Synthesis of New Tetra Triazole Functionalized Calix[4]resorcinarene and Chemosensing of Copper Ions in Aqueous Medium,” *Curr Org Chem*, vol. 24, no. 3, pp. 332–337, May 2020, doi: 10.2174/1385272824666200211114211.
- [54] E. Galante *et al.*, “Glycoclusters presenting lactose on calix[4]arene cores display trypanocidal activity,” *Tetrahedron*, vol. 67, no. 33, pp. 5902–5912, 2011, doi: 10.1016/j.tet.2011.06.065.
- [55] A. Dondoni and A. Marra, “C-glycoside clustering on calix[4]arene, adamantane, and benzene scaffolds through 1,2,3-triazole linkers,” *Journal of Organic Chemistry*, vol. 71, no. 20, pp. 7546–7557, 2006, doi: 10.1021/jo0607156.
- [56] A. A. Husain and K. S. Bisht, “Synthesis of a novel resorcin[4]arene-glucose conjugate and its catalysis of the CuAAC reaction for the synthesis of 1,4-disubstituted 1,2,3-triazoles in water,” *RSC Adv*, vol. 9, no. 18, pp. 10109–10116, 2019, doi: 10.1039/c9ra00972h.
- [57] C. Gao *et al.*, “Synthesis and characterization of resorcinarene-centered amphiphilic A 8B4 miktoarm star copolymers based on poly(ϵ - caprolactone) and poly(ethylene glycol) by combination of CROP and ‘click’ chemistry,” *J Polym Sci A Polym Chem*, vol. 51, no. 13, pp. 2824–2833, 2013, doi: 10.1002/pola.26670.
- [58] W. Liu, M. A. Minier, A. H. Franz, M. Curtis, and L. Xue, “Synthesis of nucleobase-calix[4]arenes via click chemistry and evaluation of their complexation with alkali metal ions and molecular assembly,” *Supramol Chem*, vol. 23, no. 12, pp. 806–818, 2011, doi: 10.1080/10610278.2011.632824.
- [59] T. Lämpchen *et al.*, “Novel analogs of antitumor agent calixarene 0118: Synthesis, cytotoxicity, click labeling with 2-[^{18}F]fluoroethylazide, and in vivo evaluation,” *Eur J Med Chem*, vol. 89, pp. 279–295, 2015, doi: 10.1016/j.ejmech.2014.10.048.
- [60] R. Hosseinzadeh, E. Domehri, M. Tajbakhsh, and A. Bekhradnia, “New fluorescent sensor based on a calix[4]arene bearing two triazole–coumarin units for copper ions: application for Cu $^{2+}$ detection in human blood serum,” *J Incl Phenom Macrocycl Chem*, vol. 93, no. 3–4, pp. 245–252, 2019, doi: 10.1007/s10847-018-0872-3.

- [61] J. Mo, P. K. Eggers, Z. X. Yuan, C. L. Raston, and L. Y. Lim, "Paclitaxel-loaded phosphonated calixarene nanovesicles as a modular drug delivery platform," *Sci Rep*, vol. 6, no. March, pp. 1–12, 2016, doi: 10.1038/srep23489.
- [62] B. Garska, M. Tabatabai, and H. Ritter, "Calix[4]arene-click-cyclodextrin and supramolecular structures with watersoluble NIPAAM-copolymers bearing adamantyl units: 'Rings on ring on chain,'" *Beilstein Journal of Organic Chemistry*, vol. 6, pp. 784–788, 2010, doi: 10.3762/bjoc.6.83.
- [63] R. Nag, S. Polepalli, M. Althaf Hussain, and C. P. Rao, "Ratiometric Cu²⁺ Binding, Cell Imaging, Mitochondrial Targeting, and Anticancer Activity with Nanomolar IC50 by Spiro-Indoline-Conjugated Calix[4]arene," *ACS Omega*, vol. 4, no. 8, pp. 13231–13240, 2019, doi: 10.1021/acsomega.9b01402.
- [64] M. Charnley *et al.*, "Generation of bioactive materials with rapid self-assembling resorcinarene-peptides," *Advanced Materials*, vol. 21, no. 28, pp. 2909–2915, Jul. 2009, doi: 10.1002/adma.200802731.
- [65] D. Astruc, E. Boisselier, and C. Ornelas, "Dendrimers designed for functions: From physical, photophysical, and supramolecular properties to applications in sensing, catalysis, molecular electronics, photonics, and nanomedicine," *Chem Rev*, vol. 110, no. 4, pp. 1857–1959, 2010, doi: 10.1021/cr900327d.
- [66] S. Kajouj *et al.*, "Synthesis and photophysical studies of a multivalent photoreactive Ru II -calix[4]arene complex bearing RGD-containing cyclopentapeptides," *Beilstein Journal of Organic Chemistry*, vol. 14, no. li, pp. 1758–1768, 2018, doi: 10.3762/bjoc.14.150.
- [67] M. Li *et al.*, "Metal ion-responsive nanocarrier derived from phosphonated calix[4]arenes for delivering dauricine specifically to sites of brain injury in a mouse model of intracerebral hemorrhage," *J Nanobiotechnology*, vol. 18, no. 1, pp. 1–19, 2020, doi: 10.1186/s12951-020-00616-3.
- [68] B. A. Makwana, K. Bhatt, D. Vyas, H. S. Gupte, and V. K. Jain, "Synthesis , Characterisation , Binding Behaviour and Antimicrobial Activity of Azocalix [4] Resorcine dye derived from 8-aminoquinoline," vol. 3, no. 6, pp. 463–470, 2014.
- [69] R. R. Kashapov *et al.*, "N-Methyl-d-glucamine–Calix[4]resorcinarene Conjugates: Self-assembly and biological properties," *Molecules*, vol. 24, no. 10, pp. 1–15, 2019, doi: 10.3390/molecules24101939.
- [70] Roxane. Salvatierra-González, Yehuda. Benguigui, Pan American Health Organization., Pan American Sanitary Bureau., and World Health Organization., *Resistencia antimicrobiana en las Américas magnitud del problema y su contención.*

Organización Panamericana de la Salud, Oficina Sanitaria Panamericana, Oficina Regional de la Organización Mundial de la Salud, 2000.

- [71] J. Castañeda-casimiro *et al.*, "Péptidos antimicrobianos: péptidos con múltiples funciones," *Alergia, asma e inmunología*, vol. 18, no. 1, pp. 16–29, 2009, [Online]. Available: <http://www.medigraphic.com/pdfs/alergia/al-2009/al091d.pdf>
- [72] N. Bruni *et al.*, "Antimicrobial activity of lactoferrin-related peptides and applications in human and veterinary medicine," *Molecules*, vol. 21, no. 6, 2016, doi: 10.3390/molecules21060752.
- [73] J. L. Gifford, H. N. Hunter, and H. J. Vogel, "Lactoferricin: A lactoferrin-derived peptide with antimicrobial, antiviral, antitumor and immunological properties," *Cellular and Molecular Life Sciences*, vol. 62, no. 22, pp. 2588–2598, 2005, doi: 10.1007/s00018-005-5373-z.
- [74] S. Farnaud and R. W. Evans, "Lactoferrin - A multifunctional protein with antimicrobial properties," *Mol Immunol*, vol. 40, no. 7, pp. 395–405, 2003, doi: 10.1016/S0161-5890(03)00152-4.
- [75] D. J. Schibli, P. M. Hwang, and H. J. Vogel, "The structure of the antimicrobial active center of lactoferricin B bound to sodium dodecyl sulfate micelles," *FEBS Lett*, vol. 446, no. 2–3, pp. 213–217, 1999, doi: 10.1016/S0014-5793(99)00214-8.
- [76] L. H. Vorland, H. Ulvatne, J. Andersen, H. Haukland, Ø. Rekdal, and J. S. Svendsen, "Lactoferricin of Bovine Origin is More Active than Lactoferricins of Human , Murine and Caprine Origin," pp. 513–517, 1998.
- [77] N. D. J. Huertas Méndez *et al.*, "Synthetic Peptides Derived from Bovine Lactoferricin Exhibit Antimicrobial Activity against E. coli ATCC 11775, S. maltophilia ATCC 13636 and S. enteritidis ATCC 13076," *Molecules*, vol. 22, no. 3, pp. 1–10, 2017, doi: 10.3390/molecules22030452.
- [78] Y. Vargas-Casanova *et al.*, "Synergistic bactericide and antibiotic effects of dimeric, tetrameric, or palindromic peptides containing the RWQWR motif against Gram-positive and Gram-negative strains," *RSC Adv*, vol. 9, no. 13, pp. 7239–7245, 2019, doi: 10.1039/c9ra00708c.
- [79] N. De Jesús Huertas, Z. J. R. Monroy, R. F. Medina, and J. E. G. Casta, "Antimicrobial activity of truncated and polyvalent peptides derived from the FKRRWQWRMKKGLA sequence against Escherichia coli ATCC 25922 and staphylococcus aureus ATCC 25923," *Molecules*, vol. 22, no. 6, 2017, doi: 10.3390/molecules22060987.
- [80] Y. Vargas Casanova *et al.*, "Antibacterial Synthetic Peptides Derived from Bovine Lactoferricin Exhibit Cytotoxic Effect against MDA-MB-468 and MDA-MB-231 Breast

- Cancer Cell Lines,” *Molecules*, vol. 22, no. 10, p. 1641, Sep. 2017, doi: 10.3390/molecules22101641.
- [81] J. H. Cho, B. H. Sung, and S. C. Kim, “Buforins: Histone H2A-derived antimicrobial peptides from toad stomach,” *Biochim Biophys Acta Biomembr*, vol. 1788, no. 8, pp. 1564–1569, 2009, doi: 10.1016/j.bbamem.2008.10.025.
- [82] G. Tonarelli and A. Simonetta, “Péptidos antimicrobianos de organismos procariotas y eucariotas como agentes terapéuticos y conservantes de alimentos,” *Fabricib*, vol. 17, pp. 137–177, 2014, doi: 10.14409/fabricib.v17i0.4316.
- [83] E. Fleming, N. P. Maharaj, J. L. Chen, R. B. Nelson, and D. E. Elmore, “Effect of lipid composition on buforin II structure and membrane entry,” *Proteins: Structure, Function, and Bioinformatics*, vol. 73, no. 2, pp. 480–491, 2008, doi: 10.1002/prot.22074.
- [84] H. S. Lee *et al.*, “Mechanism of anticancer activity of buforin IIb, a histone H2A-derived peptide,” *Cancer Lett*, vol. 271, no. 1, pp. 47–55, 2008, doi: 10.1016/j.canlet.2008.05.041.
- [85] C. B. Park, K.-S. Yi, K. Matsuzaki, M. S. Kim, and S. C. Kim, “Structure-activity analysis of buforin II, a histone H2A-derived antimicrobial peptide: The proline hinge is responsible for the cell-penetrating ability of buforin II,” *Proceedings of the National Academy of Sciences*, vol. 97, no. 15, pp. 8245–8250, 2000, doi: 10.1073/pnas.150518097.
- [86] H. S. Lee *et al.*, “Mechanism of anticancer activity of buforin IIb, a histone H2A-derived peptide,” *Cancer Lett*, vol. 271, no. 1, pp. 47–55, 2008, doi: 10.1016/j.canlet.2008.05.041.
- [87] S. A. Jang *et al.*, “Mechanism of action and specificity of antimicrobial peptides designed based on buforin IIb,” *Peptides (N.Y.)*, vol. 34, no. 2, pp. 283–289, 2012, doi: 10.1016/j.peptides.2012.01.015.
- [88] H. M. Pineda-Castañeda, L. D. Bonilla-Velásquez, A. L. Leal-Castro, R. Fierro-Medina, J. E. García-Castañeda, and Z. J. Rivera-Monroy, “Use of Click Chemistry for Obtaining an Antimicrobial Chimeric Peptide Containing the LfcinB and Buforin II Minimal Antimicrobial Motifs,” *ChemistrySelect*, vol. 5, no. 5, pp. 1655–1657, 2020, doi: 10.1002/slct.201903834.
- [89] K. Fosgerau and T. Hoffmann, “Peptide therapeutics: Current status and future directions,” *Drug Discov Today*, vol. 20, no. 1, pp. 2–8, 2015, doi: 10.1016/j.drudis.2014.10.003.

- [90] Ministerio de salud, "Proceso De Investigación, Desarrollo Y Aprobación De Un Fármaco," *MSDsalud*, pp. 1–9, 2016.
- [91] S. B. Levy and M. Bonnie, "Antibacterial resistance worldwide: Causes, challenges and responses," *Nature Medicine*, vol. 10, no. 12S. Nat Med, pp. S122–S129, 2004. doi: 10.1038/nm1145.
- [92] M. C. Maranan, B. Moreira, S. Boyle-Vavra, and R. S. Daum, "Antimicrobial resistance in staphylococci. Epidemiology, molecular mechanisms, and clinical relevance," *Infect Dis Clin North Am*, vol. 11, no. 4, pp. 813–849, 1997, doi: 10.1016/S0891-5520(05)70392-5.
- [93] C. L. Ventola, "The Antibiotic Resistance Crisis," *Pharmacy and Therapeutics*, vol. 40, no. 4, pp. 1–7, 2015, doi: 10.5796/electrochemistry.82.749.
- [94] F. Pasteran, A. Corso, M. Monsalvo, J. Frenkel, and J. Lazovski, "Resistencia a los antimicrobianos : causas , consecuencias y perspectivas en Argentina," *Whonet-Argentina*, vol. 4, pp. 1–4, 2013.
- [95] L. Morrison and T. R. Zembower, "Antimicrobial Resistance," *Gastrointestinal Endoscopy Clinics of North America*, vol. 30, no. 4. W.B. Saunders, pp. 619–635, Oct. 01, 2020. doi: 10.1016/j.giec.2020.06.004.
- [96] "OMS | Prevención y control de los brotes de cólera: política y recomendaciones de la OMS." <https://www.who.int/topics/cholera/control/es/> (accessed Nov. 06, 2020).
- [97] M. Ali, A. R. Nelson, A. L. Lopez, and D. A. Sack, "Updated global burden of cholera in endemic countries," *PLoS Negl Trop Dis*, vol. 9, no. 6, Jun. 2015, doi: 10.1371/journal.pntd.0003832.
- [98] R. Laxminarayan and G. M. Brown, "Economics of antibiotic resistance: A theory of optimal use," *J Environ Econ Manage*, vol. 42, no. 2, pp. 183–206, Sep. 2001, doi: 10.1006/jeem.2000.1156.
- [99] A. Giuliani, G. Pirri, and S. F. Nicoletto, *Antimicrobial peptides: an overview of a promising class of therapeutics*, vol. 2, no. 1. 2007. doi: 10.2478/s11535-007-0010-5.
- [100] N. J. Afacan, A. T.Y. Yeung, O. M. Pena, and R. E.W. Hancock, "Therapeutic Potential of Host Defense Peptides in Antibiotic-resistant Infections," *Curr Pharm Des*, vol. 18, no. 6, pp. 807–819, 2012, doi: 10.2174/138161212799277617.
- [101] J. L. Lau and M. K. Dunn, "Therapeutic peptides: Historical perspectives, current development trends, and future directions," *Bioorg Med Chem*, vol. 26, no. 10, pp. 2700–2707, 2018, doi: 10.1016/j.bmc.2017.06.052.
- [102] O. E. Akanbi, H. A. Njom, J. Fri, A. C. Otigbu, and A. M. Clarke, "Antimicrobial Susceptibility of Staphylococcus aureus Isolated from Recreational Waters and

- Beach Sand in Eastern Cape Province of South Africa,” *Int J Environ Res Public Health*, vol. 14, no. 9, p. 1001, Sep. 2017, doi: 10.3390/ijerph14091001.
- [103] T. A. Taylor and C. G. Unakal, *Staphylococcus Aureus*. StatPearls Publishing, 2017.
- [104] F. P. A. Robinson and M. Shalit, “Características generales del *Staphylococcus aureus*,” *Anti-Corrosion Methods and Materials*, vol. 1, no. 4, pp. 11–14, 2014, doi: 10.1108/eb020168.
- [105] R. Camarena, J; Roberto, “INFECCIÓN POR *Staphylococcus aureus* RESISTENTE A METICILINA,” *Control calidad SEIMC*, pp. 1–5, 2000.
- [106] R. AGUILAR and J. OLARTE, “*Escherichia coli* como causa de diarrea infantil,” *Rev Cubana Pediatr*, vol. 22, no. 6, pp. 334–33448, 2003.
- [107] BETELGEUX, “*Escherichia Coli*: características, patogenicidad y prevención (I) -,” *BETELGEUX*, 2016.
- [108] R. AGUILAR and J. OLARTE, “*Escherichia coli* como causa de diarrea infantil,” *Rev Cubana Pediatr*, vol. 22, no. 6, pp. 334–33448, 2003.
- [109] S. Mosquito, J. Ruiz, and T. J. Ochoa, “MECANISMOS MOLECULARES DE RESISTENCIA ANTIBIÓTICA EN *Escherichia coli* ASOCIADAS A DIARREA *Escherichia coli*- ASSOCIATED DIARRHEA,” vol. 28, no. 4, pp. 9–11, 2011.
- [110] A. T. Pavia *et al.*, “Hemolytic-uremic syndrome during an outbreak of *Escherichia coli* O157:H7 infections in institutions for mentally retarded persons: Clinical and epidemiologic observations,” *J Pediatr*, vol. 116, no. 4, pp. 544–551, 1990, doi: 10.1016/S0022-3476(05)81600-2.
- [111] J. M. Sánchez Merino, C. Guillán Maquieira, C. Fuster Foz, F. J. Madrid García, M. Jiménez Rodríguez, and J. García Alonso, “Sensibilidad microbiana de *escherichia coli* en infecciones urinarias extrahospitalarias,” *Actas Urol Esp*, vol. 27, no. 10, pp. 3–7, 2003, doi: 10.1016/S0210-4806(03)73014-9.
- [112] Z. Rivera *et al.*, “Double dimer peptide constructs are immunogenic and protective against *Plasmodium falciparum* in the experimental Aotus monkey model,” *Journal of Peptide Research*, vol. 59, no. 2, pp. 62–70, 2002, doi: 10.1046/j.1397-002x.2001.00001_957.x.
- [113] A. G. S. Hogberg, “Two stereoisomeric macrocyclic resorcinol-acetaldehyde condensation products,” *Journal of Organic Chemistry*, vol. 45, no. 22, pp. 4498–4500, 2002, doi: 10.1021/JO01310A046.
- [114] A. Kivrak, C. Yilmaz, M. Konus, H. Koca, S. Aydemir, and J. A. Oagaz, “Synthesis and biological properties of novel 1-methyl-2-(2-(prop-2-yn-1-yloxy)benzylidene)

- hydrazine analogues,” *Turk J Chem*, vol. 42, no. 2, pp. 306–316, Apr. 2018, doi: 10.3906/kim-1701-42.
- [115] V. Rodríguez *et al.*, “Efficient Fmoc Group Removal Using Diluted 4-Methylpiperidine: An Alternative for a Less-Polluting SPPS-Fmoc/tBu Protocol,” *Int J Pept Res Ther*, no. 0123456789, pp. 4–6, 2019, doi: 10.1007/s10989-019-09865-9.
- [116] X. Li, “Click to join peptides/proteins together,” *Chem Asian J*, vol. 6, no. 10, pp. 2606–2616, 2011, doi: 10.1002/asia.201100329.
- [117] O. Avrutina *et al.*, “Application of copper(I) catalyzed azide-alkyne [3+2] cycloaddition to the synthesis of template-assembled multivalent peptide conjugates,” *Org Biomol Chem*, vol. 7, no. 20, pp. 4177–4185, 2009, doi: 10.1039/b908261a.
- [118] A. Suárez, “Reacciones de cicloadición 1,3-dipolares a alquinos catalizadas por cobre,” *An. Quím*, vol. 108, no. 4, pp. 306–313, 2012, [Online]. Available: file:///C:/Users/Usuario/Downloads/pag_306.pdf
- [119] M. D. C. C. S. Arthur L. Barry, Ph.D. William A. Craig, M.D. Harriette Nadler, Ph.D. L. Barth Reller, “M26-A: Methods for Determining Bactericidal Activity of Antimicrobial Agents; Approved Guideline,” *Clinical and laboratory standards institute*, vol. 19, no. 1, pp. 56–78, 1999.
- [120] L. Saiman, “Clinical utility of synergy testing for multidrug-resistant *Pseudomonas aeruginosa* isolated from patients with cystic fibrosis: ‘the motion for,’” *Paediatr Respir Rev*, vol. 8, no. 3, pp. 249–255, 2007, doi: 10.1016/j.prrv.2007.04.006.
- [121] “M27-A3 Reference Method for Broth Dilution Antifungal Susceptibility Testing of Yeasts; Approved Standard-Third Edition,” 2008, Accessed: Sep. 07, 2022. [Online]. Available: www.clsi.org.
- [122] Y. Vargas-Casanova *et al.*, “Synergistic bactericide and antibiotic effects of dimeric, tetrameric, or palindromic peptides containing the RWQWR motif against Gram-positive and Gram-negative strains,” *RSC Adv*, vol. 9, no. 13, pp. 7239–7245, 2019, doi: 10.1039/c9ra00708c.
- [123] V. Solarte, J. Rosas, Z. Rivera, J. E. García, M. Arango, and J.-P. Vernot, “A tetrameric peptide derived from bovine lactoferricin exhibits specific cytotoxic effects against Oral Squamous-Cell Carcinoma cell lines,” *Biomed Res Int*, p. 13, 2015, doi: 10.1155/2015/630179.
- [124] T. Langan, K. Rodgers, and R. Chou, “Synchronization of Mammalian Cell Cultures by Serum Deprivation,” *Methods in Cell Science*, vol. 1524, pp. 97–105, 2017, doi: 10.1023/A:1009872403440.

- [125] S. Alfei and A. M. Schito, "From nanobiotechnology, positively charged biomimetic dendrimers as novel antibacterial agents: A review," *Nanomaterials*, vol. 10, no. 10, pp. 1–50, 2020, doi: 10.3390/nano10102022.
- [126] P. Patel, V. Patel, and P. M. Patel, "Synthetic strategy of dendrimers: A review," *Journal of the Indian Chemical Society*, vol. 99, no. 7, p. 100514, Jul. 2022, doi: 10.1016/J.JICS.2022.100514.
- [127] A. Velásquez-Silva, B. Cortés, Z. J. Rivera-Monroy, A. Pérez-Redondo, and M. Maldonado, "Crystal structure and dynamic NMR studies of octaacetyl-tetra(propyl)calix[4]resorcinarene," *J Mol Struct*, vol. 1137, pp. 380–386, Jun. 2017, doi: 10.1016/j.molstruc.2017.02.059.
- [128] M. He *et al.*, "Chromophore formation in resorcinarene solutions and the visual detection of mono- and oligosaccharides," *J Am Chem Soc*, vol. 124, no. 18, pp. 5000–5009, May 2002, doi: 10.1021/JA017713H/SUPPL_FILE/JA017713H_S2.CIF.
- [129] N. K. Beyeh and K. Rissanen, "Tetranitroresorcin[4]arene: synthesis and structure of a new stereoisomer," *Tetrahedron Lett*, vol. 50, no. 52, pp. 7369–7373, Dec. 2009, doi: 10.1016/J.TETLET.2009.10.075.
- [130] H. Mu, R. Zhou, J. Sun, and C. Yan, "Syntheses and crystal structures of functionalized tetramethyl resorcinarenes," *Chem Res Chin Univ*, vol. 31, no. 6, pp. 925–929, 2015, doi: 10.1007/s40242-015-5235-7.
- [131] H. Ito, T. Nakayama, M. Sherwood, D. Miller, and M. Ueda, "Characterization and Lithographic Application of Calix[4]resorcinarene Derivatives," *Chemistry of Materials*, vol. 20, no. 1, pp. 341–356, Jan. 2007, doi: 10.1021/CM7021483.
- [132] A. A. Castillo-Aguirre, Z. J. Rivera Monroy, and M. Maldonado, "Analysis by RP-HPLC and Purification by RP-SPE of the C -Tetra(p -hydroxyphenyl)resorcinolarene Crown and Chair Stereoisomers," *J Anal Methods Chem*, vol. 2019, 2019, doi: 10.1155/2019/2051282.
- [133] D. S. Insuasty Cepeda *et al.*, "Synthetic Peptide Purification via Solid-Phase Extraction with Gradient Elution: A Simple, Economical, Fast, and Efficient Methodology," *Molecules*, vol. 24, no. 7, 2019, doi: 10.3390/molecules24071215.
- [134] H. M. Pineda-Castañeda, M. Maldonado, and Z. J. Rivera-Monroy, "Efficient Separation of C-Tetramethylcalix[4]resorcinarene Conformers by Means of Reversed-Phase Solid-Phase Extraction," *ACS Omega*, vol. 8, no. 1, pp. 231–237, Jan. 2023, doi: 10.1021/acsomega.2c03218.

- [135] I. R. Knyazeva *et al.*, “Synthesis of novel highly functionalized triazole-linked calix[4]resorcinols via click reaction,” *Mendeleev Communications*, vol. 27, no. 6, pp. 556–558, 2017, doi: 10.1016/j.mencom.2017.11.005.
- [136] H. Wenschuh, M. Beyermann, R. Winter, M. Bienert, D. Ionescu, and L. A. Carpino, “Fmoc amino acid fluorides in peptide synthesis — Extension of the method to extremely hindered amino acids,” *Tetrahedron Lett*, vol. 37, no. 31, pp. 5483–5486, Jul. 1996, doi: 10.1016/0040-4039(96)01160-4.
- [137] G. B. Fields and R. L. Noble, “Solid phase peptide synthesis utilizing 9-fluorenylmethoxycarbonyl amino acids,” *Int J Pept Protein Res*, vol. 35, no. 3, pp. 161–214, 1990, doi: 10.1111/j.1399-3011.1990.tb00939.x.
- [138] R. Behrendt, P. White, and J. Offer, “Advances in Fmoc solid-phase peptide synthesis,” *Journal of Peptide Science*, vol. 22, no. 1, pp. 4–27, 2016, doi: 10.1002/psc.2836.
- [139] P. E. Schneggenburger, B. Worbs, and U. Diederichsen, “Azide reduction during peptide cleavage from solid support—the choice of thioscavenger?,” *Journal of Peptide Science*, vol. 16, no. 1, pp. 10–14, Jan. 2010, doi: 10.1002/PSC.1202.
- [140] M. Arias, L. J. McDonald, E. F. Haney, K. Nazmi, J. G. M. Bolscher, and H. J. Vogel, “Bovine and human lactoferricin peptides: Chimeras and new cyclic analogs,” *BioMetals*, vol. 27, no. 5, pp. 935–948, 2014, doi: 10.1007/s10534-014-9753-4.
- [141] M. A. León-Calvijo, A. L. Leal-Castro, G. A. Almanzar-Reina, J. E. Rosas-Pérez, J. E. García-Castañeda, and Z. J. Rivera-Monroy, “Antibacterial Activity of Synthetic Peptides Derived from Lactoferricin against *Escherichia coli* ATCC 25922 and *Enterococcus faecalis* ATCC 29212,” *Biomed Res Int*, vol. 2015, pp. 1–8, Mar. 2015, doi: 10.1155/2015/453826.
- [142] V. Solarte, J. Rosas, Z. Rivera, J. E. García, M. Arango, and J.-P. Vernot, “A tetrameric peptide derived from bovine lactoferricin exhibits specific cytotoxic effects against Oral Squamous-Cell Carcinoma cell lines,” *Biomed Res Int*, vol. 2015, p. 13, 2015, doi: 10.1155/2015/630179.
- [143] B. Fang, H. Y. Guo, M. Zhang, L. Jiang, and F. Z. Ren, “The six amino acid antimicrobial peptide bLFcin6 penetrates cells and delivers siRNA,” *FEBS Journal*, vol. 280, no. 4, pp. 1007–1017, 2013, doi: 10.1111/febs.12093.
- [144] K. Aguirre-Guataqui *et al.*, “Chimeric Peptides Derived from Bovine Lactoferricin and Buforin II: Antifungal Activity against Reference Strains and Clinical Isolates of *Candida* spp.,” *Antibiotics*, vol. 11, no. 11, p. 1561, Nov. 2022, doi: 10.3390/antibiotics11111561.
- [145] S. K. Carvajal, Y. Vargas-Casanova, H. M. Pineda-Castañeda, J. E. García-Castañeda, Z. J. Rivera-Monroy, and C. M. Parra-Giraldo, “In Vitro Antifungal Activity

- of Chimeric Peptides Derived from Bovine Lactoferricin and Buforin II against *Cryptococcus neoformans* var. *grubii*,” *Antibiotics* 2022, Vol. 11, Page 1819, vol. 11, no. 12, p. 1819, Dec. 2022, doi: 10.3390/ANTIBIOTICS11121819.
- [146] H. M. Pineda-Castañeda *et al.*, “Designing Chimeric Peptides: A Powerful Tool for Enhancing Antibacterial Activity,” *Chem Biodivers*, vol. 18, no. 2, 2021, doi: 10.1002/cbdv.202000885.
- [147] J. R. Guerra *et al.*, “The tetrameric peptide LfcinB (20-25)₄ derived from bovine lactoferricin induces apoptosis in the MCF-7 breast cancer cell line,” *RSC Adv*, vol. 9, no. 36, pp. 20497–20504, 2019, doi: 10.1039/c9ra04145a.